

The Behavior of Structures Composed of Composite Materials

SOLID MECHANICS AND ITS APPLICATIONS

Volume 105

Series Editor: G.M.L. GLADWELL
Department of Civil Engineering
University of Waterloo
Waterloo, Ontario, Canada N2L 3G1

Aims and Scope of the Series

The fundamental questions arising in mechanics are: *Why?*, *How?*, and *How much?*
The aim of this series is to provide lucid accounts written by authoritative researchers giving vision and insight in answering these questions on the subject of mechanics as it relates to solids.

The scope of the series covers the entire spectrum of solid mechanics. Thus it includes the foundation of mechanics; variational formulations; computational mechanics; statics, kinematics and dynamics of rigid and elastic bodies; vibrations of solids and structures; dynamical systems and chaos; the theories of elasticity, plasticity and viscoelasticity; composite materials; rods, beams, shells and membranes; structural control and stability; soils, rocks and geomechanics; fracture; tribology; experimental mechanics; biomechanics and machine design.

The median level of presentation is the first year graduate student. Some texts are monographs defining the current state of the field; others are accessible to final year undergraduates; but essentially the emphasis is on readability and clarity.

For a list of related mechanics titles, see final pages.

The Behavior of Structures Composed of Composite Materials

Second Edition

by

JACK R. VINSON

*H. Fletcher Brown Professor of Mechanical & Aerospace Engineering,
The Center for Composite Materials and The College of Marine Studies,
Department of Mechanical Engineering,
University of Delaware,
Newark, Delaware, U.S.A.*

and

ROBERT L. SIERAKOWSKI

*Chief Scientist,
AFRL/MN Eglin AFB,
Florida, U.S.A.*

KLUWER ACADEMIC PUBLISHERS

NEW YORK, BOSTON, DORDRECHT, LONDON, MOSCOW

eBook ISBN: 0-306-48414-5
Print ISBN: 1-4020-0904-6

©2004 Kluwer Academic Publishers
New York, Boston, Dordrecht, London, Moscow

Print ©2002 Kluwer Academic Publishers
Dordrecht

All rights reserved

No part of this eBook may be reproduced or transmitted in any form or by any means, electronic, mechanical, recording, or otherwise, without written consent from the Publisher

Created in the United States of America

Visit Kluwer Online at: <http://kluweronline.com>
and Kluwer's eBookstore at: <http://ebooks.kluweronline.com>

To my beautiful wife, Midge, for providing the wonderful environment, love, patience and encouragement to complete this text - JRV

In loving memory of Nina, and also to my wonderful children, Sandy and Steve - RLS

Preface to the Second Edition

The purpose of this text is to educate the engineering reader in the various aspects of mechanics for using composite materials in the design and analysis of composite structures and products.

In Chapter 1, the text acquaints the reader with the description of a composite material, and its constituents. Then, methods by which to manufacture composite materials are discussed, followed by a description of the uses of composite materials early in the twenty-first century.

Chapter 2 provides the fundamentals of anisotropic elasticity, and the methods to characterize and mathematically describe composite laminae and laminates which are the “building blocks” of composite structures. Also discussed are thermal, hygrothermal, high strain rate and piezoelectric considerations in modern composites.

Chapter 3 then deals exclusively with the static and dynamic response of composite plates and panels subjected to a variety of mechanical and environmental loads in great detail. This includes stresses, deformations, buckling loads, natural frequencies and response to blast loads. Chapter 4 analogously treats a special case of the above, namely beams, columns and rods.

In Chapter 5, cylindrical composite shells are discussed, both in determining the stresses and deformations due to static loads, but in treating the buckling of these shells under various loads and their combinations. The peculiar behavior of shells, (such as the bending boundary layer) compared to plates and beams is discussed in detail.

Because so many practical structural problems are too difficult or complex to obtain analytical solutions, Chapter 6 provides in-depth knowledge of attacking real life structural design problems using energy principles and variational methods. Thus, the engineer can always obtain a solution to a problem.

Chapter 7 provides various strength and failure theories widely used today, and their comparison. Chapter 8 provides suggested ways to analyze and design adhesive bonded joints and mechanically fastened joints.

Chapter 9 has been added to provide a needed introduction to composite design philosophy.

Appendix 1 provides a discussion of micromechanics basics; Appendix 2 lists all or most of the test standards for polymer matrix composite and Appendix 3 lists the mechanical properties of many composite in use today.

At the end of each chapter are numerous problems, which can be useful as homework problems or modified for examination problems. Professors may contact the authors for solutions to these problems.

Appreciation is hereby expressed to James T. Arters, an engineering student at the University of Delaware, who meticulously typed the text through its evolution. His accuracy, stamina and diligence are greatly appreciated. Appreciation is also expressed to Dr. Gregg Schoeppner for his contributions to Chapter 1 and the Appendices, and to Ms. Jill O'Donnell for her manuscript reading.

Jack R. Vinson
Robert L. Sierakowski

Preface to the First Edition

While currently available tests dealing with the subject of high performance composite materials touch upon a spectra of topics such as mechanical metallurgy, physical metallurgy, micromechanics and macromechanics of such systems, it is the specific purpose of this text to examine elements of the mechanics of structural components composed of composite materials. This text is intended for use in training engineers in this new technology and rational thought processes necessary to develop a better understanding of the behavior of such material systems for use as structural components. The concepts are further exploited in terms of the structural format and development to which the book is dedicated. To this end the development progresses systematically by first introducing the notion and concepts of what these new material classes are, the fabrication processes involved and their unique features relative to conventional monolithic materials. Such introductory remarks, while far too short in texts of this type, appear necessary as a precursor for engineers to develop a better understanding for design purposes of both the threshold limits to which the properties of such systems can be pushed as well as the practical limitations on their manufacture.

Following these introductory remarks, an in-depth discussion of the important differences between composites and conventional monolithic material types is discussed in terms of developing the concepts associated with directional material properties. That is, the ideas of anisotropic elasticity for initially homogeneous bodies in the phenomenological sense are described and presented. The use of such analytical tools is then presented through exemplification of selected problems for a number of classical type problems of various geometric shapes including plane stress, plane strain and the bending of a simply supported beam.

These ideas are carried forward and developed for continuous fiber composites in Chapter Two which discusses both single ply laminae and multi-ply laminate theory. This is then followed by a series of chapters, each of which deals with functional aspect of structural design in which the basic building blocks of a structural system are made. That is, plates and panels; beams, columns and rods; and cylindrical and spherical shells are each discussed within the framework of their potential use in a functional environment. Thus the traditional topics of conventional monolithic (isotropic) material structural elements such as structures subjected to static loads, thermal and other environmental loads, structural instability and vibratory response are included along with chapters on energy methods and failure theories of composite materials.

Energy methods have been included to present a tool for solving difficult problems of various types encountered in practice. Indeed, in many instances closed form solutions are not possible and approximate solutions must be sought. Energy methods thus provide both an alternative for the formulation of such problems plus a means of generating approximate solutions.

The chapter on failure theories is a generic presentation in the senses that any and/or all of the above structural components consisting of various multi-ply construction can fail when subjected to a sufficiently large loading combination. It is emphasized that the failure of composites is a complicated, changing issue because of the diverse ways in which such structural systems can fail due both to the geometric ply arrangement of the

components, complicated load paths, and the diversity of failure mechanisms which can be activated. Therefore, this chapter should serve in a global sense at best as a guide to the prediction of structural integrity, while more common and acceptable phenomenological failure theories are being developed.

Finally, a chapter on joining is included to discuss to some detail the two methods by which composite material structural components can be joined: namely, adhesive bonding and mechanical fastening. Again, the material presented is an introduction to the subject which is rapidly changing and developing.

At the end of each chapter are several problems, characteristic of the material covered which can be used. Some answers are given in an appendix.

Knowing that nothing is perfect, the authors welcome any notification of errors and ambiguities, and if addresses are provided, authors will forward errata sheets periodically.

Appreciation is hereby expressed to many students at the University of Delaware, University of Florida, Ohio State University, The Ballistics Research Laboratory, and the Argentine Air Force who have helped directly or indirectly in refining, improving and correcting the text, as well as working various problems and examples. In addition appreciation is expressed to Dr. W.J. Renton, Vought Corporation, who has used portions of the text at the University of Texas-Arlington, and made suggestions and corrections.

Jack R. Vinson
Robert L. Sierakowski

Contents

Preface to the Second Edition	VII
Preface to the First Edition	IX
1. Introduction to Composite Materials	1
1.1. General History	1
1.2. Composite Material Description	2
1.3. Types of Composite Materials	6
1.4. Constituent Properties	8
1.5. Composite Manufacturing, Fabrication and Processing	11
1.6. Uses of Composite Materials	21
1.7. Design and Analyses with Composite Materials	33
1.8. References	36
1.9. Journals	36
1.10. Problems	37
2. Anisotropic Elasticity and Composite Laminate Theory	39
2.1. Introduction	39
2.2. Derivation of the Anisotropic Elastic Stiffness and Compliance Matrices	40
2.3. The Physical Meaning of the Components of the Orthotropic Elasticity Tensor	46
2.4. Methods to Obtain Composite Elastic Properties from Fiber and Matrix Properties	50
2.5. Thermal and Hygrothermal Considerations	53
2.6. Time-Temperature Effects on Composite Materials	57
2.7. High Strain Rate Effects on Material Properties	58
2.8. Laminae of Composite Materials	59
2.9. Laminate Analyses	66
2.10. Piezoelectric Effects	76
2.11. References	77
2.12. Problems	79
3. Plates and Panels of Composite Materials	87
3.1. Introduction	87
3.2. Plate Equilibrium Equations	87
3.3. The Bending of Composite Material Laminated Plates: Classical Theory	91
3.4. Classical Plate Theory Boundary Conditions	94
3.5. Navier Solutions for Rectangular Composite Material Plates	95
3.6. Navier Solution for a Uniformly Loaded Simply Supported Plate – An Example Problem	98
3.7. Levy Solution for Plates of Composite Materials	102

3.8. Perturbation Solutions for the Bending of a Composite Material Plate With Mid-Plane Symmetry and No Bending-Twisting Coupling	106
3.9. Quasi-Isotropic Composite Panels Subjected to a Uniform Lateral Load	109
3.10. A Static Analysis of Composite Material Panels Including Transverse Shear Deformation Effects	111
3.11. Boundary Conditions for a Plate Using the Refined Plate Theory Which Includes Transverse Shear Deformation	114
3.12. Composite Plates on an Elastic Foundation	115
3.13. Solutions for Plates of Composite Materials Including Transverse-Shear Deformation Effects, Simply Supported on All Four Edges	116
3.14. Dynamic Effects on Panels of Composite Materials	119
3.15. Natural Flexural Vibrations of Rectangular Plates: Classical Theory	120
3.16. Natural Flexural Vibrations of Composite Material Plate Including Transverse-Shear Deformation Effects	122
3.17. Forced-Vibration Response of a Composite Material Plate Subjected to a Dynamic Lateral Load	124
3.18. Buckling of a Rectangular Composite Material Plate – Classical Theory	130
3.19. Buckling of a Composite Material Plate Including Transverse-Shear Deformation Effects	132
3.20. Some Remarks on Composite Structures	135
3.21. Methods of Analysis for Sandwich Panels With Composite Material Faces, and Their Structural Optimization	138
3.22. Governing Equations for a Composite Material Plate With Mid-Plane Asymmetry	138
3.23. Governing Equations for a Composite Material Plate With Bending-Twisting Coupling	139
3.24. Concluding Remarks	140
3.25. References	141
3.26. Problems and Exercises	143
4. Beams, Columns and Rods of Composite Materials	155
4.1. Development of Classical Beam Theory	155
4.2. Some Composite Beam Solutions	160
4.3. Composite Beams With Abrupt Changes in Geometry or Load	165
4.4. Solutions by Green's Functions	171
4.5. Composite Beams of Continuously Varying Cross-Section	173
4.6. Rods	177
4.7. Vibration of Composite Beams	179
4.8. Beams With Mid-Plane Asymmetry	183
4.9. Advanced Beam Theory for Dynamic Loading Including Mid-Plane Asymmetry	184
4.10. Advanced Beam Theory Including Transverse Shear Deformation Effects	193
4.11. Buckling of Composite Columns	197
4.12. References	200
4.13. Problems	200

5. Composite Material Shells	215
5.1. Introduction	215
5.2. Analysis of Composite Material Circular Cylindrical Shells	215
5.3. Some Edge Load and Particular Solutions	222
5.4. A General Solution for Composite Cylindrical Shells Under Axially Symmetric Loads	228
5.5. Response of a Long Axi-Symmetric Laminated Composite Shell to an Edge Displacement	230
5.6. Sample Solutions	232
5.7. Mid-Plane Asymmetric Circular Cylindrical Shells	239
5.8. Buckling of Circular Cylindrical Shells of Composite Materials Subjected to Various Loads	243
5.9. Vibrations of Composite Shells	252
5.10. Additional Reading On Composite Shells	253
5.11. References	253
5.12. Problems	254
6. Energy Methods For Composite Material Structures	259
6.1. Introduction	259
6.2. Theorem of Minimum Potential Energy	260
6.3. Analysis of a Beam Using the Theorem of Minimum Potential Energy	261
6.4. Use of Minimum Potential Energy for Designing a Composite Electrical Transmission Tower	268
6.5. Minimum Potential Energy for Rectangular Plates	272
6.6. A Rectangular Composite Material Plate Subjected to Lateral and Hygrothermal Loads	274
6.7. In-Plane Shear Strength Determination of Composite Materials in Laminated Composite Panels	276
6.8. Use of the Theorem of Minimum Potential Energy to Determine Buckling Loads in Composite Plates	282
6.9. Trial Functions for Various Boundary Conditions for Composite Material Rectangular Plates	285
6.10. Reissner's Variational Theorem and its Applications	286
6.11. Static Deformation of Moderately Thick Beams	289
6.12. Flexural Vibrations of Moderately Thick Beams	293
6.13. Flexural Natural Frequencies of a Simply Supported Beam Including Transverse Shear Deformation and Rotatory Inertia Effects	295
6.14. References	299
6.15. Problems	299
7. Strength and Failure Theories	303
7.1. Introduction	303
7.2. Failure of Monolithic Isotropic Materials	306
7.3. Anisotropic Strength and Failure Theories	309
7.3.1. Maximum Stress Theory	310
7.3.2. Maximum Strain Theory	310

7.3.3. Interactive Failure Theories	311
7.4. Lamina Strength Theories	315
7.5. Laminate Strength Analysis	328
7.6. References	331
7.7. Problems	332
8. Joining of Composite Material Structures	333
8.1. General Remarks	333
8.2. Adhesive Bonding	333
8.3. Mechanical Fastening	348
8.4. Recommended Reading	354
8.5. References	354
8.6. Problems	357
9. Introduction to Composite Design	361
9.1. Introduction	361
9.2. Structural Composite Design Procedures	368
9.3. Engineering Analysis	371
Appendices	375
A-1 Micromechanics	375
A-2 Test Standards for Polymer Matrix Composites	391
A-3 Properties of Various Polymer Composites	393
Author Index	397
Subject Index	401

CHAPTER 1

INTRODUCTION TO COMPOSITE MATERIALS

1.1 General History

The combining of materials to form a new material system with enhanced material properties is well documented in history. For example, the ancient Israelite workers during their tenure under the Pharaohs incorporated chopped straw in bricks as a means of enhancing their structural integrity (see Exodus 5). The Japanese Samurai warriors were known to use laminated metals in the forging of their swords to obtain desirable material properties. More recently, in the 20th century civil engineers placed steel rebars in cement and aggregate to make a well-known composite material, i.e., reinforced concrete. One could say that the modern era of composite materials began with fiberglass polymer matrix composites about the time of World War II.

In order to introduce the reader to the subject matter of new high-performance composite materials it is necessary to begin by defining precisely what constitutes such a class of materials. Furthermore, one must also define the level or scale of material characterization to adequately describe such systems for discussion. This is done with the understanding that any definition and classification scheme introduced is somewhat arbitrary.

For introductory purposes, many workers in the field of composites use a somewhat loose description for defining a composite material as simply being the combination of two or more materials formed to obtain some useful new material or specific material property. In some cases the addition of the words microscopic and macroscopic are added to describe the level of material characterization.

The definition posed above is to a large extent broad-based, in that it encompasses any number of material systems for which different levels of characterization must be used to specify the system and for which different analytical tools may be necessary for modeling purposes. As a simplistic example of the definition used above we can consider a beam consisting of clad copper and titanium material elements used in a switching strip. Such a composite system can be considered at the macroscopic level as providing enhanced temperature-dependent material behavior due to the mismatch in coefficients of thermal expansion between the copper and titanium metallic elements. This material system, while consisting of two dissimilar materials and falling within the realm of satisfying the definition of a composite material would not be acceptable as being representative of modern definitions of composites for current applications in the aerospace, automotive and other technical areas. A representative list of journals dealing with composite materials is given in Section 1.9.

1.2 Composite Material Description

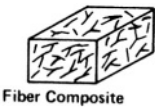
In order that agreement may be reached at the outset on a suitable modern day definition for advanced composite materials a structural classification according to the use of the following typical constituent elements is tabulated below.

STRUCTURAL LEVELS
(I) BASIC/ELEMENTAL Single molecules, crystal cells
(II) MICROSTRUCTURAL Crystals, Phases, Compounds
(III) MACROSTRUCTURAL Matrices, Particles, Fibers

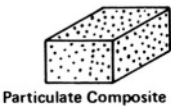
Of the structural types cited above, Type (III), or the Macrostructural type is the most important for further discussion herein. Continuing with this, next consider a further classification within the structural framework adopted. A classification of combinations of materials is described and shown in Table 1.1.

TABLE 1.1. Classification of Composite Materials

Fiber. Either continuous (long or chopped whiskers) suspended in a matrix material



Particulate. Composed of particles suspended in a matrix material.



Flake. Composed of flakes which have large ratios of platform area to thickness and are suspended in a matrix material.



Filled/Skeletal. Composed of a continuous skeletal matrix filled by a second material.



Laminar. Composed of layers (lamina) bonded together by a matrix material.



The fiber composite classification in Table 1.1 can be further structured for identification by noting the direction and placement of fibers. This results in Figure 1.1 for classification of fiber-reinforced composite types.

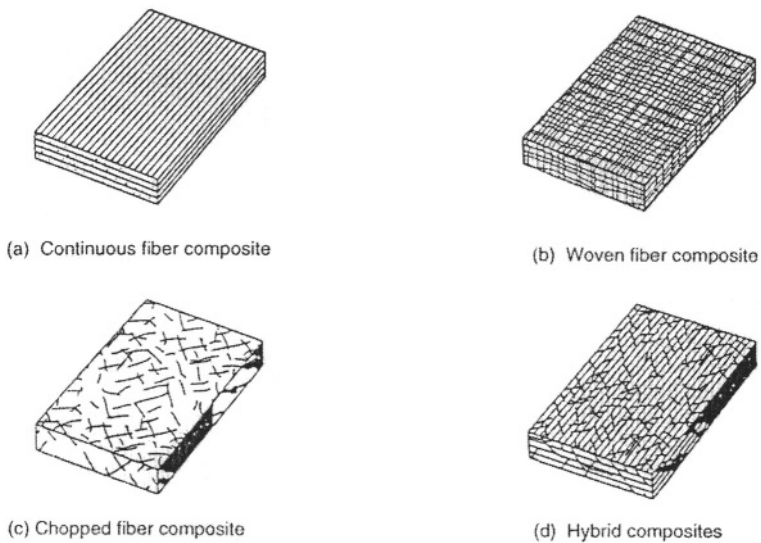


FIGURE 1.1. Types of Fiber-Reinforced Composites

A further classification of the woven composite configurations, shown in (b) above, is illustrated in the geometric architectures shown below in Figure 1.2.

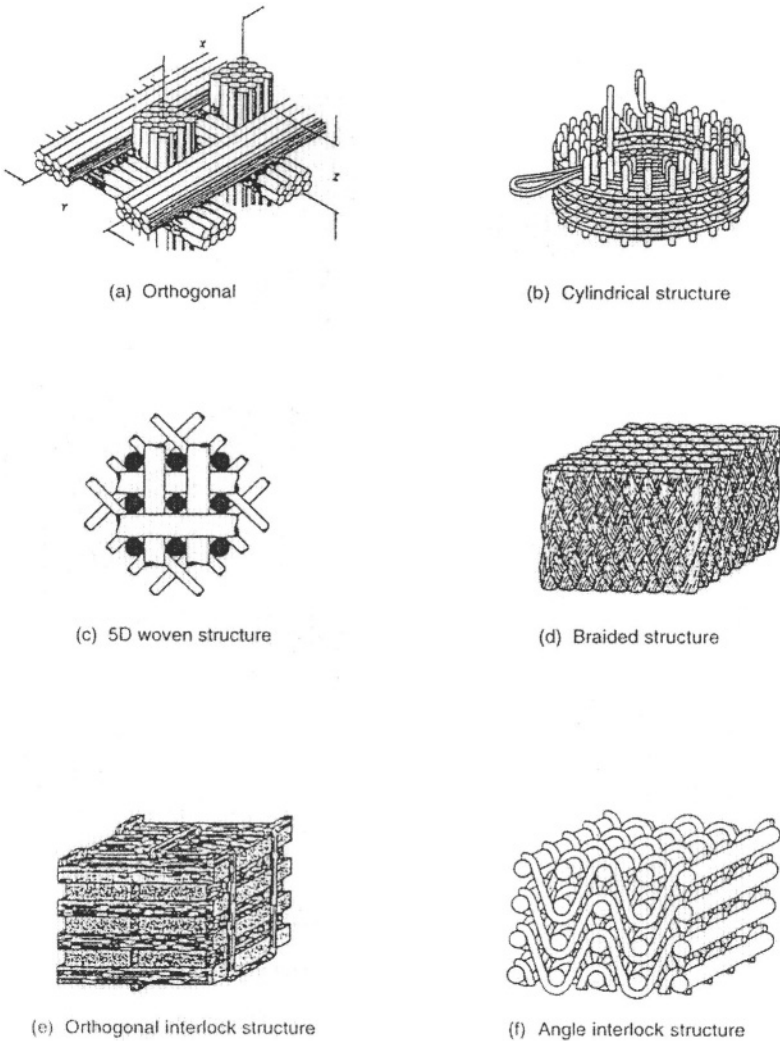


FIGURE 1.2. Types of Woven Fiber-Reinforced Composites

Of the composite material types described in Table 1.1, fiber composites have received considerable attention in recent years due to the development of advanced fiber types such as glass, Kevlar and graphite, which have moduli in excess of 3×10^6 psi/20 GPa. The incorporation of these fiber types into suitable binders/matrices, which may be metals, non-metals or ceramics, leads to a synergism in which the new material possesses unique properties compared to the properties of either of the constituent elements. The acceleration of this material's revolution is depicted in Figure 1.3, which shows the state a maturity of various materials and, in particular, the status of composite materials.

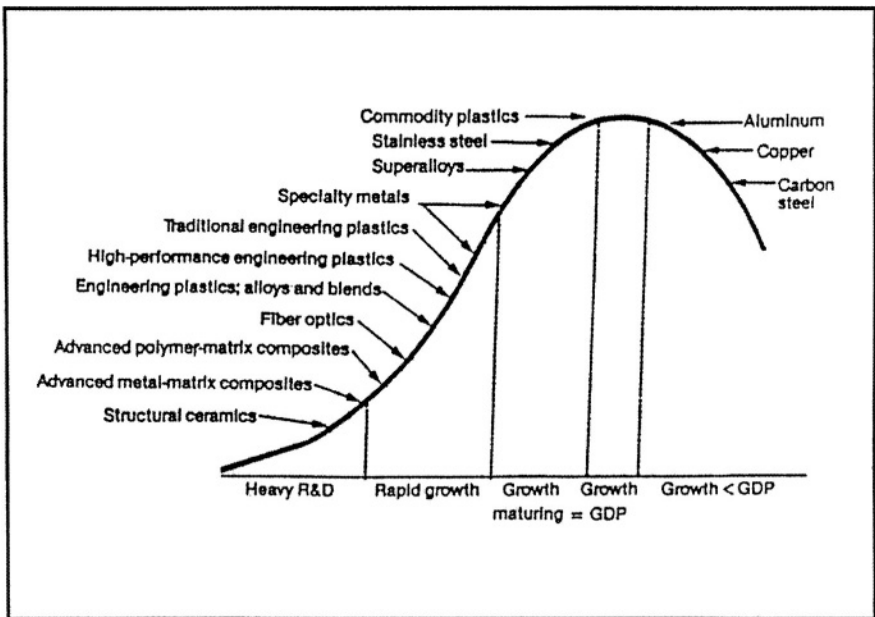


FIGURE 1.3. State of Materials Maturity

This leads to a definition of a composite material, which has been defined in ASTM D 3878-95c as:

“Composite Material. A substance consisting of two or more materials, insoluble in one another, which are combined to form a useful engineering material possessing certain properties not possessed by the constituents.”

As previously discussed, the way in which the constituents of a composite material are engineered is critical to the performance of the material system. Composites consisting of fibers embedded in a suitable matrix (binder) material can consist of several configurations dependent upon whether the embedded fibers are continuous or discontinuous. The configurations are:

- Discontinuous, fiber-reinforced composite – A composite material which consists of chopped fibers or whiskers embedded within a matrix material.
- Fabric reinforced composite – A composite material in which the embedded fiber assembly consists of a fabric, which may be woven, knitted or braided.
- Fiber-reinforced composite – A composite material which consists of embedded continuous/discontinuous fibers in a matrix material.

- Filamentary composite – A composite material reinforced by continuous fibers embedded in a matrix material.
- Unidirectional fiber-reinforced composite – A composite material in which all the embedded fibers are all aligned in a single direction.

1.3 Types of Composite Materials

The important types of advanced composites can be depicted in the pie chart shown in Figure 1.4 below, which describes the five principal types of advanced composite material in wide use.

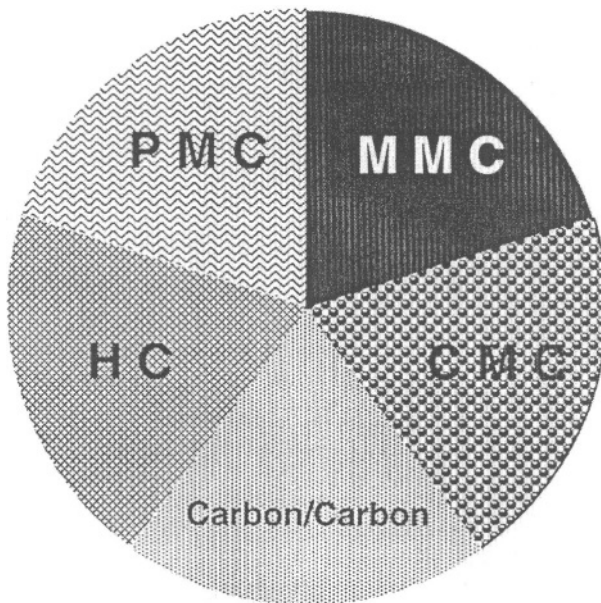


FIGURE 1.4. Principal Composite Materials

The composite types cited in Figure 1.4 include Polymer Matrix Composites (PMC), Metal Matrix Composites (MMC), Ceramic Matrix Composites (CMC), Carbon-Carbon (CC) and Hybrids consisting of a combination of the previously mentioned matrices and/or fibers.

In composite materials in 2001, glass fibers are the most used, and electrical or E-glass fibers account for more than 90% of all glass fibers used. S-glass fibers comprise the other 10% and are typically forty to seventy percent stronger than E-glass. Also, S-2 glass fibers were developed in the 1960's for military applications.

The other two fiber types most often used in composite materials today are carbon and aramid (Kevlar) fibers.

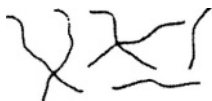
As to matrix materials by far the most often used are polymeric resins. Metal and ceramic matrix materials are used only for special applications. The polymeric resins fall into two categories: thermosets and thermoplastics. Thermoset resins become cross-linked during cure and the result is a final rigid configuration. Thermoplastic resins are processed at higher temperatures and remain plastic, can be reheated and can be reshaped. However, the majority of polymeric resins used in composites in 2001 are thermosets.

- Thermosets – This matrix can be characterized by having polymer chains that become highly cross-linked during cure. Once it is cured, it is in a final rigid configuration and there is nothing that will change it (short of a failure of the matrix). These matrices are advantageous for high temperature applications of composites.



Among the most often used thermoset resins are unsaturated polyester, halogenated polyester, vinylester, epoxy, phenolic, polyurethane and polybutadiene.

- Thermoplastics – This matrix can be characterized by having polymer chains that are not cross-linked. It can be remolded to a new shape when heated to approximately the same temperature at which it was cured. When using these matrices, the operating temperature should be kept below the cure temperature.



Among the thermoplastic resins the most often used include polyethylene, polystyrene, polypropylene, acrylonitrile-butadiene styrene (ABS), acetal, polycarbonate (PC), polyvinyl chloride (PVC), polysulfone (PSF), polyphenylene sulfide (PPS) and nylon (semi-crystalline polyimide).

1.4 Constituent Properties

The mechanical properties of a composite material are determined by the properties of the constituent materials. As a starting point, the basic properties of commonly used constituents in composite material construction are discussed.

1.4.1 MATRIX PROPERTIES

The matrix represents the binding material of the composite, which supports and protects the fibers. It also provides a mechanism for the transfer of loads in the event of fiber breakage. Typically, the matrix has a lower density, stiffness and strength than the fibers. The response characteristics for polymeric matrix materials are usually viscoelastic or viscoplastic and therefore the matrix is affected by time, temperature and moisture. Indeed, the stress-strain response of polymeric matrices is influenced by all these factors. A summary tabulation of the properties of typical polymeric matrices is included in Table 1.2 below, and Table 1.3 provides properties of some structural matrix materials.

TABLE 1.2. Typical Matrix Properties

Material	Density (kg/m ³)	E_t (GPa)	E_c (GPa)	σ_t (MPa)	σ_c (MPa)	ν	α (10 ⁻⁶ /°C)
Polyester	1200-1400	2.5-4.0	---	45-90	100-250	0.37-0.40	100-200
Epoxy	1100-1350	3.0-5.5	---	40-100	100-200	0.38-0.40	45-65
NARMCO 2387 (epoxy)	1210	3.38	3.86	29	158	---	---
PVC	1400	2.8	---	58	---	---	50
Nylon	1140	2.8	---	70	---	---	100
Polyethylene	960	1.2	---	32	---	---	120

In Table 1.2, E_T and E_C are the tensile and compressive moduli of elasticity respectively, σ_T and σ_C are the ultimate strengths, ν is the Poisson's ratio and α is the coefficient of thermal expansion.

TABLE 1.3. Typical Structural Matrix Resins

Resin	Tensile Strength (MPa)	Tensile Modulus (GPa)	T _g (K) *
<i>Thermosets</i>			
Epoxy (TSMDA)	103.4	4.1	463
Bismaleimide	82.7	4.1	547
Polyimide	137.9	4.8	630
<i>Thermoplastics</i>			
Polyphenylene sulfide	65.5	4.3	366 (555 mp)
Polyetheretherketone	70.3	1.1	400

*Glass Transition Temperature

1.4.2 FIBER PROPERTIES

Reinforcement of the matrix, to provide the majority of the strength and stiffness of a composite is accomplished by the fibers, which carry the majority of the loading and which inherently have superior properties to the bulk fiber material. The fiber can be of one of the following types:

- Organic
- Metallic
- Synthetic
- Mineral

Fibers, as used for reinforcement, can also be classified according to their geometrical properties. For reinforcement in a composite, characteristic fiber dimensions are seen below:

	Fibers	Whiskers
Length	5 mm (.20) inches > 100 × dia.	1 mm (.04 inches) 10 × dia.
Cross Sectional Area	$1.975 \times 10^{-3} \text{ mm}^2$ ($3.6 \times 10 \text{ in}^2$)	
Diameter	.25 mm (.01 inches)	

A typical demand curve for carbon fibres is shown in Figure 1.5[1]*.

* Numbers in brackets refer to references at the end of the Chapter.

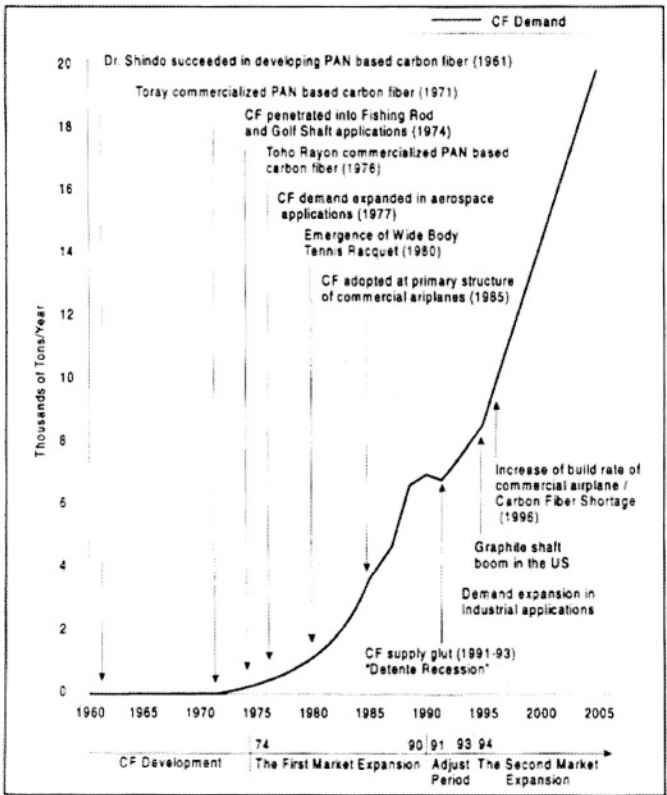


FIGURE 1.5. Demand for Carbon Fiber 1971-2005

1.5 Composite Manufacturing, Fabrication and Processing

Composite fabrication can be considered to be related to three basic manufacturing techniques shown in Table 1.4.

TABLE 1.4. Basic Manufacturing Techniques

Process	Description	Limitations
Laminating	Material, usually in form of reinforcing cloth, paper, foil, metal, wood, glass fiber, plastic, etc., preimpregnated or coated with thermoset resin (sometimes a thermoplastic) is molded under pressure greater than 6895 kPa into sheet, rod, tube or other simple shapes. Excellent dimensional stability of finished product; very economical in large production of parts.	High tool and die costs. Limited to simple shapes and cross section profiles.
Pultrusion	This process is similar to profile extrusion, however, it does not provide flexibility and uniformity of product control, and automation. Used for continuous production of simple shapes (rods, tubes and angles) principally incorporating fiberglass or other reinforcement. High output possible.	Close tolerance control requires diligence. Unidirectional strength usually the rule
Filament winding	Excellent strength-to-weight ratio. Continuous, reinforced filaments, usually glass, in the form of roving are saturated with resin and machine wound onto mandrels having shape of desired finished part. Once winding is completed, part and mandrel are cured; mandrel can then be removed through porthole at end of wound part. High strength reinforcements can be oriented precisely in direction where strength is required. Good uniformity of resin distribution in finished part; mainly circular objects such as pressure bottles, pipes and rocket cases.	Limited to shapes of positive curvature; openings and holes can reduce strength if not properly designed into molding operations.

Comparisons of various composite manufacturing processes are shown in Table 1.5(a) and (b).

TABLE 1.5(a). Comparison of FRP Composite Manufacturing Processes, Production Factors
(adapted from Wittman and Shook, 1982)

Manufacturing Process	Equipment Costs	Rate of Production	Part Strength	Operator Skill Required	Part complexity	Reproducibility	Possible Fibre Forms (R-Random/C-Continuous)
Hand Lay-up	L	L	L	H	H	L	R,C
Spray-up	M	M	L	H	H	L	R
Tape Lay-up (Manual)	L	L	---	H	N	L	C
Tape Lay-up (Automated)	H	H	---	L	M	H	C
Vacuum Bag Moulding (Wet Lay-up)	L	M	M	H	H	L	R,C
Autoclave Moulding (Tape Lay-up)	H	M	H	M	M	H	C
Filament Winding	M	M	H	L	L	H	C
Pultrusion	H	H	H	L	L	H	C
Compression Moulding	H	H	*	M	H	H	R,C
Resin Transfer Moulding	M	M	*	M	H	H	R,C
Reaction Injection Moulding	M	H	*	M	H	H	R,C
Injecting Moulding	H	H	L	H	H	H	R
Stitched/Thermoform Preforms	M	H	M	M	M	H	R,C
Random Fibre Preforms	M	L	L	H	H	L	R
3-D Woven/Braided Preforms	H	M	H	L	H	H	C

Legend: H – high
M – medium
L – low

TABLE 1.5(b). Comparison of FRP Composite Manufacturing Processes, Materials
(Rosato and Rosato 1990)

	Thermosets					Thermoplastics									
	Polyester	Polyester SMC	Polyester BMC	Epoxy	Polyurethane	Acetal	Nylon 6	Nylon 6/6	Polycarbonate	Polypropylene	Polyphenylene Sulfide	ABS	Polyphenylene Oxide	Polystyrene	Polyester
Injection Moulding	*		*	*	*	*	*	*	*	*	*	*	*	*	*
Hand Lay-up	*			*											
Spray-up	*			*											
Compression Moulding	*	*	*	*	*										
Preform Moulding	*			*											
Filament Winding	*			*											
Pultrusion	*			*											
Resin Transfer Moulding	*			*											
Reinforced Reaction Injection Moulding	*			*	*		*								

1.5.1 COMPRESSION MOLDING

For most high-volume fiber reinforced polymer matrix (FRP) composite parts compression molding is the primary choice. The high-pressure molding process produces high-strength, complex parts of a variety of sizes. Matched molds are mounted in a hydraulic or mechanical molding press. A weighed charge of bulk or sheet molding compound or a preform is placed in the open mold, along with a measured charge of resin. The heated mold halves are closed, and pressure is applied. Molding time, depending on part size and thickness, ranges from about one to five minutes. Inserts and attachments can be molded in. Compression-molded composites are characterized by good mechanical and chemical properties, superior color and excellent surface finish. Trimming and finishing costs are minimal. See Figure 1.6.

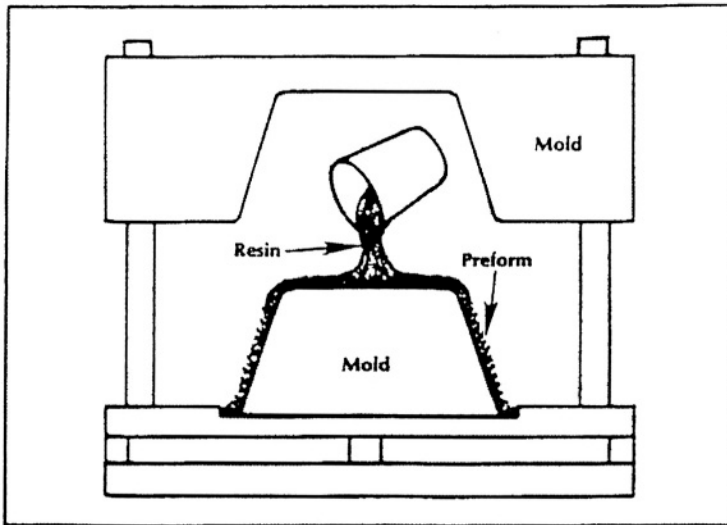


FIGURE 1.6. Compression Molding

1.5.2 RESIN TRANSFER MOLDING (RTM)

Suitable for medium-volume production of rather large FRP components, resin transfer molding is usually considered an intermediate process between the relatively slow spray-up and the faster compression-molding methods, which require higher tooling costs. RTM parts, like compression-molded parts, have two finished surfaces, but molded parts require trimming. Gel coats may be used. Abrate [2] provides an overall view of resin flow in fiber preforms.

Reinforcement mat or woven roving is placed in the bottom half of the mold, which is then closed and clamped. Catalyzed, low-viscosity resin is pumped in under pressure, displacing the air and venting it at the edges, until the mold is filled. Molds for this low-pressure system are usually made from reinforced plastics.

Vacuum-Assisted Resin Transfer Molding (VARTM): after the composite material is entered into the mold, and the part is vacuum bagged, a vacuum of \geq to 14 psi and cure temperature of less than 350° F is applied. The vacuum compacts the composite and helps the resin wet out the preformed composite part. See Figure 1.7.

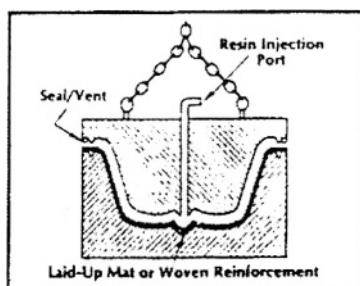


FIGURE 1.7. Resin Transfer Molding (RTM)

1.5.3 INJECTION MOLDING

Reinforced thermoset molding compounds can be injection molded, Figure 1.8, in equipment similar to that commonly used for thermoplastic resins. The principal difference lies in the temperatures maintained in various areas of the system. With thermoplastics, the injection screw and chamber are maintained at a relatively high temperature, and the die is cooled so the molded part sets up. In contrast, for a thermoset FRP, the screw and chamber are cooled so that the resin does not cross-link and gel, and the die is heated so it does cross-link and cure.

Injection molding offers high-speed production and low direct labor costs. Combined with the excellent mechanical properties available from long fibered BMC, the result is a capability for high volumes of complex parts with properties comparable to those of compression or transfer molded parts.

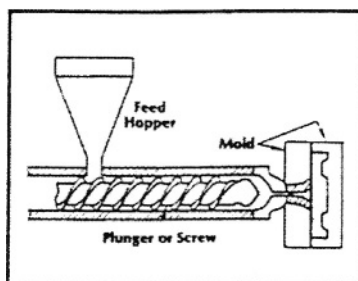


FIGURE 1.8. Injection Molding

1.5.4 COLD PRESS MOLDING

Cold press molding does not use external heat to effect part cure because the compound cures at room temperature, aided by the self-generated exothermic heat. Cold molding is an economical press-molding method, providing two finished surfaces on parts made, for manufacturing intermediate volumes of products using a low-pressure cure and inexpensive molds of plaster or glass reinforced plastic. These molds do not have sharp edges, so trimming after molding is required.

Preform or mat reinforcement is placed on the lower mold half and a resin/filler mixture is added. The mold is closed under moderate pressure or 20 to 50 psi, and the FRP part cures. Cold molding is suited mainly for relatively simple shapes, without ribs or bosses.

1.5.5 STRUCTURAL REACTION INJECTION MOLDING (SRIM)

Structural reaction injection molding shown in Figure 1.9, is suitable for medium-to-high volume composite parts requiring superior strength with no loss in toughness or flexibility. The SRIM process also produces parts with high impact resistance and lower weight, and is excellent for larger part sizes.

Like injection molding, resin is injected into a closed mold. However, the SRIM process utilizes a directed-fiber preform or reinforcing mat, which is placed into the mold prior to closure, resulting in even distribution of glass and uniform mechanical properties.

SRIM parts offer two finished surfaces, but the polyurethane systems typically used do not provide a Class A surface finish and are generally considered unsuitable for applications where cosmetics are important. For structural application, however, the low temperature and pressure characteristics of SRIM lead to lower equipment and manufacturing costs compared to similar processes.

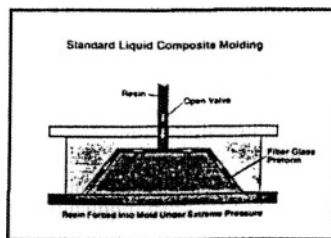


FIGURE 1.9. Structural Reaction Injection Molding (SRIM)

1.5.6 HAND LAY-UP

The simplest and oldest of the fabrication processes for FRP composites, hand lay-up, is a labor-intensive method suited especially for low-volume production of large components such as boat hulls and associated parts. See Figure 1.10.

A pigmented gel coat is first sprayed onto the mold for a high-quality surface finish. When the gel coat has become tacky, glass reinforcing mat and/or woven roving is placed on the mold, and resin is poured, brushed or sprayed on. Manual rolling then removes entrapped air, densifies the composite and thoroughly wets the reinforcement with the resin. Additional layers of mat or woven roving and resin are added for thickness. Curing is initiated by a catalyst or accelerator in the resin system, which hardens the composite without external heat.

Hand lay-up offers low-cost tooling, simple processing and a wide range of part size potential. Design changes are made easily. Parts have one finished surface and require trimming.

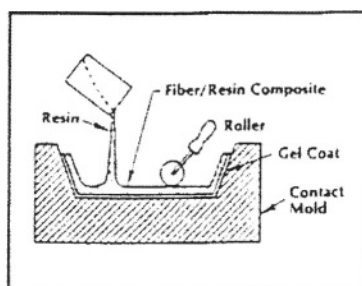


FIGURE 1.10. Hand Lay-Up

1.5.7 SPRAY LAY-UP

Similar to hand lay-up in simplicity, spray lay-up, shown in Figure 1.11, offers greater shape complexity and faster production. It too uses a low-cost open mold (one finished part surface), room temperature curing resin and is suited for producing large FRP parts such as tub/shower units and vent hoods in low to moderate quantities. Cure is usually at room temperature, but it can be accelerated by application of moderate heat.

Chopped fiber reinforcement and catalyzed resin are deposited in the mold from a combination chopper/spray gun. As with lay-up, manual rolling removes entrapped air and wets the fiber reinforcement. Woven roving is often added in specific areas for thickness or greater strength. Pigmented gel coats can be used to produce a smooth, colorful surface.

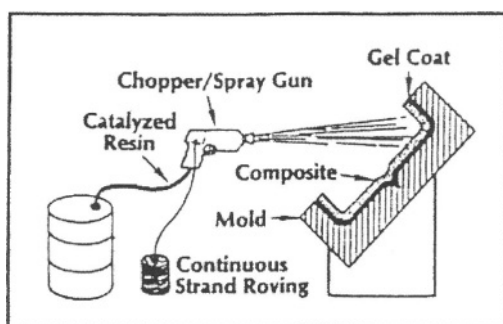


FIGURE 1.11. Spray Lay-Up

Mechanical properties and off mold surfaces or contact-molding FRP components can be improved by a number of techniques. These techniques speed the cure of parts made by lay-up and spray-up, but they also add to processing costs.

1.5.8 VACUUM BAG PROCESSING

Vacuum bag processing, Figure 1.12, uses a vacuum to eliminate entrapped air and excess resin from a lay-up from on either a male or female mold. A non-adhering film (usually polyvinyl alcohol or nylon) is placed over the lay-up and sealed at its edges. A vacuum is drawn on the bag formed by the film, and the FRP composite is cured, either at room temperature or with heat to speed the process. Compared to hand lay-up, the vacuum method provides higher reinforcement concentration and better adhesion between layers.

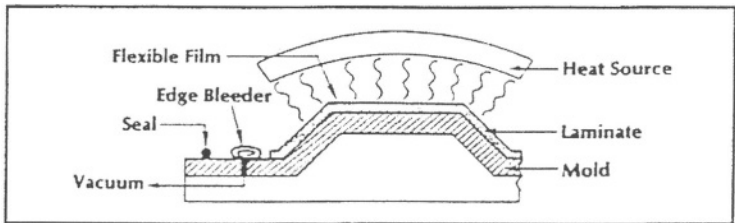


FIGURE 1.12. Vacuum Bag Processing

1.5.9 PRESSURE BAG MOLDING

Pressure bag molding is similar to the vacuum bag method except that air pressure of 30 to 50 psi is applied to a rubber bag or sheet that covers the laid-up assembly to force out entrapped air and excess resin. Pressurized steam may be used instead to accelerate the cure. This process is practical only with female molds. See Figure 1.13 below.

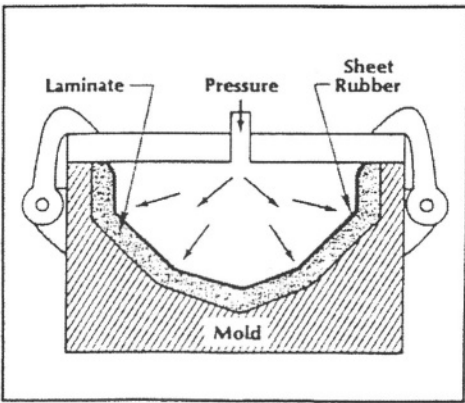


FIGURE 1.13. Pressure Bag Molding

1.5.10 AUTOCLAVE MOLDING

Autoclave molding is a further modification of either vacuum bag or pressure bag molding. The process produces denser, void-free composites because higher heat and pressure are used in the cure. Autoclaves, Figure 1.14, are essentially heated pressure vessels (usually equipped with vacuum systems) into which bagged lay-ups, on their molds, are taken to be cured at pressure of 50 to 100 psi. Autoclaves are normally used to process high-performance components based on epoxy-resin systems for aircraft and aerospace applications.

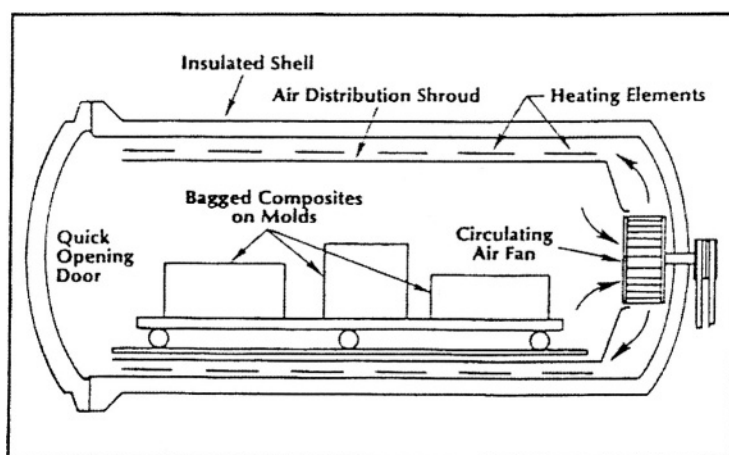


FIGURE 1.14. Autoclave

1.5.11 FILAMENT WINDING

Some FRP production methods involve specialized approaches to making parts requiring unusual properties or configurations such as very large size, extremely high strength, highly directional fiber orientation, unusual shape or constant cross section. In most cases, these methods are the only ones suitable for the conditions of configurations for which they were designed.

Continuous, resin-impregnated fibers or roving are wound on a rotating mandrel in a predetermined pattern, providing maximum control over fiber placement and uniformity of structure. See Figure 1.15. In the wet method, the fiber picks up the low viscosity resin either by passing through a trough or from a metered application system. In the dry method, the reinforcement is impregnated with resin prior to winding.

Integral fittings and vessel closings can be wound into the structure. When sufficient layers have been applied, the FRP composite is cured on the mandrel and the mandrel is removed.

Filament winding is traditionally used to produce cylindrical and spherical FRP products such as chemical and fuel storage tanks and pipe, pressure vessels and rocket

motor cases. However, the technology has been expanded, and with computer controlled winding machines, other shapes are now being made.

Today, computerized numerical control can provide up to 11 axes of motion for single and multiple spindles. Examples are helicopter tail booms and rotor blades, wind turbine blades and aircraft cowl.

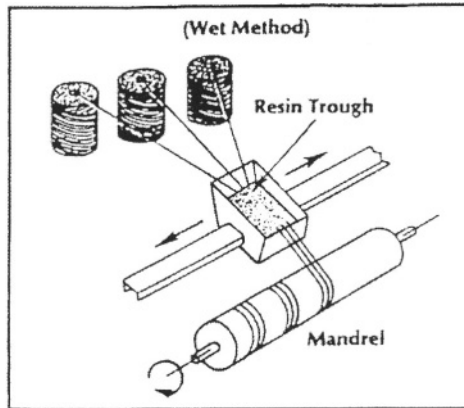


FIGURE 1.15. Filament Winding

1.5.12 PULTRUSION

Constant section-reinforced FRP shapes such as structural members (I-beams, channels, etc.), solid rod, pipe and ladder side rails are produced in continuous lengths by pultrusion. The reinforcement, consisting of a combination of roving, mat, cloth and surfacing veil, is pulled through a resin bath to wet-out the fibers, then drawn through a forming block that sets the shape of the composite and removes excess resin, and through a heated steel die to cure the resin. See Figure 1.16. Temperature control and time in the die are critical for proper curing. The finished shape is cut to lengths by a traveling cutoff saw.

Very high strengths are possible in pultruded shapes because of high fiber content (to 75 percent) and orientation parallel to the length of the FRP shape. Pultrusion is easily automated, and there is no practical limit to product length manufactured by the process.

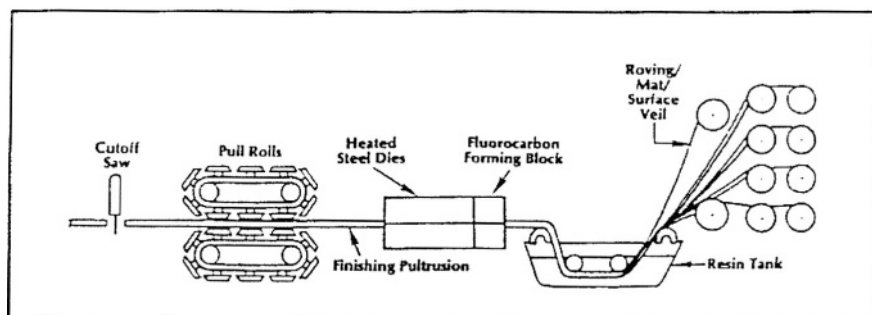


FIGURE 1.16. Pultrusion

1.5.13 CONTINUOUS LAMINATING PROCESSES

Sheet FRP products such as glazing panels, flat and corrugated construction panels are made by a continuous laminating process. Glass fiber chopped rovings, reinforcing mat and fabric are combined with resin and sandwiched between two carrier film sheets. The material then passes between steel rollers to eliminate entrapped air and to establish finished laminate thickness, then through a heated zone to cure the resin. Wall thickness can be closely controlled.

A wide variety of surface finishes and textures can be applied and panel length is unlimited. Corrugations are produced by molds or by rollers just prior to the curing stage.

1.6 Uses of Composite Materials

Since the publication of the first edition of this text in 1986, the use of composite materials has grown enormously both in quantity and variety. In 1999 composite usage was increasing at 4% in North America and 6% worldwide. According to the Freedonia Group, Inc. of Cleveland, reinforced thermoset resin demand will increase at an annual rate of 3% to 2.37 billion pounds by 2001. Faster growth is predicted for thermoplastics, 3.8% to 1.44 billion pounds by 2001. They also see increasing demand for glass fibers because of automotive market growth and in construction to 2.4 billion pounds by 2003. The shipment of U.S. composite materials, showing the growth with time, is given in Figure 1.17 [1].

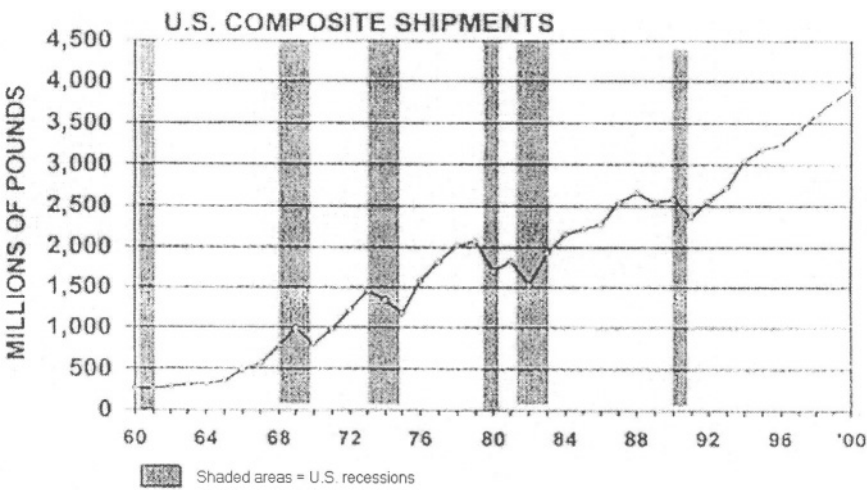


FIGURE 1.17.

1.6.1 AIRCRAFT

The increasing use of composite materials in commercial and military aircraft are clearly seen in Figures 1.18 and 1.19 [1].

Advanced Composites by Commercial Aircraft Model
(% empty structural weight)

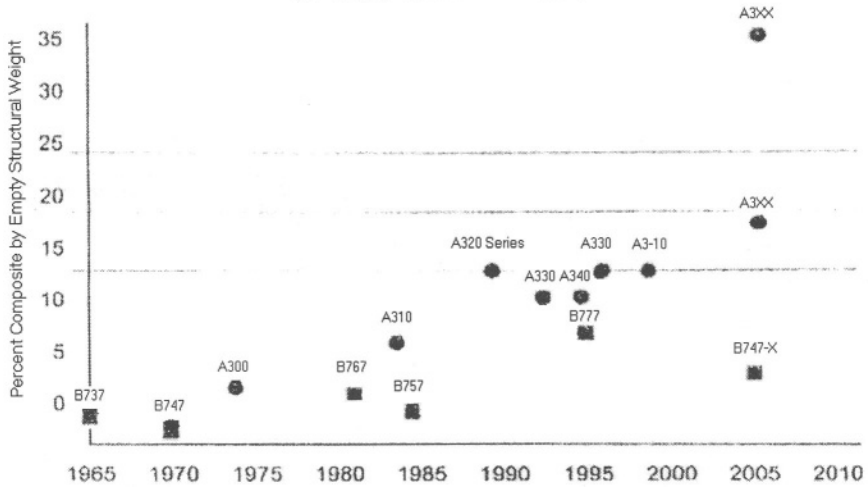


FIGURE 1.18. Composite Weight Growth in Commercial Aircraft as a Percentage of Empty Structural Weight.

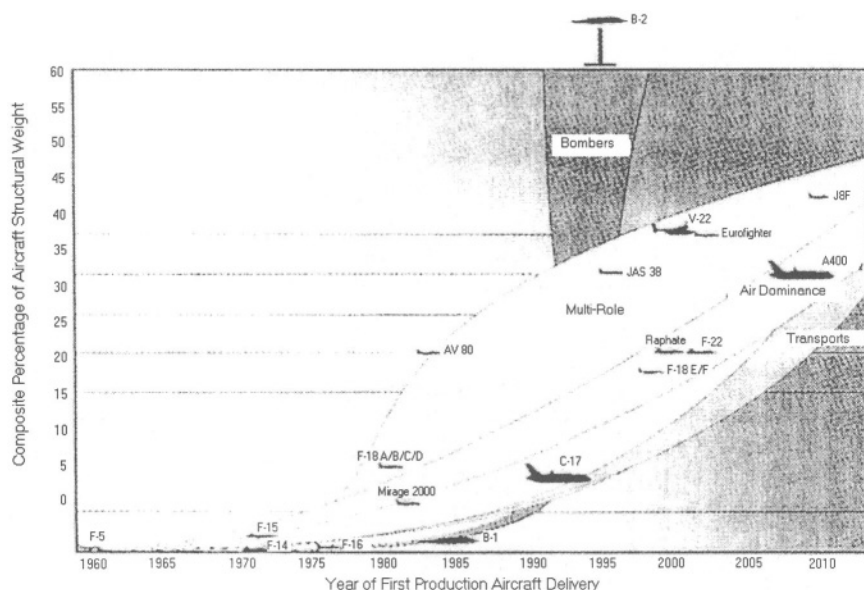


FIGURE 1.19. Composite Weight Growth in Military Aircraft as a Percentage of Empty Structural Weight.

Airbus Industries, in its new A380 super jumbo jet will use a considerable amount of glass composite laminate, with an S-2 glass fiber reinforced epoxy prepreg sandwiched within either aluminum sheets or carbon fiber polymeric laminates.

The X-29 aircraft has forward swept wings, made possibly only by the use of advanced composite materials. The X-36 advanced research vehicle that takes vertical and horizontal empennage components is largely covered by a carbon fiber/epoxy composite material.

Lockheed Martin, using RTM, is building an all composite vertical tail for an advanced fighter aircraft. The RTM process reduces part count from 13 to one, elementary more than 1000 fasteners, manufacturing costs were reduced by more than 60%. The twelve foot tail weight almost 200 lbs, with skins more than 100 plies and thickness variation of force.

Boeing recently unveiled a Sonic Cruiser program, which is being treated as the first real product breakthrough in air transport construction since the widebody. This aircraft will be the size of 100-300 seat jets with a totally different configuration offering costs only slightly higher than current subsonic planes. The designs will use largely composite materials.

One of the newest fighter aircraft of the United States Air Force is the F-22, Raptor. Thirty six percent of its wing by weight is a composite material while thirty five percent of its vertical stabilizers is a composite material.

Also, in 2001, Harris, Starnes and Shuart have provided an assessment for design and manufacturing of large composite material structures for use in aerospace vehicles [3].

1.6.2 AUTOMOBILES, BUSES and TRUCKS

According to the Automotive Composite Alliance, Troy, Michigan, the use of thermoset composites by automobile companies has nearly doubled in the past decade, to 318 million pounds by 2000, and a projected 467 million pounds by 2004. Reinforced thermoplastics are in even greater demand.

An example is the 2000 Ford Excursion SUV which uses SMC for the tailgate and cargo door assembly to reduce weight. As a result tooling cost investment was reduced by 75% from tooling costs for metal components, and designers were able to eliminate several components.

The Los Angeles County Metropolis Transportation Authority has introduced a composite bus designed to extend service life from 12 to 25 years, reduce expensive brake wear and increase fuel efficiency. It weighs 21,800 lbs, 9,000 lbs lighter than a conventional bus. The composite used is stitched glass fiber fabric with an epoxy vinylester resin system produced by the VARTM process.

Composite drive shafts for World Rally cars will soon be used, as well as carbon fiber/epoxy laminate clutch disks for manual gear shaft systems, which provides superior traction with minimum slippage.

The commercial trucking industry started replacing welded steel components with molded hoods, roofs and other body parts with composite materials in the 1970's. Today all major commercial truck manufacturers use composites for weight reduction, design flexibility and improved durability.

The U.S. Department of Energy is leading a multi-agency program to develop the 21st century truck. One of its goals is to take 15% to 20% of the weight out of a truck/trailer combination. This DOE program includes assessment of the most feasible applications of lightweight carbon fiber composites in these vehicles.

Composite hydrogen storage cylinders reaching 10,000 psi (700 Bar) pressure have recently been achieved. This is a major milestone because 80% more hydrogen fuel can be stored in a given volume at 10 ksi than at 5 ksi, thus significantly increasing the range of fuel cell vehicles.

1.6.3 NAVAL VESSELS

According to a recent review by Mouritz, Gellert, Burchill and Challis [4], for naval vessels composites were first introduced immediately after World War II in the construction of small personnel boat for the U.S. Navy. By the time of the Vietnam War, there were over 3,000 composite personnel boats, patrol boats, landing craft and reconnaissance craft in service. Prior to 1950 composite boats were some 16 meters in length, however, in recent years the lengths have increased until today there are all composite naval ships up to 80-90 meters long.

Studies have shown that the structural weight of composite sandwich patrol boats should be up to 10% lighter than an aluminum boat and 36% lighter than a steel boat of similar size. The reduced weight can provide an increase in payload, greater range and/or reduced fuel consumption. It is predicted that the operating costs will be less than those of a steel design because of less maintenance (corrosion) and lower fuel consumption.

The largest all composite naval patrol boats currently in service is the Skjold surface effect ship of the Royal Norwegian Navy, commissioned in 1999. It is 46.8 meters long and 270 tonnes full-load displacement and operates at a maximum speed of 57 knots with a catamaran hull. It is worth noting that the Skjold has been filled with a large array of imbedded sensors in the hull to provide real-time information at strain levels generated during sea trials – another advantage of using composite sandwich construction.

In the late 1980's the Swedish Navy built a 30 meter long surface effect ship, the Smyge MPC2000 of sandwich construction using carbon, glass and Kevlar vinylester skins and a PVC foam core.

These lightweight materials provide, excellent corrosion resistance, good damage resistance against underwater shock loading (UNDEX) and stealth properties including low thermal and magnetic signatures and good noise suppression properties.

Mine countermeasure vessels (MCMV) made of a composite have resulted in innovative designs capable of resisting local buckling, due to hull girder stiffness and excellent underwater shock resistance. The hull structures most commonly used are frame single-skin, unframed monocoque and sandwich constructions. In the monocoque construction thick skins of 0.15-0.20 meters of composite are used. The composite sandwich construction has been used on the Landsort and Flyvefisker Swedish MCMV's. The Royal Norwegian Navy has laminated the Oksoy, Alta, and Hinnoy. In the latter, sensors to monitor strains in the hull and deck have been used to determine the structural behavior of the ship when compared to design predictions and for hull condition monitoring to provide warning of structural overloads. Other sensors monitor vibrations generated by the engines, water jet propulsors and other machinery.

The longest composite naval ship built is the Swedish Visby (YS-2000) corvette, shown in Figure 1.20, launched in June 2000. The ship is 72 meters long, with a full-load displacement of 620 tonnes. Because the Visby is to be used for surveillance, combat, mine-lay up, mine countermeasures and anti-submarine warfare operations the Royal Swedish Navy chose to construct the entire ship of composite materials rather than with traditional steel or aluminum. It is built of sandwich construction consisting of faces of hybrid carbon and glass polymer laminates covering a PVC foam core. The Visby is the first naval ship to significantly use carbon fiber composites in the hull. The introduction of carbon fibers increases the cost five fold compared to glass fibers, however, design studies have shown that by using some carbon fibers in the composite skins the hull weight can be reduced by 30% without increasing fabrication costs greatly. Not only does the use of carbon fibers improve the ships' performance by increasing the range and reducing the operating costs, but the carbon fibers provide adequate electromagnetic shielding in the Visby superstructure.

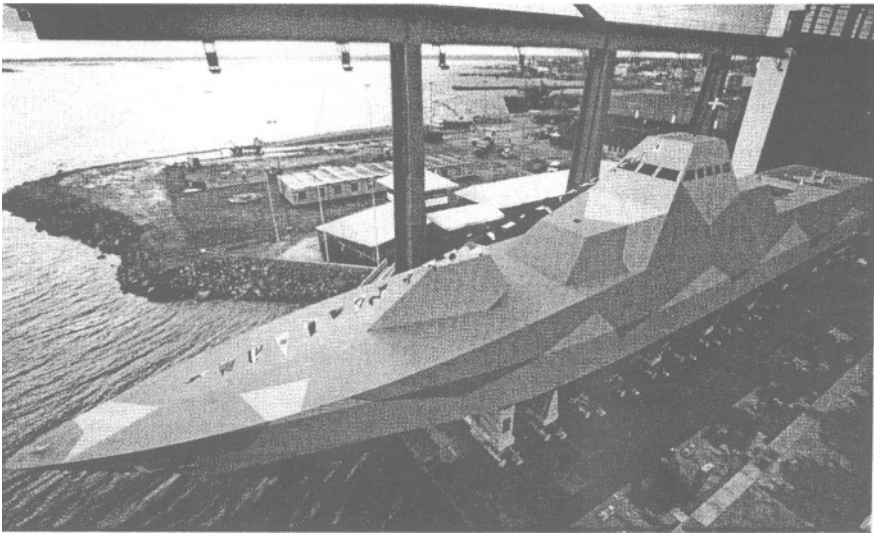


FIGURE 1.20. Visby.

By using composite materials weight savings of up to 65% have been achieved in the superstructure of naval vessels by replacing equivalent steel members.

It has been found that the yield strain in fiberglass composites is about 10 times that of steel, hence fatigue cracking in composite superstructures on a steel hull is expected to be reduced considerably.

Some naval studies have shown that composite superstructures would be 15-70% lighter than a steel superstructure of similar size. The Royal Navy has estimated that replacing an all steel helicopter hanger on a frigate by using a hybrid composite panel and steel frame construction will result in a weight saving of 31% (i.e., 9 tons). Another study has shown that for a frigate, an all composite superstructure with stiffened sandwich composite panels will save 40% weight over a steel construction without greatly increasing the construction costs.

The French Navy is the first to operate large warships with a composite superstructure, this being the La Fayette frigate launched in 1992. The aft section of the superstructure is made of fiberglass sandwich composite panels, with a length of 38 meters, width of 15 meters, height of 6.5-8.5 meters and a weight of 85 tons. This makes it the largest composite superstructure on a warship. Additionally, the funnels on the La Fayette are also composite.

Based on a study by Critchfield [5] in the early 1990's, the U.S. Navy has designed, fabricated and put in use an all composite mast, designated as the Advanced Enclosed Mast/Sensor (AEM/S), on the USS Radford. The AEM/S system is 28 meters tall and 10.7 meters in diameter, hexagonal in shape and is the largest topside structure in place on a U.S. Navy ship. It is made of a frequency tunable hybrid composite material, which allows for the passage of the ship's own frequencies through the composite structure with little loss while reflecting all other frequencies. Thus, the performance of the antenna and other on board sensors is improved while the radar & cross-section

signature of the mast are reduced. Again, this result is achieved only by the introduction of composites. Other benefits include that the mast structure encloses all major antennas and other sensitive electronic equipment, protecting them from the elements and thus reducing maintenance.

Propellers for naval ships and submarines have traditionally been made of a nickel-aluminum-bronze alloy because of the requirements for corrosion resistance and high yield strength. Although recent design and performance of composite propeller systems is classified, the use of modern composites manufacturing allows for continuous fibers to be aligned with the major hydrodynamic and centripetal forces along the blade, and thus the potential for application in this area.

The use of composites is now being introduced for propeller shafts on large ships (frigates and destroyers) where they account for 2% (100-200 tons) of total ship weight. Carbon fiber/epoxy and glass fiber/epoxy composite shafts have the potential to be 25-80% lighter than steel shafts for the same purpose, while also providing noise suppression due to the intrinsic dampening properties of composites, and thus reducing the ship's acoustic signature. Also, the non-magnetic properties of composite shafts reduce that signature. The Navy also anticipates fewer problems with corrosion, bearing loads, fatigue with a corresponding 25% reduction in cost over the service life of the components.

For ship funnels, composites have been introduced on MCMV craft for many years. Composite stacks of course are used on the Visby. The U.S. Navy is also considering using composite stacks on the (DDG51) Arleigh Burke class destroyers. The advantages include weight savings, reduced radar cross-section and reduced infrared (thermal) signature. It has been reported that composite funnels in two Italian cruise liners resulted in a weight saving of 50% and a cost saving of 20% when compared to aluminum and steel funnels they replaced.

Composite steel rudders are also being developed because they are expected to be 50% lighter and 20% cheaper than metal rudders. One such application is the use of composite rudders on the Avenger class MCMV's.

In the case of composite applications for submarines, the United Kingdom has investigated the feasibility of lining the outside wall of steel pressure hulls with a sandwich composite. This effort is expected to increase the overall buckling strength, lower fatigue strains, reduce corrosion and lower acoustic, magnetic and electrical signatures. Furthermore, antennas and sensors may be imbedded in the composites.

Considering all of the aforementioned applications, Mouritz et al [4] point out the following. "Despite the use of composite in naval craft for fifty years, the information and tools needed by naval architects is not complete. For example, simple analysis tools for determining failure modes of complex naval composite structures, particularly under blast, shock, collision and fire events, are virtually non-existent. Furthermore, the scaling laws for composites are complex due to their anisotropic properties, which makes the design of load-bearing structures more difficult than designing with metals. To overcome the lack of information, it is common procedure to design composite ship structures with safety factors that are higher than when designing for metals. Most composite structures are designed with safety factors between 4 and 6, although values up to 10 are applied when the structure must carry impact loads. The high safety factors result in structures

that are heavy and bulky, and this seriously erodes the strength to weight advantages offered by composites.”

Mouritz [4] goes on to say that “stringent performance requirements have hindered the use of composites in naval vessels. Large-scale structures are required to pass a series of strict regulations relating to a blast and underwater shock damage resistance, fire performance (flammability, fire, smoke, toxicity, structural integrity) fragment/ballistic protection and radar/sonar capabilities. The data needed to assess the survivability of composite structures are extremely limited, and conducting tests to determine their performance under blast, shock, ballistic and fire conditions is time consuming and expensive.”

1.6.4 BOATS AND SHIPS

According to a marine industry market report, the total annual shipments in 2000 was \$13.6 billion in the USA for the boating industry, with at an annual growth rate of 7.5 % since 1990. In 2000, 466,900 boats were sold in the USA, of which 70% were made of composite materials. Fiberglass boat manufacturers use a variety of materials including glass roving, woven fabrics, mats, vinylester and polyester resins, epoxy, balsa, foam and honeycomb cores, E-glass, S-Glass, Carbon and Kevlar fibers, with E-glass being the fiber of choice. The manufacturing techniques used for boats include hand lay-up, spray-up, RTM, SCRIMP and SMC processes. Currently the majority of fiberglass boats are produced using an open mold process.

The marine industry consumed 422 million pounds of composite materials in the USA in 2000, and grew at a rate of 5.2% compared to 1999. Boat builders use composite materials for the boat hulls, as well as decks, showers, bulkheads, cockpit covers, hatches, etc. The demand for high performance fibers is increasing in order to reduce weight, gain speed and save fuel. There is growing interest in carbon and Kevlar fibers for high performance applications such as power and racing boats.

1.6.5 INFRASTRUCTURE – BRIDGES, HIGHWAYS AND BUILDINGS

According to Composites Worldwide, Inc. in 2001 composites are expected to grow at a rate of at least 35% per year in infrastructure applications, primarily in bridges and the repair and strengthening of reinforced concrete structures.

More than 40% of the bridges in the United States (> 250,000) are either structurally unsound or are operationally inadequate. To repair or replace these bridges with conventional material solutions exceeds the dollars available from taxes, so composites are being recognized as the better (if not only) solution. Already over 1500 reinforced concrete bridges around the world have been reinforced by composite laminates and jacket wrap systems.

Composite decks are being used increasingly to replace bridge decks because they weigh only 20% of the conventional deck, have great corrosion resistance and not only are easier to install, but require only a fraction of the time for the installation. Such composite bridge decks are already in use in California, Delaware, Kansas, New York, Ohio and Virginia.

Pultruded profiles are a dominant feature in composite construction. The “Eyecatcher” five story building in Basel, Switzerland has an all composite primary structure. Its structural profiles were made from fiber-glass reinforced isopolyester pultruded with resin injection. This provides a structure with high thermal insulation, lightweight and corrosion resistance.

The introduction of fiber reinforced composites as structural members/systems can be considered to be an orderly transfer of technology from the aerospace industry. The inherent desirable features of light weight and high strength associated with advanced fiber composites can be considered to be one of the biggest attributes of composite technology. The unique properties of these materials, particularly polymer matrix composites (PMC's), appear to be especially adaptive to a large number of civil infrastructure applications, a number of which are cited in the accompanying paragraphs.

Mild steel reinforcing bars are recognized to corrode rapidly in some environments. The development of a lightweight, non-conductive, environmentally compatible and economically competitive rebar is a desirable design objective. Such systems have been started and recent developments show considerable promise in meeting required design objectives. An example of a bridge deck slab that employs prestressed carbon fiber/epoxy strands and rebars made with either glass or carbon fibers in select polymer matrices is currently being tested for environmental conditioning in Michigan and is shown below in Figure 1.21.

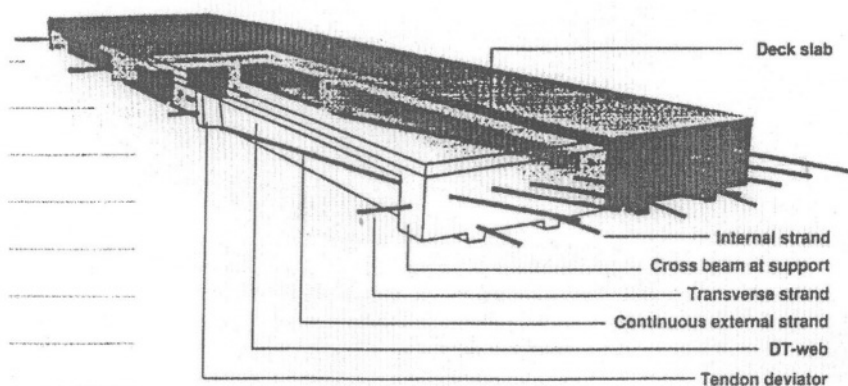


FIGURE 1.21. Slab with Prestressed Composite Reinforcements.

An example of a portable, rapidly deployable bridge is shown in Figure 1.22. This structure provides an emergency rescue venue for mass transit emergencies, is portable, load bearing to 1200 lbs. and electrically insulated. A hybrid of glass, aramid and carbon fibers in an epoxy matrix provides tough, stiff surface skins for top thread and shoulder, as well as strength/load bearing in bottom corrugation of this portable emergency evacuation bridge.

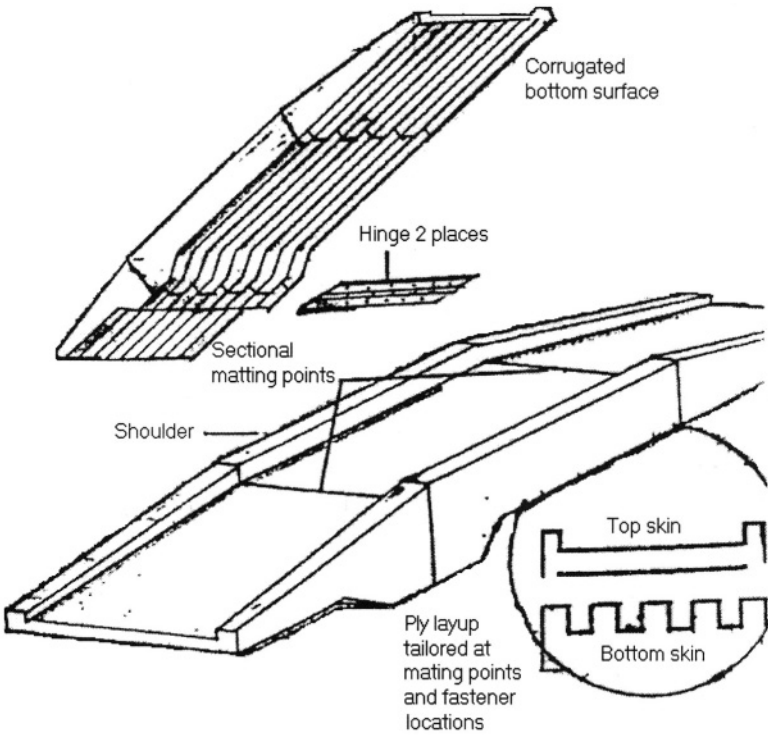


FIGURE 1.22. Portable Deployable Bridge.

A schematic concept of a cable stayed bridge for use in interstate deployment is shown in Figure 1.23 below. Such a bridge would utilize cable and deck construction using advanced high strength graphite/epoxy composites.

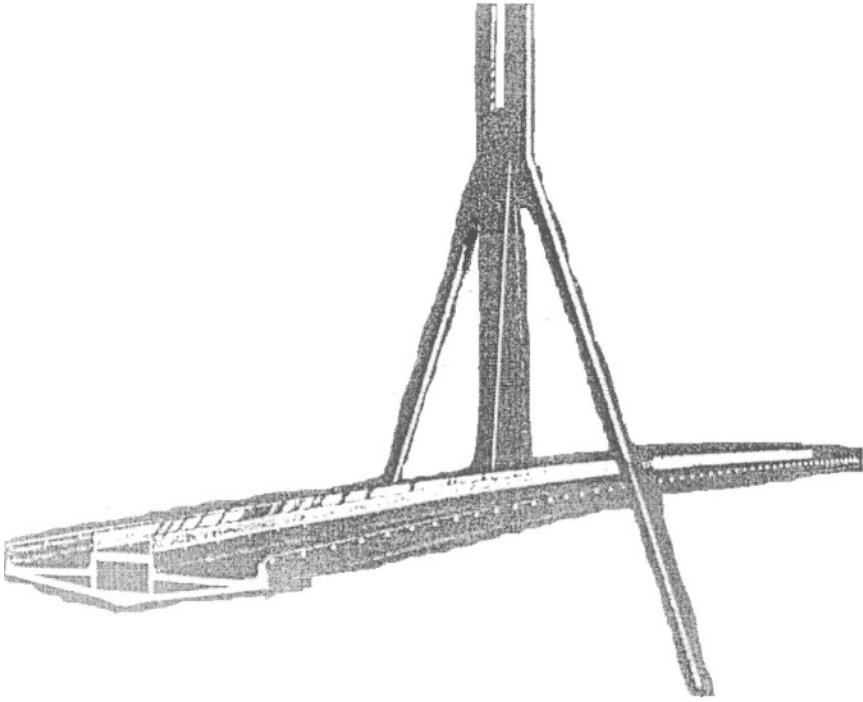


FIGURE 1.23. Composite Cable Stayed Bridge.

1.6.6 COASTAL USE

Composite materials are being used increasingly as marine fenders, pilings and outfall structures in water based upon their excellent corrosion resistance.

1.6.7 SPORTS AND RECREATION

Composite materials are now used extensively in products involving seven of the top ten most popular sports and recreational activities. Composite use in recreational goods grew more than 40% in the first six months of 1999 alone. Fishing rods, tennis rackets, golf clubs, kayak paddles, masts, kits and bicycles all employ composites.

In 2001 thermoplastic golf club shafts are being made. An important attribute of thermoplastic composites over thermosets is that since they do not cure, cycle times are minimized and scrap can be recycled.

1.6.8 AGRICULTURE

The agricultural equipment maker, John Deere, has designed and manufactured a composite material 6 foot by 6 foot, 56 pound component of a combine using RIM, because it is more resistant to impact and corrosion than metal designs, and is lighter and with significant cost efficiencies.

1.6.9 ARMORED VEHICLES

Europe's first composite armored fighting vehicle was tested in Great Britain in early 2001. It has shown that composites will probably be the armor of choice in future battlefields.

1.6.10 WIND ENERGY

The blades for wind energy systems are increasingly being fabricated from composite materials. As an example one project which will accommodate the energy needs of 50,000 American homes will use blades 24m. to 37m. long. These blades will be of unidirectional and biaxial +45/-45 fiberglass mat using an epoxy matrix. The blades are constructed using a hand lay-up, vacuum bag and resin infusion process. Both solid laminate and cored sandwich construction are also planned for fabrication.

1.6.11 MUSICAL INSTRUMENTS

Guitar makers were among the first instrument makers to use composites. Also, composite violin bows are now being used.

1.6.12 AND THE LATEST.....IN 2002

- Smart materials (piezoelectric) are being incorporated into laminated composites. Piezoelectric materials are smart materials such that when an electric voltage is applied the materials can extend, compress or shear, depending upon their orientation. As such by applying a voltage the fins and canards of in-flight projectiles can undergo mid-course trajectory corrections for greater accuracy.

- Carbon nanotubes are being incorporated into composites to increase their mechanical properties.

- Researchers Scott White and Nancy Sottos at the University of Illinois have developed a method by which composites may heal themselves if a localized fracture occurs.

- Biodegradable composite materials are being used for both fibers and matrices for some composite structures so that in time the machine will simply decompose rather than rust in place.

- Multifunctional or functionally graded materials involving composite materials.

1.7 Design and Analysis with Composite Materials

In the theory of elasticity there are three sets of equations that are used [6]

- Equilibrium
- Stress-Strain (Constitutive Equations)
- Strain-Displacement Relations/Compatibility equations

To illustrate these equations consider a prismatic bar as shown in Figure 1.24 below subjected to a load P ,

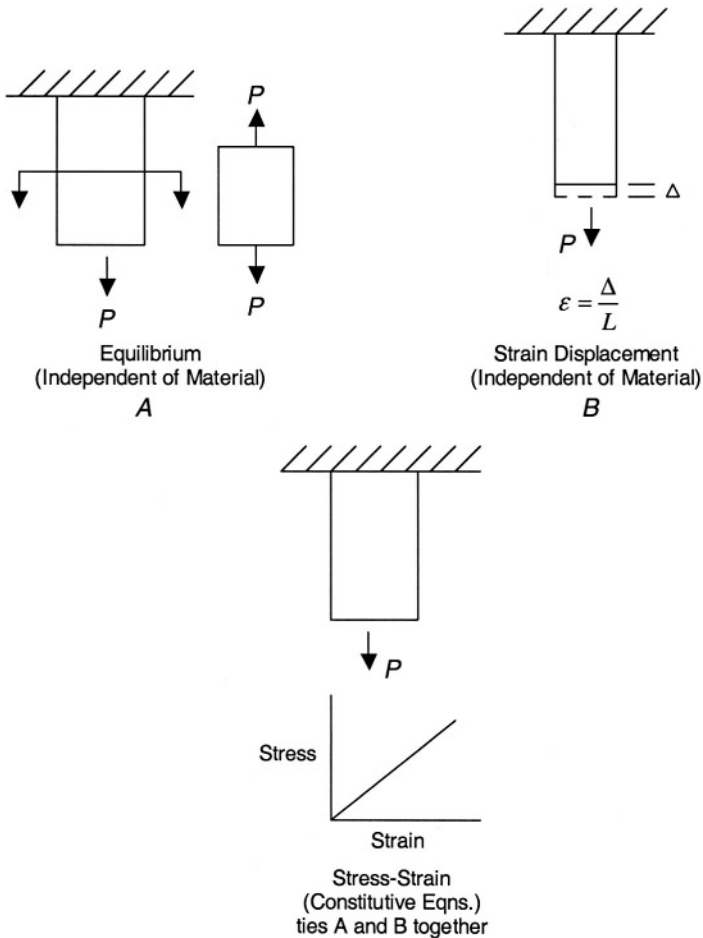


FIGURE 1.24. Simple Tensile Test

In the above all but the stress-strain relations are independent of the material used in the structure. Therefore, the equilibrium equations, the strain-displacement relations and the compatibility equations are the same for an isotropic (where the material properties are the same in every direction) structure as for an anisotropic (where properties differ with direction) composite material structure. The compatibility equations insure that all deflections are single valued and continuous.

The composite configuration is a key element in the selection of appropriate constitutive equations for determining the stresses and deformations in a specific structural member. Whether a composite material is unidirectional, cross-ply, angle ply, woven, braided, or any other configuration, as well as the properties of the fibers and matrix used, all determine the details of the constitutive equations.

Using these sets of equations, the design and analysis of composite structures can be carried out. It is the purpose of this text to provide information, techniques of solutions, some actual solutions and the knowledge to find many other solutions.

In design and analysis, there are four primary things to determine for any structure:

1. The location and magnitude of the maximum stresses.

Only by determining these maximum values can a comparison be made with the strength of the composite material at that location in each principal direction to determine if the structure is over-stressed (area will fail) or under-stressed (hence, too heavy). In performing these calculations a few general concepts can be used.

A factor of safety (F.S.) is a number that is used and/or mandated to account for unknown considerations such as unanticipated loads, material aberrations, unanticipated uses, etc. A factor of safety could be as low as, for example, 1.5 for fighter aircraft, and as high as 10 for elevator cables. The factor of safety is used to relate the strength of the material to an allowable stress (σ_{all}) to which a structure is designed and analyzed.

$$\sigma_{all} = \frac{\text{strength of the material}}{\text{F.S.}} \quad \text{or} \quad \sigma_{all} = \frac{\text{buckling stress}}{\text{F.S.}} \quad (1.1)$$

In this case the stress and strength are taken at the locations of maximum stress in each principle direction.

Likewise, another often used measure of structural integrity is the margin of safety (M.S.) defined by

$$\text{M.S.} = 1 - \frac{\sigma_{\max}}{\sigma_{all}} \quad (1.2)$$

In this equation the σ_{all} could be associated with the strength of the material or the buckling stress (see below).

Generally if a structure has a positive margin of safety for the critical load condition at the region of maximum stress it is considered to be structurally adequate.

2. The location and magnitude of maximum deflections.

This calculation indicates whether the structure is adequately stiff. Many structures are stiffness critical; among these are aircraft wings, gyroscopes and the chassis of automobiles. If the structure is too flexible or compliant, it cannot perform its intended tasks.

3. Determination of natural frequencies.

Almost every structure is subjected to dynamic loads. When a structure is subjected to dynamic loads, whether cyclical or one time impact, every natural frequency of the structure is excited. Therefore, it is important to determine the important natural frequencies, and this will be discussed later.

If a cyclic loading occurs at one or more given frequencies it is important that no natural frequency of the structure be close to these imposed frequencies. Otherwise, the resonances that will occur will cause structural failure with time, or if failure does not occur, fatigue problems will most likely occur.

4. Determination of buckling loads.

When a structure is subject to compressive and/or shear loading, an elastic instability can occur, termed buckling. Usually buckling is synonymous with collapse and termination of the usefulness of the structure. Depending upon the slenderness or frailty of the structure, the buckling (internal) stresses associated with the buckling load can be a fraction of the strength of the material.

Therefore, in analyzing a structural design, an analyst must check out each of the above four important criteria to insure that the structure is sound.

In designing a structure, one must therefore insure that the materials, stacking sequences, thickness and configuration details (stress concentrations) are such that the structure is adequate for the four important design considerations outlined above.

To complicate matters one must also consider temperature considerations in order to use the mechanical properties at temperature extremes, consider any potential corrosion effects, weathering, damage, moisture and other environmental effects, and if the material is exposed to dynamic loads, consider high strain rate effects.

For composites, design and manufacturing are inextricably entwined. The selection of a manufacturing process may be automatic, however, in many instances this selection is based on available equipment and/or prior experience. This affects the type of composite material used in the design. The geometry of the component, the number of parts to be made, surface finish and dimensional stability can have a pronounced effect on material selection and the resulting composite configuration.

1.8 References

1. *Composites Fabrication* (2001) Vol. 17, No. 1, January, pp. 28-31.
2. Abrate, S. (2002) Resin Flow in Fiber Preforms, *Applied Mechanics Reviews*.
3. Harris, C.E., Starnes, Jr. J.H. and Shuart, M.J. (2001) An Assessment of the State-of-the-Art in Design and Manufacturing of Large Composite Structures for Aerospace Vehicles, *NASA/TM-2001-210844*, April.
4. Mouritz, A.P., Gellart, E., Burchill, P. and Challis, K. (2001) *Review of Advanced Composite Structures for Naval Ships and Submarines*, Composite Structures.
5. Critchfield, M.O., Morgan, S.L. and Potter, P.C. (1991) *GRP Deckhouse Development for Naval Ships*, *Advances in Marine Structures*, Elsevier, London, pp. 372-391.
6. Sokolnikoff, I.S. (1956) *Mathematical Theory of Elasticity*, McGraw Hill Book Co., Inc., New York.
7. Bogdanovich, A.E. and Sierakowski, R.L. (1999) Composite Materials and Structures: Science, Technology and Applications, *Applied Mechanics Reviews*, Vol. 52, No. 12, Part 1, December.

1.9 Journals

The developments in the area of composite materials structures is developing so rapidly that one can only attempt to keep current through extensive Journal readings. However, a recent review article by Bogdanovich and Sierakowski [7] is suggested for those interested in learning more about composite materials.

Below is a representative sample of Journals to read by which to keep current.

1. AIAA Journal
2. Advanced Composites
3. Advanced Composites Bulletin
4. Advanced Composites Letters
5. Applied Composite Materials
6. Applied Mechanics Reviews
7. Cement & Concrete Composites
8. Composite Interfaces
9. Composite Material Technology
10. Composite Materials Science
11. Composite Structures
12. Composites
13. Composites & Adhesives
14. Composites Design & Application
15. Composites Fabrication
16. Composites Manufacturing
17. Composites Science and Technology
18. Composites Technology
19. Composites Technology & Research

20. Composites Technology Review
21. Composites. Part A: Applied Science and Manufacturing
22. Composites. Part B: Engineering
23. Computers & Structures
24. Experimental Mechanics
25. Fibre Science and Technology
26. High-Performance Composites
27. International Journal of Cement Composites & Lightweight Concrete
28. International Journal of Composite Structures
29. International Journal of Engineering Science
30. International Journal of Polymeric Materials
31. International Journal of Solids & Structures
32. Journal of Applied Mechanics
33. Journal of Applied Polymer Science
34. Journal of Composite Materials
35. Journal of Composite Technology & Research
36. Journal of Composites in Construction
37. Journal of Engineering Materials and Technology
38. Journal of Material Science
39. Journal of Materials Research
40. Journal of Mechanics and Physics of Solids
41. Journal of Reinforced Plastics and Composites
42. Journal of Sandwich Structures and Materials
43. Journal of Sound and Vibration
44. Journal of Testing and Evaluation
45. Journal of Thermoplastic Composite Materials
46. Mechanics of Composite Materials
47. Mechanics of Composite Materials and Structures
48. Mechanics of Materials
49. Polymer Composites
50. Polymer Engineering and Science
51. Polymers & Polymer Composites
52. Reinforced Plastics
53. SAMPE Journal
54. SAMPE Quarterly
55. Shock and Vibration Digest

1.10 Problems

1. Select an area of composite materials science and technology that interests you, and scan several of the above journals for papers written in the last two years. Read at least eight of them and provide a bibliography of these papers.
2. Select three papers from the above that you feel are the best, describe what the authors did, how they did it and tell why you consider these papers to be the best.

3. From the materials listed in Table 2.2, construct a graph in which the ordinate is the ratio of strength in the fiber direction to density (σ_{11}/ρ) and the abscissa is the ratio of modulus of elasticity in the fiber direction to density (E_{11}/ρ). Plot a point on the graph for each material.
- Which material will be the lightest to use in a strength critical structure?
 - Which material will be the lightest to use in a stiffness critical structure?
 - Which material would be the heaviest to use in a strength critical structure?
 - Which material would be the heaviest to use in a stiffness critical structure?

CHAPTER 2

Anisotropic Elasticity and Composite Laminate Theory

When research began on composite materials, as described in Chapter 1, definitions and nomenclature were developed that formed a vocabulary and approach specialized to composite materials structures. To systematically develop a theory for composite materials structures, one should begin with the following derivations [1-3]*.

2.1 Introduction

An isotropic material is one that has identical mechanical, physical, thermal and electrical properties in every direction. Isotropic materials involve only four elastic constants, the modulus of elasticity, E , the shear modulus, G , the bulk modulus K and Poisson's ratio, ν . However, only two are independent, and the following relationships exist:

$$G = \frac{E}{2(1+\nu)}, \quad K = \frac{E}{3(1-2\nu)} \quad (\text{Isotropic only}) \quad (2.1)$$

Most engineers and material scientists are well schooled in the behavior and design of isotropic materials, which include the family of most metals and pure polymers. The rapidly increasing use of anisotropic materials such as composite materials has resulted in a materials revolution and requires a new knowledge base of anisotropic material behavior.

Before understanding the physical behavior of composite material structures and before being able to quantitatively determine the stresses, strains, deformations, natural frequencies, and buckling loads in such structures, a clear understanding of anisotropic elasticity is necessary. In general, isotropic materials are mathematical approximations to the true situation. For instance, in polycrystalline metals, the structure is usually made up of numerous anisotropic grains, wherein macroscopic isotropy exists in a statistical sense only because the anisotropic individual grains are randomly oriented. However, the same materials could be macroscopically anisotropic due to cold working, forging or spinning during a fabrication process. Other materials such as wood, human and animal bone, and all fiber reinforced materials are anisotropic.

Fiber reinforced composite materials are unique in application because the use of long fibers results in a material which has a higher strength-to-density ratio and/or stiffness-to-density ratio than any other material system at moderate temperature, and there exists the opportunity to uniquely tailor the fiber orientations to a given geometry,

* Number in brackets refers to the number of the reference in Section 2.11.

applied load and environment. For short fiber composites, used mainly in high production, low cost systems, the use of fibers makes the composites competitive and superior to plastic and metal alternatives. Finally, the use of two or more kinds of dissimilar fibers within one matrix is termed a hybrid composite, where one fiber is stronger or stiffer while the other fiber is less expensive but desirable for less critical locations in an overall structural component. Other examples of a hybrid composite involve stronger and stiffer (but more brittle) fibers that are protected by outer plies of a tougher fiber composite to protect the composite from impact and other deleterious effects. Therefore through the use of composite materials, the engineer is not merely a materials selector, but is also a materials designer.

For small deflections, the linear elastic analysis of anisotropic composite material structures requires the use of the equilibrium equations, strain-displacement relations, and compatibility equations, which remain the same whether the structure is composed of an isotropic material or an anisotropic composite material. However, it is very necessary to drastically alter the stress-strain relations, also called the constitutive relations, to account for the anisotropy of the composite material structure.

A quantitative understanding of the virtues of using composite materials in a structure is found through deriving systematically the anisotropic elasticity tensor matrix, as discussed in Section 2.2.

2.2 Derivation of the Anisotropic Elastic Stiffness and Compliance Matrices

Consider an elastic solid body of any general shape, and assume it is composed of an infinity of *material points* within it. In order to deal with a *continuum*, one also assumes that the material points are infinitely large compared to the molecular lattice spacing of the particular material. If one assigns a Cartesian reference frame to the elastic body shown in Figure 2.1, one then calls this rectangular parallelepiped material point a *control element* or control volume of dimension dx , dy and dz in a Cartesian coordinate system.

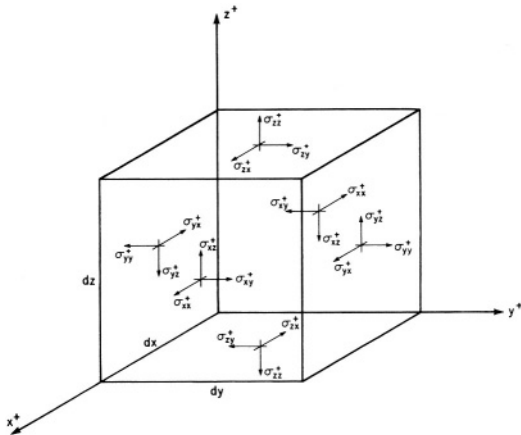


FIGURE 2.1. Positive Stresses on a Control Element of an Elastic Body

On the surface of the control element there can exist both normal stresses (those perpendicular to the plane of the face) and shear stresses (those parallel to the plane of the face). On any one face the three mutually orthogonal stress components comprise a vector, which is called a *surface traction*.

It is important to note the sign convention and the meaning of the subscripts of these surface stresses. For a stress component on a face whose outward normal is in the direction of a positive axis, the stress component is positive when it is in the direction of a positive axis. Also, when a stress component is on a face whose outward normal is in the direction of a negative axis, the stress component is positive when it is in the direction of a negative axis. This can be seen clearly in Figure 2.1.

The first subscript of any stress component on any face of the control element signifies the axis to which the outward normal of the face is parallel; the second subscript refers to the axis to which that stress component is parallel. Again, see Figure 2.1.

The strains occurring in an elastic body have the same subscripts as the stress components but are of two types. Dilatational or extensional strains are denoted by ϵ_{ii} , where $i = x, y, z$, and are a measure of the change in dimension of the control volume in the subscripted direction due to normal stresses, σ_{ii} , acting on the control volume. Shear strains ϵ_{ij} ($i \neq j$) are proportional to the change in angles of the control volume from 90° , changing the rectangular control volume into a parallelogram due to the shear stresses, σ_{ij} , $i \neq j$. For example, looking at the control volume x - y plane shown in Figure 2.2 below, shear stresses σ_{xy} and σ_{yx} cause the square control element with 90° corner angles to become a parallelogram with the corner angle ϕ as shown. Here, the change in angle γ_{xy} is

$$\gamma_{xy} = \frac{\pi}{2} - \phi \quad (2.2)$$

The shear strain ϵ_{xy} , a tensor quantity is defined by

$$\epsilon_{xy} = \gamma_{xy} / 2 \quad (2.3)$$

Similarly, $\epsilon_{xz} = \gamma_{xz} / 2$ and $\epsilon_{yz} = \gamma_{yz} / 2$.

Having defined all of the elastic stress and strain tensor components, the stress-strain relations are now used to derive the anisotropic stiffness and compliance matrices.

The following derivation of the stress-strain relations for an anisotropic material parallels the derivation of Sokolnikoff [1], Vinson and Chou [2], and Vinson [3]. Although the derivation is very formal mathematically to the reader who is primarily interested with the end result, the systematic derivation does provide confidence in the extended use of the results.

From knowledge of basic strength of materials [4], both the stresses, σ_{ij} , and the strains ϵ_{ij} , are second order tensor quantities, where in three dimensional space they have

$3^2 = 9$ components. They are equated by means of the fourth order elasticity tensor, C_{ijkl} , which therefore has $3^4 = 81$ components, with the resulting constitutive equation:

$$\boxed{\sigma_{ij} = C_{ijkl} \varepsilon_{kl}} \quad (2.4)$$

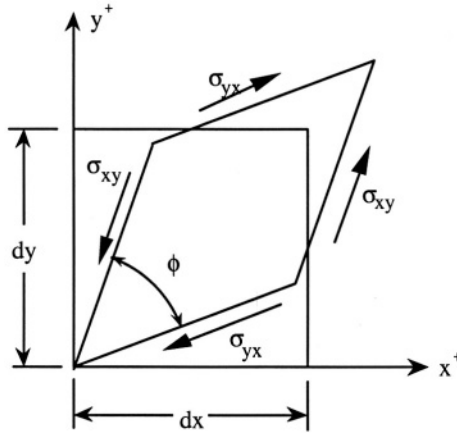


FIGURE 2.2. Shearing of a Control Element

where i, j, k and l assume values of 1, 2, 3 or x, y, z in a Cartesian coordinate system. Fortunately, there is no actual material that has eighty-one elastic constants. Both the stress and strain tensors are symmetric, i.e., $\sigma_{ij} = \sigma_{ji}$ and $\varepsilon_{kl} = \varepsilon_{lk}$, and therefore the following shorthand notation may be used:

$$\begin{array}{llll} \sigma_{11} = \sigma_1 & \sigma_{23} = \sigma_4 & \varepsilon_{11} = \varepsilon_1 & 2\varepsilon_{23} = \varepsilon_4 \\ \sigma_{22} = \sigma_2 & \sigma_{31} = \sigma_5 & \varepsilon_{22} = \varepsilon_2 & 2\varepsilon_{31} = \varepsilon_5 \\ \sigma_{33} = \sigma_3 & \sigma_{12} = \sigma_6 & \varepsilon_{33} = \varepsilon_3 & 2\varepsilon_{12} = \varepsilon_6 \end{array} \quad (2.5)$$

At the outset it is noted that $\varepsilon_4, \varepsilon_5$ and ε_6 , which are quantities widely used in composite analyses, are not tensor quantities and therefore do not transform from one set of axes to another by affine transformation relationships. Care must also be taken regarding whether or not to use the factor of "two" when using shear strain relations. Using Equation (2.5), Equation (2.4) can be written:

$$\boxed{\sigma_i = C_{ij} \epsilon_j} \quad (i, j = 1 \dots 6) \quad (2.6)$$

It should be noted that the contracted C_{ij} quantities are also not tensor quantities, and therefore cannot be transformed as such.

Hence by the symmetry in the stress and strain tensors the elasticity tensor immediately reduces to the 36 components shown by Equation (2.6). In addition, if a strain energy density function, W , exists [1 through 4], i.e.,

$$\boxed{W = \frac{1}{2} \sigma_{ij} \epsilon_{ij},}$$

in such a way that

$$\frac{\partial W}{\partial \epsilon_{ij}} = C_{ijkl} \epsilon_{kl} = \sigma_{ij}, \quad (2.7)$$

then the independent components of C_{ijkl} are reduced to 21 elastic constants, since $C_{ijkl} = C_{klij}$ and now it can be written $C_{ij} = C_{ji}$.

Next, to simplify the general mathematical anisotropy to the cases of very practical importance, consider the Cartesian coordinate system only. (However, the results are applicable to any curvilinear orthogonal coordinate system of which there are twelve, some of which are spherical, cylindrical, elliptical, etc.).

First, consider an elastic body whose properties are symmetric with respect to the $X_1 - X_2$ plane. The resulting symmetry can be expressed by the fact that the C_{ij} 's discussed above must be invariant under the transformation $x_1 = x_1'$, $x_2 = x_2'$ and $x_3 = -x_3'$, shown in Figure 2.3.

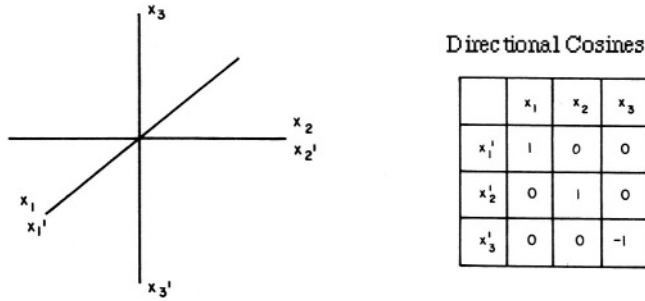


FIGURE 2.3. One Plane of Symmetry

Also shown in the table above are the direction cosines, t_{ij} , associated with this transformation. The stresses and strains of the primed coordinate system are related to those of the original (unprimed) coordinate system by the well-known relationships:

$$\sigma'_{\alpha\beta} = t_{\alpha i} t_{\beta j} \sigma_{ij} \quad \text{and} \quad \epsilon'_{\alpha\beta} = t_{\alpha i} t_{\beta j} \epsilon_{ij}.$$

where, for $i=1, 2, 3$, $\sigma'_i = \sigma_i$ and $\epsilon'_i = \epsilon_i$, i.e., $\sigma'_{11} = t_{11} t_{11} \sigma_{11} = \sigma_{11}$. However, from the direction cosines, $\epsilon'_{23} = -\epsilon_{23}$ or $\epsilon'_4 = -\epsilon_4$, and $\sigma'_4 = -\sigma_4$; likewise $\epsilon'_{31} = -\epsilon_{31}$, hence $\epsilon'_5 = -\epsilon_5$ and $\sigma'_5 = -\sigma_5$. For example, $\sigma'_{23} = \sigma'_4 = t_{22} t_{33} \sigma_{23} = (1)(-1)\sigma_{23} = -\sigma_{23} = -\sigma_4$.

If one looks in detail at Equation (2.4) then,

$$\begin{aligned} \sigma'_4 &= C_{41}\epsilon'_1 + C_{42}\epsilon'_2 + C_{43}\epsilon'_3 + C_{44}\epsilon'_4 + C_{45}\epsilon'_5 + C_{46}\epsilon'_6, \\ \sigma_4 &= C_{41}\epsilon_1 + C_{42}\epsilon_2 + C_{43}\epsilon_3 + C_{44}\epsilon_4 + C_{45}\epsilon_5 + C_{46}\epsilon_6. \end{aligned}$$

It is evident from these two equations that $C_{41}=C_{42}=C_{43}=C_{46}=0$. From similar examinations of the other two axial symmetries, it can be seen that $C_{25}=C_{35}=C_{64}=C_{65}=0$, $C_{51}=C_{52}=C_{53}=C_{56}=0$, and $C_{14}=C_{15}=C_{16}=C_{24}=C_{34}=0$.

So, for a material having only one plane of symmetry the number of elastic constants is now reduced to 13. Note that from a realistic engineering point of view this would still require thirteen independent physical tests (at each temperature and humidity condition!) - an almost impossible task both in manpower and budget.

Now, materials that have three mutually orthogonal planes of elastic symmetry are called "orthotropic" (a shortened term for orthogonally anisotropic). In such a case, other terms in the elasticity matrix are also zero, namely

$$C_{16} = C_{26} = C_{36} = C_{45} = 0.$$

Therefore, the elastic stiffness matrix for orthotropic materials is shown below, remembering that $C_{ij} = C_{ji}$,

$$C_{ij} = \begin{bmatrix} C_{11} & C_{12} & C_{13} & 0 & 0 & 0 \\ C_{21} & C_{22} & C_{23} & 0 & 0 & 0 \\ C_{31} & C_{32} & C_{33} & 0 & 0 & 0 \\ 0 & 0 & 0 & C_{44} & 0 & 0 \\ 0 & 0 & 0 & 0 & C_{55} & 0 \\ 0 & 0 & 0 & 0 & 0 & C_{66} \end{bmatrix} \quad (2.8)$$

Thus, for orthotropic elastic bodies, such as most composite materials in a three dimensional configuration, there are nine elastic constants.

Hence, with Equations (2.8) and (2.6), the explicit stress-strain relations for an orthotropic, three dimensional material are: $\sigma_i = C_{ij}\epsilon_j$ ($i, j = 1, 2, \dots, 6$) or more explicitly,

$$\begin{aligned} \sigma_1 &= C_{11}\epsilon_1 + C_{12}\epsilon_2 + C_{13}\epsilon_3 \\ \sigma_2 &= C_{21}\epsilon_1 + C_{22}\epsilon_2 + C_{23}\epsilon_3 \\ \sigma_3 &= C_{31}\epsilon_1 + C_{32}\epsilon_2 + C_{33}\epsilon_3 \\ \sigma_4 &= \sigma_{23} = C_{44}\epsilon_4 = 2C_{44}\epsilon_{23} \\ \sigma_5 &= \sigma_{31} = C_{55}\epsilon_5 = 2C_{55}\epsilon_{31} \\ \sigma_6 &= \sigma_{12} = C_{66}\epsilon_6 = 2C_{66}\epsilon_{12} \end{aligned} \quad (2.9)$$

It should be noted that in the latter three relationships, which involve shear relations, the factor of two is present because of the widely used definitions of ϵ_4 , ϵ_5 and ϵ_6 shown in Equation (2.5).

If the Equations (2.9) are inverted, then, through standard matrix transformation:

$$\begin{aligned} \epsilon_1 &= a_{11}\sigma_1 + a_{12}\sigma_2 + a_{13}\sigma_3 \\ \epsilon_2 &= a_{21}\sigma_1 + a_{22}\sigma_2 + a_{23}\sigma_3 \\ \epsilon_3 &= a_{31}\sigma_1 + a_{32}\sigma_2 + a_{33}\sigma_3 \\ \epsilon_4 &= 2\epsilon_{23} = a_{44}\sigma_{23} = a_{44}\sigma_4 \\ \epsilon_5 &= 2\epsilon_{31} = a_{55}\sigma_{31} = a_{55}\sigma_5 \end{aligned} \quad (2.10)$$

$$\epsilon_6 = 2\epsilon_{12} = a_{66}\sigma_{12} = a_{66}\sigma_6.$$

The a_{ij} matrix, called the compliance matrix, involves the transpose of the cofactor (C_0) matrix of the C_{ij} 's divided by the determinant of the C_{ij} matrix with each term defined as

$$a_{ij} = \frac{[C_0 C_{ij}]^T}{|C_{ij}|} \tag{2.11}$$

Again, the a_{ij} quantities are not tensors, and cannot be transformed as such. In fact, factors of 1, 2 and 4 appear in various terms when relating the tensor compliance quantities a_{ijkl} and the contracted compliance quantities a_{ij} .

It can be easily shown that $a_{ij} = a_{ji}$ and that

$$\epsilon_i = a_{ij}\sigma_j \text{ (where } i, j = 1, 2, \dots, 6). \tag{2.12}$$

Table 2.1 is useful for listing the number of elastic coefficients present in both two and three dimensional elastic bodies.

2.3 The Physical Meaning of the Components of the Orthotropic Elasticity Tensor

So far, the components of both the stiffness matrix, C_{ij} , and the compliance matrix, a_{ij} , are mathematical symbols relating stresses and strains. By performing hypothetical simple tensile and shear tests all of the components above can be related to physical or mechanical properties.

Class of Material	Number of nonzero coefficients	Number of independent coefficients
<i>Three - Dimensional Case</i>		
General anisotropic	36	21
One-plane of symmetry	20	13
Two-planes of symmetry	12	9
Transversely isotropic	12	5
Isotropic	12	2
<i>Two - Dimensional Case</i>		
General anisotropic	9	6
One-plane of symmetry	9	6
Two-planes of symmetry	5	4
Transversely isotropic	5	4
Isotropic	5	2

TABLE 2.1. Summary of the Number of Elastic Coefficients Involved for Certain Classes of Materials

Class of Material	Number of nonzero coefficients	Number of independent coefficients
Three-Dimensional Case		
General Anisotropy	36	21
One-plane of symmetry	20	13
Two-planes of symmetry	12	9
Transverse isotropy	12	5
Isotropy	12	2
Two-Dimensional Case		
General anisotropy	9	6
One-plane of symmetry	9	6
Two-planes of symmetry	5	4
Transverse isotropy	5	4
Isotropy	5	2

Consider a simple, standard tensile test in the x_1 direction. The resulting stress and strain tensors are

$$\sigma_{ij} = \begin{bmatrix} \sigma_{11} & 0 & 0 \\ 0 & 0 & 0 \\ 0 & 0 & 0 \end{bmatrix}, \quad \epsilon_{ij} = \begin{bmatrix} \epsilon_{11} & 0 & 0 \\ 0 & -\nu_{12}\epsilon_{11} & 0 \\ 0 & 0 & -\nu_{13}\epsilon_{11} \end{bmatrix} \quad (2.13)$$

where the Poisson's ratio, ν_{ij} , is very carefully defined as the negative of the ratio of the strain in the x_j direction to the strain in the x_i direction due to an applied stress in the x_i direction. In other words in the above it is seen that $\epsilon_{22} = -\nu_{12}\epsilon_{11}$ or $\nu_{12} = -\epsilon_{22}/\epsilon_{11}$.

Also, the constant of proportionality between stress and strain in the 1 direction is denoted as E_{11} (or E_1), the modulus of elasticity in the x_i direction. Thus,

$$\epsilon_1 = a_{11}\sigma_1 = \frac{\sigma_1}{E_1}$$

$$\epsilon_2 = a_{21}\sigma_1 = -\nu_{12}\epsilon_1 = -\left(\frac{\nu_{12}\sigma_1}{E_1}\right)$$

$$\epsilon_3 = a_{31}\sigma_1 = -\nu_{13}\epsilon_1 = -\left(\frac{\nu_{13}\sigma_1}{E_1}\right)$$

Therefore,

$$a_{11} = 1/E_1, \quad a_{21} = -\nu_{12}/E_1, \quad a_{31} = -\nu_{13}/E_1 \quad (2.14)$$

For a simple tensile test in the x_2 direction, it is found that

$$a_{12} = -\nu_{21}/E_2, \quad a_{22} = 1/E_2, \quad a_{32} = -\nu_{23}/E_2. \quad (2.15)$$

Likewise, a tensile test in the x_3 direction yields

$$a_{13} = -\nu_{31}/E_3, \quad a_{23} = -\nu_{32}/E_3, \quad a_{33} = 1/E_3. \quad (2.16)$$

From the fact that $a_{ij} = a_{ji}$, then

$$\boxed{\frac{\nu_{ij}}{E_i} = \frac{\nu_{ji}}{E_j}} \quad (i, j = 1, 2, 3) \quad (2.17)$$

The Equation (2.17) is most valuable and widely used in the analysis of all composite material bodies.

Next, consider a hypothetical simple shear test as shown in Figure 2.4. In this case the stress, strain, and displacement tensor components are:

$$\sigma_{ij} = \begin{bmatrix} 0 & \sigma_{12} & 0 \\ \sigma_{21} & 0 & 0 \\ 0 & 0 & 0 \end{bmatrix}, \quad \epsilon_{ij} = \begin{bmatrix} 0 & \epsilon_{12} & 0 \\ \epsilon_{21} & 0 & 0 \\ 0 & 0 & 0 \end{bmatrix},$$

$$u_{i,j} = \begin{bmatrix} 0 & 0 & 0 \\ \sigma_{21}/G_{21} & 0 & 0 \\ 0 & 0 & 0 \end{bmatrix}$$

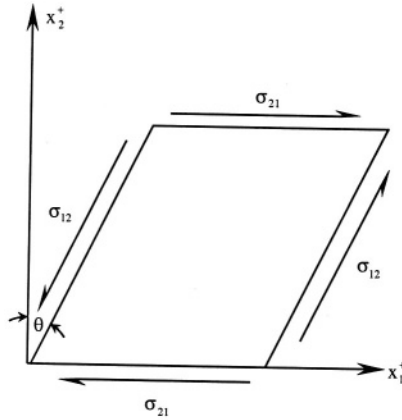


FIGURE 2.4. Shear Stresses and Strains

In the above, u_i is the displacement and $u_{i,j} = (\partial u_i / \partial x_j)$. From elementary strength of materials the constant of proportionality between the shear stress σ_{21} and the angle θ is G_{21} , the shear modulus in the $x_1 - x_2$ plane.

From the theory of elasticity

$$\epsilon_{12} = \frac{1}{2}(u_{1,2} + u_{2,1}) = \frac{\sigma_{21}}{2G_{21}} = \frac{\tan \theta}{2} \quad (2.18)$$

From Equation (2.10), $\epsilon_6 = a_{66}\sigma_6$, or

$$\epsilon_{12} = \frac{a_{66}\sigma_{21}}{2} = \frac{\sigma_{21}}{2G_{21}} \quad (2.19)$$

Hence,

$$a_{66} = \frac{1}{G_{21}} = \frac{1}{G_{12}} \quad (2.19)$$

Similarly,

$$a_{44} = \frac{1}{G_{23}} \quad \text{and} \quad a_{55} = \frac{1}{G_{13}} \quad (2.20)$$

Thus, all a_{ij} components have now been related to mechanical properties, and it is seen that to characterize a three dimensional orthotropic body, nine physical quantities are needed (that is $E_1, E_2, E_3, G_{12}, G_{23}, G_{31}, \nu_{12}, \nu_{13}, \nu_{21}, \nu_{23}, \nu_{31}$ and ν_{32} , and using Equation (2.17). However, because of (2.17) only six separate tests are needed to obtain the nine physical quantities. The standardized tests used to obtain these anisotropic elastic constants are given in ASTM standards, and are described in a text by Carlsson and Pipes [5]. For convenience, the compliance matrix is given explicitly as:

$$a_{ij} = \begin{bmatrix} \frac{1}{E_1} & -\frac{\nu_{21}}{E_2} & -\frac{\nu_{31}}{E_3} & 0 & 0 & 0 \\ -\frac{\nu_{12}}{E_1} & \frac{1}{E_2} & -\frac{\nu_{32}}{E_3} & 0 & 0 & 0 \\ -\frac{\nu_{13}}{E_1} & -\frac{\nu_{23}}{E_2} & \frac{1}{E_3} & 0 & 0 & 0 \\ 0 & 0 & 0 & \frac{1}{G_{23}} & 0 & 0 \\ 0 & 0 & 0 & 0 & \frac{1}{G_{13}} & 0 \\ 0 & 0 & 0 & 0 & 0 & \frac{1}{G_{12}} \end{bmatrix} \quad (2.21)$$

2.4 Methods to Obtain Composite Elastic Properties from Fiber and Matrix Properties

There are several sets of equations for obtaining the composite elastic properties from those of the fiber and matrix materials. These include those of Halpin and Tsai [6], Hashin [7], and Christensen [8]. In 1980, Hahn [9] codified certain results for fibers of circular cross section which are randomly distributed in a plane normal to the unidirectionally oriented fibers. For that case the composite is macroscopically, transversely isotropic, that is $(\)_{12} = (\)_{13}$, $(\)_{22} = (\)_{33}$ and $(\)_{55} = (\)_{66}$, where in the parentheses the quantity could be E, G, or ν ; hence, the elastic properties involve only five independent constants, namely $(\)_{11}, (\)_{22}, (\)_{12}, (\)_{23}$ and $(\)_{66}$.

For several of the elastic constants, Hahn states that they all have the same functional form:

$$P = \frac{(P_f V_f + \eta P_m V_m)}{(V_f + \eta V_m)} \quad (2.22)$$

where for the elastic constant P , the P_f , P_m and η are given in Table 2.2 below, and where V_f and V_m are the volume fractions of the fibers and matrix respectively (and whose sum equals unity):

TABLE 2.2. Determination of Composite Properties From Fiber and Matrix Properties

Elastic Constant	P	P_f	P_m	η
E_{11}	E_{11}	E_{11f}	E_m	1
ν_{12}	ν_{12}	ν_{12f}	ν_m	1
G_{12}	$1/G_{12}$	$1/G_{12f}$	$1/G_m$	η_6
G_{23}	$1/G_{23}$	$1/G_{23f}$	$1/G_m$	η_4
K_T	$1/K_T$	$1/K_f$	$1/K_m$	η_K

The expressions for E_{11} and ν_{12} are called the Rule of Mixtures. In the above K_T is the plane strain bulk modulus, $K_f = [E_f/2(1-\nu_f)]$ and $K_m = [E_m/2(1-\nu_m)]$. Also, the η 's are given as follows:

$$\eta_6 = \frac{1 + G_m/G_{12f}}{2}, \quad \eta_4 = \frac{3 - 4\nu_m + G_m/G_{23f}}{4(1-\nu_m)}, \quad \eta_K = \frac{1 + G_m/K_f}{2(1-\nu_m)}.$$

The shear modulus of the matrix material, G_m , if isotropic, is given by $G_m = E_m/2(1+\nu_m)$.

The transverse moduli of the composite, $E_{22} = E_{33}$, are found from the following equation:

$$E_{22} = E_{33} = \frac{4K_T G_{23}}{K_T + mG_{23}}, \quad (2.23)$$

where

$$m = 1 + \frac{4K_T \nu_{12}^2}{E_{11}}.$$

The equations above have been written in general for composites reinforced with anisotropic fibers such as some graphite and aramid (Kevlar) fibers. If the fibers are isotropic, the fiber properties involve E_f , G_f and ν_f , where $G_f = \frac{E_f}{2(1+\nu_f)}$. In that case

also η_K becomes

$$\eta_K = \frac{1 + (1-2\nu_f)G_m/G_f}{2(1-\nu_m)} \quad (2.24)$$

Hahn notes that for most polymeric matrix structural composites, $G_m/G_f < 0.05$. If that is the case then the η parameters are approximately:

$$\eta_6 \approx 0.5; \quad \eta_4 = \frac{3-4\nu_m}{4(1-\nu_m)}; \quad \eta_K = \frac{1}{2(1-\nu_m)} \quad (2.25)$$

Finally, noting that $\nu_m = 0.35$ for most epoxies, then $\eta_4 = .62$ and $\eta_K = 0.77$.

Also, the Poisson's ratio, ν_{23} , can be written as

$$\nu_{23} = \nu_{12f} V_f + \nu_m (1-V_f) \left[\frac{1 + \nu_m - \nu_{12} \left(\frac{E_m}{E_{11}} \right)}{1 - \nu_m^2 + \nu_m \nu_{12} \left(\frac{E_m}{E_{11}} \right)} \right] \quad (2.26)$$

where ν_{12f} is the fiber Poisson's ratio and for ν_f , see Table 2.2.

The above equations along with Equation (2.17) provide the engineer with the wherewithal to estimate the elastic constants for a composite material if the constituent properties and volume fractions are known. In a few instances only the weight fraction of the fiber, W_f , is known. In that case the volume fraction is obtained from the following equation, where W_m is the weight fraction of the matrix, and ρ_m and ρ_f are the respective densities:

$$V_f = \frac{\rho_m W_f}{\rho_m W_f + \rho_f W_m} \quad (2.27)$$

For determining the composite elastic constants for short fiber composites, hybrid composites, textile composites, and very flexible composites, Chou [10] provides a comprehensive treatment.

2.5 Thermal and Hygrothermal Considerations

In the previous two sections, the elastic relations developed pertain only to an anisotropic elastic body at one temperature, that temperature being the "stress free" temperature, i.e. the temperature at which the body is considered to be free of stress if it is under no mechanical static or dynamic loadings.

However, in both metallic and composite structures changes in temperature are commonplace both during fabrication and during structural usage. Changes in temperature result in two effects that are very important. First, most materials expand when heated and contract when cooled, and in most cases this expansion is proportional to the temperature change. If, for instance, one had a long thin bar of a given material then with change in temperature, the ratio of the change in length of the bar, ΔL , to the original length, L , is related to the temperature of the bar, T , as shown in Figure 2.5.

Mathematically, this can be written as

$$\epsilon_{\text{thermal}} = \frac{\Delta L}{L} = \alpha \Delta T \quad (2.28)$$

where α is the coefficient of thermal expansion i.e., the proportionality constant between the "thermal" strain ($\Delta L/L$) and the change in temperature, ΔT , from some reference temperature at which there are no thermal stresses or thermal strains.

The second major effect of temperature change relates to stiffness and strength. Most materials become softer, more ductile, and weaker as they are heated. Typical plots of ultimate strength, yield stress and modulus of elasticity as functions of temperature are shown in Figure 2.6. In performing a stress analysis, determining the natural frequencies, or finding the buckling load of a heated or cooled structure one must use the strengths and the moduli of elasticity of the material at the temperature at which the structure is expected to perform.

In an orthotropic material, such as a composite, there can be up to three different coefficients of thermal expansion, and three different thermal strains, one in each of the orthogonal directions comprising the orthotropic material [Equation (2.28) would then have subscripts of 1, 2 and 3 on both the strains and the coefficients of thermal expansion]. Notice that, for the primary material axes, all thermal effects are dilatational only; there are no thermal effects in shear.

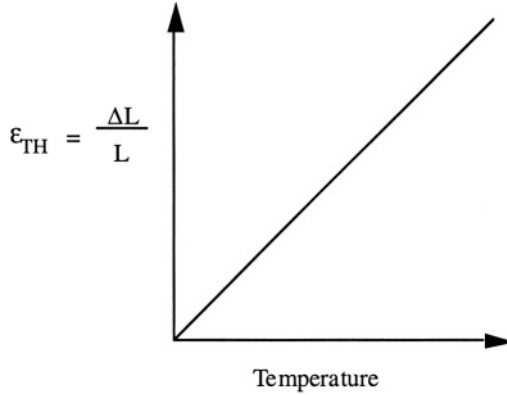


FIGURE 2.5. Change in Length of a Bar or Rod as a Function of Temperature

Some recent general articles and monographs on thermomechanical effects on composite material structures include those by Tauchert [11], Argyris and Tenek [12], Turvey and Marshall [13], Noor and Burton [14] and Huang and Tauchert [15].

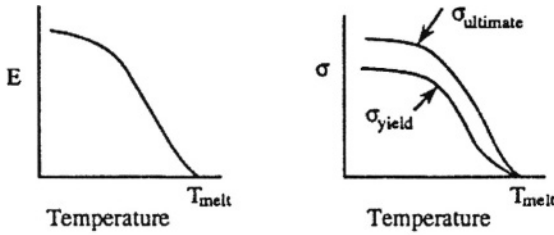


FIGURE 2.6. Modulus of Elasticity and Strengths as Functions of Temperature

During the mid-1970's another physical phenomenon associated with polymer matrix composites was recognized as important. It was found that the combination of high temperature and high humidity caused a doubly deleterious effect on the structural performance of these composites. Engineers and material scientists became very concerned about these effects, and considerable research effort was expended in studying this new phenomenon. Conferences [16] were held which discussed the problem, and both short range and long range research plans were proposed. The twofold problem involves the fact that the combination of high temperature and high humidity results in the entrapment of moisture in the polymer matrix, with attendant weight increase ($\leq 2\%$) and more importantly, a swelling of the matrix. It was realized [17] that the ingestion of moisture varied linearly with the swelling so that in fact

$$\epsilon_{\text{hygrothermal}} = \frac{\Delta L}{L} = \beta \Delta m \quad (2.29)$$

where Δm is the increase from zero moisture measured in percentage weight increase, and β is the coefficient of hygrothermal expansion, analogous to the coefficient of thermal expansion, depicted in Equation (2.28). This analogy is a very important one because one can see that the hygrothermal effects are entirely analogous mathematically to the thermal effect. Therefore, if one has the solutions to a thermoelastic problem, merely substituting $\beta\Delta m$ for or adding it to the $\alpha\Delta T$ terms provides the hygrothermal solution. The test methods to obtain values of the coefficient of hygrothermal expansion β are given in [18].

The second effect (i.e. the reduction of strength and stiffness) is also similar to the thermal effect. This is shown qualitatively in Figure 2.7. Dry polymers have properties that are usually rather constant until a particular temperature is reached, traditionally called by polymer chemists the "glass transition temperature," above which both strength and stiffness deteriorate rapidly. If the same polymer is saturated with moisture, not only are the mechanical properties degraded at any one temperature but the glass transition temperature for that polymer is significantly lower.

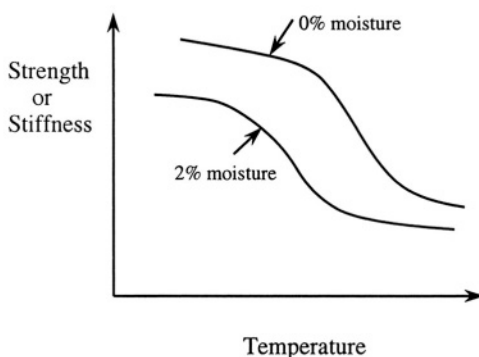


FIGURE 2.7. Mechanical Properties as a Function of Temperature and Moisture Absorption

As a quantitative example, Figure 2.8 clearly shows the diminution in tensile and shear strength due to a long term hygrothermal environment. Short time tensile and shear tests were performed on random mat glass/polyester resin specimens. It is clearly seen that there is a significant reduction in tensile strength, and a 29.3% and a 37.1% reduction in ultimate shear strength of these materials over a 100⁺ day soak period. If these effects are not accounted for in design analysis, catastrophic failures can and have occurred.

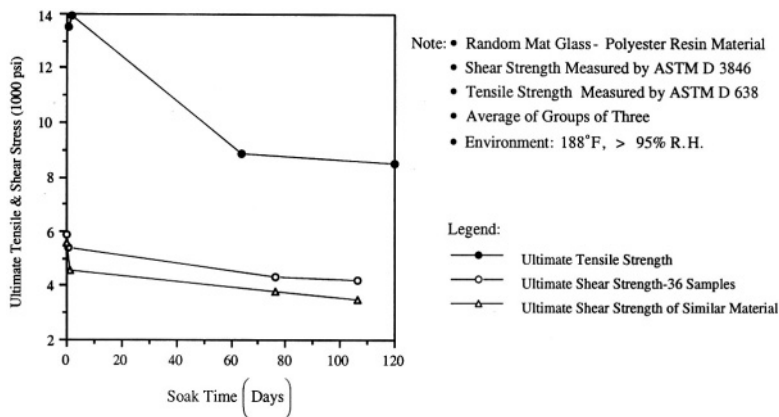


FIGURE 2.8. Strength as a Function of Soak Time in a Hot, Wet Environment

Thus, for modern polymer matrix composites one must include not only the thermal effects but also the hygrothermal effects or the structure can be considerably under designed, resulting in potential failure.

Thus, to deal with the real world of polymer composites, Equation (2.12) must be modified to read

$$\epsilon_i = a_{ij}\sigma_j + \alpha_i\Delta T + \beta_i\Delta m \quad (i = 1, 2, 3) \tag{2.30}$$

$$\epsilon_i = a_{ij}\sigma_j \quad (i = 4, 5, 6) \tag{2.31}$$

where in each equation $j = 1 - 6$.

Two types of equations are shown above because in the primary materials system of axes ($i, j = 1, 2, \dots, 6$) both thermal and hygrothermal effects are dilatational only, that is, they cause an expansion or contraction, but do not affect the shear stresses or strains. This is important to remember.

Although the thermal and moisture effects are analogous, they have significantly different time scales. For a structure subjected to a change in temperature that would require minutes or at most hours to come to equilibrium at the new temperature, the same structure would require weeks or months to come to moisture equilibrium (saturation) if that dry structure were placed in a 95-100% relative humidity environment. Figure 2.9 illustrates the point, as an example. A 1/4" thick random mat glass polyester matrix material requires 49 days of soak time at 188°F and 95% relative humidity to become saturated.

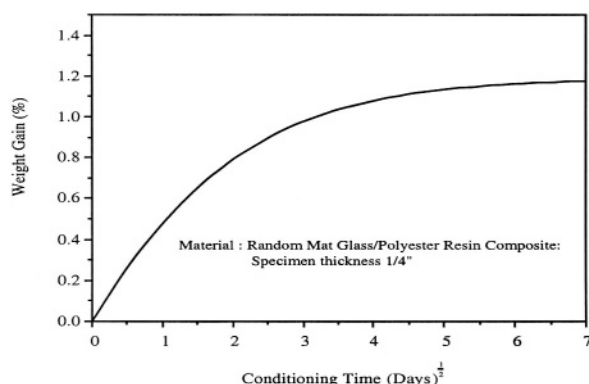


FIGURE 2.9. Moisture Absorption as a Function of Soak Time

Recently, Woldesenbet [19] soaked a large number of IM7/8551-7 graphite epoxy unidirectional test pieces, some in room temperature water to saturation. For the 1/4" diameter by 3/8" long cylinders soaked at room temperature the time required to reach saturation was 55 weeks. Other test pieces were soaked at an elevated temperature to reduce soak time.

For additional reading on this subject, see Shen and Springer [20].

2.6 Time-Temperature Effects on Composite Materials

In addition to the effects of temperature and moisture on the short time properties discussed above, if a structure is maintained under a constant load for a period of time, then creep and viscoelastic effects can become very important in the design and analysis of that structure. The subject of creep is discussed in numerous materials science and strength of materials texts and will not be described here in detail.

Creep and viscoelasticity can become significant in any material above certain temperatures, but can be particularly important in polymer matrix materials whose operating temperatures must be kept below maximum temperatures of 250°F, 350°F, or in some cases 600°F for short periods of time, dependent upon the specific polymer material. See Christensen [21].

From a structural mechanics point of view, almost all of the viscoelastic effects occur in the polymer matrix, while little or no creep occurs in the fibers. Thus, the study of creep in the polymeric materials, which comprise the matrix, provides the data necessary to study creep in composites. Jurf and Vinson [22] experimentally studied the effects of temperature and moisture (hygrothermal effects) on various epoxy materials (FM 73M and FM 300M adhesives). They established that at least for some epoxy materials it is possible to construct a master creep curve using a temperature shift factor, and established the fact that a moisture shift factor can also be employed. The importance of this is that by these experimentally determined temperature and moisture

shift factors, for the shear modulus of the epoxy, the results of short time creep tests can be used for a multitude of time/temperature/moisture combinations over the lifetime and environment of a structure comprised of that material. Wilson [23,24] studied the effects of viscoelasticity on the buckling of columns and rectangular plates and found that significant reductions of the buckling loads can occur. Wilson found that for the materials he studied, the buckling load diminished over the first 400 hours, then stabilized at a constant value. However that value may be a small fraction of the elastic buckling load if the composite properties in the load direction were matrix dominated properties (described later in the text). Wilson also established that for the problems studied it was quite satisfactory to bypass the complexities of a full-scale viscoelastic analysis using the Correspondence Principle and Laplace transformations. The use of the appropriate short time stiffness properties of the composite experimentally determined with specimens that have been held at the temperature and until the time for which the structural calculations are being made.

2.7 High Strain Rate Effects on Material Properties

Another consideration in the analysis of all composite material structures is the effect of high strain rate on the strength and stiffness properties of the materials used. Most materials have significantly different strengths, moduli, and strains to failure at high strain rates compared to static values. However most of the major finite element codes such as those which involve 10^5 - 10^6 elements using 10^1 - 10^2 hours of computer time to describe underwater and other explosion effects on structures, still utilize static material properties. High strain rate properties of materials are sorely needed. Some dynamic properties have been found, and test techniques established. For more information see Lindholm [25], Daniel, La Bedz, and Liber [26], Nicholas [27], Zukas [28], and Sierakowski [29,30], Rajapakse and Vinson [31], and Abrate [32,33].

Vinson and his colleagues have found through testing over thirty various composite materials over the range of strain rates tested up to 1600/sec, that in comparing high strain rate values to static values, the yield stresses can increase by a factor up to 3.6, the yield strains can change by factors of 3.1, strains to failure can change by factors up to 4.7, moduli of elasticity can change by factors up to 2.4, elastic strain energy densities can change by factors up to 6, while strain energy densities to failure can change by factors up to 8.1. Thus the use of static material properties to analyze and design structures subjected to impact, explosions, crashes, or other dynamic loads should be carefully reviewed.

2.8 Laminae of Composite Materials

Almost all practical composite material structures are thin in the thickness direction because the superior material properties of composites permit the use of thin walled structures. Many polymeric matrix composites are made in the form of a uniaxial set of fibers surrounded by a polymeric matrix in the form of a tape several inches wide termed as a "prepreg." The basic element in most long fiber composite structures is a lamina of fiber plus matrix, all fibers oriented in one direction, made by laying the prepreg tape of a certain length side by side. In the next section, 2.9, the stacking of various laminae to form a superior structure termed a laminate will be discussed. In modern manufacturing methods, such as many liquid injection molding techniques, the fibers are placed in the mold as a "preform". In that case the analyst must decide whether the molded composite can best be modeled as one lamina or a laminate. Also if a composite lamina has a thermal gradient across the thickness such that the material properties vary significantly from one surface to the other, then the analyst could model the composite as a laminate with differing material properties in each lamina.

To describe this, consider a small element of a lamina of constant thickness h , wherein the principal material axes are labeled 1 and 2, that is the 1 direction is parallel to the fibers, the 2 direction is normal to them, and consider that the beam, plate or shell geometric axes are x and y as depicted in Figure 2.10. For the material axes 1 and 2, the 1 axis is always in the direction involving the stiffer and stronger material properties, compared to the 2 direction.

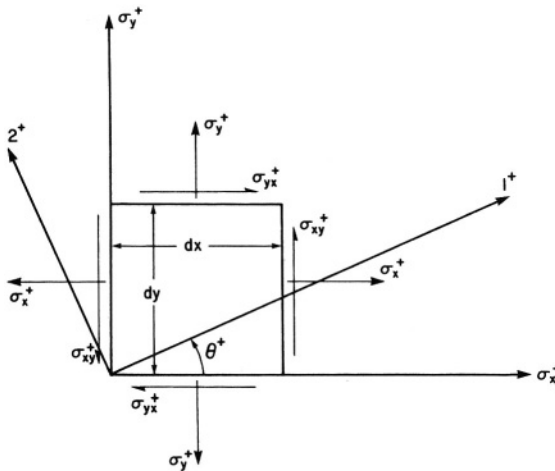


FIGURE 2.10. Lamina Coordinate System

The element shown in Figure 2.10 has the stresses shown in the positive directions consistent with references [2,3,34-36]. If one performs a force equilibrium study to relate σ_x , σ_y and σ_{xy} to σ_1 , σ_2 , and σ_{12} , it is exactly analogous to the Mohr's circle analysis in basic strength of materials with the result that, in matrix form,

$$\begin{bmatrix} \sigma_1 \\ \sigma_2 \\ \sigma_6 \end{bmatrix} = [T]_{CL} \begin{bmatrix} \sigma_x \\ \sigma_y \\ \sigma_{xy} \end{bmatrix} \quad (2.32)$$

where

$$[T]_{CL} = \begin{bmatrix} m^2 & n^2 & +2mn \\ n^2 & m^2 & -2mn \\ -mn & mn & (m^2 - n^2) \end{bmatrix} \quad (2.33)$$

and where here $m = \cos \theta$, $n = \sin \theta$, and θ is defined positive as shown in Figure 2.10, and the subscripts CL refer to the classical two-dimensional case only, that is, in the 1-2 plane or the x - y plane only.

Analogously, a strain relationship also follows for the classical isothermal case

$$\begin{bmatrix} \epsilon_1 \\ \epsilon_2 \\ \epsilon_{12} \end{bmatrix} = [T]_{CL} \begin{bmatrix} \epsilon_x \\ \epsilon_y \\ \epsilon_{xy} \end{bmatrix} \quad (2.34)$$

However, these classical two-dimensional relationships must be modified to treat a composite material to include thermal effects, hygrothermal effects, and the effects of transverse shear deformation treated in detail elsewhere [2, 3, 4, 6, 7]. The effects of transverse shear deformation, shown through the inclusion of the $\sigma_4 - \epsilon_4$ and $\sigma_5 - \epsilon_5$ relations shown in Equations (2.32) and (2.34), must be included in composite materials, because in the fiber direction the composite has many of the mechanical properties of the fiber itself (strong and stiff) while in the thickness direction the fibers are basically ineffective and the shear properties are dominated by the weaker matrix material. Similarly, because quite often the matrix material has much higher coefficients of thermal and hygrothermal expansion (α and β), thickening and thinning of the lamina cannot be ignored in some cases. Hence, without undue derivation, the Equations (2.32) through (2.34) are modified to be:

$$\begin{bmatrix} \sigma_1 \\ \sigma_2 \\ \sigma_3 \\ \sigma_4 \\ \sigma_5 \\ \sigma_6 \end{bmatrix} = \begin{bmatrix} \sigma_x \\ \sigma_y \\ \sigma_z \\ \sigma_{yz} \\ \sigma_{xz} \\ \sigma_{xy} \end{bmatrix} \quad \text{and} \quad \begin{bmatrix} \varepsilon_1 \\ \varepsilon_2 \\ \varepsilon_3 \\ \varepsilon_{4/2} \\ \varepsilon_{5/2} \\ \varepsilon_{6/2} \end{bmatrix} = [T] \begin{bmatrix} \varepsilon_x \\ \varepsilon_y \\ \varepsilon_z \\ \varepsilon_{yz} \\ \varepsilon_{xz} \\ \varepsilon_{xy} \end{bmatrix} \quad (2.35)$$

where

$$[T] = \begin{bmatrix} m^2 & n^2 & 0 & 0 & 0 & 2mn \\ n^2 & m^2 & 0 & 0 & 0 & -2mn \\ 0 & 0 & 1 & 0 & 0 & 0 \\ 0 & 0 & 0 & m & -n & 0 \\ 0 & 0 & 0 & n & m & 0 \\ -mn & mn & 0 & 0 & 0 & (m^2 - n^2) \end{bmatrix} \quad (2.36)$$

Please note the introduction of the factor of $\frac{1}{2}$ as noted in the strain expressions, because of the way ε_4 , ε_5 and ε_6 are defined in Equation (2.5).

For completeness, the reverse transformations are given.

$$\begin{bmatrix} \sigma_x \\ \sigma_y \\ \sigma_z \\ \sigma_{yz} \\ \sigma_{xz} \\ \sigma_{xy} \end{bmatrix} = [T]^{-1} \begin{bmatrix} \sigma_1 \\ \sigma_2 \\ \sigma_3 \\ \sigma_4 \\ \sigma_5 \\ \sigma_6 \end{bmatrix} \quad \text{and} \quad \begin{bmatrix} \varepsilon_x \\ \varepsilon_y \\ \varepsilon_z \\ \varepsilon_{yz} \\ \varepsilon_{xz} \\ \varepsilon_{xy} \end{bmatrix} = [T]^{-1} \begin{bmatrix} \varepsilon_1 \\ \varepsilon_2 \\ \varepsilon_3 \\ \left\{ \frac{\varepsilon_4}{2} \right\} \\ \left\{ \frac{\varepsilon_5}{2} \right\} \\ \left\{ \frac{\varepsilon_6}{2} \right\} \end{bmatrix} = [T]^{-1} \begin{bmatrix} \varepsilon_{11} \\ \varepsilon_{22} \\ \varepsilon_{33} \\ \varepsilon_{23} \\ \varepsilon_{13} \\ \varepsilon_{12} \end{bmatrix} \quad (2.37)$$

where*

$$[T]^{-1} = \begin{bmatrix} m^2 & n^2 & 0 & 0 & 0 & -2mn \\ n^2 & m^2 & 0 & 0 & 0 & 2mn \\ 0 & 0 & 1 & 0 & 0 & 0 \\ 0 & 0 & 0 & m & n & 0 \\ 0 & 0 & 0 & -n & m & 0 \\ mn & -mn & 0 & 0 & 0 & (m^2 - n^2) \end{bmatrix} \quad (2.38)$$

Again, please note that the transformations can be made only with *tensor* strains. Hence, from Equation (2.5), it is necessary to divide ϵ_4 , ϵ_5 and ϵ_6 by two.

If one systematically uses these expressions, and utilizes Hooke's Law relating stress and strain, and includes the thermal and hygrothermal effects, one can produce the following overall general equations for a lamina of a fiber reinforced composite material in terms of the principal material directions (1, 2, 3); see Equations (2.8) - (2.21).

$$\begin{Bmatrix} \sigma_1 \\ \sigma_2 \\ \sigma_3 \\ \sigma_4 \\ \sigma_5 \\ \sigma_6 \end{Bmatrix} = \begin{bmatrix} Q_{11} & Q_{12} & Q_{13} & 0 & 0 & 0 \\ Q_{12} & Q_{22} & Q_{23} & 0 & 0 & 0 \\ Q_{13} & Q_{23} & Q_{33} & 0 & 0 & 0 \\ 0 & 0 & 0 & Q_{44} & 0 & 0 \\ 0 & 0 & 0 & 0 & Q_{55} & 0 \\ 0 & 0 & 0 & 0 & 0 & Q_{66} \end{bmatrix} \begin{Bmatrix} \epsilon_1 - \alpha_1 \Delta T - \beta_1 \Delta m \\ \epsilon_2 - \alpha_2 \Delta T - \beta_2 \Delta m \\ \epsilon_3 - \alpha_3 \Delta T - \beta_3 \Delta m \\ 2\epsilon_{23} \\ 2\epsilon_{31} \\ 2\epsilon_{12} \end{Bmatrix} \quad (2.39)$$

In the above, the Q_{ij} quantities are used for the stiffness matrix quantities obtained directly from Equation (2.8) through (2.21). One should also remember that $\epsilon_{23} = (1/2G_{23})\sigma_4$, $\epsilon_{31} = (1/2G_{31})\sigma_5$ and $\epsilon_{12} = (1/2G_{12})\sigma_6$, hence the coefficients of "two" appearing with the tensor shear strains ϵ_{23} , ϵ_{31} , and ϵ_{12} above. Using the notation of Sloan [36], the stiffness matrix quantities can be written as follows:

* $[T]^{-1}$ can be found by replacing θ by $(-\theta)$ in $[T]$.

$$\begin{aligned}
Q_{11} &= E_{11}(1-v_{23}v_{32})/\Delta, \quad Q_{22} = E_{22}(1-v_{31}v_{13})/\Delta \\
Q_{33} &= E_{33}(1-v_{12}v_{21})/\Delta, \quad Q_{44} = G_{23}, \quad Q_{55} = G_{13}, \quad Q_{66} = G_{12} \\
Q_{12} &= (v_{21} + v_{31}v_{23})E_{11}/\Delta = (v_{12} + v_{32}v_{13})E_{22}/\Delta \\
Q_{13} &= (v_{31} + v_{21}v_{32})E_{11}/\Delta = (v_{13} + v_{12}v_{23})E_{33}/\Delta \quad (2.40) \\
Q_{23} &= (v_{32} + v_{12}v_{31})E_{22}/\Delta = (v_{23} + v_{21}v_{13})E_{33}/\Delta \\
\Delta &= 1 - v_{12}v_{21} - v_{23}v_{32} - v_{31}v_{13} - 2v_{21}v_{32}v_{13}
\end{aligned}$$

Incidentally in the above expressions, if the lamina is transversely isotropic, i.e. has the same properties in both the 2 and 3 directions, then $v_{12} = v_{13}$, $G_{12} = G_{13}$, $E_{22} = E_{33}$ with resulting simplification.

For preliminary calculations in design or where great accuracy is not needed, simpler forms [2, 3] for some of the expressions in Equation (2.40) can be used, as shown below, with little loss in numerical accuracy:

$$\begin{aligned}
Q_{11} &= E_{11}/(1 - v_{12}v_{21}), \quad Q_{22} = E_{22}/(1 - v_{12}v_{21}) \\
Q_{12} &= Q_{21} = v_{21}E_{11}/(1 - v_{12}v_{21}) = v_{12}E_{22}/(1 - v_{12}v_{21}) \quad (2.41) \\
Q_{66} &= G_{12}
\end{aligned}$$

If these simpler forms are used then one would use the classical form of the constitutive relations instead of Equation (2.39), neglecting transverse shear deformation and transverse normal stress, i.e., letting σ_3, σ_4 and σ_5 equal zero, thus obtaining

$$\begin{Bmatrix} \sigma_1 \\ \sigma_2 \\ \sigma_3 \end{Bmatrix} = \begin{bmatrix} Q_{11} & Q_{12} & 0 \\ Q_{12} & Q_{22} & 0 \\ 0 & 0 & Q_{66} \end{bmatrix} \begin{Bmatrix} \varepsilon_1 - \alpha_1 \Delta T - \beta_1 \Delta m \\ \varepsilon_2 - \alpha_2 \Delta T - \beta_2 \Delta m \\ 2\varepsilon_{12} \end{Bmatrix} \quad (2.42)$$

where one should remember also that $2\varepsilon_{12} = \varepsilon_6$, hence the appearance of the factor of two before ε_{12} . As stated above for many cases it is sufficient to use Equations (2.41) and (2.42) rather than Equations (2.39) and (2.40) for faster and easier calculation.

When the structural axes, x, y and z , are not aligned with the principle materials axes, 1, 2, 3, as described in Figure 2.10, then a coordinate transformation is necessary.

To relate these relationships to the x - y - z coordinate system, one utilizes Equations (2.37) through (2.39). The result is

$$\begin{Bmatrix} \sigma_x \\ \sigma_y \\ \sigma_z \\ \sigma_{yz} \\ \sigma_{xz} \\ \sigma_{xy} \end{Bmatrix} = \begin{bmatrix} \bar{Q}_{11} & \bar{Q}_{12} & \bar{Q}_{13} & 0 & 0 & \bar{Q}_{16} \\ \bar{Q}_{12} & \bar{Q}_{22} & \bar{Q}_{23} & 0 & 0 & \bar{Q}_{26} \\ \bar{Q}_{13} & \bar{Q}_{23} & \bar{Q}_{33} & 0 & 0 & \bar{Q}_{36} \\ 0 & 0 & 0 & \bar{Q}_{44} & \bar{Q}_{45} & 0 \\ 0 & 0 & 0 & \bar{Q}_{45} & \bar{Q}_{55} & 0 \\ \bar{Q}_{16} & \bar{Q}_{26} & \bar{Q}_{36} & 0 & 0 & \bar{Q}_{66} \end{bmatrix} \begin{Bmatrix} \epsilon_x - \alpha_x \Delta T - \beta_x \Delta m \\ \epsilon_y - \alpha_y \Delta T - \beta_y \Delta m \\ \epsilon_z - \alpha_z \Delta T - \beta_z \Delta m \\ 2\epsilon_{yz} \\ 2\epsilon_{xz} \\ 2(\epsilon_{xy} - \alpha_{xy} \Delta T - \beta_{xy} \Delta m) \end{Bmatrix} \quad (2.43)$$

where $[\bar{Q}] = [T]^{-1}[Q][T]$, or more explicitly,

$$\bar{Q}_{11} = Q_{11}m^4 + 2(Q_{12} + 2Q_{66})m^2n^2 + Q_{22}n^4$$

$$\bar{Q}_{12} = (Q_{11} + Q_{22} - 4Q_{66})m^2n^2 + Q_{12}(m^4 + n^4)$$

$$\bar{Q}_{13} = Q_{13}m^2 + Q_{23}n^2$$

$$\bar{Q}_{16} = -mn^3Q_{22} + m^3nQ_{11} - mn(m^2 - n^2)(Q_{12} + 2Q_{66})$$

$$\bar{Q}_{22} = Q_{11}n^4 + 2(Q_{12} + 2Q_{66})m^2n^2 + Q_{22}m^4$$

$$\bar{Q}_{23} = n^2Q_{13} + m^2Q_{23}$$

$$\bar{Q}_{33} = Q_{33}$$

$$\bar{Q}_{26} = -m^3nQ_{22} + mn^3Q_{11} + mn(m^2 - n^2)(Q_{12} + 2Q_{66}) \quad (2.44)$$

$$\bar{Q}_{36} = (Q_{13} - Q_{23})mn$$

$$\bar{Q}_{44} = Q_{44}m^2 + Q_{55}n^2$$

$$\bar{Q}_{45} = (Q_{55} - Q_{44})mn$$

$$\bar{Q}_{55} = Q_{55}m^2 + Q_{44}n^2$$

$$\bar{Q}_{66} = (Q_{11} + Q_{22} - 2Q_{12})m^2n^2 + Q_{66}(m^2 - n^2)^2$$

$$\alpha_x = \alpha_1m^2 + \alpha_2n^2 \quad \beta_x = \beta_1m^2 + \beta_2n^2$$

$$\alpha_y = \alpha_2m^2 + \alpha_1n^2 \quad \beta_y = \beta_2m^2 + \beta_1n^2$$

$$\alpha_z = \alpha_3 \quad \beta_z = \beta_3$$

$$\alpha_{xy} = (\alpha_1 - \alpha_2)mn \quad \beta_{xy} = (\beta_1 - \beta_2)mn.$$

It should be remembered that although the coefficients of both thermal and hygrothermal expansion are purely dilatational in the material coordinate system 1-2, rotation into the structural coordinate system x - y , results in an α_{xy} and a β_{xy} , simply because the composite materials will probably have $\alpha_1 \neq \alpha_2$ and $\beta_1 \neq \beta_2$.

Again, for preliminary design purposes or for approximate but usually accurate calculations one can use the simpler classical form of

$$\begin{Bmatrix} \sigma_x \\ \sigma_y \\ \sigma_{xy} \end{Bmatrix} = \begin{bmatrix} \bar{Q}_{11} & \bar{Q}_{12} & \bar{Q}_{16} \\ \bar{Q}_{12} & \bar{Q}_{22} & \bar{Q}_{26} \\ \bar{Q}_{16} & \bar{Q}_{26} & \bar{Q}_{66} \end{bmatrix} \begin{Bmatrix} \epsilon_x - \alpha_x \Delta T - \beta_x \Delta m \\ \epsilon_y - \alpha_y \Delta T - \beta_y \Delta m \\ 2(\epsilon_{xy} - \alpha_{xy} \Delta T - \beta_{xy} \Delta m) \end{Bmatrix} \quad (2.45)$$

where the \bar{Q}_{ij} are defined in Equation (2.44), but one can use the Q_{ij} of Equation (2.41) instead of Equation (2.40) for consistency with the simpler expressions above.

One interesting variation of the above classical quantities of Equation (2.43) resulted when Tsai and Pagano [37] rewrote many of the quantities in terms of material invariants and trigonometric functions involving (20) and (40). Their method provides an alternative formulation or a check of numerical results.

At this point, given a lamina of a unidirectional composite of known elastic properties, if used in a plate or panel, (as well as a beam, ring or shell, discussed later) with the 1-2 material axis at an angle θ from the plate or panel x-y axes, all stiffness quantities Q_{ij} and \bar{Q}_{ij} can be determined relating stresses and strains in either coordinate system.

2.9 Laminate Analysis

In the previous section the generalized constitutive equations for one lamina of a composite material were formulated. Many structures of composite materials including sandwich structures are composed of numerous laminae, which are bonded and/or cured together. In fact, over and above the superior properties in strength and stiffness that composites possess, the ability to stack laminae one on the other in a varied but unique fashion to result in the optimum laminate material properties for a given structural size and set of loadings is one of the major advantages that composites have over more conventional structures. Up to this point, the concentration has been on the stress-strain or constitutive relations. Now the other three sets of equations comprising the equations of elasticity will be considered: the strain-displacement relations, the equilibrium equations and the compatibility equations.

Consider a laminate composed of N laminae. For the k^{th} lamina of the laminate, Equation (2.43) can be written as:

$$\begin{Bmatrix} \sigma_x \\ \sigma_y \\ \sigma_z \\ \sigma_{yz} \\ \sigma_{xz} \\ \sigma_{xy} \end{Bmatrix}_k = [\tilde{Q}]_k \begin{Bmatrix} \epsilon_x - \alpha_x \Delta T - \beta_x \Delta m \\ \epsilon_y - \alpha_y \Delta T - \beta_y \Delta m \\ \epsilon_z - \alpha_z \Delta T - \beta_z \Delta m \\ 2\epsilon_{yz} \\ 2\epsilon_{xz} \\ 2(\epsilon_{xy} - \alpha_{xy} \Delta T - \beta_{xy} \Delta m) \end{Bmatrix}_k, \quad (2.46)$$

where all of the above matrices must have the subscript k due to the material and its orientation for each particular lamina with respect to the structural x - y coordinates and therefore its unique $[\tilde{Q}]_k$, $[\alpha_i]_k$ and $[\beta_i]_k$.

For any elastic body the strain-displacement equations, i.e., those kinematic relations describing the functional relations between the elastic strains in the body and its displacements, are given by the following expression when considering linear elastic deformation:

$$\epsilon_{ij} = \frac{1}{2} (u_{i,j} + u_{j,i}) \quad (2.47)$$

where $i, j = x, y, z$ in a Cartesian coordinate frame, and the comma denotes partial differentiation with respect to the coordinate denoted by the symbol after the comma. Explicitly, the relations are:

$$\begin{aligned} \epsilon_x &= \frac{\partial u}{\partial x}, & \epsilon_y &= \frac{\partial v}{\partial y}, & \epsilon_z &= \frac{\partial w}{\partial z} \\ \epsilon_{xz} &= \frac{1}{2} \left(\frac{\partial u}{\partial z} + \frac{\partial w}{\partial x} \right), & \epsilon_{yz} &= \frac{1}{2} \left(\frac{\partial v}{\partial z} + \frac{\partial w}{\partial y} \right) \\ \epsilon_{xy} &= \frac{1}{2} \left(\frac{\partial u}{\partial y} + \frac{\partial v}{\partial x} \right) \end{aligned} \quad (2.48)$$

In the above u , v , and w are the displacements in the structural x , y , and z directions, respectively. In linear elastic beam, plate, ring and shell theory, it is assumed that a lineal element extending through the thickness of a thin plate and perpendicular to the middle surface (that is, the x - y plane in Figure 2.11 below) prior to loading, upon the application of a load undergoes at most a translation and a rotation with respect to the original coordinate system. Based upon that one assumption the functional form of the displacements for a laminated plate is:

$$u(x, y, z) = u_0(x, y) + z\bar{\alpha}(x, y)$$

$$v(x, y, z) = v_0(x, y) + z\bar{\beta}(x, y) \quad (2.49)$$

$$w(x, y, z) = w(x, y)$$

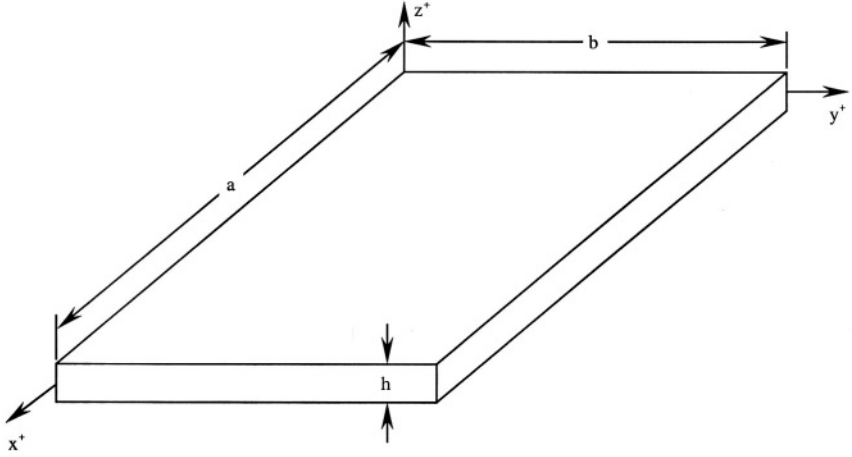


FIGURE 2.11. Typical Rectangular Plate

where u_0 , v_0 and w are the middle surface displacements, i.e., the translations of the lineal element, and the second terms in the first two equations are the rotations of a lineal element through the thickness. In classical beam and plate theory $\bar{\alpha}$ and $\bar{\beta}$ are the negative of the first derivative of the lateral displacement with respect to the x and y coordinates respectively (i.e., $\bar{\alpha} = -(\partial w / \partial x)$ and $\bar{\beta} = -(\partial w / \partial y)$, the negative of the slope), but if transverse shear deformation is included, $\bar{\alpha}$ and $\bar{\beta}$ are unknown dependent variables which must be solved for; this will be discussed later. Also, in classical theory, it is assumed that the lineal element across the thickness of the beam, plate or shell cannot extend nor shrink because at most it undergoes a translation and rotation, hence $w = w(x, y)$ only. Sloan [36] has shown that for many practical composites, plate thickening (where the lateral deflection is a function of z) is unimportant and can be neglected, hence it is not included here, but can be found in detail in [30].

Substituting Equation (2.49) into Equation (2.48) results in:

$$\varepsilon_x = \frac{\partial u_0}{\partial x} + z \frac{\partial \bar{\alpha}}{\partial x}, \quad \varepsilon_y = \frac{\partial v_0}{\partial y} + z \frac{\partial \bar{\beta}}{\partial y}, \quad \varepsilon_z = 0$$

$$\begin{aligned}\varepsilon_{xz} &= \frac{1}{2} \left(\bar{\alpha} + \frac{\partial w}{\partial x} \right), \quad \varepsilon_{yz} = \frac{1}{2} \left(\bar{\beta} + \frac{\partial w}{\partial y} \right) \\ \varepsilon_{xy} &= \frac{1}{2} \left(\frac{\partial u_0}{\partial y} + \frac{\partial v_0}{\partial x} \right) + \frac{z}{2} \left(\frac{\partial \bar{\alpha}}{\partial y} + \frac{\partial \bar{\beta}}{\partial x} \right)\end{aligned}\tag{2.50}$$

The mid-surface strains can be written as:

$$\varepsilon_{x_0} = \frac{\partial u_0}{\partial x}, \quad \varepsilon_{y_0} = \frac{\partial v_0}{\partial y}, \quad \varepsilon_{xy_0} = \frac{1}{2} \left(\frac{\partial u_0}{\partial y} + \frac{\partial v_0}{\partial x} \right)\tag{2.51}$$

The curvatures can be written as

$$\kappa_x = \frac{\partial \bar{\alpha}}{\partial x}, \quad \kappa_y = \frac{\partial \bar{\beta}}{\partial y}, \quad \kappa_{xy} = \frac{1}{2} \left(\frac{\partial \bar{\alpha}}{\partial y} + \frac{\partial \bar{\beta}}{\partial x} \right)\tag{2.52}$$

The classical and first order shear deformation theories utilize displacements and strains to describe the strains and displacements of a laminated or sandwich structure composed of composite material, because all of the individual laminae are bonded together, therefore the same assumptions are made regarding the lineal element through the laminate thickness. Thus, a continuity of strains and displacements occurs across the laminated structure regardless of the orientation of individual laminae.

Substituting (2.50) through (2.52) into Equation (2.46) results in Equation (2.53); wherein because it is assumed that $\varepsilon_z = 0$, (because plate thickening is neglected), σ_z for a thin walled structure of composite material is usually negligible and will not be considered further.

$$\begin{Bmatrix} \sigma_x \\ \sigma_y \\ \sigma_{yz} \\ \sigma_{xz} \\ \sigma_{xy} \end{Bmatrix}_k = [\bar{Q}]_k \begin{Bmatrix} \varepsilon_{x_0} + z\kappa_x - \alpha_x \Delta T - \beta_x \Delta m \\ \varepsilon_{y_0} + z\kappa_y - \alpha_y \Delta T - \beta_y \Delta m \\ 2\varepsilon_{yz} \\ 2\varepsilon_{xz} \\ 2(\varepsilon_{xy_0} + \kappa_{xy}z - \alpha_{xy} \Delta T - \beta_{xy} \Delta m) \end{Bmatrix}_k\tag{2.53}$$

Note that without the hygrothermal terms, the strain-curvature matrix at the right in Equation (2.53) would suffice for the entire laminate independent of orientation, because the displacements, and strains are continuous over the thickness of the laminate. In that case the subscript k on that matrix would not be needed. However, even though there is continuity of the mid-surface strains and curvatures across the thickness of the laminate, the stresses are discontinuous across the laminate thickness because of the

various orientations of each lamina, hence, the subscript k in the stress matrix above. It is seen from Equation (2.53) that if all quantities on the right hand side are known, one can easily calculate each stress component in each lamina comprising the laminate.

Consider a laminated plate or panel of thickness h as shown below, in Figure 2.12. It is seen that h_k is the *vectorial* distance from the panel mid-plane, $z = 0$, to the upper surface of the k^{th} lamina, i.e., *any dimension below the midsurface is a negative dimension* and any dimension above the midsurface is positive. For example, consider a laminate 0.52 mm (0.020") thick, composed of four equally thick laminae, each being 0.13 mm (0.005") thick. Then $h_0 = -0.26$ mm (-0.010"), $h_1 = -0.13$ mm (-0.005"), $h_2 = 0$, $h_3 = 0.13$ mm (0.005") and $h_4 = 0.26$ mm (0.010").

As in classical beam, plate and shell theory [2, 3, 34-36], one defines and uses stress resultants (N), stress couples (M), and transverse shear resultants (Q) per unit width, with appropriate subscript, for the overall structure regardless of the number and the orientation of the laminae, hence:

$$\begin{Bmatrix} N_x \\ N_y \\ N_{xy} \\ Q_x \\ Q_y \end{Bmatrix} = \int_{-h/2}^{+h/2} \begin{Bmatrix} \sigma_x \\ \sigma_y \\ \sigma_{xy} \\ \sigma_{xz} \\ \sigma_{yz} \end{Bmatrix} dz, \quad \begin{Bmatrix} M_x \\ M_y \\ M_{xy} \end{Bmatrix} = \int_{-h/2}^{+h/2} \begin{Bmatrix} \sigma_x \\ \sigma_y \\ \sigma_{xy} \end{Bmatrix} z dz \quad (2.54)$$

It must be emphasized that all of the above quantities are a force per unit width and a couple per unit width because in plate and shell structures these quantities vary in both the x and y directions.

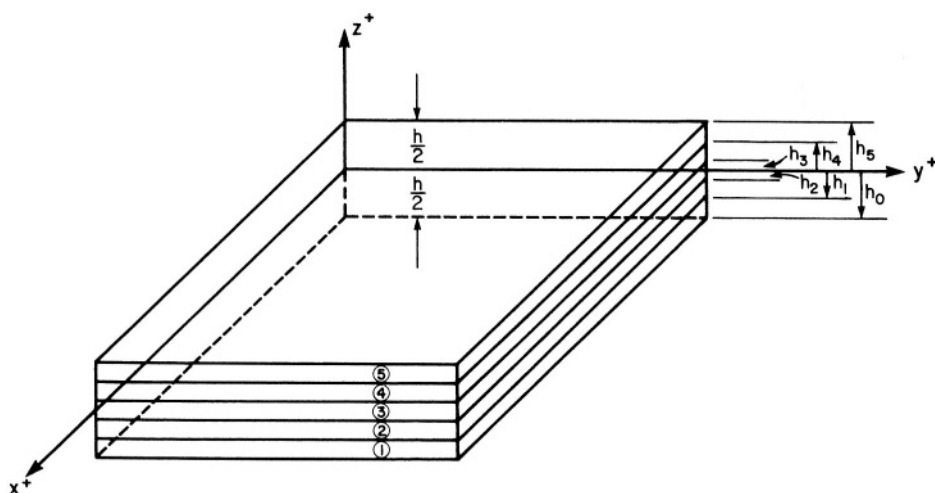


FIGURE 2.12. Nomenclature for the Stacking Sequence

On the plate shown in Figure 2.13, the positive directions of all the stress resultants and stress couples are shown, consistent with the definitions of the quantities given in Equation (2.54).

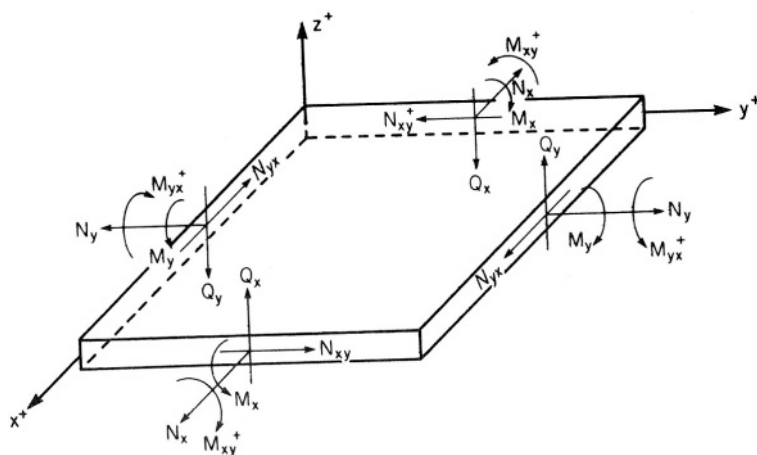


FIGURE 2.13. Positive directions for Stress Resultants and Stress Couples for a Plate

For a laminated plate, the stress components can be integrated across each lamina, but must then be added together across the laminae as follows; employing Equations (2.47) and (2.50) through Equation (2.52):

$$\begin{aligned}
\begin{bmatrix} N_x \\ N_y \\ N_{xy} \end{bmatrix} &= \sum_{k=1}^N \int_{h_{k-1}}^{h_k} \begin{bmatrix} \sigma_x \\ \sigma_y \\ \sigma_{xy} \end{bmatrix} dz \\
\begin{bmatrix} N_x \\ N_y \\ N_{xy} \end{bmatrix} &= \sum_{k=1}^N \left\{ \int_{h_{k-1}}^{h_k} [\bar{Q}]_k \begin{bmatrix} \varepsilon_{x_0} \\ \varepsilon_{y_0} \\ \varepsilon_{xy_0} \end{bmatrix} dz + \int_{h_{k-1}}^{h_k} [\bar{Q}]_k \begin{bmatrix} \kappa_x \\ \kappa_y \\ \kappa_{xy} \end{bmatrix} z dz \right. \\
&\quad \left. - \int_{h_{k-1}}^{h_k} [\bar{Q}]_k \begin{bmatrix} \alpha_x \\ \alpha_y \\ \alpha_{xy} \end{bmatrix}_k \Delta T dz - \int_{h_{k-1}}^{h_k} [\bar{Q}]_k \begin{bmatrix} \beta_x \\ \beta_y \\ \beta_{xy} \end{bmatrix}_k \Delta m dz \right\} \quad (2.55)
\end{aligned}$$

where only the pertinent portions of the $[\bar{Q}]_k$ matrix are used.

Since the derivatives of the mid-surface displacements (u_0 and v_0), the rotations ($\bar{\alpha}$ and $\bar{\beta}$) and the \bar{Q} 's are not functions of z , Equation (2.55) can be rewritten as:

$$\begin{aligned}
\begin{bmatrix} N_x \\ N_y \\ N_{xy} \end{bmatrix} &= \sum_{k=1}^N \left\{ [\bar{Q}]_k \begin{bmatrix} \varepsilon_{x_0} \\ \varepsilon_{y_0} \\ \varepsilon_{xy_0} \end{bmatrix}_k \int_{h_{k-1}}^{h_k} dz + [\bar{Q}]_k \begin{bmatrix} \kappa_x \\ \kappa_y \\ \kappa_{xy} \end{bmatrix}_k \int_{h_{k-1}}^{h_k} z dz \right. \\
&\quad \left. - \int_{h_{k-1}}^{h_k} [\bar{Q}]_k \begin{bmatrix} \alpha_x \\ \alpha_y \\ \alpha_{xy} \end{bmatrix}_k \Delta T dz - \int_{h_{k-1}}^{h_k} [\bar{Q}]_k \begin{bmatrix} \beta_x \\ \beta_y \\ \beta_{xy} \end{bmatrix}_k \Delta m dz \right\} \quad (2.56)
\end{aligned}$$

Finally, Equation (2.56) can be written succinctly as:

$$[N] = [A][\varepsilon_0] + [B][\kappa] - [N]^T - [N]^m, \quad (2.57)$$

where it is shown later in Equation (2.66) that a factor of 2 is necessary in some terms, and where

$$A_{ij} = \sum_{k=1}^N (\bar{Q}_{ij})_k [h_k - h_{k-1}], \quad [i, j = 1, 2, 6] \quad (2.58)$$

$$B_{ij} = \frac{1}{2} \sum_{k=1}^N (\bar{Q}_{ij})_k [h_k^2 - h_{k-1}^2], \quad [i, j = 1, 2, 6] \quad (2.59)$$

$$N_{ij}^T = \sum_{k=1}^N \int_{h_{k-1}}^{h_k} (\bar{Q}_{ij})_k [\alpha_{ij}]_k \Delta T dz \quad [i, j = 1, 2, 6] \quad (2.60)$$

$$N_{ij}^m = \sum_{k=1}^N \int_{h_{k-1}}^{h_k} (\bar{Q}_{ij})_k [\beta_{ij}]_k \Delta m dz \quad [i, j = 1, 2, 6] \quad (2.61)$$

where it is obvious from Equation (2.56) how the $[\alpha_{ij}]_k$ and $[\beta_{ij}]_k$ matrices are defined.

From Equation (2.57), it is seen that the in-plane stress resultants for a laminated thin walled structure are not only functions of the mid-plane strains ($\epsilon_{x_0} = \partial u_0 / \partial x$, etc.) as they are in a homogeneous beam, plate or shell, but they can also be functions of the curvatures and twists ($\kappa_x = \partial^2 w / \partial x^2$, etc.) as well. Therefore in-plane forces can cause curvatures or twisting deformations in composite laminated structures.

Similar to the above, but multiplying Equation (2.53) through by z first before integrating, as in Equation (2.55), the following can be found:

$$\begin{aligned} \begin{bmatrix} M_x \\ M_y \\ M_{xy} \end{bmatrix} &= \sum_{k=1}^N \left\{ \begin{bmatrix} \bar{Q} \end{bmatrix}_k \begin{bmatrix} \epsilon_{x_0} \\ \epsilon_{y_0} \\ \epsilon_{xy_0} \end{bmatrix} \right\}_{h_{k-1}}^{h_k} z dz + \begin{bmatrix} \bar{Q} \end{bmatrix}_k \begin{bmatrix} \kappa_x \\ \kappa_y \\ \kappa_{xy} \end{bmatrix} \right\}_{h_{k-1}}^{h_k} z^2 dz \\ &- \int_{h_{k-1}}^{h_k} \begin{bmatrix} \bar{Q} \end{bmatrix}_k \begin{bmatrix} \alpha_x \\ \alpha_y \\ \alpha_{xy} \end{bmatrix} \Delta T z dz - \int_{h_{k-1}}^{h_k} \begin{bmatrix} \bar{Q} \end{bmatrix}_k \begin{bmatrix} \beta_x \\ \beta_y \\ \beta_{xy} \end{bmatrix} \Delta m z dz \Big\} \\ [M] &= [B] [\epsilon_0] + [D] [\kappa] - [M]^T - [M]^m \end{aligned} \quad (2.62)$$

where it will be shown in Equation (2.66) that factors of 2 are necessary in some terms, and where

$$D_{ij} = \frac{1}{3} \sum_{k=1}^N (\bar{Q}_{ij})_k [h_k^3 - h_{k-1}^3], \quad [i, j = 1, 2, 6] \quad (2.63)$$

$$M_{ij}^T = \sum_{k=1}^N \int_{h_{k-1}}^{h_k} (\bar{Q}_{ij})_k [\alpha_{ij}]_k (\Delta T) z dz \quad [i, j = 1, 2, 6] \quad (2.64)$$

$$M_{ij}^m = \sum_{k=1}^N \int_{h_{k-1}}^{h_k} (\bar{Q}_{ij})_k [\beta_{ij}]_k (\Delta m) z dz \quad [i, j = 1, 2, 6] \quad (2.65)$$

It is noted that in Equations (2.60), (2.61), (2.64) and (2.65) the Q_{ij} , α_{ij} and β_{ij} could have been placed outside of the integral sign since in a lamina, they are not functions of z .

Finally, the results of (2.57) and (2.62) can be written succinctly as follows to form perhaps the most important and most used equation in this text.

$$\begin{bmatrix} N_x \\ N_y \\ N_{xy} \\ \vdots \\ M_x \\ M_y \\ M_{xy} \end{bmatrix} = \begin{bmatrix} A_{11} & A_{12} & A_{16} & | & B_{11} & B_{12} & B_{16} \\ A_{12} & A_{22} & A_{26} & | & B_{12} & B_{22} & B_{26} \\ A_{16} & A_{26} & A_{66} & | & B_{16} & B_{26} & B_{66} \\ \vdots & \vdots & \vdots & & \vdots & \vdots & \vdots \\ B_{11} & B_{12} & B_{16} & | & D_{11} & D_{12} & D_{16} \\ B_{12} & B_{22} & B_{26} & | & D_{12} & D_{22} & D_{26} \\ B_{16} & B_{26} & B_{66} & | & D_{16} & D_{26} & D_{66} \end{bmatrix} \begin{bmatrix} \epsilon_{x0} \\ \epsilon_{y0} \\ 2\epsilon_{xy0} \\ \vdots \\ \kappa_x \\ \kappa_y \\ 2\kappa_{xy} \end{bmatrix} - \begin{bmatrix} N_x^T \\ N_y^T \\ N_{xy}^T \\ \vdots \\ M_x^T \\ M_y^T \\ M_{xy}^T \end{bmatrix} - \begin{bmatrix} N_x^m \\ N_y^m \\ N_{xy}^m \\ \vdots \\ M_x^m \\ M_y^m \\ M_{xy}^m \end{bmatrix} \quad (2.66)$$

The $[A]$ matrix represents the extensional stiffness matrix relating the in-plane stress resultants (N 's) to the mid-surface strains (ϵ_0 's) and the $[D]$ matrix is the flexural stiffness matrix relating the stress couples (M 's) to the curvatures (κ 's). Since the $[B]$ matrix relates the M 's to ϵ_0 's and N 's to κ 's, it is called the bending-stretching coupling matrix. It should be noted that a laminated structure can have bending-stretching coupling even if all laminae are isotropic. For example, a laminate composed of one lamina of steel and another of polyester will have bending-stretching coupling. In fact, only when the structure is exactly symmetric about its middle surface are all of the B_{ij} components equal to zero, and this requires symmetry in laminae properties, orientation, and distance from the middle surface.

It is seen that stretching-shearing coupling occurs when A_{16} and A_{26} are non-zero. Twisting-stretching coupling as well as bending-shearing coupling occurs when the B_{16} and B_{26} terms are non-zero, and bending-twisting coupling comes from non-zero values of the D_{16} and D_{26} terms. Usually the $(\)_{16}$ and $(\)_{26}$ terms are avoided by proper stacking sequences, but there could be some structural applications where these effects could be used to advantage, such as in aeroelastic tailoring.

Examples of these effects in several cross-ply laminates (i.e., combinations of 0° and 90° plies), angle ply laminates (combinations of $+\theta$ and $-\theta$ plies), and unidirectional laminates (all 0° plies) are involved in problems at the end of this chapter. It is seen in Equation (2.58) that $(h_k - h_{k-1})$ is always positive, and from Equation (2.63) $(h_k^3 - h_{k-1}^3)$ is

always positive, hence, in all symmetric cross-ply laminates, all $()_{16}$ and $()_{26}$ terms are zero.

The inclusion of transverse shear deformation effects on the structural behavior, results in an improved theory as follows. To determine the transverse shear resultants Q_x and Q_y , defined in Equation (2.54), it is assumed that the transverse shear stresses are distributed parabolically across the laminate thickness. In spite of the discontinuities at the interface between laminae, a continuous function $f(z)$ is used as a weighting function by some authors, which includes a factor of $5/4$ so that the shear factor calculated for a layered orthotropic shell wall is consistent with the established shear factor from the previous work of Reissner [38] and Mindlin [39] for the homogeneous case.

$$f(z) = \frac{5}{4} \left[1 - \left(\frac{z}{h/2} \right)^2 \right] \quad (2.67)$$

Then from Equations (2.40), (2.43), (2.50), (2.54), and (2.67)

$$\sigma_{xz_k} = 2\bar{Q}_{55_k} \epsilon_{xz} + 2\bar{Q}_{45_k} \epsilon_{yz} \quad \sigma_{yz_k} = 2\bar{Q}_{45_k} \epsilon_{xz} + 2\bar{Q}_{44_k} \epsilon_{yz} \quad (2.68)$$

where,

$$\bar{Q}_{44} = Q_{44}m^2 + Q_{55}n^2, \bar{Q}_{45} = (Q_{55} - Q_{44})mn, \bar{Q}_{55} = Q_{55}m^2 + Q_{44}n^2,$$

$$Q_{44} = G_{23}, \text{ and } Q_{55} = G_{13},$$

Hence, the transverse shear resultants Q_x and Q_y are as follows:

$$Q_x = 2(A_{55} \epsilon_{xz} + A_{45} \epsilon_{yz}) \quad (2.69)$$

$$Q_y = 2(A_{45} \epsilon_{xz} + A_{44} \epsilon_{yz}) \quad (2.70)$$

where,

$$A_{ij} = \frac{5}{4} \sum_{k=1}^N (\bar{Q}_{ij})_k \left[h_k - h_{k-1} - \frac{4}{3} (h_k^3 - h_{k-1}^3) \frac{1}{h^2} \right] \quad (ij = 4, 5 \text{ only}) \quad (2.71)$$

where h is the total thickness of the laminated plate. Some authors use other weighting functions. As an example if one considers the laminate to be only one lamina,

$-\frac{h}{2} \leq z \leq \frac{h}{2}$, then $A_{ss} = \left(\frac{5}{6}\right) Q_{ss} h$, illustrating clearly the weighting factor introduced by Reissner of $\frac{5}{6}$ [38].

At this point the stress-strain relations, or constitutive relations Equation (2.66) can be combined with the appropriate stress equations of equilibrium, and the strain-displacement relations to form an appropriate beam, plate or shell theory including thermal and hygrothermal effects as well as transverse shear deformation.

2.10 Piezoelectric Effects

A piezoelectric material is one of several intelligent or “smart” materials (others include shape memory alloys, electro-rheological fluids, etc.) used to develop adaptive structures. Piezoelectric materials are those which produce strains if an electrical potential is applied, or if strained it produces an electric potential. At present, piezoelectric materials are in the form of thin layers of polymer or ceramic, and can be integrated into or onto structures for both sensing deformations on one hand or controlling structural deformations and damping vibrations on the other hand. Most work in this area has been performed since 1985, but is developing rapidly. In 1990, Lee and Moon [40] treated the beams and plates with thin piezoelectric PVDF layers. The linear vibrations of piezoelectric laminates were also treated in [40]. Yu [41] has also presented the nonlinear equations for a sandwich plate with a thin piezoelectric face layer.

Basically the piezoelectric effect can be described by

$$\epsilon_{ij}^P = d_{kij} E_k', \quad (i, j, k, = 1, 2, 3) \quad (2.72)$$

where ϵ_{ij}^P is the usual strain tensor, caused by a piezoelectric effect, E_k' is the electrical field intensity vector, and d_{kij} is the piezoelectric tensor. It is of rank three, and hence has twenty-seven (3^3) components in three dimensional space. It is easily seen that it is symmetric with respect to i and j because the strain tensor ϵ_{ij} is symmetric. It is the only third order tensor having any application to structural mechanics.

It has been found, see Leibowitz and Vinson [42], Larson [43] and Newill [44], that the piezoelectric effect is analogous to thermal and hygrothermal effects. This means the total strain equals the sum of the isothermal strain plus any thermal strain plus any moisture (hygrothermal) strain plus the strains caused by the piezoelectric effect, and therefore a piezoelectric stress resultant and a piezoelectric stress couple can be defined exactly analogous to thermal and moisture stress resultants and couples. These are, using the quantities defined above,

$$N_{ij}^P = \sum_{k=1}^N (\bar{Q}_{ij})_k \int_{h_{k-1}}^{h_k} d_{kij} E_k' dz \quad (2.73)$$

$$\mathbf{M}_{ij}^P = \sum_{k=1}^N (\bar{\mathbf{Q}}_{ij})_k \int_{h_{k-1}}^{h_k} \mathbf{d}_{kij} \mathbf{E}_k' \zeta \, dz \quad (2.74)$$

and they can appear as another column matrix on the right hand side of Equation (2.66).

This analogy is extremely important because it enables the analyst and designer to utilize all available thermoelastic and hygrothermal solutions to solve composite structure (as well as other) problems that involve piezoelectric materials.

Other recent references for study are papers by Hilton and Yi, e.g. [45].

2.11 References

1. Sokolnikoff, I.S. (1956) *The Mathematical Theory of Elasticity*, McGraw-Hill Book Company, Inc., New York, Second Edition.
2. Vinson, J.R. and Chou, T.-W. (1975) *Composite Materials and Their Use in Structures*. Applied Science Publishers, London.
3. Vinson, J.R. (1993) *The Behavior of Shells Composed of Isotropic and Composite Materials*, Kluwer Academic Publisher, Dordrecht, The Netherlands.
4. Shames, I.H. (1975) *Introduction to Solid Mechanics*. New York: Prentice-Hall, Inc.
5. Carlsson, L.A. and Pipes, R.B. (1996) *Experimental Characterization of Advanced Composite Materials*, Prentice-Hall Publishing Co., Inc., Englewood Cliffs, N.J., Second Edition.
6. Halpin, J.C. and Tsai, S.W. (1967) Environmental Factors in Composite Materials Design, *Air Force Materials Laboratory Technical Report*, pp. 67-423.
7. Hashin, Z. (1972) Theory of Fiber Reinforced Materials, *National Aeronautics and Space Administration Contractors Report 1974*.
8. Christensen, R.M. (1979) *Mechanics of Composite Materials*. New York: John Wiley and Sons, Inc.
9. Hahn, H.T. (1980) Simplified Formulas for Elastic Moduli of Unidirectional Continuous Fiber Composites, *Composites Technology Review*, Fall.
10. Chou, T.-W. (1992) *Microstructural Design of Fiber Composites*, Cambridge University Press.
11. Tauchert, T.R. (1991) Thermally Induced Flexure, Buckling and Vibration of Composite Laminated Plates, *Applied Mechanics Reviews*, Vol. 44, No. 8, pp. 347-360.
12. Argyris, J. and Tenek, L. (1997) Recent Advances in Computational Thermostructural Analysis of Composite Plate and Shells with Strong Nonlinearities, *Applied Mechanics Reviews*, Vol. 50, No. 5, pp. 285-305.
13. Turvey, O.J. and Marshall, I.H. (1995) *Buckling and Local Buckling of Composite Plates*, Chapman and Hall, London.
14. Noor, A.K. and Burton, W.S. (1992) Computational Models for High Temperature Multilayered Composite Plates and Shells, *Applied Mechanics Reviews*, Vol. 45, No. 10, pp. 414-446.
15. Huang, N.N. and Tauchert, T.R. (1988) Large Deformation of Antisymmetric Angle Ply Laminates Resulting from Non-uniform Temperature Loadings, *Journal of Thermal Stresses*, Vol. 11, pp. 287-297.

16. Vinson, J.R., Walker, W.J., Pipes, R.B. and Ulrich, O.R. (1977) The Effects of Relative Humidity and Elevated Temperatures on Composite Structures, *Air Force Office of Scientific Research Technical Report 77-0030*, February.
17. Pipes, R.B., Vinson, J.R. and Chou, T.W. (1976) On the Hygrothermal Response of Laminated Composite Systems, *Journal of Composite Materials*, April, pp. 130-148.
18. ASTM Standard D5229-92 Test Method for Moisture Absorption Properties and Equilibrium Conditioning of Polymer Matrix Composite Materials.
19. Woldesenbet, E. (1995) High Strain Rate Properties of Composites, *Ph.D. Dissertation*, Department of Mechanical Engineering, University of Delaware, January.
20. Shen, C. and Springer, G.S. (1981) Environmental Effect on the Elastic Moduli of Composite Material, Ed. G.S. Springer, Technomic Publishing Co., Inc.
21. Christensen, R.M. (1981) Theory of Viscoelasticity. An Introduction, Academic Press, New York, 2nd Edition.
22. Jurf, R.A. and Vinson, J.R. (1985) Effect of Moisture on the Static and Viscoelastic Shear Properties of Epoxy Adhesives, *Journal of Materials Science*, Vol. 20, pp. 2979-2989.
23. Wilson, D.W. and Vinson, J.R. (1982) Viscoelastic Effects on Buckling of Laminated Plates Subjected to Hygrothermal Conditions, *ASME Publications AD-03*, "Advances in Aerospace Structures and Materials".
24. Wilson, D.W. and Vinson, J.R. (1985). Viscoelastic Effects on the Buckling Response of Laminated Columns, *ASTM Special Publication*, 864, "Recent Advances in Composites in the United States and Japan.
25. Lindholm, V.S. (1964) Some Experiments With the Split Hopkinson Pressure Bar, *Journal of Mechanics and Physics of Solids*, Vol. 12, pp. 317-335.
26. Daniel, I.M., La Bedz, R.H. and Liber, T. (1981) New Method for Testing Composites at Very High Strain Rates, *Experimental Mechanics*, February.
27. Nicholas, T. (1981) Tensile Testing of Materials at High Rates of Strain, *Experimental Mechanics*, pp. 177-185, May.
28. Zukas, J.A. (1982) *Impact Dynamics*, John Wiley and Sons, New York, N.Y.
29. Sierakowski, R.L. and Chaturvedi, S.K. (1997) *Dynamic Loading and Characterization of Fiber-Reinforced Composites*, Wiley Interscience.
30. Sierakowski, R.L. (1997) Strain Rate Effects in Composites, *Applied Mechanics Reviews*, Vol. 50, No. 12, pp. 741-761, December.
31. Rajapakse, Y. and Vinson, J.R. (1995) High Strain Rate Effects on Polymer, Metal and Ceramic Matrix Composites and Other Advanced Materials, *ASME Bound Volume AD-Vol. 48*.
32. Abrate, S. (1991) Impact on Laminated Composite Materials, *Applied Mechanics Reviews*, Vol. 44, No. 4, pp. 155-190, April.
33. Abrate, S. (1994) Impact on Laminated Composites: Recent Advances, *Applied Mechanics Reviews*, Vol. 47, No. 11, pp. 517-544, November.
34. Vinson, J.R. (1974) *Structural Mechanics: The Behavior of Plates and Shells*. New York: Wiley-Interscience, John Wiley and Sons, Inc.
35. Vinson, J.R. (1989) *The Behavior of Thin Walled Structures: Beams, Plates and Shells*, Kluwer Academic Publishers, Dordrecht.

36. Sloan, J.G. (1979) The Behavior of Rectangular Composite Material Plates Under Lateral and Hygrothermal Loads, *MMAE Thesis*, University of Delaware (also AFOSR-TR-78-1477, July 1978).
37. Tsai, S.W. and Pagano, N.J. (1968) Invariant Properties of Composite Materials, Tsai, S.W. et al., eds., *Composite Materials Workshop*, Technomic Publishing Co., Inc., Lancaster, PA, pp. 233-253.
38. Reissner, E. (1950) On a Variational Theorem in Elasticity, *J. Math. Phys.*, 29, pp. 90.
39. Mindlin, R.D. (1951) Influence of Rotatory Inertia and Shear on Flexural Motions of Isotropic Elastic Plates, *Journal of Applied Mechanics*, pg. 73.
40. Lee, C.K. and Moon, F.C. (1990) Modal Sensors/Actuators, *Journal of Applied Mechanics*, Vol. 57, pp. 434-441.
41. Yu., Y.Y. (1977) Dynamics for Large Deflection of a Sandwich Plate With Thin Piezoelectric Face Layers, Ed. G.S. Simites, *Analysis and Design Issues for Modern Aerospace Vehicles*, ASME AD-Vol. 55, pp. 285-292.
42. Leibowitz, M. and Vinson, J.R. (1991) Intelligent Composites: Design and Analysis of Composite Material Structures Involving Piezoelectric Material Layers. Part A-Basic Formulation, *Center for Composite Materials Technical Report 91-54*, University of Delaware, November.
43. Larson, P.H. (1993) The Use of Piezoelectric Materials in Creating Adaptive Shell Structures, *Ph.D. Dissertation*, Mechanical Engineering, University of Delaware.
44. Newill, J.F. (1996) Composite Sandwich Structures Incorporating Piezoelectric Materials, *Ph.D. Dissertation*, Mechanical Engineering, University of Delaware.
45. Hilton, H.H., Yi, S. and Vinson, J.R. (1998) Probabilistic Structural Integrity of Piezoelectric Viscoelastic Composite Structures, *Proceedings of the 39th AIAA/ASME/ASCE/AHS/ASC SDM Conference*, April.

2.12 Problems

1. Consider a laminate composed of boron-epoxy with the following properties:

$Q_{11} = 2.43 \times 10^5 \text{ MPA}$ $(35.32 \times 10^6 \text{ psi})$	$Q_{12} = 2.43 \times 10^4 \text{ MPA}$ $(1.06 \times 10^6 \text{ psi})$
$Q_{22} = 2.43 \times 10^4 \text{ MPA}$ $(3.532 \times 10^6 \text{ psi})$	$Q_{66} = 1.034 \times 10^3 \text{ MPA}$ $(1.5 \times 10^6 \text{ psi})$

If the laminate is a cross-ply with $[0^\circ/90^\circ/90^\circ/0^\circ]$, with each ply being 0.25 mm (0.11") thick, and if the laminate is loaded in tension in the x direction (i.e., the 0° direction):

- (a) What percentage of the load is carried by the 0° plies? The 90° plies?
- (b) If the strength of the 0° plies is $1.364 \times 10^3 \text{ MPA}$ (198,000 psi), and the strength of the 90° plies is 44.8 MPA (6,500psi) which plies will fail first?
- (c) What is the maximum load, N_{\max} , that the laminate can carry at incipient failure? What stress exists in the remaining two plies, at the failure load of the other two others?

- (d) If the structure can tolerate failure of two plies, what is the maximum load, N_{\max} that the other two plies can withstand to failure?
2. A laminate is composed of graphite epoxy (GY70/339) with the following properties: $E_{11} = 2.89 \times 10^5$ MPA (42×10^6 psi), $E_{22} = 6.063 \times 10^3$ MPA (0.88×10^6 psi), $G_{12} = 4.134 \times 10^3$ MPA (0.6×10^6 psi) and $\nu_{12} = 0.31$. Determine the elements of the A, B and D matrices for a two-ply laminate $[+45^\circ/-45^\circ]$, where each ply is 0.15 mm (0.006") thick.
3. Consider a square panel composed of one ply with the fibers in the directions as shown in Figure 2.12. Which of the orientations above would be the stiffest for the loads given in Figure 2.13?
4. For a panel consisting of boron-epoxy with the properties of Problem 1 above, and a stacking sequence of $[0^\circ/+45^\circ/-45^\circ/0^\circ]$, and a ply thickness of 0.14 mm (0.005"), determine the elements of the elements of the A, B and D matrices.
5. The properties of graphite fibers and a polyimide matrix are as follows:

$$E = 2.756 \times 10^5 \text{ MPA}$$

$$(40 \times 10^6 \text{ psi})$$

$$\nu = 0.2$$

$$E = 2.756 \times 10^3 \text{ MPA}$$

$$(0.4 \times 10^6 \text{ psi})$$

$$\nu = 0.33$$

- (a) Find the modulus of elasticity in the fiber direction, E_{11} , of a laminate of graphite-polyimide composite with 60% fiber volume ratio.
- (b) Find the Poisson's ratio, ν_{12} ?
- (c) Find the modulus of elasticity normal to the fiber direction, E_{22} .
- (d) What is the Poisson's ratio, ν_{21} ?
6. Consider a laminate composed of GY70/339 graphite epoxy whose properties are given above in Problem 2. For a lamina thickness of 0.127 mm (0.005"), calculate the elements of the A, B and D matrices for the following:
- (a) $[0^\circ, 0^\circ, 0^\circ, 0^\circ]$ (unidirectional);
- (b) $[0^\circ, 90^\circ, 90^\circ, 0^\circ]$ (across-ply);
- (c) $[\pm 45^\circ]$, i.e. $[+45^\circ/-45^\circ/-45^\circ/+45^\circ]$ (an angle-ply);
- (d) $[0^\circ/+45^\circ/-45^\circ/90^\circ]$, (a quasi-isotropic, 8 plies);
- (e) Compare the various stiffness quantities for the four laminates above.

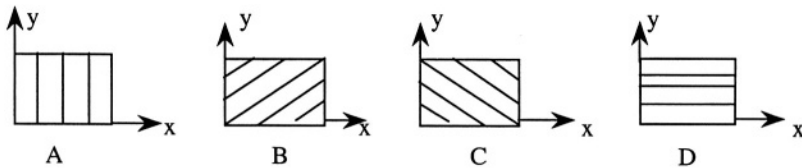


Figure 2.12.

7. Consider a laminate composed of GY70/339 graphite epoxy whose properties are given above in Problem 2. For a lamina thickness of 0.127 mm (0.005") cited in Problem 6, calculate the elements of the [A], [B] and [D] matrices for the following laminates:
- (a) $[\pm(45)2]_s$, $[+45^\circ/-45^\circ/+45^\circ/-45^\circ]$,
- (b) $[\pm 45]_s$, $[+45^\circ/-45^\circ/-45^\circ/+45^\circ]$
- (c) $[\pm 45]_Q$, $[+45^\circ/-45^\circ/+45^\circ/-45^\circ]$

(d) $[\pm(45)_2]_{0s}$, $[+45/-45/+45/-45]_{0s}$

Compare the forms of the A, B and D matrices between laminate type.

8. What type of coupling would you expect in the (B) matrix for (a) and (b) below:
 - (a) $0^\circ/90^\circ$ laminate
 - (b) $+\theta/-\theta$ laminate
9. Given a composite laminate composed of continuous fiber laminate laminae of High Strength Graphite/Epoxy with properties of Table 2.2, if the laminate architecture is $[0^\circ, 90^\circ, 90^\circ, 0^\circ]$, determine A_{11} if $\nu_{12} = 0.3$, and each ply thickness is 0.006".
10. Consider a plate composed of a 0.01" thick steel plate joined perfectly to an aluminum plate, 0.01" thick. Using the properties of Table 2.2 calculate B_{11} , if the Poisson's Ratio of each material is $\nu = 0.3$.
11. Consider a unidirectional composite composed of a polyimide matrix and graphite fibers with properties given in Problem 5 above. In the fiber direction, what volume fraction is required to have a composite stiffness of $E_{11} = 10 \times 10^6$ psi to match an aluminum stiffness.
12. A laminate is composed of ultra high modulus graphite epoxy with properties given in Table 2.2 below. Determine the elements of the [A], [B] and [D] matrices for a two ply laminate $[+45^\circ/-45^\circ]$, where each ply is 0.006" thick. For the material $\nu_{12} = 0.31$.
13. A laminate is composed of boron-epoxy with the properties of Problem 2.1 and a stacking sequence of $[0/+45^\circ/-45^\circ/0^\circ]$, and a ply thickness of 0.006". Determine the elements of the A, B and D matrices.

TABLE 2.2. Unidirectional properties

Material	Elastic moduli			Ultimate strength			Density
	Axial E_{11}	Transverse E_{22}	Shear G_{12}	Axial tens. σ_{11}	Trans. tens. σ_{22}	Shear tens. τ_{12}	
High strength GR/epoxy	20 (138)	1.0 (6.9)	0.65 (4.5)	220 (1517)	6 (41)	14 (97)	0.057 (1.57)
High Modulus GR/epoxy	32 (221)	1.0 (6.9)	0.7 (4.8)	175 (1206)	5 (34)	10 (69)	0.058 (1.60)
Ultra high modulus GR/epoxy	44 (303)	1.0 (6.9)	0.95 (6.6)	110 (758)	4 (28)	7 (48)	0.061 (1.68)
Kevlar49/ epoxy	12.5 (86)	0.8 (5.5)	0.3 (2.1)	220 (1517)	4 (28)	6 (41)	0.050 (1.38)
S glass epoxy	8 (55)	1.0 (6.9)	0.5 (3.4)	260 (1793)	6 (41)	10 (69)	0.073 (2.00)
Steel	30 (207)	30 (207)	11.5 (79)	60 (414)	60 (414)	35 (241)	0.284 (7.83)
Aluminum 6061-T6	10.5 (72)	10.5 (72)	3.8 (26)	42 (290)	42 (290)	28 (193)	0.098 (2.70)

Moduli in Msi (GPa); Stress in Ksi (MPa); Density in lb/in³(g/cm³)

14. Consider a composite laminae made up of continuous Boron fibers imbedded in an epoxy matrix. The volume fraction of the Boron fibers in the composite is 40%. Assuming that the modulus of elasticity of the Boron fiber is 5×10^7 psi and the epoxy is 5×10^5 psi, find:
- The Young's moduli of the composite in the 1 and 2 direction.
 - Consider an identical second lamina to be glued to the first so that the fibers of the second lamina are parallel to the 2 direction. Assuming the thickness of each lamina to be 0.1" and neglecting Poisson's Ratio, what are the new moduli in the 1 and 2 directions.
15. The properties of graphite fibers and a polyimide matrix are as follows:
- | GRAPHITE | POLYIMIDE |
|--------------------------|---------------------------|
| $E = 40 \times 10^6$ psi | $E = 0.4 \times 10^6$ psi |
| $\nu = 0.2$ | $\nu = 0.33$ |
- Find the modulus of elasticity in the fiber direction, E_{11} , of a lamina of graphite – polyimide composite with 70% fiber volume ratio.
 - Find the Poisson's Ratio, ν_{12} .
 - Find the modulus of elasticity normal to the fiber direction, E_{22} .
 - What is the Poisson's Ratio, ν_{22} .
 - Compare these properties with those obtained for the same material system but with $\nu_F = 60\%$ in problem 2.5.
16. In a given composite, the coefficient of thermal expansion for the epoxy and the graphite fibers are $+30 \times 10^{-6}$ in/in/°F and -15×10^{-6} in/in/°F respectively. For space application where no thermal distortion can be tolerated what volume fractions of each component are required to make zero expansion and contraction in the fiber direction for an all 0° construction? (Hint: Use the Rule of Mixtures).
17. Find the A, B and D matrices for the following composite: 50% volume Fraction Boron- Epoxy Composite
- $$E_{11} = 30.0 \times 10^6$$
- $$E_{22} = 3.0 \times 10^6$$
- $$G_{12} = 1.0 \times 10^6$$
- $$\nu_{12} = 0.22$$

Stacking Sequence (each lamina is 0.0125" thick)

$\theta=45^\circ$
$\theta=0^\circ$
$\theta=90^\circ$
$\theta=-45^\circ$
$\theta=-45^\circ$
$\theta=90^\circ$
$\theta=0^\circ$
$\theta=45^\circ$

18. Three composite plates are under uniform transverse loading. All the conditions, such as materials, boundary conditions and geometry, etc. are the same except the

stacking sequence as shown below. Without using any calculation, indicate which plate will have maximum deflection and will have minimum deflection.

19. Consider a Kevlar 49/epoxy composite, whose properties are given on p303 in the text. A plate whose stacking sequence is [0,90,90,0] (i.e. a cross ply laminate) is fabricated wherein each thickness is 0.0055 inches
 - (a) Determine the A, B, and D matrix component.
 - (b) What if any are the couplings in this cross-ply construction that are decided below Equation (2.62)?
 - (c) If only in-plane loads are applied, is the plate stiffer in the x direction or y direction, or are they the same?
 - (d) If only plate bending is considered, is the plate stiffer in the x direction, the y direction, or are they equally stiff?
20. Given the following fiber and matrix properties for HM-S/epoxy composite components:

Epoxy
 $E_m=0.5\text{Msi}=3.45\text{Gpa}$
 $G_m=0.185\text{Msi}=1.27\text{Gpa}$
 $\rho_m=0.0440\text{ lb/in}^3=1.218\text{ gr./cm}^3$

HM-S/Graphite
 $E_{f11}=55.0\text{Msi}=379.3\text{Gpa}$
 $E_{f22}=0.9\text{Msi}=6.2\text{Gpa}$
 $\nu_{f22}=0.20$
 $\rho_{f12}=0.0703\text{ lb/in}^3=1.946\text{ gr./cm}^3$

Determine each of the following properties for a unidirectional composite:

E_{11} , E_{12} , E_{33} , G_{12} , G_{13} , ν_{12} , ν_{21} , ν_{13} , ν_{31} , ν_{23} and ν_{32} for the fiber volume fractions of $V_f=0\%$, 30%, 60%. Which properties increase linearly with volume fraction? Which do not increase linearly with volume fraction?

21. Given a cross-ply construction of four lamina of the same composite material system oriented as 0° , 90° , 90° , 0° , each lamina being equally thick, which elements of the [A], [B] and [D] matrices of Equation (2.66) will be equal to zero.
22. Given an angle-ply construction of five plies of the same composite material oriented as $+0^\circ/-0^\circ/+0^\circ/-0^\circ/+0^\circ$, each of equal thickness, which elements of the [A], [B] and [D] matrices of Equation (2.66) will be equal to zero.
23. Determine the elements of the C_{ij} matrix analogous to the a_{ij} of Equation (2.10) through (2.12) for orthotropic materials. (Hint: start with Equation (2.17) and solve for the σ_{ij}).

$$C_{ij} = \begin{bmatrix} C_{11} & C_{12} & C_{13} & 0 & 0 & 0 \\ C_{21} & C_{22} & C_{23} & 0 & 0 & 0 \\ C_{31} & C_{32} & C_{33} & 0 & 0 & 0 \\ 0 & 0 & 0 & C_{44} & 0 & 0 \\ 0 & 0 & 0 & 0 & C_{55} & 0 \\ 0 & 0 & 0 & 0 & 0 & C_{56} \end{bmatrix}$$

24. A laminate is composed of graphite epoxy (GY70/339) with the following properties:

$E_{11}=2.89 \times 10^5\text{MPa}(42 \times 10^6\text{psi})$
 $E_{22}=60.63 \times 10^3\text{MPa}(0.88 \times 10^6\text{psi})$

$$G_{12}=4.134 \times 10^3 \text{MPa}(0.60 \times 10^6 \text{psi})$$

$$\nu_{12}=0.31$$

- (a) Determine the elements of the [A], [B], and [D] matrices for a two-ply laminate [+45/-45], where each ply is 0.15mm. (0.006 inches) thick.
- (b) What couplings exist as discussed below Equation (2.66) for this laminate?
25. For a panel consisting of Boron-Epoxy with the properties

$$Q_{11}=35.32 \times 10^6 \text{psi}$$

$$Q_{22}=3.532 \times 10^6 \text{psi}$$

$$Q_{12}=1.06 \times 10^6 \text{psi}$$

$$Q_{66}=1.50 \times 10^6 \text{psi}$$

and a stacking sequence of $[0^\circ, +45^\circ, -45^\circ, 0^\circ]$, and a ply thickness of 0.006 inches, determine the elements of the A, B and D matrices. What would the elements be if the ply thickness were 0.0055 inches?

26. Determine how the A, B, D matrices are populated for the following two stacking sequences $[0^\circ, \pm 45^\circ, 90^\circ]_{QS}$ and $[0^\circ, \pm 45^\circ, 90^\circ]_S$. The subscript QS mean symmetric Q times where Q=2, 3,...

The composite material is orthotropic and has the properties E_{11} , E_{22} , G_{12} , ν_{12} , with each lamina having thickness h_k . In the [A], [B], and [D] matrices, place an x or an O for each element, where an x shows that the component is non zero, and O shows that the component is zero.

27. What type of couplings, as discussed below Equation (2.66) would you expect in the B matrix for (a) and (b) below: (that is, identify the non-zero terms)
- (a) $0^\circ/90^\circ$ laminate
- (b) $+0^\circ/-0^\circ$ laminate
28. Find the [A], [B] and [D] for the following laminates.

0°	0°	0°	90°	$0.1''$
90°	1°	90°	0°	$0.1''$
90°	90°	0°	0°	$0.1''$
0°	90°	90°	90°	$0.1''$

Given: $E_{11}=30 \times 10^6 \text{psi}$, $E_{22}=3 \times 10^6 \text{psi}$, $G_{12}=1 \times 10^6 \text{psi}$, $\nu_{12}=0.3$.

29. In problem 2.28 which laminate is stiffest and which is the least stiff for
- (a) In-plane loads in the 0° direction.
- (b) In-plane loads in the 90° direction.
- (c) Bending in the 0° direction.
- (d) Bending in the 90° direction.
30. Consider a laminate composed of GY 70/339 graphite/epoxy with the following properties,

$$E_{11}=2.89 \times 10^5 \text{MPa} (42 \times 10^6 \text{psi})$$

$$E_{22}=6.063 \times 10^3 \text{MPa}(0.88 \times 10^6 \text{psi})$$

$$G_{12}=40134 \times 10^3 \text{MPa}(0.60 \times 10^6 \text{psi})$$

$$\nu_{12}=0.31$$

Using the laminate thickness as 0.127mm (0.005 inches) calculate the elements of the [A], [B], and [D] matrices for the following laminates.

- (a) $[\pm (45)_2]_s$, $[+45/-45/+45/-45]_s$
- (b) $[\pm 45]_s$, $[+45/-45/+45/-45]_s$
- (b) $[\pm 45]_{Qs}$, $[+45/-45/+45/-45]_{Qs}$
- (c) $[\pm (45)_2]_{Qs}$, $[+45/-45/+45/-45]_{Qs}$

Compare the forms of the [A], [B] and [D] matrices between laminate types.

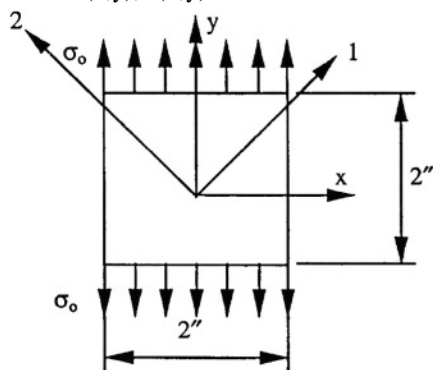
31. A composite material has stiffness matrix as follows,

$$[C] = \begin{bmatrix} 100 & -10 & 0 & 0 & 0 & 10 \\ -10 & 50 & 0 & 0 & 0 & 10 \\ 0 & 0 & 50 & 0 & 0 & 0 \\ 0 & 0 & 0 & 20 & 0 & 0 \\ 0 & 0 & 0 & 0 & 20 & 0 \\ 0 & 0 & 0 & 0 & 0 & 20 \end{bmatrix} \times 10^5 \text{ psi}$$

Determine the state of stress if the strains are given by,

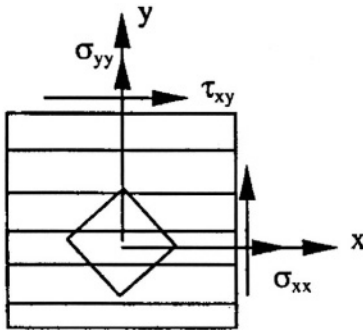
$$\epsilon_x = 100 \mu\text{in/in}, \epsilon_y = 50 \mu\text{in/in}, \gamma = -100 \mu\text{in/in}.$$

32. Consider the stress acting on an element of a composite material to be as shown below. The material axes 1,2 are angle θ with respect to the geometry loading axes for the element. Taking the material properties as noted below, find the m-plane displacements $u(x,y)$, $v(x,y)$.



$$\begin{aligned} \sigma_{yy} &= \sigma_o = 25 \text{ Ksi} \\ \theta &= 45^\circ \\ E_{11} &= 25 \times 10^6 \text{ psi} \\ E_{22} &= 1 \times 10^6 \text{ psi} \\ G_{12} &= 0.5 \times 10^6 \text{ psi} \\ \nu_{12} &= 0.25 \end{aligned}$$

33. A 50% boron-epoxy orthotropic material is subjected to combined stress as shown below.



$$\sigma_{xx} = 10,000 \text{ psi}$$

$$\sigma_{yy} = 10,000 \text{ psi}$$

$$\tau_{xy} = 10,000 \text{ psi}$$

- Find the stress on the material element for a 45° rotation about the z-axis in a positive sense.
- (a) If the strain components in the non-rotated system are given by:
 $\epsilon_x = 260 \mu\text{in/in}$, $\epsilon_y = 3110 \mu\text{in/in}$, $\gamma = -9090 \mu\text{in/in}$
 Find the corresponding strains in the rotated system.
- (b) Comment on the corresponding stresses and strains in the rotated system.

CHAPTER 3

PLATES AND PANELS OF COMPOSITE MATERIALS

3.1 Introduction

In Chapter 2, the constitutive equations were developed in detail, describing the relationships between integrated stress resultants (N_x, N_y, N_{xy}) , integrated stress couples (M_x, M_y, M_{xy}) , in-plane mid-surface strains $(\epsilon_x^0, \epsilon_y^0, \epsilon_{xy}^0)$, and the curvatures $(\kappa_x, \kappa_y, \kappa_{xy})$, as seen in Equation (2.66). These will be utilized with the strain-displacement relations of Equations (2.48) and (2.50) and the equilibrium equations to be developed in Section 3.2 to develop structural theories for thin walled bodies, the configuration in which composite materials are most generally employed. Plates and panels are discussed in this chapter. Beams, rods and columns are discussed in Chapter 4. Shells will be the subject of Chapter 5. The use of energy methods for solving structures problems is discussed in Chapter 6. However to study any of the structural equations it is necessary to first develop suitable equilibrium equations.

3.2 Plate Equilibrium Equations

The integrated stress resultants (N), shear resultants (Q) and stress couples (M), with appropriate subscripts, are defined by Equation (2.54), and their positive directions are shown in Figure 2.13, for a rectangular plate, defined as a body of length a in the x -direction, width b in the y -direction, and thickness h in the z -direction, where $h \ll b$, $h \ll a$, i.e. a thin plate.

In mathematically modeling solid materials, including the laminates of Chapter 2, a continuum theory is generally employed. In doing so, a representative material point within the elastic solid or lamina is selected as being macroscopically typical of all material points in the body or lamina. The material point is assumed to be infinitely smaller than any dimension of the structure containing it, but infinitely larger than the size of the molecular lattice spacing of the structured material comprising it. Moreover, the material point is given a convenient shape; and in a Cartesian reference frame that convenient shape is a small cube of dimensions dx , dy , and dz as shown in Figure 3.1 below.

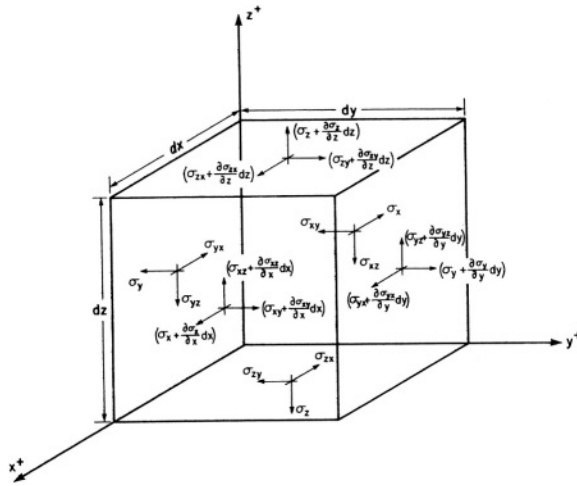


Figure 3.1. Coordinate systems, geometry, and nomenclature.

This cubic material point of dimension dx , dy and dz is termed a control element. The positive values of all stresses acting on each surface of the control element are shown in Figure 3.1, along with how they vary from one surface to another, using the positive sign convention consistent with most scientific literature, and consistent with Figure 2.1. Details of the nomenclature can be found in any text on solid mechanics, including Vinson [1,2]. In addition to the surface stresses acting on the control element shown in Figure 3.1, body force components F_x , F_y and F_z can also act on the body. These body force components such as gravitational, magnetic or centrifugal forces are proportional to the control element volume, i.e., its mass.

A force balance can now be made in the x , y and z directions resulting in three equations of equilibrium. For instance, a force balance in the x -direction would yield

$$\left(\sigma_x + \frac{\partial \sigma_x}{\partial x} dx \right) dydz + \left(\sigma_{yx} + \frac{\partial \sigma_{yx}}{\partial y} dy \right) dx dz + \left(\sigma_{zx} + \frac{\partial \sigma_{zx}}{\partial z} dz \right) dx dy - \sigma_x dydz - \sigma_{yx} dx dz - \sigma_{zx} dy dx + F_x dx dy dz = 0$$

Canceling terms and dividing the remaining terms by the volume results in the following

$$\frac{\partial \sigma_x}{\partial x} + \frac{\partial \sigma_{yx}}{\partial y} + \frac{\partial \sigma_{zx}}{\partial z} + F_x = 0 \quad (3.1)$$

Similarly, equilibrium in the y and z directions yields:

$$\frac{\partial \sigma_{xy}}{\partial x} + \frac{\partial \sigma_y}{\partial y} + \frac{\partial \sigma_{zy}}{\partial z} + F_y = 0 \quad (3.2)$$

$$\frac{\partial \sigma_{xz}}{\partial x} + \frac{\partial \sigma_{yz}}{\partial y} + \frac{\partial \sigma_z}{\partial z} + F_z = 0 \quad (3.3)$$

Using Einsteinian notation, these three equations can be consolidated to the following:

$$\sigma_{ji,j} + F_i = 0 \quad i, j = x, y, z$$

These three equations comprise the equilibrium equations for a three dimensional elastic body. However, for beam, plate and shell theory, whether involving composite materials or not, one must integrate the stresses across the thickness of the thin walled structures to obtain solutions.

Recalling the definitions of Chapter 2, the stress resultants and stress couples defined previously are:

$$\begin{bmatrix} N_x \\ N_y \\ N_{xy} \\ Q_x \\ Q_y \end{bmatrix} = \int_{-h/2}^{+h/2} \begin{bmatrix} \sigma_x \\ \sigma_y \\ \sigma_{xy} \\ \sigma_{xz} \\ \sigma_{yz} \end{bmatrix} dz = \sum_{k=1}^N \int_{h_{k-1}}^{h_k} \begin{bmatrix} \sigma_x \\ \sigma_y \\ \sigma_{xy} \\ \sigma_{xz} \\ \sigma_{yz} \end{bmatrix}_k dz_k \quad (3.4)$$

$$\begin{bmatrix} M_x \\ M_y \\ M_{xy} \end{bmatrix} = \int_{-h/2}^{h/2} \begin{bmatrix} \sigma_x \\ \sigma_y \\ \sigma_{xy} \end{bmatrix} z dz = \sum_{k=1}^N \int_{h_{k-1}}^{h_k} \begin{bmatrix} \sigma_x \\ \sigma_y \\ \sigma_{xy} \end{bmatrix}_k z_k dz_k \quad (3.5)$$

The first form of each is applicable to a single layer plate, while the second form is necessary for a laminated plate due to the stress discontinuities associated with different materials and/or differing orientations in the various plies.

Turning now to (3.1), neglecting the body force term, F_x , for simplicity of this example, integrating term by term across each ply, and summing across the plate provides

$$\sum_{k=1}^N \int_{h_{k-1}}^{h_k} \frac{\partial \sigma_{xk}}{\partial x} dz + \sum_{k=1}^N \int_{h_{k-1}}^{h_k} \frac{\partial \sigma_{yxk}}{\partial y} dz + \sum_{k=1}^N \int_{h_{k-1}}^{h_k} \frac{\partial \sigma_{zxk}}{\partial z} dz = 0 \quad (3.6)$$

In the first two terms integration and differentiation can be interchanged, hence:

$$\frac{\partial}{\partial x} \left[\sum_{k=1}^N \int_{h_{k-1}}^{h_k} \sigma_{x_k} dz \right] + \frac{\partial}{\partial y} \left[\sum_{k=1}^N \int_{h_{k-1}}^{h_k} \sigma_{yx_k} dz \right] + \sum_{k=1}^N \sigma_{zx} \Big|_{h_{k-1}}^{h_k} = 0 \quad (3.7)$$

In the first two terms N_x and N_{yx} appear explicitly as the bracketed quantities. In the third term it is clear that between all plies of a laminated composite plate and between the face and core materials of a sandwich panel the interlaminar shear stresses will cancel each other, and one can define the applied surface shear stresses on the top ($z = h_N$) and bottom ($z = h_0$) surfaces as shown below (see Figure 2.1)

$$\sigma_{zx}(h_N) \equiv \tau_{1x} \quad \text{and} \quad \sigma_{zx}(h_0) \equiv \tau_{2x} \quad (3.8)$$

Equation (3.7) can then be written as:

$$\frac{\partial N_x}{\partial x} + \frac{\partial N_{yx}}{\partial y} + \tau_{1x} - \tau_{2x} = 0 \quad (3.9)$$

Similarly, integrating the equilibrium equation in the y-direction provides

$$\frac{\partial N_{xy}}{\partial x} + \frac{\partial N_y}{\partial y} + \tau_{1y} - \tau_{2y} = 0 \quad (3.10)$$

where

$$\sigma_{zy}(h_N) \equiv \tau_{1y} \quad \text{and} \quad \sigma_{zy}(h_0) \equiv \tau_{2y} \quad (3.11)$$

Likewise equilibrium in the z-direction upon integration and summing provides

$$\frac{\partial Q_x}{\partial x} + \frac{\partial Q_y}{\partial y} + p_1 - p_2 = 0 \quad (3.12)$$

where

$$\sigma_z(h_N) \equiv p_1 \quad \text{and} \quad \sigma_z(h_0) \equiv p_2 \quad (3.13)$$

In addition to the integrated force equilibrium equations above, two equations of moment equilibrium are also needed, one for the x-direction and one for the y-direction. Multiplying equation 3.1 through by zdz , integrating across each ply and summing across all laminae results in the following

$$\sum_{k=1}^N \int_{h_{k-1}}^{h_k} \frac{\partial \sigma_{x_k}}{\partial x} z dz + \sum_{k=1}^N \int_{h_{k-1}}^{h_k} \frac{\partial \sigma_{yx_k}}{\partial y} z dz + \sum_{k=1}^N \int_{h_{k-1}}^{h_k} \frac{\partial \sigma_{zx_k}}{\partial z} z dz = 0$$

Again, in the first two terms integration and summation can be interchanged with differentiation with the result that the first two terms become $(\partial M_x / \partial x) + (\partial M_{xy} / \partial y)$. However, the third term must be integrated by parts as follows:

$$\sum_{k=1}^N \int_{h_{k-1}}^{h_k} \frac{\partial \sigma_{zx_k}}{\partial z} z dz = \sum_{k=1}^N \left\{ z \sigma_{zx} \right\}_{h_{k-1}}^{h_k} - \int_{h_{k-1}}^{h_k} \sigma_{zx} dz$$

Here the last term is clearly $-Q_x$. Again in the first term on the right, clearly the moments of all the interlaminar stresses between plies cancel each other out, and the only non-zero terms are the moments of the applied surface shear stresses hence that term becomes

$$h_N \tau_{1x} - h_0 \tau_{2x} = \frac{h}{2} [\tau_{1x} + \tau_{2x}]$$

Using the former expression, the equation of equilibrium of moments in the x -direction is

$$\frac{\partial M_x}{\partial x} + \frac{\partial M_{xy}}{\partial y} - Q_x + \frac{h}{2} [\tau_{1x} + \tau_{2x}] = 0 \quad (3.14)$$

Similarly in the y -direction the moment equilibrium equation is

$$\frac{\partial M_{xy}}{\partial x} + \frac{\partial M_y}{\partial y} - Q_y + \frac{h}{2} [\tau_{1y} + \tau_{2y}] = 0 \quad (3.15)$$

where all the terms are defined above. Thus, there are five equilibrium equations for a rectangular plate, regardless of what material or materials are utilized in the plate: (3.9), (3.10), (3.12), (3.14) and (3.15).

3.3 The Bending of Composite Material Laminated Plates: Classical Theory

Consider a plate composed of a laminated composite material that is mid-plane symmetric, i.e. $B_{ij} = 0$, and has no other coupling terms ($\epsilon_{16} = \epsilon_{26} = 0$), no surface shear stresses and no hygrothermal effects. The plate equilibrium equations for the bending of the plate, due to lateral loads given by Equations (3.14), (3.15) and (3.12) become:

$$\frac{\partial M_x}{\partial x} + \frac{\partial M_{xy}}{\partial y} - Q_x = 0 \quad (3.16)$$

$$\frac{\partial M_{xy}}{\partial x} + \frac{\partial M_y}{\partial y} - Q_y = 0 \quad (3.17)$$

$$\frac{\partial Q_x}{\partial x} + \frac{\partial Q_y}{\partial y} + p(x, y) = 0 \quad (3.18)$$

where $p(x, y) = p_1(x, y) - p_2(x, y)$. Equations (3.16) and (3.17) can be substituted into Equation (3.18) with the result that:

$$\frac{\partial^2 M_x}{\partial x^2} + 2 \frac{\partial^2 M_{xy}}{\partial x \partial y} + \frac{\partial^2 M_y}{\partial y^2} = -p(x, y) \quad (3.19)$$

The above equations are derived from equilibrium considerations alone. From Equation (2.66) and for the case of mid-plane symmetry ($B_{ij} = 0$) and no $(\)_{16}$ and $(\)_{26}$ terms, the constitutive relations are:

$$M_x = D_{11}\kappa_x + D_{12}\kappa_y \quad (3.20)$$

$$M_y = D_{12}\kappa_x + D_{22}\kappa_y \quad (3.21)$$

$$M_{xy} = 2D_{66}\kappa_{xy} \quad (3.22)$$

where from Equation (2.49)

$$\kappa_x = \frac{\partial \bar{\alpha}}{\partial x}, \quad \kappa_y = \frac{\partial \bar{\beta}}{\partial y}, \quad \kappa_{xy} = \frac{1}{2} \left(\frac{\partial \bar{\alpha}}{\partial y} + \frac{\partial \bar{\beta}}{\partial x} \right).$$

It is well known that transverse shear deformation (that is $\varepsilon_{xz} \neq 0, \varepsilon_{yz} \neq 0$) effects are important in plates composed of composite material plates in determining maximum deflections, vibration natural frequencies and critical buckling loads. However, it is appropriate to use a simpler stress analysis involving classical theory which neglects transverse shear deformation for preliminary design to determine a “first cut” for stresses, the required overall stacking sequence and required plate thickness is appropriate.

If, in fact, transverse shear deformation is ignored, then from Equation (2.48)

$$\varepsilon_{xz} = 0 = \frac{1}{2} \left(\bar{\alpha} + \frac{\partial w}{\partial x} \right) \text{ and } \varepsilon_{yz} = 0 = \frac{1}{2} \left(\bar{\beta} + \frac{\partial w}{\partial y} \right)$$

hence, from the above,

$$\bar{\alpha} = -\frac{\partial w}{\partial x}, \quad \bar{\beta} = -\frac{\partial w}{\partial y}, \quad \kappa_x = -\frac{\partial^2 w}{\partial x^2}, \quad \kappa_y = -\frac{\partial^2 w}{\partial y^2}, \quad \kappa_{xy} = -\frac{\partial^2 w}{\partial x \partial y} \quad (3.23)$$

So, substituting Equation (3.23) into Equations (3.20) through (3.22) results in the following for the case of no transverse shear deformations, i.e., classical plate theory:

$$M_x = -D_{11} \frac{\partial^2 w}{\partial x^2} - D_{12} \frac{\partial^2 w}{\partial y^2} \quad (3.24)$$

$$M_y = -D_{12} \frac{\partial^2 w}{\partial x^2} - D_{22} \frac{\partial^2 w}{\partial y^2} \quad (3.25)$$

$$M_{xy} = -2D_{66} \frac{\partial^2 w}{\partial x \partial y}. \quad (3.26)$$

Substituting these three equation in turn into Equation (3.19) results in:

$$D_{11} \frac{\partial^4 w}{\partial x^4} + 2(D_{12} + 2D_{66}) \frac{\partial^4 w}{\partial x^2 \partial y^2} + D_{22} \frac{\partial^4 w}{\partial y^4} = p(x, y). \quad (3.27)$$

The above coefficients are usually simplified to:

$$D_{11} \equiv D_1, \quad D_{22} \equiv D_2, \quad (D_{12} + 2D_{66}) \equiv D_3 \quad (3.28)$$

with the result that (3.27) becomes

$$D_1 \frac{\partial^4 w}{\partial x^4} + 2D_3 \frac{\partial^4 w}{\partial x^2 \partial y^2} + D_2 \frac{\partial^4 w}{\partial y^4} = p(x, y). \quad (3.29)$$

This is the governing differential equation for the bending of a plate composed of a composite material, excluding transverse shear deformation, with no coupling terms (that is $B_{ij} = ()_{16} = ()_{26} = 0$), and no hygrothermal terms (that is, $\Delta T = \Delta m = 0$) subjected to a lateral distributed load $p(x, y)$. As stated previously, neglecting transverse shear deformation and hygrothermal effects can lead to significant errors, as will be shown, but

in many cases their neglect results in easier solutions which are useful in preliminary design to “size” the plate initially.

Solutions of Equation (3.29) can be obtained generally in two ways: direct solution of the governing differential equation (3.29), or utilization of an energy principle solution. The latter offers more latitude in finding approximate solutions, often needed, and these will be discussed in detail later in Chapter 6.

Direct solutions of the governing differential equations for plates of composite materials fall into three categories: Navier solutions, Levy solutions and perturbation solutions. Each has its advantages and disadvantages. However prior to that, boundary conditions need to be discussed.

3.4 Classical Plate Theory Boundary Conditions

In the “classical” (that is, ignoring transverse shear deformation) plate theory of Section 3.3, two and only two boundary conditions can be satisfied at each edge of the plate because the governing differential equation (3.29) is fourth order in x and fourth order in y . The boundary conditions for a simply supported edge and a clamped edge shown below are identical to those of classical beam theory, where here n is the direction normal to the plate edge and t is the direction parallel or tangent to the edge:

Simply Supported Edge

$$w = 0 \text{ and } M_n = 0. \quad (3.30)$$

$M_n = 0$ implies $\partial^2 w / \partial n^2 = 0$, because in Equations (3.24) and (3.25), there is no curvature (that is $\partial^2 w / \partial t^2$) along the edge of the simply supported plate because $w = 0$.

Clamped Edge

$$w = 0 \text{ and } \frac{\partial w}{\partial n} = 0. \quad (3.31)$$

Free Edge

For a free edge of a plate, that is, one on which there are neither loads nor any displacement or slope requirements, it is clear that M_n , Q_n and M_{nt} all should be zero. However with classical plate theory only two boundary conditions can be satisfied. This was a major problem for the solid mechanists of the early nineteenth century. Then Kirchhoff brilliantly formulated an approximate solution to the problem, which is developed in many texts including [1, 2]. He reasoned that for the free edge

$$M_n = 0 \quad (3.32)$$

where now because there is curvature along the edge the full expressions of Equation (3.24) and Equation (3.25) must be utilized. The approximate expression for the second boundary condition is developed in detail in various texts, with the result that:

$$V_n = Q_n + \frac{\partial M_{nt}}{\partial t} = 0 \quad (3.33)$$

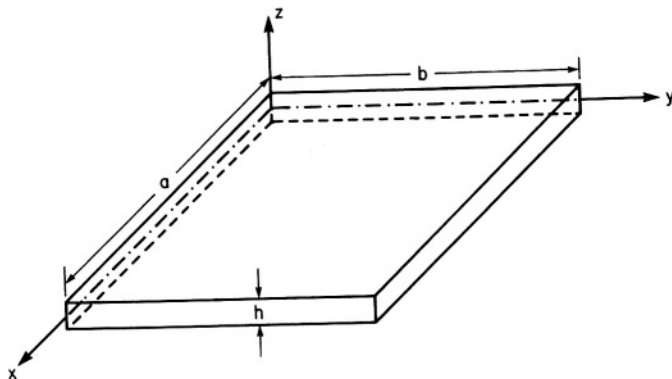


Figure 3.2.

where V_n is the “effective” shear resultant, and Q_n is given by Equation (3.16) or (3.17), M_n is given by Equation (3.24) or (3.25), and M_{nt} is given by Equation (3.26).

3.5 Navier Solutions for Rectangular Composite Material Plates

The Navier approach to these solutions involves separable solutions, as shown below, of the governing differential-plate equation shown in Equation (3.29). Thus

$$\begin{aligned} w(x, y) &= \sum_{m=1}^{\infty} \sum_{n=1}^{\infty} A_{mn} \bar{X}_m(x) \bar{Y}_n(y) \\ p(x, y) &= \sum_{m=1}^{\infty} \sum_{n=1}^{\infty} B_{mn} \bar{X}_m(x) \bar{Y}_n(y) \end{aligned} \quad (3.34)$$

In the above, the functions $\bar{X}_m(x)$ and $\bar{Y}_n(y)$ are a uniformly convergent, complete, orthogonal set of functions that satisfy the boundary conditions. Thus, when the complete summation is taken, the exact solution is obtained. From a practical point of

view, because of uniform convergence, a finite number of terms are sufficient to provide any desired accuracy.

If one assumes a plate that is simply supported on all four edges, then Equation (3.34) can be written as

$$w(x, y) = \sum_{m=1}^{\infty} \sum_{n=1}^{\infty} A_{mn} \sin\left(\frac{m\pi x}{a}\right) \sin\left(\frac{n\pi y}{b}\right) \quad (3.35)$$

$$p(x, y) = \sum_{m=1}^{\infty} \sum_{n=1}^{\infty} B_{mn} \sin\left(\frac{m\pi x}{a}\right) \sin\left(\frac{n\pi y}{b}\right) \quad (3.36)$$

These half-range sine series (the original Navier problem) satisfy the simply supported boundary conditions on all four edges of the plate shown in Figure 3.2. If the plate has other boundary conditions, then other functions must be used for $\bar{X}_m(x)$ and $\bar{Y}_n(y)$, in which case the approach is labeled the Generalized Navier approach.

To proceed it is first necessary to determine B_{mn} in Equation (3.36) in order to describe the load $p(x, y)$, whether it is continuous or discontinuous. One simply multiplies both the left- and right-hand sides of Equation (3.36) by

$\sin\left(\frac{r\pi x}{a}\right) \sin\left(\frac{s\pi y}{b}\right) dx dy$ and integrates both sides from 0 to a in the x -direction and 0 to b in the y -direction, i.e., over the planform area of the plate. It must be remembered that

$$\int_0^a \sin\left(\frac{m\pi x}{a}\right) \sin\left(\frac{r\pi x}{a}\right) dx = \begin{cases} a/2 & \text{if } m = r \\ 0 & \text{if } m \neq r \end{cases} \quad (3.37)$$

Therefore,

$$B_{mn} = \frac{4}{ab} \int_0^a \int_0^b p(x, y) \sin\left(\frac{m\pi x}{a}\right) \sin\left(\frac{n\pi y}{b}\right) dy dx \quad (3.38)$$

For example if $p(x, y) = p_0 = \text{a constant}$, a commonly occurring load,

$$B_{mn} = \frac{4p_0}{mn\pi^2} [1 - (-1)^m][1 - (-1)^n] \quad (3.39)$$

Now the above can be used for an isotropic or orthotropic plate, classical theory or advanced theory (including transverse-shear deformation) and a laminated or single-layer plate. Considering an orthotropic composite panel, using classical plate theory, simply supported on all four edges, Equation (3.29) is used.

Simply substituting Equations (3.35) and (3.36) into Equation (3.29), the equality requires that each term be equated, thus

$$A_{mn} = \frac{B_{mn}}{D_1 \left(\frac{m\pi}{a} \right)^4 + 2D_3 \left(\frac{m\pi}{a} \right)^2 \left(\frac{n\pi}{b} \right)^2 + D_2 \left(\frac{n\pi}{b} \right)^4} \quad (3.40)$$

where the flexural stiffness quantities D_1 , D_2 and D_3 are defined by Equations (3.28), for a laminated composite panel. For the isotropic case in which $E_{11} = E_{22} = 2G(1 + \nu)$, becomes Equation (3.28) $D_1 = D_2 = D_3$.

After obtaining the solution for $w(x, y)$ using Equations (3.35), (3.36) and (3.40), one may calculate the magnitude and location of the maximum deflection. By taking the derivative of $w(x, y)$, and using Equations (3.24) through (3.26), the stress couples M_x , M_y and M_{xy} are determined to find the maximum values and their location. Finally, depending upon whether the panel is a laminate or a single layer, the maximum stresses are determined through calculating the curvatures at the locations of maximum stress couples.

$$\kappa_x = -\frac{\partial^2 w}{\partial x^2}, \quad \kappa_y = -\frac{\partial^2 w}{\partial y^2} \text{ and } \kappa_{xy} = -\frac{\partial^2 w}{\partial x \partial y}$$

Knowing these, one can calculate the stresses in each of the k laminae through the following, since in this case of a lateral loading only, there is no in-plane response, i.e. $\epsilon_{x_0} = \epsilon_{y_0}$ and ϵ_{xy_0} are zero.

$$\begin{bmatrix} \sigma_x \\ \sigma_y \\ \sigma_{xy} \end{bmatrix}_k = \begin{bmatrix} \bar{Q}_{11} & \bar{Q}_{12} & 0 \\ \bar{Q}_{12} & \bar{Q}_{22} & 0 \\ 0 & 0 & \bar{Q}_{66} \end{bmatrix}_k \begin{bmatrix} \kappa_x \\ \kappa_y \\ 2\kappa_{xy} \end{bmatrix} z \quad (3.41)$$

The number of terms necessary to attain a desired accuracy depends upon the particular load $p(x, y)$, the aspect ratio of the plate (b/a), and the material system of which the plate is fabricated.

3.6 Navier Solution for a Uniformly Loaded Simply Supported Plate – An Example Problem

The case of a uniformly loaded, $p(x, y) = -p_0$ simply supported plate is solved by means of the Navier series solution of Section 3.5, for two composite materials systems: unidirectional and cross-ply, stresses σ_x , σ_y and σ_{xy} are determined for each case at the quarter points and mid-point of the plane. In addition, the solutions have been examined by utilizing one, three and five terms in the Navier series solution.

In this analysis, it is of course assumed that all plies are perfectly bonded and classical theory is used (that is, ϵ_{xy} and ϵ_{yz} , are assumed zero). This results in the in-plane stresses, σ_x , σ_y and σ_{xy} being directly determined, while the transverse shear stresses σ_{xz} and σ_{yz} are determined subsequently.

Using the methods discussed previously it is found that the stresses in each lamina for the case of $p(x, y) = -p_0$ are given by:

$$\begin{Bmatrix} \sigma_x \\ \sigma_y \\ \sigma_{xy} \end{Bmatrix}_k = + \frac{16p_0 z}{\pi^4} \sum_{m=1,3,5}^{\infty} \sum_{n=1,3,5}^{\infty} \frac{1}{mnD} \cdot \begin{bmatrix} \left[-\bar{Q}_{11}^k \left(\frac{m}{a} \right)^2 - \bar{Q}_{12}^k \left(\frac{n}{b} \right)^2 \right] \sin \frac{m\pi x}{a} \cdot \sin \frac{n\pi y}{b} \\ \left[-\bar{Q}_{12}^k \left(\frac{m}{a} \right)^2 - \bar{Q}_{22}^k \left(\frac{n}{b} \right)^2 \right] \sin \frac{m\pi x}{a} \cdot \sin \frac{n\pi y}{b} \\ 2\bar{Q}_{66}^k \left(\frac{m}{a} \right) \left(\frac{n}{b} \right) \cos \frac{m\pi x}{a} \cdot \cos \frac{n\pi y}{b} \end{bmatrix}$$

where

$$D = D_{11} \left(\frac{m}{a} \right)^4 + 2D_3 \left(\frac{mn}{ab} \right)^2 + D_{22} \left(\frac{n}{b} \right)^4$$

where D_3 is defined by Equation (3.28).

As a numerical example a square plate of $a = b = 12''$ is considered. The total plate thickness is 0.08": eight plies of 0.01" thickness ($h_k = 0.01''$).

The first material system considered is E glass/epoxy, with a fiber volume fraction $V_f = 70\%$, with the following properties:

$$E_{11} = 8.8 \times 10^6 \text{ psi}$$

$$\nu_{12} = 0.23$$

$$E_{22} = 3.6 \times 10^6 \text{ psi}$$

$$G_{12} = 1.74 \times 10^6 \text{ psi}$$

The stiffnesses Q_{ij} are

0° ply (psi)	90° ply (psi)
$\bar{Q}_{11} = 9.0 \times 10^6$	$\bar{Q}_{11} = 3.68 \times 10^6$
$\bar{Q}_{12} = 0.85 \times 10^6$	$\bar{Q}_{12} = 0.85 \times 10^6$
$\bar{Q}_{22} = 3.68 \times 10^6$	$\bar{Q}_{22} = 9.0 \times 10^6$
$\bar{Q}_{66} = 1.74 \times 10^6$	$\bar{Q}_{66} = 1.74 \times 10^6$

In the following figures, the stresses have been normalized as $\bar{\sigma}_{ij} = \sigma_{ij} / p_0$. In Figure 3.3, the normalized stresses are shown at the plate midpoint ($x = a/2$, $y = b/2$) for a unidirectional ($\theta = 0^\circ$) laminate. In this case the stresses are proportional to the distance from the plate mid-plane. In Figure 3.4, the normalized stresses at plate midpoint are shown for a mid-plane symmetric cross-ply laminate. Here, because the plies alternate between 0° and 90° , the stresses are discontinuous from ply to ply, and in each ply the stresses are larger in the fiber direction than in the 90° direction. In Figure 3.5, these stresses are shown at the quarter point location for the cross-ply plate. Because of symmetry, at the plate center in-plane shear stresses are zero, while at the quarter points a non-zero σ_{xy} exists as shown in Figure 3.5.

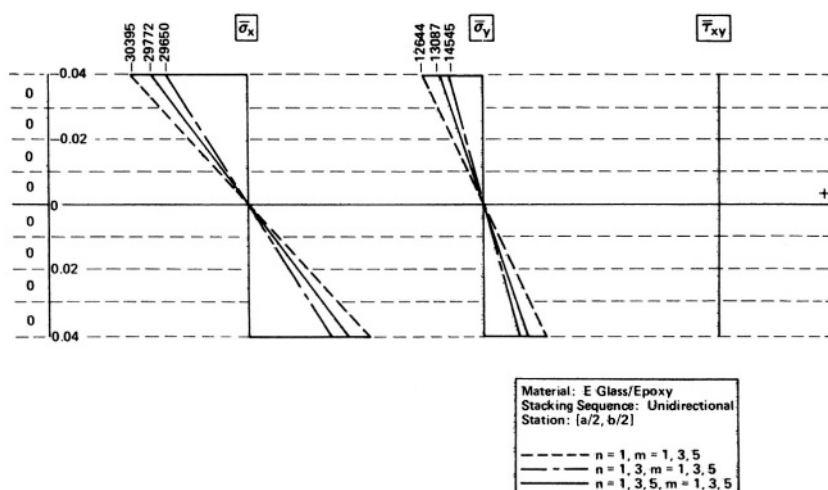


Figure 3.3. Normalized stresses at center of the plate for an E glass/epoxy unidirectional composite.

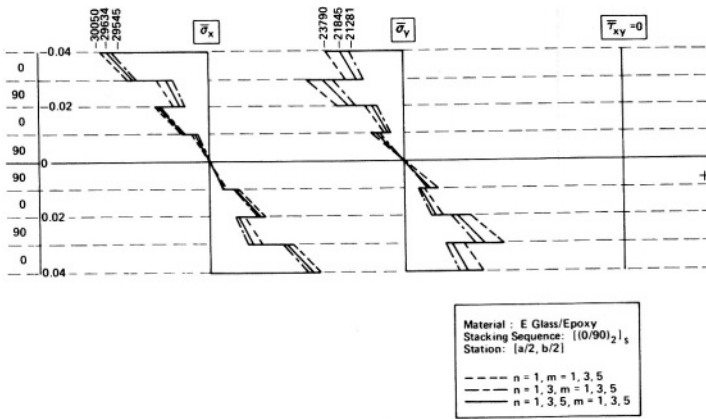


Figure 3.4. Normalized stresses at center of plate for an E glass/epoxy cross-ply composite.

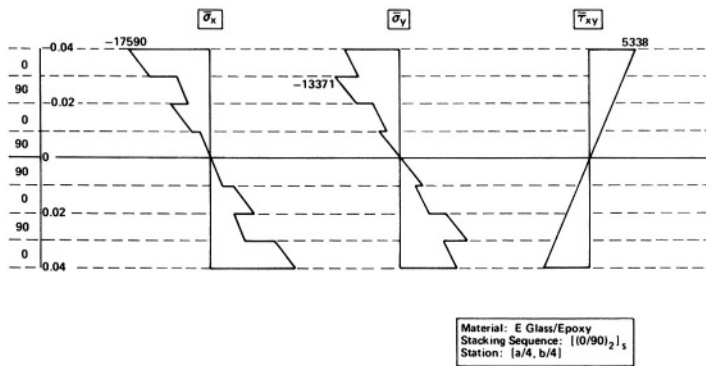


Figure 3.5. Normalized stresses at quarter point of plate for an E glass/epoxy cross-ply composite.

A cross-ply laminate of T300-5208 graphite-epoxy has been used for comparison with the E glass/epoxy laminate. Properties of the graphite-epoxy laminate are as follows for $V_f = 70\%$:

$$\begin{aligned} E_{11} &= 22.2 \times 10^6 \text{ psi} & \nu_{12} &= 0.12 \\ E_{22} &= 1.58 \times 10^6 \text{ psi} & G_{12} &= 0.81 \times 10^6 \text{ psi} \end{aligned}$$

Again normalized stresses have been shown in Figures 3.6 and 3.7 at both plate quarter point and mid-point.

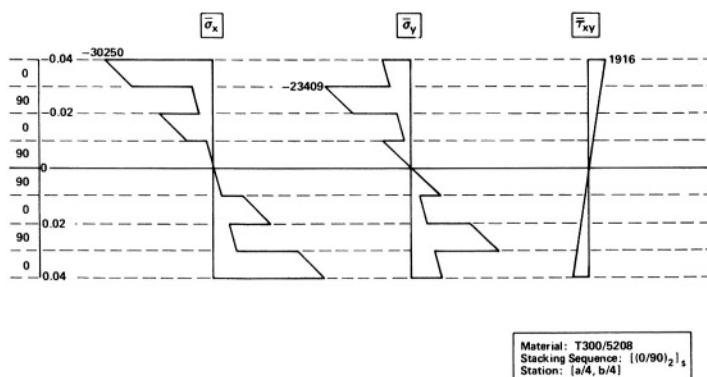


Figure 3.6. Normalized stresses at quarter point of plate of a graphite/epoxy cross-ply composite.

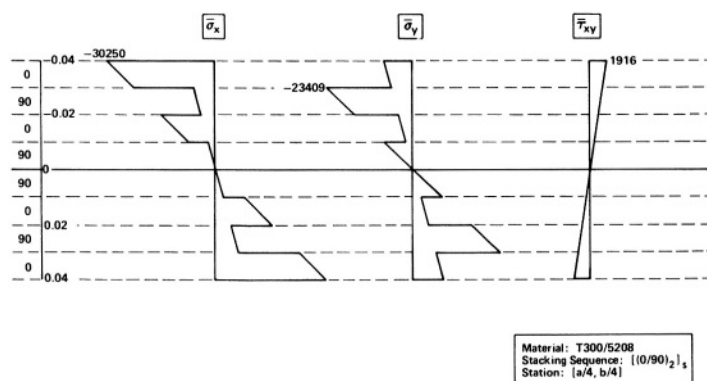


Figure 3.7. Normalized stresses at center of plate of a cross-ply graphite/epoxy composite.

Some conclusions can be drawn from this example set.

1. Solution convergence is rapid within the framework of taking three terms for both m and n for evaluating $\bar{\sigma}_x$, but is not as rapid in calculating $\bar{\sigma}_y$.
2. For the same material there is little difference between the maximum value of the $\bar{\sigma}_x$ stress for both the unidirectional and cross-ply composites at similar plate locations, however, the $\bar{\sigma}_y$ stresses differ significantly.
3. The stress $\bar{\sigma}_y$ at a fixed location for the graphite/epoxy laminate is much smaller relative to the $\bar{\sigma}_x$ value (10%), compared to that in the E glass/epoxy laminate where $\bar{\sigma}_y$ is 33% of the value of $\bar{\sigma}_x$ at the same location.

This example was the work of Wenn-Jinn Liou, a student at the University of Florida.

3.7 Levy Solution for Plates of Composite Materials

The second direct method of solution for the bending of rectangular plates due to lateral loads, is due to Maurice Levy [3] who, in 1899, introduced a single infinite-series method of solution for isotropic plate problems. The method can also be used to solve Equation (3.29) for an orthotropic composite material plate.

Consider the plate, shown in Figure 3.2, with edges $y = 0$ and $y = b$ simply supported. The boundary conditions for those edges are

$$\begin{aligned} w(x, 0) = w(x, b) &= 0 \\ M_y(x, 0) = M_y(x, b) &= 0 \end{aligned} \quad (3.42)$$

The latter implies that

$$\frac{\partial^2 w(x, 0)}{\partial y^2} = \frac{\partial^2 w(x, b)}{\partial y^2} = 0 \quad (3.43)$$

Levy assumed the following solution form: a single infinite half-range sine series that satisfies the simply supported boundary conditions on both y edges:

$$w(x, y) = \sum_{n=1}^{\infty} \phi_n(x) \sin\left(\frac{n\pi y}{b}\right) \quad (3.44)$$

where $\phi_n(x)$ is at this point an unknown function of x . A laterally distributed load $p(x, y)$ can be expressed as follows:

$$p(x, y) = g(x)h(y) \quad (3.45)$$

where $g(x)$ and $h(y)$ are specified. The form of Equation (3.44) requires that the $h(y)$ portion of the load also be expanded in terms of a half range sine series, such as

$$h(y) = \sum_{n=1}^{\infty} A_n \sin\left(\frac{n\pi y}{b}\right) \quad (3.46)$$

where

$$A_n = \frac{2}{b} \int_0^b h(y) \sin\left(\frac{n\pi y}{b}\right) dy \quad (3.47)$$

Substituting Equations (3.44) through (3.46) into (3.29) and observing that the equation exists only if it is true term by term, it is seen that, after dividing by D_1 and the trigonometric function:

$$\frac{d^4 \phi_n(x)}{dx^4} - \frac{2D_3}{D_1} \lambda_n^2 \frac{d^2 \phi_n(x)}{dx^2} + \frac{D_2}{D_1} \lambda_n^4 \phi_n(x) = \frac{A_n g_n(x)}{D_1} \quad (3.48)$$

where $\lambda_n = n\pi/b$. Note that Equation (3.48) was derived without specifying any boundary conditions on the x -edges. In fact, the homogeneous solution of Equation (3.48) yields four constants of integration, which are determined through satisfying boundary conditions on those edges.

To obtain the homogeneous solution of Equation (3.48) the right-hand side is set equal to zero:

$$\frac{d^4 \phi_n(x)}{dx^4} - \frac{2D_3}{D_1} \lambda_n^2 \frac{d^2 \phi_n(x)}{dx^2} + \frac{D_2}{D_1} \lambda_n^4 \phi_n(x) = 0 \quad (3.49)$$

After letting $\phi_n(x) = e^{sx}$, and dividing the result by e^{sx} , the indicial equation, from (3.49) becomes:

$$s^4 - \frac{2D_3}{D_1} \lambda_n^2 s^2 + \frac{D_2}{D_1} \lambda_n^4 = 0 \quad (3.50)$$

Unlike the case of an isotropic plate where $D_1 = D_2 = D_3$, such that the roots are easily seen to be $\pm \lambda_n$ and $\pm \lambda_n$ (repeated roots), for this case there are three sets of roots depending upon whether $(D_2/D_1)^{1/2}$ is greater than, equal to or less than D_3/D_1 . Hence, for the orthotropic composite plate, sandwich or laminate, using the Levy-type solution requires three different forms for the homogeneous solution of $\phi_n(x)$ to be put in Equation (3.44) depending on the relative stiffness of the plate in various directions.

For the case, $(D_2/D_1)^{1/2} < (D_3/D_1)$

$$\phi_{n_h}(x) = C_1 \cosh(\lambda_n s_1 x) + C_2 \sinh(\lambda_n s_1 x) + C_3 \cosh(\lambda_n s_2 x) + C_4 \sinh(\lambda_n s_2 x) \quad (3.51)$$

where the roots are

$$s_1 = \sqrt{\left(\frac{D_3}{D_1}\right) + \sqrt{\left(\frac{D_3}{D_1}\right)^2 - \frac{D_2}{D_1}}}, \quad s_2 = \sqrt{\left(\frac{D_3}{D_1}\right) - \sqrt{\left(\frac{D_3}{D_1}\right)^2 - \frac{D_2}{D_1}}}$$

For the case, $(D_2/D_1)^{1/2} = (D_3/D_1)$

$$\phi_{n_h}(x) = (C_5 + C_6 x) \cosh(\lambda_n s_3 x) + (C_7 + C_8 x) \sinh(\lambda_n s_3 x) \quad (3.52)$$

where the roots are

$$s_3 = \pm \sqrt{\frac{D_3}{D_1}}$$

For the case $(D_2/D_1)^{1/2} > (D_3/D_1)$

$$\begin{aligned} \phi_{n_h}(x) = & (C_9 \cos \lambda_n s_5 x + C_{10} \sin \lambda_n s_5 x) \cosh(\lambda_n s_4 x) \\ & + (C_{11} \cos \lambda_n s_5 x + C_{12} \sin \lambda_n s_5 x) \sinh(\lambda_n s_4 x) \end{aligned} \quad (3.53)$$

where the roots are

$$s_4 = \sqrt{\frac{1}{2} \left[\left(\frac{D_2}{D_1} \right)^{1/2} + \frac{D_3}{D_1} \right]}, \quad s_5 = \sqrt{\frac{1}{2} \left[\left(\frac{D_2}{D_1} \right)^{1/2} - \frac{D_3}{D_1} \right]}$$

Obviously, for a given plate whose materials and orientation have already been specified (the analysis problem) only one of the three cases needs to be solved. However, if one is trying to determine the best material and orientation (the design problem), then more than one case may need to be solved, with the necessity of determining not just four constants, but eight or all twelve to satisfy the edge boundary conditions to determine which construction is best for the design.

Concerning the particular solution, it is noted that if the lateral load, $p(x, y)$, is at most linear in x , hence from Equation (3.45), $g_n(x)$ is at most linear in x , then from Equation (3.48) the particular solution is

$$\phi_{n_p}(x) = \frac{A_n g_n(x)}{\lambda_n^4 D_2} \quad (3.54)$$

Otherwise, one must seek another particular solution. In any case, one must then add the relevant homogeneous ϕ_{n_h} to the particular ϕ_{n_p} to satisfy any set of boundary conditions on the x -edges of the plate. For example, suppose the $x = 0$ edge is simply supported, then from Equation (3.30) the boundary conditions are

$$w(0, y) = 0, \text{ and } M_x(0, y) = 0 \rightarrow \frac{\partial^2 w}{\partial x^2}(0, y) = 0 \quad (3.55)$$

However, when $w(x, y)$ has the form of Equation (3.44) this then implies that:

$$\phi_n(0) = \phi_n''(0) = 0 \quad (3.56)$$

where primes denote differentiation with respect to x .

Similarly, appropriate expressions can be found if the x -edges are clamped or free. Then whatever the relevant form of the boundary conditions on $x = 0$ and $x = a$, the total $\phi_n(x) = \phi_{n_h} + \phi_{n_p}$ and hence $w(x, y)$ is known from Equation (3.44). Then, for a composite-material laminated plate, one must calculate the curvatures, as was done in the previous section for the Navier approach:

$$\kappa_x = -\frac{\partial^2 w}{\partial x^2}, \quad \kappa_y = -\frac{\partial^2 w}{\partial y^2} \text{ and } 2\kappa_{xy} = -\frac{\partial^2 w}{\partial x \partial y}$$

Knowing these, one can calculate the bending stresses in each of the k laminae through the following:

$$\begin{bmatrix} \sigma_x \\ \sigma_y \\ \sigma_{xy} \end{bmatrix}_k = \begin{bmatrix} \bar{Q}_{11} & \bar{Q}_{12} & 0 \\ \bar{Q}_{12} & \bar{Q}_{22} & 0 \\ 0 & 0 & \bar{Q}_{66} \end{bmatrix}_k \begin{bmatrix} \kappa_x \\ \kappa_y \\ \kappa_{xy} \end{bmatrix} z \quad (3.57)$$

The stresses thus derived for each lamina must then be compared with the allowable stresses, determined through some failure criterion to see if structural integrity is retained under a given load (the analysis problem), or if this set of materials and orientation is sufficient for a given load (the design problem).

It is seen that the Levy-type solution is fine for a composite plate with no bending-stretching coupling, i.e., with midplane symmetry, and with two opposite edges simply supported. If two opposite edges are not simply supported then the complexity of the functions necessary to satisfy the boundary conditions on the $y = \text{constant}$ edges cause problems.

3.8 Perturbation Solutions for the Bending of a Composite Material Plate With Midplane Symmetry and No Bending-Twisting Coupling

As shown in the previous two sections, the Navier approach is excellent for composite material plates with all four edges simply supported, and the Levy approach is fine for composite material plates with two opposite edges simply supported, regardless of the boundary conditions on the other two edges. But for a composite plate with two opposite edges simply supported, even the Levy approach yields three distinct solutions depending on the relative magnitudes of D_1 , D_2 and $D_3 = D_{12} + 2D_{66}$. In addition, there are numerous books and papers available for the solution of isotropic plate problems [4].

Aware of all of the above, and based upon the fact that the solution of the second case of the Levy solution of (3.52) has the same form as that of the isotropic case, Vinson showed that the cases of (3.51) and (3.53) can be dealt with as perturbations about the solution of the same plates composed of isotropic materials [5,6].

Consider the governing equation for the bending of a composite material plate exhibiting mid-plane symmetry ($B_{ij} = 0$), no bending-twisting coupling ($D_{16} = D_{26} = 0$), and no transverse shear deformation (classical theory). Then Equation (3.29) becomes, after dividing both sides by D_1 :

$$\frac{\partial^4 w}{\partial x^4} + \frac{2D_3}{D_1} \frac{\partial^4 w}{\partial x^2 \partial y^2} + \frac{D_2}{D_1} \frac{\partial^4 w}{\partial y^4} = \frac{p(x, y)}{D_1} \quad (3.58)$$

Coordinate stretching is employed by defining the following:

$$\bar{y} = \left(\frac{D_2}{D_1} \right)^{-1/4} \cdot y, \quad \bar{b} = \left(\frac{D_2}{D_1} \right)^{-1/4} \cdot b \quad (3.59)$$

Substituting Equation (3.59) into Equation (3.58) yields

$$\frac{\partial^4 w}{\partial x^4} + 2 \left(\frac{D_2}{D_1} \right)^{-1/2} \cdot \left(\frac{D_3}{D_1} \right) \frac{\partial^4 w}{\partial x^2 \partial \bar{y}^2} + \frac{\partial^4 w}{\partial \bar{y}^4} = \frac{p(x, \bar{y})}{D_1} \quad (3.60)$$

Next defining a quantity α to be

$$\alpha = 2 \left[1 - \left(\frac{D_2}{D_1} \right)^{-1/2} \left(\frac{D_3}{D_1} \right) \right] \quad (3.61)$$

it is seen that substituting Equation (3.61) into Equation (3.60) yields

$$\frac{\partial^4 w}{\partial x^4} + \frac{2\partial^4 w}{\partial x^2 \partial \bar{y}^2} + \frac{\partial^4 w}{\partial \bar{y}^4} - \alpha \frac{\partial^4 w}{\partial x^2 \partial \bar{y}^2} = \frac{p(x, \bar{y})}{D_1} \quad (3.62)$$

If one defines the biharmonic operator, used in all isotropic plate problems, to be (in the stretched coordinate system)

$$\nabla^4 w = \frac{\partial^4 w}{\partial x^4} + \frac{2\partial^4 w}{\partial x^2 \partial \bar{y}^2} + \frac{\partial^4 w}{\partial \bar{y}^4} \quad (3.63)$$

then Equation (3.62) becomes

$$\nabla^4 w - \alpha \frac{\partial^4 w}{\partial x^2 \partial \bar{y}^2} = \frac{p(x, \bar{y})}{D_1} \quad (3.64)$$

Finally, assume the form of the solution for $w(x, \bar{y})$ to be

$$w(x, \bar{y}) = \sum_{n=0}^{\infty} w_n(x, \bar{y}) \alpha^n \quad (3.65)$$

which is a perturbation solution employing the “small” parameter α defined in Equation (3.61). Substituting Equation (3.65) into Equation (3.64) and equating all coefficients of α^n to zero, it is easily found that:

$$\nabla^4 w_0 = \frac{p(x, \bar{y})}{D_1} \quad (3.66)$$

$$\nabla^4 w_n = -\frac{\partial^4 w_{n-1}(x, \bar{y})}{\partial x^2 \partial \bar{y}^2} \quad n \geq 1 \quad (3.67)$$

It is seen that Equation (3.66) is the governing differential equation for an isotropic composite material plate of stiffness D_1 , subjected to the actual lateral load $p(x, \bar{y})$ with the stretched coordinate \bar{y} defined in Equation (3.59). It is probable that, regardless of boundary conditions on any edge, the solution of Equation (3.66) is available in the literature, either exactly or approximately. Subsequently w_1, w_2, w_3 , and so on are available from solving Equation (3.67), a plate whose lateral load is $-D_1 \left(\partial^4 w_{n-1} / \partial x^2 \partial \bar{y}^2 \right)$, where w_{n-1} is known, whose flexural stiffness is D_1 and whose

boundary conditions are homogeneous; if not the nonhomogeneity should be accounted for in the w_0 solution.

This technique is very useful because the “small” perturbation parameter need not be so small; it has been proven that when $|\alpha| < 1$, Equation (3.65) is another form of the exact solution, and $|\alpha| < 1$ covers much of the practical composite material construction regime. Also from a computational point of view, it is seldom necessary to include terms past $n = 1$, in Equation (3.65).

The above technique can be very useful. However, even if $|\alpha| \geq 1$, then the composite may fall within another range where for $(D_2 / D_1) \ll 1$. In that case, the plate behaves as a plate in the x -direction, but because $(D_2 / D_1) \ll 1$, it behaves as a membrane in the y -direction, with the following simpler governing differential equation,

$$\frac{\partial^4 w}{\partial x^4} + 2 \frac{D_3}{D_1} \frac{\partial^4 w}{\partial x^2 \partial y^2} = \frac{p(x, y)}{D_1} \quad (3.68)$$

with the solution in the form of the following for a plate simply supported on the y edges

$$w(x, y) = \sum_{n=1}^{\infty} \phi_n(x) \sin \lambda_n^* y^* \quad (3.69)$$

where

$$y^* = \left(\frac{2D_3}{D_1} \right)^{-1/2} \cdot y, \quad \lambda_n^* = \frac{n\pi}{b^*}, \quad b^* = \left(\frac{2D_3}{D_1} \right)^{-1/2} \cdot b \quad (3.70)$$

Even if the perturbation technique described by Equations (3.69) and (3.70) is not used it still provides physical insight by showing that if $D_2 \ll D_1$, then the structure behaves as a plate in the stiffer direction and acts only as a membrane in the weaker direction.

Finally, if $(\bar{b}/a) = (D_2 / D_1)^{-1/4} (b/a) > 3$, then the plate behaves purely as a beam in the x -direction as discussed later in Chapter 4, regardless of the boundary conditions on the y edge, as far as maximum deflection and maximum stresses. Hence, beam solutions have easy application to the solution of many composite plate problems. All of the details on the last two techniques are give in detail in References [5] and [6].

Incidentally, the techniques described in this section are the first use of perturbation techniques involving material property perturbation, even though geometric perturbations have been utilized for many decades.

3.9 Quasi-Isotropic Composite Panels Subjected to a Uniform Lateral Load

When a composite laminate has a stacking sequence in which $D_{11} = D_{22}$, it is referred to as quasi-isotropic. In that case it behaves as an isotropic plate in the determination of lateral deformations, $w(x, y)$, and stress couples, M_x , M_y and M_{xy} .

For isotropic plate monocoque plates several textbooks such as Timoshenko and Woinowsky-Krieger [4] and Vinson [7] have provided expressions for the maximum deflection, w_{\max} , and the maximum stress couple, M , a plate attains when subjected to a constant laterally distributed load p_0 , such as,

$$w_{\max} = \frac{C_0 p_0 a^4}{Eh^3} \quad (3.71)$$

$$M_{\max} = C_1 p_0 a^2 \quad (3.72)$$

where a is the smaller plate dimension; b is the longer plate dimension, $b \geq a$; E is the modulus of elasticity of the plate; h is the plate thickness; and $\nu = 0.3$.

The dimensionless constants C_0 and C_1 are given in tabular form for various boundary conditions, and these are repeated herein for completeness in Tables 3.1 through 3.4. Table 3.5 also provides information for the case wherein the plate is subjected to a hydraulic head. These tables and procedures are well known and well used.

TABLE 3.1. Coefficients for determining Maximum Deflections and Maximum Stresses for a Rectangular Plate, with $b > a$, Simply Supported at the Edges, under Uniform Pressure Loading p_0 with Sufficient Corner Forces to Hold it Down on the Foundation ($\nu = 0.3$).

b/a	1	1.2	1.4	1.6	1.8	2	3	4	5	∞
C_0	0.044	0.062	0.077	0.091	0.102	0.111	0.134	0.140	0.142	0.142
C_1	0.048	0.063	0.075	0.086	0.095	0.102	0.119	0.124	0.125	0.125

TABLE 3.2. Coefficients for determining Maximum Deflections and Maximum Stresses for a Rectangular Plate, under Uniform Load p_0 , with the a Edges Clamped and b Edges Simply Supported ($\nu = 0.3$).

b/a	∞	3	2	1.6	1.3	1	0.75	0.50	0.25
C_0	0.142	0.128	0.099	0.066	0.042	0.021	0.0081	0.00177	0.00011
C_1	0.125	0.125	0.119	0.109	0.094	0.070	0.045	0.021	0.0052

TABLE 3.3. Coefficients for Determining Maximum Deflections and Maximum Stresses for a Rectangular Plate, under Uniform Loading p_0 , Clamped along the a Edge, and Simply Supported along the Three Remaining Edges ($\nu = 0.3$).

b/a	∞	2	1.5	1.2	1	0.75	0.50	0.25
C_0	0.142	0.101	0.070	0.047	0.030	0.0133	0.0033	0.0002
C_1	0.125	0.122	0.112	0.098	0.084	0.058	0.031	0.0077

TABLE 3.4. Coefficients for determining Maximum Deflections and Maximum Stresses for a Rectangular Plate, under Uniform Loading p_0 , Clamped on All Four Edges ($\nu = 0.3$).

b/a	1	1.2	1.4	1.6	1.8	2.0	2.2
C_0	0.0138	0.0188	0.0226	0.0251	0.0267	0.0277	0.0285
C_1	0.0513	0.0639	0.0726	0.0780	0.0812	0.0829	0.0833

TABLE 3.5. Coefficients for determining Maximum Deflections and Maximum Stresses for a Rectangular Plate, Simply Supported on All Four Sides, Subjected to a Linearly Increasing Hydraulic Pressure along the a Edges, one b side having Zero Pressure, the Opposite b side having p_0 . [The Maximum Deflections occurs just off the middle of the plate toward the p_0 side (at about $0.55a$), the Maximum Stress somewhat farther off to the side ($\nu = 0.3$).]

b/a	∞	4	3	2	1.5	1	0.75	0.50	0.25
C_0	0.071	0.070	0.067	0.055	0.042	0.022	0.012	0.0037	0.0004
C_1	0.064	0.063	0.061	0.053	0.043	0.026	0.021	0.0139	0.0051

Of course, for the isotropic plate, the flexural stiffness is given by

$$D = \frac{Eh^3}{12(1-\nu^2)} \quad (3.73)$$

and the maximum bending stress, which occurs on the top and bottom surfaces of the plate, is

$$\sigma_{\max}(\pm h/2) = \pm \frac{6M_{\max}}{h^2} \quad (3.74)$$

Also for Tables 3.1 through 3.5, the numerical coefficients correspond to a Poisson's ratio of $\nu = 0.3$ wherein $1-\nu^2 = 0.91$. Therefore, for materials with other Poisson ratios, ν , Equation (3.71) must be changed to

$$w_{\max} = \frac{C_0 p_0 a^4}{Eh^3} \left(\frac{1-\nu^2}{0.91} \right) \quad (3.75)$$

With Equations (3.75) and (3.72), the well-used Tables 3.1 through 3.4 for monocoque plates can be used to analyze quasi-isotropic composite plates as well. It must be remembered that for these classical theory solutions no transverse-shear deformation effects are included. Table 3.5 can be used to analyze and design composite material plates subjected to a hydraulic head.

It is seen that for a *monocoque* quasi-isotropic plate design,

- (1) The plate must not be overstressed, i.e., the maximum stress is determined from the use of Equation (3.72) to determine the maximum stress couple, M , and the procedures described earlier to determine the stresses in each lamina. The determined maximum stress cannot exceed some allowable stress, σ_{all} , defined by the material's ultimate stress or yield stress divided by a factor of safety on ultimate stress or yield stress, whichever is smaller. This requires a certain value of plate thickness, h .
- (2) The monocoque plate must not be over deflected determined by Equation (3.75). This is sometimes specified, but in other cases the plate deflection cannot exceed the plate thickness or some fraction thereof. If the maximum plate deflection reaches a value of the plate thickness, h , the equations discussed herein become inapplicable because the plate behavior becomes increasingly nonlinear which requires that other equations be used. Again, to prevent over deflection, a plate thickness, h , is required as determined by Equation (3.75).

Therefore, in monocoque plate design, the plate thickness, h , is determined either from a strength or stiffness requirement, whichever requires the larger thickness.

3.10 A Static Analysis of Composite Material Panels Including Transverse Shear Deformation Effects

The previous derivations have involved "classical" plate theory, i.e., they have neglected transverse shear deformation effects. Because in many composite material laminated plate constructions, transverse-shear deformation effects are important, a more refined theory will now be developed. However, because of its simplicity, and the number of solutions available, classical theory is still useful for preliminary design and analysis to size the structure required in minimum time and effort.

In the simpler classical theory, the neglect of transverse shear deformation effects means that $\epsilon_{xz} = \epsilon_{yz} = 0$. To include transverse shear deformation effects, one uses

$$\epsilon_{xz} = \frac{1}{2} \left(\frac{\partial u}{\partial z} + \frac{\partial w}{\partial x} \right) \quad (3.76)$$

$$\varepsilon_{yz} = \frac{1}{2} \left(\frac{\partial v}{\partial z} + \frac{\partial w}{\partial y} \right) \quad (3.77)$$

Now substituting the admissible forms of the displacement for a plate or panel, Equation (2.49) into Equations (3.76) and (3.77), shows that

$$\varepsilon_{xz} = \frac{1}{2} \left(\bar{\alpha} + \frac{\partial w}{\partial x} \right) \quad (3.78)$$

$$\varepsilon_{yz} = \frac{1}{2} \left(\bar{\beta} + \frac{\partial w}{\partial y} \right) \quad (3.79)$$

No longer are the rotations $\bar{\alpha}$ and $\bar{\beta}$ explicit functions of the derivatives of the lateral deflection w , as shown by Equation (3.23) for classical plate theory. The result is that for this refined theory there are five geometric unknowns, u_0 , v_0 , w , $\bar{\alpha}$ and $\bar{\beta}$, instead of just the first three in classical theory.

Now one needs to look again at the equilibrium equations, the constitutive equations (stress-strain relations), the strain-displacement relations and the compatibility equations. For the plate, the equilibrium equations are given by Equations (3.9) through (3.15), because they do not change from classical theory. The constitutive equations for a composite material laminated plate and sandwich panel are given by Equations (2.58) through (2.66). The new cogent strain-displacement (kinematic) relations are given above in Equation (3.78) and (3.79). Because the resulting governing equations are in terms of displacements and rotations, any single valued, continuous solution will by definition satisfy the compatibility equations.

As an example consider a plate that is mid-plane symmetric ($B_{ij} = 0$) and has no coupling terms [$(\)_{16} = (\)_{26} = (\)_{45} = 0$]; the constitutive equations for this orthotropic plate can be written as follows, where κ is a transverse shear coefficient to be discussed later.

$$N_x = A_{11}\varepsilon_x^0 + A_{12}\varepsilon_y^0 \quad (3.80)$$

$$N_y = A_{12}\varepsilon_x^0 + A_{22}\varepsilon_y^0 \quad (3.81)$$

$$N_{xy} = 2A_{66}\varepsilon_{xy}^0 \quad (3.82)$$

$$M_x = D_{11}\kappa_x + D_{12}\kappa_y \quad (3.83)$$

$$M_y = D_{12}\kappa_x + D_{22}\kappa_y \quad (3.84)$$

$$M_{xy} = 2D_{66}\kappa_{xy} \quad (3.85)$$

$$Q_x = 2A_{55}\epsilon_{xz} = \kappa A_{55}\left(\bar{\alpha} + \frac{\partial w}{\partial x}\right) \quad (3.86)$$

$$Q_y = 2A_{44}\epsilon_{yz} = \kappa A_{44}\left(\bar{\beta} + \frac{\partial w}{\partial y}\right) \quad (3.87)$$

Because the plate is mid-plane symmetric there is no bending-stretching coupling, hence the in-plane loads (N_x, N_y, N_{xy}) and deflections (u_o, v_o) are uncoupled (separate) from the lateral loads, deflections and rotations. Hence, for the lateral distributed static loading, $p(x, y)$, Equations (3.16) through (3.18) and Equations (3.83) through (3.87) are utilized: 8 equations and 8 unknowns.

Substituting Equations (3.83) through (3.87) into Equations (3.16) through (3.18) and using Equation (2.66) results in the following set of governing differential equations for a laminated composite plate subjected to a lateral load, with $B_{ij} = 0$, $(\)_{16} = (\)_{26} = (\)_{45} = 0$, and no applied surface shear stresses (for simplicity)

$$D_{11}\frac{\partial^2\bar{\alpha}}{\partial x^2} + D_{66}\frac{\partial^2\bar{\alpha}}{\partial y^2} + (D_{12} + D_{66})\frac{\partial^2\bar{\beta}}{\partial x\partial y} - \kappa A_{55}\left(\bar{\alpha} + \frac{\partial w}{\partial x}\right) = 0 \quad (3.88)$$

$$(D_{12} + D_{66})\frac{\partial^2\bar{\alpha}}{\partial x\partial y} + D_{66}\frac{\partial^2\bar{\beta}}{\partial x^2} + D_{22}\frac{\partial^2\bar{\beta}}{\partial y^2} - \kappa A_{44}\left(\bar{\beta} + \frac{\partial w}{\partial y}\right) = 0 \quad (3.89)$$

$$\kappa A_{55}\left(\frac{\partial\bar{\alpha}}{\partial x} + \frac{\partial^2 w}{\partial x^2}\right) + \kappa A_{44}\left(\frac{\partial\bar{\beta}}{\partial y} + \frac{\partial^2 w}{\partial y^2}\right) + p(x, y) = 0 \quad (3.90)$$

The inclusion of transverse shear deformation effects results in three coupled partial differential equations with three unknowns, $\bar{\alpha}$, $\bar{\beta}$ and w , contrasted to having one partial differential equation with one unknown, w , in classical plate (panel) theory; see Equation (3.29). Incidentally if one specified that $\bar{\alpha} = -\frac{\partial w}{\partial x}$ and $\bar{\beta} = -\frac{\partial w}{\partial y}$, substituting that into Equations (3.88) through (3.90) reduces the three equations to Equation (3.29), the classical theory equation. The κ symbol with no subscript in (3.88) through (3.90) is a transverse shear deformation shape factor which varies from 1 to 2 depending upon the geometry.

The classical plate theory governing partial differential equation is fourth order in both x and y , and therefore requires two and only two boundary conditions on each of the four edges, as discussed in Section 3.4. This refined theory, including transverse shear

deformation, is really sixth order in both x and y , and therefore requires three boundary conditions on each edge as discussed in Section 3.11 below.

If the laminated plate is orthotropic but not mid-plane symmetric, i.e., $B_{ij} \neq 0$, the governing equations are more complicated than Equations (3.88) through (3.90) and are given by Whitney [8], Vinson [9] and are discussed briefly in Section 3.23 below.

3.11 Boundary Conditions for a Plate Using the Refined Plate Theory Which Includes Transverse Shear Deformation

3.11.1. SIMPLY-SUPPORTED EDGE

Again Equation (3.30) holds, but now a third boundary condition is required for the plate bending because it can be shown that Equations (3.88) through (3.90) are sixth order in w with respect to x and y . In addition, since the in-plane and lateral behavior are coupled, a fourth boundary condition enters the picture as well. This has resulted in the use of two different simply supported boundary conditions, both of which are mathematically admissible as natural boundary conditions (to be discussed later) and are practical structural boundary conditions. By convention the simply supported boundary conditions are given as follows:

$$\begin{aligned}
 S1(x = \text{constant edge}): \quad w = M_x = u_0 = N_{xy} = 0 \\
 S1(y = \text{constant edge}): \quad w = M_y = v_0 = N_{yx} = 0 \\
 S2(x = \text{constant edge}): \quad w = M_x = N_x = v_0 = 0 \\
 S2(y = \text{constant edge}): \quad w = M_y = N_y = u_0 = 0
 \end{aligned} \tag{3.91}$$

where u_0 is the mid-surface displacement in the x -direction and v_0 is the mid-surface displacement in the y -direction.

Whether one uses S1 or S2 boundary conditions is determined by the physical aspects of the plate problem being studied.

3.11.2. CLAMPED EDGE

Similarly, for a clamped edge the lateral deflection w and the rotation $\bar{\alpha}$ or $\bar{\beta}$ (for an $x = \text{constant}$ edge or a $y = \text{constant}$ edge, respectively) are zero (note: the slope is not zero) and the other boundary conditions are analogous to Equation (3.31).

$$C1(x = \text{constant edge}): \quad w = \bar{\alpha} = u_0 = N_{xy} = 0$$

$$\text{C1}(y = \text{constant edge}): w = \bar{\beta} = v_0 = N_{yx} = 0 \quad (3.92)$$

$$\text{C2}(x = \text{constant edge}): w = \bar{\alpha} = N_x = v_0 = 0$$

$$\text{C2}(y = \text{constant edge}): w = \bar{\beta} = N_y = u_0 = 0$$

3.11.3. FREE EDGE

The free edge requires three boundary conditions on each edge; therefore, it is no longer necessary to resort to the difficulties of the Kirchhoff boundary conditions for the bending of the plate needed for classical plates. The boundary conditions for the bending of the plate are simply:

$$M_n = Q_n = M_{nt} = 0 \quad (3.93)$$

where n and t are directions normal to and tangential with the edge. Again, the in-plane boundary conditions for the free edge are $N_n = N_{nt} = 0$.

3.11.4. OTHER BOUNDARY CONDITIONS

In addition to the above boundary conditions, which are widely used to approximate the actual structural boundary conditions, sometimes it is desirable to consider an edge whose lateral deflection is restrained, whose rotation is restrained or both. The means by which to describe these boundary conditions is given for example in [7, pp. 20-21].

3.12 Composite Plates on An Elastic Foundation

Consider a composite material plate that is supported on an elastic foundation. In most cases an elastic foundation is modeled as an elastic medium with a constant foundation modulus, i.e., a spring constant per unit planform area, of k in units such as lbs./in.². Therefore, the elastic foundation acts on the plate as a force in the negative direction proportional to the local lateral deflection $w(x,y)$. The force per unit area is $-kw$, because when w is positive the foundation modulus is acting in a negative direction, and vice versa. In order to incorporate the effect of the elastic foundation modeled as above one simply adds another force to the $p(x,y)$ load term. The results are, that for classical theory, Equation (3.29) is modified to (3.94), and for the refined theory, Equation (3.90) is modified to Equation (3.95):

$$D_1 \frac{\partial^4 w}{\partial x^4} + 2D_3 \frac{\partial^4 w}{\partial x^2 \partial y^2} + D_2 \frac{\partial^4 w}{\partial y^4} + kw = p(x, y) \quad (3.94)$$

$$\kappa A_{55} \left(\frac{\partial \bar{\alpha}}{\partial x} + \frac{\partial^2 w}{\partial x^2} \right) + \kappa A_{44} \left(\frac{\partial \bar{\beta}}{\partial y} + \frac{\partial^2 w}{\partial y^2} \right) - \kappa w + p(x, y) = 0 \quad (3.95)$$

3.13 Solutions for Plates of Composite Materials Including Transverse-Shear Deformation Effects, Simply Supported on All Four Edges

Some solutions are now presented for the equations in Section 3.10 and 3.11, using the governing differential equations (3.88) through (3.90). In the following κ with no subscript is a transverse shear factor, often given as $\pi^2/12$ or $5/6$.

Dobyns [10] has employed the Navier approach to solving these equations for a composite plate simply supported on all four edges subjected to a lateral load, using the following functions:

$$w(x, y) = \sum_{m=1}^{\infty} \sum_{n=1}^{\infty} C_{mn} \sin\left(\frac{m\pi x}{a}\right) \sin\left(\frac{n\pi y}{b}\right) \quad (3.96)$$

$$\bar{\alpha}(x, y) = \sum_{m=1}^{\infty} \sum_{n=1}^{\infty} A_{mn} \cos\left(\frac{m\pi x}{a}\right) \sin\left(\frac{n\pi y}{b}\right) \quad (3.97)$$

$$\bar{\beta}(x, y) = \sum_{m=1}^{\infty} \sum_{n=1}^{\infty} B_{mn} \sin\left(\frac{m\pi x}{a}\right) \cos\left(\frac{n\pi y}{b}\right) \quad (3.98)$$

$$p(x, y) = \sum_{m=1}^{\infty} \sum_{n=1}^{\infty} q_{mn} \sin\left(\frac{m\pi x}{a}\right) \sin\left(\frac{n\pi y}{b}\right) \quad (3.99)$$

It is seen that Equations (3.96) through (3.98) satisfy the simply supported boundary conditions on all edges given in Equation (3.91).

Substituting these functions into the governing differential equations (3.88) through (3.90) results in the following:

$$\begin{bmatrix} L_{11} & L_{12} & L_{13} \\ L_{12} & L_{22} & L_{23} \\ L_{13} & L_{23} & L_{33} \end{bmatrix} \begin{Bmatrix} A_{mn} \\ B_{mn} \\ C_{mn} \end{Bmatrix} = \begin{Bmatrix} 0 \\ 0 \\ q_{mn} \end{Bmatrix} \quad (3.100)$$

if $\lambda_m \equiv m\pi/a$, $\lambda_n \equiv n\pi/b$ and q_{mn} is the lateral load coefficient of (3.99) above, then the operators L_{ij} ($i, j = 1, 2, 3$) are given by the following:

$$L_{11} = D_{11}\lambda_m^2 + D_{66}\lambda_n^2 + \kappa A_{55} \quad L_{12} = (D_{12} + D_{66})\lambda_m\lambda_n$$

$$L_{13} = \kappa A_{55} \lambda_m, \quad L_{22} = D_{66} \lambda_m^2 + D_{22} \lambda_n^2 + \kappa A_{44}$$

$$L_{23} = \kappa A_{44} \lambda_n, \quad L_{33} = \kappa A_{55} \lambda_m^2 + \kappa A_{44} \lambda_n^2.$$

Solving Equation (3.100), one obtains

$$A_{mn} = \frac{(L_{12}L_{23} - L_{22}L_{13})q_{mn}}{\det} \quad (3.101)$$

$$B_{mn} = \frac{(L_{12}L_{13} - L_{11}L_{23})q_{mn}}{\det} \quad (3.102)$$

$$C_{mn} = \frac{(L_{11}L_{22} - L_{12}^2)q_{mn}}{\det} \quad (3.103)$$

where \det is the determinant of the $[L]$ matrix in Equation (3.100).

Having solved the problem to obtain $\bar{\alpha}$, $\bar{\beta}$ and w , the curvatures $\kappa_x = (\partial \bar{\alpha} / \partial x)$, $\kappa_y = (\partial \bar{\beta} / \partial y)$ and $\kappa_{xy} = 1/2[(\partial \bar{\alpha} / \partial y) + (\partial \bar{\beta} / \partial x)]$ may be obtained. These then can be substituted back into Equations (3.20) through (3.22) to obtain the stress couples M_x , M_y and M_{xy} to determine the location where they are maximum, to help in determining where the stresses are maximum.

For a laminated composite plate, to find the bending stresses in each lamina one must use the above equations to find the values for κ_x , κ_y and κ_{xy} in Equation (3.23). Finally, for each lamina the bending stresses can be found using:

$$\begin{bmatrix} \sigma_x \\ \sigma_y \\ \sigma_{xy} \end{bmatrix} = \begin{bmatrix} \bar{Q}_{11} & \bar{Q}_{12} & 0 \\ \bar{Q}_{12} & \bar{Q}_{22} & 0 \\ 0 & 0 & \bar{Q}_{66} \end{bmatrix}_k \begin{bmatrix} \kappa_x \\ \kappa_y \\ 2\kappa_{xy} \end{bmatrix} z \quad (3.104)$$

The stresses in each lamina in each direction must be compared to the strength of the lamina material in that direction. Keep in mind that quite often the failure occurs in the weaker direction in a composite material.

Looking at the load $p(x,y)$ in Equation (3.99), if the lateral load $p(x,y)$ is distributed over the entire lateral surface, then the Euler coefficient, q_{mn} is found to be

$$q_{mn} = \frac{4}{ab} \int_0^a \int_0^b p(x,y) \sin\left(\frac{m\pi x}{a}\right) \sin\left(\frac{n\pi y}{b}\right) dx dy \quad (3.105)$$

If that load is uniform then,

$$q_{mn} = \frac{4p_0}{mn\pi^2} (1 - \cos m\pi) (1 - \cos n\pi). \quad (3.106)$$

For a concentrated load located at $x = \xi$ and $y = \eta$,

$$q_{mn} = \frac{4P}{ab} \sin\left(\frac{m\pi\xi}{a}\right) \sin\left(\frac{n\pi\eta}{b}\right) \quad (3.107)$$

where P is the total load.

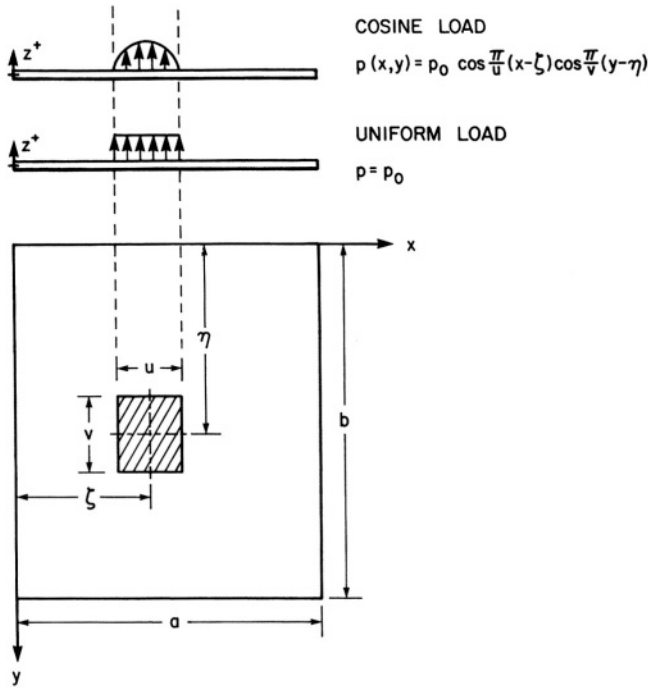


FIGURE 3.8. Load over a rectangular area. (Reprinted from Reference [8]).

For loads over a rectangular area of side lengths u and v whose center is at ξ and η , as shown in Figure 3.8, q_{mn} is given as follows:

$$q_{mn} = \frac{4P \sin\left(\frac{m\pi\eta}{b}\right) \sin\left(\frac{m\pi\xi}{a}\right) \cos\left(\frac{n\pi v}{2b}\right) \cos\left(\frac{m\pi u}{2a}\right)}{abu^2v^2 \left(\frac{n}{b} - \frac{1}{v}\right) \left(\frac{n}{b} + \frac{1}{v}\right) \left(\frac{m}{a} - \frac{1}{u}\right) \left(\frac{m}{a} + \frac{1}{u}\right)} \quad (3.108)$$

where P is the total load. Note that when $n/b = 1/v$, $m/a = 1/u$, then $q_{mn} = 0$. Of course, any other lateral load can be characterized by the use of Equation (3.105).

3.14 Dynamic Effects on Panels of Composite Materials

Seldom in real life is a structure subjected only to static loads. More often products and structures are subjected to vehicular, impact, crash, earthquake, handling, or fabricating dynamic loads. In the linear-elastic range, dynamic effects can be divided into two categories: natural vibrations and forced vibrations, and the latter can be further subdivided into one-time events (an impact) or recurring loads (such as cyclic loading). These will be discussed in turn.

Physically every elastic continuous body has an infinity of natural frequencies, only a few of which are of practical significance. When a structure is excited cyclically at a natural frequency, it takes little input energy for the amplitude to grow until one of four things happens:

- (1) The amplitude of vibration grows until the ultimate strength of a brittle material is exceeded and the structure fails.
- (2) Portions of the structure exceed the yield strength, plastically deform and the behavior changes drastically.
- (3) The amplitude grows until nonlinear effects become significant, and there is no natural frequency.
- (4) Due to damping or other mechanism the amplitude is limited, but as the natural vibration continues, fatigue failures may occur.

Physically, when a structure is undergoing a natural vibration the sum of the potential energy and kinetic energy remains constant if no damping is present. This can be termed a conservative system. However, the energy is compartmentalized, i.e., if a structure is truly vibrating in one mode of natural vibration it will not change and commence vibration in some other mode of natural vibration at some other natural frequency. In a complex structure if two components have vibrational natural frequencies that are identical, then when one component is excited, the other component will also be excited. It is for this very reason that duplicative natural frequencies are to be avoided. Also in complex structures of course the structural natural frequencies can be coupled involving all components.

Mathematically, natural vibration problems are called eigenvalue problems. They are represented by homogeneous equations, for which nontrivial solutions only occur at certain characteristic (*eigen*, in German) values of a parameter, from which the natural frequencies are determined. In a natural vibration the displacement field comprises a

normal mode. At any two different natural frequencies the corresponding normal modes are orthogonal to each other hence the compartmentalization of the energy). The normal modes comprise the solutions to the homogeneous governing differential equations, which are now zero only at the eigenvalues for those equations and boundary conditions.

If there is a forcing function, then the particular solution for the specific forcing function (which can be cyclical or a one time dynamic impact load) is added onto the homogeneous solution, which involves the natural frequencies and mode shapes. Physically, any dynamic load excites each and every one of the normal modes and corresponding natural frequencies. Usually, only a relatively few are large enough to be of concern. The largest amplitude of response will be in those mode shapes whose natural frequency is closest to the oscillatory component of the forcing functions.

When there are no natural frequencies close to the oscillatory portion of the dynamic load, then the structure will respond in deflection and stresses corresponding only to the magnitude and spatial distribution of the load. Such a condition results in solving the worst-case static problem in which the biggest load at some time, t , is applied. This is termed a quasistatic case. However, if the dynamic load oscillatory component is close to one of more natural frequencies, then the structural response can be much larger than the value obtained from a quasistatic calculation, and that increase can be represented by a dynamic load factor.

In what follows natural frequencies are treated first, then forced linear vibrations and finally nonlinear large-amplitude vibrations are discussed.

3.15 Natural Flexural Vibrations of Rectangular Plates: Classical Theory

Consider a rectangular composite material plate that is mid-plane symmetric such that $B_{ij} = 0$. If this plate is isotropic, i.e., $D_1 = D_2 = D_3 = D$, then the governing differential equation is given by Equation (3.29) for the classical theory, i.e., no transverse-shear deformation, and repeated here as

$$D \left[\frac{\partial^4 w}{\partial x^4} + 2 \frac{\partial^4 w}{\partial x^2 \partial y^2} + \frac{\partial^4 w}{\partial y^4} \right] = p(x, y) \quad (3.109)$$

For dynamic loads, using d'Alembert's Principle, the equation is written as

$$D \left[\frac{\partial^4 w}{\partial x^4} + 2 \frac{\partial^4 w}{\partial x^2 \partial y^2} + \frac{\partial^4 w}{\partial y^4} \right] = p(x, y, t) - \rho_m h \frac{\partial^2 w}{\partial t^2} \quad (3.110)$$

where the last term is the mass per unit planform area times the acceleration. For natural vibrations the load (the forcing function) can be ignored and the resulting homogeneous equation is

$$D \left[\frac{\partial^4 w}{\partial x^4} + 2 \frac{\partial^4 w}{\partial x^2 \partial y^2} + \frac{\partial^4 w}{\partial y^4} \right] + \rho_m h \frac{\partial^2 w}{\partial t^2} = 0 \quad (3.111)$$

This equation yields all of the natural frequencies for plates with any boundary conditions. For the easiest case, consider the composite material plate to be simply supported on all four edges. In that case, one may guess the following form for the deflection function because it satisfies all boundary conditions:

$$w(x, y, t) = A_{mn} \sin\left(\frac{m\pi x}{a}\right) \sin\left(\frac{n\pi y}{b}\right) \cos(\omega_{mn} t) \quad (3.112)$$

where ω_{mn} is the natural circular frequency in radians per unit time. Note that instead of $\cos(\omega_{mn} t)$, one may use either $\sin(\omega_{mn} t)$ or $e^{i(\omega_{mn} t)}$, where $i = \sqrt{-1}$, and the results will be the same.

Substituting Equation (3.112) into Equation (3.111) one sees that the nontrivial solution exists only when

$$\omega_{mn} = \left[\frac{\pi^4 D}{\rho_m h} \left(\frac{m^2}{a^2} + \frac{n^2}{b^2} \right)^2 \right]^{1/2} \quad (3.113)$$

In the above m and n are integers only. In this case, the lowest natural frequency occurs when $m = n = 1$, and this lowest frequency is always termed the fundamental natural frequency. To obtain the natural frequency in terms of cycles per second (Hz)

$$f_{mn} = \frac{\omega_{mn}}{2\pi} \quad (3.114)$$

Equation (3.113) is more accurate at low values of m and n , but as these integers increase, i.e., higher mode shapes, the calculated values increasingly exceed measured values. This is because transverse shear deformation effects increase with increased values of m and n , i.e., with the increased ratio of plate thickness to the wavelength of the m -nth mode of vibration. One major reference on the free vibrations of rectangular isotropic plates is Leissa [11].

If the composite plate is specially orthotropic and mid-plane symmetric, then for the natural vibration problem the governing differential equation is written as in Equation (3.29),

$$D_1 \frac{\partial^4 w}{\partial x^4} + 2D_3 \frac{\partial^4 w}{\partial x^2 \partial y^2} + D_2 \frac{\partial^4 w}{\partial y^4} = -\rho_m h \frac{\partial^2 w}{\partial t^2} \quad (3.115)$$

Again, if all four edges are simply supported then the mode shapes are give by Equation (3.112) with the result that the natural circular frequency in radians per second is given by

$$\omega_{mn} = \frac{\pi^2}{\sqrt{\rho_m h}} \left[D_1 \left(\frac{m}{a} \right)^4 + 2D_3 \left(\frac{m}{a} \right)^2 \left(\frac{n}{b} \right)^2 + D_2 \left(\frac{n}{b} \right)^4 \right]^{1/2} \quad (3.116)$$

Again, the natural frequency in Hz is given by Equation (3.114).

Keep in mind that for Equation (3.116) and other equations for the frequencies for natural vibrations to accurately describe the motion, the maximum deflection must be a fraction of the plate thickness since the theory is linear. Above that level of motion, nonlinear effects become increasingly significant.

3.16 Natural Flexural Vibrations of Composite Material Plates Including Transverse-Shear Deformation Effects

The governing partial differential equations for a composite plate or panel that is specially orthotropic and mid-plane symmetric subjected to a lateral static load $p(x,y)$ are given in Equations (3.88) through (3.90). If one now wishes to find the natural frequencies of this composite plate, that has mid-surface symmetry ($B_{ij} = 0$), no other couplings ($\epsilon_{16} = \epsilon_{26} = \epsilon_{45} = 0$), but includes transverse shear deformation, $\epsilon_{xz} \neq 0$, $\epsilon_{yz} \neq 0$, then one sets $p(x,y) = 0$ in Equation (3.90), but adds $-\rho_m(\partial^2 w / \partial t^2)$ to the right-hand side. In addition, because $\bar{\alpha}$ and $\bar{\beta}$ are both dependent variables that are independent of w , there will be an oscillatory motion of the lineal element across the plate thickness about the mid-surface of the plate. This results in the last term on the left-hand side of Equations (3.88) and (3.90) becoming $I(\partial^2 \bar{\alpha} / \partial t^2)$ and $I(\partial^2 \bar{\beta} / \partial t^2)$ respectively, as shown below:

$$D_{11} \frac{\partial^2 \bar{\alpha}}{\partial x^2} + D_{66} \frac{\partial^2 \bar{\alpha}}{\partial y^2} + (D_{12} + D_{66}) \frac{\partial^2 \bar{\beta}}{\partial x \partial y} - \kappa A_{55} \left(\bar{\alpha} + \frac{\partial w}{\partial x} \right) - I \frac{\partial^2 \bar{\alpha}}{\partial t^2} = 0 \quad (3.117)$$

$$(D_{12} + D_{66}) \frac{\partial^2 \bar{\alpha}}{\partial x \partial y} + D_{66} \frac{\partial^2 \bar{\beta}}{\partial x^2} + D_{22} \frac{\partial^2 \bar{\beta}}{\partial y^2} - \kappa A_{44} \left(\bar{\beta} + \frac{\partial w}{\partial y} \right) - I \frac{\partial^2 \bar{\beta}}{\partial t^2} = 0 \quad (3.118)$$

$$\kappa A_{55} \left(\frac{\partial \bar{\alpha}}{\partial x} + \frac{\partial^2 w}{\partial x^2} \right) + \kappa A_{44} \left(\frac{\partial \bar{\beta}}{\partial y} + \frac{\partial^2 w}{\partial y^2} \right) - \rho_m h \frac{\partial^2 w}{\partial t^2} = 0 \quad (3.119)$$

where ρ_m is given by

$$\rho_m = \frac{1}{h} \sum_{k=1}^N \rho_k (h_k - h_{k-1}) \quad (3.120)$$

where ρ_k is the mass density of the k th lamina, and here I is

$$I = \sum_{k=1}^N \rho_m z_k^2 dz_k. \quad (3.121)$$

In Equations (3.117) through (3.119) the κ 's are transverse-shear deformation parameters, as discussed earlier.

Similar to the Navier procedure used in previous analyses and following Dobyns [10] for the simply supported plate let

$$w(x, y, t) = \sum_{m=1}^{\infty} \sum_{n=1}^{\infty} C'_{mn} \sin\left(\frac{m\pi x}{a}\right) \sin\left(\frac{n\pi y}{b}\right) e^{i\omega t} \quad (3.122)$$

$$\bar{\alpha}(x, y, t) = \sum_{m=1}^{\infty} \sum_{n=1}^{\infty} A'_{mn} \cos\left(\frac{m\pi x}{a}\right) \sin\left(\frac{n\pi y}{b}\right) e^{i\omega t} \quad (3.123)$$

$$\bar{\beta}(x, y, t) = \sum_{m=1}^{\infty} \sum_{n=1}^{\infty} B'_{mn} \sin\left(\frac{m\pi x}{a}\right) \cos\left(\frac{n\pi y}{b}\right) e^{i\omega t} \quad (3.124)$$

Substituting these into the dynamic governing equations above results in a set of homogeneous equations that can be solved for the natural frequencies of vibration

$$\begin{bmatrix} L'_{11} & L_{12} & L_{13} \\ L_{12} & L'_{22} & L_{23} \\ L_{13} & L_{23} & L'_{33} \end{bmatrix} \begin{Bmatrix} A'_{mn} \\ B'_{mn} \\ C'_{mn} \end{Bmatrix} = \begin{Bmatrix} 0 \\ 0 \\ 0 \end{Bmatrix} \quad (3.125)$$

where the unprimed L quantities were defined below Equation (3.100) and

$$L'_{11} = L_{11} - \frac{\rho_m h^3}{12} \omega_{mn}^2$$

$$L'_{22} = L_{22} - \frac{\rho_m h^3}{12} \omega_{mn}^2$$

$$\dot{L}_{33}' = L_{33} - \rho_m h \omega_{mn}^2$$

Three eigenvalues (natural frequencies) result from solving Equation (3.125) for each value of m and n . However, two of the frequencies are significantly higher than the other because they are associated with the rotatory inertia terms, which are the last terms on the left-hand sides of Equations (3.117) and (3.118) and are very seldom important in structural responses. If they are neglected then $\dot{L}_{11}' = L_{11}$ and $\dot{L}_{22}' = L_{22}$ above, and the square of the remaining natural frequency can be easily found to be

$$\omega_{mn}^2 = [QL_{33} + 2L_{12}L_{23}L_{13} - L_{22}L_{13}^2 - L_{11}L_{23}^2] / \rho_m h Q \quad (3.126)$$

where, here, $Q = L_{11}L_{22} - L_{12}^2$. Also,

$$A_{mn}' = \frac{L_{12}L_{23} - L_{22}L_{13}}{Q} C_{mn}'$$

$$B_{mn}' = \frac{L_{12}L_{13} - L_{11}L_{23}}{Q} C_{mn}'$$

If transverse-shear deformation effects were neglected, Equation (3.126) would reduce to the following result for the case of a mid-plane symmetric, specially orthotropic composite laminated classical plate, simply supported on all four edges.

$$\omega_{mn} = \frac{\pi^2}{\sqrt{\rho_m h}} \sqrt{D_1 \left(\frac{m}{a}\right)^4 + 2D_3 \left(\frac{m}{a}\right)^2 \left(\frac{n}{b}\right)^2 + D_2 \left(\frac{n}{b}\right)^4} \quad (3.127)$$

where $\rho_m h$ is the mass density per unit planform area. If this plate is isotropic (3.127) becomes identical to (3.113).

3.17 Forced-Vibration Response of a Composite Material Plate Subjected to a Dynamic Lateral Load

Dobyns [10] then goes on to develop the solutions for the simply supported laminated composite plate subjected to a dynamic lateral load $p(x,y,t)$, neglecting the rotatory inertia terms discussed above, utilizing a convolution integral $P(t)$ as seen below in (3.131). Incidentally, the convolution integral is also known as the superposition integral and the Duhamel integral.

His solutions are also applicable to specially orthotropic composite material plates using the proper stiffness matrix quantities. The solutions to Equations (3.117) through

(3.119), modified to include a dynamic distributed lateral load $p(x,y,t)$ and neglecting the rotatory inertia terms are given by

$$w(x, y, t) = \frac{1}{\rho_m h} \sum_{m=1}^{\infty} \sum_{n=1}^{\infty} \left(\frac{q_{mn}}{\omega_{mn}} \right) \sin\left(\frac{m\pi x}{a}\right) \sin\left(\frac{n\pi y}{b}\right) P(t) \quad (3.128)$$

$$\bar{\alpha}(x, y, t) = \frac{1}{\rho_m h} \sum_{m=1}^{\infty} \sum_{n=1}^{\infty} \left(\frac{q_{mn}}{\omega_{mn}} \right) \frac{(L_{12}L_{23} - L_{22}L_{13})}{Q} \cos\left(\frac{m\pi x}{a}\right) \sin\left(\frac{n\pi y}{b}\right) P(t) \quad (3.129)$$

$$\bar{\beta}(x, y, t) = \frac{1}{\rho_m h} \sum_{m=1}^{\infty} \sum_{n=1}^{\infty} \left(\frac{q_{mn}}{\omega_{mn}} \right) \frac{(L_{12}L_{13} - L_{11}L_{23})}{Q} \sin\left(\frac{m\pi x}{a}\right) \cos\left(\frac{n\pi y}{b}\right) P(t) \quad (3.130)$$

where

$$P(t) = \int_0^t F(\tau) \sin[\omega_{mn}(t - \tau)] d\tau \quad (3.131)$$

and q_{mn} is the coefficient of the lateral-load function expanded in series form [see Equation (3.105)].

So for a given lateral distributed load $p(x,y,t)$, if a solution of the form given by Equations (3.128) through (3.130) is applicable, then the curvatures κ_x , κ_y and κ_{xy} for the plate can be found from Equation (3.23), and the stresses in each lamina are found from Equation (3.104). The function $P(t)$ has been solved analytically for several representative forcing functions shown in Figure 3.9.

For the sine pulse, the forcing function $F(t)$ and the convolution integral $P(t)$ are

$$\begin{aligned} F(t) &= F_0 \sin(\pi t / t_1) & 0 \leq t \leq t_1 \\ F(t) &= 0 & t > t_1 \\ P(t) &= \int_0^t F(t) \sin[\omega_{mn}(t - \tau)] d\tau = \frac{F_0 t_1 [\pi \sin \omega_{mn} t - \omega_{mn} t_1 \sin(\pi t / t_1)]}{\pi^2 - t_1^2 \omega_{mn}^2} \text{ for} \\ & & 0 \leq t \leq t_1 \end{aligned} \quad (3.132)$$

$$P(t) = \frac{F_0 \pi t_1 [\sin \omega_{mn} t - \sin \omega_{mn} (t - t_1)]}{\pi^2 - t_1^2 \omega_{mn}^2} \quad \text{for } t \geq t_1 \quad (3.133)$$

For the stepped pulse the forcing function $F(t)$ and the convolution integral $P(t)$ are given

$$F(t) = F_0 \quad 0 \leq t \leq t_1$$

$$F(t) = 0 \quad t > t_1$$

$$P(t) = \int_0^t F(\tau) \sin[\omega_{mn}(t - \tau)] d\tau = \frac{F_0}{\omega_{mn}} [1 - \cos(\omega_{mn} t)] \quad \text{for } 0 \leq t \leq t_1 \quad (3.134)$$

$$P(t) = \frac{F_0}{\omega_{mn}} \{ \cos[\omega_{mn}(t - t_1)] - \cos(\omega_{mn} t) \} \quad \text{for } t > t_1 \quad (3.135)$$

For a triangular pulse:

$$F(t) = F_0 (1 - t/t_1) \quad 0 \leq t \leq t_1$$

$$F(t) = 0 \quad t > t_1$$

$$\begin{aligned} P(t) &= \int_0^t F(\tau) \sin[\omega_{mn}(t - \tau)] d\tau \\ &= \frac{F_0}{\omega_{mn}} \left[1 - \cos(\omega_{mn} t) + \frac{1}{\omega_{mn} t_1} \sin(\omega_{mn} t) - \frac{t}{t_1} \right] \quad \text{for } 0 \leq t \leq t_1 \end{aligned} \quad (3.136)$$

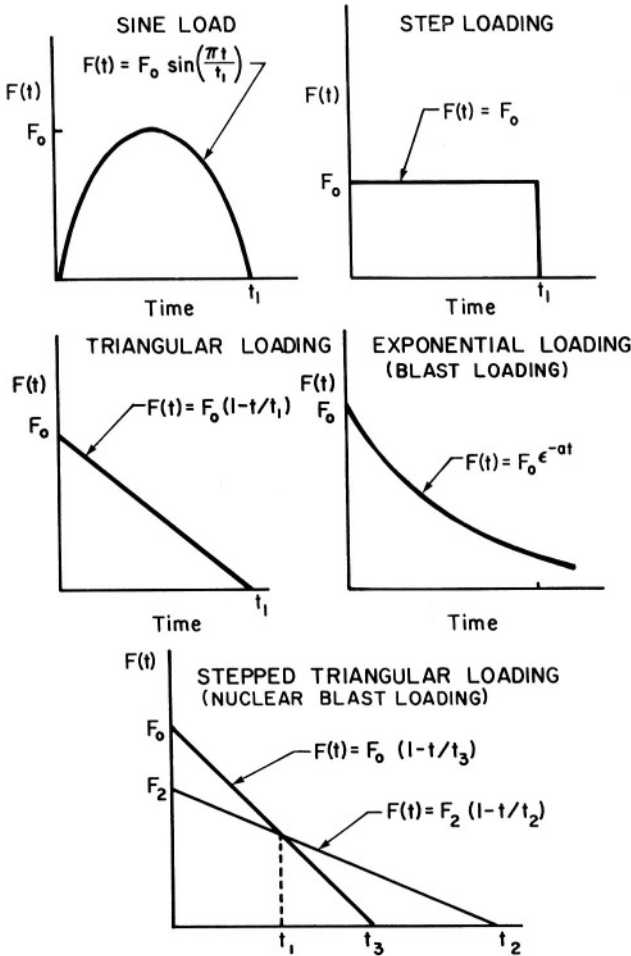


FIGURE 3.9. Representative forcing functions. (Reprinted from Reference [10].)

$$P(t) = F_0 \left\{ -\frac{1}{\omega_{mn}} \cos(\omega_{mn}t) + \frac{2}{\omega_{mn}^2 t_1} \cos \omega_{mn} \left(t - \frac{t_1}{2} \right) \sin \omega_{mn} \left(\frac{t_1}{2} \right) \right\} \text{ for } t > t_1 \quad (3.137)$$

The stepped triangular pulse of Figure 3.9 simulates a nuclear-blast loading [10] where the pressure pulse consists of a long-duration phase of several seconds due to the overpressure and a short-duration phase of a few milliseconds due to the shock wave reflection. The short-duration phase has twice the pressure of the long-duration phase.

$$F(t) = F_0(1 - t/t_3) \quad 0 \leq t \leq t_1$$

$$F(t) = F_2(1 - t/t_2) \quad t \leq t \leq t_2$$

$$F(t) = 0 \quad t > t_2$$

$$P(t) = \int_0^t F(\tau) \sin[\omega_{mn}(t - \tau)] d\tau$$

$$= \frac{F_0}{\omega_{mn}} \left[1 - \cos(\omega_{mn}t) + \frac{1}{\omega_{mn}t_3} \sin(\omega_{mn}t) - \frac{t}{t_3} \right] \text{ for } 0 < t \leq t_1 \quad (3.138)$$

$$\begin{aligned} P(t) = F_0 & \left\{ \frac{1}{\omega_{mn}} \left(1 - \frac{t}{t_3} \right) \cos[\omega_{mn}(t - t_1)] - \frac{1}{\omega_{mn}} \cos(\omega_{mn}t) \right. \\ & \left. - \frac{1}{\omega_{mn}^2 t_3} \sin[\omega_{mn}(t - t_1)] + \frac{1}{\omega_{mn}^2 t_3} \sin(\omega_{mn}t) \right\} \\ & + F_2 \left\{ \frac{1}{\omega_{mn}} \left(1 - \frac{t}{t_2} \right) - \frac{1}{\omega_{mn}} \left(1 - \frac{t}{t_2} \right) \cos[\omega_{mn}(t - t_1)] \right. \\ & \left. + \frac{1}{\omega_{mn}^2 t_2} \sin[\omega_{mn}(t - t_1)] \right\} \quad \text{for } t_1 \leq t \leq t_2 \end{aligned} \quad (3.139)$$

$$\begin{aligned} P(t) = F_0 & \left[\frac{1}{\omega_{mn}} \left(1 - \frac{t_1}{t_3} \right) \cos[\omega_{mn}(t - t_1)] - \frac{1}{\omega_{mn}} \cos(\omega_{mn}t) \right. \\ & \left. + \frac{1}{\omega_{mn}^2 t_3} \{ \sin(\omega_{mn}t) - \sin[\omega_{mn}(t - t_1)] \} \right] \\ & + F_2 \left[\frac{1}{\omega_{mn}} \left(\frac{t_1}{t_2} - 1 \right) \cos[\omega_{mn}(t - t_1)] \right. \\ & \left. - \frac{1}{\omega_{mn}^2 t_2} \{ \sin[\omega_{mn}(t - t_2)] - \sin[\omega_{mn}(t - t_1)] \} \right] \quad \text{for } t > t_2 \end{aligned} \quad (3.140)$$

Lastly, the exponential pulse of Figure 3.9 may be used to simulate a high explosive (non-nuclear) blast loading when the decay parameter α is empirically determined to fit the pressure pulse of the actual blast. The equations are

$$F(t) = F_0 e^{-\alpha t} \quad 0 \leq t \leq \infty$$

$$P(t) = \int_0^t F(\tau) \sin[\omega_{mn}(t - \tau)] d\tau$$

$$= \frac{F_0 [\omega_{mn} e^{-\alpha t} + \alpha \sin(\omega_{mn} t) - \omega_{mn} \cos(\omega_{mn} t)]}{\alpha^2 + \omega_{mn}^2} \quad \text{for } t > 0 \quad (3.141)$$

It should be noted that although the forcing-function equations given above are used herein to investigate the dynamic response of a composite material plate, these equations are useful for many other purposes.

Dobyns [10] concludes that the equations presented in this section allow one to analyze a composite material panel subjected to dynamic loads with only a little more effort than is required for the same panel subjected to static loads. He stated that one does not have to rely upon approximate design curves or arbitrary dynamic-magnification load factors.

With the information presented to this point, the necessary equations for the study of a composite plate without various couplings, but that include transverse-shear deformation, have been developed. The plate may be subjected to various static loads and a variety of dynamic loads. These loads and solutions can be used singly-or superimposed-to describe a complex dynamic input. (Those same load functions can be used for beams, shells and many other structural configurations.) With the solutions for $\bar{\alpha}(x, y)$, $\bar{\beta}(x, y)$ and w , maximum deflections and stresses can be determined for deflection stiffness-critical and strength-critical structures.

Vibration Damping

Damping of composite structures is clearly beyond the scope of this basic textbook. However, it would be a mistake not to mention that composite structures incorporate significant damping through the intrinsic properties of composite materials compared to metallic structures.

For the study of vibration damping, the text by Nashif, Jones, and Henderson [12] is excellent. Also, the text by Inman [13] concerning vibrations, vibrations damping, control, measurement and stability provides much needed information useful to the study of composite material structural vibrations.

3.18 Buckling of a Rectangular Composite Material Plate – Classical Theory

In addition to looking at maximum deflections, maximum stresses and natural frequencies when analyzing a structure, one must investigate under what loading conditions an instability can occur, which is also generically referred to as buckling.

For a mid-plane symmetric plate there are five equations associated with the in-plane loads N_x , N_y and N_{xy} and the in-plane displacements they cause, u_0 and v_0 . These equations are given by (3.9), (3.10) and (2.66), for the case of mid-plane symmetry ($B_{ij} = 0$) it is seen that

$$N_x = A_{11}\epsilon_x^0 + A_{12}\epsilon_y^0 + 2A_{16}\epsilon_{xy}^0 \quad (3.142)$$

$$N_y = A_{12}\epsilon_x^0 + A_{22}\epsilon_y^0 + 2A_{26}\epsilon_{xy}^0 \quad (3.143)$$

$$N_{xy} = A_{16}\epsilon_x^0 + A_{26}\epsilon_y^0 + 2A_{66}\epsilon_{xy}^0 \quad (3.144)$$

Likewise the six governing equations involving $M_x, M_y, M_{xy}, Q_x, Q_y$ and w , are given by Equations (3.12), (3.14), (3.15), (3.24), (3.25) and (3.26). At any rate there is no coupling between in-plane and lateral action for the plate with mid-plane symmetry. Yet is it well known and often observed that in-plane loads through buckling do cause lateral deflections, which are usually disastrous.

The answer to the paradox is the following: Through this Chapter up to this point we have used a *linear* elasticity theory, and the physical event of buckling is a non-linear problem. Because buckling is a non-linear effect, the in-plane strains are given by the following, where it is seen that the next (non-linear) term in the McLaurin series has been included:

$$\begin{aligned} \epsilon_x &= \frac{\partial u}{\partial x} + \frac{1}{2} \left(\frac{\partial w}{\partial x} \right)^2, & \epsilon_y &= \frac{\partial v}{\partial y} + \frac{1}{2} \left(\frac{\partial w}{\partial y} \right)^2 \\ \epsilon_{xy} &= \frac{\gamma_{xy}}{2} = \frac{1}{2} \left(\frac{\partial u}{\partial y} + \frac{\partial v}{\partial x} + \frac{\partial w}{\partial x} \frac{\partial w}{\partial y} \right) \end{aligned} \quad (3.145)$$

The results of including the terms to predict the advent or inception of buckling for the plate are given in the following equations, which is Equation (3.29) for a specially orthotropic plate; modified to include buckling effects:

$$\begin{aligned}
D_1 \frac{\partial^4 w}{\partial x^4} + 2D_3 \frac{\partial^4 w}{\partial x^2 \partial y^2} + D_2 \frac{\partial^4 w}{\partial y^4} &= p(x, y) + N_x \frac{\partial^2 w}{\partial x^2} \\
&+ 2N_{xy} \frac{\partial^2 w}{\partial x \partial y} + N_y \frac{\partial^2 w}{\partial y^2}
\end{aligned}
\tag{3.146}$$

It is clearly seen that there is a coupling between the in-plane loads and the lateral deflection.

The buckling loads like the natural frequencies are independent of the lateral loads, which will be disregarded in what follows. However, in actual structural analysis, the effect of lateral loads, along with the in-plane loads could cause overstressing and failure before the buckling load is reached. However, the buckling load is independent of the lateral load, as are the natural frequencies. Incidentally, common sense dictates that if one is designing a structure to withstand compressive loads, with the possibility of buckling being the failure mode, one had better design the structure to be mid-plane symmetric, so that $B_{ij} = 0$, otherwise the bending-stretching coupling could cause overstressing before the buckling load is reached.

Looking now at Equation (3.146) for the buckling of the composite plate under an axial load per unit width N_x only, and ignoring $p(x, y)$ Equation (3.146) becomes:

$$D_1 \frac{\partial^4 w}{\partial x^4} + 2D_3 \frac{\partial^4 w}{\partial x^2 \partial y^2} + D_2 \frac{\partial^4 w}{\partial y^4} - N_x \frac{\partial^2 w}{\partial x^2} = 0 \tag{3.147}$$

Again assuming the buckling mode for a laminated composite material plate to be that of an isotropic plate with the same boundary conditions, then for the case of the plate simply supported on all four edges one assumes the Navier solution:

$$w(x, y) = \sum_{m=1}^{\infty} \sum_{n=1}^{\infty} A_{mn} \sin \frac{m\pi x}{a} \sin \frac{n\pi y}{b} \tag{3.148}$$

Substituting Equation (3.148) into Equation (3.147) it is seen that for the critical load $N_{x_{cr}}$

$$N_{x_{cr}} = -\frac{\pi^2 a^2}{m^2} \left[D_1 \left(\frac{m}{a} \right)^4 + 2D_3 \left(\frac{m}{a} \right)^2 \left(\frac{n}{b} \right)^2 + D_2 \left(\frac{n}{b} \right)^4 \right] \tag{3.149}$$

where again several things are clear: Equation (3.147) is a homogeneous equation, one cannot determine the value of A_{mn} , and only the lowest value of $N_{x_{cr}}$ is of any importance usually. However, it is not clear which value of m and n result in the lowest critical buckling load. All values of n appear in the numerator, so $n = 1$ is the necessary

value for this case of all four edges simply supported. But m appears several places, and depending upon the value of the flexural stiffness D_1, D_2 and D_3 , and the length to width ratio of the plate, a/b , it is not clear which value of m will provide the lowest value of $N_{x_{cr}}$. However, for a given plate it is easily determined computationally.

Thus, it is seen that the eigenvalue problems differ from the considerations in previous sections because either event, natural vibration or buckling, occurs at only certain values. Hence, the natural frequencies and the buckling load are the eigenvalues; the vibrational mode and the buckling mode are the eigenfunctions.

In analyzing any structure one therefore should determine four things: the maximum deflection, the maximum stresses, the natural frequencies (if there is any dynamic loading to the structure – or nearby to the structure) and the buckling loads (if there are any compressive loads or in-plane shear loads).

What about the natural vibrations and buckling loads of composite material plates with boundary conditions other than simply supported? It is seen that for the cases treated in this section that double sine series were used because those are the vibrational modes and buckling modes of plates simply supported on all edges.

All combinations of beam vibrational mode shapes are applicable for the study of plates with various boundary conditions. These have been developed by Warburton [14], and all derivatives and integrals of those functions catalogued conveniently by Young and Felgar [15, 16] for easy use.

Expressions for buckling and vibrational modes for other boundary conditions are available in many texts. They can be used instead of Equation (3.148) for the buckling mode.

It must again be stated that in buckling loads calculated in this section do not include transverse shear effects, and are therefore only approximate – but they are useful for preliminary design, because of their relative simplicity. If the transverse shear deformation were included, see the next section, the buckling loads would be lower than those calculated in this section – so the buckling loads calculated, neglecting transverse shear deformation, are not conservative.

3.19 Buckling of a Composite Material Plate Including Transverse Shear Deformation Effects.

Consider the same composite material plate discussed in Section 3.18. However, herein the effects of transverse shear deformation will be included. The constitutive equations are given in (2.66), where the curvatures are defined by (3.23).

For the buckling of the plate due to in-plane loads, the equilibrium equations for a buckled plate are [17]:

$$\frac{\partial N_x}{\partial x} + \frac{\partial N_{xy}}{\partial y} = 0 \quad \frac{\partial N_{xy}}{\partial x} + \frac{\partial N_y}{\partial y} = 0$$

$$\frac{\partial Q_x}{\partial x} + \frac{\partial Q_y}{\partial y} + N_x \frac{\partial^2 w}{\partial x^2} + 2N_{xy} \frac{\partial^2 w}{\partial x \partial y} + N_y \frac{\partial^2 w}{\partial y^2} = 0 \quad (3.150)$$

$$\frac{\partial M_x}{\partial x} + \frac{\partial M_{xy}}{\partial y} = Q_x \quad \frac{\partial M_{xy}}{\partial x} + \frac{\partial M_y}{\partial y} = Q_y$$

The five equilibrium equations can be written in terms of the five unknowns, the three displacements, u , v and w , and the two rotations, $\bar{\alpha}$ and $\bar{\beta}$. Solving the five coupled partial differential equations with the proper boundary conditions provide the solution. However, only a few cases have been solved analytically. Moh and Hwu [17] have given an analytical solution for the composite plate with a cross-ply symmetric laminate.

Substituting the constitutive equations and the strain displacement relations into the equilibrium equations provide the following results:

$$N_x \frac{\partial^2 w}{\partial x^2} + N_y \frac{\partial^2 w}{\partial y^2} + 2N_{xy} \frac{\partial^2 w}{\partial x \partial y} + A_{55} \frac{\partial \bar{\alpha}}{\partial x} + A_{44} \frac{\partial \bar{\beta}}{\partial y} = 0 \quad (3.151)$$

$$D_{11} \frac{\partial^3 w}{\partial x^3} + D_3 \frac{\partial^3 w}{\partial x \partial y^2} - \left[D_{11} \frac{\partial^2 \bar{\alpha}}{\partial x^2} + D_{66} \frac{\partial^2 \bar{\alpha}}{\partial y^2} - A_{55} \bar{\alpha} \right] \\ (3.152)$$

$$-(D_{12} + D_{66}) \frac{\partial^2 \bar{\beta}}{\partial x \partial y} = 0$$

$$D_{22} \frac{\partial^3 w}{\partial y^3} + D_3 \frac{\partial^3 w}{\partial x^2 \partial y} - \left[D_{22} \frac{\partial^2 \bar{\beta}}{\partial x^2} + D_{66} \frac{\partial^2 \bar{\beta}}{\partial y^2} - A_{55} \bar{\beta} \right] \\ (3.153)$$

$$-(D_{12} + D_{66}) \frac{\partial^2 \bar{\alpha}}{\partial x \partial y} = 0$$

In these equations the N_x , N_y and N_{xy} are treated as constants that are known and remain unchanged during bending. Using the usual assumptions for the deflections and rotations. Consider the plate to be simply supported on all four edges and subjected to a biaxial compressive load per unit edge distance such that

$$N_x = -\bar{N}_x, \quad N_y = -k\bar{N}_x \quad \text{and} \quad N_{xy} = 0 \quad (3.154)$$

$$\begin{aligned}
w &= W \sin\left(\frac{m\pi x}{a}\right) \sin\left(\frac{n\pi y}{b}\right) \\
\bar{\alpha} &= \Gamma_x \cos\left(\frac{m\pi x}{a}\right) \sin\left(\frac{n\pi y}{b}\right) \\
\bar{\beta} &= \Gamma_y \sin\left(\frac{m\pi x}{a}\right) \cos\left(\frac{n\pi y}{b}\right)
\end{aligned} \tag{3.155}$$

Three simultaneous linear equations in W , Γ_x and Γ_y result from substituting Equation (3.155) into Equations (3.151) through (3.153). Since nontrivial solutions exist only when the determinant of the coefficients is zero, $N_{x_{cr}}$, the buckling load is found.

Moh and Hwu [17] found that

$$N_{x_{cr}} = \frac{(1+\eta)P_0}{\left[1 + k(an/bm)^2\right](1+\eta_x+\eta_y+\eta_0)} \tag{3.156}$$

where

$$\begin{aligned}
\eta &= \pi^2 D^* \left[\frac{1}{A_{44}} \left(\frac{m}{a}\right)^2 + \frac{1}{A_{55}} \left(\frac{n}{b}\right)^2 \right] \\
\eta_x &= \frac{\pi^2}{A_{55}} \left[D_{11} \left(\frac{m}{a}\right)^2 + D_{66} \left(\frac{n}{b}\right)^2 \right] \\
\eta_y &= \frac{\pi^2}{A_{44}} \left[D_{66} \left(\frac{m}{a}\right)^2 + D_{22} \left(\frac{n}{b}\right)^2 \right] \\
\eta_0 &= \frac{D^* P_0 m^2 n^2}{a^2 A_{55} A_{44}} \\
P_0 &= \frac{\pi^2 a^2}{m^2} \left[D_{11} \left(\frac{m^4}{a^4}\right) + 2D_3 \left(\frac{m}{a}\right)^2 \left(\frac{n}{b}\right)^2 + D_{22} \left(\frac{n}{b}\right)^4 \right]
\end{aligned}$$

$$D^*P_0 = \frac{\pi^2 a^2}{m^2} \left\{ D_{11}D_{66} \left(\frac{m}{a} \right)^4 + [D_{11}D_{22} - D_{12}D_{33}] \left(\frac{m}{a} \right)^2 \left(\frac{n}{b} \right)^2 + D_{22}D_{66} \left(\frac{n}{b} \right)^4 \right\}$$

It is seen that for classical theory (where A_{44} and A_{55} are infinite) the buckling load is simplified and is identical to that found using classical theory. It can also be seen that with the inclusion of transverse shear deformation effects that the buckling load is lower than that predicted by classical theory.

Also if the composite plate is on an elastic foundation, as discussed in Section 3.12, Kerr [18] has treated this problem for an applied lateral load and Paliwal and Ghosh [19] have treated this problem for buckling.

3.20 Some Remarks On Composite Structures

So far in this chapter, plates made of composite materials have been discussed. However, there are complicated constructions, which are made either from composite materials or from isotropic materials, which can be referred to as composite structures. One such structure is a box beam shown below in Figure 3.10, which could be the cross-section of a windmill blade, a water ski, or other representative structural components.

Such a structure will be subjected to tensile or compressive loads in the x -direction, to bending loads about the structural mid-surface, and to torsional loads about the x -axis. In each case one needs to develop the extensional stiffness matrix EA , the flexural stiffness matrix EI and the torsional stiffness matrix GJ , for the rectangular cross-section.

It is probable that in the structural component considered, the top and bottom panels would be identical, as well as each side panel perpendicular to the other one – that will be assumed here, and therefore the subscripts 1 and 2 will be used.

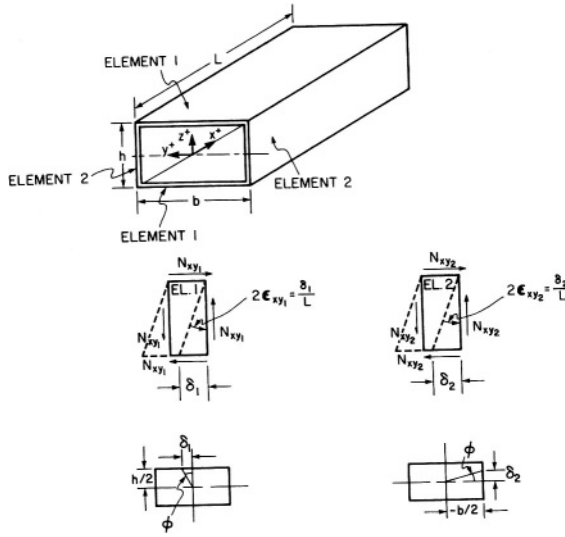


Figure 3.10. Box Beam.

For each panel the extensional relationship in the x -direction involves, for a construction without couplings

$$N_x = A_{11} \epsilon_x^0, \text{ where } N_x \text{ is the force per unit width}$$

Simply adding the contribution of each unit width, the overall load P carried by the overall construction can be written as

$$P = 2N_{x1}b + 2N_{x2}h = [2(A_{11})_1b + 2(A_{11})_2h]\epsilon_x^0$$

Hence, the structural extensional stiffness EA for the rectangular construction of Figure 3.10 is simply

$$EA = 2(A_{11})_1b + 2(A_{11})_2h$$

Similarly if the box beam is bent in the x - z plane the overall bending moment M will be related to the overall curvature κ_x , by

$$M = \left[2(D_{11})_1b + 2(A_{11})_1b\left(\frac{h}{2}\right)^2 + \frac{2(A_{11})_2h^3}{12} \right] \kappa_x \quad (3.158)$$

However, if the top and bottom surfaces are thin compared to the overall box height h , then the first term is negligible compared to the other ones, so

$$(EI)_{\text{box beam}} = 2(A_{11})_1 b \left(\frac{h}{2}\right)^2 + \frac{(A_{11})_2 h^3}{6} \quad (3.159)$$

Similar expressions can easily be constructed for the torsional stiffness. Consider the construction of Figure 3.10 subjected to a torsional load T in inch-lbs. about the x -axis.

Then it is clear that

$$T = 2(N_{xy_1})_1 b \left(\frac{h}{2}\right) + 2(N_{xy_2})_2 h \left(\frac{b}{2}\right) \quad (3.160)$$

Now from Equation (2.66), for both elements,

$$N_{xy_i} = 2A_{66_i} \varepsilon_{xy_i}^0 \quad (i=1,2)$$

If ϕ is the angle of twist caused by the torque T over the length L , then for element 1 and 2

$$\phi = \frac{\delta_1}{(h/2)} \quad \text{and} \quad \phi = \frac{\delta_2}{(b/2)} \quad (3.161)$$

It is also seen that

$$\varepsilon_{xy_1} = \frac{\delta_1}{2L} \quad \text{and} \quad \varepsilon_{xy_2} = \frac{\delta_2}{2L} \quad (3.162)$$

$$\begin{aligned} T &= 2(N_{xy})_1 b \left(\frac{h}{2}\right) + 2(N_{xy})_2 h \left(\frac{b}{2}\right) = 2bh(A_{66})_1 \varepsilon_{xy_1} + 2bh(A_{66})_2 \varepsilon_{xy_2} \\ &= \frac{bh}{L}(A_{66})_1 \delta_1 + \frac{bh}{L}(A_{66})_2 \delta_2 \end{aligned}$$

$$T = \frac{bh}{2L} [(A_{66})_1 h + (A_{66})_2 b] \phi$$

So the GJ, the torsional stiffness of the construction of Figure 3.10 is

$$GJ = \frac{bh}{2} [(A_{66})_1 h + (A_{66})_2 b] \quad (3.163)$$

The above merely illustrates what one can and must do to develop the basic mechanics of materials gross formulation for the extension, bending or twisting of a rectangular section, perhaps composed of very esoteric composite materials but used for a water ski, windmill blade or other shapes for many other purposes.

3.21 Methods of Analysis for Sandwich Panels with Composite Material Faces, and Their Structural Optimization

The analysis and design of sandwich panels may be accomplished in many cases simply by using the equations for the laminated composite material panels discussed herein. Merely by using the A, B and D matrix formulation for a sandwich all of the equations in Chapter 3 apply. For example, if the faces can be considered as a homogeneous material, then the lower face can be considered as lamina 1, the core as lamina 2, and the upper face as lamina 3. If the face were, for example made of a four ply cross-ply, then the lower face can be considered as laminae 1 through 4, the core is lamina 5 and the top face is laminae 5 through 9.

Either classical theory of the inclusion of transverse shear deformation can be incorporated.

Only when buckling must be considered are the methods of Chapter 3 incomplete. The methods of this chapter can predict overall buckling. However, in a sandwich panel, other buckling modes can occur and must be considered. These include core shear instability, face wrinkling, and face dimpling.

For further reading on this subject the texts by Zenkert [20] and Vinson [9] and papers by Sierakowski [21-24] are suggested.

3.22 Governing Equations for a Composite Material Plate With Mid-Plane Asymmetry

Consider a rectangular plate in which there are no $(\)_{16}$ nor $(\)_{26}$ coupling terms, but which has bending stretching coupling, i.e. $B_{ij} \neq 0$. In that case the equilibrium Equations (3.9) through (3.15), and the strain-displacement Equations (2.51) and (3.23) remain the same.

However, from Equation (2.66) it is seen that the constitutive equations change as shown below.

$$\begin{aligned} N_x &= A_{11}\epsilon_{x_0} + A_{12}\epsilon_{y_0} + B_{11}\kappa_x + B_{12}\kappa_y \\ N_y &= A_{12}\epsilon_{x_0} + A_{22}\epsilon_{y_0} + B_{11}\kappa_x + B_{22}\kappa_y \\ N_{xy} &= 2A_{66}\epsilon_{xy_0} + 2B_{66}\kappa_{xy} \end{aligned} \quad (3.164)$$

Proceeding as before for the mid-plane symmetric rectangular plate of Section 3.3, the resulting three coupled equations using classical plate theory, i.e. no transverse shear deformation, have the following form:

$$A_{11} \left(\frac{\partial^2 u_0}{\partial x^2} \right) + [A_{12} + A_{66}] \frac{\partial^2 v_0}{\partial x \partial y} + A_{66} \frac{\partial^2 u_0}{\partial y^2} - B_{11} \frac{\partial^3 w}{\partial x^3} - [B_{12} + B_{66}] \frac{\partial^3 w}{\partial x \partial y^2} = 0 \quad (3.165)$$

$$[A_{12} + A_{66}] \frac{\partial^2 u_0}{\partial x \partial y} + A_{22} \frac{\partial^2 v_0}{\partial y^2} + A_{66} \frac{\partial^2 v_0}{\partial x^2} - [B_{12} + B_{66}] \frac{\partial^3 w}{\partial x^2 \partial y} - B_{22} \frac{\partial^3 w}{\partial y^3} = 0 \quad (3.166)$$

$$-B_{11} \frac{\partial^3 u_0}{\partial x^3} - [B_{12} + 2B_{66}] \left(\frac{\partial^3 u_0}{\partial x \partial y^2} + \frac{\partial^3 v_0}{\partial x^2 \partial y} \right) - B_{22} \frac{\partial^3 v_0}{\partial y^3} + D_1 \frac{\partial^4 w}{\partial x^4} + 2D_3 \frac{\partial^4 w}{\partial x^2 \partial y^2} + D_2 \frac{\partial^4 w}{\partial y^4} = p(x, y) \quad (3.167)$$

Because of the bending-stretching coupling not only are lateral displacements, $w(x, y)$, induced but in-plane displacements, u_0 and v_0 , as well; hence, three coupled equations (3.165) through (3.167).

3.23 Governing Equations for a Composite Material Plate With Bending-Twisting Coupling

Looking at Equation (2.66), the moment curvature relations for a rectangular mid-plane symmetric plate with bending-twisting coupling are:

$$\begin{aligned} M_x &= D_{11} \kappa_x + D_{12} \kappa_y + 2D_{16} \kappa_{xy} \\ M_y &= D_{12} \kappa_x + D_{22} \kappa_y + 2D_{26} \kappa_{xy} \\ M_{xy} &= D_{16} \kappa_x + D_{26} \kappa_y + 2D_{66} \kappa_{xy} \end{aligned} \quad (3.168)$$

Of course if transverse shear deformation is ignored, i.e. classical theory then the curvatures are given by (3.23), and the moment curvature relations become:

$$\begin{aligned}
 M_x &= -D_{11} \frac{\partial^2 w}{\partial x^2} - D_{12} \frac{\partial^2 w}{\partial y^2} - 2D_{16} \frac{\partial^2 w}{\partial x \partial y} \\
 M_y &= -D_{12} \frac{\partial^2 w}{\partial x^2} - D_{22} \frac{\partial^2 w}{\partial y^2} - 2D_{26} \frac{\partial^2 w}{\partial x \partial y} \\
 M_{xy} &= -D_{16} \frac{\partial^2 w}{\partial x^2} - D_{26} \frac{\partial^2 w}{\partial y^2} - 2D_{66} \frac{\partial^2 w}{\partial x \partial y}
 \end{aligned} \tag{3.169}$$

Substituting these into (3.19), provides the following governing differential equation.

$$\begin{aligned}
 D_{11} \frac{\partial^4 w}{\partial x^4} + 4D_{16} \frac{\partial^4 w}{\partial x^3 \partial y} + 2D_{33} \frac{\partial^4 w}{\partial x^2 \partial y^2} + 4D_{26} \frac{\partial^4 w}{\partial x \partial y^3} \\
 + D_{22} \frac{\partial^4 w}{\partial y^4} = p(x, y)
 \end{aligned} \tag{3.170}$$

Comparing (3.170) with (3.29), it is seen that due to the presence of the D_{16} and D_{26} bending-twisting coupling terms, odd numbered derivatives appear in the governing differential equation. That precludes the use of both the Navier approach of Section 3.5, and the use of the Levy approach of Section 3.7 in obtaining solutions for plate with bending-twisting coupling. With these complications one may want to obtain solutions using the Theorem of Minimum Potential Energy discussed in Chapter 6 below.

3.24 Concluding Remarks

It appears that there is no end in trying to more adequately describe mathematically the behavior of composite materials utilized in structural components. Unfortunately, the more sophisticated one gets in such descriptions the more difficult the mathematics becomes, as is evidenced in the increasing difficulty observed as one progresses through the sections of Chapter 3.

One additional complication that is important in some composite material structures is that the stiffness (and other properties) are different in tension than they are in compression. This occurs because (1) sometimes the tensile and compressive mechanical properties of both fiber and matrix materials, differ and (2) sometimes it occurs because the matrix material is very weak compared to the fiber (that is $E_m \ll E_f$), such that the fibers buckle in compression under a small load so that for

the composite the stiffness in compression differs markedly than the stiffness in tension. Hence, one can idealize a little and say that one has one set of elastic properties in tension and another set of elastic properties in compression. Bert [25] has termed this a bimodular material, typical of some composites, certainly typical of aramid (Kevlar) fibers in a rubber matrix as used in tires, and also typical of certain biological tissues modeled in biomedical engineering. In this context

$$\begin{bmatrix} A & B \\ B & D \end{bmatrix}_{\text{Tension}} \neq \begin{bmatrix} A & B \\ B & D \end{bmatrix}_{\text{Compression}} \quad (3.171)$$

and all of the complications that result therefrom are too difficult to treat in this text for first year students trying to learn the fundamentals of composite materials.

Lastly, time dependent effects in the stresses, deformation and strains of composite materials are becoming more important design considerations. Viscoelasticity and creep are respected disciplines about which entire books have been written. These effects have been deemed important in some composite material structures. Crossman, Flaggs, Vinson and Wilson have all commented thereupon. Wilson and Vinson [26] have shown that the effects of viscoelasticity on the buckling resistance of polymer matrix composite material plates is very significant. Similarly, the effect of viscoelasticity on the natural vibration frequencies will also be significant. Many of these effects have been included in a survey article by Reddy [27] who has focused primarily on plates composed of composite materials.

3.25 References

1. Vinson, J.R. (1974) *Structural Mechanics: The Behavior of Plates and Shells*, Wiley-Interscience, John Wiley and Sons, New York.
2. Vinson, J.R. and Chou, T.W. (1975) *Composite Materials and Their Use in Structures*, Applied Science Publishers, London.
3. Levy, M. (1899) Sur L'équilibre Elastique d'une Plaque Rectangulaire, *Compt Rend* 129, pp. 535-539.
4. Timoshenko, S. and Woinowsky-Krieger, S. (1959) *Theory of Plates and Shells*, McGraw-Hill Book Co. Inc., 2nd edition, New York.
5. Vinson, J.R. (1961) New Techniques of Solutions for Problems in Orthotropic Plates, *Ph.D. Dissertation*, University of Pennsylvania.
6. Vinson, J.R. and Brull, M.A. (1962) New Techniques of Solutions of Problems in Orthotropic Plates, *Transactions of the Fourth United States Congress of Applied Mechanics*, Vol. 2, pp. 817-825.
7. Vinson, J.R. (1989) *The Behavior of Thin Walled Structures: Beams, Plates and Shells*, Kluwer Academic Publishers, Dordrecht, The Netherlands.
8. Whitney, J.M. (1987) *Structural Analysis of Laminated Anisotropic Plates*, Technomic Publishing Co. Inc., Lancaster, Pa.
9. Vinson, J.R. (1999) *The Behavior of Sandwich Structures of Isotropic and Composite Materials*, Technomic Publishing Co. Inc., Lancaster, Pa.

10. Dobyns, A.L., (1981) The Analysis of Simply-Supported Orthotropic Plates Subjected to Static and Dynamic Loads, *AIAA Journal*, May, pp. 642-650.
11. Leissa, A.W. (1973) The Free Vibration of Rectangular Plates, *Journal of Sound and Vibration*, Vol. 31, No. 3, pp. 257-293.
12. Nashif, A.D., Jones, D.I.G. and Henderson, J. (1985) *Vibration Damping*, Wiley Interscience.
13. Inman, D.J. (1989) *Vibration with Control Measurement and Stability*, Prentice Hall, Englewood Cliffs, New Jersey.
14. Warburton, G. The Vibration of Rectangular Plates, *Proceedings of the Institute of Mechanical Engineers*, 1968 (1954), pg. 371-384.
15. Young, D. and Felgar, R., Jr. (1944) Tables of Characteristic Functions Representing Normal Modes of Vibration of a Beam, *The University of Texas Publication Number 4913*.
16. Felgar, R., Jr. (1950) Formulas for Integral Containing Characteristic Functions of a Vibrating Beam, *Bureau of Engineering Research, The University of Texas Publication*.
17. Moh, J-S and Hwu, C. (1997) Optimization for Buckling of Composite Sandwich Plates, *AIAA Journal*, Vol. 35, pp. 863-868.
18. Kerr, A.D. (1964) Elastic and Viscoelastic Foundation Models, *Journal of Applied Mechanics*, Vol. 31, pp. 491-498.
19. Paliwal, D.N. and Ghosh, S.K. (1944) Stability of Orthotropic Plates on a Kerr Foundation, *AIAA Journal*, Vol. 38, pp. 1993-1997.
20. Zenkert, D. (1995) *An Introduction to Sandwich Construction*, EMAS Publications, West Midlands, UK.
21. Sierakowski, R.L. and Mukhopadhyay, A.K. (1990) On Sandwich Beams With Laminate Facings and Honeycomb - Cores Subjected to Hygrothermal Loads: Part I – Analysis, *Journal of Composite Materials*, Vol. 24, No. 4, pp. 382-400.
22. Sierakowski, R.L. and Mukhopadhyay, A.K. (1990) On Sandwich Beams With Laminate Facings and Honeycomb – Cores Subjected to Hygrothermal Loads: Part II – Application, *Journal of Composite Materials*, Vol. 24, No. 4, pp. 401-418.
23. Sierakowski, R.L., Mukhopadhyay, A.K., and Yu, Y.Y. (1994) On Sandwich Beams With Laminate Facings and Honeycomb – Cores Subjected to Hygrothermal and Mechanical Loads: Part III – Timoshenko Beam Theory, *Journal of Composite Materials*, Vol. 28, No. 11, pp. 1057-1075.
24. Sierakowski, R.L. and Mukhopadhyay, A.K. (2000) On Thermoelastic and Hygrothermal Response of Sandwich Beams With Laminate Facings and Honeycomb – Cores: Part IV – A Dynamic Theory, *Journal of Composite Materials*, Vol. 34, pp. 174-199.
25. Bert, C.W., Reddy, J.N. Reddy, V.S. and Chao, W.C. (1981) Analysis of Thick Rectangular Plates Laminated of Bimodulus Composite Materials, *AIAA Journal*, Vol. 19, No. 10, October, pp. 1342-1349.
26. Wilson, D.W. and Vinson, J.R. (1984) Viscoelastic Analysis of Laminated Plate Buckling, *AIAA Journal*, Vol. 22, No. 7, July, pp. 982-988.
27. Reddy, J.N. (1982) Survey of Recent Research in the Analysis of Composite Plates, *Composite Technology Review*, Fall.

3.26 Problems and Exercises

- 3.1. Find the critical buckling load, N_{xcr} in lbs./in. for a plate simply supported on all four edges made of a material whose flexural stiffness properties are given as follows and whose thickness is 1 inch.

$$[D] = \begin{bmatrix} 1.63 & 0.028 & 0 \\ 0.028 & 0.160 & 0 \\ 0 & 0 & 0.037 \end{bmatrix} \times 10^6 \text{ lb.} \cdot \text{in.}$$

- (a) If $a = 30$ inches and $b = 20$ inches.
 (b) If $a = 50$ inches and $b = 12$ inches.

- 3.2. Find the fundamental natural frequency in Hz (cps) for each of the plates of Problem 3.1, if the mass density of the material is

$$\rho_m = 1.8 \times 10^{-4} \frac{\text{lb.} \cdot \text{sec.}^2}{\text{in.}^4}$$

- 3.3. The following material properties are given for a unidirectional, 4 ply laminate, $h = 0.020''$

$$A = \begin{bmatrix} 0.84 & 0.00547 & 0 \\ 0.00547 & 0.0176 & 0 \\ 0 & 0 & 0.012 \end{bmatrix} \times 10^6 \text{ lb./in.}$$

$$B = 0$$

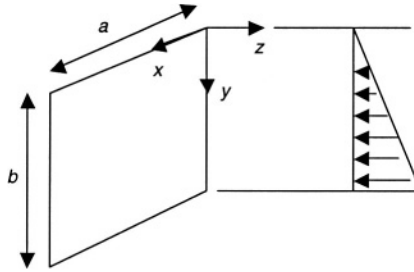
$$D = \begin{bmatrix} 28.053 & 0.1824 & 0 \\ 0.1824 & 0.5879 & 0 \\ 0 & 0 & 2 \end{bmatrix} \text{ lb.} \cdot \text{in.}$$

ρ , the mass density (corresponding to 0.06 lb./in.^3) = $1.554 \times 10^{-4} \text{ lb. sec.}^2/\text{in.}^4$

Consider a plate made of the above material with dimensions $a = 20''$, $b = 30''$, $h = 0.020''$. For the first perturbation method of Section 3.8 determine \bar{b} and α . Is α a proper value to use this perturbation technique?

- 3.4. Consider the plate of problem 3.3. If it is simply supported on all four edges, what is its fundamental natural frequency in cycles per seconds neglecting transverse shear deformation?

- 3.5. For a box beam whose dimensions are $b = 4''$, $h = 2''$, $L = 20''$, composed of T300/934 graphite/epoxy, whose properties are given in Appendix 2, determine the extensional stiffness, EA ; the flexural stiffness, EI , and the torsional stiffness, GJ , if the box beam is made of a 4 laminae, unidirectional composite, with a lamina thickness of $0.0055''$, all fibers being in the length direction.
- 3.6. Consider a composite material plate of dimensions $0 \leq x \leq a$, $0 \leq y \leq b$, of thickness h , composed of an E Glass/epoxy, which is modeled as being simply supported on all four edges. It is part of a structural system, which is subjected to a hydraulic load as shown below.



The load is $p(x, y) = \rho y$ where ρ is the weight density of the water.

- (a) To utilize the Navier approach determine B_{mn} which is given by

$$B_{mn} = \frac{4}{ab} \int_0^a \int_0^b p(x, y) \sin\left(\frac{m\pi x}{a}\right) \sin\left(\frac{n\pi y}{b}\right) dy dx.$$

- (b) At what value of x will the maximum deflection occur?
- (c) At what value of x will the maximum stress σ_x occur?
- 3.7. Consider a square plate in which $a = b = 20''$ made of a unidirectional Kevlar/epoxy composite, $V_f = 60\%$, whose properties are:

$$E_{11} = 11.02 \times 10^6 \text{ psi}$$

$$E_{22} = 0.798 \times 10^6 \text{ psi}$$

$$G_{12} = 0.334 \times 10^6 \text{ psi}$$

$$\nu_{12} = 0.34$$

$$\rho_w = 0.07 \text{ lb/in}^3$$

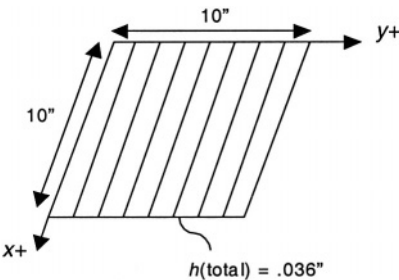
- (a) Determine the flexural stiffness matrix $[D]$.
 - (b) In the first perturbation technique of Section 3.8, calculate \bar{b} and α .
 - (c) Can this perturbation technique be used for this problem?
 - (d) What is the total weight of this plate?
 - (e) If this plate is simply supported on all four edges at what location (i.e., $x = ?$ and $y = ?$) will the maximum deflection occur?
 - (f) For the plate in e. above at what location will the maximum bending-stress occur?
- 3.8. Consider a plate composed of aluminum, an isotropic material of modulus of elasticity E , shear modulus G , and Poisson's ratio ν . The plate is of thickness h . Analogous to the stiffness matrix of Equation (2.66) determine the values of A_{ij} , B_{ij} and D_{ij} for this construction.
- 3.9. Consider a plate measuring 16" x 16" in planform of $[0^\circ, 90^\circ, 90^\circ, 0^\circ]$, of total thickness 0.022". The $[D]$ matrix for this construction is

$$D = \begin{bmatrix} 8.70 & 0.242 & 0 \\ 0.242 & 1.854 & 0 \\ 0 & 0 & 0.296 \end{bmatrix} \text{ lb.} - \text{in.}$$

If the plate is subjected to an in-plane compressive load in the $\theta = 0^\circ$ direction, what is the critical buckling load per inch of the edge distance, $N_{x_{cr}}$, using classical plate theory?

- 3.10. What is the fundamental natural frequency of the plate of Problem 3.9 in Hz (i.e. cycles per second), using classical plate theory? The weight density of the composite is 0.06 lb./in.^3 .
- 3.11. In designing a test facility to demonstrate the buckling of the plate of Problem 3.9, what load cell capacity (force capability) is needed to attain the loads necessary to buckle the plate?
- 3.12. (a) The plate of Problems 3.9 through 3.11 above will be used in an environment in which it will be exposed to a sinusoidal frequency of 6 Hz. Is it likely there will be a vibration problem requiring detailed study? Why?
 (b) What about 12 Hz? Why?
- 3.13. Could the first perturbation solution technique of Section 3.8 be used to obtain solution for the plate of Problem 3.9 subjected to a static lateral load, $p(x,y)$?
- 3.14. Consider a rectangular plate of composite materials which is part of a space vehicle structure. Its dimensions are 10" x 10". It is composed of Kevlar 49/epoxy

(properties are given in Appendix 2 of the text). It is composed of six laminae, unidirectional (all 0°), with ply thickness $h_k = 0.006 \text{ in.}$ The density of the material is 0.06 lbs./in.^3 .



The plate is simply supported on all four edges.

- (a) What are the flexural stiffnesses D_{11}, D_{12}, D_{22} and D_{66} ?
 - (b) Because the panel is part of a large space vehicle structure, care must be taken to identify all natural frequencies in the 0-1.5 Hz. Range. What, if any natural frequencies fall in this range?
 - (c) If the plate is subjected to a uniform in-plane compressive load in the x -direction, what is the critical buckling load, $N_{x_{cr}}$.
 - (d) Will the plate buckle before it is overstressed or will it be overstressed before it buckles?
- 3.15. For a plate or panel, what are the four ways in which it may fail or become subjected to a condition which may terminate its usefulness?
- 3.16. A panel simply supported on all four edges, measuring $a = 30''$, $b = 10''$, composed of T300-5208 graphite epoxy, composed of laminae with the following properties:

$$\begin{aligned}
 Q_{11} &= 22.36 \times 10^6 \text{ psi} & \rho_w &= 0.05 \text{ lb./in.}^3 \\
 Q_{22} &= 1.591 \times 10^6 \text{ psi} \\
 Q_{12} &= 0.4773 \times 10^6 \text{ psi} & h_k &= 0.0055'' \\
 Q_{66} &= 0.81 \times 10^6 \text{ psi}
 \end{aligned}$$

In the October 1986 issue of the AIAA Journal, M.P. Nemeth discusses the conditions in which one can ignore D_{16} and D_{26} in determining the buckling load

for a composite plate. He defines:

$$\gamma = \frac{D_{16}}{(D_{11}^3 D_{22})^{1/4}} \text{ and } \delta = \frac{D_{26}}{(D_{11} D_{22}^3)^{1/4}}$$

If both of these ratios are less than 0.18, one can use Equation (3.149) to determine the buckling load within 2% of the correct value for a plate simply supported on all four edges. If either of the ratios is greater than 0.18 one must replace the left hand side of Equation (3.146) with the left hand side of Equation (3.170), which negates the use of the Navier and Levy methods being used, thus complicating the solution.

For a four ply panel with stacking sequence of $[+45^\circ, -45^\circ, -45^\circ, +45^\circ]$, determine γ and δ to see if the simpler solution can be used.

- 3.17. Determine the fundamental natural frequency in Hertz (cycles per second) for the panel of Problem 3.16 made of four plies, unidirectionally oriented (all 0° plies).
- 3.18. Determine the critical buckling load, $N_{x_{cr}}$, for the same panel as in Problem 3.16.
- 3.19. For the panel of Problems 3.16 and 3.17, could the perturbation method of Section 3.8 be used to solve for deflections and stresses, i.e., is $\alpha < 1$?
- 3.20. Consider a plate of dimensions $a = 18''$ and $b = 12''$, composed of a laminated composite material whose lamina properties are:

$$\begin{array}{ll} E_1 = 18.5 \times 10^6 \text{ psi} & \nu_{12} = 0.30 \\ E_2 = 1.64 \times 10^6 \text{ psi} & G_{12} = 0.87 \times 10^6 \text{ psi} \end{array}$$

The stacking sequence of the plate is $[0^\circ, 90^\circ, 90^\circ, 0^\circ]$ in which each lamina is $0.006'' = h_k$. The plate is simply supported on each edge.

What are A_{11} , B_{11} and D_{11} for this plate?

- 3.21. For the plate of Problem 3.20, at what values of x and y will the maximum deflection occur if the plate is subjected to a uniform lateral load $p(x, y) = p_0$ (a constant)?
- 3.22. For the plate of Problems 3.20 and 3.21 above at which values of x and y would maximum ply stresses occur?
- 3.23. For the plate of Problem 3.20, calculate the critical buckling load per unit width,

$N_{x_{cr}}$, if the plate is subjected to a uniform compressive load in the x direction.

- 3.24. What is the fundamental natural vibration frequency in Hz for the plate of Problem 3.20. Assume a weight density for the composite to be $\rho_w = 0.06 \text{ lb./in.}^3$.
- 3.25. Suppose the plate of Problem 3.24 were designed to be subjected to a continuing harmonic forcing function at:
- (a) 38 to 48 Hz
 - (b) 10 Hz.

Would there be a problem structurally with this due to dynamic effects? Why?

- 3.26. Consider a Kevlar 49/epoxy composite, whose properties are given in Appendix 2 of the text, and whose weight density is $\rho_w = 0.06 \text{ lbs./in.}^3$. A plate whose stacking sequence is $[0^\circ, 90^\circ, 90^\circ, 0^\circ]$ is fabricated wherein each ply is $0.0055''$ thick. The plate is $20'' \times 16''$ in planform dimensions, and is simply supported on all four edges.

Determine $A_{11}, A_{12}, A_{22}, A_{66}, D_{11}, D_{12}, D_{22}$ and D_{66} .

- 3.27. Could the perturbation solution technique of Section 3.8 be used to solve problems for the plate of Problem 3.26?
- 3.28. If the plate of Problem 3.26 is subjected to an in-plane compressive load in the x -direction only, what is the critical buckling load per inch of edge distance, $N_{x_{cr}}$, using classical plate theory?
- 3.29. What is the fundamental natural frequency of the plate of Problem 3.26 in Hz., using classical plate theory?
- 3.30. If the fundamental natural frequency were calculated including the effects of transverse shear deformation, would that frequency be higher, lower or equal to the frequency calculated in Problem 3.29 above?
- 3.31. Consider a Kevlar 49/3501-6 epoxy composite with the following properties:

$$E_{11} = 10.5 \times 10^6 \text{ psi}$$

$$\nu_{12} = 0.366$$

$$E_{22} = 0.778 \times 10^6 \text{ psi}$$

$$G_{12} = 0.273 \times 10^6 \text{ psi}$$

For a unidirectional composite of thickness 0.1 inches, calculate D_{12} .

- 3.32. A square plate, simply supported on all four edges is composed of GY70/339 graphite epoxy. If this square plate is made of four plies with the A and D matrix values shown on the accompanying page, which stacking sequence would you choose for a design to have the highest fundamental natural frequency? Which stacking sequence has the lowest fundamental natural frequency?

GY70/339 graphite epoxy composite

[A] matrix

[D] matrix

- a. Unidirectional four ply

$$\begin{bmatrix} 842 & 5.46 & 0 \\ 5.46 & 17.6 & 0 \\ 0 & 0 & 12 \end{bmatrix} \times 10^3 \text{ lb./in.}$$

$$\begin{bmatrix} 28.1 & 0.182 & 0 \\ 0.182 & 0.588 & 0 \\ 0 & 0 & 0.4 \end{bmatrix} \text{ lb.-in.}$$

- b. Crossply $[0^\circ, 90^\circ, 90^\circ, 0^\circ]$ four ply

$$\begin{bmatrix} 4.30 & 5.46 & 0 \\ 5.46 & 4.30 & 0 \\ 0 & 0 & 12 \end{bmatrix} \times 10^3 \text{ lb./in.}$$

$$\begin{bmatrix} 24.6 & 0.182 & 0 \\ 0.182 & 4.02 & 0 \\ 0 & 0 & 0.4 \end{bmatrix} \text{ lb.-in.}$$

- c. Angle ply $[\pm 45^\circ]_s$, four ply

$$\begin{bmatrix} 230 & 206 & 0 \\ 206 & 230 & 0 \\ 0 & 0 & 212 \end{bmatrix} \times 10^3 \text{ lb./in.}$$

$$\begin{bmatrix} 7.67 & 6.87 & 5.15 \\ 6.87 & 7.67 & 5.15 \\ 5.15 & 5.15 & 7.07 \end{bmatrix} \text{ lb.-in.}$$

- 3.33. For a plate simply supported on all four edges that is 6 inches wide and 15 inches long made up of the unidirectional four ply graphite epoxy described in (a) above of Problem 3.32, what is the critical buckling load, $N_{x_{cr}}$, if the compressive load is applied parallel to the longer direction of the plate?
- 3.34. If the plate of Problem 3.33 were subjected only to a uniform lateral load, $p_0 = -5 \text{ psi}$, where would the maximum value of the tensile stress be located (i.e. where would you place a strain gage to measure the largest tensile strain, $x = ?$, $y = ?$, $z = ?$) ?
- 3.35. The following properties are given for T300/934 graphite epoxy unidirectional composite:

$$E_x = 23.69 \times 10^6 \text{ psi}$$

$$E_y = 1.7 \times 10^6 \text{ psi}$$

$$\nu_{xy} = 0.30$$

What is ν_{yx} ?

- 3.36. Consider a boron-epoxy material with the following properties:

$$Q_{11} = 35.3 \times 10^6 \text{ psi}$$

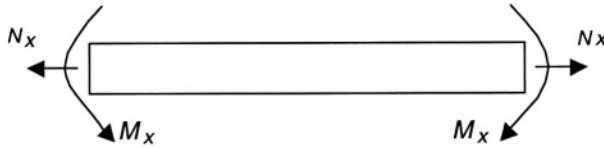
$$Q_{12} = 1.06 \times 10^6 \text{ psi}$$

$$Q_{22} = 3.53 \times 10^6 \text{ psi}$$

$$Q_{66} = 1.5 \times 10^6 \text{ psi}$$

Consider a two ply laminate wherein lamina 1 is oriented at 0° , and lamina 2 is oriented at 90° . Each ply is 0.01" thick. Calculate A_{11} , B_{11} and D_{11} .

- 3.37. For a two ply laminate of materials and ply thickness of Problem 3.36 above, wherein lamina 1 is $+45^\circ$ and lamina 2 is oriented at -45° , calculate B_{11} .
- 3.38. Consider a square plate with length and width of 12 inches, and thickness of $h = 0.020$ ", composed of graphite/epoxy whose stiffness matrix properties are given in Problem 3.32a. Calculate the natural frequency f_{23} in cycles per second (i.e., $m = 2$, $n = 3$, $f_{mn} = w_{mn} / 2\pi$).
- 3.39. (a) Does a natural frequency of vibration of a plate clamped on all four edges, subjected to a lateral distributed load $p(x, y) = p_0$, where p_0 is a constant, depend on the value of the load p_0 ?
- (b) Does a plate of lamina stacking sequence $[+45^\circ, -45^\circ, -45^\circ, +45^\circ]$, where each ply has the same material and same thickness have a non-zero $[B]$ matrix?
- (c) Does bending-twisting coupling involve the A_{16} and A_{26} terms?
- 3.40. You have been asked to replace an existing aluminum plate structure by a unidirectional Kevlar/epoxy structure using the material properties given in Problem 3.7. The loading on the aluminum plate is all in one direction, both an in-plane tensile load and a bending moment as shown below, and the structure is stiffness critical. Therefore, you must design a unidirectional fiberglass structure to have an extensional stiffness, A_{11} and a flexural stiffness, D_{11} , that equals or exceeds those values for the aluminum structure. The aluminum properties are $E = 10.1 \times 10^6 \text{ psi}$, $\nu = 0.3$, $\rho = 0.10 \text{ lb./in.}^3$ and the aluminum plate is 0.101 inches thick.



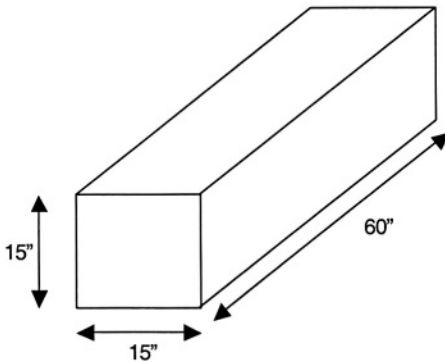
- For the existing aluminum structure, what is the extensional stiffness per unit width, $Eh/(1-\nu^2)$?
- In the existing structure what is the flexural stiffness per unit width, $Eh^3/12(1-\nu^2)$?
- If you replace the aluminum structure with the Kevlar/epoxy structure, what thickness h is required of your composite plate to have A_{11} equal the extensional stiffness of the aluminum structure?
- What thickness h is required to your composite plate to have D_{11} equal the flexural stiffness of the aluminum structure?
- Which h must your composite design be to achieve the stated design requirement?
- Will your composite design be heavier or lighter than the aluminum structure and by what percentage?

3.41. Consider a rectangular panel simply supported on all four edges. The panel measure $a = 25''$, $b = 10''$, where $0 \leq x \leq a$, $0 \leq y \leq b$. The laminated plate is composed of unidirectional boron/aluminum with the following properties:

$E_{11} = 32 \times 10^6 \text{ psi}$	$\rho = 0.0915 \text{ lb./in.}^3$
$E_{22} = 20 \times 10^6 \text{ psi}$	$\sigma_{lu} = 250,000 \text{ psi}$
$G_{12} = 8 \times 10^6 \text{ psi}$	$\nu_f = 50\%$
ply thickness $h_k = 0.007 \text{ in.}$	$\nu_{12} = 0.35$

- Determine Q_{11} , Q_{22} , Q_{12} and Q_{66} for a lamina (ply) of this material.
- Determine the flexural stiffness D_{11} , D_{22} , D_{12} and D_{66} for a plate made of four ply, unidirectionally oriented (all 0° plies).
- Determine the fundamental natural frequency in Hertz (cycles per second) for the panel.

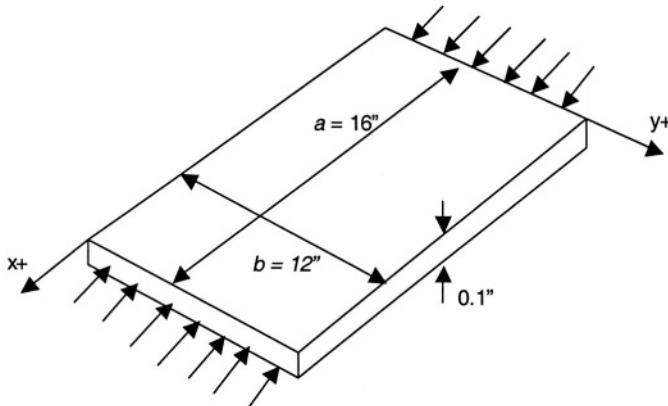
- (d) Determine the critical buckling load, $N_{x_{cr}}$, for the panel, when it is subjected to a uniform compressive load in the x -direction.
- (e) If the panel were made of one ply with the fibers oriented at $\theta = +30^\circ$, what is \bar{Q}_{11} ?
- 3.42. Consider a laminated plate composed of the first graphite/epoxy composite whose properties are given in Appendix 2 of the text. The laminate consists of four laminae, stacked as $[0^\circ, 90^\circ, 90^\circ, 0^\circ]$, where each ply is 0.0055 inches thick. Calculate a) A_{66} , b) B_{66} , c) D_{66} and d) ν_{21} .
- 3.43. Consider a rectangular composite plate whose stiffness matrices are given in Problem 3.3 above. The plate is 15 inches wide, 60 inches long, simply supported on all four edges, is 0.020 inches thick, whose weight density is 0.06 lbs./in.^3 , and the fibers are in the long direction.
- (a) If an in-plane compressive load, N_x , is applied in the direction parallel to the longer dimension, what is the critical buckling load, $N_{x_{cr}}$, using classical plate theory?
- (b) Using classical plate theory what is the fundamental natural frequency in Hz.?
- (c) If transverse shear deformation effects were included in the above calculations would the buckling load and fundamental natural frequency be higher, the same, or lower?
- 3.44. Consider that four plates identical to the one in Problem 3.41 above are used to fabricate a box beam 60 inches long as shown below.



- (a) Calculate the axial stiffness, EA , of this box beam.
- (b) Calculate the flexural stiffness, EI , of this box beam.

(c) Calculate the torsional stiffness, GJ , of this box beam.

- 3.45. Given a Kevlar/epoxy rectangular plate, with the unidirectional material properties given in Problem 3.7 above, for a plate of dimensions 16" x 12", and a thickness of 0.1", as shown below, simply supported on all four edges.



- What is the critical load per unit inch, $N_{x_{cr}}$, to cause plate buckling of the plate.
- What is the stress in the load direction at buckling?
- Will the plate be overstressed before it could buckle?
- What is the total weight of this plate?
- What thickness would this plate have to be to have the buckling stress equal to the compressive strength of the composite material?

CHAPTER 4

Beams, Columns and Rods of Composite Materials

4.1 Development of Classical Beam Theory

A beam, column or rod is a long thin structural component of width b , height h and length L , where $b/L \ll 1$ and $h/L \ll 1$, as shown in Figure 4.1. Its loading and its response to that loading occur in the x - z plane only. It should be noted that if there are loads in the y - z plane, those are treated exactly analogous to the loadings and response in the x - z plane. Subsequently, superposition is used to analyze the response to both loadings.

Furthermore, if the $()_{16}$ and $()_{26}$ coupling terms exist in the constitutive relations, then x - z , y - z plane coupling exist and the structure of Figure 4.1 does not behave as a beam.

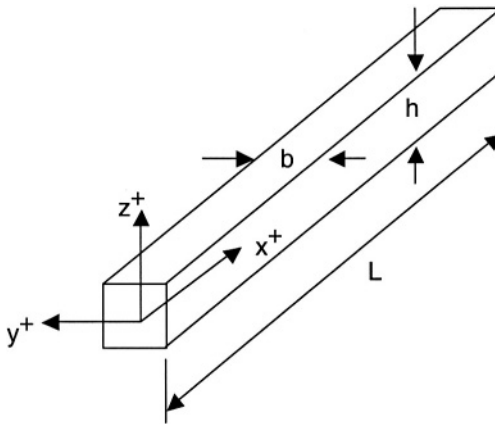


FIGURE 4.1. Nomenclature for a Beam, Column or Rod.

The term “beam” is utilized when the structure of Figure 4.1 is subjected to a lateral load in the x - z plane, in the z -direction, distributed and/or concentrated, applied to the upper and/or lower surface (that is, $z = \pm h/2$), such that bending (curvature, in the x, z plane) occurs. The term “rod” is used when the structure of Figure 4.1 is loaded in the axial direction (the x -direction) by tensile forces which try to “stretch” the structure. The term “column” is used when the structure shown is subjected to compressive forces in the x -direction which reduces the length of the structure, resulting in the compressive stresses, and/or the elastic instability (buckling) of the structure, a topic which will be discussed

later in this chapter. Combination of these loads may occur, such as when the first and third types of loads occur simultaneously, resulting in the structure being referred to as a “beam column”.

As a simple first example, consider the beam to be loaded in the x - z plane only, whether the loading is lateral, in-plane tensile, in-plane compressive or combinations thereof. Also, for simplicity, ignore the thermal and moisture effects (that is, hygrothermal effects) which add on to the strain terms in the constitutive equations given in Chapter 2. Because a beam is so narrow ($b \ll L$), strains are ignored in the y -direction, implying that all Poisson’s ratio effects can be ignored (that is a classical beam assumption). Lastly, as stated previously, there is no y -direction dependence on any quantity involved in the set of governing equations.

Looking then at Equation (2.66), the above assumptions dictate that the remaining constitutive equations for this beam are

$$\begin{bmatrix} N_x \\ M_x \end{bmatrix} = \begin{bmatrix} A_{11} & B_{11} \\ B_{11} & D_{11} \end{bmatrix} \begin{bmatrix} \epsilon_x^0 \\ \kappa_x \end{bmatrix} \quad (4.1)$$

and from Equation (2.69), if transverse shear deformation effects are considered,

$$Q_x = 2A_{55}\epsilon_{xz} \quad (4.2)$$

If the beam has mid-plane symmetry, as the majority of composite constructions do, then $B_{ij} = 0$, hence $B_{11} = 0$, and the equations above in Equation (4.1) become uncoupled, i.e.,

$$N_x = A_{11}\epsilon_x^0 \quad (4.3)$$

$$M_x = D_{11}\kappa_x \quad (4.4)$$

Note that without B_{11} , the in-plane load, N_x , and its resulting strain ϵ_x^0 are completely uncoupled from the stress couple, M_x , and its resulting curvature, κ_x .

In most composite constructions, transverse shear deformation cannot be ignored (that is, $\epsilon_{xz} \neq 0$), because it significantly affects the lateral deformation, w ; the natural frequencies of vibration; and the buckling loads. Yet, stress levels are only moderately affected by its inclusion and the simplified analytical methods, neglecting transverse shear deformation can be used for preliminary or approximate design to “size” the structure initially. So for this initial example, assume $\epsilon_{xz} = 0$, and hence Equation (4.2) will be ignored in what follows.

Looking now to the plate equilibrium equations of the previous chapter, (3.9, 3.12 and 3.14), from the beam assumptions made, it is seen that

$N_y = N_{xy} = M_y = M_{xy} = Q_y = \tau_{1y} = \tau_{2y} = 0$; hence the remaining equilibrium equations become:

$$\frac{dN_x}{dx} + \tau_{1x} - \tau_{2x} = 0 \quad (4.5)$$

$$\frac{dQ_x}{dx} + p_1 - p_2 = 0 \quad (4.6)$$

$$\frac{dM_x}{dx} - Q_x + \frac{h}{2}[\tau_{1x} + \tau_{2x}] = 0. \quad (4.7)$$

Again, for simplicity of example, assume the surface shear stresses τ_{1x} and τ_{2x} are zero. Also it is seen that the beam will only react to the difference between p_1 and p_2 the normal surface traction on the top and bottom surface, hence:

$$p(x) = p_1 - p_2. \quad (4.8)$$

The result is that Equations (4.5) through (4.8) become

$$\frac{dN_x}{dx} = 0 \quad (4.9)$$

$$\frac{dQ_x}{dx} + p(x) = 0 \quad (4.10)$$

$$\frac{dM_x}{dx} - Q_x = 0. \quad (4.11)$$

It should be remembered that in the above, the N_x , Q_x and M_x quantities are respectively plate type quantities which are per unit edge distance in the y -direction, and hence apply directly to a beam of "unit" width. However, since nothing varies in the y -direction for the beam in question, it is both traditional and easy to multiply all of the above equations by the beam width b . Hence, one can define the usual beam resultants, moments and loadings to be:

$$P \equiv N_x b, \quad V \equiv Q_x b, \quad M_b \equiv M_x b, \quad q(x) \equiv p(x)b \quad (4.12)$$

Therefore, using Equations (2.57), (2.62), (4.3), (4.4) and (4.9) through (4.12) the governing equations for a beam of composite materials or even a simple isotropic single layer beam, with mid-plane symmetry subjected to lateral and in-plane loads, ignoring hygrothermal effects and transverse shear deformation are:

$$P = bA_{11}\varepsilon_x^0 = bA_{11} \frac{du_0}{dx} \quad (4.13)$$

$$M_b = bD_{11}\kappa_x = -bD_{11} \frac{d^2w}{dx^2} \quad (4.14)$$

$$\frac{dP}{dx} = 0 \quad (4.15)$$

$$\frac{dV}{dx} + q(x) = 0 \quad (4.16)$$

$$\frac{dM_b}{dx} - V = 0 \quad (4.17)$$

From Equation (4.15) it is seen that $P = \text{constant}$ (as can also be seen from a simple free-body diagram of a beam), and therefore integration of Equation (4.13) gives the solution for the mid-surface in-plane displacement, u_0 :

$$u_0(x) = \left(\frac{P}{bA_{11}} \right) x + C_0 \quad (4.18)$$

wherein C_0 is a constant of integration determined by where $u_0(x)$ is specified. If the rod is loaded by a tensile axial load P only, Equation (4.18) provides the displacement, from which all stresses in every ply can be determined by

$$(\sigma_x)_k = (\bar{Q}_{11})_k (\varepsilon_x^0) = (\bar{Q}_{11})_k \left(\frac{du_0}{dx} \right) \quad (4.19)$$

If P is a compressive load, the same equations apply, except that if the load P_{cr} that would cause buckling is sought, a more refined theory is needed, which will be discussed later in this chapter in Section 4.10.

Analogously, substituting Equation (4.14) into (4.17) and the result into Equation (4.16) results in the following differential equation for the bending of the beam:

$$bD_{11} \frac{d^4w}{dx^4} = q(x). \quad (4.20)$$

This is the governing differential equation for a composite material beam with $B_{11} = \Delta T = \Delta m = \varepsilon_{xz} = 0$. Four straightforward integrations of Equation (4.20) yield the entire solution including four constants of integration with which to satisfy the boundary conditions. It can easily be shown that under these conditions if the beam involves only a one layer, isotropic material, then $bA_{11} = EA = Ebh$ and $bD_{11} = EI = Ebh^3/12$, for a beam of rectangular cross-section, remembering that in beam theory, Poisson's ratio effects are ignored.

From Equation (4.20), the governing differential beam equation for the mid-plane symmetric beam can be written as:

$$\frac{d^4 w}{dx^4} = \frac{q(x)}{bD_{11}} \quad (4.21)$$

$$\frac{d^3 w}{dx^3} = \frac{1}{bD_{11}} \int q(x) dx + C_1 \quad (4.22)$$

$$\frac{d^2 w}{dx^2} = \frac{1}{bD_{11}} \iint q(x) dx dx + C_1 x + C_2 \quad (4.23)$$

$$\frac{dw}{dx} = \frac{1}{bD_{11}} \iiint q(x) dx dx dx + \frac{C_1 x^2}{2} + C_2 x + C_3 \quad (4.24)$$

$$w(x) = \frac{1}{bD_{11}} \iiint q(x) dx dx dx dx + \frac{C_1 x^3}{6} + \frac{C_2 x^2}{2} + C_3 x + C_4 \quad (4.25)$$

Once the solution of $w(x)$ is found, the bending stresses in each of the laminae are found by

$$(\sigma_x)_k = z(\bar{Q}_{11})_k (\kappa_x) = -(\bar{Q}_{11})_k z \frac{d^2 w}{dx^2} \quad (4.26)$$

Obviously if both in-plane and lateral loads occur simultaneously, then the stresses are found by the sum of Equations (4.19) and (4.26)

$$(\sigma_x)_k = (\bar{Q}_{11})_k \frac{du_0}{dx} - (\bar{Q}_{11})_k z \frac{d^2 w}{dx^2}. \quad (4.27)$$

Thus the theory for the classical beam, i.e., no transverse shear deformation, with composite materials or isotropic materials, single layer or multi-ply, has been developed; now for some solutions.

4.2 Some Composite Beam Solutions

From the theory for a composite beam-rod-column developed in Section 4.1, solutions to all such problems can be found directly.

For the bending of a beam, the equations (4.21) through (4.25) result in four constants of integration, which are used to satisfy the boundary conditions at each end of the beam. Discussions of classical boundary conditions are found in any undergraduate mechanics textbook and so will not be developed herein. There are three classical edge boundary conditions: simple-support, clamped and free. For each, the explicit boundary conditions are:

<i>Simple Support:</i>	<i>Clamped:</i>	<i>Free:</i>
$w = 0$	$w = 0$	$M_b = 0$
$M_b = 0$	$\frac{dw}{dx} = 0$	$V_b = 0$

(4.28)

As an example, consider a composite beam clamped at each end subjected to a uniform lateral load $q(x) = -q_0$, where q_0 is a constant as shown in Figure 4.2.

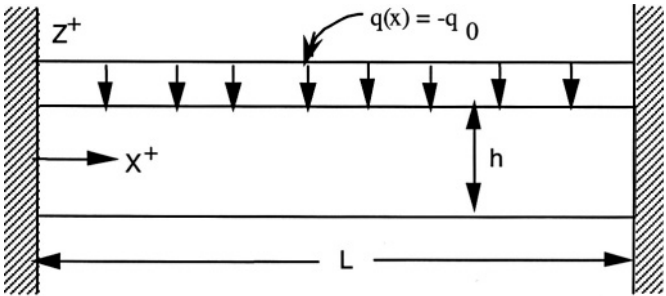


FIGURE 4.2. Clamped - Clamped beam with a uniform lateral load.

The clamped boundary conditions are used now to solve for the constants C_1 through C_4 .

$$w(0) = 0 = C_4$$

$$\frac{dw}{dx}(0) = 0 = C_3$$

$$w(L)=0=-\frac{q_0 L^4}{24bD_{11}}+\frac{C_1 L^3}{6}+\frac{C_2 L^2}{2}$$

$$\frac{dw}{dx}(L)=0=-\frac{q_0 L^3}{6bD_{11}}+\frac{C_1 L^2}{2}+C_2 L$$

Therefore,

$$C_1 = \frac{q_0 L}{2bD_{11}} \text{ and } C_2 = -\frac{q_0 L^2}{12bD_{11}}$$

Finally,

$$w(x) = -\frac{q_0}{24bD_{11}} [x^4 - 2Lx^3 + L^2 x^2] \quad (4.29)$$

One objective of such analysis is to determine the maximum deflection, because some structures are deflection or stiffness critical. Therefore, it is seen (in this case through symmetry) that

$$w_{\max} = w(L/2) = -\frac{q_0 L^4}{384bD_{11}} \quad (4.30)$$

Similarly, the location of the maximum stress must be determined in order to calculate that value because quite often structures are strength critical. From Equations (4.14) and (4.29),

$$M_b = -bD_{11} \frac{d^2 w}{dx^2} = \frac{q_0}{12} [6x^2 - 6Lx + L^2] \quad (4.31)$$

Note that the bending moment M_b is not dependent upon any elastic material property. It is seen that the maximum value occurs at $x = 0$ and L , and is

$$M_{b_{\max}} = M_b(0) = M_b(L) = \frac{q_0 L^2}{12} = -bD_{11} \frac{d^2 w(0)}{dx^2} = -bD_{11} \frac{d^2 w(L)}{dx^2} \quad (4.32)$$

To tie in the mechanics of single layer isotropic classical beams, with the mechanics of a symmetric laminated composite beam or rectangular cross-section, the following analyses are made.

Suppose the beam were of a one layer, isotropic material then the maximum stress would be at the top and bottom of the beam at each end, that is, $z = \pm h/2$, and the traditional equation would be used

$$\sigma_x = \frac{Mbz}{I} \text{ where } I = bh^3/12 \text{ for a rectangular beam}$$

So

$$\sigma_{x_{\max}} = \sigma_x(0, \pm h/2) = \sigma_x(L, \pm h/2) = \pm \frac{6M b_{\max}}{bh^2} = \pm \frac{q_0 L^2}{2bh^2} \quad (4.33)$$

from which the maximum stress can be calculated, and compared to the allowable stress properties for the material.

For a beam of a given composite material, the calculation is not so simple. Having found $M_{b_{\max}}$ through Equation (4.32), Equation (4.14) must be utilized to find the maximum curvature $\kappa_{x_{\max}}$,

$$\kappa_{x_{\max}} = \kappa_x \begin{pmatrix} 0 \\ L \end{pmatrix} = \frac{M_{b_{\max}}}{bD_{11}} = + \frac{q_0 L^2}{12bD_{11}} = \left(- \frac{d^2 w}{dx^2} \right) \quad (4.34)$$

Then, and only then, can the maximum stress be calculated for each lamina through the use of Equations (4.26) and (4.34)

$$[\sigma_x]_{k_{\max}} = [\bar{Q}_{11}]_k [\kappa_{x_{\max}}] z = -[\bar{Q}_{11}]_k \left(\frac{d^2 w}{dx^2} \right)_{\max} z = \frac{[\bar{Q}_{11}]_k q_0 L^2 z}{12bD_{11}} \quad (4.35)$$

Then, this $[\sigma_x]_{k_{\max}}$ must be compared with the allowable stress values (that is, failure stress) for each lamina with its specific orientation and composite material system.

Keep in mind that all of the above analysis could be much more complicated even for a composite beam, if the composite beam were not mid-plane symmetric ($B_{11} \neq 0$) or if hygrothermal effects were present (that is, $\epsilon_x^0 + z\kappa_x - \alpha_x \Delta T - \beta_x \Delta m$), all of which will be discussed in later sections of this chapter.

As a second example of solutions to beam problems, consider a beam cantilevered from the end $x = 0$ as shown in Figure 4.3 where the load $q(x) = -q_0$, a constant.

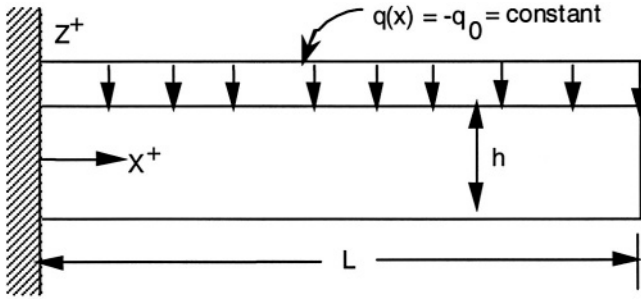


FIGURE 4.3. Clamped - Free Beam Subjected to a Uniform Load.

Again, the solution is (see Equation 4.25),

$$w(x) = -\frac{q_0 x^4}{24bD_{11}} + \frac{C_1 x^3}{6} + \frac{C_2 x^2}{2} + C_3 x + C_4. \quad (4.36)$$

Again, as before, because $w(0) = 0$ and $dw/dx(0) = 0$,

$$C_3 = C_4 = 0.$$

The other two boundary conditions are $M_b(L) = 0$ and $V(L) = 0$, which is analogous to saying

$$\begin{aligned} \frac{d^2 w}{dx^2}(L) &= 0 = -\frac{q_0 L^2}{2bD_{11}} + C_1 L + C_2 \\ \frac{d^3 w}{dx^3}(L) &= 0 = -\frac{q_0 L}{bD_{11}} + C_1. \end{aligned}$$

Hence:

$$C_1 = \frac{q_0 L}{bD_{11}} \text{ and } C_2 = -\frac{q_0 L^2}{2bD_{11}}.$$

Thus:

$$w(x) = -\frac{q_0}{24bD_{11}} [x^4 - 4Lx^3 + 6L^2x^2]. \quad (4.37)$$

It is easily seen that again for maximum deflection and maximum stress couple (bending moment) that

$$w_{\max} = w(L) = -\frac{q_0 L^4}{8bD_{11}} \quad (4.38)$$

$$M_{b_{\max}} = M_b(0) = \frac{q_0 L^2}{2} \quad (4.39)$$

Again, one can use the above to investigate the maximum stresses in a single layer isotropic beam, a mid-plane symmetric composite laminate and a mid-plane symmetric composite or isotropic sandwich beam.

If this beam were of a one ply, isotropic material

$$\sigma_{x_{\max}} = \pm \frac{6M_{b_{\max}}}{bh^2} = \pm \frac{3q_0 L^2}{bh^2} \quad (4.40)$$

If the beam is made of a laminated composite material then from Equations (4.14) and (4.39)

$$\kappa_{\max} = \kappa_x(0) = \frac{M_b}{bD_{11}} = \frac{q_0 L^2}{2bD_{11}},$$

and again from Equation (4.26)

$$\sigma_{x_{\max}} = [\bar{Q}_{11}]_k z \kappa_{x_{\max}}. \quad (4.41)$$

Many more examples for beams could be given, but they would be repetitive; for these classical cases, many solutions are available in several texts, e.g., Gere and Timoshenko [1] which provide beam deflections and the location and magnitude of maximum deflections for over 20 different load-boundary condition combinations for isotropic beams. Then using the methods described above one can determine maximum deflections and stresses in isotropic and composite beams. In all cases for these composite beams $EA = bA_u$ and $EI = bD_u$ wherein Poisson's ratio effects are neglected in the A_u and D_u terms here because the structure is a beam.

4.3 Composite Beams With Abrupt Changes in Geometry or Load

It is not unusual for beams to have either abrupt discontinuities in load or geometry such as shown in Figures 4.4 or 4.5 below.

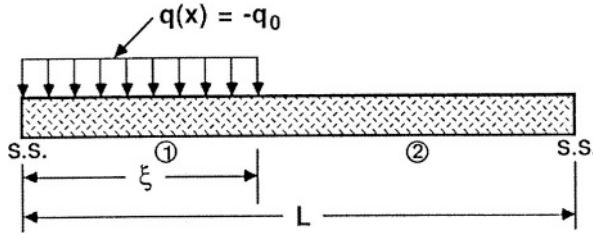


FIGURE 4.4. Uniform Beam with Discontinuous Load.

One complication arises when a beam of flexural stiffness EI or bD_{11} over the entire length is subjected to a distributed load $q(x)$ over only one portion of its length. For example, if $q(x) = -q_0$ over $0 \leq x \leq \xi$, and $q(x) = 0$ over the portion $\xi \leq x \leq L$. Because of this load discontinuity, the beam must be divided into two parts as shown in Figure 4.4. In what follows the beam equations under the load will be subscripted 1, and those dealing with the unloaded portion are subscripted 2. The boundary conditions at the ends can be easily written as follows:

$$\begin{aligned} w_1(0) &= 0 & w_2(L) &= 0 \\ M_{b_1}(0) \text{ or } \frac{d^2 w_1(0)}{dx^2} &= 0 & M_{b_2} \text{ or } \frac{d^2 w_2(L)}{dx^2} &= 0. \end{aligned} \quad (4.42)$$

Four other boundary conditions must be determined, and they describe the compatibilities that must exist at the junction of beam parts 1 and 2, namely

$$w_1(\xi) = w_2(\xi) \quad (4.43)$$

$$\frac{dw_1(\xi)}{dx} = \frac{dw_2(\xi)}{dx} \quad (4.44)$$

$$M_{b_1}(\xi) = M_{b_2}(\xi) \text{ or } \frac{d^2 w_1(\xi)}{dx^2} = \frac{d^2 w_2(\xi)}{dx^2} \quad (4.45)$$

$$V_1(\xi) = V_2(\xi) \text{ or } \frac{d^3 w_1(\xi)}{dx^3} = \frac{d^3 w_2(\xi)}{dx^3}. \quad (4.46)$$

Using the above, it is seen that there are eight equations to determine the eight boundary constants $C_{11}, C_{21}, C_{31}, C_{41}, C_{12}, C_{22}, C_{32}$ and C_{42} in Equations (4.22) through (4.25), where the second subscript is used to denote Section 1 or Section 2. The equations to solve involve solving an 8×8 set of algebraic equations and lengthy manipulations. The final constants in this example are:

$$\begin{aligned}
 C_{11} &= \frac{q_0}{bD_{11}} \left[\xi - \frac{\xi^2}{2L} \right] & C_{12} &= -\frac{q_0 \xi^2}{2bD_{11}L} \\
 C_{21} &= 0 & C_{22} &= \frac{q_0 \xi^2}{2bD_{11}} \\
 C_{31} &= \frac{q_0}{24bD_{11}} \left(-4L\xi^2 - \frac{\xi^4}{L} + \xi^3 \right) & C_{32} &= -\frac{q_0}{24bD_{11}} \left[4L\xi^2 + \frac{\xi^4}{L} \right] \\
 C_{41} &= 0 & C_{42} &= \frac{q_0 \xi^4}{24bD_{11}}.
 \end{aligned}$$

The resulting displacement equations are:

$$w_1(x) = -\frac{q_0}{24bD_{11}} \left[x^4 - 4x^3\xi + \frac{4x^3\xi^2}{L} + 4Lx\xi^2 + \frac{x\xi^4}{L} - x\xi^3 \right], \quad 0 \leq x \leq \xi \quad (4.47)$$

$$w_2(x) = -\frac{q_0}{24bD_{11}} \left[\frac{2x^3\xi^2}{L} - 6x^2\xi^2 + 4Lx\xi^2 - \frac{x\xi^4}{L} - \xi^4 \right], \quad \xi \leq x \leq L \quad (4.48)$$

The location and magnitude of the maximum deflection will occur in either Section 1 or 2 depending upon the extent of the load, i.e., where ξ is located. Then by taking second derivatives of the deflections function one can determine the curvatures and bending moments in Sections 1 and 2, and subsequently determine the locations and magnitude of the maximum stress for a given ξ .

From Equations (4.47) and (4.48), it can be seen that $\xi = 0$, if i.e. no load, the beam consists only of Section 2, and since each term has ξ in the numerator, $w = 0$, i.e., the beam is not loaded. Similarly, if $\xi = L$, the beam consists only of Section 1, the

problem is that of a simple supported beam subjected to a uniform load over the entire length of $q(x) = -q_0$, with the result that:

$$w(x) = -\frac{q_0}{24bD_{11}}[x^4 - 2Lx^3 + L^3x] \quad (4.49)$$

wherein

$$w_{\max} = w\left(\frac{L}{2}\right) = -\frac{5q_0L^4}{384bD_{11}}. \quad (4.50)$$

Subsequently, the stresses in each lamina are given by Equation (4.26), where obviously the maximum stresses occur at $x = \frac{L}{2}$ in this case.

Similarly, consider the beam shown in Figure 4.5, wherein the dimensions change from h_1 to h_2 , hence in the Section 1, the flexural stiffness is $(bD_{11})_1$, on the right $(bD_{11})_2$.

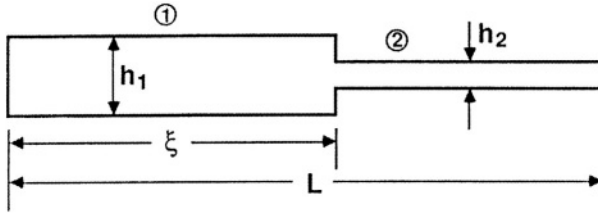


FIGURE 4.5. Beam of discontinuous flexural stiffness.

Again, Equations (4.22) through (4.25) are used for each section, satisfying C_{11} through C_{42} , as in the previous section by solving for the boundary conditions at each end, and the four matching boundary conditions at $x = \xi$, wherein for Section 1, $(bD_{11})_1$ is used and for the right section $(bD_{11})_2$ is used.

It is now seen that in general, for each load discontinuity and/or each structural discontinuity, the beam must be divided into sections involving continuous loads and continuous geometry, with rational matching of conditions at each boundary. For example, if there were three load discontinuities and two abrupt changes in geometry, all at different axial locations, the beam must be divided into six sections, and twenty-four equations must be solved to obtain twenty-four boundary value constants. Then, an investigation must be made of candidate sections to determine in which the maximum deflection and in which the maximum stress occurs. This can become quite lengthy.

Another approach to these complicated problems will be illustrated in Chapter 6, Energy Methods.

Finally, consider a beam of length L , subjected to a concentrated load P located at $x = \xi$, as shown in Figure 4.6.

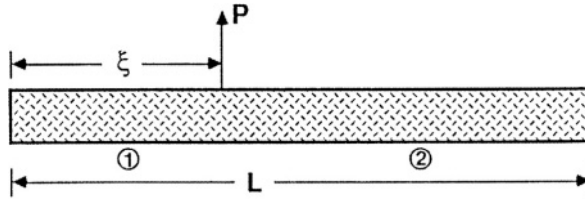


FIGURE 4.6. Beam Subjected to a Concentrated Lateral Load.

Again, because of the discontinuity, the beam must be divided into sections at each discontinuity, such as Section 1 from $0 \leq x \leq \xi$, and Section 2 at $\xi \leq x \leq L$, as shown in Figure 4.6.

Here, there is no lateral distributed load, $q(x)$, so only the homogeneous solution of Equation (4.25) is used for each of the two sections, or

$$w_i(x) = \frac{C_{1i}x^3}{6} + \frac{C_{2i}x^2}{2} + C_{3i}x + C_{4i} \quad (i = 1, 2). \quad (4.51)$$

For this class of problems, again there are eight boundary conditions; four to be determined to satisfy the boundary conditions at the ends of the beam, and four to properly match conditions at the load P .

At the ends, the boundary conditions such as simple support, clamped, free, etc. can be imposed using Equations (4.22) through (4.25) for example.

At $x = \xi$, the load position, it is clear that for Sections 1 and 2, the deflection, slope, and bending moment must match. Therefore,

$$w_1(\xi) = w_2(\xi) \quad (4.52)$$

$$\frac{dw_1(\xi)}{dx} = \frac{dw_2(\xi)}{dx} \quad (4.53)$$

$$M_{b_1}(\xi) = M_{b_2}(\xi) \quad \text{or} \quad \frac{d^2w_1(\xi)}{dx^2} = \frac{d^2w_2(\xi)}{dx^2}. \quad (4.54)$$

Looking at the vertical equilibrium, it is seen that the last boundary condition is

$$V_1(\xi) - V_2(\xi) = P \quad \text{or} \quad -\frac{d^3 w_1(\xi)}{dx^3} + \frac{d^3 w_2(\xi)}{dx^3} = \frac{P}{bD_{11}}. \quad (4.55)$$

Using Equations (4.22) through (4.25) to satisfy the above boundary conditions, the solutions for a beam with various boundary conditions are:

BEAM CLAMPED AT EACH END

$$w_1(x) = \frac{P\xi}{2bD_{11}} \left[1 - \left(\frac{\xi}{L} \right)^2 \right] x^2 \quad (4.56)$$

$$- \frac{P}{6bD_{11}} \left[1 - 3 \left(\frac{\xi}{L} \right)^2 + 2 \left(\frac{\xi}{L} \right)^3 \right] x^3, \quad 0 \leq x \leq \xi$$

$$w_2(x) = -\frac{P\xi^3}{6bD_{11}} + \frac{P\xi^2 x}{2bD_{11}} + \frac{P\xi x^2}{2bD_{11}} \left[-2 + \frac{\xi}{L} \right] \quad (4.57)$$

$$+ \frac{Px^3}{6bD_{11}} \left(\frac{\xi}{L} \right)^2 \left[3 - 2 \left(\frac{\xi}{L} \right) \right], \quad \xi \leq x \leq L.$$

BEAM CLAMPED AT $x = 0$, SIMPLY SUPPORTED AT $x = L$

$$w_1(x) = \frac{PL}{4bD_{11}} \left(\frac{\xi}{L} \right) \left[2 - 3 \left(\frac{\xi}{L} \right) + \left(\frac{\xi}{L} \right)^2 \right] x^2 \quad (4.58)$$

$$- \frac{P}{12bD_{11}} \left[2 - 3 \left(\frac{\xi}{L} \right)^2 + \left(\frac{\xi}{L} \right)^3 \right] x^3, \quad 0 \leq x \leq \xi$$

$$w_2(x) = -\frac{P\xi^3}{6bD_{11}} + \frac{P\xi^2 x}{2bD_{11}} - \frac{PLx^2}{4bD_{11}} \left(\frac{\xi}{L} \right)^2 \left[3 - \left(\frac{\xi}{L} \right) \right] \quad (4.59)$$

$$+ \frac{Px^3}{12bD_{11}} \left(\frac{\xi}{L} \right)^2 \left[3 - \frac{\xi}{L} \right], \quad \xi \leq x \leq L.$$

BEAM CLAMPED AT $x = 0$, FREE AT $x = L$

$$w_1(x) = \frac{P\xi x^2}{2bD_{11}} - \frac{Px^3}{2bD_{11}}, \quad 0 \leq x \leq \xi \quad (4.60)$$

$$w_2(x) = -\frac{P\xi x^3}{6bD_{11}} + \frac{P\xi^2 x}{2bD_{11}}, \quad \xi \leq x \leq L. \quad (4.61)$$

BEAM SIMPLY SUPPORTED AT EACH END

$$w_1(x) = \frac{PL^2 x}{6bD_{11}} \left(\frac{\xi}{L} \right) \left[2 + \left(\frac{\xi}{L} \right) - 3 \left(\frac{\xi}{L} \right)^2 \right] \quad (4.62)$$

$$- \frac{Px^3}{6bD_{11}} \left[1 - \frac{\xi}{L} \right], \quad 0 \leq x \leq \xi$$

$$w_2(x) = -\frac{P\xi^3 x}{6bD_{11}} + \frac{PL^2 x}{6bD_{11}} \left(\frac{\xi}{L} \right) \left[2 + \frac{\xi}{L} \right] \quad (4.63)$$

$$- \frac{P\xi x^2}{2bD_{11}} + \frac{Px^3}{6bD_{11}} \left(\frac{\xi}{L} \right), \quad \xi \leq x \leq L.$$

These equations are quite general for a beam of uniform flexural stiffness bD_{11} , subjected to any concentrated load P acting at $x = \xi$. For instance, Equation (4.60) can be used for a clamped-free beam with a load P acting at the tip of $x = L$ by letting $\xi = L$.

Also because the equations evolve from linear theory, superposition can be used if there are two concentrated loads at two different locations, but care must be used to accurately depict regions to the left and right of each load to insure correct solutions.

After the solutions $w_i(x)$ are found, Equations (4.14) and (4.17) are used to obtain bending moments and shear resultants, and Equation (4.26) is used to determine stresses everywhere.

4.4 Solutions by Green's Functions

From Section 4.3, consider a composite beam subjected to a unit concentrated load, i.e., $P = 1$. By way of example, consider the beam simply supported at each end given by Equations (4.62) and (4.63). In this case,

$$w_1(x) = \frac{L^2 x}{6bD_{11}} \left(\frac{\xi}{L} \right) \left[2 + \left(\frac{\xi}{L} \right) - 3 \left(\frac{\xi}{L} \right)^2 \right] - \frac{x^3}{6bD_{11}} \left[1 - \left(\frac{\xi}{L} \right) \right] = G_1(x, \xi), \quad 0 \leq x \leq \xi \quad (4.64)$$

$$w_2(x) = -\frac{\xi^3}{6bD_{11}} + \frac{L^2 x}{6EI} \left(\frac{\xi}{L} \right) \left[2 + \frac{\xi}{L} \right] - \frac{\xi x^2}{2bD_{11}} + \frac{x^3}{6EI} \left(\frac{\xi}{L} \right) = G_2(x, \xi), \quad \xi \leq x \leq L. \quad (4.65)$$

Note that $G_1(x)$ is the deflection to the left of the load, $G_2(x)$ to the right of the load. Green's function G_1 and G_2 can be defined as the deflection at x due to a unit load at ξ .

It can be reasoned that any distributed load $q(x)$ is in fact an infinity of concentrated loads, which can be summed to obtain the solution of the response to a distributed load. Because of the infinity of concentrated loads, the infinite summation can be replaced by an integration such that the following is correct.

$$w(x) = \int_x^L G_1(x, \xi) q(\xi) d\xi + \int_0^x G_2(x, \xi) q(\xi) d\xi. \quad (4.66)$$

For a beam simply supported at each end Equations (4.66) and (4.67) would be inserted for G_1 and G_2 , and other analogous expressions from Section 4.3 would be used for beams with other boundary conditions.

As an example, solving Equations (4.68), (4.66) and (4.67) with $q(x) = -q_0$, a uniform load over the entire length, results in

$$w(x) = -\frac{q_0}{24bD_{11}} (x^4 - 2Lx^3 + L^3x) \quad (4.67)$$

which is the solution obtained through solving the governing differential equation (4.20) and satisfying the appropriate boundary conditions, with the explicit solution shown in

Equation (4.49). Likewise, using the Green's function approach discussed above for a uniform load results in Equation (4.29) for the clamped-clamped beam, and Equation (4.37) for the cantilevered beam.

Thus, with the use of Green's functions one uses an integral equation where the Green's functions satisfy the boundary conditions, rather than solving the governing differential equation and matching boundary conditions. This alternative approach

1. is general for any governing differential equation such as a beam, plate or shell.
2. can save great computational difficulty for complicated problems.

As an example of the latter, consider the following problem (Figure 4.7):

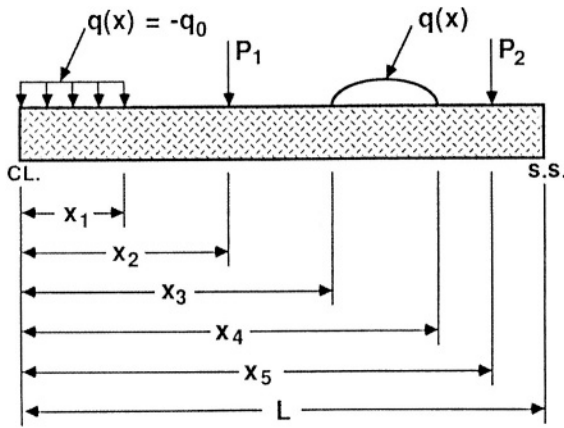


FIGURE 4.7. Beam subjected to several lateral loads.

To solve the problem above, developing a solution requires solving the governing differential equations and matching boundary conditions involves dividing the beam into six sections, wherein twenty-four boundary value constants must be solved for, and particular solutions obtained for each of the distributed loads. As a result, $w(x)$ is determined everywhere after all constants are solved for simultaneously.

Using the Green's function approach, suppose that one hypothesizes that the maximum deflection and bending moment occurs in the region $x_3 \leq x \leq x_4$. One obtains $G_1(x, \xi)$ and $G_2(x, \xi)$ for the clamped-simply supported beam from Equations (4.58) and (4.59). Then for $x_3 \leq x \leq x_4$, $w(x)$ is given by

$$\begin{aligned}
w(x) = & \int_0^{x_1} G_2(x, \xi)(-q_0) d\xi - G_2(x, x_2)P_1 \\
& - \int_{x_3}^x G_2(x, \xi)q(\xi) d\xi - \int_x^{x_4} G_1(x, \xi)q(\xi) d\xi \\
& - G_1(x, \xi)P_2 \quad \text{for } x_3 \leq x \leq x_4.
\end{aligned} \tag{4.68}$$

To check that the maxima occur in this region, one could easily investigate adjoining regions, i.e., $x_2 \leq x \leq x_3$, and $x_4 \leq x \leq x_5$. Having obtained Equation (4.78), maximum deflections and stresses are determined straightforwardly as shown before.

4.5 Composite Beams of Continuously Varying Cross-Section

There are many applications in which beams can be better designed and utilized through having a variable cross-section rather than a constant cross-section discussed in Sections 4.1 through 4.4. In that case, the $EI = bD_{11}$ and $EA = bA_{11}$ are functions of x , the length dimension, i.e., $bD_{11}(x)$ and $bA_{11}(x)$.

In that case, it is straightforward to derive the governing equation of beam bending, analogous to the derivation leading to Equation (4.20). The result is

$$\frac{d^2}{dx^2} \left[EI(x) \frac{d^2 w}{dx^2} \right] = q(x) \tag{4.69}$$

where here $I(x)$ is a continuously varying function of x , and the mid-surface of the beam is $z = 0$. Depending on what that function of x is, the solution could be rather complicated and/or tedious.

For these types of problems, Galerkin's method is well suited. No attempt is made here to provide a detailed comprehensive introduction of Galerkin's method, which is well treated in numerous other texts. However, consider an ordinary differential equation (although the method is equally useful for partial differential equations as well as nonlinear equations).

$$L[w(x)] - q(x) = 0 \tag{4.70}$$

where L is any differential operator, and $q(x)$ is a forcing function. Boundary conditions must be homogeneous; if not, a transformation of variables must be made first to attain homogeneous boundary conditions.

In Galerkin's method one assumes a complete set of coordinate functions $X_n(x)$, $n = 1, 2, 3, \dots, N$, which satisfies the prescribed homogeneous boundary conditions. Although these functions need not be an orthogonal set, if they are, the procedure is much simpler. Therefore, assume

$$w_n(x) = \sum_{n=1}^N C_n X_n(x) \quad (4.71)$$

where the C_n are constants.

By using only the first N terms, an error $\varepsilon_N(x)$ can be defined from Equations (4.73) and (4.72), as

$$\varepsilon_N(x) = L(w_N) - q(x). \quad (4.72)$$

If $\varepsilon_N(x)$ is sufficiently small, then $w_n(x)$ of Equation (4.73) is considered to be a satisfactory approximation to $w(x)$. So $\varepsilon_n(x)$ can be viewed as an error function, and the task is to select proper values of C_n to minimize $\varepsilon_n(x)$. In the Galerkin method, this is done by the following orthogonality condition:

$$\int_0^L \varepsilon_N(x) X_m(x) dx = 0 \quad \text{where } 1 \leq m \leq N. \quad (4.73)$$

This is equivalent to minimizing the mean square error and insures that $w_n(x)$ will converge to $w(x)$ in the mean.

From above, this is equivalent to stating:

$$\int_0^L \left[L \left(\sum_{n=1}^N C_n X_n(x) - q(x) \right) \right] X_m(x) dx = 0, \quad m = 1, 2, 3, \dots, N. \quad (4.74)$$

Therefore, Equation (4.76) is a set of N algebraic equations through which one can determine the C_n to minimize $\varepsilon_n(x)$. This is a powerful technique.

As an example, consider a tapered beam subjected to a lateral distributed load $q(x)$, as developed by R.L. Daugherty when he taught a course using the first edition of this text. Assume the variable stiffness can be written as:

$$EI(x) = EI_0 f(x). \quad (4.75)$$

Equation (4.71) can then be written as

$$(fw'')'' = \frac{q(x)}{EI_0} \quad (4.76)$$

where primes denote differentiation with respect to x . Hence,

$$fw^{iv} + 2f'w''' + f''w'' = \frac{q(x)}{EI_0} \quad (4.77)$$

If the beam is simply supported, i.e. $w = w'' = 0$ at $x=0, L$, coordinate functions can be chosen as follows:

$$X_n(x) = \sin \frac{n\pi x}{L} = \sin \alpha_n x \text{ where } \alpha_n = n\pi / L. \quad (4.78)$$

These are a complete set of functions, which satisfy the boundary conditions. Thus,

$$w_n(x) = \sum_{n=1}^{\infty} C_n \sin \alpha_n x \quad (4.79)$$

and from Equation (4.74)

$$\begin{aligned} \varepsilon_n(x) = \sum_{n=1}^{\infty} \{ & C_n f \alpha_n^4 \sin \alpha_n x - 2C_n f' \alpha_n^3 \cos \alpha_n x - f'' C_n \alpha_n^2 \sin \alpha_n x \} \\ & - \frac{q(x)}{EI_0}. \end{aligned} \quad (4.80)$$

From Equations (4.75) and (4.76), Galerkin's procedure requires

$$\begin{aligned} \sum_{n=1}^N C_n \left\{ \int_0^L f \alpha_n^4 \sin \alpha_n x \sin \alpha_m x dx - \int_0^L f' \alpha_n^3 \cos \alpha_n x \sin \alpha_m x dx \right. \\ \left. - \int_0^L f'' \alpha_n^2 \sin \alpha_n x \sin \alpha_m x dx \right\} - \int_0^L \frac{q(x)}{EI_0} \sin \alpha_m x dx = 0. \end{aligned} \quad (4.81)$$

To continue the example, let $f(x) = 1 + (x/L)$, then Equation (4.83) becomes:

$$\begin{aligned} \sum_{n=1}^N C_n \left\{ \int_0^L \alpha_n^4 \left(1 + \frac{x}{L} \right) \sin \alpha_n x \sin \alpha_m x dx \right. \\ \left. - \int_0^L \left(\frac{1}{L} \right) 2\alpha_n^3 \cos \alpha_n x \sin \alpha_m x dx \right\} - \int_0^L \frac{q(x)}{EI_0} \sin \alpha_m x dx = 0. \end{aligned} \quad (4.82)$$

For $n \neq m$

$$\int_0^L \left(1 + \frac{x}{L}\right) \sin \alpha_n x \sin \alpha_m x dx = \frac{[(-1)^{n+m} - 1] 2\alpha_n \alpha_m}{(\alpha_n^2 - \alpha_m^2)^2} \frac{1}{L}$$

$$\int_0^L \cos \alpha_n x \sin \alpha_m x dx = \frac{\alpha_m}{(\alpha_n^2 - \alpha_m^2)} [(-1)^{n+m} - 1]$$

So Equation (4.82) is, for $n \neq m$

$$\sum_{n=1}^N C_n \left\{ \frac{2\alpha_n^5 \alpha_m}{L} \frac{[(-1)^{n+m} - 1]}{(\alpha_n^2 - \alpha_m^2)^2} - \frac{2\alpha_n^3 \alpha_m}{L} \frac{[(-1)^{n+m} - 1]}{\alpha_n^2 - \alpha_m^2} \right\}$$

(4.83)

$$= \int_0^L \frac{q(x)}{EI_0} \sin \alpha_m x dx.$$

For $n = m$

$$\int_0^L \left(1 + \frac{x}{L}\right) \sin \alpha_n x \sin \alpha_m x dx = 3L/4$$

(4.84)

$$\int_0^L \cos \alpha_n x \sin \alpha_m x dx = 0.$$

Thus, Equation (4.82) becomes for $n = m$

$$\sum_{n=1}^N C_n \left(\frac{3L\alpha_n^4}{4} \right) = \int_0^L \frac{q(x)}{EI_0} \sin \alpha_m x dx.$$

If N is taken as 3 for example, the final set of three non-homogeneous algebraic equations are written as follows to obtain C_1 , C_2 and C_3 . The first, second and third equations are for $m = 1, 2, 3$, respectively.

$$C_1 \left(\frac{3L\alpha_1^4}{4} \right) + C_2 \left[\frac{2\alpha_2^5 \alpha_1 (-2)}{L(\alpha_2^2 - \alpha_1^2)^2} - \frac{2\alpha_2^3 \alpha_1 (-2)}{L(\alpha_2^2 - \alpha_1^2)} \right] = \int_0^L \frac{q(x)}{EI_0} \sin \alpha_1 x dx$$

$$\begin{aligned}
& C_1 \left[\frac{2\alpha_1^5 \alpha_2 (-2)}{L(\alpha_1^2 - \alpha_2^2)^2} - \frac{2\alpha_1^3 \alpha_2 (-2)}{L(\alpha_1^2 - \alpha_2^2)} \right] + C_2 \left(\frac{3L\alpha_2^4}{4} \right) \\
& + C_3 \left[\frac{2\alpha_3^5 \alpha_2 (-2)}{L(\alpha_3^2 - \alpha_2^2)^2} - \frac{2\alpha_3^3 \alpha_2 (-2)}{L(\alpha_3^2 - \alpha_2^2)} \right] = \int_0^L \frac{q(x)}{EI_0} \sin \alpha_2 x dx \\
& C_2 \left[\frac{2\alpha_2^5 \alpha_3 (-2)}{L(\alpha_2^2 - \alpha_3^2)^2} - \frac{2\alpha_2^3 \alpha_3 (-2)}{L(\alpha_2^2 - \alpha_3^2)} \right] + C_3 \left(\frac{3L\alpha_3^4}{4} \right) = \int_0^L \frac{q(x)}{EI_0} \sin \alpha_3 x dx.
\end{aligned}$$

To complete the problem for any distributed load, $q(x)$, is straightforward.

To know what value of N to take can only be determined by solving the problem with one higher integer and determining that the previous approximation is sufficient.

One thing to remember is that the result of this method is the determination of an approximate deflection $w(x)$. To determine stresses requires solving for w'' since the bending stresses are proportional to w'' . Taking derivatives of an approximative function causes an increase in the error through differentiation. Hence, for stress critical structural members, N must be determined by suitably approximate the maximum stress. This may require a higher value of N than that required to achieve a certain accuracy in maximum deflection.

4.6 Rods

Consider the rod shown in Figure 4.1 and 4.8 subjected to a uniform tensile axial load in the x -direction.

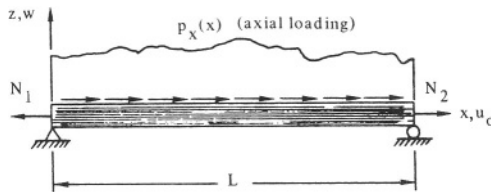


FIGURE 4.8. Axial Loading of a Simply Supported Rod.

One wishes to determine the in-plane mid-plane displacement $u_0(x)$ and the axial stresses in each lamina σ_{x_k} .

The assumptions are:

- Individual plies (laminae) are perfectly bonded (no slip).

- b. The thickness dimensions of the rod are small compared to the length of the rod.
- c. Displacements and strains are small compared to all beam/rod dimensions.
- d. A balanced, mid-plane symmetric laminate is used, i.e., $B_{11} = 0$.
- e. The loading is static.
- f. For simplicity of example hygrothermal effects are ignored.
- g. The loading is in the x - z plane.
- h. Since $b \ll L$, strains in the y -direction are ignored.

The governing equation for axial equilibrium is easily shown to be as follows, where here an axial component has been added to (4.5)

$$\frac{dN_x}{dx} + p(x) = 0 \quad (4.85)$$

where from Figure 4.8, $p(x)$ is the axial distributed force per unit area, which can be a function of x .

The mid-plane strain-axial displacement equation is again seen to be

$$\epsilon_{x_0} = \frac{\partial u_0}{\partial x} \quad (4.86)$$

The constitutive equation can be given by the following for each ply,

$$\sigma_{x_k} = E_{x_k} \epsilon_{x_k} \quad (4.87)$$

where E_{x_k} is the ply stiffness in the x -direction of the k th lamina, and is equivalent to $(Q_{11})_k$ if Poisson's ratio effects are ignored.

It has been shown in many texts that E_x can be written as follows:

$$\frac{1}{E_{x_k}} = \frac{\cos^4 \theta_k}{E_{11}} + \left(\frac{1}{G_{12}} - \frac{2\nu_{12}}{E_{11}} \right) \cos^2 \theta_k \sin^2 \theta_k + \frac{\sin^4 \theta_k}{E_{22}} \quad (4.88)$$

where all quantities have been defined previously. *Note that as alternative to using Equations (4.87) and (4.88) to obtain the stress in the k th lamina, one could use Equation (4.19) where of course $\bar{Q}_{11_k} = E_{x_k}$ because with a beam $\nu_{xy} = \nu_{yx} = 0$.

The integrated axial stress resultant N_x is seen to be, as in (4.3)

$$N_x = A_{11} \epsilon_x^0 \quad (4.89)$$

Utilizing the above equations the governing differential equation is found to be

$$\frac{d^3 u_0}{dx^3} = -\frac{1}{A_{11}} \left(\frac{dp(x)}{dx} \right) \quad (4.90)$$

If the rod is held fixed at $x = 0$ in Figure 4.8, then the boundary conditions are:

$$u_0(0) = 0$$

$$\frac{du_0}{dx}(0) = 0 \quad (4.91)$$

$$\frac{du_0(L)}{dx} = \frac{p_0 L}{A_{11}}$$

The solution is found straightforwardly to be

$$u_0(x) = \frac{p_0 L^2}{A_{11}} \left[-\frac{1}{2} \left(\frac{x}{L} \right)^2 + \frac{x}{L} \right] \quad (4.92)$$

and the stress in the k th lamina is

$$\sigma_{x_k} = \frac{p_0 L}{A_{11}} E_{x_k} \left[1 - \frac{x}{L} \right] \quad (4.93)$$

4.7 Vibration of Composite Beams

In Sections 4.1 through 4.5 the problems studied have concentrated on (1) finding the maximum deflection in composite beams to insure that they are not too large for a deflection-limited or stiffness-critical structure, and (2) determining the maximum stresses in the beam structure for those structures, which are strength critical. However, there are two other ways in which a structure can become damaged or useless; one is through a dynamic response to time-dependent loads, and the other is through the occurrence of an elastic instability (buckling).

In the former, dynamic loading on a structure can vary from a recurring cyclic loading of the same repeated magnitude, such as a structure supporting an unbalanced motor that is turning at a specified number of revolutions per minute (for example), to the other extreme of a short time, intense, nonrecurring load, termed shock or impact loading, such as a bird striking an aircraft component during flight. A continuous infinity of dynamic loads exists between these extremes of harmonic oscillation and impact.

Whole volumes are written on the dynamic response of composite structures to time-dependent loads, but that is beyond the scope of this text. There are a number of texts dealing with dynamic response of isotropic structures. However, one common thread to all dynamic responses are the natural frequencies of vibration and their associated mode shapes.

Mathematically, any continuous structure has an infinity of natural frequencies and mode shapes. If a structure is oscillated at a frequency that corresponds to a natural frequency, it will respond by a rapidly growing amplitude with time, requiring very little input energy, until such time as the structure becomes overstressed and fails, or until the oscillations become so large that nonlinear effects may limit the amplitude to a large but usually unsatisfactory value, and then considerable fatigue damage can occur.

Thus, to insure the structural integrity of any structure being designed or analyzed, the natural frequencies should be determined in order to compare them with any time-dependent loadings to which the structure will be subjected. This is to insure that the frequencies imposed and the natural frequencies differ considerably. Conversely, in designing a structure, over and above insuring that the structure will not over-deflect, or become overstressed, care should be taken to avoid resonances (that is, imposed loads having the same frequency as one or more natural frequencies).

The easiest example to illustrate this behavior is that of the bending of a beam previously studied, with mid-plane symmetry ($B_{ij} = 0$) so that there is no bending-stretching coupling and no transverse shear deformation ($\epsilon_{xz} = 0$). In this case the governing equation (4.20), is repeated below:

$$bD_{11} \frac{d^4 w}{dx^4} = q(x) \quad (4.94)$$

In Equation (4.94), it is seen that the imposed static load is written as a force per unit length. For dynamic loading, if d'Alembert's Principle were used then one can add a term to Equation (4.94) equal to the product mass and acceleration per unit length. In that case Equation (4.94) becomes

$$bD_{11} \frac{\partial^4 w(x,t)}{\partial x^4} = q(x,t) - \frac{\rho_m A \partial^2 w(x,t)}{\partial t^2} \quad (4.95)$$

where w and q both become functions of time as well as space, and derivatives therefore become partial derivatives, ρ_m is the mass density of the beam material, and here A is the beam cross-sectional area. In the above, $q(x,t)$ is now the spatially varying time-dependent forcing function causing the dynamic response, and could be anything from a harmonic oscillation to an intense one-time impact.

For a composite beam in which different laminae have differing mass densities, then in the above equations use, for a beam of rectangular cross-section,

$$\rho_m A = \rho_m b h = \sum_{k=1}^N \rho_{m_k} b (h_k - h_{k-1}) \quad (4.96)$$

However, natural frequencies for the beam occur as functions of the material properties and the geometry and hence are not affected by the forcing functions; therefore, for this study let $q(x,t)$ be zero. Thus Equation (4.94) becomes

$$bD_{11} \frac{\partial^4 w}{\partial x^4} + \rho_m A \frac{\partial^2 w}{\partial t^2} = 0 \quad (4.97)$$

One sees that this is the homogeneous equation associated with Equation (4.94). For a simple case, (the easiest one) assume the composite beam to be simply supported at each end. One may assume a spatial component of the lateral deflection to satisfy the simply-supported boundary conditions, a harmonic temporal component, and an amplitude A_n such that

$$w(x,t) = \sum_{n=1}^{\infty} A_n \sin \frac{n\pi x}{L} \cos \omega_n t \quad (4.98)$$

Here ω_n is called the natural circular frequency in radians per unit time for the n th vibrational mode. Note that in this case there is one natural frequency for each natural mode shape, for $n = 1, 2, 3, \dots$, etc.

For this to be true, then by substituting Equation (4.98) into (4.97) and solving for ω_n , it is seen that for each value of n ,

$$\omega_n = \frac{n^2 \pi^2}{L^2} \sqrt{\frac{bD_{11}}{\rho_m A}} \quad (4.99)$$

Thus, for each n there is a different natural frequency, and a different mode shape, as shown in Figure 4.9.

For each value of n , the natural frequency is important because if the beam were forced to oscillate at that particular frequency, a resonance would occur, and the amplitude would grow until some form of structural failure would occur, as discussed previously.

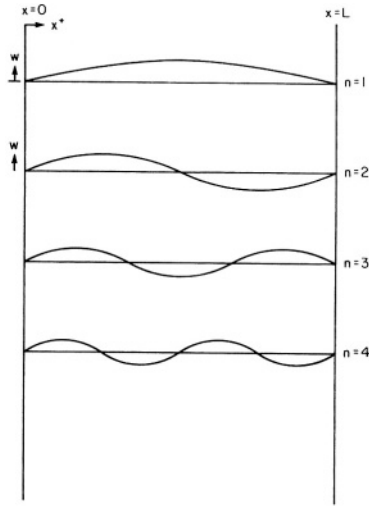


FIGURE 4.9. Simply Supported Beam Mode Shapes.

The lowest natural frequency, corresponding to $n = 1$ in this simply supported beam case, is termed the fundamental frequency. It should be noted that n could go from a value of one to infinity. However, the governing differential equation (4.97) is only applicable over a portion of this range, i.e., it applies to those mode shapes in which the classical beam equations apply. For an isotropic single-layer beam, the equation breaks down when the half wavelength becomes close to the height, h , of the beam, because then transverse shear deformation effects ($\epsilon_{xz} \neq 0$) become important, and the classical theory of Equations (4.94) and (4.97) yields increasingly inaccurate frequencies. In composite material beams, transverse-shear deformation effects can be important even for the fundamental natural frequency; but to include transverse shear deformation and rotatory inertia effects involves considerable analytical complications, that will be dealt with later in this chapter. Natural frequencies using classical beam theory, such as Equation (4.99) for the case of both ends simply supported, are useful for preliminary design and forensic analyses.

It is handy to know the natural frequencies of beams for various practical boundary conditions in order to insure that no recurring forcing functions are close to any of the natural frequencies, because that would result almost certainly in a structural failure. In each case below, the natural circular frequency ω_n in radians/unit time are given as

$$\omega_n = \alpha^2 (bD_{11} / \rho_m AL^4)^{1/2} \quad (4.100)$$

where all terms have been explained earlier except the coefficient α^2 . Once ω_n is known then the natural frequency in cycles per second (Hertz) is given by $f_n = \omega_n / 2\pi$.

The values of α^2 have been catalogued by Warburton [2], Young and Felgar [3] and Felgar [4]. Some values are given in Table 4.1 for ease of use.

Incidentally, the natural frequencies of a free-free beam equal those of a clamped-clamped beam. Also if transverse-shear deformation effects were included, each of the above natural frequencies would be lower. This will be discussed later.

TABLE 4.1. Tabulation of α^2 Values for Use in Determining Beam-Natural Frequencies

n	Simple-Simple	Simple-Clamped	Clamped-Clamped	Clamped-Free
1	9.870	15.42	22.37	3.516
2	39.48	49.96	61.67	22.03
3	88.83	104.25	120.90	61.70

4.8 Beams With Mid-Plane Asymmetry

In considering a beam that is not mid-plane symmetric, the equilibrium equations remain the same as given by Equations (4.5), (4.6) and (4.7).

However, because of mid-plane asymmetry, bending-stretching coupling occurs, and therefore the extensional and bending behavior are coupled. From Equation (2.66) it is seen that the constitutive equations for the asymmetric beam are

$$N_x = A_{11}\epsilon_{x_0} + B_{11}\kappa_x \quad (4.101)$$

$$M_x = B_{11}\epsilon_{x_0} + D_{11}\kappa_x$$

Likewise the in-plane and lateral displacements are given by the usual translation plus rotation only for classical theory:

$$u(x, z) = u_0(x) + z\bar{\alpha}(x) \quad (4.102)$$

$$w(x, z) = w(x) \text{ only}$$

Proceeding as before for the symmetric beam the two coupled differential equations can be written as follows:

$$\frac{d^4 w}{dx^4} = \frac{q(x)}{bD_{11}(1-\phi^2)} \quad (4.103)$$

$$\frac{d^2 u_0}{dx^2} = \frac{B_{11}}{A_{11}} \frac{d^3 w}{dx^3} \quad (4.104)$$

where all terms have been explained previously except for ϕ . This term is a mid-plane asymmetry parameter [5]. It is defined as

$$\phi = \frac{B_{11}}{\sqrt{A_{11}D_{11}}} \quad (4.105)$$

It is zero for a mid-plane symmetric structure, and it can be shown that physically the limits of ϕ are

$$-1 < \phi < +1. \quad (4.106)$$

In (4.103) the term $bD_{11}(1-\phi^2)$ is the reduced flexural stiffness defined by Whitney [6].

One then solves Equation (4.103) above analogous to the solutions for the mid-plane symmetric beam.

For a beam that is subjected to a uniform load per unit length q_0 , the maximum deflection can be written as [7].

$$w_{\max} = \frac{q_0 L^4}{K_2 b D_{11} (1 - \phi^2)} \quad (4.107)$$

where values of K_2 are 12 for a clamped-clamped beam; 8 for a simple-simple beam and 2 for a cantilevered beam.

When considering mid-plane asymmetric beams, the asymmetry could be due to using different composite materials for the upper and lower portions, which of course would have different mechanical properties. Alternatively, even if the same composite is used throughout the beam, there may be differing strengths and moduli in tension and compression. So care must be taken to ensure the allowable stress is not exceeded either in tension or compression.

4.9 Advanced Beam Theory for Dynamic Loading Including Mid-Plane Asymmetry

Consider the elasticity equilibrium equations in the x and z directions and the moment equilibrium equations where now, using d'Alemberts' Principle, the initial terms are included. The results are, without derivation, where in this section $p(x,t)$ is the axial load per unit cross-sectional area, and $q(x,t)$ is the lateral load per unit length of the beam.

$$\frac{\partial N_x}{\partial x} + p_x(x,t) = \rho_1 \frac{\partial^2 u_0}{\partial t^2} + \bar{\rho}_2 \frac{\partial^2 \bar{\alpha}}{\partial t^2} \quad (4.108)$$

$$\frac{\partial Q_x}{\partial x} + q(x, t) = \bar{\rho}_1 \frac{\partial^2 w}{\partial t^2} \quad (4.109)$$

$$\frac{\partial M_x}{\partial x} - Q_x + m'(x, t) = \bar{\rho}_2 \frac{\partial^2 u_0}{\partial t^2} + \bar{\rho}_3 \frac{\partial^2 \bar{\alpha}}{\partial t^2} \quad (4.110)$$

where $\bar{\rho}_1$, $\bar{\rho}_2$ and $\bar{\rho}_3$ are the longitudinal inertia, the bending-stretching coupling inertia and the rotatory inertia respectively defined as:

$$\bar{\rho}_1 = \sum_{k=1}^N \int_{h_{k-1}}^{h_k} b \rho_k dz = \sum_{k=1}^N \rho_k b (h_k - h_{k-1}) \quad (4.111)$$

$$\bar{\rho}_2 = \sum_{k=1}^N \int_{h_{k-1}}^{h_k} b \rho_k z dz = \sum_{k=1}^N \rho_k \frac{b}{2} (h_k^2 - h_{k-1}^2) \quad (4.112)$$

$$\bar{\rho}_3 = \sum_{k=1}^N \int_{h_{k-1}}^{h_k} b \rho_k z^2 dz = \sum_{k=1}^N \rho_k \frac{b}{3} (h_k^3 - h_{k-1}^3) \quad (4.113)$$

where ρ_k is the mass density of each ply, e.g. lb. - sec² / in.⁴.

These equations can be simplified to the following coupled equations:

$$\begin{aligned} \frac{\partial^2 M_x}{\partial x^2} + \frac{\partial m'(x, t)}{\partial x} + q(x, t) &= \bar{\rho}_1 \frac{\partial^2 w}{\partial t^2} + \bar{\rho}_2 \frac{\partial^3 u_0}{\partial x \partial t^2} + \bar{\rho}_3 \frac{\partial^3 \bar{\alpha}}{\partial x \partial t^2} \\ \frac{\partial N_x}{\partial x} + p_x(x, t) &= \bar{\rho}_1 \frac{\partial^2 u_0}{\partial t^2} + \bar{\rho}_3 \frac{\partial^2 \bar{\alpha}}{\partial t^2} \end{aligned} \quad (4.114)$$

Making use of the constitutive equations of (2.66), and the strain displacement relations, the following dynamic equations can be obtained in terms of the displacements:

$$A_{11} \frac{\partial^2 u_0}{\partial x^2} - B_{11} \frac{\partial^3 w}{\partial x^3} + p_x(x, t) - \frac{\partial N_T}{\partial x} - \frac{\partial N_m}{\partial x} = \bar{\rho}_1 \frac{\partial^2 u_0}{\partial t^2} - \bar{\rho}_2 \frac{\partial^3 w}{\partial x \partial t^2} \quad (4.115)$$

$$B_{11} \frac{\partial^3 u_0}{\partial x^3} - D_{11} \frac{\partial^4 w}{\partial x^4} + q(x, t) + \frac{\partial m'}{\partial x} - \frac{\partial^2 M_T}{\partial x^2} - \frac{\partial^2 M_m}{\partial x^2} =$$

$$\bar{\rho}_1 \frac{\partial^2 w}{\partial t^2} + \bar{\rho}_2 \frac{\partial^3 u_0}{\partial x \partial t^2} - \bar{\rho}_3 \frac{\partial^4 w}{\partial x^2 \partial t^2} \quad (4.116)$$

If the loads are static, these equations become

$$A_{11} \frac{d^2 u_0}{dx^2} - B_{11} \frac{d^3 w}{dx^3} + p(x) - \frac{dN_T}{dx} - \frac{dN_m}{dx} = 0 \quad (4.117)$$

$$B_{11} \frac{d^3 u_0}{dx^3} - D_{11} \frac{d^4 w}{dx^4} + q(x) + \frac{dm'}{dx} - \frac{d^2 M_T}{dx^2} - \frac{d^2 M_m}{dx^2} = 0 \quad (4.118)$$

Note, in the above the subscript T denotes thermal terms, and the subscript m denotes moisture effects. m' represents the axial moment distribution.

Solving the first equation above for the function of u_0 , which is then substituted into the second equation, the result is:

$$\left[\frac{A_{11} D_{11} - B_{11}^2}{A_{11}} \right] \frac{d^4 w}{dx^4} = q(x) + \frac{dm'}{dx} - \frac{d^2 M_T}{dx^2} - \frac{d^2 M_m}{dx^2}$$

$$- \frac{B_{11}}{A_{11}} \left[\frac{dp(x)}{dx} - \frac{d^2 N_T}{dx^2} - \frac{d^2 N_m}{dx^2} \right] \quad (4.119)$$

One sees immediately that the reduced bending stiffness is

$$\left[\frac{A_{11} D_{11} - B_{11}^2}{A_{11}} \right] = \bar{D}_{11} = b D_{11} (1 - \phi^2) \quad (4.120)$$

It is seen that if the beam is mid-plane symmetric, the last term on the right hand side of Equation (4.119) is zero.

As an example, consider a mid-plane asymmetric beam simply supported at each end, where there is a lateral load per unit length $q(x)$ only. The above equations are simply:

$$\bar{D}_{11} \frac{d^4 w}{dx^4} = q(x) \quad (4.121)$$

$$\frac{d^3 u_0}{dx^3} = \frac{q(x)}{\bar{B}_{11}} \quad (4.122)$$

$$\text{where } \bar{B}_{11} = \frac{A_{11}D_{11} - B_{11}^2}{B_{11}} \quad (4.123)$$

In this case the solution is:

$$w(x) = \frac{\bar{W}(x)}{\bar{D}_{11}} + C_1 x^3 + C_2 x^2 + C_3 x + C_4 \quad (4.124)$$

$$u_0(x) = \frac{1}{\bar{B}_{11}} \frac{d\bar{W}(x)}{dx} + C_5 x^2 + C_6 x + C_7 \quad (4.125)$$

$$\text{where } \bar{W}(x) = \iiint q(x) dx dx dx \quad (4.126)$$

In the beam simply supported at each end, with no axial load, and arbitrarily setting $u_0(0) = 0$, the solution is:

$$w(x) = \frac{1}{\bar{D}_{11}} \left\{ \bar{W}(x) + L^2 \frac{d^2 \bar{W}(0)}{dx^2} \left[\frac{1}{6} \left(\frac{x}{L} \right)^3 - \frac{1}{2} \left(\frac{x}{L} \right)^2 + \frac{1}{3} \left(\frac{x}{L} \right) \right] \right. \\ \left. + L^2 \frac{d^2 \bar{W}(L)}{dx^2} \left[\frac{1}{6} \left(\frac{x}{L} \right) - \frac{1}{6} \left(\frac{x}{L} \right)^3 \right] + \bar{W}(0) \left[\frac{x}{L} - 1 \right] - \bar{W}(L) \left(\frac{x}{L} \right) \right\} \quad (4.127)$$

$$u_0(x) = \frac{1}{\bar{B}_{11}} \left\{ \frac{d\bar{W}(x)}{dx} + L \frac{d^2 \bar{W}(0)}{dx^2} \left[\frac{1}{2} \left(\frac{x}{L} \right)^2 - \left(\frac{x}{L} \right) \right] \right. \\ \left. - \frac{L}{2} \frac{d^2 \bar{W}(L)}{dx^2} \left(\frac{x}{L} \right)^2 - \frac{d\bar{W}(0)}{dx} \right\} \quad (4.128)$$

Using now the following equations for the stress in the axial direction in the k th lamina

$$\sigma_{x_k} = E_{x_k} \left[\frac{du_0}{dx} - z \frac{d^2 w}{dx^2} \right] \quad (4.129)$$

From the foregoing $\bar{Q}_{11_k} = Q_{11_k} = E_{x_k}$, where Poisson's ratio effects are ignored for a beam. Thus, one finds that

$$\sigma_{x_k} = E_{x_k} \left[\frac{1}{\bar{B}_{11}} - \frac{z}{\bar{D}_{11}} \right] \left[\frac{d^2 \bar{W}(x)}{dx^2} + \frac{d^2 W(0)}{dx^2} \left(\frac{x}{L} - 1 \right) - \frac{d^2 W(L)}{dx^2} \left(\frac{x}{L} \right) \right] \quad (4.130)$$

From beam theory if one uses the relationship

$$\frac{d\sigma_x}{dx} = -\frac{d\sigma_{xz}}{dz} \quad (4.131)$$

one can conclude that

$$\sigma_{zx_k} = \frac{1}{b} \int_{h_1}^z \frac{d\sigma_{x_k}}{dx} dz \quad (4.132)$$

then from above

$$\tau_{zx_k} = \frac{1}{b} \left[\frac{d^3 \bar{W}(x)}{dx^3} + \frac{1}{L} \left(\frac{d^2 W(0)}{dx^2} - \frac{d^2 W(L)}{dx^2} \right) \right] \int_{h_0}^z E_{x_k} \left(\frac{1}{\bar{B}_{11}} - \frac{z}{\bar{D}_{11}} \right) dz \quad (4.133)$$

where h_0 is a negative number associated with the bottom of lamina 1, i.e., the lower face of the beam.

Now for the specific case of $q(x) = q_0$ (a constant).

$$\bar{W}(x) = \frac{q_0 x^4}{24} \quad (4.134)$$

$$w(x) = \frac{q_0 L^4}{24 \bar{D}_{11}} \left[\left(\frac{x}{L} \right)^4 - 2 \left(\frac{x}{L} \right)^3 + \frac{x}{L} \right] \quad (4.135)$$

$$u_0(x) = \frac{q_0 L^4}{24 \bar{B}_{11}} \left[4 \left(\frac{x}{L} \right)^3 - 6 \left(\frac{x}{L} \right)^2 \right] \quad (4.136)$$

and the stresses are

$$\sigma_{x_k} = \frac{q_0 L^2}{2(A_{11}D_{11} - B_{11}^2)} \left[\left(\frac{x}{L} \right)^2 - \frac{x}{L} \right] E_{x_k} [B_{11} - zA_{11}] \quad (4.137)$$

$$\tau_{xz_k} = \frac{q_0 L}{2b(A_{11}D_{11} - B_{11}^2)} \left[2 \left(\frac{x}{L} \right) - 1 \right] \int_{h_0}^z E_{x_k} [B_{11} - zA_{11}] dA \quad (4.138)$$

Now as an example problem consider the mid-plane asymmetric beam subjected only to a static hygrothermal loading, and no mechanical loads.

From above, the governing differential equations are

$$\frac{d^4 w}{dx^4} = -\frac{1}{\bar{D}_{11}} \left[\frac{d^2 M_{x_T}}{dx^2} + \frac{d^2 M_{x_H}}{dx^2} \right] + \frac{1}{\bar{B}_{11}} \left[\frac{d^2 N_{x_T}}{dx^2} + \frac{d^2 N_{x_H}}{dx^2} \right] \quad (4.139)$$

$$\frac{d^3 u_0}{dx^3} = -\frac{1}{\bar{B}_{11}} \left[\frac{d^2 M_{x_T}}{dx^2} + \frac{d^2 M_{x_H}}{dx^2} \right] + \frac{1}{\bar{A}_{11}} \left[\frac{d^2 N_{x_T}}{dx^2} + \frac{d^2 N_{x_H}}{dx^2} \right] \quad (4.140)$$

Integrating these equations straightforwardly produces the solutions for the deflection.

$$w(x) = -\frac{1}{\bar{D}_{11}} [M_T(x) + M_H(x)] + \frac{1}{\bar{B}_{11}} [N_T(x) + N_H(x)] + C_1 x^3 + C_2 x^2 + C_3 x + C_4 \quad (4.141)$$

$$u_0(x) = -\frac{1}{\bar{B}_{11}} \left[\frac{dM_T(x)}{dx} + \frac{dM_H(x)}{dx} \right] + \frac{1}{\bar{A}_{11}} \left[\frac{dN_T(x)}{dx} + \frac{dN_H(x)}{dx} \right] + C_5 x^2 + C_6 x + C_7 \quad (4.142)$$

where

$$M_T(x) = \iint M_{x_T}(x) dx dx$$

$$M_H(x) = \iint M_{x_H}(x) dx dx \quad (4.143)$$

$$N_T(x) = \iint N_{x_T}(x) dx dx$$

$$N_H(x) = \iint N_{x_H}(x) dx dx$$

For this example problem consider the beam to be simply supported at each end, hence the boundary conditions are

$$w(0) = w(L) = M_x(0) = M_x(L) = N_x(0) = N_x(L) = u_0(0) = 0$$

The values of the seven constants are easily found to be

$$C_1 = C_2 = C_5 = C_6 = 0$$

$$C_3 = \frac{M_T(L) + M_H(L) - [M_T(0) + M_H(0)]}{\bar{D}_{11}L} - \frac{N_T(L) + N_H(L) - [N_T(0) + N_H(0)]}{\bar{B}_{11}L}$$

$$C_4 = \frac{M_T(0) + M_H(0)}{\bar{D}_{11}} - \frac{N_T(0) + N_H(0)}{\bar{B}_{11}}$$

$$C_7 = \frac{1}{\bar{B}_{11}} \left[\frac{dM_T}{dx} + \frac{dM_H}{dx} \right] - \frac{1}{\bar{A}_{11}} \left[\frac{dN_T}{dx} + \frac{dN_H}{dx} \right]$$

Therefore, for this case the displacements are seen to be

$$\begin{aligned} w(x) = & -\frac{1}{\bar{D}_{11}} \left\{ M_T(x) + M_H(x) - [M_T(L) + M_H(L)] \left(\frac{x}{L} \right) \right. \\ & - [M_T(0) + M_H(0)] \left(1 - \frac{x}{L} \right) + \frac{1}{\bar{B}_{11}} [N_T(x) + N_H(x)] \\ & \left. - [N_T(L) + N_H(L)] \left(\frac{x}{L} \right) - [N_T(0) + N_H(0)] \left(1 - \frac{x}{L} \right) \right\} \quad (4.144) \end{aligned}$$

$$u_0(x) = -\frac{1}{\bar{B}_{11}} \left[\frac{dM_T(x)}{dx} + \frac{dM_T(0)}{dx} + \frac{dM_H(x)}{dx} - \frac{dM_H(0)}{dx} \right] + \frac{1}{\bar{A}_{11}} \left[\frac{dN_T(x)}{dx} - \frac{dN_T(0)}{dx} + \frac{dN_H(x)}{dx} - \frac{dN_H(0)}{dx} \right] \quad (4.145)$$

One general observation can be made: The thermal effects and the moisture effects on this and every other structure are identical. So as long as one is using linear theory, the two effects obviously are superposed as seen above. But the important thing to remember is that if one has the thermal effect solution to any solid mechanics (linear, problem, then through superposition one has the solution of the hygrothermal problem for the same structure and boundary conditions.

Finally, consider the following numerical example. It provides the reader with the opportunity to perform numerical calculations to insure that everything previously discussed is understood.

Consider a beam of quasi-isotropic $[0/\pm 45/90]_s$, i.e., $[0, +45, -45, 90, 90, -45, +45, 0]$ laminate of E-glass/epoxy composite of width $b = 1''$, and ply thickness 0.01 inches. The composite mechanical properties are:

$$\begin{aligned} E_1 &= 7.8 \times 10^6 \text{ psi} & \nu_{12} &= 0.25 \\ E_2 &= 2.6 \times 10^6 \text{ psi} & \alpha_1 &= 3.5 \times 10^{-6} / ^\circ \text{F} \\ G_{12} &= 1.25 \times 10^6 \text{ psi} & \alpha_2 &= 11.4 \times 10^{-6} / ^\circ \text{F} \end{aligned}$$

The axial mechanical properties are obtained from using

$$\frac{1}{E_{x_k}} = \frac{\cos^4 \theta_k}{E_1} + \left(\frac{1}{G_{12}} - \frac{2\nu_{12}}{E_{11}} \right) \cos^2 \theta_k \sin^2 \theta_k + \frac{\sin^4 \theta_k}{E_{22}} \quad (4.146)$$

So

$$E_x^0 = 7.8 \times 10^6 \text{ psi} \quad E_x^{90} = 2.6 \times 10^6 \text{ psi}$$

$$E_x^{+45} = 3.203 \times 10^6 \text{ psi}$$

$$A_x = \sum_{k=1}^N E_{x_k} (h_k - h_{k-1}) = 3.3608 \times 10^5 \text{ lbs.}$$

$$B_x = \sum_{k=1}^N E_{x_k} \frac{b}{2} (h_k^2 - h_{k-1}^2) = 0$$

$$D_x = 249.7 \text{ lb.} \cdot \text{in.}^2$$

the axial coefficients of thermal expansion are given by

$$\begin{aligned}\alpha_x &= \alpha_1 m^2 + \alpha_2 n^2 \\ \alpha_x^0 &= 3.5 \times 10^{-6} / ^\circ \text{F} & \alpha_x^{90} &= 11.4 \times 10^{-6} / ^\circ \text{F} \\ \alpha_x^{+45} &= 7.45 \times 10^{-6} / ^\circ \text{F}\end{aligned} \quad (4.147)$$

The thermal loadings are as follows

$$\begin{aligned}N_{x_T} &= \sum_{k=1}^N \int_{h_{k-1}}^{h_k} b E_{x_k} \alpha_{x_k} \Delta T z dz = 2.093 \Delta T \text{ lb.} / ^\circ \text{F} \\ M_{x_T} &= \sum_{k=1}^N \int_{h_{k-1}}^{h_k} b E_{x_k} \alpha_{x_k} \Delta T z dz = 0 \\ M_T(x) &= \iint M_{x_T}(x) dx dx = 0 \\ N_T(x) &= \iint N_{x_T}(x) dx dx = 2.093 \Delta T \left(\frac{x^2}{2} \right)\end{aligned}$$

Finally, the deformations for this problem are

$$\begin{aligned}w(x) &= 0 \\ u_0(x) &= \frac{1}{A_x} \left[\frac{dN_T(x)}{dx} - \frac{dN_T(0)}{dx} \right] \\ \frac{dN_T}{dx} &= 2.093 \Delta T x & \frac{dN_T(0)}{dx} &= 0 \\ u_0(x) &= 6.228 \times 10^{-6} \Delta T x\end{aligned}$$

4.10 Advanced Beam Theory Including Transverse Shear Deformation Effects

The effects of transverse shear deformation are discussed now so that a comparison can be made with the analyses of Section 4.8, which did not include these effects. The development of this section includes dynamic mechanical and hygrothermal loadings.

As stated previously, in almost all cases transverse shear deformation effects are significant in composite material structures because in almost all cases the fibers, which strengthen and stiffen the matrix are in the x - y plane, so the transverse shear stiffnesses closely resemble the shear stiffness of the matrix material only, hence more compliant than many in-plane properties.

The equilibrium equations can be written as

$$\frac{\partial N_x}{\partial x} + p(x, t) = \bar{\rho}_1 \frac{\partial^2 u_0}{\partial t^2} + \bar{\rho}_2 \frac{\partial^2 \bar{\alpha}}{\partial t^2} \quad (4.148)$$

$$\frac{\partial Q_x}{\partial x} + q(x, t) = \bar{\rho}_1 \frac{\partial^2 w}{\partial t^2} \quad (4.149)$$

$$\frac{\partial M_x}{\partial x} - Q_x + m'(x, t) = \bar{\rho}_2 \frac{\partial^2 u_0}{\partial t^2} + \bar{\rho}_3 \frac{\partial^2 \bar{\alpha}}{\partial t^2} \quad (4.150)$$

where

$$\bar{\rho}_1, \bar{\rho}_2, \bar{\rho}_3 = \int_{-h/2}^{h/2} b(l, z, z^2) \rho \, dz = \sum_{k=1}^N \int_{h_{k-1}}^{h_k} b(l, z, z^2) \rho_k \, dz \quad (4.151)$$

For the above, the deflections are still given as

$$u(x, z, t) = u_0(x, t) + z \bar{\alpha}(x, t) \quad (4.152)$$

$$w(x, z, t) = w(x, t) \quad \text{only} \quad (4.153)$$

The strain displacement relations are

$$\epsilon_x = \frac{\partial u}{\partial x} = \frac{\partial u_0}{\partial x} + z \frac{\partial \bar{\alpha}}{\partial x} \quad (4.154)$$

$$\epsilon_{xz} = \frac{1}{2} \gamma_{xz} = \frac{1}{2} \left(\frac{\partial u}{\partial z} + \frac{\partial w}{\partial x} \right) = \frac{1}{2} \left(\bar{\alpha} + \frac{\partial w}{\partial x} \right) \quad (4.155)$$

The stress-strain relations are for each ply

$$\sigma_{x_k} = E_{x_k} \varepsilon_{x_k} \quad (4.156)$$

The integrated constitutive equations are

$$\begin{aligned} N_x &= A_x \varepsilon_x^0 + B_x \kappa_x \\ M_x &= B_x \varepsilon_x^0 + D_x \kappa_x \\ Q_x &= 2\kappa^2 A_{55} \varepsilon_{xz} \end{aligned} \quad (4.157)$$

where here κ^2 is a transverse shear correction factor described previously. For the static loading case, the governing equations are given as:

$$A_x \frac{d^2 u_0}{dx^2} + B_x \frac{d^2 \bar{\alpha}}{dx^2} + p_x(x) = 0 \quad (4.158)$$

$$\kappa^2 A_{55} \left(\frac{d\bar{\alpha}}{dx} + \frac{d^2 w}{dx^2} \right) + q(x) = 0 \quad (4.159)$$

$$B_x \frac{d^2 u_0}{dx^2} + D_x \frac{d^2 \bar{\alpha}}{dx^2} - \kappa^2 A_{55} \left(\bar{\alpha} + \frac{dw}{dx} \right) + m'(x) = 0 \quad (4.160)$$

Substituting (4.158) into (4.160), and taking the first derivative of the result, results in

$$\frac{d^3 \bar{\alpha}}{dx^3} = -\frac{1}{D_x} q(x) + \frac{1}{B_x} \frac{dp_x(x)}{dx} - \frac{1}{D_x} \frac{dm'(x)}{dx}$$

Now taking the second derivative of Equation (4.159) and substituting it into the above, results in

$$\frac{d^3 \bar{\alpha}}{dx^3} = -\frac{1}{\kappa^2 A_{55}} \left[\frac{d^2 q(x)}{dx^2} \right] - \frac{d^4 w}{dx^4}$$

Thus the right hand side of the above two equations can be written as

$$\frac{d^4 w}{dx^4} = \frac{q(x)}{\overline{D}_x} - \frac{1}{\kappa^2 A_{55}} \left[\frac{d^2 q(x)}{dx^2} \right] - \frac{1}{\overline{B}_x} \frac{dp_x(x)}{dx} + \frac{1}{\overline{D}_x} \frac{dm'(x)}{dx} \quad (4.161)$$

Similarly,

$$\frac{d^3 u_0}{dx^3} = -\frac{1}{A_{xx}} \frac{dp(x)}{dx} + \frac{1}{\overline{B}_x} q(x) + \frac{1}{\overline{B}_x} \frac{dm'(x)}{dx} \quad (4.162)$$

These two equations can be solved for any static problem. Consider a simply supported beam with a uniform transverse loading q_0 only. From Equations (4.158) through (4.160)

$$A_x \frac{d^2 u_0}{dx^2} + B_x \frac{d^2 \bar{\alpha}}{dx^2} = 0 \quad (4.163)$$

$$\kappa^2 A_{55} \left(\frac{d\bar{\alpha}}{dx} + \frac{d^2 w}{dx^2} \right) + q_0 = 0 \quad (4.164)$$

$$B_x \frac{d^2 u_0}{dx^2} + D_x \frac{d^2 \bar{\alpha}}{dx^2} - \kappa^2 A_{55} \left(\bar{\alpha} + \frac{dw}{dx} \right) = 0 \quad (4.165)$$

from which it can be found that

$$\frac{d^4 w}{dx^4} = \frac{q_0}{\overline{D}_x} \quad \text{and} \quad \frac{d^3 u_0}{dx^3} = \frac{q_0}{\overline{B}_x} \quad (4.166)$$

The constitutive equations are

$$N_x = A_x \frac{du_0}{dx} + B_x \frac{d\bar{\alpha}}{dx}$$

$$M_x = B_x \frac{du_0}{dx} + D_x \frac{d\bar{\alpha}}{dx}$$

Therefore, the displacements $u_0(x)$ and $w(x)$ as well as the rotation $\bar{\alpha}(x)$ are found by integrating the expressions above in Equations (4.166) and (4.163), and found to be

$$w(x) = \frac{q_0 x^4}{24 \overline{D}_x} + \frac{C_1 x^3}{6} + \frac{C_2 x^2}{2} + C_3 x + C_4 \quad (4.167)$$

$$u_0(x) = \frac{q_0 x^3}{6 \overline{B}_x} + \frac{C_5 x^2}{2} + C_6 x + C_7 \quad (4.168)$$

$$\overline{\alpha}(x) = -\frac{q_0 x}{\kappa^2 A_{55}} - \frac{q_0 x^3}{6 D_x} - \frac{C_1 x^2}{2} - C_2 x + C_3 \quad (4.169)$$

Note that in the above if transverse shear deformation effects were ignored or suppressed, then $A_{55} = \infty$, and $\overline{\alpha} = -\frac{dw}{dx}$, and the results are identical to those derived previously.

Now for this simply supported beam the boundary conditions are

$$w(0) = w(L) = M_x(0) = M_x(L) = N_x(0) = N_x(L) = u_0(0) = 0$$

identical to those studied in the previous section. The resulting constants are

$$\begin{aligned} C_1 &= -\frac{q_0 L}{2 \overline{D}_x} & C_2 &= -\frac{q_0}{\kappa^2 A_{55}} \\ C_3 &= \frac{q_0 L^3}{24 \overline{D}_x} + \frac{q_0 L}{2 \kappa^2 A_{55}} & C_5 &= -\frac{q_0 L}{2 \overline{B}_x} \\ C_4 &= C_6 = C_7 = 0 \end{aligned}$$

Therefore, the displacements are

$$w(x) = \frac{q_0 L^4}{24 \overline{D}_x} \left[\left(\frac{x}{L} \right)^4 - 2 \left(\frac{x}{L} \right)^3 + \left(\frac{x}{L} \right) \right] + \frac{q_0 L^2}{2 \kappa^2 A_{55}} \left[\frac{x}{L} - \left(\frac{x}{L} \right)^2 \right] \quad (4.170)$$

$$\overline{\alpha}(x) = \frac{q_0 L^3}{24 \overline{D}_x} \left[1 - 4 \left(\frac{x}{L} \right)^3 + 6 \left(\frac{x}{L} \right)^2 \right] + \frac{q_0 L}{2 \kappa^2 A_{55}} \quad (4.171)$$

$$u_0(x) = \frac{q_0 L^3}{12 \bar{B}_x} \left[2 \left(\frac{x}{L} \right)^3 - 3 \left(\frac{x}{L} \right)^2 \right] \quad (4.172)$$

Note once more that if transverse shear deformation effects were ignored,

$A_{55} = \infty$ and $\bar{\alpha} = -\frac{dw}{dx}$, and if the beam were mid-plane symmetric, then $u_0(x) = 0$ and $\bar{D}_x = D_x$ (or D_{11}), and those are the classical beam results derived earlier.

Now in this example the maximum displacement occurs at mid-span and is seen to be

$$w(x/2) = w_{\max} = \frac{5q_0 L^4}{384 \bar{D}_x} + \frac{q_0 L^2}{8\kappa^2 A_{55}} \quad (4.173)$$

where it is clear the second term on the right hand side is the transverse shear contribution.

4.11 Buckling of Composite Columns

When analyzing a structure, in addition to looking at maximum deflections, maximum stresses and natural frequencies, one must investigate under what loading conditions an instability can occur, which is also genetically referred to as buckling.

Looking at the governing equations for a composite beam with mid-plane symmetry ($B_{ij} = 0$) given by Equations (4.13) through (4.17), it is seen that there are

only two equations dealing with in-plane loads P and in-plane deflections u_0 , namely, Equations (4.13) and (4.15) with (4.18) being the resulting solution. The remaining three equations deal only with the lateral load $q(x)$ and the lateral deflection w that occurs, with Equation (4.20) being the governing differential equation for the lateral loading $q(x)$. Therefore, it is seen that the in-plane action is entirely independent of the lateral action.

Yet it is well known and often observed that in-plane loads (through buckling) do cause lateral deflections, which are usually disastrous. The answer to the paradox is that up to this point in this chapter only linear elasticity theory has been used, and the physical event of buckling is a nonlinear theory problem. The development of the nonlinear theory will not be included herein because it is covered in so many other texts [7,8], except to say that for a beam the strain-displacement relation is modified to include a non-linear term as seen below.

$$\epsilon_x = \frac{du}{dx} + \frac{1}{2} \left(\frac{dw}{dx} \right)^2$$

The result of including the terms to predict the advent or inception of buckling for the beam is the following:

$$bD_{11} \frac{d^4 w}{dx^4} = q(x) + P \frac{d^2 w}{dx^2} \quad (4.174)$$

where there is a coupling between the in-plane load P and the lateral deflection, w .

Some items should be noted. The buckling loads, like the natural frequencies in vibration, are independent of the lateral loads, which will be disregarded in what follows. However, in actual structural analysis, the effect of lateral loads, along with the in-plane loads could cause overstressing and failure before the in-plane buckling load is reached. Incidentally, common sense dictates that if one is designing a structure to withstand compressive loads, with the possibility of buckling being the important failure mode, one had better design the structure to be mid-plane symmetric, so that $B_{ij} = 0$. Otherwise, the bending-stretching coupling would likely cause overstressing before the buckling load is reached, as well as reduce the buckling load itself; see Equation (4.179) below.

Looking at the buckling of a column only, Equation (4.174) can be written as

$$bD_{11} \frac{d^4 w}{dx^4} + P \frac{d^2 w}{dx^2} \quad (4.175)$$

One can determine that the buckling mode shapes $w(x)$ for the column, simply supported at each end, are as follows:

$$w(x) = \sum_{n=1}^{\infty} A_n \sin \frac{n\pi x}{L} \quad (4.176)$$

Substituting Equation (4.176) into (4.175) yields

$$\sum_{n=1}^{\infty} A_n \left[bD_{11} \frac{n^4 \pi^4}{L^4} + P \frac{n^2 \pi^2}{L^2} \right] \sin \frac{n\pi x}{L} = 0$$

and for this to be true for all n , the critical values of P , called P_{cr} are

$$P_{cr} = -\frac{n^2 \pi^2}{L^2} bD_{11} \quad (4.177)$$

Several things are clear: Equation (4.175) is a homogeneous equation; one cannot obtain the magnitude A_n of the buckling mode, and unlike in vibrations where many values of n are important, here only the one giving the lowest value of P_{cr} is important,

(in this case, $n = 1$) because after buckling the column is usually permanently deformed or fails, and finally, P_{cr} is a negative value which means a compressive in-plane load.

Thus, it is seen that the eigenvalue problems differ from the considerations in previous sections because the event, natural vibration or buckling, occurs only at certain values. Hence, the natural frequencies and the buckling load are the eigenvalues; while the vibrational mode and the buckling mode are the eigenfunctions.

In analyzing any structure, one should therefore determine four things: the maximum deflection, the maximum stresses, the natural frequencies (if there is any dynamic loading to the structure, or nearby to the structure), and the buckling loads (if there are any compressive or shear loads).

Mathematically, one can see that the effects of transverse shear deformation occur because of the finite values of A_{55} in Equation (2.159). In classical theory, A_{55} is taken to be infinite since $\epsilon_{xz} = 0$ and Q_x is finite. It is also seen that in the natural frequency calculations, the transverse shear deformation effects increase with the integer n .

All combinations of beam vibrational mode shapes applicable for use here have been developed by Warburton [2], and all derivatives and integrals of those functions catalogued conveniently by Young and Felgar [3] and Felgar [4] for easy use. Similar expressions for buckling modes are available in many texts, and can likewise be used to obtain buckling loads with other boundary conditions, analogous to Equation (4.177).

It must again be stated that the natural frequencies and buckling loads calculated in this section; do not include transverse shear effects, and are therefore only approximate, but they are useful for preliminary design because of their relative simplicity. If transverse shear deformation were included (see the next section), both natural frequencies and buckling loads would be lower than those calculated in this section – so the buckling loads calculated, neglecting transverse shear deformation, are not conservative.

It has been shown that the simple expressions for approximate natural frequencies and buckling loads, which do not include transverse shear deformation (tsd) effects, can be modified to initiate such effects for the columns discussed previously. The result is an approximate but useful expression

$$\left\{ \begin{matrix} \omega_n \\ P_{cr} \end{matrix} \right\}_{\text{with tsd}} = \frac{\left\{ \begin{matrix} \omega_n \\ P_{cr} \end{matrix} \right\}_{\text{previously determined (classical)}}}{\left(1 + \frac{D_{11} n^2 \pi^2}{A_{55} L^2} \right)^{1/2}} \quad (4.178)$$

It has been shown by (4.118) that in the beam equation, if the laminate is asymmetric with respect to the middle surface (that is, $B_{11} \neq 0$), then the D_{11} terms in those equations can be replaced by

$$\frac{A_{11} D_{11} - B_{11}^2}{A_{11}} \quad (4.179)$$

Equation (4.179) has been termed the “reduced” or “apparent” flexural stiffness.

4.12 References

1. Gere, J. and Timoshenko, S. (1984) *Mechanics of Materials*, Second Edition, PWS-Kent Publishing Company, Boston, MA, Appendix G.
2. Warburton, G. (1968) “The Vibration of Rectangular Plates,” *Proceedings of the Institute of Mechanical Engineers*, Institute of Mechanical Engineers, London, U.K., 371.
3. Young, D. and Felgar, R.F. Jr., “Tables of Characteristic Functions Representing Normal Modes of Vibration for a Beam,” The University of Texas Engineering Research Series Report No. 44, July 1, 1949.
4. Felgar, R.P. Jr. (1950) “Formulas for Integrals Containing Characteristic Functions of a Vibrating Beam,” The University of Texas Bureau of Engineering Research Circular No. 14.
5. Vinson, J.R. and Dee, A.T. (1998) Use of Asymmetric Sandwich Construction to Minimize Bending Stresses, *Sandwich Constructions 4*, ed. K.-A. Olson, Vol. 1, EMAS Publishers, Ltd. UK, pp 391-402.
6. Whitney, J.M. (1969) The Effect of Transverse Shear Deformation on the Bending of Laminated Plates, *Journal of Composite Materials*, Vol. 3, pp. 534-547.
7. Timoshenko, S.P. and Gere, J.M. (1961) *Theory of Elastic Stability*, McGraw-Hill Book Co., Inc., 2nd Edition.
8. Bleich, H.H. (1952) *Buckling of Metal Structures*, McGraw-Hill Book Co., Inc.

4.13 Problems

- 4.1. The governing differential equation for a beam composed of a composite material in which $B_{ij} = 0$ and $D_{16} = D_{26} = 0$ is

$$bD_{11} \frac{d^4 w}{dx^4} = q(x)$$

where b is the beam width, D_{11} is the flexural stiffness in the x -direction, and $q(x)$ is the lateral load per unit length. If the beam is of length L , and the beam is simply supported at $x = 0$, clamped at $x = L$, and the lateral load is a constant $q(x) = q_0$, determine explicitly the expression $w(x)$.

- 4.2. Given a beam made of T300/5208 graphite epoxy with the following mechanical properties at 70° F

$$E_1 = 14.5 \times 10^4 \text{ MPa} = 21 \times 10^6 \text{ psi}$$

$$E_2 = 1.17 \times 10^4 \text{ MPa} = 1.76 \times 10^6 \text{ psi}$$

$$G_{12} = 0.45 \times 10^4 \text{ MPa} = 0.65 \times 10^6 \text{ psi}$$

$$\nu_{12} = 0.21 \quad \nu_{21} = 0.017$$

$$\rho = 0.06 \text{ lbs./in.}^3, \text{ the weight density}$$

$$g = 386 \text{ in./sec.}^2$$

assume $\sigma_{\text{allowable}} = 100,000 \text{ psi}$.

Consider the beam to be made of an all 0° layup, of 30 laminae, each $0.006''$ thick, such that the total beam thickness is $h = 0.18''$. The beam is one inch wide ($b = 1''$) and twelve inches long ($L = 12''$).

- (a) If the beam is simply supported at each end, and subjected to a uniform lateral load of 10 lbs./in. of length, what is the maximum deflection?
 - (b) What is its maximum stress?
 - (c) What is its fundamental natural frequency in bending?
 - (d) If the beam were subjected to a compressive end load what would the critical buckling load be?
- 4.3. Consider a beam of length $20''$, width $1''$ of the material of Problem 4.2. If the beam is simply supported at each end, what minimum beam thickness, h , is necessary to insure that the beam is not overstressed when it is subjected to a uniform lateral load of $q_0 = 20 \text{ lbs./in.}$?
- 4.4. For a beam of the material of Problem 4.2, with $L = 15''$, $b = 1''$ and $h = 0.020''$, what is the fundamental natural frequency in cycles per second (Hz) if the beam is simply supported at each end? Neglect transverse shear deformation.
- 4.5. For the beam of Problem 4.4 above, what is the critical buckling load, P_{cr} , neglecting transverse shear deformation?
- 4.6. For a clamped-clamped composite beam of uniform cross-section but mid-plane asymmetric subjected to mechanical and hygrothermal loads, determine explicit expressions for the lateral (transverse) deflection, $w(x)$, and the in-plane stresses.
- 4.7. For a composite beam simply supported at each end, made of a laminate of $[0, 90]_s$, i.e., $[0/90/90/0]$ whose ply thickness is 0.01 inches, subjected to a uniform lateral load q_0 , determine the following stress profiles of
- (a) $\sigma_x / (q_0 L^2 / 8)$ at both $x = L/2$ and $x = L/4$.
 - (b) $\sigma_{xz} / (q_0 L / 4)$ at both $x = 0$ and $x = L/4$.

The material properties are:

$$E_{11} = 8.8 \times 10^6 \text{ psi}$$

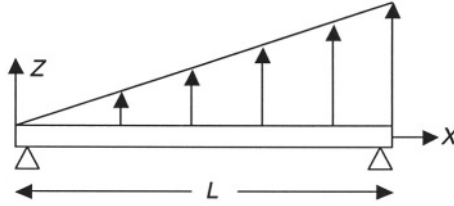
$$E_{22} = 3.6 \times 10^6 \text{ psi}$$

$$G_{12} = 1.74 \times 10^6 \text{ psi}$$

$$\nu_{12} = 0.23$$

$$V_F = 0.72$$

- 4.8. Consider the following simply supported beam subjected to the loading shown, where the beam is mid-plane asymmetric



So from the equilibrium equations, prove that

$$w(x) = \frac{A_{11}KL^5}{120(A_{11}D_{11} - B_{11}^2)} \left[\left(\frac{x}{L} \right)^5 - \frac{10}{3} \left(\frac{x}{L} \right)^3 + \frac{7}{3} \left(\frac{x}{L} \right) \right]$$

$$u_0(x) = \frac{B_{11}KL^5}{24(A_{11}D_{11} - B_{11}^2)} \left[\left(\frac{x}{L} \right)^4 - 2 \left(\frac{x}{L} \right)^2 \right]$$

- 4.9. Consider a composite material beam, with constant flexural stiffness, bD_{11} , simply supported at each end, and subjected to a lateral load per unit length given by

$$q(x) = q_0 \sin \frac{\pi x}{L}$$

Solving the governing differential equation and satisfying the boundary conditions, determine the location and the magnitude of the maximum displacement.

- 4.10. Consider a composite material beam, with constant flexural stiffness, bD_{11} , simply supported at each end, and subjected to a lateral load per unit length given by

$$q(x) = \bar{q} \left[1 - \sin \frac{\pi x}{L} \right]$$

Solving the governing differential equation and satisfying the boundary conditions,

determine the location and the magnitude of the maximum displacement.

- 4.11. For a beam of the material below where $L = 15''$, $b = 1''$ and $h = 0.020''$, shown in Figure 4.1, what is the fundamental natural frequency in cycles per second (Hz) if the beam is simply supported on each end. Neglect transverse shear deformation.

The following material properties are given for a unidirectional, 4 ply laminate.

$$A = \begin{bmatrix} 0.84 & 0.00547 & 0 \\ 0.00547 & 0.0176 & 0 \\ 0 & 0 & 0.012 \end{bmatrix} \times 10^6 \text{ lb./in.}$$

$$B = 0$$

$$D = \begin{bmatrix} 28.053 & 0.1824 & 0 \\ 0.1824 & 0.5874 & 0 \\ 0 & 0 & 0.4 \end{bmatrix} \text{ lb.-in.}$$

$$\rho, \text{ the mass density (corresponding to } 0.061 \text{ lb./in.}^3) = 1.554 \times 10^{-4} \frac{\text{lb. sec.}^2}{\text{in.}^4}$$

- 4.12. For the same beam as in Problem 4.11 above, what is the critical compressive buckling load, P_{cr} , neglecting transverse shear deformation.
- 4.13. A beam is made of unidirectional Spectra 900 fibers in a Metton matrix. The properties are:

Spectra 900 fiber ($\nu_f = 24\%$)

$$E = 24.8 \times 10^6 \text{ psi}$$

$$\nu = 0.30$$

$$\rho = \text{assume } 0.06 \text{ lb./in.}^3$$

Metton

$$E = 0.141 \times 10^6 \text{ psi}$$

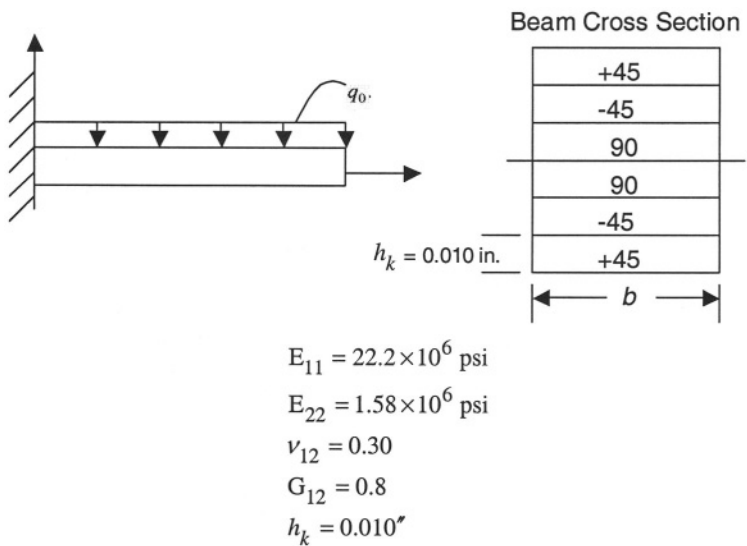
$$\nu = 0.4$$

$$\rho = \text{assume } 0.037 \text{ lb./in.}^3$$

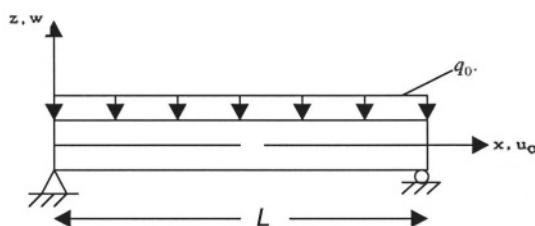
The beam is made by injection molding, hence is uniform in construction.

- What is the longitudinal stiffness in the fiber direction?
 - If the beam is $1/8''$ thick, $1''$ wide, $20''$ long what is its fundamental natural frequency if it is simply supported at each end?
 - What is its critical buckling load when subjected to an axial compressive load?
 - If subjected to a unit uniform lateral pressure of 1 psi, what is the maximum deflection?
- 4.14. Consider a composite beam of T300/5208 graphite/epoxy, composed of 4 unidirectional laminae each of $0.0055''$ thickness whose properties are given in Problem 4.2. The beam is $1''$ wide and $20''$ long, simply supported at the end $x = 0$ and clamped at the end $x = L$. A later load of $q = 10 \text{ lbs./in.}$ of length is imposed.
- What is the maximum stress (which occurs at the clamped end, incidentally)?
 - Is the beam overstressed?

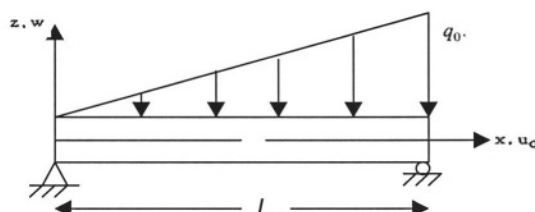
- (c) If so, how many plies are needed for an adequate design so that the maximum stress is not greater than the strength of the material?
- 4.15. What is the fundamental natural frequency of the beam of Problem 4.14 if the weight density is 0.06 lbs./cubic inch, and the gravitational constant is 386 in./second squared?
- 4.16. For a clamped-clamped beam, the axial buckling load is four times that of a beam simply supported at each end. For the beam of Problem 4.14, clamped at each end, what is the axial buckling load?
- 4.17. A cantilever beam of length L , composed of a graphite/epoxy composite material T300/5208 with the stacking sequence shown is subjected to a uniform mechanical load $q(x) = -q_0$. For the beam shown plot the stress distribution at the section of maximum moment. Compare the shape of this stress distribution with that of an isotropic beam.



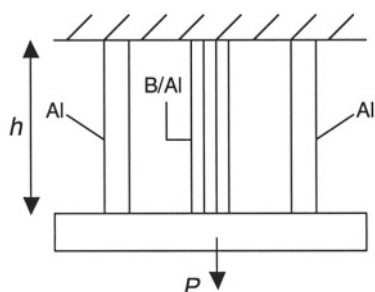
- 4.18. Calculate the bending and shear stresses at $x = L/2$ for a simply supported $[0^\circ / 90^\circ]_s$, $[0/90/90/0]$, composite beam composed of the following materials, whose properties are given in Appendix 2:
- E-glass/Epoxy
 - Graphite/Epoxy (T300/5208)
- for the mechanical loads shown. Each ply is $0.01''$ thick and the beam width is $1''$.
- (a) Uniform transverse load



(b) Triangular transverse load



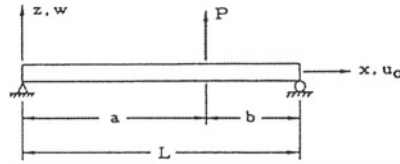
- 4.19. A load P is supported by three vertical bars as shown below. The horizontal bar remains horizontal during deformation. Consider the middle bar to be made from a composite material consisting of an aluminum matrix with boron fibers continuous and aligned parallel to the load. Assume a 50% volume fraction of fibers to matrix and a structurally contiguous bond between fibers and matrix.
- Find the fiber and matrix stresses for the middle bar
 - If all bars were made of aluminum, what would the middle load stress be? Compare to the composite bar.



Note: Area $A_{Al} = \text{Area}_{B/Al}$, and use the rule of mixtures to find E_{comp} , i.e.,

$$E_{comp} = E_f V_f + E_m V_m, \quad E_B = 60 \times 10^6 \text{ psi}, \quad \text{and} \quad E_{Al} = 10 \times 10^6 \text{ psi}$$

- 4.20. Consider a simply supported laminated beam subjected to a single concentrated load as shown



For this beam find:

(a) The displacements u_0, w

(b) Forces and Moments

(c) Strains

(d) If the beam consists of a $[0/\pm 45/90]_s$, $[0/+45/-45/90/90/-45/+45/0]$, laminate, find the stress distribution at $x = a$. Consider the beam to be made of a Kevlar-epoxy composite. Use properties from Appendix 2. Each ply thickness is 0.010 inches.

- 4.21. Find the stress distribution in the $[\pm 45/90]_s$ cantilever beam shown below at the section of maximum moment. The beam is made of T300/5208 Graphite-epoxy with the following properties

$$E_{11} = 22.2 \times 10^6 \text{ psi}$$

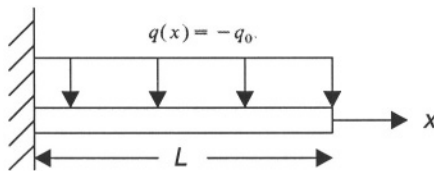
$$E_{22} = 1.58 \times 10^6 \text{ psi}$$

$$\nu_{12} = 0.30$$

$$G_{12} = 0.81 \times 10^6 \text{ psi}$$

$$t = 0.010''$$

Compare the shape of the stress distribution with the case of an isotropic beam.



- 4.22. Consider a beam simply supported at each end under a constant (uniform) load q_0 as shown below. Find the stresses and plot the stress distribution at the mid-span $L/2$ and at $L/4$.

Kevlar/Epoxy Composite

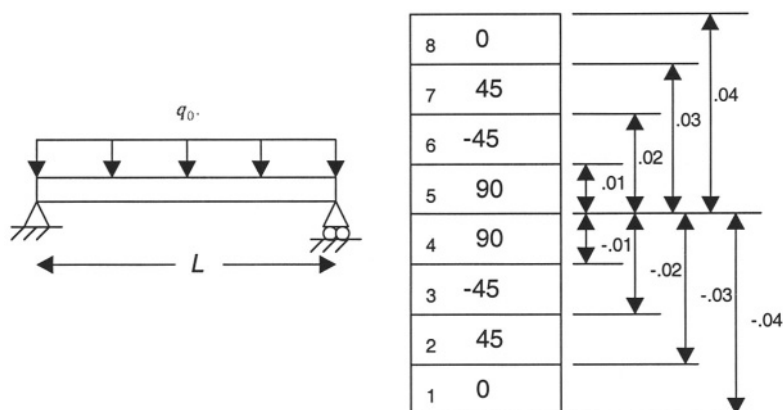
$$E_1 = 11.02 \times 10^6 \text{ psi}$$

$$E_2 = 0.798 \times 10^6 \text{ psi}$$

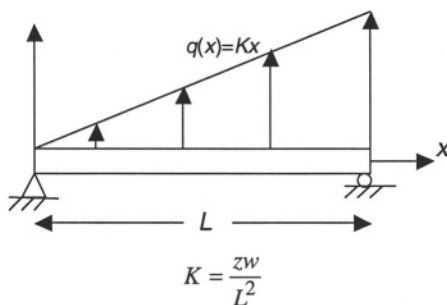
$$G_{12} = 0.334 \times 10^6 \text{ psi}$$

$$\nu_{12} = 0.34$$

Stacking sequence $[0/\pm 45/90]_s$ with $h_k = 0.010''$.



- 4.23 Consider a simply supported beam under a transverse ramp loading. Find the lateral deflection and in-plane displacement.



The governing differential equations can be reduced to

$$w_{,xxxx} = \frac{1}{D_x} q_x = \frac{Kx}{D_x}$$

$$u_{0,xxx} = \frac{1}{B_x} q_x = \frac{Kx}{B_x}$$

- 4.24. A graphite-epoxy structure with fiber orientation 30° from the x -axis is loaded by a

triangular loading as shown below. Assume for this problem that it is a beam. Obtain the expressions for the in-plane displacement u_0 , normal displacement w and the rotation $\bar{\alpha}$. Find the maximum deflection w and identify the shear correction.

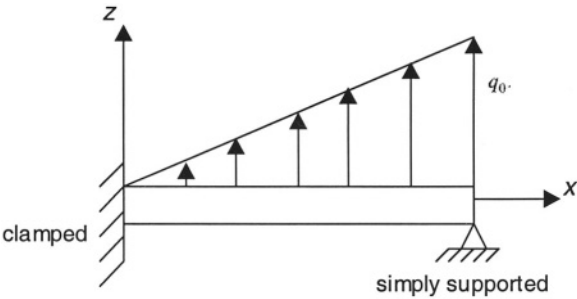
- Assume no axial loading, no hygrothermal effects, and mid-plane symmetry.
- Assume the displacement field is:

$$u(x,z,t) = u_0(x,t) + z\bar{\alpha}(x,t)$$
$$w(x,z,t) = w(x,t)$$

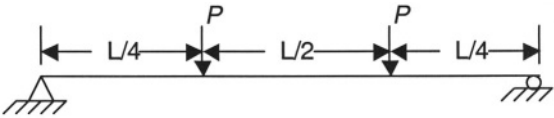
- Assume $Q_x = 2K^2 A_{55} h$

$$\varepsilon_{xz} = \frac{1}{2} \left(\bar{\alpha} + \frac{\partial w}{\partial x} \right)$$

- Make sure to clearly write down the governing equations and all the boundary conditions.



4.25. Consider a simply supported beam with two equal concentrated loads symmetrically placed as shown below, i.e., four point bending.



For a composite laminated stacking sequence of $[0/90/0/90]$ with each ply of thickness $h_k = 0.1''$ and properties given by

$$\begin{aligned}
 E_{11} &= 30 \times 10^6 \text{ psi} \\
 E_{22} &= 3 \times 10^6 \text{ psi} \\
 G_{12} &= 1 \times 10^6 \text{ psi} \\
 \nu_{12} &= 0.30
 \end{aligned}$$

Find the maximum stresses in the beam for each ply.

- 4.26. For a clamped-clamped beam, the axial buckling load is 4 times that of a beam simply supported at each end. Consider a composite beam made of T300/5208 (see Problem 4.2) graphite/epoxy composed of 4 unidirectional laminae each of thickness $0.0055''$, the beam being $1''$ wide and $20''$ in length, find the axial buckling load.
- 4.27. Find the variation in the flexural stress σ_x for the beam shown below and compare the solution with that of a homogeneous/isotropic beam. Use the material properties given in Problem 4.17.

$h_k = 0.010 \text{ in.}$

+45
-45
90
90
-45
+45

- 4.28. Find the variation in the flexural stress σ_x for the laminated beam cross-section shown below, subjected to a bending moment M .

$h_k = 0.010 \text{ in.}$

0
+45
-45
90
90
-45
+45
0

Take each ply as $0.01''$ thick and consider two composite materials, with the properties indicated below.

<u>E - Glass/Epoxy</u>	<u>Graphite/Epoxy</u>
$E_{11} = 7.569 \times 10^6 \text{ psi}$	$E_{11} = 2.03 \times 10^7 \text{ psi}$
$E_{22} = 2.03 \times 10^6 \text{ psi}$	$E_{22} = 1.3 \times 10^6 \text{ psi}$
$G_{12} = 9.135 \times 10^5 \text{ psi}$	$G_{12} = 9.71 \times 10^5 \text{ psi}$
$\nu_{12} = 0.21$	$\nu_{12} = 0.32$

- 4.29. A laminated $[0/90]_2$, $[0/90/0/90/0/90/0]$, composite beam simply supported at each end, made from graphite/epoxy is 1mm. thick, 20mm. wide and has plies of 0.125mm thickness. The lamina properties are as follows, where the S values are strength, the L and T refer to fiber and transverse directions, and $+$ and $-$ refer to tension and compression values, respectively.

$E_{11} = 180 \text{ GPa}$	$S_L^+ = 1700 \text{ MPa}$
$E_{22} = 10 \text{ GPa}$	$S_L^- = 1400 \text{ MPa}$
$G_{12} = 7 \text{ GPa}$	$S_T^+ = 40 \text{ MPa}$
$\nu_{12} = 0.28$	$S_T^- = 230 \text{ MPa}$

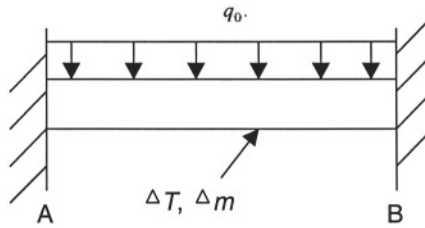
The beam is subjected to a uniformly distributed mechanical q_0 . Find the following:

- The bending stress σ_x and the shear stress τ_{xz} through the thickness of the beam.
 - For a constant temperature gradient ΔT and a constant hygrometric gradient Δm , each applied separately, find the σ_x and τ_{xz} through the thickness.
 - Compare the temperature and hygrometric loading stress distributions with the mechanical loading case.
- 4.30. Consider a simply supported composite beam of length L with a symmetric stacking sequence given by $[(0/90)_2]_s$. Find the transverse deflection at $L/4$ and $L/2$ for each of the following loadings.
- A constant thermal load ΔT
 - A constant hygrometric load Δm

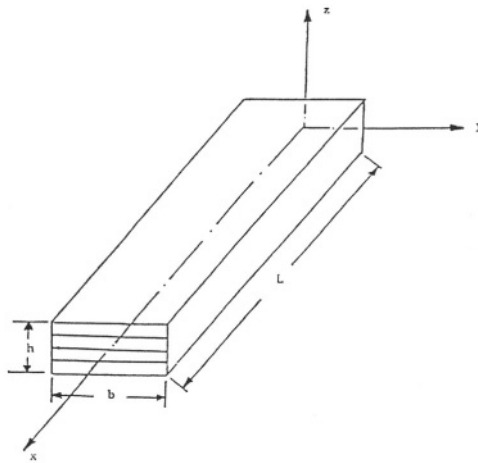
Consider the following two composite materials, whose properties are given in Appendix 2.

- E-Glass/Epoxy
- T300/5208 Graphite/Epoxy

- 4.31. Find the flexural stresses and maximum displacement in a composite beam with clamped boundaries subjected to a uniform mechanical load q_0 , a constant thermal gradient ΔT and a constant moisture gradient Δm .



- 4.32. Consider a 4 ply composite laminated beam with geometry as shown below. The beam is simply supported on elastic springs of equal spring stiffness K . For ply sequences of $[0, 0/90, 45/-45]_s$, with a mid-span load P , find the stress distribution at the quarter span and at the center of the beam. For the same system if the beam is subjected to a hygrometric load only (1% moisture), what would the corresponding stress distribution be at the quarter and mid-span of the beam. Use the governing equations for simple laminated beam theory. For a composite material use AS4/3501 Graphite whose properties are given in Appendix 2.



- 4.33. (a) Design a simply supported polymer matrix composite beam of laminate construction such that the maximum allowable deflection due to a uniform lateral load of 12 lb./in. is less than 0.10 inches. The beam length is 6 feet. Consider the beam to be initially designed for the indicated mechanical load only. Variables for the design include
- Material Type
 - Stacking Sequence
 - Beam Depth and Breadth
- (b) Ignoring moisture effects, how would the design change if the beam was

subjected to both the specified mechanical load and a temperature of 25° F above ambient room temperature, taken as 75° F

- 4.34. Consider a beam of length 20", width 1" of the following material.

$$E_{11} = 14.5 \times 10^4 \text{ MPa} = 21 \times 10^6 \text{ psi}$$

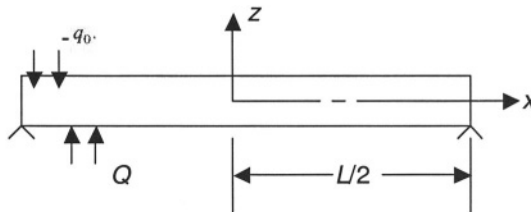
$$E_{22} = 1.17 \times 10^4 \text{ MPa} = 1.76 \times 10^6 \text{ psi}$$

$$G_{12} = 0.45 \times 10^4 \text{ MPa} = 0.65 \times 10^6 \text{ psi}$$

$$\nu_{12} = 0.21, \quad \nu_{21} = 0.017$$

If the beam is simply supported at each end, what minimum beam thickness, h , is necessary to insure that the beam is not overstressed when it is subjected to a uniform lateral load of $q_0 = 20 \text{ lbs./in.}$?

- 4.35. Consider a beam on an elastic foundation as shown below with two rigid end supports. The beam is subjected to a uniform mechanical load $-q_0$ in lb./in. Take the elastic foundation as $Q = Kw(x)$ lb./in.
- Discuss approaches to solving the problem.
 - Write the governing differential equations.
 - Find the deflection $w(x)$.
 - Find the deflection at the center of the beam.
 - Discuss the effects of the end supports.



- 4.36. Plot the first five vibration mode shapes for a beam simply supported at each end with a stacking sequence $[0/\pm 45/90]_s$ and a ply thickness of 0.010".

Assume the material is E-Glass/Epoxy

$$E_{11} = 8.8 \times 10^6 \text{ psi}$$

$$E_{22} = 3.6 \times 10^6 \text{ psi}$$

$$G_{12} = 1.74 \times 10^6 \text{ psi}$$

$$\nu_{12} = 0.23$$

$$\rho_k = 0.050 \text{ lb./in.}^3$$

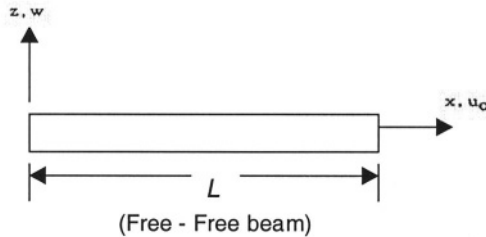
- 4.37. Consider a composite beam made of T300/5208 Graphite/epoxy (see Problem 4.2),

and composed of 4 unidirectional lamina each of thickness $0.0055''$. The beam is $1''$ wide, $20''$ long, carries a uniform lateral load of $q = 10$ lbs./in. of length, has a weight density of 0.05 lbs./in.³ and the gravitational constant is 386 in./sec.². Find the fundamental natural frequency.

- 4.38. Starting from general equations for the free-free vibrations of a composite beam shown below, obtain the frequency equations, expressions for the natural circular frequencies (ω_n) and mode shapes ($w_n(x)$) for the flexural vibrations.

Make the following assumptions:

- Classical beam theory
- No coupling between the extensional and flexural deformation
- Effects of rotatory inertia is negligible
- No hygrothermal loads
- Uniform beam



CHAPTER 5

COMPOSITE MATERIAL SHELLS

5.1 Introduction

A shell is a thin walled body, just as a beam or plate is, whose middle surface is curved in at least one direction. For instance a cylindrical shell and a conical shell have only one direction in which the middle surface is curved. On the other hand in a spherical shell there is curvature in both directions. Such mundane shells as a front fender of a car and an eggshell are examples of shells with double curvature.

Shell theory is greatly complicated, compared to beam and plate theory, because of this curvature. The treatment of shell theory in its proper detail is the subject of a graduate level full semester or full year course, and hence, well beyond the scope of this book. One recent textbook dealing with shells of composite materials as well as isotropic materials is that of Reference [1]. Even to derive the governing differential equations for a shell of general curvature from first principles require several lectures in topology.

Then, to complicate shell theory all of the material complexities associated with laminated composite materials makes the shell theory of composite materials very complicated, and a great challenge.

In this text, the shell geometries will be restricted to circular cylindrical shells; for other geometries see Reference [1].

5.2 Analysis of Composite Material Circular Cylindrical Shells

5.2.1 GENERAL EQUATIONS

The simplest of all shell geometries is that of the circular cylindrical shell shown below in Figure 5.1. The positive directions of the displacements u , v , and w are shown, as well as the positive directions of the coordinates x and ζ . The remaining coordinate is the circumferential coordinate θ . The positive value of all stress resultants and stress couples are shown in Figure 5.2 below.

In the classical shell theory discussed in this section, all of the assumptions used in classical plate theory of Chapters 2 and 3 are utilized:

$$\begin{aligned}\sigma_{\zeta} &= \varepsilon_{\zeta} = \varepsilon_{x\zeta} = \varepsilon_{\theta\zeta} = 0 \\ u(x, \theta, \zeta) &= u_0(x, \theta) + \zeta \beta_x(x, \theta) \\ v(x, \theta, \zeta) &= v_0(x, \theta) + \zeta \beta_{\theta}(x, \theta)\end{aligned}\tag{5.1}$$

where all of the terms have been explained in the previous chapters.

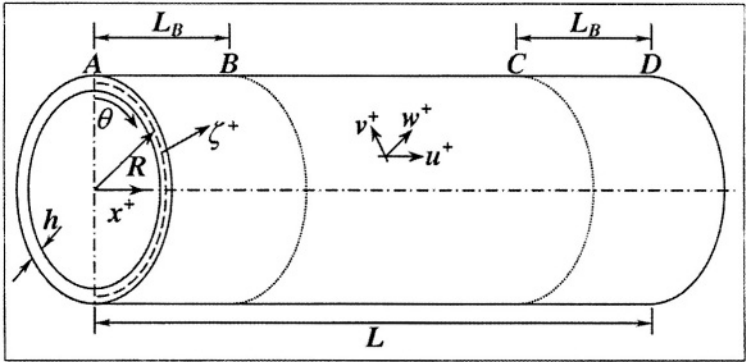


FIGURE 5.1. Circular Cylindrical Shell Geometry

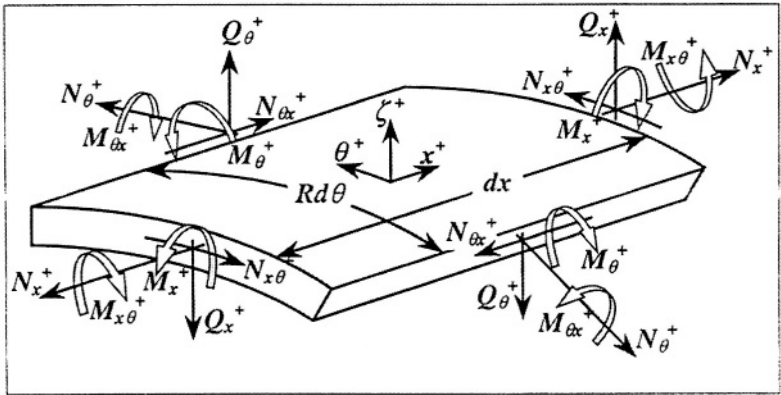


FIGURE 5.2. Positive directions of Integrated Stress Quantities

In addition, there is one other assumption known as Love's First Approximation, which is consistent with the neglect of transverse shear deformation:

$$h/R \ll 1. \quad (5.2)$$

It is true that the accurate analysis of shells of composite materials should include transverse shear deformation because of the fact that the modulus of elasticity in the fiber direction is a fiber dependent property, while the transverse shear modulus is a matrix dominated property. However, for preliminary design, one can often neglect transverse shear deformation effects with resulting simplifications in the governing equations.

To derive the governing differential equations for cylindrical shells, one begins with introducing the elasticity equations in a curvilinear coordinate system, just as the elasticity equations were derived using a Cartesian coordinate system in Chapter 3 for plates. One can proceed to develop the governing equations for a shell of general shape, then specialize the shell to any particular configuration such as a circular cylindrical shell. This would require significant space, for a complete derivation and thus too involved for the scope of this text, however, it is available in Reference [1]. Therefore, the governing equations are presented below without derivation. The equilibrium equations are:

$$\frac{\partial N_x}{\partial x} + \frac{1}{R} \frac{\partial N_{x\theta}}{\partial \theta} + q_x = 0 \quad (5.3)$$

$$\frac{\partial N_{x\theta}}{\partial x} + \frac{1}{R} \frac{\partial N_\theta}{\partial \theta} + \frac{Q_\theta}{R} + q_\theta = 0 \quad (5.4)$$

$$\frac{\partial Q_x}{\partial x} + \frac{1}{R} \frac{\partial Q_\theta}{\partial \theta} - \frac{1}{R} N_\theta + p(x, \theta) = 0 \quad (5.5)$$

$$\frac{\partial M_x}{\partial x} + \frac{1}{R} \frac{\partial M_{x\theta}}{\partial \theta} - (Q_x - m_x) = 0 \quad (5.6)$$

$$\frac{\partial M_{x\theta}}{\partial x} + \frac{1}{R} \frac{\partial M_\theta}{\partial \theta} - (Q_\theta - m_\theta) = 0 \quad (5.7)$$

where

$$q_x = \sigma_{\zeta x}(h/2) - \sigma_{\zeta x}(-h/2) = \tau_{1x} - \tau_{2x}$$

$$q_\theta = \sigma_{\zeta \theta}(h/2) - \sigma_{\zeta \theta}(-h/2) = \tau_{1\theta} - \tau_{2\theta}$$

$$m_x = \frac{h}{2} [\sigma_{\zeta x}(h/2) + \sigma_{\zeta x}(-h/2)] = \frac{h}{2} [\tau_{1x} + \tau_{2x}]$$

$$m_\theta = \frac{h}{2} [\sigma_{\zeta \theta}(h/2) + \sigma_{\zeta \theta}(-h/2)] = \frac{h}{2} [\tau_{1\theta} + \tau_{2\theta}]$$

These equilibrium equations are independent of the material system. The circumferential terms can also be written in terms of ds , the arc distance where $ds = R d\theta$. The quantities q_x, q_θ, m_x and m_θ are functions of the surface shear stresses on the outer and inner surfaces of the composite shell wall, and $p(x, \theta)$ is the laterally distributed load per unit area, positive in the positive ζ direction.

For the case where the transverse shear deformation is ignored (i.e. classical theory) the relations between the rotations β_x and β_θ and the displacements are given by:

$$\beta_x + \frac{\partial w}{\partial x} = 0 \quad (5.8)$$

$$\beta_\theta + \frac{1}{R} \frac{\partial w}{\partial \theta} - \frac{v_0}{R} = 0. \quad (5.9)$$

The material properties enter through the constitutive equations. For simplicity, it is assumed that the lamination stacking sequence is mid-plane symmetric such that there is no bending-stretching coupling, i.e. $[B] = 0$, and that there are no other coupling terms, i.e. $(\)_{16} = (\)_{26} = 0$.

Also, for the following derivation, the simplest case will be studied – that of a shell of one lamina only. Subsequently, generalizations are made to the configurations. In the current case, the stress-strain relations and the strain-displacement relations, utilizing the displacement assumptions of Equation (5.1) are; for the case of one ply

$$\epsilon_x = \frac{1}{E_x} [\sigma_x - \nu_{x\theta} \sigma_\theta] = \frac{\partial u_0}{\partial x} + \zeta \left(\frac{\partial \beta_x}{\partial x} \right) \quad (5.10)$$

$$\epsilon_\theta = \frac{1}{E_\theta} [\sigma_\theta - \nu_{\theta x} \sigma_x] = \frac{1}{R} \left[\frac{\partial v_0}{\partial \theta} + w \right] + \zeta \left(\frac{\partial \beta_\theta}{\partial \theta} \right) \quad (5.11)$$

$$\epsilon_{x\theta} = \frac{1}{2G_{x\theta}} \sigma_{x\theta} \quad (5.12)$$

The in-plane stiffnesses and the flexural stiffnesses are given as follows:

$$\begin{aligned} K_x &= \frac{E_x h}{(1 - \nu_{x\theta} \nu_{\theta x})}, & K_\theta &= \frac{E_\theta h}{(1 - \nu_{x\theta} \nu_{\theta x})} \\ D_x &= \frac{E_x h^3}{12(1 - \nu_{x\theta} \nu_{\theta x})}, & D_\theta &= \frac{E_\theta h^3}{12(1 - \nu_{x\theta} \nu_{\theta x})}. \end{aligned} \quad (5.13)$$

Remember that if the fibers are in the axial direction then $K_x = A_{11}$, $K_\theta = A_{22}$, $D_x = D_{11}$ and $D_\theta = D_{22}$. If the fibers are in the circumferential direction then the subscripts are reversed. The orthotropic relationship of course holds, given in Equation (2.17), and repeated here:

$$\frac{\nu_{x\theta}}{E_x} = \frac{\nu_{\theta x}}{E_\theta}. \quad (5.14)$$

5.2.2 AXIAL SYMMETRY

For simplicity, assume that the loads are axially symmetric hence, $\partial(\)/\partial\theta = 0$ in all equations.

Performing the usual integration of Equations (5.10) and (5.11) by multiplying each equation by $d\zeta$ and integrating from $-h/2$ to $h/2$, and utilizing the definitions of the stress resultants, results in:

$$N_x - \nu_{x\theta} N_\theta = E_x h \frac{\partial u_0}{\partial x}, \quad N_\theta - \nu_{\theta x} N_x = E_\theta h \frac{w}{R}.$$

Rearranging these equations, the following results are obtained,

$$N_x = K_x \left[\frac{\partial u_0}{\partial x} + \nu_{\theta x} \frac{w}{R} \right] \quad (5.15)$$

$$N_\theta = K_\theta \left[\nu_{x\theta} \frac{\partial u_0}{\partial x} + \frac{w}{R} \right]. \quad (5.16)$$

Similarly, multiplying Equations (5.10) and (5.11) by $\zeta d\zeta$ and integrating from $-h/2$ to $h/2$, results in:

$$M_x - \nu_{x\theta} M_\theta = -\frac{E_x h^3}{12} \frac{\partial^2 w}{\partial x^2}, \quad M_\theta - \nu_{\theta x} M_x = 0.$$

Rearranging these equations yields the following:

$$M_x = -D_x \frac{\partial^2 w}{\partial x^2}, \quad M_\theta = \nu_{\theta x} M_x \quad (5.17, 5.18)$$

Further assume for simplicity in the following derivation that there are no surface shear stresses, hence,

$$q_x = q_\theta = m_x = m_\theta = 0.$$

The above shell equations can be simplified to the following:

$$\frac{dN_x}{dx} = 0 \quad (5.19)$$

$$\frac{dQ_x}{dx} - \frac{N_\theta}{R} + p(x) = 0, \quad \frac{dM_x}{dx} - Q_x = 0 \quad (5.20, 5.21)$$

$$\beta_x + \frac{dw}{dx} = 0, \quad \beta_\theta = 0 \quad (5.22, 5.23)$$

$$N_x = K_x \left[\varepsilon_{x_0} + \nu_{\theta x} \varepsilon_\theta \right] = K_x \left[\frac{du_0}{dx} + \frac{\nu_{\theta x}}{R} w \right] \quad (5.24)$$

$$N_\theta = K_\theta \left[\varepsilon_\theta + \nu_{x\theta} \varepsilon_{x_0} \right] = K_\theta \left[\nu_{x\theta} \frac{du_0}{dx} + \frac{w}{R} \right] \quad (5.25)$$

$$M_x = -D_x \frac{d^2 w}{dx^2}, \quad M_\theta = \nu_{\theta x} M_x \quad (5.26, 5.27)$$

$$Q_x = -D_x \frac{d^3 w}{dx^3}. \quad (5.28)$$

From Equations (5.19) and (5.24),

$$\frac{d^2 u_0}{dx^2} + \frac{\nu_{\theta x}}{R} \frac{dw}{dx} = 0. \quad (5.29)$$

From Equations (5.20), (5.25) and (5.28), one obtains:

$$-D_x \frac{d^4 w}{dx^4} - \frac{K_\theta}{R} \left[\nu_{x\theta} \frac{du_0}{dx} + \frac{w}{R} \right] + p(x) = 0. \quad (5.30)$$

From Equations (5.29) and (5.30) the resulting governing equation is:

$$\frac{d^4 w}{dx^4} + \frac{K_\theta}{D_x R^2} (1 - \nu_{x\theta} \nu_{\theta x}) w = \frac{1}{D_x} \left[p(x) - \nu_{\theta x} \frac{N_x}{R} \right]. \quad (5.31)$$

Now defining

$$\varepsilon^4 \equiv \frac{3(1-\nu_{x\theta}\nu_{\theta x})}{h^2 R^2} \frac{D_\theta}{D_x}. \quad (5.32)$$

the governing differential equations for the lateral deflection w , and the in-plane displacements u_0 become

$$\frac{d^4 w}{dx^4} + 4\varepsilon^4 w = \frac{1}{D_x} \left[p(x) - \frac{\nu_{\theta x}}{R} N_x \right] \quad (5.33)$$

$$\frac{d^2 u_0}{dx^2} + \frac{\nu_{\theta x}}{R} \frac{dw}{dx} = 0. \quad (5.34)$$

The form of (5.33) is desirable since it is uncoupled from the other governing equation (5.34). From (5.19), N_x is seen to be a constant as determined by the applied load, P , in the axial direction, i.e. $N_x = P/2\pi R$. In fact, it is seen from (5.33) that the presence of an axial in-plane force is that of an equivalent lateral pressure as far as the lateral displacement w is concerned.

Upon determining w and u_0 from Equations (5.33) and (5.34), the stress resultants and stress couples can be obtained from Equations (5.24) through (5.28). Stresses can then be determined from the following equations for a composite shell of one ply only.

$$\sigma_x = \frac{N_x}{h} + \frac{M_x \zeta}{h^3/12} \quad (5.35)$$

$$\sigma_\theta = \frac{N_\theta}{h} + \frac{M_\theta \zeta}{h^3/12} \quad (5.36)$$

$$\sigma_{xz} = \frac{3Q_x}{2h} \left[1 - \left(\frac{\zeta}{h/2} \right)^2 \right] \quad (5.37)$$

It is noted that the governing differential equation (5.33) has the same form as that of a beam on an elastic foundation, that is, by replacing D_x with the flexural stiffness of a beam, EI , and replacing $4\varepsilon^4 D_x$ by k , the beam foundation modulus. Thus, the physical intuition of all of the solutions for beams on an elastic foundation can be utilized.

By standard methods, the roots of the fourth order equation (5.33) are obtained to be $\pm \varepsilon(1 \pm i)$ where $i = \sqrt{-1}$. The general solution can therefore be written as

$$w(x) = Ae^{-\varepsilon x} \cos \varepsilon x + Be^{-\varepsilon x} \sin \varepsilon x + Ce^{\varepsilon x} \cos \varepsilon x + Ee^{\varepsilon x} \sin \varepsilon x + w_p(x) \quad (5.38)$$

where A , B , C and E are constants of integration determined by the boundary conditions, and $w_p(x)$ is the particular integral.

The in-plane displacement $u_0(x)$ can be obtained through integrating Equation (5.24) as follows

$$u_0(x) = \frac{N_x x}{K_x} - \frac{\nu \theta_x}{R} \int w dx + F \quad (5.39)$$

where N_x is constant and F is a constant of integration.

It is seen, therefore, that for circular cylindrical shells subjected to axially symmetric loads there are six boundary conditions, three at each end. The natural boundary conditions are thus given by,

- 1) Either u_x is prescribed or $N_x = 0$.
- 2) Either $\frac{dw}{dx}$ is prescribed or $M_x = 0$.
- 3) Either w is prescribed or $Q_x = 0$.

In the above set of boundary conditions, the simply supported, clamped and free edge boundary conditions are contained.

5.3 Some Edge Load and Particular Solutions

5.3.1. CIRCULAR CYLINDRICAL SHELL, SEMI-INFINITE IN LENGTH SUBJECTED TO A STRESS COUPLE M_0 AT $x = 0$

Figure 5.3 provides a description for this problem in which the shell extends from $0 \leq x \leq \infty$, and $p(x) = 0$. Hence, only the homogeneous portion of Equation (5.38) is used, and it is easily seen that $C = E = 0$ in order to have finite deflections. The constants A and B are determined from Equations (5.26) and (5.28).

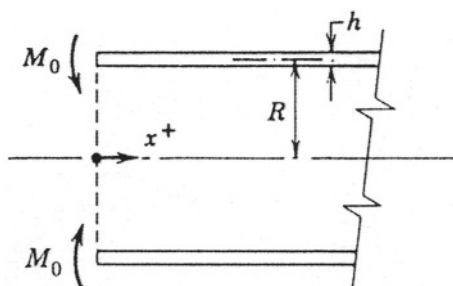


FIGURE 5.3. Circular cylindrical shell subjected to an edge moment at one end

$$M_x(0) = M_0 = -D_x \frac{d^2 w(0)}{dx^2} \quad (5.40)$$

$$Q_x(0) = 0 = -D_x \frac{d^3 w(0)}{dx^3} \quad (5.41)$$

Using the above with Equation (5.38) it is easily determined that the solution is

$$w(x) = \frac{M_0}{2\varepsilon^2 D_x} e^{-\varepsilon x} (\sin \varepsilon x - \cos \varepsilon x) \quad (5.42)$$

It is seen that the effect of this edge moment decays exponentially away from the edge.

5.3.2. CIRCULAR CYLINDRICAL SHELL, SEMI-INFINITE IN LENGTH SUBJECTED TO TRANSVERSE SHEAR FORCE Q_0 AT $x = 0$

Figure 5.4 illustrates this problem.

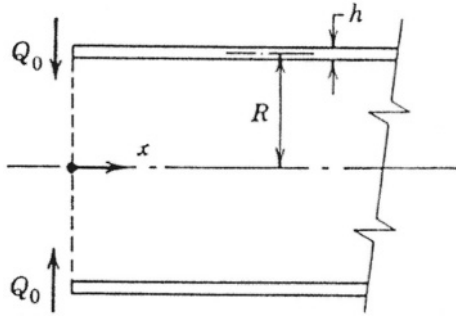


FIGURE 5.4. Circular cylindrical shell subjected to an edge shear resultant at one end

Again, the shell geometry ranges from $0 \leq x \leq \infty$ and $p(x) = 0$ with $C = E = 0$ a given. The constants A and B are determined from the applied load conditions at the edge, namely;

$$M_x(0) = 0 = -D_x \frac{d^2 w(0)}{dx^2} \quad (5.43)$$

$$Q_x(0) = Q_0 = -D_x \frac{d^3 w(0)}{dx^3} \quad (5.44)$$

Using these results with Equation (5.38) the solution is found to be

$$w(x) = -\frac{Q_0}{2\epsilon^3 D_x} e^{-\epsilon x} (\cos \epsilon x) \quad (5.45)$$

Again, one sees that the effect of the edge shear load exponentially decays away from the edge.

5.3.3. CIRCULAR CYLINDRICAL SHELL, SEMI-INFINITE IN LENGTH SUBJECTED TO AN EDGE MOMENT AND A TRANSVERSE SHEAR FORCE AT $x = L$

Here, one considers the semi-infinite shell to exist from $-\infty \leq x \leq L$ and $p(x) = 0$. The positive directions of the loadings are shown in Figure 5.5.

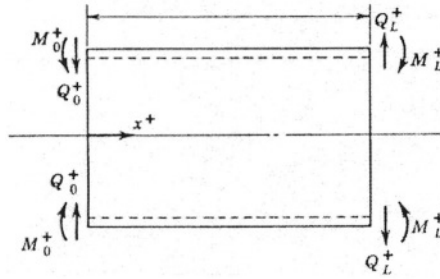


FIGURE 5.5. Positive directions for edge loads on a circular cylindrical shell

One follows the procedures of the previous two sub-sections, where for an edge moment, M_L

$$M_x(L) = -D_x \frac{d^2 w(L)}{dx^2} = M_L \quad (5.46)$$

$$Q_x(L) = -D_x \frac{d^3 w(L)}{dx^3} = 0 \quad (5.47)$$

The result can be written as follows following some trigonometric manipulations:

$$w(x) = \frac{M_L}{2\varepsilon^2 D_x} e^{-\varepsilon(L-x)} (\sin \varepsilon(L-x) - \cos \varepsilon(L-x))$$

(5.48)

Notice the similarity between Equations (5.48) and (5.42), and again the effect of the edge moment decays exponentially from the loaded edge.

Finally, applying an edge transverse shear force, Q_L , to the end $x = L$ of the shell produces a problem defined as

$$M_x(L) = -D_x \frac{d^2 w(L)}{dx^2} = 0 \quad (5.49)$$

$$Q_x(L) = -D_x \frac{d^3 w(L)}{dx^3} = Q_L \quad (5.50)$$

with the solution given by

$$w(x) = \frac{Q_L}{2\epsilon^3 D_x} e^{-\epsilon(L-x)} (\cos \epsilon(L-x)) \quad (5.51)$$

Again, notice the similarity with Equation (5.45) where the exponential decay is identical at each end, but note the change in sign due to the earlier definitions of the signs of shear stresses on faces, see Figure 5.5.

5.3.4. GENERALIZATION

Looking once again at the shell solution for a circular cylindrical shell subjected to axially symmetric in-plane and lateral loads, for a specially orthotropic, mid-plane symmetric composite given by Equation (5.38) one notices that the terms containing the constants A and B are well behaved going to zero as x increases, but the terms containing the constants C and E blow up as x increases. This can cause a major problem computationally and even at best, in solving for the boundary value constants A , B , C and E will involve terms involving $e^{-\epsilon x}$ and $e^{-\epsilon(L-x)}$ and $e^{+\epsilon x}$ and $e^{+\epsilon(L-x)}$ where the exponent can be quite large.

However, this unpleasant situation can be circumvented. Note that one can consider Equations (5.42), (5.45), (5.48) and (5.51) also as solutions to the homogeneous shell equation just as the first four terms of Equations (5.38) are, but in each case the lateral deflection decays away from an edge, and does not blow up. All that is required is to consider M_0 , M_L , Q_0 and Q_L as boundary value constants, analogous to A , B , C and E . So instead of Equation (5.38) the following equation, (5.54) below is found to be more convenient to use. It is of course exactly the same as Equation (5.38) and can be obtained through suitable manipulations.

5.3.5. PARTICULAR SOLUTIONS

Examining Equation (5.33) it is seen that if the fourth derivative of the applied lateral load is zero the particular solution can easily be written as

$$w_p(x) = \frac{1}{4\epsilon^4 D_x} \left[p(x) - \frac{v_{\theta x} N_x}{R} \right] \quad (5.52)$$

This is the particular solution for most practical cases of real structures and loads for axially symmetrically loaded circular cylindrical shells.

For a laminated structure, with $v_{\theta x} = A_{12}/A_{11}$, the particular solution can be written as

$$w_p(x) = \frac{1}{4\varepsilon^4 D_x} \left[p(x) - \frac{A_{12}}{A_{11}} \frac{N_x}{R} \right] \quad (5.53)$$

5.3.6. BEST FORM OF SOLUTION UTILIZING THE BENDING BOUNDARY LAYER

$$\begin{aligned} w(x) = & \frac{M_0}{2\varepsilon^2 D_x} e^{-\varepsilon x} (\sin \varepsilon x - \cos \varepsilon x) - \frac{Q_0}{2\varepsilon^3 D_x} e^{-\varepsilon x} \cos \varepsilon x \\ & + \frac{M_L}{2\varepsilon^2 D_x} e^{-\varepsilon(L-x)} [\sin \varepsilon(L-x) - \cos \varepsilon(L-x)] \\ & + \frac{Q_L}{2\varepsilon^3 D_x} e^{-\varepsilon(L-x)} \cos \varepsilon(L-x) + w_p(x) \end{aligned} \quad (5.54)$$

Instead of using A , B , C and E in Equation (5.38) as the constants of integration, one employs M_0 , Q_0 , M_L and Q_L as the integration constants.

The particular advantage of using Equation (5.54) rather than Equation (5.38) is easily seen. It can be shown that each term of the homogeneous solution contains trigonometric terms, which oscillate between ± 1 , multiplied by an exponential term with a negative exponent, hence an exponential decay. If one assumes that any term is negligible when $e^{-\varepsilon x} \leq 0.006$ or $e^{-\varepsilon(L-x)} \leq 0.006$, that condition occurs whenever εx or $\varepsilon(L-x)$ is greater than 5.15. If $\nu_{\theta x} \nu_{x\theta}$ is taken as 0.09 then, that condition is met exactly whenever

$$\begin{aligned} x &> 4\sqrt{Rh(D_x/D_\theta)^{1/2}} \\ L-x &> 4\sqrt{Rh(D_x/D_\theta)^{1/2}} \end{aligned} \quad (5.55)$$

[Note: For other products of Poisson ratios, changing the values of 0.006 above very slightly still allows the integer 4 to be used in (5.55)]

This is important because at a distance greater than $4\sqrt{Rh(D_x/D_\theta)^{1/2}}$ away from either end of the shell, the entire homogeneous solution of (5.54) essentially goes to zero, and can be neglected. In the case of continuous loads, $p(x)$, the particular solution is one leading to

membrane stresses and displacements. Because of this the region $0 \leq x \leq 4\sqrt{Rh(D_x/D_\theta)^{1/2}}$ and $0 \leq L-x \leq 4\sqrt{Rh(D_x/D_\theta)^{1/2}}$ is called the "bending boundary layer." It is seen that the length of the bending boundary layer is a function of the flexural stiffnesses D_x and D_θ .

Computationally, Equation (5.54) is very useful. For a shell longer than the bending boundary layer, that is, $L \geq 4\sqrt{Rh(D_x/D_\theta)^{1/2}}$ in the region $0 \leq x \leq 4\sqrt{Rh(D_x/D_\theta)^{1/2}}$, the terms involving M_L and Q_L are neglected; in the region $0 \leq (L-x) \leq 4\sqrt{Rh(D_x/D_\theta)^{1/2}}$ the terms involving M_0 and Q_0 can be ignored; in the region $4\sqrt{Rh(D_x/D_\theta)^{1/2}} \leq x \leq L-4\sqrt{Rh(D_x/D_\theta)^{1/2}}$, the terms involving M_0, Q_0, M_L, Q_L can be ignored. Also, when the shell is longer than the bending boundary layer and when $d^2 p(x)/dx^2 = d^3 p(x)/dx^3 = 0$, then and only then,

$$\begin{aligned} M_0 &= M_x(0), & M_L &= M_x(L) \\ Q_0 &= Q_x(0), & Q_L &= Q_x(L). \end{aligned}$$

Even though the above derivation is for a single-layer orthotropic material, it can be easily extended to that of a laminated composite shell, if all couplings are zero. In that case, the general solution can be written as follows in Section 5.4.

5.4 A General Solution for Composite Cylindrical Shells Under Axially Symmetric Loads

The following is a recipe giving all the equations an analyst or designer needs to analyze or design a circular cylindrical shell subjected to axially symmetric static loads made of a specially orthotropic, mid-plane symmetric composite laminate. In the following, the D_{ij} and Q_{ij} quantities defined previously are employed.

$$\begin{aligned} w(x) = & \frac{M_0}{2\varepsilon^2 D_{11}} e^{-\varepsilon x} (\sin \varepsilon x - \cos \varepsilon x) - \frac{Q_0}{2\varepsilon^3 D_{11}} e^{-\varepsilon x} \cos \varepsilon x \\ & + \frac{M_L}{2\varepsilon^2 D_{11}} e^{-\varepsilon(L-x)} [\sin \varepsilon(L-x) - \cos \varepsilon(L-x)] \\ & + \frac{Q_L}{2\varepsilon^3 D_{11}} e^{-\varepsilon(L-x)} \cos \varepsilon(L-x) + \frac{1}{4\varepsilon^4 D_{11}} \left[p(x) - \frac{A_{12}}{A_{11}} \frac{N_x}{R} \right] \end{aligned} \quad (5.56)$$

where

$$\varepsilon^4 = \frac{3(1 - \nu_{x\theta}\nu_{\theta x})}{R^2 h^2} \frac{D_{22}}{D_{11}} \quad (5.57)$$

$$\begin{aligned} \frac{dw}{dx} = & \frac{M_0}{\varepsilon D_{11}} e^{-\varepsilon x} \cos \varepsilon x + \frac{Q_0}{2\varepsilon^2 D_{11}} e^{-\varepsilon x} (\sin \varepsilon x + \cos \varepsilon x) \\ & - \frac{M_L}{\varepsilon D_{11}} e^{-\varepsilon(L-x)} \cos \varepsilon(L-x) \\ & + \frac{Q_L}{2\varepsilon^2 D_{11}} e^{-\varepsilon(L-x)} [\sin \varepsilon(L-x) + \cos \varepsilon(L-x)] \\ & + \frac{1}{4\varepsilon^4 D_{11}} \frac{dp(x)}{dx} \end{aligned} \quad (5.58)$$

$$\begin{aligned} M_x = -D_{11} \frac{d^2 w}{dx^2} = & M_0 e^{-\varepsilon x} (\sin \varepsilon x + \cos \varepsilon x) + \frac{Q_0}{\varepsilon} e^{-\varepsilon x} \sin \varepsilon x \\ & + M_L e^{-\varepsilon(L-x)} [\sin \varepsilon(L-x) + \cos \varepsilon(L-x)] \\ & - \frac{Q_L}{\varepsilon} e^{-\varepsilon(L-x)} \sin \varepsilon(L-x) - \frac{1}{4\varepsilon^4} \frac{d^2 p(x)}{dx^2} \end{aligned} \quad (5.59)$$

$$\begin{aligned} Q_x = -D_{11} \frac{d^3 w}{dx^3} = & -2M_0 \varepsilon e^{-\varepsilon x} \sin \varepsilon x + Q_0 e^{-\varepsilon x} (\cos \varepsilon x - \sin \varepsilon x) \\ & + 2M_L \varepsilon e^{-\varepsilon(L-x)} \sin \varepsilon(L-x) \\ & - Q_L e^{-\varepsilon(L-x)} [-\cos \varepsilon(L-x) + \sin \varepsilon(L-x)] - \frac{1}{4\varepsilon^4} \frac{d^3 p(x)}{dx^3} \end{aligned} \quad (5.60)$$

$$N_x = \text{constant} \quad (5.61)$$

In the case of axially symmetric loading $\kappa_\theta = 0$, the stresses in each lamina are given by

$$\begin{Bmatrix} \sigma_x \\ \sigma_\theta \end{Bmatrix}_k = \begin{bmatrix} Q_{11} & Q_{12} \\ Q_{12} & Q_{22} \end{bmatrix}_k \begin{Bmatrix} \varepsilon_x^0 \\ \varepsilon_\theta^0 \end{Bmatrix} + \begin{bmatrix} Q_{11} & Q_{12} \\ Q_{12} & Q_{22} \end{bmatrix}_k \begin{Bmatrix} \kappa_x \\ 0 \end{Bmatrix} \zeta \quad (5.62)$$

where $\epsilon_x^0 = \frac{\partial u_0}{\partial x}$, $\epsilon_\theta^0 = \frac{w}{R}$ and $\kappa_x = -\frac{\partial^2 w}{\partial x^2}$. If the shell is of one orthotropic layer, u_0 is given by Equation (5.39).

Waltz and Vinson [2] have shown that in a laminated cylindrical shell wherein $\frac{d^2 p(x)}{dx^2} = 0$, all interlaminar shear stresses also go to zero outside of the bending boundary layer, that is, $4\sqrt{Rh(D_{11}/D_{22})^{1/2}} \leq x \leq L - 4\sqrt{Rh(D_{11}/D_{22})^{1/2}}$. This is an extremely important and useful result.

5.5 Response of a Long Axi-Symmetric Laminated Composite Shell to an Edge Displacement

As an illustrative example, consider a long $\left(L > 4\sqrt{(D_x/D_\theta)^{1/2}Rh} \right)$ shell, composed of a laminated construction, $[0, \pm 45^\circ / 90^\circ]_S$, composed of two composite materials, subjected to an edge displacement $w(0) = w_0$, and $du(0)/dx = 0$ at one edge. Each of the eight plies are $h_k = 0.01''$, and the two materials are T300/5208 graphite/epoxy and E-glass/epoxy with the following properties:

	T300/5208	E-glass/epoxy
E_1	22.2×10^6 psi	8.8×10^6 psi
E_2	1.58×10^6 psi	3.6×10^6 psi
ν_{12}	0.30	0.23
ν_{21}	0.021	0.0941
G_{12}	0.81×10^6 psi	1.74×10^6 psi
ν_f	0.70	0.72

Using the methods of Chapter 2, the components of the stiffness matrices are:

	T300/5208	E-glass/epoxy
A_{11} (lb./in.)	0.76×10^6	0.4667×10^6
A_{12} (lb./in.)	0.2355×10^6	0.1079×10^6
A_{22} (lb./in.)	0.76×10^6	0.4667×10^6
$A_{16} = A_{26}$	0	0
A_{66} (lb./in.)	0.2622×10^6	0.1794×10^6
B_{ij}	0	0
D_{11} (lb. - in.)	6.74×10^2	3.1673×10^2

The terms D_{12}, D_{22} are omitted in the above for brevity, and $D_{16} = D_{26} = 0$.

Stresses in each lamina are calculated at two axial locations to show the stress distributions that occur in the bending boundary layer.

Stresses are calculated at an axial location where the deflection is on half of the imposed edge displacement, i.e. $w = w_0/2$. Secondly, stresses are calculated at an axial location of $x = l/2$, where l is the axial distance at which $w = 0$, nearest to the end of the shell. Results are shown in Figure 5.6. It is seen that the σ_x stresses are tensile on the outer layers and compressive on the inner layers. It is also seen that the circumferential stresses, σ_θ , are maximum in the $\theta = 90^\circ$ layers, which is logical because the circumferential stiffness is greatest in these layers and hence the circumferential load is carried in the 90° layers analogous to a stiff spring in a collection of parallel springs. Lastly, even though the deflections and stresses are axially symmetric, in-plane shear stresses, $\tau_{x\theta}$, do exist because of the stacking sequence of the laminate.

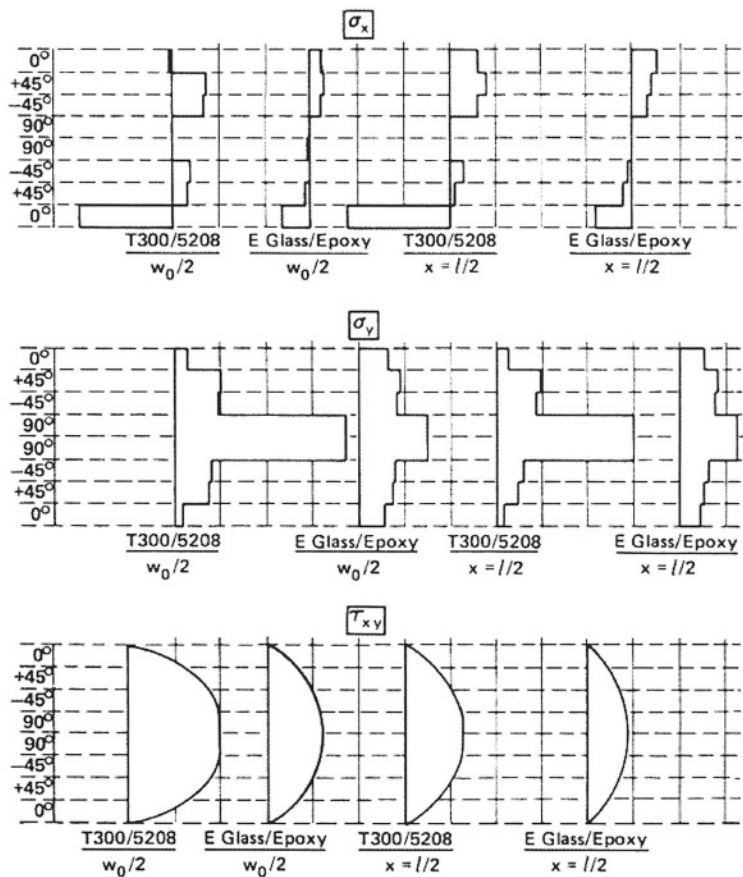


FIGURE 5.6. Stresses at selected points and/or displacements within the bending boundary layer

5.6 Sample Solutions

5.6.1 EFFECTS OF SIMPLE AND CLAMPED SUPPORTS

Consider the circular cylindrical shell composed of a transversely isotropic composite shown in Figure 5.7, typical of many RTM fabric composites today. The end of the shell $x = 0$ is simply supported, the end $x = L$ is clamped. The ends of the shell are assumed to be rigid plates. The internal pressure is p_0 , and A_{12}/A_{11} is written simply as ν in this example. The following information is desired:

- What is the magnitude and exact location of the maximum stress that occurs in the bending boundary layer at the simply supported end?
- The same information near the clamped end?
- What is the magnitude of the maximum stress occurring outside the bending boundary layers, say at $x = L/2$?
- If the maximum principal stress failure theory is used, would the shell be structurally sound if in the design the thickness had been determined by membrane shell theory? (Membrane shell theory neglects all bending effects, see Section 5.10).

From the external axial force equilibrium, $N_x = p_0 R / 2$. The boundary conditions at $x = 0$ are $w(0) = 0$ and $M(0) = 0$. From Equations (5.56) and (5.59), the boundary conditions are:

$$w(0) = -\frac{M_0}{2\varepsilon^2 D} - \frac{Q_0}{2\varepsilon^3 D} + \frac{1}{4\varepsilon^4 D} p_0 (1 - \nu/2) \quad (5.63)$$

$$M_x(0) = M_0 = 0 \quad (5.64)$$

Hence,

$$Q_0 = \frac{p_0}{2\varepsilon} (1 - \nu/2) \quad (5.65)$$

where because of the composite configuration, the material is quasi-isotropic $D_1 = D_2 = D$, and for this example $D_3 = D$ for simplicity.

It is worthwhile to point out that for a cylindrical shell closed at the ends by a structure of any shape, when there is an internal pressure, then $N_x = \frac{p_0 R}{2}$, and this appears in the $(-\nu/2)$ terms in equations (5.63), (5.65), (5.73) and (5.74). If the cylindrical shell were a nozzle (i.e. no ends), then $N_x = 0$ and the $(-\nu/2)$ term would not appear.

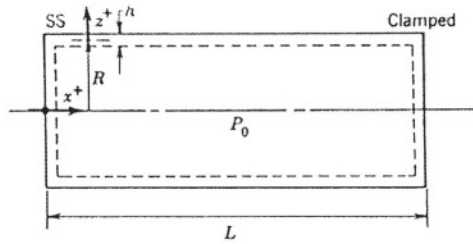


FIGURE 5.7. Example problem of shell of constant internal pressure with one end simply supported and the other end clamped

To determine the location of the maximum value of σ_x , the location of the maximum value of $M(x)$ is required, since N_x is a constant. Since M_x is zero at $x = 0$, and again it is zero for $x \geq L_B$, extreme values lie somewhere in the bending boundary layer. They occur at values of x where $dM_x/dx = 0$. Since $dM_x/dx = Q_x$, therefore the extrema occur at $Q_x = 0$. From Equation (5.64) and (5.65), the fact that $p_0 = \text{constant}$, and since the shell is long, the effects of M_L and Q_L are negligible. Equation (5.60) becomes

$$Q_x = (p_0/2)(1-\nu/2)e^{-\epsilon x}(\cos \epsilon x - \sin \epsilon x) = 0.$$

For this condition to exist, $\cos \epsilon x = \sin \epsilon x$, or $\epsilon x = \pi/4, 3\pi/4, 5\pi/4$, etc. Since there is an exponential decay with increasing x , the largest extreme value, the maximum, occurs at $\epsilon x = \pi/4$. Hence,

$$M_{x_{\max}} = M_x\left(\frac{\pi}{4\epsilon}\right) = p_0(1-\nu/2)\frac{\sqrt{2}}{4\epsilon^2}e^{-\pi/4} \quad (5.66)$$

Equations (5.35) and (5.36) can be used instead of (5.62) since the shell is made of a transversely isotropic composite material, such as many RTM fabric composites.

$$\sigma_{x_{\max}} = \frac{N_x}{h} \pm \frac{6M_{x_{\max}}}{h^2} = \frac{p_0 R}{2h} \pm 0.498 \frac{p_0 R}{h}, \quad \text{for } \nu = 0.3$$

$$\sigma_{x_{\max}} = \sigma_x\left(\frac{\pi}{4\epsilon}, +h/2\right) = 0.998 \frac{p_0 R}{h} \quad (5.67)$$

From Equations (5.64), (5.65), (5.56) and (5.59)

$$w(x) = \frac{p_0(1-\nu/2)}{4\epsilon^4 D} [1 - e^{-\epsilon x} \cos \epsilon x] \quad \text{for } x \leq L_B \quad (5.68)$$

$$M_x(x) = \frac{p_0(1-\nu/2)}{2\epsilon^2} e^{-\epsilon x} \sin \epsilon x \quad \text{for } x \leq L_B \quad (5.69)$$

Therefore from Equations (5.18), (5.36), (5.62), (5.68) and (5.69)

$$\sigma_{\theta} = \frac{Rp_0}{h} \pm \frac{3\nu(1-\nu/2)Rp_0 e^{-\varepsilon x} \sin \varepsilon x}{h[3(1-\nu^2)]^{1/2}} - \frac{p_0(1-\nu/2)R e^{-\varepsilon x} \cos \varepsilon x}{h} \quad \text{for } z = \pm h/2 \quad (5.70)$$

For $\nu = 0.3$, this reduces to

$$\sigma_{\theta} = \frac{Rp_0}{h} [1 \pm 0.464 e^{-\varepsilon x} \sin \varepsilon x - 0.85 e^{-\varepsilon x} \cos \varepsilon x] \quad \text{for } x \leq L_B, z = \pm h/2$$

Extreme values occur for the condition $\partial \sigma_{\theta} / \partial x = 0$, which requires that

$$\pm 0.464(-\sin \varepsilon x + \cos \varepsilon x) + 0.85(\sin \varepsilon x + \cos \varepsilon x) = 0. \quad (5.71)$$

The + requirement occurs for $\varepsilon x = 1.875$; the negative when $\varepsilon x = 2.845$. Of these two, σ_{θ} is a maximum in the former case. The maximum value of σ_{θ} in the range $x \leq L_B$, is

$$\sigma_{\theta_{\max}} = \sigma_{\theta} \left(\frac{1.875}{\varepsilon}, +h/2 \right) = 1.1072 \frac{p_0 R}{h} \quad \text{for } \nu = 0.3. \quad (5.72)$$

At the clamped end, the boundary conditions are $w(L) = w'(L) = 0$. From Equations (5.56) and (5.58) and making use of the fact that the shell is long ($L > 4\sqrt{Rh}$)

$$w(L) = 0 = -\frac{M_L}{2\varepsilon^2 D} + \frac{Q_L}{2\varepsilon^3 D} + \frac{p_0}{4\varepsilon^4 D} (1 - \nu/2) = 0$$

$$\frac{dw(L)}{dx} = 0 = -\frac{M_L}{\varepsilon D} + \frac{Q_L}{2\varepsilon^3 D} = 0.$$

Hence,

$$M_L = -\frac{p_0(1-\nu/2)}{2\varepsilon^2} \quad (5.73)$$

$$Q_L = -\frac{p_0(1-\nu/2)}{\varepsilon} \quad (5.74)$$

It can be shown and is physically obvious that at the clamped end, $M_{\zeta_{\max}} = M(L) = M_L$. Hence, at $x = L$,

$$\sigma_x = \frac{N_x}{h} + \frac{M_L \zeta}{h^3/12} = \frac{p_0 R}{2h} - \frac{p_0(1-\nu/2)\zeta}{2\varepsilon^2(h^3/12)} \quad (5.75)$$

$$\sigma_{x_{\max}} = \sigma_x(L, -h/2) = 2.04 \frac{p_0 R}{h} \text{ for } \nu = 0.3.$$

However, $\sigma_{\theta_{\max}}$ occurs away from the end of the shell. Analogous to the procedures used at the previous end, it is found that

$$\sigma_{\theta_{\max}} = \sigma_{\theta} \left(L - \frac{2.65}{\varepsilon}, +h/2 \right) = 1.069 \frac{p_0 R}{h}. \quad (5.76)$$

At $x = L/2$, which is outside either bending boundary layer, it is seen from Equation (5.35) that $M_x = 0$, hence,

$$\sigma_x = \frac{N_x}{h} = \frac{p_0 R}{2h} \quad (5.77)$$

which is recognized as the membrane solution. Likewise,

$$\sigma_{\theta} = \nu \sigma_x + \frac{Ew}{R} = \frac{p_0 R}{h}. \quad (5.78)$$

This is also the membrane solution.

It is seen that the maximum principal stress occurring in the boundary layer at the simply supported end is, from Equation (5.72) $1.1072 p_0 R/h$; correspondingly, at the clamped end it is $2.04 p_0 R/h$ [see (5.75)]. The maximum stress predicted by membrane theory is $1.0 p_0 R/h$, in the hoop direction seen in (5.78). Hence, stresses greater than the membrane stresses occur in both boundary layers; 10% higher in the simply supported area, and 104% higher in the clamped edge. Thus, this shell if designed on a basis of membrane shell theory would be woefully inadequate.

In the above example, the location of the maximum axial stress and the maximum circumferential stress at each end of the shell have been determined. It should be remembered that a biaxial stress state exists everywhere. Hence, when dealing with a material which follows yield or fracture criteria such as a maximum distortion energy criteria, maximum shear stress, or one of several others, then that criteria must be used to find the location of the maximum value of the equivalent uniaxial stress state as discussed in Chapter 7. Quite often a very simple digital

computer routine can be employed to do the arithmetic, using the analytical solution, to determine the location and magnitude of the maximum stress state.

As pictorial examples of the stress couples, M_x , are the transverse shear resultants, Q_x , that exist in the bending boundary layers, Figures 5.8 and 5.9 illustrate that for a simply supported edge at $x = 0$ the stress couple is zero at the edge and peaks a short distance away, while the maximum value of the shear resultant occurs at the edge. Both M_x and Q_x go to zero in the bending boundary layer, and at greater distances from the edge only membrane stresses and deflections occur.

Figures 5.10 and 5.11 show analogous results for the clamped edge at $x = L = 200$ inches where it is seen that both the stress couple, M_x , and the transverse shear resultant, Q_x , are maximum at the clamped edge, but diminish to zero in the bending boundary layer.

Figures 5.8 through 5.11 are from a paper by Preissner [3] in which the values of ϕ are defined by (5.88) in the next section, and was defined also in Chapter 4 for an asymmetric composite beam.

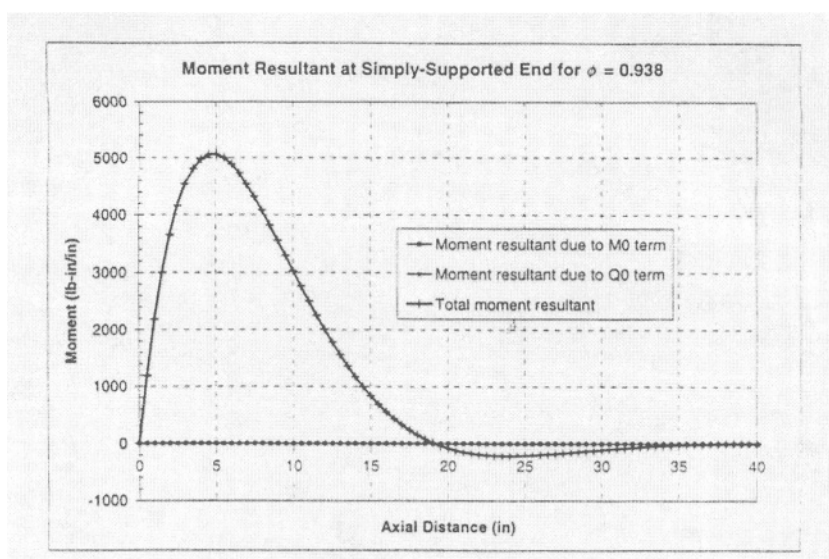


Figure 5.8. Stress Couple, M_x , as a function of distance from a simply-supported edge

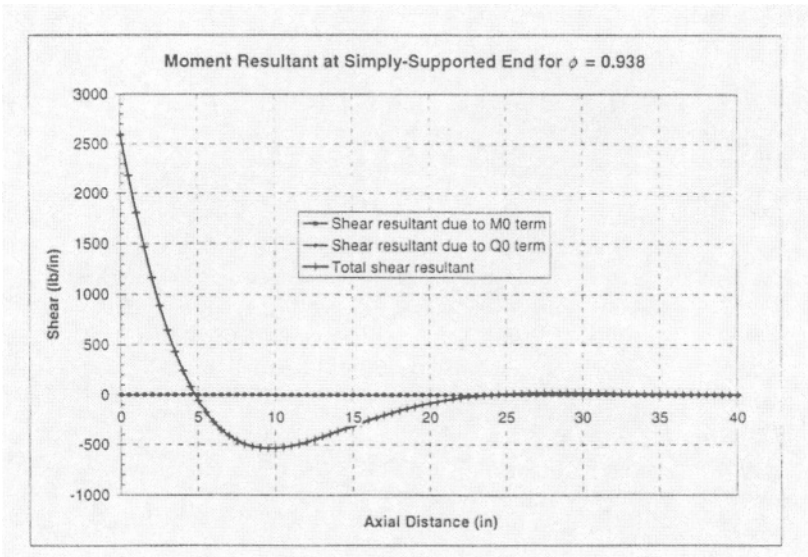


Figure 5.9. Transverse Shear Resultant, Q_x , as a function of distance for a simply-supported edge

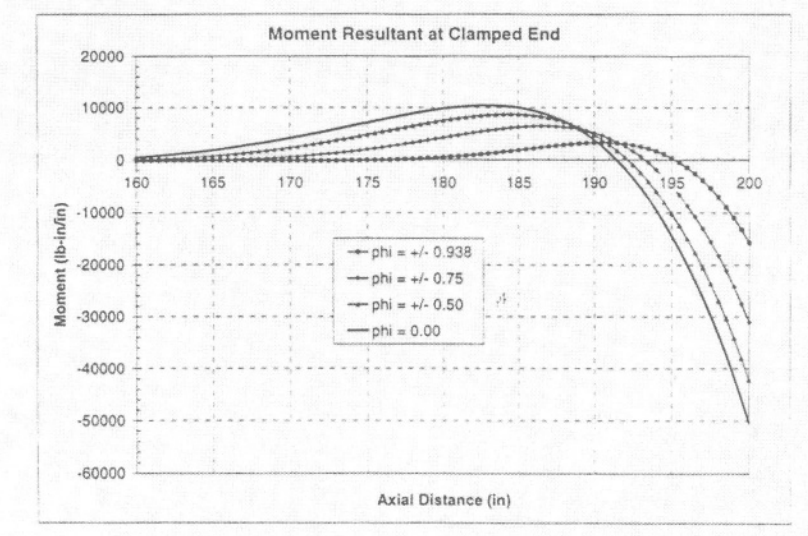


Figure 5.10. Stress Couple, M_x , as a function of distance from a clamped edge

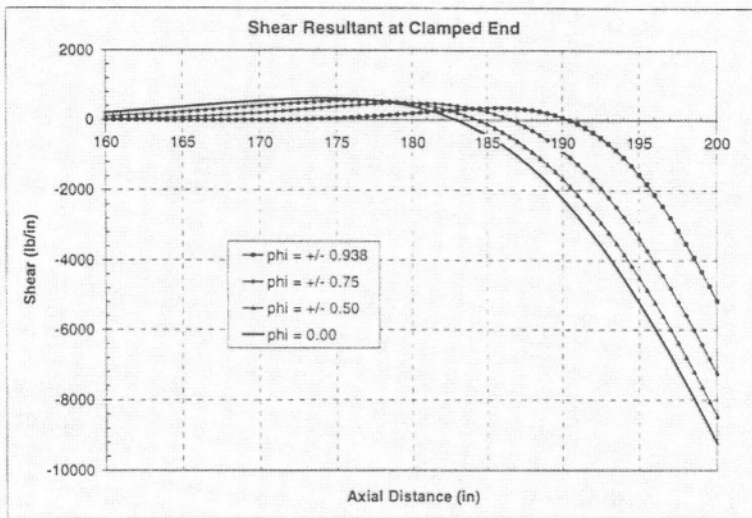


Figure 5.11. Transverse Shear Resultant, Q_x , as a function of distance for a clamped edge

5.7 Mid-Plane Asymmetric Circular Cylindrical Shells

In many applications there are good reasons to have the shell structure be mid-plane asymmetric with respect to the materials used. The exterior environment may differ markedly from the interior environment to which the shell is exposed the outer environment may have extremes of temperature and humidity, blast damage, etc. while the inner environment may have chemical, abrasive, esthetic or other considerations. Also stealth considerations may play a role in some shell structures.

5.7.1 GOVERNING DIFFERENTIAL EQUATIONS

To study the shell with mid-plane asymmetry under axially symmetric loads, the equilibrium equations and the strain displacement relations remain the same as in Section 5.2.2, in Equation (5.19) through (5.28).

However, the constitutive equations for the mid-plane asymmetric composite, which is specially orthotropic so that the material axes 1-2-3 coincide with the $x-\theta-\epsilon$ axes are found from Equation (2.66) to be

$$N_x = A_{11}\epsilon_{x_0} + A_{12}\epsilon_{\theta_0} + B_{11}\kappa_x + B_{12}\kappa_\theta \quad (5.79)$$

$$N_\theta = A_{12}\epsilon_{x_0} + A_{22}\epsilon_{\theta_0} + B_{12}\kappa_x + B_{22}\kappa_\theta \quad (5.80)$$

$$M_x = B_{11}\varepsilon_{x_0} + B_{12}\varepsilon_{\theta_0} + D_{11}\kappa_x + D_{12}\kappa_\theta \quad (5.81)$$

$$M_\theta = B_{12}\varepsilon_{x_0} + B_{22}\varepsilon_{\theta_0} + D_{12}\kappa_x + D_{22}\kappa_\theta \quad (5.82)$$

As before, substituting derivatives of these results into the equilibrium equations and using the strain-displacement relations results in the following equation analogous to Equation (5.34).

$$A_{11} \frac{d^2 u_0}{dx^2} + \frac{A_{12}}{R} \frac{dw}{dx} - B_{11} \frac{d^3 w}{dx^3} = 0 \quad (5.83)$$

The second governing differential equation analogous to Equation (5.33) is

$$\begin{aligned} & \left(\frac{A_{11}D_{11} - B_{11}^2}{A_{11}} \right) \frac{d^4 w}{dx^4} + \frac{2}{R} \left(\frac{A_{12}B_{11}}{A_{11}} - B_{12} \right) \frac{d^2 w}{dx^2} + \frac{1}{R^2} \left(\frac{A_{11}A_{22} - A_{12}^2}{A_{11}} \right) w \\ & = p(x) - \frac{A_{12}}{A_{11}} \frac{N_x}{R} \end{aligned} \quad (5.84)$$

Defining a reduced or effective flexural stiffness D_e as:

$$D_e \equiv \frac{A_{11}D_{11} - B_{11}^2}{A_{11}} \quad (5.85)$$

and introducing the following definition

$$4\varepsilon^4 \equiv \frac{1}{D_e R^2} \left(\frac{A_{11}A_{22} - A_{12}^2}{A_{11}} \right) \quad (5.86)$$

Equation (5.84) can now be written as:

$$\frac{d^4 w}{dx^4} + \frac{2}{D_e R} \left(\frac{A_{12}B_{11}}{A_{11}} - B_{12} \right) \frac{d^2 w}{dx^2} + 4\varepsilon^4 w = \frac{1}{D_e} \left[p(x) - \frac{A_{12}}{A_{11}} \frac{N_x}{R} \right] \quad (5.87)$$

Except for the second term on the left-hand side of Equation (5.87), this is the usual governing equation for an axially symmetric cylindrical shell of flexural stiffness D_e , subjected to axially symmetric loads as given in Equation (5.33). It is also noted that the second term of Equation (5.87) varies directly with the asymmetry quantities, B_{11} and B_{12} .

Recall that a mid-plane asymmetry parameter ϕ was defined previously in Chapter 4 as

$$\phi \equiv \frac{B_{11}}{\sqrt{A_{11}D_{11}}} \quad (5.88)$$

It is convenient to solve this relationship for B_{11} , and substitute the result into the second term in Equation (5.87), with the result that

$$\frac{d^4 w}{dx^4} + C\phi \frac{d^2 w}{dx^2} + 4\varepsilon^4 w = \frac{1}{D_e} \left[p(x) - \frac{A_{12}}{A_{11}} \frac{N_x}{R} \right] \quad (5.89)$$

where:

$$C \equiv \frac{2}{D_e R} \sqrt{\frac{D_{11}}{A_{11}}} \frac{(A_{12}B_{11} - A_{11}B_{12})}{B_{11}} \quad (5.90)$$

Thus, Equations (5.83) and (5.89) are the two governing differential equations to solve for the circular cylindrical shell of a mid-plane asymmetric composite subjected to axially symmetric lateral and axial loads.

5.7.2 PERTURBATION SOLUTION

Since ϕ is bounded to be less than ± 1 , it is possible to let the lateral deflection of Equation (5.89) take the form of a perturbation series solution given by:

$$w(x) = \sum_{n=0}^{\infty} w_n(x) \phi^n \quad (5.91)$$

If one substitutes this series into Equation (5.89), noting that the differentiation and summation can be interchanged, the result is:

$$\begin{aligned} & \frac{d^4 w_0(x)}{dx^4} + \phi \frac{d^4 w_1(x)}{dx^4} + \dots + \phi^n \frac{d^4 w_n(x)}{dx^4} \\ & + C\phi \left[\frac{d^2 w_0(x)}{dx^2} + \phi \frac{d^2 w_1(x)}{dx^2} + \dots + \phi^n \frac{d^2 w_n(x)}{dx^2} \right] \\ & + 4\varepsilon^4 w_0(x) + 4\varepsilon^4 \phi w_1(x) + \dots + 4\varepsilon^4 \phi^n w_n(x) = \frac{1}{D_e} \left[p(x) - \frac{A_{12}}{A_{11}} \frac{N_x}{R} \right] \end{aligned} \quad (5.92)$$

This can now be separated into a series of differential equations by collecting on powers of ϕ where $\phi^0 = 1$.

$$\begin{aligned}
 n=0, \quad & \frac{d^4 w_0(x)}{dx^4} + 4\varepsilon^4 w_0(x) = \frac{1}{D_e} \left[p(x) - \frac{A_{12}}{A_{11}} \frac{N_x}{R} \right] \\
 n=1, \quad & \frac{d^4 w_1(x)}{dx^4} \phi^1 + C \frac{d^2 w_0(x)}{dx^2} \phi^1 + 4\varepsilon^4 w_1(x) \phi^1 = 0 \\
 n=n, \quad & \frac{d^4 w_n(x)}{dx^4} \phi^n + C \frac{d^2 w_{n-1}(x)}{dx^2} \phi^n + 4\varepsilon^4 w_n(x) \phi^n = 0
 \end{aligned} \tag{5.93}$$

Note the important feature of this perturbation approach. If the problems are solved successively from $n = 0$, it is first seen that the differential equation for $n = 0$ is the customary axially- and mid-plane symmetric cylindrical shell equation. There are many solutions available for this problem. For $n \geq 1$, it is seen that the term involving the second derivative is actually known as it involves the w -solution for $n-1$. Thus these terms can be moved to the right-hand side and the Equations (5.93) can be written as:

$$\begin{aligned}
 n=0, \quad & \frac{d^4 w_0(x)}{dx^4} + 4\varepsilon^4 w_0(x) = \frac{1}{D_e} \left[p(x) - \frac{A_{12}}{A_{11}} \frac{N_x}{R} \right] \\
 n=1, \quad & \frac{d^4 w_1(x)}{dx^4} \phi^1 + 4\varepsilon^4 w_1(x) \phi^1 = -C \frac{d^2 w_0(x)}{dx^2} \phi^1 \\
 n>1, \quad & \frac{d^4 w_n(x)}{dx^4} \phi^n + 4\varepsilon^4 w_n(x) \phi^n = -C \frac{d^2 w_{n-1}(x)}{dx^2} \phi^n
 \end{aligned} \tag{5.94}$$

Thus, by canceling the ϕ terms it is found for $n = 0$:

$$\frac{d^4 w_0(x)}{dx^4} + 4\varepsilon^4 w_0(x) = \frac{1}{D_e} \left[p(x) - \frac{A_{12}}{A_{11}} \frac{N_x}{R} \right] \tag{5.95}$$

and for $n \geq 1$:

$$\frac{d^4 w_n(x)}{dx^4} + 4\varepsilon^4 w_n(x) = -C \frac{d^2 w_{n-1}(x)}{dx^2} \tag{5.96}$$

The forcing function of the $n = 0$ equation, (5.95), is the actual applied load to the shell. For $n \geq 1$, the forcing function involves derivatives of the $(n-1)$ equation solution, and is therefore a known quantity.

It has been shown previously by Vinson and Brull [4] that whenever $|\phi| < 1$, Equation (5.91) is another form of the exact solution to equations such as Equation (5.87). Also, in practice, it is seldom necessary to utilize more than the first two terms of the perturbation solution, i.e., $w(x) \cong w_0(x) + w_1(x)\phi$. Through this perturbation technique, the solution of Equation (5.87) can be treated as a successive set of solutions of the customary axially symmetric, mid-plane symmetric, cylindrical shell. There are many solutions available for such problems.

5.7.3 EDGE LOAD SOLUTIONS AND THE BENDING BOUNDARY LAYER FOR A MID-PLANE ASYMMETRIC SHELL

It has been shown that for the mid-plane asymmetric shell the boundary layer exists and has the same length as it is for the usual mid-plane symmetric shell as given by Equation (5.55).

As in the case of beams and plates, when loads applied to circular cylindrical shells are compressive, are in beam type bending, involve an external pressure or are torsional about the longitudinal axis, buckling can occur. Such buckling can result in shell failure, and if the buckling stress is lower than the allowable stress from a strength point of view, then that value is the limit to the useful load carrying capability of the shell.

5.8 Buckling of Circular Cylindrical Shells of Composite Materials Subjected to Various Loads

5.8.1 APPLIED LOADS

Consider a circular cylindrical shell as shown in Figure 5.12 below of mean radius, R , wall thickness, h and length, L , subjected to a compressive load, P , a beam-type bending moment, M , a torque, T and an external pressure, p . For ease of presentation the compression stress resultants resulting from some of these loads will be denoted as positive quantities, as opposed to the usual conventions used previously throughout this book.

$$N_{x_{\text{comp}}} = \frac{P}{2\pi R} \quad (5.97)$$

$$\left(N_{x_{\text{bend}}} \right)_{\text{max}} = \frac{M}{\pi R^2} \quad (5.98)$$

where N_x is the axial load per unit circumference.

Each of the above results represent the applied loads. If for these applied loads, the external pressure p or the applied torque T , equal or exceed a critical value, buckling will result, which for most practical purposes is synonymous to collapse and thus failure of the shell.

The following sections are based on Reference [5].

Concerning the buckling or elastic stability of beams and plates discussed in previous chapters, the analytical predictions are quite accurate compared to the experimental values obtained over many decades. This is not true of shell structures.

Shell structures have little respect for solid mechanicians trying to develop analytical solutions for shells buckling under most loads! Physically, shell structures are very sensitive to initial imperfections when it comes to their stability. Also, in any shell there are slight variations in the shell wall thickness, the value of the radius, any seams resulting from their manufacturing and such things as the inability to have a compressive load, for example, be uniformly distributed around the entire circumference. As a result the experimentally determined buckling loads are often significantly diminished from the analytically determined predictions.

Hence, in any analyses, the analytical values must have an empirical factor relating the analytical prediction to the experimental values of test data. Without such empirical factors the analytical predictions are not conservative.

This means that any new buckling analyses methods should also have an empirical “knockdown” factor in order to relate analyses to the same experimental data.

So from this very practical point of view the NASA methods presented here are current, and have been validated over time.

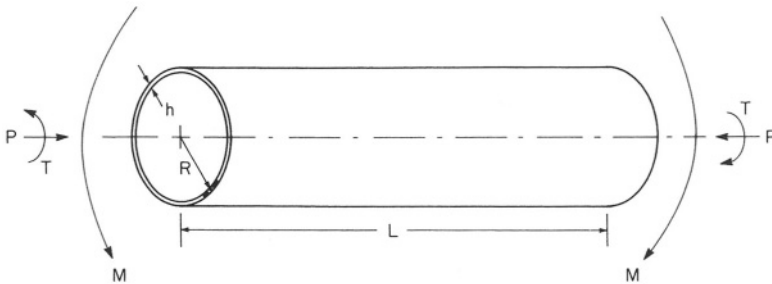


FIGURE 5.12.

5.8.2 BUCKLING DUE TO AXIAL COMPRESSION

Assumptions

- Special anisotropy [that is $(\)_{16} = (\)_{26} = 0$]
- Prebuckled deformations are not taken into account
- Ends of the cylindrical shell are supported by rings rigid in their planes, but offer no resistance to rotation or bending out of their plane.

5.8.2.1 General Case, No Mid-Plane Symmetry, and $n > 4$

$$N_{x_{cr}} = \left(\frac{L}{m\pi} \right)^2 \frac{\begin{vmatrix} C_{11} & C_{12} & C_{13} \\ C_{21} & C_{22} & C_{23} \\ C_{31} & C_{32} & C_{33} \end{vmatrix}}{\begin{vmatrix} C_{11} & C_{12} \\ C_{21} & C_{22} \end{vmatrix}} \quad (5.99)$$

where

$N_{x_{cr}}$ critical compressive load per unit circumference

L cylinder length

R cylinder radius

m number of buckle *half waves* in the axial direction

n number of buckle *waves* in the circumferential direction

$$C_{11} = A_{11} \left(\frac{m\pi}{L} \right)^2 + A_{66} \left(\frac{n}{R} \right)^2 \quad (5.100)$$

$$C_{22} = A_{22} \left(\frac{n}{R} \right)^2 + A_{66} \left(\frac{m\pi}{L} \right)^2 \quad (5.101)$$

$$\begin{aligned} C_{33} = & D_{11} \left(\frac{m\pi}{L} \right)^4 + (4D_{66} + 2D_{12}) \left(\frac{m\pi}{L} \right)^2 \left(\frac{n}{R} \right)^2 + D_{22} \left(\frac{n}{R} \right)^4 \\ & + \frac{A_{22}}{R^2} + \frac{2B_{22}}{R} \left(\frac{n}{R} \right)^2 + \frac{2B_{12}}{R} \left(\frac{m\pi}{L} \right)^2 \end{aligned} \quad (5.102)$$

$$C_{12} = C_{21} = (A_{12} + A_{66}) \left(\frac{m\pi}{L} \right) \left(\frac{n}{R} \right) \quad (5.103)$$

$$C_{23} = C_{32} = (B_{12} + 2B_{66}) \left(\frac{m\pi}{L} \right)^2 \left(\frac{n}{R} \right) + \frac{A_{22}}{R} \left(\frac{n}{R} \right) + B_{22} \left(\frac{n}{R} \right)^3 \quad (5.104)$$

$$C_{13} = C_{31} = \frac{A_{12}}{R} \left(\frac{m\pi}{L} \right) + B_{11} \left(\frac{m\pi}{L} \right)^3 + (B_{12} + 2B_{66}) \left(\frac{m\pi}{L} \right) \left(\frac{n}{R} \right)^2 \quad (5.105)$$

$$A_{ij} = \sum_{k=1}^N [\bar{Q}_{ij}]_k (h_k - h_{k-1}) \quad (5.106)$$

$$B_{ij} = \frac{1}{2} \sum_{k=1}^N [\bar{Q}_{ij}]_k (h_k^2 - h_{k-1}^2) \quad (5.107)$$

$$D_{ij} = \frac{1}{3} \sum_{k=1}^N [\bar{Q}_{ij}]_k (h_k^3 - h_{k-1}^3) \quad (5.108)$$

Here, (5.106) through (5.108) are repeated from Chapter 2 for the reader's convenience.

It is seen that the A_{ij} comprise the extensional stiffness matrix of the composite shell, B_{ij} comprise the bending – extension coupling matrix, and the D_{ij} comprise the flexural or bending stiffness matrix of the shell material. This notation is discussed previously in Chapter 2.

It should be noted that if the fiber orientation is circumferential, then $\theta = 90^\circ$ in determining the values of A_{ij} , B_{ij} and D_{ij} in Equations (5.106) through (5.108).

To determine the critical load $N_{x_{cr}}$ for a cylindrical shell with given dimensions and a given material system, one determines those integer values of m and n which make $N_{x_{cr}}$ a minimum. If choices can be made regarding the ply orientation and number of plies, then an optimization analysis can be performed to determine the construction that provides the highest buckling load per unit weight.

After the buckling load has been determined, a check must be made to see that the final construction is not overstressed at a load below the critical buckling load, because if that is the case the cylinder is limited to a load that will result in overstressing rather than buckling. For a laminated composite construction, the most general constitutive equation for the cylinder is given by the following, which is a repeat of Equation (2.66).

$$\begin{bmatrix} N_x \\ N_\theta \\ N_{x\theta} \\ \hline M_x \\ M_\theta \\ M_{x\theta} \end{bmatrix} = \begin{bmatrix} A_{11} & A_{12} & A_{16} & B_{11} & B_{12} & B_{16} \\ A_{12} & A_{22} & A_{26} & B_{12} & B_{22} & B_{26} \\ A_{16} & A_{26} & A_{66} & B_{16} & B_{26} & B_{66} \\ \hline B_{11} & B_{12} & B_{16} & D_{11} & D_{12} & D_{16} \\ B_{12} & B_{22} & B_{26} & D_{12} & D_{22} & D_{26} \\ B_{16} & B_{26} & B_{66} & D_{16} & D_{26} & D_{66} \end{bmatrix} \begin{bmatrix} \epsilon_x^0 \\ \epsilon_\theta^0 \\ 2\epsilon_{x\theta}^0 \\ \hline \kappa_x \\ \kappa_\theta \\ 2\kappa_{x\theta} \end{bmatrix} \quad (5.109)$$

In this case of buckling due to axial compression, $N_\theta = N_{x\theta} = M_x = M_\theta = M_{x\theta} = 0$, $N_x = N_{x_{cr}}$ one can obtain the $[\epsilon^0]$ and $[\kappa]$ matrices from the above. Then, using these matrices each stress component $\sigma_x, \sigma_\theta, \sigma_{x\theta}$ in each lamina and ply can be calculated using

$$\begin{bmatrix} \sigma_x \\ \sigma_\theta \\ \sigma_{x\theta} \end{bmatrix}_k = [\bar{Q}]_k \begin{bmatrix} \epsilon_x^0 \\ \epsilon_\theta^0 \\ \epsilon_{x\theta}^0 \end{bmatrix} + z[\bar{Q}]_k \begin{bmatrix} \kappa_x \\ \kappa_\theta \\ 2\kappa_{x\theta} \end{bmatrix} \quad (5.110)$$

Remember that if the shell wall is one ply or is unidirectional, then and only then can (5.35) through (5.37) be used instead of (5.110) to determine the shell stresses.

These stresses can then be compared to the allowable or failure stress in each ply as discussed in Chapter 7 below.

5.8.2.2 Special Case, Mid-Plane Symmetry ($B_{ij} = 0$)

For this case the appropriate equation to use is

$$\begin{aligned} \frac{N_{x_{cr}} L^2}{\pi^2 D_{11}} = m^2 & \left(1 + 2 \frac{D_{12}}{D_{11}} \beta^2 + \frac{D_{22}}{D_{11}} \beta^4 \right) \\ & + \frac{\gamma^2 L^4}{\pi^4 m^2 D_{11} R^2} \cdot \frac{A_{11} A_{22} - A_{12}^2}{A_{11} + \left(\frac{A_{11} A_{22} - A_{12}^2}{A_{66}} + 2 A_{12} \right) \beta^2 + A_{22} \beta^4} \end{aligned} \quad (5.111)$$

where

$$\beta = \frac{nL}{\pi R m} \quad (5.112)$$

$$\gamma = 1.0 - 0.901(1 - e^{-\phi}) \quad (5.113)$$

$$\phi = \frac{1}{29.8} \left[\frac{R}{\left(\frac{D_{11} D_{22}}{A_{11} A_{22}} \right)^{1/4}} \right]^{1/2} \quad (5.114)$$

Here γ is an empirical (knockdown) factor that insures that the calculated buckling load will be conservative with respect to all experimental data that are available to date.

To determine the critical buckling load, $N_{x_{cr}}$, the integers m and n are varied to determine the minimum value of $N_{x_{cr}}$, which results in the actual buckling load. Again, one may perform an optimization calculation to insure that overstressing of some ply or plies have not occurred at a load below the critical buckling load, using Equations (5.109) and (5.110) above.

5.8.3 BUCKLING DUE TO BENDING OF THE CYLINDRICAL SHELL (SYMMETRICAL CASE $B_{ij} = 0$)

The equations to use are given by (5.111), (5.112) and (5.114) where the empirical factor γ is given by:

$$\gamma = 1.0 - 0.731(1 - e^{-\phi}) \quad (5.115)$$

The procedures to find the critical buckling load $N_{x_{cr}}$ for a given geometry and construction, the procedures to optimize the construction, and the procedures to insure there is no overstressing are identical to the procedures discussed in Section 5.8.2.1.

5.8.4 BUCKLING DUE TO EXTERNAL LATERAL PRESSURE AND HYDROSTATIC PRESSURE

For a lateral external pressure, the critical value of pressure, p_{cr} , that will cause buckling is determined by:

$$p_{cr} = \frac{R}{n^2} \frac{\begin{vmatrix} C_{11} & C_{12} & C_{13} \\ C_{21} & C_{22} & C_{23} \\ C_{31} & C_{32} & C_{33} \end{vmatrix}}{\begin{vmatrix} C_{11} & C_{12} \\ C_{21} & C_{22} \end{vmatrix}} \quad (5.116)$$

where the C_{ij} are defined by (5.100) through (5.105).

In this case $m = 1$, and one varies the integer n ($n \geq 2$) to find the minimum value of p_{cr} for a given construction because that is the physical buckling load.

For long cylinders subjected to a lateral pressure, the critical buckling pressure is given by:

$$p_{cr} = \frac{3 \left(D_{22} - \frac{B_{22}^2}{A_{22}} \right)}{R^3} \quad (5.117)$$

In the case where $B_{11} = B_{22} = B_{12} = B_{66} = 0$, p_{cr} is found by the following,

$$p_{cr} = \frac{5.513}{LR^{3/2}} \left[\frac{D_{22}^3 (A_{11}A_{22} - A_{12}^2)}{A_{22}} \right]^{1/4} \quad (5.118)$$

which is valid only when

$$\left(\frac{D_{22}}{D_{11}} \right)^{3/2} \left(\frac{A_{11}A_{22} - A_{12}^2}{12A_{22}D_{11}} \right)^{1/2} \left(\frac{L^2}{R} \right) > 500 \quad (5.119)$$

If the external pressure is hydrostatic, use Equation (5.116) but replace n^2 by

$$n^2 + \frac{1}{2} \left(\frac{m\pi R}{L} \right)^2 \quad (5.120)$$

One varies the integers m and n to obtain the combination that gives the lowest (physical) buckling pressure that will occur.

NOTE: In all cases above it is recommended in Reference [5] that the calculated critical pressure, p_{cr} , be multiplied by 0.75 for use in design.

Again, if this number of plies can be varied as well as their orientation then an optimization can be achieved to obtain the highest buckling pressure per unit weight.

To insure that overstressing does not occur at a pressure lower than the critical pressure:

For the case of an external lateral pressure only:

$$N_{\theta} = pR, \quad N_x = N_{x\theta} = M_x = M_{\theta} = M_{x\theta} = 0 \quad (5.121)$$

For a hydrostatic pressure:

$$N = pR, \quad N_x = p \frac{R}{2}, \quad N_{x\theta} = M_x = M_{\theta} = M_{x\theta} = 0 \quad (5.122)$$

These results are used in Equation (5.109) to obtain the $[\epsilon^0]$ and $[\kappa]$ matrices, and then they are substituted into Equation (5.110) to find the stress in each ply, and thus compare the stresses to

an allowable or failure stress, as discussed in Chapter 7, in order to insure that no overstressing occurs.

5.8.5 BUCKLING DUE TO A TORSIONAL LOAD

When $[B_{ij} \approx 0]$, the critical torque T_{cr} that can be applied is:

$$T_{cr} = 21.75(D_{22})^{5/8} \left(\frac{A_{11}A_{22} - A_{12}^2}{A_{22}} \right)^{3/8} \frac{R^{5/4}}{L^{1/2}} \quad (5.123)$$

Another restriction on this equation is that

$$\left(\frac{D_{22}}{D_{11}} \right)^{5/6} \left(\frac{A_{11}A_{22} - A_{12}^2}{12A_{22}D_{11}} \right)^{1/2} \frac{L^2}{R} \geq 500 \quad (5.124)$$

It is recommended in Reference [5] that the T_{cr} determined by Equation (5.123) above be multiplied by 0.67 for use in design.

T_{cr} is obtained from Equation (5.123) directly. An optimized structure can be obtained by varying the θ 's in each ply as well as the number of plies to obtain a construction that is minimum weight for a given T_{cr} . To insure that there is no overstressing in any ply at T_{cr} in Equation (5.92) insert

$$N_{x\theta} = \frac{T_{cr}}{2\pi R^2}, \quad N_x = N_\theta = M_x = M_\theta = M_{x\theta} = 0$$

And determine the $[\epsilon^0]$ and the $[\kappa]$ matrices, which in turn, upon substitution into Equation (5.110) gives the stresses in each ply, to be compared to allowable or fracture values, discussed in Chapter 7.

5.8.6 BUCKLING DUE TO COMBINED AXIAL COMPRESSION AND BENDING

The interaction equations for this combined loading is

$$R_c + R_b = 1$$

where

$$R_c = \frac{N_{x_{\text{comp}}}}{N_{x_{\text{crcomp}}}}, \quad R_B = \frac{\left(N_{x_{\text{bend}}} \right)_{\text{max}}}{\left(N_{x_{\text{crbend}}} \right)_{\text{max}}} \quad (5.125)$$

For the applied loads in the numerators of Equation (5.125), use (5.97) for axial compression and (5.98) for bending. The critical values are obtained from Section 5.8.2.2 and 5.8.3, respectively.

If $R_c + R_B < 1$, the constructions will not buckle.

For a given construction, the integer m and n must both be varied simultaneously for both loadings such that the left-hand side of Equation (5.125) is a maximum for a given set of applied loads. Also a combined optimization can be made to find a construction that will be minimum weight for a given set of loads. To check overstressing Equations (5.109) and (5.110) are again employed where the only non-zero load is

$$N_x = \frac{P_{\text{applied}}}{2\pi R} + \frac{M_{\text{applied}}}{\pi R^2} \quad (5.126)$$

5.8.7 BUCKLING DUE TO COMBINED AXIAL COMPRESSION AND EXTERNAL PRESSURE

The interactive equation to employ, although it is not completely established, is:

$$R_c + R_p = 1$$

Where $R_p = p_{\text{applied}} / p_{\text{cr}}$, and R_c is given previously in Equation (5.125), and p_{cr} is determined from the equations in Section 5.8.4 for either an external lateral pressure or a hydrostatic pressure.

Recall the statements of previous sections in order to analyze the adequacy of the shell for given loads, optimize the shell for given loads, and for overstressing calculations to utilize Equations (5.92) and (5.93) where for a combination of axial compression and external lateral pressure:

$$N_x = \frac{P_{\text{applied}}}{2\pi R}, \quad N_\theta = p_{\text{applied}} R, \quad \text{all other loads}=0$$

and for axial compression and hydrostatic pressure:

$$N_x = \frac{P_{\text{applied}}}{2\pi R} + \frac{RP_{\text{applied}}}{2}, \quad N_\theta = RP_{\text{applied}}, \quad \text{all other loads}=0$$

5.8.8 BUCKLING DUE TO AXIAL COMPRESSION AND A TORSIONAL LOAD

The interaction equation to utilize, although it is still preliminary, is

$$R_c + R_T = 1 \quad (5.127)$$

where

$$R_T = \frac{T_{\text{applied}}}{T_{\text{cr}}}$$

and T_{cr} is taken from Equation (5.123). The procedure to follow is equivalent to that of Sections 5.8.6 and 5.8.7, except in checking for overstressing. The non-zero loads to employ with Equations (5.109) and (5.110) are:

$$N_x = \frac{P_{\text{applied}}}{2\pi R}, \quad N_{x\theta} = \frac{T_{\text{applied}}}{2\pi R^2}$$

5.9 Vibration of Composite Shells

The natural and forced vibration of composite shell structures is very involved, time consuming to present and study, and therefore is left to the reader. Given here are some of the basic papers for the reader to study; after which the general more recent literature will logically follow.

The free vibration of laminated orthotropic cylindrical shells using classical theory has been studied by White [6], Dong [7], Bert [8], Tasi [9,10] and Tasi and Roy [11]. Mirsky [12,13] included transverse shear deformation and transverse normal strain of orthotropic homogeneous cylindrical shells. Dong and Tso [14] analyzed the vibration of layered orthotropic cylinders including transverse shear deformation. Sun and Whitney [15] studied the axially symmetric vibration of laminated composite cylindrical shells including transverse shear deformation, transverse normal stress and strain, rotatory inertia and higher order stiffness and inertia terms.

Analytical and experimental aspects of the dynamic response of composite shells have been studied by Ross, Sierakowski and Sun [16], including various experimental techniques and models.

5.10 Additional Reading On Composite Shells

As indicated above the literature on shell theory involving composite materials is very voluminous, and only by following papers of the journals given in Chapter 1, can anyone hope to acquire a general knowledge.

One textbook covering a broad scope of the theory and analysis of shell structures is Reference [1]. A sampling of papers for recommended reading includes publications by Vizzini and Lagace [17], Whitney and Sun [18] Hsu, Reddy and Bert [19], Simitses, Shaw and Sheinman [20], Greenberg and Stavsky [21], Vinson [22], Sheinman and Ben-Yosef [23], Berman and Simitses [24], Nemeth and Smeltzer [25], Arbocz, Starnes and Nemeth [26] and Nosier and Reddy [27].

5.11 References

1. Vinson, J.R. (1992) *The Behavior of Shells Composed of Isotropic and Composite Materials*, Kluwen Academic Publishers, Dordrecht, The Netherlands.
2. Waltz, T. and Vinson, J.R. (1976) Interlaminar Stresses in Laminated Cylindrical Shells of Composite Materials, *AIAA Journal*, Vol. 14, No. 9, September, pp. 1213-1218.
3. Preissner, E.C. and Vinson, J.R. (1998) Circular Cylindrical Sandwich Shells With Mid-Plane Asymmetry Subjected to Axially Symmetric Loads, *ASME AD*, Vol. 56, Recent Advances in Mechanics of Aerospace Structures and Materials, ed. B.V. Sankar, pp. 245-252.
4. Vinson, J.R. and Brull, M.A. (1962) New Techniques of Solution for Problems in the theory of Orthotropic Plates, *Transactions of the Fourth U.S. National Congress of Applied Mechanics*, Vol. 2, pp. 817-825.
5. Anon. (1968) Buckling of Thin Walled Circular Cylinders, *NASA SP-8007*, Revised, August.
6. White, J.C. (1961) The Flexural Vibrations of Thin Laminated Cylinders, *Journal of Engineering Industry*, pp. 397-402.
7. Dong, S.B. (1968) Free Vibration of Laminated Orthotropic Cylindrical Shells, *Journal of the Acoustical Society of America*, Vol. 44, pp. 1628-1635.
8. Bert, C.W., Baker, J.L. and Egle, D. (1969) Free Vibrations of Multilayer Anisotropic Cylindrical Shells, *Journal of Composite Materials*, Vol. 3, pp. 480-499.
9. Tasi, J. (1968) Reflection of Extensional Waves at the End of a Thin Cylindrical Shell, *Journal of the Acoustical Society of America*, Vol. 44, pp. 291-292.
10. Tasi, J. (1971) Effect of Heterogeneity on the Axisymmetric Vibration of Cylindrical Shells, *Journal of Sound and Vibration*, Vol. 14, pp. 325-328.
11. Tasi, J. and Roy, B.N. (1971) Axisymmetric Vibration of Finite Heterogeneous Cylindrical Shells, *Journal of Sound and Vibration*, Vol. 17, pp. 83-94.
12. Mirsky, I. (1964) Vibration of Orthotropic, Thick, Cylindrical Shells, *Journal of the Acoustical Society of America*, Vol. 36, pp. 41-51.
13. Mirsky, I. (1964) Axisymmetric Vibrations of Orthotropic Cylinders, *Journal of the Acoustical Society of America*, Vol. 36, pp. 2106-2112.
14. Dong, S.B. and Tso, F.K.W. (1972) On a Laminated Orthotropic Shell Theory Including Transverse Shear Deformation, *Journal of Applied Mechanics*, Vol. 39, pp. 1091-1097.

15. Sun, C.T. and Whitney, J.M. (1974) Axisymmetric Vibrations of Laminated Composite Cylindrical Shells, *Journal of the Acoustical Society of America*, Vol. 55, June, pp. 1238-1246.
16. Ross, C.A., Sierakowski, R.L. and Sun, C.T. (1980) Dynamic Response of Composite Materials, *Society for Experimental Mechanics Publication S-014*.
17. Vizzini, A.J and Lagace, P.A. (1985) The Role of Ply Buckling in the Compression Failure of Graphite/Epoxy Tubes, *AIAA Journal*, Vol. 23, No. 11, November, pp. 1791-1797.
18. Whitney, J.M. and Sun, C.T. (1975) Buckling of Composite Cylindrical Characterization Specimen, *Journal of Composite Materials*, Vol. 9, April, pp. 138-148.
19. Hsu, Y.S., Reddy, J.N. and Bert, C.W. (1981) Thermoelasticity of Circular Cylindrical Shells Laminated of Bimodulus Composite Materials, *Journal of Thermal Stresses*, Vol. 4, pp. 155-177.
20. Simitses, G.J., Shaw, D. and Sheinman, I. (1985) Stability of Cylindrical Shells by Various Nonlinear Shell Theories, *ZAMM*, Vol. 65, pp. 159-166.
21. Greenberg, J.B. and Stavsky, Y., Vibrations of Axially Compressed Laminated Orthotropic Cylindrical Shells; Including Shear Deformation, *Acta Mechanica*, Vol. 37, No. 1-2, pp. 13-28.
22. Vinson, J.R. (1999) *The Behavior of Sandwich Structures of Isotropic and Composite Materials*, Technomic Publishing Company, Inc. (now CRC Publishers), Lancaster, Pa.
23. Sheinman, I. And Ben-Yosef, Y. (2002) Buckling of Laminated Cylindrical Shells in Terms of Different Shell Theories and Formulations, *AIAA Journal*, forthcoming.
24. Birman, V. and Simitses, G.J. (2000) Theory of Cylindrical Sandwich Shells With Dissimilar Facings Subjected to Thermomechanical Loads, *AIAA Journal*, Vol. 38, No. 2, February, pp. 362-367.
25. Nemeth, M.P. and Smeltzer III, S.S. (2000) Bending Boundary Layers in Laminated-Composite Circular Cylindrical Shells, November, NASA/TP-2000-210549.
26. Arbocz, J. Starnes, J.H. and Nemeth, M.P. (1998) Towards a Probabilistic Criterion for Preliminary Shell Design, *Proceedings of the AIAA/ASME/ASCE/AHS/ASC Structures Structural Dynamics and Materials Conference*, April, pp. 2941-2955.
27. Nosier, A. and Reddy, J.N. (1992) Vibration and Stability Analyses of Cross-Ply Laminated Circular Cylindrical Shells, *Journal of Sound and Vibration*, Vol. 157, No.1, pp. 139-159.

5.12 Problems

- 5.1. Consider a cylindrical shell composed of four laminae of T300/5208 unidirectional graphite-epoxy whose properties include:

$$\begin{aligned}
 E_1 &= 21 \times 10^6 \text{ psi} & \nu_{12} &= 0.21 & \nu_{21} &= 0.017 \\
 E_2 &= 1.76 \times 10^6 \text{ psi} & \rho &= 0.06 \text{ lb./in.}^3 & g &= 386 \text{ in./sec.}^2 \\
 G_{12} &= 0.65 \times 10^6 \text{ psi} & \sigma_{\text{allowable}} &= 100,000 \text{ psi}
 \end{aligned}$$

If the plies are 0.0055" thick, all oriented with $\theta = 0^\circ$, (that is, unidirectional in the axial direction), and if the radius of the shell is $R = 12"$

- (a) What is D_{11} ?

- (b) What is D_{22} ?
- (c) What is the length of the bending boundary layer at each end?
- 5.2. Consider a circular cylindrical shell of length $L = 50''$, radius $R = 10''$ and a wall thickness $h = 0.020''$, composed of a unidirectional composite of properties $D_x = D_{11} = 28.053 \text{ lb.} \cdot \text{in.}$, and $D_\theta = D_{22} = 0.5874 \text{ lb.} \cdot \text{in.}$ What is the length of the bending boundary layer?
- 5.3. For a circular cylindrical shell, composed of a the unidirectional graphite-epoxy given in Problem 5.1 for a shell of radius $15''$, wall thickness of $0.15''$ and length $30''$, what is the length of the bending boundary layer if:
- (a) The fibers are in the axial direction?
- (b) The fibers are in the circumferential direction?
- 5.4. Consider the cylindrical shell of Problem 5.3 with the material properties given in Problem 5.1, where the fibers are in the axial direction. If the shell is clamped at both ends and subjected to $p = 100 \text{ psi}$ and $N_x = 0$,
- (a) What are σ_x and σ_θ at $x = 0$?
- (c) What are σ_x and σ_θ at $x = 15''$ (i.e., $x = L/2$)?
- 5.5. Consider a circular cylindrical shell of length $L = 50''$, radius $R = 10''$ and wall thickness $h = 0.020''$, composed of the same material as in Problem 5.1 wherein $D_x = D_{11}$ and $D_\theta = D_{22}$. What is the length of the bending boundary layer for this shell?
- 5.6. Consider a shell composed of a quasi-isotropic composite material wherein $E_x = E_\theta = 17 \times 10^6 \text{ psi}$ and $\nu = 0.3$. The mean shell radius is 10 inches and the total thickness is $h = 0.3$ inches. The length is 40 inches, and the interlaminar shear strength sufficient.
- (a) What is the length of the bending boundary layer?
- (b) What is the membrane stress σ_x in the shell if it were subjected to a tensile axial load of 10^4 lbs. ?
- 5.7. Consider a composite material circular cylindrical shell subjected only to a constant lateral distributed load, $p(x) = p_0$. The axial load is $N_x = 0$. The shell and the load are axially symmetric. The shell is clamped at $x = 0$ and free at the end $x = L$. The shell is long, i.e., $L > 4\sqrt{Rh(D_x/D_\theta)^{1/2}}$. Determine explicitly the constants M_0, M_L, Q_0 , and Q_L defined in Section 5.4.
- 5.8. For a cylindrical shell of dimensions $R = 10''$ and $L = 40''$, composed of 4 laminae of T300/934 graphite/epoxy, each $0.0055''$ thick, with the fibers placed in the axial direction. What is the critical value of Torque, T_{cr} , the shell can withstand without buckling? Is the restriction on the equation satisfied?
- 5.9. For a long composite shell of a unidirectional composite material subjected to a uniform external pressure, to attain the highest buckling resistance is it better to have the fibers in the axial direction or the circumferential (hoop) direction? How did you arrive at your conclusion?
- 5.10. Consider a circular cylindrical shell composed of a wall section of 4 laminae, unidirectional in the axial direction. The material is T300/5208 graphite/epoxy whose properties are given in Problem 5.1 and each ply is $0.0055''$ thick. The shell has the

dimensions $R = 20''$ and $L = 60''$. The shell is subjected to a uniform compression.

- (a) What is the overall buckling load $N_{x_{cr}}$?
 - (b) How many lbs. of compressive load can the shell withstand before buckling?
 - (c) What are the values of the integers m and n corresponding to the minimum buckling load?
 - (d) What is the value of the axial stress?
 - (e) What is the membrane hoop stress σ_θ ?
 - (f) As the compressive load is applied, will the shell buckle first or be overstressed?
- 5.11. A piece of composite material circular cylindrical tubing is suggested for use in a laboratory apparatus. It is to be clamped at each end, and when used the air in the interior of the tube will be evacuated to a pressure of approximately 0 psi. The shell is composed to the material and thickness given by the A , B , and D matrices given by

$$A = \begin{bmatrix} 0.84 & 0.00547 & 0 \\ 0.00547 & 0.0176 & 0 \\ 0 & 0 & 2 \times 0.012 \end{bmatrix} \times 10^6 \text{ lb./in.}$$

where $A_{66} = 0.012 \times 10^6 \text{ lb./in.}$

$$B = 0$$

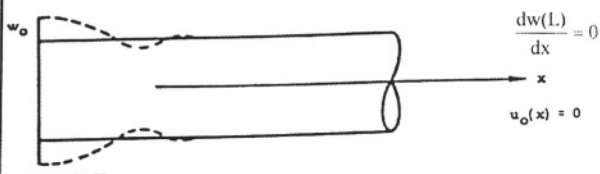
$$D = \begin{bmatrix} 28.053 & 0.1824 & 0 \\ 0.1824 & 0.5874 & 0 \\ 0 & 0 & 2 \times 0.4 \end{bmatrix} \text{ lb.-in.}$$

The tube diameter is $1''$ and its length is $6''$. Can the tubing withstand the internal vacuum in a laboratory without buckling?

- 5.12. Consider a laminated axisymmetric semi-infinite composite cylindrical shell as shown below with boundary conditions as noted.

Description of the problem:

Unit Displacement $w(o) = w_o$



Summary of Boundary Conditions:

$$\begin{aligned} u_o(o) &= 0 \\ w(o) &= w_o \\ \frac{dw(o)}{dx} &= 0 \end{aligned}$$

For the problem shown, find:

- (a) u_o and w
- (b) N_x, N_y, N_{xy}
- (c) M_x, M_y, M_{xy}
- (d) $\sigma_x^{(k)}, \sigma_y^{(k)}, \sigma_{xy}^{(k)}$

- 5.13. Consider the cylindrical shell shown in Figure 5.12. A circular cylindrical shell is of radius 15 inches and length 40 inches. This shell is composed of a quasi-isotropic composite material with the following properties:

$$E = 10 \times 10^6 \text{ psi}$$

$$\nu = 0.3$$

$$\sigma_{\text{allowable}} = 40,000 \text{ psi}$$

Calculate h only to two significant figures: e.g. 1.2", 0.12" or 0.012" etc.

- (a) If the shell is subjected to a compressive axial force of $P = 10,000$ lbs., what thickness h is required to prevent axial compression buckling?
 - (b) If the shell were internally pressurized to $p = 100$ psi, and subjected to an axial compressive load of $P = 10,000$ lbs., what thickness h is required?
 - (c) If the unpressurized shell is subjected to a bending moment of $M = 75,000$ in.-lbs., what thickness h is required?
- 5.14. A composite cylindrical shell of radius 20 inches, length 30 inches, and wall thickness 0.2 inches is subjected simultaneously to an axial compressive load $P = -10,000$ lbs. and a beam type bending load of $M = 20,000$ inch pounds as shown in Figure 5.12. Calculate the magnitude of the maximum compressive stress resultant N_x due to the combined load such that the shell will not buckle.
- 5.15. Consider a vertical smokestack of diameter 4 feet, wall thickness 0.25 inches and 100 feet in height, obviously clamped at the bottom. The stack is made of the same fiberglass described in Problem 5.14 above.

- (a) What and where is the maximum stress in the smokestack?
- (b) Give four equation numbers in the text that you would use to determine if the smokestack would buckle under its own weight.
- (c) Name one other reasonable load condition that you should analyze before constructing and putting this smokestack into operation
- (d) What is the length of the bending boundary layer at the bottom of the smokestack?
- (e) What is the length of the bending boundary layer at the top of the smokestack?

CHAPTER 6

ENERGY METHODS FOR COMPOSITE MATERIAL STRUCTURES

6.1 Introduction

Many composite material structures not only involve anisotropy, multilayer considerations and transverse shear deformation, but also have hygrothermal effects, which can be very important. True, for preliminary design one needs the simplified, easier to use analyses that have been presented earlier, but for the final design, transverse shear deformation and hygrothermal effects must be included. These thermal and moisture effects have been described in Chapter 2. Analytically they cause considerable difficulty, because with their inclusion few boundary conditions are homogeneous, hence separation of variables, used throughout the plate and shell solutions to this point, cannot be utilized in a straightforward manner. Only through the laborious process of transformation of variables can the procedures discussed herein be used [1]. Therefore, energy principles are much more convenient for use in design and analyses of plate and shell structures when hygrothermal effects are present.

In solving beam, plate and shell problems it is seen that in order to obtain a solution one must solve the differential equations and satisfy the boundary conditions; if that cannot be accomplished, there is no solution. With energy methods, one can always obtain a good approximate solution, no matter what the structural complications, the loads or the boundary conditions.

In structural mechanics three energy principles are used: Minimum Potential Energy, Minimum Complementary Energy and Reissner's Variational Theorem [2]. The first two are discussed at length in Sokolnikoff [1] and many other references. The Reissner Variational Theorem, likewise, is widely referenced. In solid mechanics, Minimum Complementary Energy is rarely used, because it requires assuming functions that insure stresses satisfy boundary conditions and equilibrium. It is usually far easier to make assumptions about functions that can represent displacements.

Minimum Potential Energy is widely used in solutions to problems involving beams, plates and shells. In fact, the more complicated the loading, the more complicated the material (e.g., laminated, anisotropic composite material), the more complicated the geometry and the more complicated the boundary conditions (e.g., discontinuous or concentrated boundary conditions), the more desirable it is to use Minimum Potential Energy to obtain an approximate solution, compared to attempting to solve the governing differential equations and to satisfy the boundary conditions exactly.

In addition, in some cases energy principles can be useful for eigenvalue problems such as in the buckling and vibration problems as shall be shown.

The Theorem of Minimum Potential Energy is discussed in Sections 6.2 through 6.9, and Reissner's Variational Theorem is discussed in Sections 6.10 through 6.13, in each case illustrated by beam theory, as was done in References 3 and 4 of Chapter 2.

There are numerous books dealing with energy theorems and variational methods. One of the more recent is that by Mura and Koya [3].

6.2 Theorem of Minimum Potential Energy

For any generalized elastic body, the potential energy of that body can be written as follows:

$$V = \int_R W dR - \int_{S_T} T_i u_i dS - \int_R F_i u_i dR \quad (6.1)$$

where

W = strain energy density function, defined in Equation (6.4) below

R = volume of the elastic body

T_i = i th component of the surface traction

u_i = i th component of the deformation

F_i = i th component of a body force

S_T = portion of the body surface over which tractions are prescribed

We see that the first term on the right-hand side of Equation (6.1) is the strain energy of the elastic body. The second and third terms are the work done by the surface tractions; and the body forces, respectively. The Theorem of Minimum Potential Energy can be stated as described in [1]: "Of all the displacements satisfying compatibility and the prescribed boundary conditions, those that satisfy the equilibrium equations make the potential energy a minimum."

Mathematically, the operation is simply stated as,

$$\delta V = 0 \quad (6.2)$$

The lowercase delta is a mathematical operation known as a variation. Operationally, it is analogous to partial differentiation. To employ variational operations in structural mechanics, only the following three operations are usually needed:

$$\frac{d(\delta y)}{dx} = \delta \left(\frac{dy}{dx} \right), \quad \delta(y^2) = 2y\delta y, \quad \int \delta y dx = \delta \int y dx \quad (6.3)$$

In Equation (6.1) the strain energy density function, W , is defined as follows in a Cartesian coordinate frame:

$$W = \frac{1}{2} \sigma_{ij} \epsilon_{ij} = \frac{1}{2} \sigma_x \epsilon_x + \frac{1}{2} \sigma_y \epsilon_y + \frac{1}{2} \sigma_z \epsilon_z$$

$$+ \sigma_{xy} \epsilon_{xy} + \sigma_{xz} \epsilon_{xz} + \sigma_{yz} \epsilon_{yz}$$

(6.4)

To utilize the Theorem of Minimum Potential Energy, the stress-strain relations for the elastic body are employed to change the stresses in Equation (6.4) to strains, and the strain-displacement relations are employed to change all strains to displacements. Thus, it is necessary for the analyst to select the proper stress-strain relations and strain-displacement relations for the problem being solved.

Although this text is dedicated to composite material structures of all types, it is best to introduce the subject using isotropic monocoque beams, a much simpler structural component, to first illustrate energy principles.

6.3 Analysis of a Beam Using the Theorem of Minimum Potential Energy

As the simplest example of the use of Minimum Potential Energy, consider a beam in bending, shown in Figure 6.1. To make it more simple consider a beam of an isotropic material. In this section, Minimum Potential Energy methods are used to show that if one makes beam assumptions, one obtains the beam equation. However, the most useful employment of the Minimum Potential Energy Theorem is through making assumptions for the dependent variables (the deflection) and using the theorem to obtain approximate solutions.

From Figure 6.1 it is seen that the beam is of length L , in the x -direction, width b and height h . It is subjected to a lateral distributed load, $q(x)$ in the positive z -direction, in units of force per unit length. The modulus of elasticity of the isotropic beam materials is E , and the stress-strain relation is

$$\sigma_x = E \epsilon_x \quad (6.5)$$

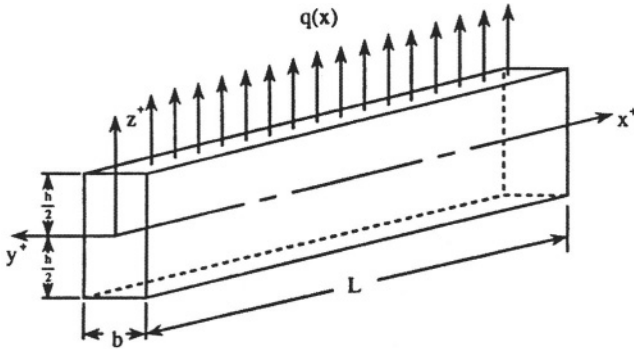


FIGURE 6.1. Beam in bending

The corresponding strain displacement relation is

$$\epsilon_x = \frac{du_x}{dx} = -\frac{d^2w}{dx^2}z \quad (6.6)$$

since in the bending of beams, $u = -z(dw/dx)$ only, as discussed in Chapter 4.

Looking at Equations (6.4) through (6.6) and remembering that in elementary beam theory

$$\sigma_y = \sigma_z = \sigma_{xy} = \epsilon_{xz} = \epsilon_{yz} = \sigma_{xy} = 0$$

then

$$W = \frac{1}{2} \sigma_x \epsilon_x = \frac{1}{2} E \epsilon_x^2 = \frac{1}{2} E \left(\frac{d^2w}{dx^2} \right)^2 z^2 \quad (6.7)$$

Therefore, the strain energy, U , which is the volume integral of the strain energy density function, W , is

$$U = \int_0^L \int_{-b/2}^{+b/2} \int_{-h/2}^{+h/2} \frac{1}{2} E \left(\frac{d^2w}{dx^2} \right)^2 z^2 dz dy dx = \frac{EI}{2} \int_0^L \left(\frac{d^2w}{dx^2} \right)^2 dx \quad (6.8)$$

where, $I = bh^3/12$, the flexural stiffness for a beam of rectangular cross-section.

Similarly, from the surface traction work term in Equation (6.1) it is seen that

$$\int_{s_r} T_i u_i ds = \int_0^L q(x) w(x) dx$$

Equation (6.1) then becomes

$$\boxed{V = \frac{EI}{2} \int_0^L \left(\frac{d^2 w}{dx^2} \right)^2 dx - \int_0^L q(x) w(x) dx} \quad (6.9)$$

Following Equation (6.2) and remembering Equation (6.3) then

$$\delta V = 0 = \frac{EI}{2} \int_0^L \delta \left(\frac{d^2 w}{dx^2} \right)^2 dx - \int_0^L q(x) \delta w(x) dx \quad (6.10)$$

The variation δ can be included under the integral, because the order of variation and integration can be interchanged. Also, there is no variation of E , I or $q(x)$ because they are all specified quantities.

Integrating by parts the first term on the right-hand side of Equation (6.10).

$$\begin{aligned} \frac{EI}{2} \int_0^L \delta \left(\frac{d^2 w}{dx^2} \right)^2 dx &= EI \int_0^L \left(\frac{d^2 w}{dx^2} \right) \delta \left(\frac{d^2 w}{dx^2} \right) dx \\ &= EI \int_0^L \frac{d^2 w}{dx^2} \frac{d^2 (\delta w)}{dx^2} dx \\ &= \left[EI \frac{d^2 w}{dx^2} \delta \left(\frac{dw}{dx} \right) \right]_0^L - EI \int_0^L \frac{d^3 w}{dx^3} \frac{d(\delta w)}{dx} dx \\ &= \left[EI \frac{d^2 w}{dx^2} \delta \left(\frac{dw}{dx} \right) \right]_0^L - \left[EI \frac{d^3 w}{dx^3} \delta w \right]_0^L \\ &\quad + EI \int_0^L \frac{d^4 w}{dx^4} \delta w dx \end{aligned} \quad (6.11)$$

Substituting Equation (6.11) into (6.10) and rearranging, it is seen that:

$$\delta V = 0 = \left[EI \frac{d^2 w}{dx^2} \delta \left(\frac{dw}{dx} \right) \right]_0^L - \left[EI \frac{d^3 w}{dx^3} \delta w \right]_0^L + \int_0^L \left[EI \frac{d^4 w}{dx^4} - q(x) \right] \delta w dx \quad (6.12)$$

For this to be true, the following equation must be satisfied for the integral above to be zero:

$$\boxed{EI \frac{d^4 w}{dx^4} = q(x)} \quad (6.13)$$

This is obviously the governing equation for the bending of a beam under a lateral load. So, it is seen that if one considers a beam-type structure, uses beam assumptions, and uses proper stress-strain relations and strain-displacement relations, the result is the beam bending equation. However, it can be emphasized that if a nonclassical-shaped elastic structure were being analyzed, by using physical intuition, experience or some other reasoning to formulate stress-strain relations, and strain-displacement relations for the body, then through the Theorem of Minimum Potential Energy one can formulate the governing differential equations for the structure and load analogous to Equation (6.13). Incidentally, the resulting governing differential equations derived from the Theorem of Minimum Potential Energy are called the Euler-Lagrange equations.

Note also for Equation (6.12) to be true, each of the first two terms must be zero. Hence, at $x = 0$ and $x = L$ (at each end) either $EI \left(d^2 w / dx^2 \right) = -M_x = 0$ or (dw / dx) must be specified (that is, its variation must be zero), also either $EI \left(d^3 w / dx^3 \right) = -V_x = 0$ or w must be specified. These are the natural boundary conditions. All of the classical boundary conditions, including simple supported, clamped and free edges are contained in the above "natural boundary conditions." This is a nice byproduct from using the variational approach for deriving governing equations for analyzing any elastic structure.

The above discussion shows that if in using The Theorem of Minimum Potential Energy one makes all of the assumptions of classical beam theory, the resulting Euler-Lagrange equation is the classical beam equation (6.13) and the natural boundary conditions given in (6.12) as discussed above.

Equally or more important the Theorem of Minimum Potential Energy provides a means to obtain an approximate solution to practical engineering problems by assuming good deflection functions which satisfy the boundary conditions. As the simplest example consider a beam simply supported at each end subjected to a uniform lateral load per unit length $q(x) = -q_0$, a constant. As shown in Figure 4.4, if $\zeta = L$, the exact solution for this problem is given by Equation (4.49), which is seen to be a polynomial.

Here, an example, assume a deflection which satisfies the boundary conditions for a beam simply supported at each end, where A is a constant to be determined.

$$w(x) = A \sin \frac{\pi x}{L} \quad (6.14)$$

This is not the exact solution, but should lead to a good approximation because (6.14) is a continuous single valued function which satisfies the boundary conditions of the problem. Proceeding,

$$\begin{aligned} w' &= A \frac{\pi}{L} \cos \frac{\pi x}{L}, & w'' &= -\frac{A \pi^2}{L^2} \sin \frac{\pi x}{L} \\ (w'')^2 &= A^2 \frac{\pi^4}{L^4} \sin^2 \frac{\pi x}{L} \end{aligned} \quad (6.15)$$

Substituting (6.14) into (6.9) results in

$$\begin{aligned} V &= \frac{bD_{11}}{2} \int_0^L \frac{A^2 \pi^4}{L^4} \sin^2 \frac{\pi x}{L} dx - \int_0^L (-q_0) A \sin \frac{\pi x}{L} dx \\ &= \frac{bD_{11}}{2} \frac{A^2 \pi^4}{L^4} \left(\frac{L}{2} \right) - (-q_0) A \frac{L}{\pi} \left[-\cos \frac{\pi x}{L} \right]_0^L \\ &= \frac{\pi^4}{4L^3} bD_{11} A^2 + q_0 A \frac{L}{\pi} [-\cos \pi + 1] \end{aligned} \quad (6.16)$$

$$\delta V = 0 = \frac{\pi^4}{4L^3} bD_{11} 2A \delta A + \frac{2q_0 L}{\pi} \delta A = \delta A \left[\frac{\pi^4}{2L^3} bD_{11} A + \frac{2q_0 L}{\pi} \right]$$

Therefore,

$$A = -\frac{4q_0 L^4}{\pi^5 bD_{11}} = w(L/2) \quad (6.17)$$

The exact solution is (4.50)

$$w(L/2) = -\frac{5}{384} \frac{q_0 L^4}{bD_{11}} \quad (6.18)$$

The difference is seen to be 0.386%. So the Minimum Potential Energy solution is seen to be almost exact in determining the maximum deflection.

In determining maximum stresses the accuracy of the energy solution is less, because bending stresses are proportional to second derivatives of deflection. By taking derivatives the errors increase (conversely, integrating is an averaging process and errors decrease) so the stresses from the approximate solution differ more from the exact solution than do the deflections.

To continue this example for a one lamina composite beam, simply supported at each end, subjected to a constant uniform lateral load per unit length of $-q_0$, it is clear that the maximum stress occurs at $x = L/2$. From (4.26) and (4.49) the exact value of the maximum stress is

$$\sigma_{\max} = \sigma_x \left(\frac{L}{2}, \pm \frac{h}{2} \right) = \pm \frac{q_0 L^2}{8} \quad (6.19)$$

Likewise, for the Minimum Potential Energy solution, using (4.26) and (6.14)

$$\sigma_{\max} = \sigma_x \left(\frac{L}{2}, \pm \frac{h}{2} \right) = \pm \frac{4q_0 L^2}{\pi^3} \quad (6.20)$$

The difference between the two is 3.2%, so the energy solution is quite accurate for many applications.

If one wishes to increase the accuracy, instead of using (6.14) one could use

$$w(x) = \sum_{n=1}^N A_n \sin \frac{n\pi x}{L} \quad (6.21)$$

If N were chosen to be three, for example, the expression for $w(x)$ is given by $w(x) = A_1 \sin \frac{\pi x}{L} + A_2 \sin \frac{2\pi x}{L} + A_3 \sin \frac{3\pi x}{L}$ and one would proceed as before, taking variations with respect to A_1 , A_2 and A_3 which provides three algebraic equations for determining the three A_n . Of course as N increases, the accuracy of the solution increases until as N approaches infinity it is another form of the exact solution.

As a second example, examine the same beam, this time subjected to a concentrated load P at the mid-length, $x = L/2$. From Chapter 4, to obtain an exact solution, one must divide the beam into two parts, as discussed in Section 4.3, so that the load discontinuity can be accommodated, with the result that there are two fourth order differential equations and eight boundary conditions. Not so with the case of Minimum Potential Energy to obtain an approximate solution, as follows. Again assume (6.14) as the approximate deflection because it is single valued, continuous and satisfies the boundary conditions at the end of the beam. There,

$$\begin{aligned}
 V &= \frac{1}{2} \int_0^L bD_{11} \left(\frac{d^2 w}{dx^2} \right)^2 dx - Pw(L/2) \\
 &= \frac{\pi^4}{4L^3} bD_{11} A^2 - PA
 \end{aligned}$$

$$\delta V = 0 = \frac{\pi^4 bD_{11} A \delta A}{2L^3} - P \delta A$$

$$\text{or, } A = \frac{2PL^3}{\pi^4 bD_{11}} = w(L/2) = w_{\max}$$

Again, instead of (6.14) one could have chosen (6.21) as the trial function to use in solving this problem.

Thus, the Theorem of Minimum Potential Energy can be used easily for complicated laterally distributed loads, concentrated lateral loads, any boundary conditions, and/or variable or discontinuous beam thicknesses. One only needs to select a form of the lateral displacement such as the following examples.

Clamped Clamped Beam

$$w(x) = A \left[1 - \cos \frac{2\pi x}{L} \right] \quad (6.22)$$

Clamped-Simple Beam

$$w(x) = A \left[L^3 x - 3Lx^3 + 2x^4 \right] \quad (6.23)$$

Cantilevered Beam

$$w(x) = Ax^2 \quad (6.24)$$

6.4 Use of The Theorem of Minimum Potential Energy for Designing a Composite Electrical Transmission Tower

Consider as an example a tapered beam of hollow circular cross-section as shown below in Figure 6.2.

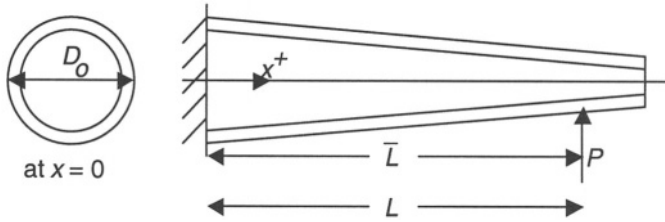


Figure 6.2. Transmission Tower

This beam can be tapered or not, can have a varying wall thickness or not, the material has an axial modulus of elasticity E , is subjected to a load P at $x = \bar{L}$ as shown, is clamped at $x = 0$ and free at $x = L$. A factor of safety is applied to the maximum stress, and a maximum tip deflection at $x = L$ is specified.

For the case shown above the potential energy, V , can be written as:

$$V = \frac{E}{2} \int_0^L I(x) \left(\frac{d^2 w}{dx^2} \right)^2 dx - Pw(\bar{L}) \quad (6.25)$$

where $I(x)$ is included in the integral because it may be a function of the length coordinate x .

For a uniform cantilever beam with an end load P the exact beam solution is

$$w(x) = \frac{P}{6EI} (2Lx^2 - x^3) \quad (6.26)$$

In the Theorem of Minimum Potential Energy, the analyst may choose any trial function he wishes as long as it is single valued, continuous and satisfies the boundary conditions. In this case the following is chosen rather than (6.24). From (6.26) above let the trial function be:

$$w(x) = A(3Lx^2 - x^3) \quad (6.27)$$

therefore,

$$(w'')^2 = 36A^2(L^2 - 2Lx + x^2) \quad (6.28)$$

If the beam has a uniform taper, then the beam diameter can be written as:

$$D(x) = D_0 - Cx \quad (6.29)$$

where D_0 is the base diameter and C is a constant describing the taper. At any axial location, the cross-sectional area can be written as:

$$\text{Area} = \pi D(x)h(x) = \pi D_0 h_0 \quad (6.30)$$

For a constant cross-sectional area of $\pi D_0 h_0$, substituting (6.29) into (6.30), it is seen that the beam wall thickness is

$$h(x) = D_0 h_0 / (D - Cx) \quad (6.31)$$

For the case described above, then the area moment of inertia is:

$$I(x) = \frac{\pi D(x)^3 h(x)}{8} = \frac{\pi D_0^3 h_0}{8} (D_0 - Cx)^2 \quad (6.32)$$

Using (6.32) and (6.28), (6.25) can be written as:

$$V = \frac{E}{2} \int_0^L \frac{\pi D_0^3 h_0}{8} (D_0 - Cx)^2 \cdot 36A^2 (L^2 - 2Lx + x^2) dx - PA(3L\bar{L}^2 - \bar{L}^3) \quad (6.33)$$

After manipulating the above,

$$V = \frac{3}{4} E \pi D_0^3 h_0 L^3 A^2 \left\{ 1 - \frac{CL}{2D_0} + \frac{1}{10} \frac{C^2 L^2}{D_0^2} \right\} - PA(3L\bar{L}^2 - \bar{L}^3) \quad (6.34)$$

Setting the variation of the potential energy to zero, by varying A , results in

$$A = \frac{P(3L\bar{L}^2 - \bar{L}^3)}{12EI_0 L^3 K} \quad (6.35)$$

where

$$I_0 = \frac{\pi D_0^3 h_0}{8} \quad \text{and} \quad K = 1 - \frac{CL}{2D_0} + \frac{1}{10} \frac{C^2 L^2}{D_0^2} \quad (6.36)$$

So
$$w(x) = A(3Lx^2 - x^3) = \frac{P(3L\bar{L}^2 - \bar{L}^3)(3Lx^2 - x^3)}{12EI_0L^3K} \quad (6.37)$$

and

$$w(L) = \frac{P(3L\bar{L}^2 - \bar{L}^3)}{6EI_0K} = \frac{4P(3L\bar{L}^2 - \bar{L}^3)}{3E\pi D_0^3 h_0 K} \quad (6.38)$$

This is the expression to use for displacement restrictions.

The maximum stress occurs at $x = 0$ for this cantilevered beam and can be written as

$$\sigma(0) = \frac{Mc}{I_0} = \frac{M(D_0/2)8}{\pi D_0^3 h_0} \text{ or } \frac{4M}{\pi D_0^2 h_0} \quad (6.39)$$

This is the expression to use for a strength requirement. If the strength requirement has a factor of safety of 4, consider the load applied in Figure 6.2 to be $4P$, in which case (6.39) becomes

$$\sigma(0) = \frac{16P\bar{L}}{\pi D_0^2 h_0} \quad (6.40)$$

Equations (6.38) and (6.40) provide two equations with which to determine h_0 and D_0 . The results are:

$$D_0 = \frac{\sigma_{\max}(3L\bar{L}^2 - \bar{L}^3)}{12Ew(L)\bar{L}K} \quad (6.41)$$

$$h_0 = \frac{16P\bar{L}}{\pi D_0^2 \sigma_{\max}} \quad (6.42)$$

Because (6.41) involves D_0 in the K term, an iteration is necessary to determine D_0 .

As a design example, let $L = 360''$, $\bar{L} = 336''$, $P = 475$ lbs, $E = 3.3 \times 10^6$ psi, $\sigma_{\max} = 15,000$ psi and when $C \neq 0$, $C = .14''/\text{ft}$ or $0.01167''/\text{in}$, $w(L) = 9.5''$ when $P = 475''$ at $\bar{L} = 336''$.

Design 1. Tapered tower, tapered wall thickness, constant weight per unit length.

$$D(x) = D_0 - Cx, \quad h = h(x)$$

In this case $D_0 = 11.92''$, $h_0 = .3814''$
 $D(L) = 7.719''$, $h(L) = .5890''$
 Total volume = 5141 in³ of material used in the design.

Design 2. Straight tower, constant diameter and wall thickness.

$$D = D_0, \quad h = h_0, \quad C = 0$$

In this case $D = 7.719''$, $h = .5890''$
 Total volume = 6149 in³ of material used.

Design 3. Tapered tower, constant wall thickness.

Let $D(x) = D_0 - Cx$, but $h = \text{constant} = h_0$.

Then

$$\begin{aligned} I(x) &= \frac{\pi D(x)^3 h}{8} \\ &= \frac{\pi h_0}{8} [D_0^3 - 3D_0^2 Cx + 3D_0 C^2 x^2 - C^3 x^3] \end{aligned} \quad (6.43)$$

In this case, (6.25) is written as

$$\begin{aligned} V &= \frac{9\pi h_0}{4} A^2 \left\{ \frac{D_0^3 L^3}{3} - \frac{1}{4} D_0^2 L^4 C + \frac{D_0 L^5 C^2}{10} - \frac{C^3 L^6}{60} \right\} \\ &\quad - PA \left[\bar{L}^3 - 3L\bar{L}^2 \right] \end{aligned} \quad (6.44)$$

From $\delta V = 0$

$$A = \frac{P \left[\bar{L}^3 - 3L\bar{L}^2 \right]}{12EI_0 L^3 \left\{ 1 - \frac{3}{4} \frac{LC}{D_0} + \frac{3}{10} \frac{L^2 C^2}{D_0^2} - \frac{1}{20} \frac{L^3 C^3}{D_0^3} \right\}} \quad (6.45)$$

Following the same procedures as noted earlier,

$$D_0 = \frac{\sigma_{\max} \left[\bar{L}^3 - 3L\bar{L}^2 \right]}{12E\bar{L}w(L)_{\{\text{from (6.45)}\}}} \quad (6.46)$$

$$h_0 = \frac{16P\bar{L}}{\pi D_0^2 \sigma_{\max}}$$

Again in (6.46) because K involves D_0 an iteration is necessary. The result is

$$D_0 = 12.724'' \quad h_0 = .3347''$$

$$\text{Total Volume} = \int_0^L \pi D(x) h_0 dx = 4021 \text{ in}^3 \text{ of material used.}$$

Summary: It is seen that Design 3 is the best, being 21.8% lighter than Design 1 and 34.6% lighter than Design 2.

6.5 Minimum Potential Energy for Rectangular Plates

Turning now to the more complicated problem of rectangular plates, and employing the Theory of Minimum Potential Energy, the strain-energy-density function, W , for a three-dimensional solid in rectangular coordinates is given by Equation (6.4). The assumptions associated with the classical plate theory of Chapter 3 are now employed in Equation (6.4) for a rectangular plate. If transverse shear deformation is neglected, then $\epsilon_{xz} = \epsilon_{yz} = 0$. If transverse normal strains are neglected then $\epsilon_z = 0$. Stresses are written in terms of strains, such that for the classical plate

$$\sigma_x = \frac{E}{(1-\nu^2)} [\epsilon_x + \nu\epsilon_y], \quad \sigma_y = \frac{E}{(1-\nu^2)} [\epsilon_y + \nu\epsilon_x]$$

$$\sigma_{xy} = \frac{E}{(1+\nu)} \epsilon_{xy}$$

Therefore, Equation (6.4) becomes

$$W = \frac{E\epsilon_x}{2(1-\nu^2)} (\epsilon_x + \nu\epsilon_y) + \frac{E\epsilon_y}{2(1-\nu^2)} (\epsilon_y + \nu\epsilon_x) + \frac{E}{(1+\nu)} \epsilon_{xy}^2 \quad (6.47)$$

If the plate is subjected to bending and stretching, the deflection functions are given by Equation (2.49). Substituting these into Equation (6.47) results in the following:

$$\begin{aligned}
 W = \frac{1}{2} \frac{E}{(1-\nu^2)} & \left\{ \left(\frac{\partial u_0}{\partial x} \right)^2 + \left(\frac{\partial v_0}{\partial y} \right)^2 + 2\nu \left(\frac{\partial u_0}{\partial x} \right) \left(\frac{\partial v_0}{\partial y} \right) + \frac{1+\nu}{2} \left[\frac{\partial u_0}{\partial y} + \frac{\partial v_0}{\partial x} \right]^2 \right\} \\
 & + \frac{Ez^2}{2(1-\nu^2)} \left[\left(\frac{\partial^2 w}{\partial x^2} \right)^2 + \left(\frac{\partial^2 w}{\partial y^2} \right)^2 + 2\nu \left(\frac{\partial^2 w}{\partial x^2} \right) \left(\frac{\partial^2 w}{\partial y^2} \right) \right] + \frac{Ez^2}{(1+\nu)} \left(\frac{\partial^2 w}{\partial x \partial y} \right)^2
 \end{aligned} \quad (6.48)$$

From this the strain energy $U = \int_R W dR$ is found for an isotropic classical rectangular plate.

$$\begin{aligned}
 U = \frac{K}{2} \int_0^a \int_0^b & \left\{ \left(\frac{\partial u_0}{\partial x} + \frac{\partial v_0}{\partial y} \right)^2 - 2(1-\nu) \frac{\partial u_0}{\partial x} \frac{\partial v_0}{\partial y} + \frac{1-\nu}{2} \left(\frac{\partial u_0}{\partial y} + \frac{\partial v_0}{\partial x} \right)^2 \right\} dx dy \\
 & + \frac{D}{2} \int_0^a \int_0^b \left\{ \left(\frac{\partial^2 w}{\partial x^2} + \frac{\partial^2 w}{\partial y^2} \right)^2 - 2(1-\nu) \left[\left(\frac{\partial^2 w}{\partial x^2} \right) \left(\frac{\partial^2 w}{\partial y^2} \right) - \left(\frac{\partial^2 w}{\partial x \partial y} \right)^2 \right] \right\} dx dy
 \end{aligned} \quad (6.49)$$

It is seen that the first term is the extensional or in-plane strain energy of the plate, and the second is the bending strain energy of the plate. In the latter, it is seen that the first term is proportional to the square of the average plate curvature, while the second term is known as the Gaussian curvature. If Equation (6.49) is used for the usual composite plate one may use the following for the extensional stiffness $K = Eh/(1-\nu^2)$ and the flexural stiffness $D = Eh^3/12(1-\nu^2)$, as discussed previously.

For the plate the total work term due to surface loadings, $p(x,y)$, N_x , N_y and N_{xy} , is seen to be

$$\begin{aligned}
\int_{s_r} T_i u_i dS = \int_0^a \int_0^b p(x, y) w(x, y) dx dy - \int_0^a \int_0^b \left\{ N_x \left[\frac{\partial u_0}{\partial x} + \frac{1}{2} \left(\frac{\partial w}{\partial x} \right)^2 \right] \right. \\
\left. + N_y \left[\frac{\partial v_0}{\partial y} + \frac{1}{2} \left(\frac{\partial w}{\partial y} \right)^2 \right] + N_{xy} \left[\left(\frac{\partial u_0}{\partial y} + \frac{\partial v_0}{\partial x} \right) + \left(\frac{\partial w}{\partial x} \right) \left(\frac{\partial w}{\partial y} \right) \right] \right\} dx dy
\end{aligned} \quad (6.50)$$

Hence, in Equations (6.49) and (6.50) if one considers a plate subjected only to a lateral load $p(x, y)$, one assumes $u_0 = v_0 = N_x = N_y = N_{xy} = 0$. Considering in-plane loads only (except for buckling) assume $w(x, y) = p(x, y) = 0$. If one is looking for buckling loads, assume $p(x, y) = u_0 = v_0 = 0$. The rationale for each of these will be discussed in subsequent sections.

6.6 A Rectangular Composite Material Plate Subjected to Lateral and Hygrothermal Loads

A detailed study by Sloan [4] shows clearly what is involved in analyzing composite panels to accurately account for the effects of anisotropy, transverse shear deformation, thermal and hygrothermal effects.

The stress-strain equations to be considered are given by Equation (2.43), wherein the \bar{Q}_{ij} are given by Equation (2.44). The strain-displacement equations are given by Equation (2.48), the form of the panel displacements by Equation (2.49), from which Equation (2.50) results. By neglecting ϵ_z and σ_z the constitutive relations for the laminate reduce to Equation (2.66).

Employing the Theorem of Minimum Potential Energy, Equation (6.1), for the plate under discussion it is seen that summing the strain-energy-density functions for each lamina across the N laminae that comprise the plate gives the total potential energy as

$$\begin{aligned}
V = \frac{1}{2} \sum_{k=1}^N \int_A \int_{h_{k-1}}^{h_k} \{ \sigma_x [\epsilon_x - \alpha_x \Delta T - \beta_x \Delta m] \\
+ \sigma_y [\epsilon_y - \alpha_y \Delta T - \beta_y \Delta m] + \sigma_{xz} [2\epsilon_{xz}] \\
+ \sigma_{yz} [2\epsilon_{yz}] + \sigma_{xy} \left[2 \left(\epsilon_{xy} - \alpha_{xy} \Delta T - \beta_{xy} \Delta m \right) \right] \} dz dA \\
- \iint_A p(x, y) w(x, y) dA
\end{aligned} \quad (6.51)$$

Here A refers to the planform area of the plate whose dimensions are $0 \leq x \leq a, 0 \leq y \leq b$ and $h/2 \leq z \leq -h/2$. It is noted that the strains used in the strain-energy relations are the isothermal strains, hence one notes the differences between total strain and the thermal and hygrothermal strains in Equation (6.51).

Now, substituting the constitutive Equations (2.66) and the strain-displacement relations (2.50) into Equation (6.51) results in

$$\begin{aligned}
 V = \iint_A & \left\{ \frac{A_{11}}{2} \left(\frac{\partial u_0}{\partial x} \right)^2 + B_{11} \frac{\partial u_0}{\partial x} \frac{\partial \bar{\alpha}}{\partial x} + \frac{D_{11}}{2} \left(\frac{\partial \bar{\alpha}}{\partial x} \right)^2 + A_{12} \frac{\partial u_0}{\partial x} \frac{\partial v_0}{\partial y} \right. \\
 & + B_{12} \left[\frac{\partial u_0}{\partial x} \frac{\partial \bar{\beta}}{\partial y} + \frac{\partial v_0}{\partial y} \frac{\partial \bar{\alpha}}{\partial x} \right] + D_{12} \frac{\partial \bar{\beta}}{\partial y} \frac{\partial \bar{\alpha}}{\partial x} + A_{16} \left[\frac{\partial u_0}{\partial x} \frac{\partial u_0}{\partial y} + \frac{\partial u_0}{\partial x} \frac{\partial v_0}{\partial x} \right] \\
 & + D_{16} \left[\frac{\partial \bar{\alpha}}{\partial x} \frac{\partial \bar{\alpha}}{\partial y} + \frac{\partial \bar{\alpha}}{\partial x} \frac{\partial \bar{\beta}}{\partial x} \right] + B_{16} \left[\frac{\partial u_0}{\partial x} \frac{\partial \bar{\alpha}}{\partial y} + \frac{\partial u_0}{\partial x} \frac{\partial \bar{\beta}}{\partial x} + \frac{\partial u_0}{\partial y} \frac{\partial \bar{\alpha}}{\partial x} + \frac{\partial v_0}{\partial x} \frac{\partial \bar{\alpha}}{\partial x} \right] \\
 & + \frac{A_{22}}{2} \left(\frac{\partial v_0}{\partial y} \right)^2 + B_{22} \frac{\partial v_0}{\partial y} \frac{\partial \bar{\beta}}{\partial y} + \frac{D_{22}}{2} \left(\frac{\partial \bar{\beta}}{\partial y} \right)^2 + A_{26} \left[\frac{\partial v_0}{\partial y} \frac{\partial u_0}{\partial y} + \frac{\partial v_0}{\partial y} \frac{\partial v_0}{\partial x} \right] \\
 & + B_{26} \left[\frac{\partial v_0}{\partial y} \frac{\partial \bar{\alpha}}{\partial y} + \frac{\partial v_0}{\partial y} \frac{\partial \bar{\beta}}{\partial x} + \frac{\partial u_0}{\partial y} \frac{\partial \bar{\beta}}{\partial y} + \frac{\partial v_0}{\partial x} \frac{\partial \bar{\beta}}{\partial y} \right] + D_{26} \left[\frac{\partial \bar{\alpha}}{\partial y} \frac{\partial \bar{\beta}}{\partial y} + \frac{\partial \bar{\beta}}{\partial x} \frac{\partial \bar{\beta}}{\partial y} \right] \\
 & + A_{45} \left[\bar{\alpha} \bar{\beta} + \bar{\alpha} \frac{\partial w}{\partial y} + \bar{\beta} \frac{\partial w}{\partial x} + \frac{\partial w}{\partial x} \frac{\partial w}{\partial y} \right] + A_{55} \left[\frac{\bar{\alpha}^2}{2} + \bar{\alpha} \frac{\partial w}{\partial x} + \frac{1}{2} \left(\frac{\partial w}{\partial x} \right)^2 \right] \\
 & + A_{44} \left[\frac{\bar{\beta}^2}{2} + \bar{\beta} \frac{\partial w}{\partial y} + \frac{1}{2} \left(\frac{\partial w}{\partial y} \right)^2 \right] + A_{66} \left[\frac{1}{2} \left(\frac{\partial u_0}{\partial y} \right)^2 + \frac{\partial u_0}{\partial y} \frac{\partial v_0}{\partial x} + \frac{1}{2} \left(\frac{\partial v_0}{\partial x} \right)^2 \right] \\
 & + B_{66} \left[\frac{\partial u_0}{\partial y} \frac{\partial \bar{\alpha}}{\partial y} + \frac{\partial u_0}{\partial y} \frac{\partial \bar{\beta}}{\partial x} + \frac{\partial v_0}{\partial x} \frac{\partial \bar{\alpha}}{\partial y} + \frac{\partial v_0}{\partial x} \frac{\partial \bar{\beta}}{\partial x} \right] \\
 & + D_{66} \left[\frac{1}{2} \left(\frac{\partial \bar{\alpha}}{\partial y} \right)^2 + \frac{\partial \bar{\alpha}}{\partial y} \frac{\partial \bar{\beta}}{\partial x} + \frac{1}{2} \left(\frac{\partial \bar{\beta}}{\partial x} \right)^2 \right] - \frac{\partial u_0}{\partial x} (N_{1j}^T + N_{1j}^m) \\
 & - \frac{\partial v_0}{\partial y} (N_{2j}^T + N_{2j}^m) - \left(\frac{\partial u_0}{\partial y} + \frac{\partial v_0}{\partial x} \right) (N_{6j}^T + N_{6j}^m) - \frac{\partial \bar{\alpha}}{\partial x} (M_{1j}^T + M_{1j}^m) \\
 & - \frac{\partial \bar{\beta}}{\partial y} (M_{2j}^T + M_{2j}^m) - \left(\frac{\partial \bar{\alpha}}{\partial y} + \frac{\partial \bar{\beta}}{\partial x} \right) (M_{6j}^T + M_{6j}^m) \\
 & \left. + T^* + M^* + \overline{MT}^* - p(x, y)w(x, y) \right\} dA
 \end{aligned} \tag{6.52}$$

In the above, all quantities (except displacements) are defined by Equations (2.56) through (2.61), Equations (2.63) through (2.65) and the following (note that the α_i and β_i below are the coefficients of thermal and hygrothermal expansion):

$$T^* = \frac{1}{2} \sum_{k=1}^N \int_{h_{k-1}}^{h_k} [\bar{Q}_{ij}]_k [\alpha_i]_k [\alpha_j]_k (\Delta T(z, t))^2 dz$$

$$M^* = \frac{1}{2} \sum_{k=1}^N \int_{h_{k-1}}^{h_k} [\bar{Q}_{ij}]_k [\beta_i]_k [\beta_j]_k (\Delta m(z, t))^2 dz$$

$$\overline{MT}^* = \sum_{k=1}^N \int_{h_{k-1}}^{h_k} [\bar{Q}_{ij}]_k [\alpha_i]_k [\beta_j]_k \Delta T(z, t) \Delta m(z, t) dz$$

As written Equation (6.52) provides the expression to use in the analysis of monocoque or composite rectangular plates of constant thickness, wherein one uses the appropriate values of the $[A]$, $[B]$ and $[D]$ stiffness matrix quantities discussed in Chapter 2.

Equation (6.52) is the most general formulation and it is seen that without the surface load term there are 30 terms to represent the strain energy in the composite material panel. Referring to Equation (2.66) and the ensuing discussion it is seen that if the laminate has no stretching-shearing coupling ($A_{16} = A_{26} = 0$) then two terms would be dropped; if no twisting-stretching coupling ($B_{16} = B_{26} = 0$) two more would be dropped; likewise two more are dropped if there were no bending-twisting coupling ($D_{16} = D_{26} = 0$). If the laminate were symmetric about the mid-plane, a very common construction, then five B_{ij} terms would be canceled out, because there would be no bending-stretching coupling. Analogous to (6.52) the corresponding equation for the potential energy for a circular cylindrical shell of a composite material is given by Equation (22.15) pp. 454-456 in Reference [5].

6.7 In-Plane Shear Strength Determination of Composite Materials in Laminated Composite Panels

In this example problem using the Theorem of Minimum Potential Energy, consider a simple test procedure to determine the in-plane shear strength of laminated composite materials, as well as other orthotropic and isotropic advanced material systems; see Vinson [6]. The test apparatus shown in Figure 6.3 is simple, inexpensive, and the flat rectangular plate test specimen is not restricted in size or aspect ratio. In addition to its use for laminated composite materials, the test can also be used for foam core sandwich panels. In sandwich panels the tests can be used to determine the in-plane shear strengths of the faces, the core and/or the adhesive bond between face and core. The shear stresses developed vary linearly in the thickness direction and are constant over the entire planform area.

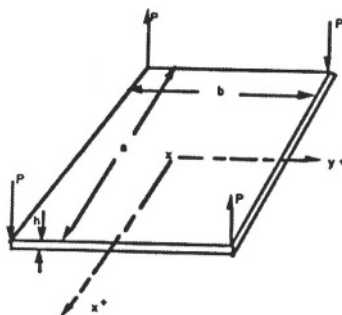


FIGURE 6.3. Test method and geometry for the determination of in-plane shear strength. (Reprinted from Reference [6].)

Consider a panel of the material to be tested to be rectangular in planform, with dimensions a in the x -direction and b in the y -direction. The panel is of constant thickness h and if anisotropic, the material principal axes 1-2, should be aligned with the structural axes x - y . The rectangular panel is placed in a test machine such that the loads P are applied at each of the four corners as shown in Figure 6.3. The loads P are recorded as applied until the test specimen fails. As a result, the in-plane shear strength of the material is easily calculated from the equations developed below.

The Theorem of Minimum Potential Energy is utilized to obtain solutions. It is assumed that the material system is specially orthotropic, i.e., the material axes (1-2) are aligned with the structural axes (x - y). It is further assumed that the test specimen is mid-plane symmetric, i.e., no bending-stretching coupling, $B_{ij} = 0$, no stretching-shearing coupling ($A_{16} = A_{26} = 0$), and no bending-twisting coupling ($D_{16} = D_{26} = 0$). The following methods of analysis can be altered to include laminates or sandwich panels asymmetric to the mid-surface, i.e., $B_{ij} \neq 0$.

The potential energy V for the structure and loading of Figure 6.3 is given by Equation (6.53), which for this case is

$$\begin{aligned}
V = & \int_{-a/2}^{a/2} \int_{-b/2}^{b/2} \left\{ \frac{A_{11}}{2} \left(\frac{\partial u_0}{\partial x} \right)^2 + \frac{D_{11}}{2} \left(\frac{\partial \bar{\alpha}}{\partial x} \right)^2 \right. \\
& + A_{12} \frac{\partial u_0}{\partial x} \frac{\partial v_0}{\partial y} + D_{12} \frac{\partial \bar{\beta}}{\partial y} \frac{\partial \bar{\alpha}}{\partial x} + \frac{A_{22}}{2} \left(\frac{\partial v_0}{\partial y} \right)^2 + \frac{D_{22}}{2} \left(\frac{\partial \bar{\beta}}{\partial y} \right)^2 \\
& + A_{66} \left[\frac{1}{2} \left(\frac{\partial u_0}{\partial y} \right)^2 + \frac{\partial u_0}{\partial y} \frac{\partial v_0}{\partial x} + \frac{1}{2} \left(\frac{\partial v_0}{\partial x} \right)^2 \right] \\
& + D_{66} \left[\frac{1}{2} \left(\frac{\partial \bar{\alpha}}{\partial y} \right)^2 + \frac{\partial \bar{\alpha}}{\partial y} \frac{\partial \bar{\beta}}{\partial x} + \frac{1}{2} \left(\frac{\partial \bar{\beta}}{\partial x} \right)^2 \right] \Bigg\} dy dx \\
& - Pw(a/2, b/2) - Pw(-a/2, -b/2) \\
& + Pw(a/2, -b/2) + Pw(-a/2, b/2)
\end{aligned} \tag{6.53}$$

where u_0 and v_0 are the mid-plane in-plane displacements in the x and y -directions, respectively, and w is the lateral displacement. All displacements are positive in the positive coordinate direction. The means to portray the concentrated loads at the corners of the plate is clearly seen in the last two lines of Equation (6.53).

Neglecting transverse-shear deformation effects, then

$$\bar{\alpha} = -\frac{\partial w}{\partial x} \text{ and } \bar{\beta} = -\frac{\partial w}{\partial y} \tag{6.54}$$

Again, the in-plane and flexural stiffness matrix quantities are given by

$$A_{ij} = \sum_{k=1}^N (\bar{Q}_{ij})_k (h_k - h_{k-1}) \tag{6.55}$$

$$D_{ij} = \frac{1}{3} \sum_{k=1}^N (\bar{Q}_{ij})_k (h_k^3 - h_{k-1}^3) \tag{6.56}$$

where $i, j = 1, 2, 6$ in the usual notation. Note that these quantities are valid for both composite laminate and sandwich construction.

To insure complete generality, the following forms for the displacements are assumed as trial functions, where the numbered coefficients are constants to be determined by boundary conditions and the variational operation:

$$\begin{aligned}
w(x, y) &= C_1 + C_2x + C_3y + C_4x^2 + C_5xy + C_6y^2 \\
&+ C_7x^3 + C_8x^2y + C_9xy^2 + C_{10}y^3 + C_{11}x^4 \\
&+ C_{12}x^3y + C_{13}x^2y^2 + C_{14}xy^3 + C_{15}y^4 \\
u_0(x, y) &= A_1 + A_2x + A_3y + A_4x^2 + A_5xy + A_6y^2 \\
v_0(x, y) &= B_1 + B_2x + B_3y + B_4x^2 + B_5xy + B_6y^2
\end{aligned} \tag{6.57}$$

When, as an analyst, one has trouble deciding on a suitable trial function for the deflection, include as many terms in the polynomial such that the highest power in the polynomial is equal to the highest order in the differential equations.

The following physical conditions are used to simplify the above assumed functions:

$$\begin{aligned}
w(0,0) &= 0; \quad u_0(0,0) = 0; \\
v_0(0,0) &= 0; \quad \frac{\partial w}{\partial x}(0,0) = 0; \quad \frac{\partial w}{\partial y}(0,0) = 0; \\
N_x = N_{xy} &= 0 \text{ on } x = \pm(a/2) \text{ edges}; \quad M_x = M_{xy} = 0 \text{ on } x = \pm(a/2) \text{ edges}; \\
N_y = N_{xy} &= 0 \text{ on } y = \pm(b/2) \text{ edges}; \quad M_y = M_{xy} = 0 \text{ on } y = \pm(b/2) \text{ edges}; \\
w(a/2, b/2) &= w(-a/2, -b/2) = -w(a/2, -b/2) = -w(-a/2, b/2)
\end{aligned}$$

The result of satisfying all of the above is that the trial functions of Equation (6.57) are reduced to the following:

$$\begin{aligned}
w(x, y) &= C_5xy \\
u_0(x, y) &= A_2x + A_3y \quad v_0(x, y) = B_2x + B_3y
\end{aligned} \tag{6.58}$$

Substituting Equation (6.58) into (6.53), and setting the variation equal to zero ($\delta V = 0$) results in the following relationships:

$$C_5 = \frac{P}{4D_{66}}, \quad A_3 = -B_2, \quad A_2 = B_3 = 0$$

Therefore:

$$w(x, y) = \frac{P}{4D_{66}}xy, \quad u_0(x, y) = A_3y, \quad v_0(x, y) = -Ax \quad (6.59)$$

From Equation (6.59) it is seen that no curvature exists in the loaded panel, and that if the panel is of monocoque construction or a laminate in which each lamina is oriented the same as all other laminae, then $D_{66} = \frac{G_{12}h^3}{12}$, where G_{12} is the in-plane shear modulus of the material, and h is the panel thickness.

For a laminated plate the in-plane shear stress for the k th lamina is given by

$$(\sigma_{xy})_k = [2\bar{Q}_{66}]_k [\epsilon_{xy}^0 + \kappa_{xy}z] = -\frac{[2\bar{Q}_{66}]_k Pz}{4D_{66}} \quad (6.60)$$

since for this test, from Equation (6.59), $\epsilon_{xy}^0 = 0$ and $\kappa_{xy} = -C_5 = -P/4D_{66}$.

In Equation (6.60), for a specially orthotropic material $\bar{Q}_{66} = G_{12}$, the in-plane shear modulus of the material, and D_{66} is given by

$$D_{66} = \frac{1}{3} \sum_{k=1}^N (\bar{Q}_{66})_k (h_k^3 - h_{k-1}^3)$$

Equation (6.60) provides an easy way to calculate the shear strength of the failed material simply by measuring the load P at failure, and the location z , i.e., the distance from the midsurface of the panel, of the initial failure site. Likewise, if one is only interested in overall panel in-plane shear strength, then knowing the load P at panel failure, and using $z = h/2$, provides the "panel" in-plane shear strength.

For instance, if the plate is an isotropic single-layer material then

$$\sigma_{xy}(\pm h/2) = \mp \frac{3P}{h^2} \quad \text{or} \quad |\sigma_{xy}| = \frac{3P}{h^2} \quad (6.61)$$

Equation (6.61) is also applicable if the plate is composed of an orthotropic single-layer material. In either case the shear modulus is not needed to calculate the in-plane shear strength.

If the in-plane shear strength of the materials in a midplane symmetric, specially orthotropic or isotropic sandwich panel is desired Equation (6.60) may again be used, where $\bar{Q}_{66_k} = G_{12_k}$ for the material being investigated and for the sandwich

$$D_{66} = \frac{G_{12_f} h_c^2 t_f}{2} \left[1 + (t_f / h_c) + \frac{4}{3} (t_f / h_c)^3 \right] + \frac{G_{12_c} h_c^3}{12} \quad (6.62)$$

where subscripts f and c refer to face and core, respectively, h_c is the depth of the core and t_f is the thickness of each face. For the usual sandwich construction in which $t_f \ll h_c$

$$D_{66} = \frac{G_{12_f} h_c^2 t_f}{2} + \frac{G_{12_c} h_c^3}{12} \quad (6.63)$$

For many sandwich panels in which $G_{12_c} \ll G_{12_f}$,

$$D_{66} = G_{12_f} h_c^2 t_f / 2 \quad (6.64)$$

For sandwich construction in which Equation (6.64) applies, the following shear strengths can be determined.

For the face material:

$$\sigma_{xy_f} = \pm P / 2 t_f h_c \quad (6.65)$$

For the core material:

$$\sigma_{xy_c} = \pm \left(\frac{P}{2 h_c t_f} \right) \left(\frac{G_{12_c}}{G_{12_f}} \right) \quad (6.66)$$

For the adhesive material:

If the adhesive being used is isotropic such that one can assume the shear strength in the x - y plane is the same as the shear strengths in the x - z and y - z planes, i.e., the transverse planes, then Equation (6.67) can be used to determine the shear strength of the adhesive material

$$\sigma_{xy_a} = \pm \left(\frac{P}{2 t_f h_c} \right) \left(\frac{G_{12_a}}{G_{12_f}} \right) \quad (6.67)$$

where the subscript a refers to the adhesive material.

In the above, after a test is conducted, one can determine where the failure first occurred (face, core or adhesive), then Equation (6.65), (6.66) or (6.67) can be used to determine that material strength.

Again, to determine the in-plane shear strength of the face material in a conventional sandwich panel, where Equation (6.64) applies, the in-plane shear moduli of the face, core and adhesive material are not required. However, to determine the in-plane shear strength of the core or adhesive material, the moduli are required, as in Equations (6.66) and (6.67).

6.8 Use of the Theorem of Minimum Potential Energy to Determine Buckling Loads in Composite Plates

Consider a specially orthotropic composite material plate shown below in Figure 6.4, where each $x = \text{constant}$ edge is simply supported, and the y edges are clamped ($y = 0$) and free ($y = b$). This is typical of a flange on a ladder side rail and many other structural applications.

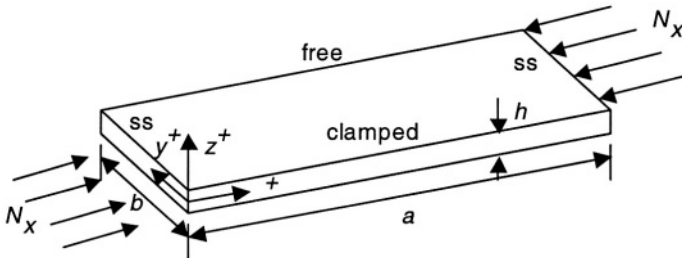


Figure 6.4. Buckling of a Flange Plate

The plate is subjected to a uniform compressive in-plane load of N_x (lbs./in. of width) in the x direction as shown in the Figure 6.4. The Theorem of Minimum Potential Energy is used to determine the critical buckling load, $N_{x_{cr}}$.

From Equation (6.52), and using classical theory i.e. $\bar{\alpha} = -\partial w / \partial x$, $\bar{\beta} = -\partial w / \partial y$, the potential energy expression is:

$$\begin{aligned}
 V = \int_0^a \int_0^b & \left\{ \frac{D_{11}}{2} \left(\frac{\partial^2 w}{\partial x^2} \right)^2 + D_{12} \left(\frac{\partial^2 w}{\partial x^2} \right) \left(\frac{\partial^2 w}{\partial y^2} \right) + \frac{D_{22}}{2} \left(\frac{\partial^2 w}{\partial y^2} \right)^2 \right. \\
 & \left. + 2D_{66} \left(\frac{\partial^2 w}{\partial x \partial y} \right)^2 \right\} dy dx - \int_0^a \int_0^b \frac{N_x}{2} \left(\frac{\partial w}{\partial x} \right)^2 dx dy
 \end{aligned} \tag{6.68}$$

In this expression the effect of the in-plane load for buckling is given by the latter integral, where the effect of an in-plane load on the lateral deflection is seen.

To use the Theorem of Minimum Potential Energy, let the deflection be a separable solution of the x and y variables

$$w(x, y) = f(x)g(y)$$

Since the edges are simply supported at $x = 0$, let

$$f(x) = A_n \sin \frac{n\pi x}{a}$$

which satisfies the boundary conditions, and let

$$g(y) = (y^4 - 4y^3b + 6b^2y^2)$$

because this is proportional to the exact deflection function for a cantilevered beam subjected to a uniform lateral load and satisfies the clamped-free boundary conditions. See (4.37).

Therefore,

$$w(x, y) = A_n \sin \frac{n\pi x}{a} (y^4 - 4y^3b + 6b^2y^2) \quad (6.69)$$

Substituting (6.69) and its derivatives into (6.68) gives

$$\begin{aligned} V = \int_0^a \int_0^b & \left\{ \frac{D_{11}}{2} \left[A_n^2 \frac{n^4 \pi^4}{a^4} \sin^2 \frac{n\pi x}{a} (y^4 - 4by^3 + 6b^2y^2) \right] \right. \\ & + D_{12} \left[\left[-A_n \frac{n^2 \pi^2}{a^2} \sin \frac{n\pi x}{a} (y^4 - 4by^3 + 6b^2y^2) \right] x \right. \\ & \left. \left[+ A_n \sin \frac{n\pi x}{a} (12y^2 - 24by + 12b^2) \right] \right] \\ & + \frac{D_{22}}{2} \left[A_n^2 \sin^2 \frac{n\pi x}{a} (12y^2 - 24by + 12b^2)^2 \right] \\ & + 2D_{66} \left[A_n^2 \frac{n^2 \pi^2}{a^2} \cos^2 \frac{n\pi x}{a} (4y^3 - 12by^2 + 12b^2y) \right] \Bigg\} dy dx \\ & - \frac{N_x}{2} \int_0^a \int_0^b A_n^2 \frac{n^2 \pi^2}{a^2} \cos^2 \frac{n\pi x}{a} (y^4 - 4by^3 + 6b^2y^2) dy dx \end{aligned} \quad (6.70)$$

Performing the spatial integration the final expression for the potential energy is:

$$V = (A_n^2) \left\{ \frac{D_{11}\pi^4 n^4 b^9}{2a^4} \left(\frac{104}{45} \right) - \frac{12}{7} D_{12} \frac{n^2 \pi^2}{a^2} b^7 + \frac{144}{2} D_{22} b^5 \left(\frac{1}{5} \right) \right. \\ \left. + 32 D_{66} n^2 \pi^2 \frac{b^7}{a^2} \left(\frac{9}{14} \right) - \frac{N_x}{2} n^2 \pi^2 \frac{b^9}{a^2} \left(\frac{104}{45} \right) \right\} \quad (6.71)$$

Taking variations of (6.71) for this eigenvalue problem one sees that the bracket must be zero.

$$\delta V = 0 = 2A_n \delta A_n \{ \} = 0, \text{ so } \{ \} = 0$$

From the above the critical buckling load $N_{x_{cr}}$ is seen to be

$$N_x = \frac{\pi^2 D_{11}}{b^2} \left[n^2 \left(\frac{b}{a} \right)^2 - \frac{(3)(45)}{(7)(13)} \frac{D_{12}}{D_{11}} + \frac{(18)(9)}{13\pi^2 n^2} \left(\frac{D_{22}}{D_{11}} \right) \left(\frac{a}{b} \right)^2 \right. \\ \left. + \frac{(36)(45)}{(7)(13)} \frac{D_{66}}{D_{11}} \right] \quad (6.72)$$

This is the solution for this case in general, written so that the relative influence for various stiffness terms can be assessed.

First, it is important to determine the wave number n yielding the lowest critical buckling load, because this is the only one of physical significance.

$$\frac{\partial N_x}{\partial n} = 0 = \frac{\pi^2 D_{11}}{b^2} \left[2n \left(\frac{b}{a} \right)^2 - \frac{2(18)(9)}{(13)(\pi^2)} \left(\frac{D_{22}}{D_{11}} \right) \left(\frac{a}{b} \right)^2 \frac{1}{n^3} \right] = 0.$$

Therefore,

$$n = \left[\frac{(18)(9)}{(13)(\pi^2)} \left(\frac{D_{22}}{D_{11}} \right) \right]^{1/4} \left(\frac{a}{b} \right) \quad (6.73)$$

Now, substituting (6.73) into (6.72) results in

$$N_{x_{cr}} = \frac{\pi^2 D_{11}}{b^2} \left\{ \left(\frac{18}{13} \right)^{1/2} \frac{3}{\pi} \left(\frac{D_{22}}{D_{11}} \right)^{1/2} - \frac{(3)(45)}{(7)(13)} \left(\frac{D_{12}}{D_{11}} \right) \right. \\ \left. + \left(\frac{18}{13} \right)^{1/2} \frac{3}{\pi} \left(\frac{D_{22}}{D_{11}} \right)^{1/2} + \frac{(36)(45)}{(7)(13)} \left(\frac{D_{66}}{D_{11}} \right) \right\} \quad (6.74)$$

Note the lowest critical buckling load for this case given in (6.74) is independent of the integer n , and the aspect ratio (a/b) !. It is also interesting to note that the first and the

third terms above are identical. This means that in (6.68) the $\frac{D_{11}}{2} \left(\frac{\partial^2 w}{\partial x^2} \right)^2$ term and the

$\frac{D_{22}}{2} \left(\frac{\partial^2 w}{\partial y^2} \right)^2$ term contribute the same strain energy. This in turn means that if D_{22} is reduced from one material to another the curvature in the y direction increases such that the strain energy remains the same, and of course the reverse is true.

6.9 Trial Functions for Various Boundary Conditions for Composite Material Rectangular Plates

To satisfy various boundary conditions for rectangular composite material plates, the lateral deflection $w(x,y)$ may take many forms as long as they are single valued and continuous.

For all combinations of clamped and simply supported boundary conditions Wu and Vinson [7] provide functions that can be used which involve characteristic beam functions that formulated by Warburton [8] and completely characterized by Young and Felgar [9,10].

Another example are the functions used by Causbie and Lagace [11] for the study of composite material rectangular plates subjected to in-plane compressive buckling loads in the x -direction. They assumed the following:

1. Simply supported on all edges

$$w = \sum_{m=1}^6 \sum_{n=1}^2 A_{mn} \sin \frac{m\pi x}{a} \sin \frac{n\pi y}{b} \quad (6.75)$$

2. SS on loaded edges, SS on one side, free on the other side

$$w = \sum_{m=1}^3 \sum_{n=1}^3 \sum_{p=1}^3 \sin\left(\frac{m\pi x}{a}\right) \left[A_{mn} \sinh\left(\frac{ny}{b}\right) + B_{mp} \sin\left(\frac{p\pi y}{b}\right) \right] \quad (6.76)$$

3. Clamped on loaded ends; simply supported on the sides

$$w = \sum_{n=1}^6 \sum_{m=1}^2 A_{mn} \left\{ \cos\left[\frac{(m+1)\pi x}{a}\right] - \cos\left[\frac{(m-1)\pi x}{a}\right] \right\} \sin\left(\frac{n\pi y}{b}\right) \quad (6.77)$$

4. Clamped on loaded ends; simply supported on one side; free on the other side

$$w = \sum_{n=1}^5 \sum_{m=1}^3 \sum_{p=1}^3 \left\{ \cos\left[\frac{(m+1)\pi x}{a}\right] - \cos\left[\frac{(m-1)\pi x}{a}\right] \right\} x + \left[A_{mn} \sinh\left(\frac{ny}{b}\right) + B_{mp} \sin\left(\frac{p\pi y}{b}\right) \right] \quad (6.78)$$

6.10 Reissner's Variational Theorem and Its Applications

Because of its broad usage in the analysis of isotropic or anisotropic thin-walled structures accounting for transverse shear deformation and transverse-normal stress, Reissner's Variational Theorem is discussed herein. A general discussion of the Variational Principle is presented, followed by a treatment of the theory of moderately thick beams, which represents a simple example of the power of this technique. The first application is the development of the governing equations for the static deformations of moderately thick rectangular beams, including the effects of transverse-shear deformation and transverse normal stress. The second application involves the use of the Theorem, together with Hamilton's Principle, to develop a theory of beam vibrations including rotatory inertia, in addition to the other effects listed above. Although dynamic effects have not previously been discussed herein, the mathematics involved is straightforward and it is convenient to discuss vibrations at this time.

The principle of Minimum Potential Energy was discussed in Sections 6.2 through 6.9. It was noted that, in carrying out the variations to minimize V , the class of admissible variations are displacements satisfying the boundary conditions. The resulting Euler-Lagrange equations of the variational problem are then equilibrium equations. When the Principle is used to formulate approximate theories (i.e., beam, plate or shell theory), it can therefore only yield approximate equilibrium equations and the stress-strain or strain-displacement relations must be obtained independently.

In 1950, Reissner [2] developed a new variational theorem of elasticity that yields as its Euler-Lagrange equations both the equilibrium equations and the stress-displacement relations. The result is the Reissner Variational Theorem, that may be stated as follows: "Of all the stress and displacement states satisfying the boundary conditions, those which also satisfy the equilibrium equations and the stress displacement relations correspond to a minimum of the functional ψ defined as,

$$\psi = \int_R H dR - \int_R F_i u_i dR - \int_{S_T} T_i u_i dS \quad (6.79)$$

Here,

$$H = \sigma_{ij} \varepsilon_{ij} - W(\sigma_{ij}) \quad (6.80)$$

S_T is the portion of S on which stresses are prescribed, and $W(\sigma_{ij})$ is the strain-energy density function in terms of stresses only. In a rectangular coordinate system $W(\sigma_{ij})$ is written as follows for an isotropic material:

$$\begin{aligned} W(\sigma_{ij}) = & \frac{1}{2E} [\sigma_x^2 + \sigma_y^2 + \sigma_z^2 - 2\nu(\sigma_x \sigma_y + \sigma_y \sigma_z + \sigma_z \sigma_x) \\ & + 2(1+\nu)(\sigma_{xy}^2 + \sigma_{zx}^2 + \sigma_{yz}^2)] \end{aligned} \quad (6.81)$$

The proof of the Theorem is as follows. Taking the variation ψ in Equation (6.79) and equating it to zero, one obtains:

$$\begin{aligned} \delta\psi = & \int_R \left[\sigma_{ij} \delta\varepsilon_{ij} + \varepsilon_{ij} \delta\sigma_{ij} - \frac{\partial W}{\partial \sigma_{ij}} \delta\sigma_{ij} \right] dR \\ & - \int_R F_i \delta u_i dR - \int_{S_T} T_i \delta u_i ds = 0 \end{aligned} \quad (6.82)$$

where

$$\varepsilon_{ij} = \frac{1}{2} \left(\frac{\partial u_i}{\partial x_j} + \frac{\partial u_j}{\partial x_i} \right)$$

It should be noted that all stress and strain components have been varied, while the body force and the surface traction components F_i and T_i , are not varied because they are prescribed functions. Rearranging the above expression, one obtains

$$\begin{aligned} \delta\psi = \int_R \left\{ \left[\varepsilon_{ij} - \frac{\partial W}{\partial \sigma_{ij}} \right] \delta\sigma_{ij} + \frac{1}{2} \sigma_{ij} \left[\frac{\partial}{\partial x_j} (\delta u_i) + \frac{\partial}{\partial x_i} (\delta u_j) \right] \right\} dR \\ - \int_R F_i \delta u_i dR - \int_{S_T} T_i \delta u_i dS = 0 \end{aligned} \quad (6.83)$$

The terms $\sigma_{ij} \frac{\partial}{\partial x_j} (\delta u_i)$ and $\sigma_{ij} \frac{\partial}{\partial x_i} (\delta u_j)$ are symmetric with respect to i and j , and one may therefore interchange these indices and obtain

$$\begin{aligned} \delta\psi = \int_R \left\{ \left[\varepsilon_{ij} - \frac{\partial W}{\partial \sigma_{ij}} \right] \delta\sigma_{ij} + \sigma_{ij} \frac{\partial}{\partial x_j} (\delta u_i) \right\} dR \\ - \int_R F_i \delta u_i dR - \int_{S_T} T_i \delta u_i dS = 0 \end{aligned} \quad (6.84)$$

Also note that $\frac{\partial}{\partial x_j} (\sigma_{ij} \delta u_i) = \sigma_{ij} \frac{\partial}{\partial x_j} (\delta u_i) + \frac{\partial \sigma_{ij}}{\partial x_j} \delta u_i$, so that Equation (6.84) may be written

$$\begin{aligned} \delta\psi = \int_R \left\{ \left[\varepsilon_{ij} - \frac{\partial W}{\partial \sigma_{ij}} \right] \delta\sigma_{ij} + \frac{\partial}{\partial x_j} (\sigma_{ij} \delta u_i) - \frac{\partial \sigma_{ij}}{\partial x_j} \delta u_i \right\} dR \\ - \int_R F_i \delta u_i dR - \int_{S_T} T_i \delta u_i dS = 0 \end{aligned}$$

Applying the Green-Gauss divergence theorem and remembering that $\delta u_i = 0$ on all surfaces where displacements are prescribed, one obtains:

$$\int_R \frac{\partial}{\partial x_j} (\sigma_{ij} \delta u_i) dR = \int_{S_T} \sigma_{ij} \nu_j \delta u_i dS = \int_{S_T} T_i \delta u_i dS \quad (6.85)$$

where the ν_j are the direction cosines. Finally, substituting Equation (6.85) into (6.84),

$$\delta\psi = \int_R \left\{ \left[\varepsilon_{ij} - \frac{\partial W}{\partial \sigma_{ij}} \right] \delta\sigma_{ij} - \left[\frac{\partial \sigma_{ij}}{\partial x_j} + F_i \right] \delta u_i \right\} dR = 0 \quad (6.86)$$

Since $\delta\sigma_{ij}$ and δu_i are arbitrary variations, Equation (6.86) is satisfied only if the stresses σ_{ij} and strains ϵ_{ij} satisfy the equations,

$$\boxed{\frac{\partial \sigma_{ij}}{\partial x_j} + F_i = 0} \quad (6.87)$$

$$\boxed{\epsilon_{ij} = \frac{\partial W(\sigma_{ij})}{\partial \sigma_{ij}}} \quad (6.88)$$

It is seen that Equations (6.87) and (6.88) are the equilibrium and stress-strain relations of elasticity. Thus, the Reissner Variational Theorem is found to be equivalent to the three-dimensional equations of elasticity and is, therefore, established. Consider now some typical applications of the Theorem to the static and dynamic deformations of beams.

6.11 Static Deformation of Moderately Thick Beams

As a first illustration, consider the development of the theory for the static deformations of moderately thick beams in which the effects of transverse shear deformation and transverse normal stress are taken into account following Reissner [2]. Consider a beam of rectangular cross-section of width b , height h and length L , as shown in Figure 6.1, subject to a distributed load $q(x)$ acting on the surface $z = +h/2$.

In order to apply the variational theorem, one must first assume functions for the stresses in the beams. In this case the following stresses are assumed for a beam of rectangular cross-section. Assume the following for this example:

$$\sigma_x = \frac{Mz}{I}, \quad \text{where } I = \frac{bh^3}{12} \quad (6.89)$$

$$\sigma_{xz} = \frac{3Q}{2A} \left[1 - \left(\frac{z}{h/2} \right)^2 \right], \quad \text{where } A = bh \quad (6.90)$$

$$\sigma_z = \frac{3q}{4b} \left[\frac{z}{h/2} + \frac{2}{3} - \frac{1}{3} \left(\frac{z}{h/2} \right)^3 \right] \quad (6.91)$$

$$\sigma_y = \sigma_{yx} = \sigma_{yz} = 0 \quad (6.92)$$

In the above, M is the beam bending moment, and Q is the beam transverse shear resultant. It should be noted that the form of the stress components σ_x and σ_{xz} is identical to that of classical theory. The form of the transverse normal stress σ_z may easily be derived from the stress equation of equilibrium in the thickness direction, as a consequence of the assumptions made above for σ_x and σ_{xz} . The expression shown in Equation (6.91) is derived for

$$\sigma_z(+h/2) = q \text{ and } \sigma_z(-h/2) = 0$$

An analogous expression can be derived easily if there were a normal stress on the lower surface.

The stress couple M and shear resultant Q are defined in the usual manner by the equations

$$M(x) = \int_{-h/2}^{h/2} b \sigma_x z dz \quad (6.93)$$

$$Q(x) = \int_{-h/2}^{h/2} b \sigma_{xz} dz \quad (6.94)$$

It should be noted that Equations (6.89) through (6.94) satisfy all of the stress boundary conditions.

As in classical beam bending theory, one assumes that beam cross-sections undergo at most a translation and a rotation. Such displacements are of the following form for bending only (no stretching), which is the simplest case to study:

$$u = z\bar{\alpha}(x) \quad (6.95)$$

$$w = w(x) \quad (6.96)$$

It should be noted that the cross-sections are not assumed to remain normal to the deformed middle surface. If they did, it would result in classical beam theory, which neglects transverse shear deformation.

The appropriate strain displacement relations may be written

$$\epsilon_x = \frac{\partial u}{\partial x} = z\bar{\alpha}'(x) \quad (6.97)$$

$$\epsilon_{xz} = \frac{1}{2} \left(\frac{\partial u}{\partial z} + \frac{\partial w}{\partial x} \right) = \frac{1}{2} (\bar{\alpha} + w') \quad (6.98)$$

$$\varepsilon_z = \frac{\partial W}{\partial z} = 0 \quad (6.99)$$

where the primes denote differentiation with respect to x .

For the present case, the Reissner functional ψ , Equation (6.79), takes the form

$$\begin{aligned} \psi = \int_0^L \int_{-h/2}^{h/2} b \{ \sigma_x z \bar{\alpha}' + \sigma_{xz} (\bar{\alpha} + w') \\ - \frac{1}{2E} [\sigma_x^2 + \sigma_z^2 - 2\nu \sigma_x \sigma_z + 2(1+\nu) \sigma_{xz}^2] \} dz dx - \int_0^L w q dx \end{aligned} \quad (6.100)$$

Substituting Equations (6.89) through (6.99) into Equation (6.100) and carrying out the integrations with respect to z , one obtains,

$$\begin{aligned} \psi = \int_0^L \left\{ M \bar{\alpha}' + Q (\bar{\alpha} + w') - \frac{M^2}{2EI} + \frac{6\nu q M}{5EA} - \frac{3Q^2}{5GA} - q w \right\} dx \\ + \int_0^L \int_{-h/2}^{h/2} \frac{\sigma_z^2}{2E} b dz dx \end{aligned} \quad (6.101)$$

It should be noted that the integration of the term in σ_z^2 has not been carried out because this term depends only on q and not on the basic unknown stresses and displacements, $\bar{\alpha}$, W , M and Q . Thus, when variations to minimize ψ are taken, the term in σ_z^2 will not contribute to the result. One may now obtain the governing equations by minimizing the functional ψ of Equation (6.101). Taking the variation of this equation and setting it equal to zero results in

$$\begin{aligned} \delta\psi = \int_0^L \left\{ M \delta(\bar{\alpha}') + \bar{\alpha}' \delta M + Q (\delta \bar{\alpha} + \delta(w')) + (\bar{\alpha} + w') \delta Q - \frac{M}{EI} \delta M \right. \\ \left. + \frac{6\nu q}{5EA} \delta M - \frac{6Q}{5GA} \delta Q - q \delta w \right\} dx = 0 \end{aligned} \quad (6.102)$$

Integrating by parts and rearranging, Equation (6.102) may be written in the form

$$\begin{aligned} \delta\psi = & [M\delta\bar{\alpha} + Q\delta w]_0^L + \int_0^L \{ [Q - M']\delta\bar{\alpha} - [Q' + q]\delta w \\ & + \left[\bar{\alpha}' - \frac{M}{EI} + \frac{6\nu q}{5EA} \right] \delta M + \left[\bar{\alpha} + w' - \frac{6Q}{5GA} \right] \delta Q \} dx = 0 \end{aligned} \quad (6.103)$$

Setting the first term equal to zero yields the natural boundary conditions; for the beam. It is seen that, either $M = 0$ or $\bar{\alpha}$ must be prescribed at $x = 0$ and L , either $Q = 0$ or w must be prescribed at $x = 0$ and L .

Finally, since the variations $\delta\bar{\alpha}$, δw , δM and δQ are all independent arbitrary functions of x , the only way in which the definite integral of Equation (6.103) can be made to vanish is by requiring the unknowns M , Q , $\bar{\alpha}$ and w to satisfy the equations.

$$\boxed{-\frac{dM}{dx} + Q = 0} \quad (6.104)$$

$$\boxed{\frac{dQ}{dx} + q = 0} \quad (6.105)$$

$$\boxed{\frac{d\bar{\alpha}}{dx} - \frac{M}{EI} + \frac{6\nu q(x)}{5EA} = 0} \quad (6.106)$$

$$\boxed{\bar{\alpha} + \frac{dw}{dx} - \frac{6Q}{5GA} = 0} \quad (6.107)$$

Note that Equations (6.104) and (6.105) are identical to the equilibrium equations of classical beam theory. This is as expected since no new stress resultants or stress couples were introduced. Considering Equation (6.107), it is seen that the quantity $\bar{\alpha} + w'$ is precisely the change in the angle between the beam cross-section and the middle surface occurring during the deformation; Equation (6.107) shows that this angular change, which is a measure of the shear deformation, is proportional to Q/A , which is the average shear stress. In addition, it should be noted that as $G \rightarrow \infty$, the transverse shear deformation tends to vanish as assumed in classical beam theory. Finally, observe that the third term of Equation (6.106) depends on the lateral load q and Poisson's ratio ν . This term would vanish if one assumed $\nu = 0$ as in classical beam theory; it is identified as the effect of the normal stress σ_z which is proportional to q , according to the initial assumptions, as seen in Equation (6.91).

Solutions of Equations (6.104) through (6.107) may easily be obtained for typical loading and boundary conditions. These solutions reveal that for beams of isotropic materials, the effects of the transverse shear deformation and transverse normal stress are negligible for sufficiently large values of L/h and become important as L/h decreases to less than ten.

As stated previously, for simplicity's sake the example treated in detail here is for a beam subjected to a lateral load. Analogous procedures could be followed to develop the equations and solutions for plates, shells and structures of other shapes using Reissner's Variational Theorem, whether in a Cartesian coordinate system or any other coordinate system, such as cylindrical or spherical coordinates.

One interesting use of beam theory including transverse shear deformation is in the development of ASTM Standard C393-62, in which the composite bending stiffness and shear modulus are measured using 3-point and 4-point bending tests. For each test the midspan deflection is measured, and is given by the following equations, respectively:

$$w_{\max} = \frac{PL^3}{48D} + \frac{PL}{4G_c(t_f + h_c)^2 / h_c b} \quad (6.108)$$

$$w_{\max} = \frac{11PL^3}{768D} + \frac{PL}{8G_c(t_f + h_c)^2 / h_c b} \quad (6.109)$$

From these simultaneous equations the flexural stiffness D , and the shear modulus of the core G_c are found.

6.12 Flexural Vibrations of Moderately Thick Beams

As a second example, a theory, developed by Reissner [2], for free flexural vibrations of moderately thick beams of rectangular cross-section is treated; this will include the effects of transverse shear deformation and rotatory inertia. Although beam vibrations were discussed previously in Section 4.6, the mathematical operations involved in the Variational Principle are presented here.

In order to derive the equations of motion, one now applies Hamilton's Principle in conjunction with Reissner's Variational Theorem. Recall that Hamilton's Principle is nothing more than a variational statement of Newton's Laws of Motion. Thus, one may state that the motion of the beam of Figure 6.1 will be such as to minimize the integral

$$\Phi = \int_{t_1}^{t_2} (T - \psi) dt \quad (6.110)$$

where T is the kinetic energy of the system, ψ is the Reissner functional, and t is time. The quantity $(T - \psi) = L$ is often called the Lagrangian. Note that the Theorem of Minimum Potential Energy could have been employed rather than using the Reissner

Variational Theorem merely by replacing ψ in Equation (6.110) by U of Equation (6.8). In that form the vibration of a classical beam would have been investigated. The equations of motion can now be obtained from the condition,

$$\delta\Phi = 0 \quad (6.111)$$

for a conservative system, and it must be remembered that all stresses, strains and displacements are now functions of time, as well as the spatial coordinates x and z .

The kinetic energy, T , for the beam of Figure 6.1 may be written in the form

$$T = \int_0^L \int_{-h/2}^{h/2} \frac{\rho_m b}{2} \left[\left(\frac{\partial u}{\partial t} \right)^2 + \left(\frac{\partial w}{\partial t} \right)^2 \right] dz dx \quad (6.112)$$

where ρ_m is the mass density of the beam material. Substituting Equations (6.95) and (6.96) in Equation (6.112) and integrating with respect to z gives

$$T = \int_0^L \frac{\rho_m}{2} \left[I \left(\frac{\partial \bar{\alpha}}{\partial t} \right)^2 + A \left(\frac{\partial w}{\partial t} \right)^2 \right] dx \quad (6.113)$$

The substitution of Equations (6.113) and (6.101) into Equation (6.110) then yields

$$\begin{aligned} \Phi = \int_{t_1}^{t_2} \int_0^L \left\{ \frac{\rho_m}{2} \left[I \left(\frac{\partial \bar{\alpha}}{\partial t} \right)^2 + A \left(\frac{\partial w}{\partial t} \right)^2 \right] - M \frac{\partial \bar{\alpha}}{\partial x} \right. \\ \left. - Q \left(\bar{\alpha} + \frac{\partial w}{\partial x} \right) + \frac{M^2}{2EI} - \frac{6\nu q M}{5EA} + \frac{3Q^2}{5GA} + qw \right\} dx dt \end{aligned} \quad (6.114)$$

where again a term in σ_z^2 has been dropped since it will not contribute to the variations (as explained previously).

The governing equations are then obtained by taking the variation of Equation (6.114) and setting the result equal to zero. It is found that the natural boundary conditions are the same as for the static case, while the initial deflection and velocity will also be specified. The equations of motion are obtained in the form

$$\boxed{Q - \frac{\partial M}{\partial x} + \rho_m I c \frac{\partial^2 \bar{\alpha}}{\partial t^2} = 0} \quad (6.115)$$

$$\boxed{\frac{\partial Q}{\partial x} - \rho_m A \frac{\partial^2 w}{\partial t^2} + q(x, t) = 0} \quad (6.116)$$

$$\boxed{\frac{\partial \bar{\alpha}}{\partial x} - \frac{M}{EI} + \frac{6vq(x, t)}{5EA} = 0} \quad (6.117)$$

$$\boxed{\bar{\alpha} + \frac{\partial w}{\partial x} - \frac{6Qk}{5GA} = 0} \quad (6.118)$$

In the above equations, two tracing constants c and k are introduced for the purpose of identifying terms. Note that Equation (6.115) is identical to the corresponding moment equilibrium condition of classical beam theory, except for the term $\rho_m Ic (\partial^2 \bar{\alpha} / \partial t^2)$ which represents the contribution of rotatory inertia. Thus, when the tracing constant $c = 1$ in the resulting solutions, rotatory inertia effects are included; when $c = 0$, the theory neglects the effect of rotatory inertia. Equation (6.116) is identical to the classical beam theory equation for transverse force equilibrium with the transverse inertia term added. Equation (6.117) exhibits the term $6vq/5EA$, which is the contribution of transverse normal stress; since this is the only term in which v appears explicitly, setting $v = 0$ is equivalent to neglecting the transverse normal stress. Equation (6.118) is nearly identical to the corresponding equation of classical theory with the term $6Qk/5GA$ representing the effect of transverse shear deformation that is included when the tracing constant $k = 1$, and neglected when $k = 0$. Now consider a simple application of this theory.

6.13 Flexural Natural Frequencies of a Simply Supported Beam Including Transverse Shear Deformation and Rotatory Inertia Effects

As an example of free vibration analysis using Reissner's Variational Theorem consider a simply supported beam undergoing a lateral vibration.

For free vibrations, Equation (6.115) through (6.118) reduce to the following by letting all applied loads go to zero.

$$\left. \begin{aligned} Q - \frac{\partial M}{\partial x} + \rho_m I_c \frac{\partial^2 \alpha}{\partial t^2} &= 0 \\ \frac{\partial Q}{\partial x} - \rho_m A \frac{\partial^2 w}{\partial t^2} &= 0 \\ \frac{\partial \bar{\alpha}}{\partial x} - \frac{M}{EI} &= 0 \\ \bar{\alpha} + \frac{\partial w}{\partial x} - \frac{6Qk}{5GA} &= 0 \end{aligned} \right\} \quad (6.119)$$

It is convenient to reduce these equations to a system of two equations in the unknown displacements w and $\bar{\alpha}$.

From the first and the third of Equations (6.119), one obtains

$$M = EI \frac{\partial \bar{\alpha}}{\partial x}, \quad Q = EI \frac{\partial^2 \bar{\alpha}}{\partial x^2} - \rho_m I_c \frac{\partial^2 \bar{\alpha}}{\partial t^2}$$

and the substitution of these expressions in the second and fourth of Equations (6.119) yields

$$\left. \begin{aligned} \frac{\partial^3 \bar{\alpha}}{\partial x^3} - \frac{\rho_m c}{E} \frac{\partial^3 \bar{\alpha}}{\partial x \partial t^2} - \frac{\rho_m A}{EI} \frac{\partial^2 w}{\partial t^2} &= 0 \\ \bar{\alpha} + \frac{\partial w}{\partial x} - \frac{kh^2}{10} \left[\frac{E}{G} \frac{\partial^2 \bar{\alpha}}{\partial x^2} - \frac{\rho_m c}{G} \frac{\partial^2 \bar{\alpha}}{\partial t^2} \right] &= 0 \end{aligned} \right\} \quad (6.120)$$

For a simply supported beam of length L , the boundary conditions are $w = M = 0$ at $x = 0$, and L . When the beam is oscillating in a normal mode, the motion is harmonic so that the solutions for $\bar{\alpha}$ and w may be taken in the form:

$$\left. \begin{aligned} w &= W_n \sin \frac{n\pi x}{L} \cos \omega_n t \\ \bar{\alpha} &= Y_n \cos \frac{n\pi x}{L} \cos \omega_n t \end{aligned} \right\} \quad (6.121)$$

Note that $\sin \omega_n t$ or $e^{i\omega_n t}$ could also have been used in Equation (6.121). Here, W_n and Y_n are the amplitudes of the displacement and rotation respectively, and ω_n is the natural frequency of the n th mode of vibration. It is easily verified that these expressions satisfy the boundary conditions. The substitution of Equations (6.121) in Equations (6.120) yields two simultaneous homogeneous algebraic equations for the amplitude W_n and Y_n . These are

$$\left\{ \begin{aligned} \left[\left(\frac{n\pi^3}{L} - \frac{\rho_m c}{E} \left(\frac{n\pi}{L} \right) \omega_n^2 \right) \right] Y_n + \frac{\rho_m A}{EI} \omega_n^2 W_n &= 0 \\ \left[1 + \frac{kh^2}{10} \left(\frac{E}{G} \frac{n^2 \pi^2}{L^2} - \frac{\rho_m c}{G} \omega_n^2 \right) \right] Y_n + \left(\frac{n\pi}{L} \right) W_n &= 0 \end{aligned} \right\} \quad (6.122)$$

Since Equations (6.115) form a homogeneous system, the condition for a nontrivial solution is that the determinant of the system vanishes; this yields the frequency equations, while the amplitude ratios are obtained from satisfying either of the two equations. Thus, the amplitude ratio is given by

$$\frac{Y_n}{W_n} = - \frac{(\rho_m A / EI) \omega_n^2}{(n\pi / L)^3 - (\rho_m c / E) \left(\frac{n\pi}{L} \right) \omega_n^2} \quad (6.123)$$

while the frequency equation may be written in the form,

$$\begin{aligned} \omega_n^4 - \left[\frac{10G}{\rho_m h^2 k c} + \left(\frac{n\pi}{L} \right)^2 \left(\frac{E}{\rho_m c} + \frac{5}{6} \frac{G}{\rho_m k} \right) \right] \omega_n^2 \\ + \frac{10}{h^2 k c} \left(\frac{G}{\rho_m} \right) \left(\frac{EI}{\rho_m A} \right) \left(\frac{n\pi}{L} \right)^4 = 0 \end{aligned} \quad (6.124)$$

As in all linear free vibration problems, one cannot determine the amplitudes of the vibration, but can determine the ratios of the amplitudes of the various components of the vibration, such as the ratio given by (6.123). The natural frequencies for the case where both transverse shear deformation and rotatory inertia are included may be obtained by solving Equation (6.124) with $k = c = 1$. The frequency equation is then of the form,

$$\omega_n^4 - \left[\frac{10G}{\rho_m h^2} + \left(\frac{n\pi}{L} \right)^2 \left(\frac{E}{\rho_m} + \frac{5}{6} \frac{G}{\rho_m} \right) \right] \omega_n^2 + \frac{10}{h^2} \left(\frac{G}{\rho_m} \right) \left(\frac{EI}{\rho_m A} \right) \left(\frac{n\pi}{L} \right)^4 = 0 \quad (6.125)$$

It is seen that there are two solutions of Equation (6.125) for every wave number n . The lower value is a frequency that is primarily a lateral displacement, corresponding to a low ratio of Y_n / W_n in Equation (6.123). The higher value is primarily a thickness shear mode in which the ratio Y_n / W_n is high.

To obtain a simplified theory neglecting the effect of rotatory inertia, but retaining transverse shear deformation, set $k = 1$ and $c = 0$ after multiplying the frequency Equation (6.124) by c . The resulting simplified frequency equation may be written

$$\left[\frac{10G}{\rho_m h^2} + \left(\frac{n\pi}{L} \right)^2 \frac{E}{\rho_m} \right] \omega_n^2 - \frac{10}{h^2} \left(\frac{G}{\rho_m} \right) \left(\frac{EI}{\rho_m A} \right) \left(\frac{n\pi}{L} \right)^4 = 0 \quad (6.126)$$

and the natural frequencies are given by

$$\omega_n^2 = \frac{\left(\frac{EI}{\rho_m A} \right) \left(\frac{n\pi}{L} \right)^4}{1 + \frac{n^2 \pi^2}{10} \left(\frac{E}{G} \right) \left(\frac{h}{L} \right)^2} \quad (6.127)$$

Finally, to obtain a frequency equation in which both transverse shear deformation and rotatory inertia are neglected, multiply Equation (6.124) by kc and set $k = c = 0$; the natural frequencies are then given by

$$\omega_n^2 = \left(\frac{EI}{\rho_m A} \right) \left(\frac{n\pi}{L} \right)^4 \quad (6.128)$$

Equation (6.128) is easily recognized as the well-known solution of the flexural natural circular frequencies of classical beam theory for a simply supported beam. A few calculations using Equations (6.125) and (6.127) will show that most of the error (approximately 90 percent) in the classical theory frequency [Equation (6.128)] is due to the neglect of transverse shear deformation. Therefore, accurate results may be obtained by using Equation (6.127), which still neglects rotatory inertia, but has the advantage of greater simplicity. Comparison of Equations (6.127) and (6.128) reveals that the effect of shear deformation is to reduce the square of the frequencies by a factor equal to

$1 + \frac{n^2 \pi^2}{10} \left(\frac{E}{G} \right) \left(\frac{h}{L} \right)^2$. It is seen that this factor increases with increasing h/L , so that the errors from using classical theory tend to become larger as the beam becomes “stubbier.” This factor also increases as n increases, indicating that classical theory is only adequate for lower modes of vibration, and it becomes increasingly inaccurate for higher modes.

6.14 References

1. Sokolnikoff, I.S. (1956) *The Mathematical Theory of Elasticity*, Second Edition, McGraw-Hill Book Company, Inc., New York.
2. Reissner, E. (1950) On a Variational Theorem in Elasticity, *J. Math. Phys.*, Vol. 29, pg. 90.
3. Mura, T. and Koya, T. (1992) *Variational Methods in Mechanics*, Oxford University Press, March.
4. Sloan, J.G. (1979) The Behavior of Rectangular Composite Material Plates Under Lateral and Hygrothermal Loads, *MMAE Thesis*, University of Delaware, (also, AFOSR-TR-78-1477, July 1978).
5. Vinson, J.R., In-Plane Shear Strength Determination of Composite Materials in Laminated and Sandwich Panels, *Applied Mechanics Reviews* (forthcoming).
6. Vinson, J.R. (1997) On Determining the In-Plane Shear Strength of Laminated Composite Materials, *Applied Mechanics in the Americas*, Vol. 4, eds. L.A. Godoy, M. Rysz and L.E. Suarez, pp. 179-182.
7. Wu, C.I. and Vinson, J.R. (1971) Nonlinear Oscillations of Laminated Specially Orthotropic Plates With Clamped and Simply Supported Edges, *Journal of the Acoustical Society of America*, Vol. 49, Part 2, May, pp. 1561-1567.
8. Warburton, G. (1954) The Vibration of Rectangular Plates, *Proceedings of the Institute of Mechanical Engineering*, 168, 371.
9. Young, D. and Felgar, Jr. R. (1944) Tables of Characteristic Functions Representing Normal Modes of Vibration of a Beam, *University of Texas Publication*, No. 4913, July.
10. Felgar, Jr. R. (1950) Formulas for Integrals Containing Characteristic Functions of a Vibrating Beam, *Bureau of Engineering Research*, University of Texas.
11. Causbie, S.M. and Lagace, P.A. (1988) Buckling and Final Failure of Graphite/PEEK Stiffened Sections, *AIAA Journal*, Vol. 26, No. 9, September, pp. 1100-1106.

6.15 Problems

- 6.1. Consider a composite beam of flexural stiffness bD_{11} clamped on each end and subjected to a uniform lateral load $q(x) = q_0$ lb./in. Using the Theorem of Minimum Potential Energy (MPE) and an assumed deflection function of

$$w(x) = A \left[1 - \cos \frac{2\pi x}{L} \right]$$

where A is the amplitude and L the beam length, find, using classical beam theory:

- a. The magnitude and location of the maximum deflection.
- b. The magnitude and location of the maximum stresses.
- c. Does this form of the deflection function satisfy all of the boundary conditions necessary to use MPE for this problem?

- 6.2. Consider an orthotropic composite panel shown in Figures 2.11 and 2.14, which has the following boundary conditions:

$$\begin{aligned}x = 0 & \quad \text{clamped} \\x = a & \quad \text{simply supported} \\y = 0 & \quad \text{clamped} \\y = b & \quad \text{free}\end{aligned}$$

Select a suitable function for the lateral deflection $w(x,y)$ with which to utilize the Theorem of Minimum Potential Energy for this composite plate to determine the deflection of the panel when it is subjected to a laterally distributed load $p(x,y)$.

- 6.3. Consider the composite beam of Problem 4.4 once again, subjected to the load

$$q(x) = \bar{q} \sin \frac{\pi x}{L}$$

where \bar{q} is a constant. Using the Theorem of Minimum Potential Energy, and letting the lateral deflection be

$$w(x) = W \sin \frac{\pi x}{L}$$

- Determine W .
 - What and where is the maximum stress?
 - Compare the above results with those obtain in Problem 4.4, i.e., what are the percentage differences and which method produces the greater deflection and stress?
- 6.4. Consider the composite beam of Problem 4.5 once again, subjected to the load

$$q(x) = \bar{q} \left[1 - \sin \frac{\pi x}{L} \right]$$

where \bar{q} is a constant. Using the Theorem of Minimum Potential Energy, and letting the lateral deflection be

$$w(x) = W \sin \frac{\pi x}{L}$$

- Determine W .
- What and where is the maximum stress?
- Compare the above results with those obtained in Problem 4.5, i.e., what are the percentage differences and which method produces the greater deflection and stress?

- 6.5. The Theorem of Minimum Potential Energy is to be used to analyze an orthotropic composite rectangular composite plate. The plate is midplane symmetric, has no moisture or thermal loading, does include transverse shear deformation effects, has no in-plane displacements, and is subjected to a lateral distributed load $p(x,y)$ only. What is the explicit expression for the potential energy V to use in solving this problem?
- 6.6. The exact solution for a simply supported beam subjected to a uniform lateral load per unit length of q_0 is:

$$w(x) = \frac{q_0 x}{24EI} (x^3 - 2Lx^2 + L^3)$$

Using the Theorem of Minimum Potential Energy and a deflection function of

$$w(x) = \sum_{n=1}^m A_n \sin\left(\frac{n\pi x}{L}\right)$$

- Determine A_n .
 - Where and what is the maximum deflection?
 - Where and what is the maximum face stress?
 - Compare these results with the exact values. What are the percentage differences?
- 6.7. Consider the sandwich beam of Problem 4.9 once again, subjected to the load

$$q(x) = q_0 \sin(\pi x / L)$$

where q is a constant. Using the Theorem of Minimum Potential Energy and letting the lateral deflection be

$$w(x) = W \sin(\pi x / L)$$

- Determine W .
- What and where is the maximum deflection?
- Compare this maximum deflection with the exact value from Problem 4.9.
- What and where is the maximum stress?

CHAPTER 7

STRENGTH AND FAILURE THEORIES

7.1 Introduction

In the past sections focus has been directed upon the functional requirements of beam, plate and shell structural elements as subjected to particular loading environments. The material presented in this section now addresses the broader based objective of having acquired a knowledge of the load analysis methodology, how can one now apply this knowledge to design a structural system to ensure a potentially safe design.

This objective, for composite structures design, is captured in the closed loop stress design profile shown below in Figure 7.1. It should be noted that as with any structural design, a key feature in the design is the selection of an appropriate failure criterion and the inherent iterative nature of the design process proper. In addition, for the case of monolithic materials such as metals it is sufficient to use one observable metric such as the ultimate tensile, compressive or shear stress to describe failure. For composites, however, the structural engineer is faced with the dilemma of selecting a suitable failure criterion based upon a number of observable stress metrics.

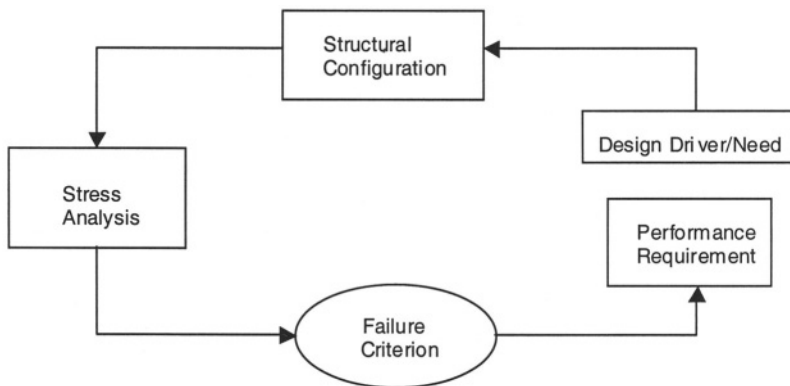


FIGURE 7.1. Closed Loop Stress Design Profile.

Thus one of the most difficult and challenging subjects to which one is exposed to in the mechanics of advanced composite materials involves finding a suitable failure criterion for these systems. This is compounded by our still limited grasp of understanding and predicting adequately the failure of all classes of monolithic materials to which we seek recourse for guidance in establishing descriptive failure criterion for a composite system. To a large degree the development of such criteria must be associated with philosophical notions of what the concept of failure is about. For example, in most

instances failure is perceived to be separation of structural components or material parts of components. This of course need not be the case since the function of the material and/or component may be the design driver and thus, for example, excessive wear in an axle joint may produce a kinematic motion no longer representative of a key design feature. In addition, any micromechanical or substructural failure features associated with early on failure initiation such as flaws and voids, surface imperfections, and built-in residual stresses are generally neglected in these design type approaches to failure. These mechanisms would serve as design drivers for initiating damage and/or degradation in the composite. Thus, failure identification can best be classified along a spectrum of disciplines and in the particular case of composites further subjugated to different levels of definition of failure dependent upon the level of material characterization. To this end, Figure 7.2 appears useful for focusing attention on the different levels of failure characterization and discipline linkage necessary for identity with each failure type. We focus attention in this section on laminate failure criteria, which are based upon lamina and micromechanical failure initiators. We do not address in this section the more global problem of failure at joints and attachments.

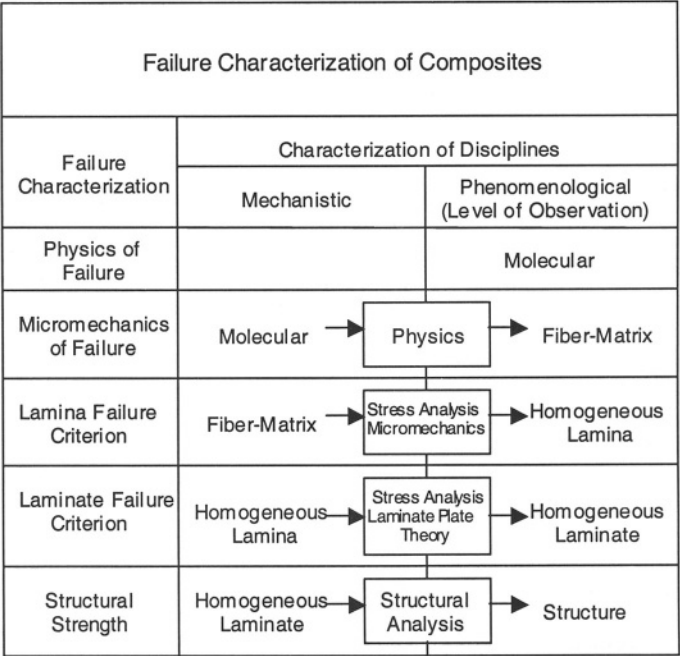
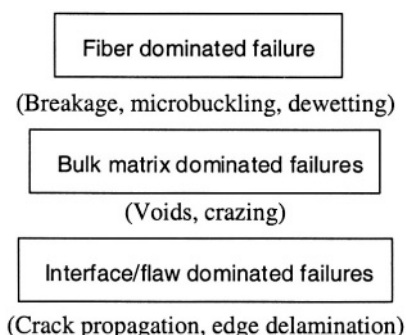


FIGURE 7.2. Classification of composite failure characterization disciplines.

At this point it is worthwhile to identify the important features and mechanisms controlling the microfailure of composite systems, which produce the damage and/or degradation leading to failure in composite laminates. First, it should be emphasized that the matrix and reinforcing fibers, the primary constituents of a composite, have in general widely different strength characteristics. Also, the interface between the fiber and matrix

is known to exhibit a response behavior different than that of the bulk matrix in general. The presence of flaws or defects, introduced into the material system during fabrication, may act as stress raisers or failure initiators. Thus, any approach to construction of a micromechanical strength theory should by necessity take into account the influence of such factors. Keeping these thoughts in mind, it appears feasible to characterize failure at the micro level by introducing such local failure modes as



Once again, such factors while being important failure initiators, are not considered as the primary or causal factors when discussing failure in a global sense. Therefore, as engineers we seek out an observational level of failure to which we can readily relate and feel comfortable with in describing the appropriate failure mechanisms. In this regard we generally attempt to specify lamina failure for an anisotropic unidirectional composite, or alternatively lamina as existing in composite orthotropic laminates.

To begin this discussion, it has been observed that failure of a laminate consisting of a number of plies oriented in different directions relative to the loading configuration occurs gradually. This occurs due to the fact that an individual lamina failure causes a redistribution of stresses within the remaining laminae of the laminate. Although the failure modes can be either fiber dominated, matrix dominated or interface/flaw dominated, these basic mechanisms would appear as more important features to material scientists or material designers. For structural designers, however, the important element to consider is the lamina, made of a chosen fiber-matrix system, which is necessary for strength and failure analysis.

Before describing the failure of isotropic materials, as a precursor to establishing failure theories for composites, it is worthwhile to indicate some relevant and distinctive features concerning the strength characteristics of composite materials. A composite lamina is known to exhibit an anisotropic strength behavior, that is, the strength is directionally dependent and thus its tensile and compressive strengths are found to be widely different. In addition, the orientation of the shear stresses with respect to the fiber direction in the lamina has been observed to have a significant influence on its strength. Finally, another consideration that merits attention for laminate failure, is that the final fracture depends not only on a failure mode or the number of interactive failure modes occurring but also depends on the failure mode which dominates the failure process. These key features of the strength and failure of composites make the subject matter both complex and challenging.

Thus, while we are able to describe the failure of isotropic materials by an allowable stress field associated with the ultimate tensile, compressive and/or shear strength of the material, the corresponding anisotropic (orthotropic) material requires knowledge of at least five principle stresses. These are the longitudinal tensile and compressive stresses, the transverse tensile and compressive stresses, and the corresponding shear stress. In order to attack a failure problem in composites, however, recourse to monolithic material or metals failure criterion are relied upon to serve as role models for both modification and suitability in predicting failure of laminates. It is therefore worthwhile to review some of the classical failure criteria associated with homogeneous isotropic materials to serve as a baseline reference to development of appropriate criteria for the case of failure of the homogeneous anisotropic or orthotropic single-ply lamina. Generally speaking, these combined loading failure (strength) theories can be categorized into three basic types of criteria as follows:

- Stress Dominated
- Strain Dominated
- Interactive

Geometrically speaking, the above criteria can be interpreted in terms of so-called failure envelopes as noted in the accompanying Table 7.1. Further, each of the failure criteria referred to in Table 7.1 can be redefined in either stress or strain space according to specific tabular schemes. We first examine, however, some general comments as related to classical developments of established failure criteria for metals and then proceed to examine these criteria further in the case of composites.

TABLE 7.1. Geometric Interpretation of Failure
One Stress Metric – Point Failure Envelope
Two Stress Metric – Two Dimensional Failure Envelope
N Dimensional Stress Metric – N Dimensional Failure Envelope

7.2 Failure of Monolithic Isotropic Materials

The ensuing brief discussion in which failure as defined by the occurrence of yielding or fracture is introduced in an attempt to establish a linkage to failure criteria used for anisotropic materials. This enables the reader to focus attention on the use of inductive approaches, based upon well founded contributions, for establishing innovative methodologies in new disciplines. To this end, one of the earliest failure criteria was suggested by Rankine (1858) [1] who proposed a theory for the yielding of homogeneous isotropic materials having unequal tensile and compressive yield strength values.

This theory known as the Maximum Principle Stress Theory simply states that when any state of stress exists in a structural element that exceeds the yield strength of the material in simple tension or compression then failure occurs. Stated mathematically in terms of principal stresses for the case of unequal tensile and compressive yield strengths in the general three dimensional case this theory can be given as:

$$\begin{aligned}
\sigma_{11} &\leq \sigma_{yp}^T & \sigma_{11} &\leq \sigma_{yp}^C \\
\sigma_{22} &\leq \sigma_{yp}^T & \sigma_{22} &\leq \sigma_{yp}^C \\
\sigma_{33} &\leq \sigma_{yp}^T & \sigma_{33} &\leq \sigma_{yp}^C
\end{aligned}
\tag{7.1}$$

For two-dimensional stresses, $\sigma_{33} = 0$ then,

$$\begin{aligned}
\sigma_{11} &\leq \sigma_{yp}^T & \sigma_{11} &\leq \sigma_{yp}^C \\
\sigma_{22} &\leq \sigma_{yp}^T & \sigma_{22} &\leq \sigma_{yp}^C
\end{aligned}
\tag{7.2}$$

If the material has the same yield point in tension and compression then,

$$\begin{aligned}
\sigma_{11} &= \pm \sigma_{yp} \\
\sigma_{22} &= \pm \sigma_{yp}
\end{aligned}
\tag{7.3}$$

The Maximum Strain Criterion states that failure occurs when at any point in a structural element the maximum strain at that point reaches the yield value equal to that occurring in a simple uniaxial tension or compression test. This result can be stated mathematically by equating the principal strains using Hooke's Law to the uniaxial strain at yield. This results in the following set of equations in terms of principal stresses:

$$\begin{aligned}
\sigma_{11} - \nu\sigma_{22} - \nu\sigma_{33} &= \sigma_{yp}^T, \sigma_{yp}^C \\
\sigma_{22} - \nu\sigma_{33} - \nu\sigma_{11} &= \sigma_{yp}^T, \sigma_{yp}^C \\
\sigma_{33} - \nu\sigma_{11} - \nu\sigma_{22} &= \sigma_{yp}^T, \sigma_{yp}^C
\end{aligned}
\tag{7.4}$$

For the case of plane stress, $\sigma_{33} = 0$, the above equations simplify to

$$\begin{aligned}
\sigma_{11} - \nu\sigma_{22} &= \sigma_{yp}^T, \sigma_{yp}^C, & \sigma_{22} - \nu\sigma_{11} &= \sigma_{yp}^T, \sigma_{yp}^C \\
-\nu(\sigma_{11} + \sigma_{22}) &= \sigma_{yp}^T, \sigma_{yp}^C
\end{aligned}
\tag{7.5}$$

Two other important failure criteria for homogeneous isotropic materials are the Maximum Shear Stress Theory often referred to as Tresca's Theory [2] and the Distortion Energy Criterion often referred to as Von Mises Criterion [3].

The first theory, that is the so-called Maximum Shear Stress Theory, suggests that yielding will occur in a material when the maximum shear stress reaches a critical value, the maximum shear stress at yielding in a uniaxial stress state. Expressed quantitatively in terms of principal stresses this result can be stated as:

$$\begin{aligned}\sigma_{11} - \sigma_{22} &= \pm \sigma_{yp} \\ \sigma_{22} - \sigma_{33} &= \pm \sigma_{yp} \\ \sigma_{33} - \sigma_{11} &= \pm \sigma_{yp}\end{aligned}\tag{7.6}$$

For the special case of plane stress, when $\sigma_{33} = 0$, the expression simplifies to read:

$$\begin{aligned}\sigma_{11} - \sigma_{22} &= \pm \sigma_{yp} \\ \sigma_{22} &= \pm \sigma_{yp} \\ \sigma_{11} &= \pm \sigma_{yp}\end{aligned}\tag{7.7}$$

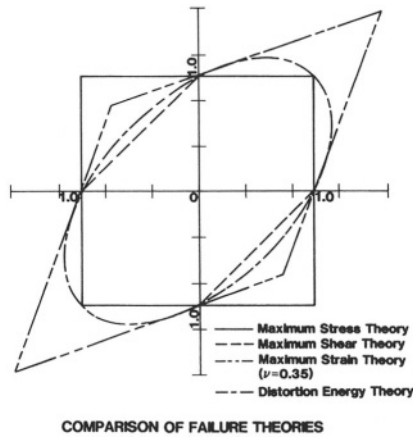


FIGURE 7.3. Comparison of failure theories.

Corresponding to Tresca's yield criterion a second popular yield criterion for homogeneous isotropic materials was attributed to von Mises (1913). This theory known as the distortion energy criterion also assumes that the principal influence on material yield is the maximum shearing stress. In this theory, the elastic energy of a material can

be considered to consist of a dilatational and distortional component. It is recognized that the dilatational part of the total work is dependent upon a hydrostatic stress state, which does not produce yielding at normal pressures in homogeneous isotropic materials. Thus, the remaining or distortional energy can be expressed in terms of principal stresses and written as:

$$\sigma_{11}^2 + \sigma_{22}^2 + \sigma_{33}^2 - \sigma_{11}\sigma_{22} - \sigma_{22}\sigma_{33} - \sigma_{33}\sigma_{11} = \sigma_{yp}^2 \quad (7.8)$$

A careful examination of this criterion with the previous Maximum Shearing Stress Theory indicates that at most the two theories deviate by no more than fifteen percent.

These four failure criterion depicted in Figure 7.3, while not exhaustive of all of the types proposed for metals, are representative models of the types often used and as such have led to the anisotropic failure criterion highlighted in the following section.

7.3 Anisotropic Strength and Failure Theories

Attention is now focused on the development of useful macroscopic yield criteria as extended from metals behavior to the case of composite (anisotropic) materials. A more comprehensive review of this subject and the individual theories can be found in Ref. [4]. In the following paragraphs, those theories, which have been most often cited in the composites literature, are reviewed in terms of their origin and salient features for the reader. This review serves as an important interface between the classical theories previously described and as a means for comparison for various composite systems analytically and experimentally.

As mentioned earlier in the text, a fundamental requirement in the design of structural systems from structural elements such as beams, plates and shells is a knowledge of the strength and/or failure of such elements subjected to complex loading states. The strength and failure of these structural elements can be associated with the yield strength of the material or correspondingly its ultimate strength. For brittle materials the ultimate or failure strength appears to be a more suitable base line reference value to determine failure while for ductile type materials the yield strength appears a more useful criterion. In the case of anisotropic materials and in particular high performance composites, the fiber reinforcements are generally elastic up to failure while the matrices can be either of the brittle or ductile type. The latter are mainly associated with metal matrix composites (MMC's), while the majority of advanced composite systems use thermosetting (epoxy) matrices for their binders. Thus, all subsequent reference to failure in this chapter as related to high performance composites will be based upon reference to the ultimate strength of the material. This should, of course, be altered if ductile matrices or fiber types other than brittle elastic are used. One other unique feature of anisotropic material failure is that modes of failure are important considerations in the design process. This is due to the fact that uniqueness in yield or failure is associated with the direction of testing.

We now proceed to examine anisotropic failure criteria in the light of the aforementioned remarks, and as extensions of failure theories based upon the three basic types established for monolithic materials, that is,

- Stress Dominated
- Strain Dominated
- Interactive

The historical development, as presented, reflects a somewhat selective one and the reader is referred to Ref. [4] for a more comprehensive discussion. In addition, the reader is cautioned that the theories, as constructed and referred to, do not include environmental factors such as temperature and humidity, and also do not include initial (residual) stresses that are usually present in composites.

7.3.1 MAXIMUM STRESS THEORY

Because of research in the forest products area, the Maximum Stress Theory was extended to orthotropic materials. It was stated that failure occurred when one or all of the orthotropic stress values exceed their maximum limits as obtained in uniaxial tension, compression, or pure shear stress tests, when the material is tested to failure. This can be stated analytically as:

$$\begin{aligned}\sigma_{11} &= X \\ \sigma_{22} &= Y \\ \sigma_{12} &= S\end{aligned}\tag{7.9}$$

Further extensions of this theory were presented by Stowell and Liu (1961) [5] and Kelly and Davies (1965) [6].

7.3.2 MAXIMUM STRAIN THEORY

The maximum strain theory states that failure occurs when the strain obtained along the principal material axes exceed their limiting values. Waddoups [7] utilized these conditions in assessing the failure strength of orthotropic materials expressing the results analytically as

$$\begin{aligned}\bar{\epsilon}_{11} &= \frac{\sigma_{11}}{E_{11}} - \nu_{12} \frac{\sigma_{22}}{E_{11}} \\ \bar{\epsilon}_{22} &= \frac{\sigma_{22}}{E_{22}} - \frac{\nu_{12}}{E_{11}} \quad \bar{\gamma}_{12} = \frac{\sigma_{12}}{G_{12}}\end{aligned}\tag{7.10}$$

$$\bar{\epsilon}_{33} = -\frac{\nu_{31}}{E_{33}}\sigma_{11} - \frac{\nu_{32}}{E_{33}}\sigma_{22}$$

The three principal strain values can be referred to modes of failure in the corresponding strain directions.

7.3.3 INTERACTIVE FAILURE THEORIES

One of the earliest interactive failure criterion for anisotropic materials was initiated by Hill [8]. This theory is a generalization of the isotropic yield behavior of ductile metals for the case of large strains. That is, as a metal is strained in a certain direction, for example in a rolling process, the material grains tend to become aligned and a self-induced anisotropy occurs. Hill thus formulated an interactive yield criterion for such materials, which can be written in terms of the stress components as:

$$\begin{aligned} F(\sigma_{22} - \sigma_{33})^2 + G(\sigma_{33} - \sigma_{11})^2 + H(\sigma_{11} - \sigma_{22})^2 \\ + 2L\sigma_{23}^2 + 2M\sigma_{13}^2 + 2N\sigma_{12}^2 = 1 \end{aligned} \quad (7.11)$$

where the quantities F, G, H, L, M and N reflect the current state of material anisotropy.

For unidirectionally reinforced composites $M = N, G = H$, we obtain

$$\begin{aligned} F(\sigma_{22} - \sigma_{33})^2 + G(\sigma_{33} - \sigma_{11})^2 + H(\sigma_{11} - \sigma_{22})^2 \\ + 2L\sigma_{23}^2 + 2M(\sigma_{31}^2 + \sigma_{12}^2) = 1. \end{aligned} \quad (7.12)$$

For a composite lamina or laminates in a plane state of stress $\sigma_{33} = 0$, the above equation reduces to

$$F\sigma_{22}^2 + G\sigma_{11}^2 + H(\sigma_{11} - \sigma_{22})^2 + 2N\sigma_{12}^2 = 1. \quad (7.13)$$

An extension of Hill's criterion to account for unequal tension and compression for anisotropic materials was introduced by Marin [9]. Stated in terms of principal stresses, failure (yielding) is assumed to occur when the following condition is satisfied

$$\begin{aligned} (\sigma_{11} - a)^2 + (\sigma_{22} - b)^2 + (\sigma_{33} - c)^2 + q[(\sigma_{11} - a)(\sigma_{22} - b) \\ + (\sigma_{22} - b)(\sigma_{33} - c) + (\sigma_{33} - c)(\sigma_{11} - a)] = \sigma^2 \end{aligned} \quad (7.14)$$

The quantities a , b , c , q and r are experimentally determined parameters.

Marin's anisotropic failure criterion was further extended by Norris (1962) [10] who introduced nine stress components to define failure. These nine properties consist of three tensile, three compressive and three shear strength values. The equations, which must be satisfied for failure to occur, are thus given by:

$$\begin{aligned} \left(\frac{\sigma_{11}}{X}\right)^2 + \left(\frac{\sigma_{22}}{Y}\right)^2 - \frac{\sigma_{11}\sigma_{22}}{XY} + \left(\frac{\sigma_{12}}{S}\right)^2 &= 1 \\ \left(\frac{\sigma_{22}}{Y}\right)^2 + \left(\frac{\sigma_{33}}{Z}\right)^2 - \frac{\sigma_{22}\sigma_{33}}{YZ} + \left(\frac{\sigma_{23}}{T}\right)^2 &= 1 \\ \left(\frac{\sigma_{33}}{Z}\right)^2 + \left(\frac{\sigma_{11}}{X}\right)^2 - \frac{\sigma_{33}\sigma_{11}}{ZX} + \left(\frac{\sigma_{13}}{R}\right)^2 &= 1 \end{aligned} \quad (7.15)$$

where the quantities X , Y and Z are the tensile or compressive yield strengths of the material which R , S and T are the corresponding shear strengths.

For the case of plane stress the above equations reduce to

$$\begin{aligned} \left(\frac{\sigma_{11}}{X}\right)^2 + \left(\frac{\sigma_{22}}{Y}\right)^2 - \frac{\sigma_{11}\sigma_{22}}{XY} + \left(\frac{\sigma_{12}}{S}\right)^2 &= 1 \\ \left(\frac{\sigma_{22}}{Y}\right)^2 &= 1 \quad \left(\frac{\sigma_{11}}{X}\right)^2 = 1 \end{aligned} \quad (7.16)$$

The plane stress results by Hill were simplified for the case of fiber reinforced composites by Azzi and Tsai [11] considering the composite to be transversely isotropic. Thus with $Z = Y$, the modified form of Hill's plane stress criterion can be written as

$$\left(\frac{\sigma_{11}}{X}\right)^2 + \left(\frac{\sigma_{22}}{Y}\right)^2 - \frac{\sigma_{11}\sigma_{22}}{X^2} + \left(\frac{\sigma_{12}}{S}\right)^2 = 1. \quad (7.17)$$

The above result is equivalent to that obtained by Norris with the distinction that the latter's data is somewhat more general in accounting for difference in yield in both tension and compression.

A generalization of this failure criterion to incorporate the effects of brittle materials was considered by Hoffman [12]. In terms of stress components, failure occurs when the following equation is satisfied:

$$\begin{aligned}
& C_1(\sigma_{22} - \sigma_{33})^2 + C_2(\sigma_{33} - \sigma_{11})^2 + C_3(\sigma_{11} - \sigma_{22})^2 + C_4\sigma_{11} + C_5\sigma_{22} \\
& + C_6\sigma_{33} + C_7\tau_{23}^2 + C_8\tau_{13}^2 + C_9\sigma_{12}^2 = 1
\end{aligned} \tag{7.18}$$

Quantities $C_1, C_2, C_3, C_4, C_5, C_6, C_7, C_8$ and C_9 are constants determined from material properties tests.

$$\begin{aligned}
C_1 &= \frac{1}{2} \left[\frac{1}{Y_T Y_C} + \frac{1}{Z_T Z_C} - \frac{1}{X_T X_C} \right] \\
C_2 &= \frac{1}{2} \left[\frac{1}{Z_T Z_C} + \frac{1}{X_T X_C} - \frac{1}{Y_T Y_C} \right] \\
C_3 &= \frac{1}{2} \left[\frac{1}{X_T X_C} + \frac{1}{Y_T Y_C} - \frac{1}{Z_T Z_C} \right] \\
C_4 &= \frac{1}{X_T} - \frac{1}{X_C} & C_7 &= \frac{1}{T^2} \\
C_5 &= \frac{1}{Y_T} - \frac{1}{Y_C} & C_8 &= \frac{1}{R^2} \\
C_6 &= \frac{1}{Z_T} - \frac{1}{Z_C} & C_9 &= \frac{1}{S^2}
\end{aligned} \tag{7.19}$$

This theory also incorporates unequal tensile and compressive failure strengths as an inherent part of the analytical development. For the case of plane stress this equation reduces to:

$$\begin{aligned}
& \frac{\sigma_{11}^2}{X_T X_C} + \frac{\sigma_{22}^2}{Y_T Y_C} - \sigma_{11}\sigma_{22} \left[\frac{1}{X_T X_C} + \frac{1}{Y_T Y_C} \right] + \frac{X_C - X_T}{X_T X_C} \sigma_{11} \\
& + \frac{Y_C - Y_T}{Y_T Y_C} \sigma_{22} + \frac{\sigma_{12}^2}{S^2} = 1
\end{aligned} \tag{7.20}$$

A generalization of the Hoffman result to incorporate a more comprehensive definition for failure was later proposed by Tsai and Wu [13]. In this criterion failure is assumed to occur when the following equations are satisfied:

$$\begin{aligned} F_i \sigma_i + F_{ij} \sigma_i \sigma_j &= 1 \quad (i, j = 1, 2, \dots, 6) \\ F_{ii} F_{jj} - F_{ij}^2 &\geq 0 \quad (i, j = 1, 2, \dots, 6) \end{aligned} \quad (7.21)$$

The quantities F_i and F_{ii} ($i = 1, 2, 3$) are related to the tensile and compressive yield strengths of the material while six shear tests both positive and negative are required to define the parameters F_4 through F_6 and F_{44} through F_{66} .

$$\begin{aligned} F_1 &= \frac{1}{X_T} - \frac{1}{X_C} & F_{11} &= \frac{1}{X_T X_C} \\ F_2 &= \frac{1}{Y_T} - \frac{1}{Y_C} & F_{22} &= \frac{1}{Y_T Y_C} \\ F_3 &= \frac{1}{Z_T} - \frac{1}{Z_C} & F_{33} &= \frac{1}{Z_T Z_C} \\ F_4 &= \frac{1}{T^+} - \frac{1}{T^-} & F_{44} &= \frac{1}{T^+ T^-} \\ F_5 &= \frac{1}{R^+} - \frac{1}{R^-} & F_{55} &= \frac{1}{R^+ R^-} \\ F_6 &= \frac{1}{S^+} - \frac{1}{S^-} & F_{66} &= \frac{1}{S^+ S^-} \end{aligned}$$

Tsai and Hahn [14] suggest the following for the constant F_{12}

$$F_{12} = -\frac{1}{2(X_T X_C Y_T Y_C)^{1/2}}$$

The ultimate test for any of the criterion as discussed above is based upon its correlation with available test data. At the present time an adequate number of tests has not been made to ascertain any deterministic values for comparative purposes. However, a survey of failure criteria, which have been proposed for use in practice, have been featured in

Ref. [15]. The results of this survey indicate that the following failure criteria appear most popular in practical use today:

- Maximum Strain
- Maximum Stress
- Interactive Criteria
 - Tsai-Hill
 - Tsai-Wu
 - Hoffman

A number of these theories will be used in selected examples in the latter part of this chapter. We begin our discussion of failure criteria by first examining failure of single-ply unidirectional fiber composites and progress to multi-ply composites consisting of variable angle ply geometries and orientations with respect to complex stress fields.

7.4 Lamina Strength Theories

We first examine the single ply strength of uniaxial lamina subjected to tensile loads. At the level of analysis being discussed and due to the success of micromechanical principles in predicting the elastic properties of composites, similar principles have been advanced for predicting the overall strength of composites as well. The problem with using this approach is that in applying a deterministic approach to the case where probabilistic events predominate, we generally obtain an invalid result. This is due to the wide variety of fiber and/or fiber bundle dominated strengths exhibited in composite networks. Further, the effects of these load perturbations can result in high stress concentrations in the vicinity of the newly failed fibers or be propagated/dispersed to remote locations in the composite. This results in a failure model, which is both dependent on the relative strength levels in the different regions of the composite as well as involvement of interactive failure modes in a broad sense. Thus in the end, a requirement for well-planned experiments appears to be a necessary building block for understanding and predicting such failure phenomena. As an example, in the case of compressive loads both material and configurational failures need to be addressed. That is both the compressive strength and buckling strengths need to be considered. Local fiber instabilities identified by in-phase and out-of-phase buckling (1), and fiber eccentricities (2) also need to be considered. The corresponding transverse tension and compression loadings are generally dominated by the so-called matrix mode of failure. In the case of compressive transverse loads, there appears to be several microscopic shear failure modes active, these being in the plane of and perpendicular to the filaments. Longitudinal and transverse shear stresses in general also result in matrix dominated failure modes although there is some theoretical evidence to suggest an increase in the in-plane shear stress.

Since most structural components are subjected to complex loading states the question of what happens to structural elements under combined loads is an important question. In the preceding qualitative discussion of strength investigation for single-ply laminae it was mentioned that material characterization was possible by obtaining data

through relatively simple uniaxial and shear tests. For the case of composites, a systematic experimental program to investigate failure for all possible complex stress states becomes prohibitive and recourse to other predictive methodologies appears necessary.

In order to establish guidelines for strength and failure of laminae, which are the building blocks of laminates, it is necessary to consider a number of fundamental features related to composite material behavior. To this end, it is important to point out that while we recognize the inherent microlevel mechanisms associated with failure in laminae we only consider failure to occur at the macrolevel. This observation is predicated to a large extent by the current state of the art in failure analysis which precludes an ability to quantitatively relate in any interactive fashion events occurring at the micro and macro level of analysis. Thus, for design purposes the engineer must resort to consideration of strength degradation as observed for laminae and relate these data subsequently to laminates.

Further, since we deal with laminae as our fundamental building units in composites we characterize their properties through means of either analytical methodologies (micromechanics) or experimental (empirical) data. The data as shown in Figures 7.4 and 7.5 serve as a means for obtaining the necessary uniaxial stress and strain allowables in tension, compression and shear. Since most laminae can be considered as either transversely isotropic or specially orthotropic, we generally need only four independent elastic compliances or stiffnesses and five strengths to define the material system.

Again, as mentioned previously a single lamina is considered to be in a plane state of stress and principal strengths are used as comparative strength criteria.

- Maximum Stress
- Maximum Strain
- Interactive Laws

Each of these theory types will be used in testing for the failure of laminae subjected to several states of stress.

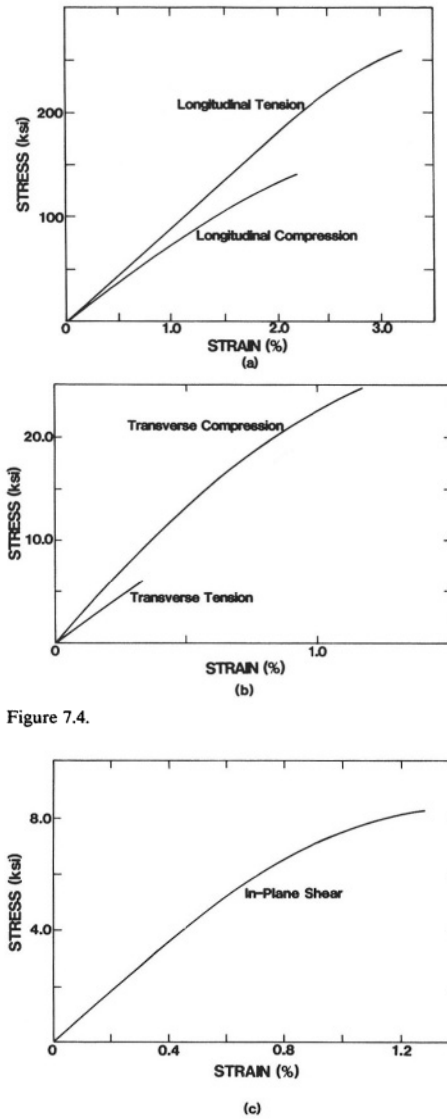


Figure 7.4.

FIGURE 7.5. Typical stress-strain curves for S-glass fibers in an epoxy matrix.

(a) Unidirectional laminate with $E_{11} = 8.8 \times 10^6$ psi for longitudinal tension and

$E_{11} = 7.2 \times 10^6$ psi for longitudinal compression.

(b) Unidirectional laminate with $E_{22} = 2.5 \times 10^6$ psi for transverse compression

$E_{22} = 1.9 \times 10^6$ psi for transverse tension.

(c) In-plane shear with $G_{12} = 0.8 \times 10^6$ psi.

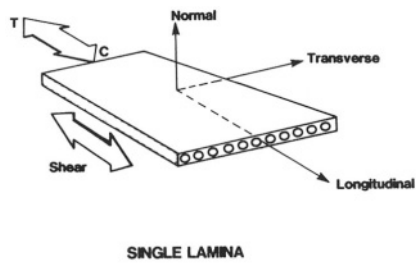


FIGURE 7.6.

Example 1

We begin by examining a single stress applied to an angle ply lamina material made of S-glass/epoxy, with stress, $\sigma_x = 500 \text{ psi}$, making an angle, $\theta = 60^\circ$, with respect to the principal fiber directions. This loading is shown in Figure 7.7 along with the design properties corresponding to this material system as indicated in Table 7.2.

We now examine each of the failure laws in turn and in terms of the loading shown.

Maximum Stress

This theory states that failure will occur if any stress along the principal directions of the lamina exceeds the specified allowables. Analytically the following set of inequalities must be satisfied to ensure a fail safe design.

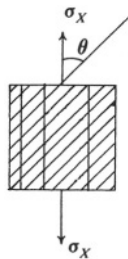


FIGURE 7.7.

TABLE 7.2. S-glass/epoxy.

$E_L = E_x = 8.42 \times 10^6$ psi		
$E_T = E_y = 2.00 \times 10^6$ psi		
$G_{LT} = 0.77 \times 10^6$ psi		
$\nu_{LT} = 0.293$		
$\nu_{TL} = 0.067$		
$\sigma_L^T = 280,000$ psi		
$\sigma_L^C = 136,000$ psi		
$\sigma_T^T = 4,000$ psi		
$\sigma_T^C = 20,000$ psi		
$\sigma_{LT}^S = 6,000$ psi		
$V_f = 0.67$		

Tension		Compression
$\sigma_L < \sigma_{LU}^t$		$\sigma_L < \sigma_{LU}^c$
$\sigma_T < \sigma_{TU}^t$		$\sigma_T < \sigma_{TU}^c$
$\sigma_{LT} < \sigma_{LTU}$		

For the present example and in order to test the failure theory, it is first necessary to transform the given stress σ_x along the direction of the principal material direction. Using the transformation equations we can thus write in a general form the following results:

$$\sigma_L = \sigma_X \cos^2 \theta = 125 \text{ psi}$$

$$\sigma_T = \sigma_X \sin^2 \theta = 375 \text{ psi}$$

$$\sigma_{LT} = \sigma_X \sin \theta \cos \theta = 216.5 \text{ psi}$$

Substituting the given values for σ_X and θ we can test the computed stresses in the material directions against the allowable stresses obtaining,

$$\sigma_L = 125 < \sigma_{LU} = 136,000 \text{ psi}$$

$$\sigma_T = 375 < \sigma_{TU} = 4,000 \text{ psi}$$

$$\sigma_{LT} = 216.5 < \sigma_{LTU} = 6,000 \text{ psi}$$

The results obtained can also be cast in terms of non-dimensional stress values and plotted as shown in Figure 7.8.

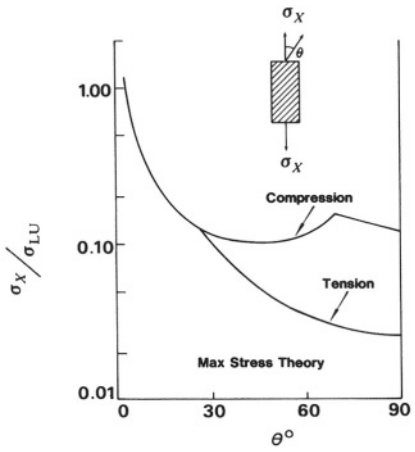


FIGURE 7.8. Analysis of an orthotropic lamina.

Maximum Strain

The maximum strain theory states that failure occurs when the strain along the material axes exceeds the allowable strain in the same principal direction as obtained in the same mode of testing. That is,

Tension		Compression
$\epsilon_L < \epsilon_{LU}^t$		$\epsilon_L < \epsilon_{LU}^c$
$\epsilon_T < \epsilon_{TU}^t$		$\epsilon_T < \epsilon_{TU}^c$
$\gamma_{LT} < \gamma_{LTU}$		

Once again, for the orthotropic lamina subjected to a load σ_X , we make use of the transformed stresses as found previously in the principal material coordinate directions. In order to calculate the corresponding strains in the principal directions (material coordinates) we use Hooke's Law for orthotropic materials. Therefore, we can write:

$$\epsilon_L = \frac{1}{E_L} [\cos^2\theta - \nu_{LT}\sin^2\theta] \sigma_X$$

$$\varepsilon_T = \frac{1}{E_T} [\sin^2 \theta - \nu_{TL} \cos^2 \theta] \sigma_X$$

$$\gamma_{LT} = \frac{1}{G_{LT}} [\sin \theta \cos \theta] \sigma_X$$

Substituting the given values of $\sigma_X, \theta, \nu_{LT}, E_L, E_T$, and G_{LT} from Table 7.2 we determine $\varepsilon_L, \varepsilon_T$ and γ_{LT} . These values are computed and tested against the allowable strain values which are given below,

$$\varepsilon_L < \varepsilon_{LU} \quad \varepsilon_L = 0.000001 < \varepsilon_{LU} = 0.033$$

$$\varepsilon_T < \varepsilon_{TU} \quad \varepsilon_T = 0.000183 < \varepsilon_{TU} = 0.002$$

$$\gamma_{LT} < \gamma_{LTU} \quad \gamma_{LT} = 0.000281 < \gamma_{LTU} = 0.0078$$

The Maximum Strain Theory can also be graphically depicted and compared with the Maximum Stress theory for the example cited. The differences in the theoretical predictions are small, this due to the fact that the material is considered to behave as linearly elastic to failure and consequently such a plot is not shown.

Interactive Theory

The third theory is of the interactive type, and states that failure occurs under some combined (multiplicative and/or additive) set of stresses. For the current examples, we select one of the interactive criteria for use specifically the Azzi/Tsai type. This failure criterion can be stated analytically for the case of plane stress as:

$$\left(\frac{\sigma_L}{\sigma_{LU}} \right)^2 - \left(\frac{\sigma_L}{\sigma_{LU}} \right) \left(\frac{\sigma_T}{\sigma_{LU}} \right) + \left(\frac{\sigma_T}{\sigma_{TU}} \right)^2 + \left(\frac{\sigma_{LT}}{\sigma_{LTU}} \right)^2 < 1$$

In the present example for an applied stress σ_X , the above equation can be written as:

$$\left(\frac{\cos^2 \theta}{\sigma_{LU}} \right)^2 - \left(\frac{\cos \theta \sin \theta}{\sigma_{LU}} \right)^2 + \left(\frac{\sin^2 \theta}{\sigma_{TU}} \right)^2 + \left(\frac{\sin \theta \cos \theta}{\sigma_{LTU}} \right)^2 < \frac{1}{\sigma_X^2}$$

Using the numbers given in Table 7.2 this equation is written as:

$$\left(\frac{0.25}{280,000}\right)^2 - \left(\frac{0.433}{280,000}\right)^2 + \left(\frac{0.75}{4,000}\right)^2 + \left(\frac{0.433}{6,000}\right)^2 < \frac{1}{(500)^2}$$

As was done in the case of the Maximum Stress Theory, a similar graphical plot of the off axis composite strength can be presented. This is shown in Figure 7.9 for comparison with the Maximum Stress (Strain) Theory. A comparison of these theories leads to the fact that the Maximum Stress Theory as does the Maximum Strain predicts somewhat higher strength values. The major discrepancy between the theories occurs in the angle at which a transition from one failure mode to an alternative mode occurs (compare curves).

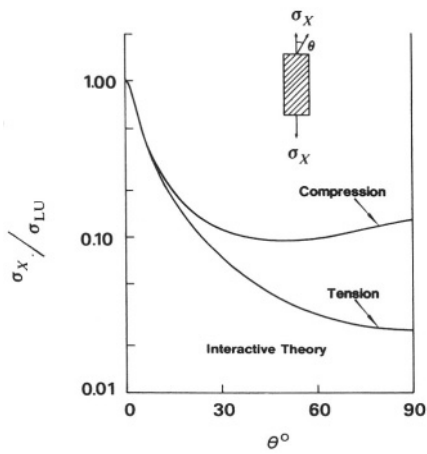


FIGURE 7.9.

Example 2

As a second example we consider the lamina composite shown in Figure 7.10 considering the material properties as given in Table 7.2.

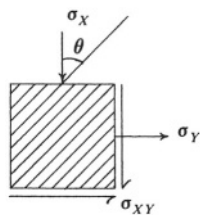


FIGURE 7.10.

Maximum Stress Theory

As stated previously, this theory predicts failure when any one of the ultimate (yield) strength values exceeds the corresponding allowable stresses in a principal axes

direction. Thus, in order to ensure a safe design once again the following inequalities must be satisfied in both tension and compression.

Tension	Compression
$\sigma_L \leq \sigma'_{LU}$	$\sigma_L \leq \sigma'_{LU}$
$\sigma_T \leq \sigma'_{TU}$	$\sigma_T \leq \sigma'_{TU}$
$\sigma_{LT} \leq \sigma_{LTU}$	

In the example given, the stresses as shown must be translated from the geometric axes to the principal material directions. This can be done through equilibrium considerations on the element or use of the transformation equations presented previously. Thus, we can use

$$\sigma_{11} = \sigma_X \cos^2 \theta + \sigma_Y \sin^2 \theta + 2\sigma_{XY} \cos \theta \sin \theta$$

$$\sigma_{22} = \sigma_X \sin^2 \theta + \sigma_Y \cos^2 \theta - 2\sigma_{XY} \cos \theta \sin \theta$$

$$\sigma_{12} = -\sigma_X \sin \theta \cos \theta + \sigma_Y \sin \theta \cos \theta + \sigma_{XY} (\cos^2 \theta - \sin^2 \theta)$$

or the transformation equations

$$\begin{bmatrix} \sigma_{11} \\ \sigma_{22} \\ \sigma_{12} \end{bmatrix} = \begin{bmatrix} T \end{bmatrix} \begin{bmatrix} \sigma_X \\ \sigma_Y \\ \sigma_{XY} \end{bmatrix}$$

Using the latter and substituting $\theta = 60^\circ$ into the transformation matrix we obtain

$$\begin{bmatrix} \sigma_{11} \\ \sigma_{22} \\ \sigma_{12} \end{bmatrix} = \begin{bmatrix} 1/4 & 3/4 & \sqrt{3}/2 \\ 3/4 & 1/4 & -\sqrt{3}/2 \\ -\sqrt{3}/4 & \sqrt{3}/4 & -1/2 \end{bmatrix} \begin{bmatrix} -500 \\ 1000 \\ -200 \end{bmatrix} = \begin{bmatrix} 451.8 \\ 48.2 \\ 749.5 \end{bmatrix} \text{ psi}$$

Comparing the stresses calculated in the right-hand column vector with the allowable values indicates that the lamina is fail safe, that is

$$\sigma_L < \sigma'_{LU}$$

$$\sigma_T < \sigma'_{TU}$$

$$\sigma_{LT} < \sigma'_{LTU}$$

Importance of Shear Stresses

Some comment on the role of the shear stress in determining the strength of lamina needs to be addressed. For homogeneous isotropic materials the direction of the shear stress can be either positive or negative and is of little consequence in determining the strength of such materials. These simplistic arguments do not carry over to orthotropic lamina and composites. Consider the lamina consisting of (-45°) oriented fibers as shown in Figure 7.11, and loaded by means of positive and negative shear stresses respectively, the signs determined from generally accepted strength of materials conventions. It can be seen that each of these laminae leads to important differences in loads along the principal material coordinate axes. In particular, for the case of positive shear tensile stresses are developed in the transverse direction and compressive stresses in the fiber direction. For the case of negative shear the reverse loading situation occurs.

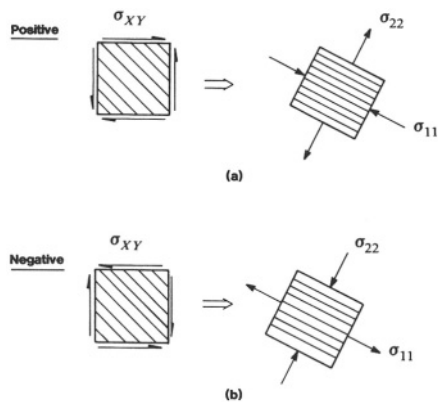


FIGURE 7.11.

Since shear strength of a lamina is controlled by the transverse strength of the composite, we can see that for the case of positive shear and negative shear fiber orientation we are led to lower predictions of apparent strength than when the reverse case prevails. Thus, the off-axis shear of laminae must be carefully examined in the light of the applied direction of the shear stress.

Maximum Strain Theory

This theory states that a fail safe design will exist when the following inequalities are satisfied:

Tension	Compression
$\epsilon_{11} \leq \epsilon_{11}^T$	$\epsilon_{11} \leq \epsilon_{11}^C$
$\epsilon_{22} \leq \epsilon_{22}^T$	$\epsilon_{22} \leq \epsilon_{22}^C$
$\epsilon_{12} \leq \epsilon_{12}$	

The Maximum Strain Theory is directly analogous to the Maximum Stress Theory in terms of correspondence in that stresses are simply replaced by allowable strain values in the fail safe procedure. This is predicated upon the assumption that the material remains elastic up to failure and thus one obtains the allowable strain from:

$$\epsilon_{LU} = \frac{\sigma_{LU}}{E_L} \quad \epsilon'_{LU} = \frac{\sigma_{LU}}{E_L}$$

$$\epsilon_{TU} = \frac{\sigma_{TU}}{E_T} \quad \gamma_{LTU} = \frac{\sigma_{LTU}}{G_{LT}} \quad \epsilon'_{TU} = \frac{\sigma'_{TU}}{E_T}$$

The strains in the L , T directions can be calculated from the Hooke's law relations using the calculated stress values for σ_L , σ_T and σ_{LT} as input values, that is:

$$\epsilon_L = \frac{\sigma_L}{E_L} - \nu_{TL} \frac{\sigma_T}{E_T} = 0.000052$$

$$\epsilon_T = \frac{\sigma_T}{E_T} - \nu_{LT} \frac{\sigma_L}{E_L} = 0.0000084$$

$$\gamma_{LT} = \frac{\sigma_{LT}}{G_{LT}} = 0.00097$$

Comparing the above values with the allowable strain we see that:

$$\epsilon_L < \epsilon_{LU}$$

$$\epsilon_T < \epsilon_{TU}$$

and,

$$\gamma_{LT} < \gamma_{LTU}$$

Interactive Theory

Two key features of the Maximum Stress and Maximum Strain failure theories should be noted. These are

- Interaction between strengths is not accounted for
- Failure is dictated by a governing inequality

The first of the above features is sometimes considered an inadequacy of these types of failure theorems and thus one attempts to define involved composite failure theories based upon homogeneous isotropic metal based systems. Due to the large number of such theories available, as discussed previously, only one of these theories will be presented and used in the present problem. The specific failure theory selected is based upon an extension of Hill's generalization of the von Mises or Distortional Energy failure theory which was further extended by Azzi and Tsai (1965). In functional form this equation is of the type,

$$\left(\frac{\sigma_L}{\sigma_{LU}} \right)^2 - \left(\frac{\sigma_L}{\sigma_{LU}} \right) \left(\frac{\sigma_T}{\sigma_{LU}} \right) + \left(\frac{\sigma_T}{\sigma_{TU}} \right)^2 + \left(\frac{\sigma_{LT}}{\sigma_{LTU}} \right)^2 < 1$$

For the present example using the calculated results for $\sigma_L, \sigma_T, \sigma_{LT}$ and the data included in Table 7.2, we can write,

$$\left(\frac{3,160}{280,000} \right)^2 + \left(\frac{340}{4,000} \right)^2 - \frac{(3,160)(340)}{(280,000)^2} + \left(\frac{5,240}{6,000} \right)^2 < 1$$

The failure criteria described in the preceding paragraphs can be summarized in terms of the three types mentioned earlier in the chapter. That is stress dominated, strain dominated and so-called stress interactive types. A graphical interpretation of these yield criteria for the case of equal tensile and compressive yield points can be graphically displayed, while an analytical description couched in terms of either strain or stress space follows in the accompanying tables.

TABLE 7.3. Failure Criteria
(Theories with and without Independent Failure Modes)
Maximum Stress Criterion

Stress Space	Strain Space
$\sigma_{LU}^1 \leq \sigma_1 \leq \sigma_{LU}$	$\varepsilon_1 = -\frac{C_{12}}{C_{11}} \varepsilon_2 - \frac{C_{16}}{C_{11}} \varepsilon_6 + \frac{\sigma_{LU}}{C_{11}}$
$\sigma_{TU}^1 \leq \sigma_2 \leq \sigma_{TU}$	$\varepsilon_1 = -\frac{C_{12}}{C_{11}} \varepsilon_2 - \frac{C_{16}}{C_{11}} \varepsilon_6 - \frac{\sigma'_{LU}}{C_{11}}$
$\sigma_{LTU}^1 \leq \sigma_6 \leq \sigma_{LTU}$	$\varepsilon_3 = -\frac{C_{12}}{C_{22}} \varepsilon_1 - \frac{C_{26}}{C_{22}} \varepsilon_6 + \frac{\sigma_{TU}}{C_{22}}$
	$\varepsilon_4 = -\frac{C_{12}}{C_{22}} \varepsilon_1 - \frac{C_{26}}{C_{22}} \varepsilon_6 - \frac{\sigma'_{TU}}{C_{22}}$
	$\varepsilon_6 = -\frac{C_{16}}{C_{66}} \varepsilon_1 - \frac{C_{26}}{C_{66}} \varepsilon_2 + \frac{\sigma_{LTU}}{C_{66}}$
	$\varepsilon_6 = -\frac{C_{16}}{C_{66}} \varepsilon_1 - \frac{C_{26}}{C_{66}} \varepsilon_2 - \frac{\sigma_{LTU}}{C_{66}}$

TABLE 7.4. Maximum Strain Criterion

Strain Space	Stress Space
$\varepsilon_{LU} = S_{11} \sigma_{LU} \geq \varepsilon_1$	$\sigma_1 = -\frac{S_{12}}{S_{11}} \sigma_2 - \frac{S_{16}}{S_{11}} \sigma_6 + \sigma_{LU}$
$\varepsilon'_{LU} = S_{11} \sigma'_{LU} \geq -\varepsilon_1$	$\sigma_1 = -\frac{S_{12}}{S_{11}} \sigma_2 - \frac{S_{16}}{S_{11}} \sigma_6 - \sigma'_{LU}$
$\varepsilon_{TU} = S_{22} \sigma_{TU} \geq \varepsilon_2$	$\sigma_2 = -\frac{S_{12}}{S_{22}} \sigma_1 - \frac{S_{26}}{S_{22}} \sigma_6 + \sigma_{TU}$
$\varepsilon'_{TU} = S_{22} \sigma'_{TU} \geq -\varepsilon_2$	$\sigma_2 = -\frac{S_{12}}{S_{22}} \sigma_1 - \frac{S_{26}}{S_{22}} \sigma_6 - \sigma'_{TU}$
$\varepsilon_{LTU} = S_{66} \sigma_{LTU} \geq \varepsilon_6$	$\sigma_6 = -\frac{S_{16}}{S_{66}} \sigma_1 - \frac{S_{26}}{S_{66}} \sigma_2 + \sigma_{LTU}$
$\varepsilon'_{LTU} = S_{66} \sigma'_{LTU} \geq -\varepsilon_6$	$\sigma_6 = -\frac{S_{16}}{S_{66}} \sigma_1 - \frac{S_{26}}{S_{66}} \sigma_2 - \sigma'_{LTU}$

TABLE 7.5. Interactive Failure Criterion

Stress Space	Strain Space
$f(\tau_i) = F_i \sigma_i + F_{ij} \sigma_i \sigma_j$ $+ F_{ijk} \sigma_i \sigma_j \sigma_k + \dots$	$g(\varepsilon_i) = G_i \varepsilon_i + G_{ij} \varepsilon_i \varepsilon_j$ $+ G_{ijk} \varepsilon_i \varepsilon_j \varepsilon_k + \dots$

F's and G's are material constants

7.5 Laminate Strength Analysis

We now turn our attention from single lamina strength analysis to the failure behavior of multiple laminae or laminates. The objective of this analysis is to determine the strength behavior of each lamina in the laminate assuming that a plane state of stress exists for each lamina independent of its orientation and position within the laminate. The application of a suitable failure criterion must be adopted, the stress on each lamina calculated and transformed to the material axes of the lamina, and a fail safe measure of each lamina determined. Several points must therefore be addressed in terms of general laminate strength analysis. We begin by examining several approaches to laminate strength analysis, which have been advanced.

In the broadest context of laminate strength interrogation, one is generally knowledgeable of either,

- Knowing the loads/Testing the design
- Knowing the design/Testing for allowable loads

For the first case indicated, so-called knowledge of the loads may be available, however, generally this is more in the realm of the designer's province to determine by experience rather than by rigorous deterministic methods. In the second case, many times the design is fixed and knowledge of what loads the structural elements can safely withstand is the challenge. Each of these issues will be examined through examples in this section. An awareness of the semi-global failure analysis of a laminate raises the following issues, that is,

- First Ply Failure
- Behavior after First Ply Failure

First ply failure occurs when the given or calculated loads exceed the ply specified failure criterion. Should this test be met then it is still possible for the system to carry additional loads after first ply failure and several approaches to accounting for ply failure can be introduced. Among these are,

- Total Ply Discount
- Ply Failure Distribution

The first approach, that of total ply discount, implies that the ply still remains within the system as a volume entity but that it no longer carries any load. This represents a conservative approach to failure analysis. The second approach implies that some knowledge of the failure mechanisms of the ply are known. For example, if matrix failure in a particular ply is known to occur, then the transverse properties of that ply can be omitted. Alternatively, if fiber failure occurs within a given ply, then that ply can be treated as having zero stiffness for subsequent analysis.

In addition to examining the effects of ply failure within the laminate, it is sometimes equally advantageous to establish failure envelopes based upon various combinations of a given set of applied loads. The most widely used loading for these

latter schemes appear to be that of membrane type loads. Both interrogation of ply failure and failure interaction envelopes will be discussing in the examples to follow. Before discussing these examples, however, it is appropriate to review that pertinent laminate equations, including generalizations to incorporate both temperature and humidity effects, required for analysis of composite failure. These equations will be useful to the reader in examining more complex failure situations where residual stresses or environmental conditions may be important as well as in establishing interactive failure envelopes. Considering a plane state of stress and referring to an arbitrary axes x and y with respect to the principal coordinate material directions, we can write the following stress-strain equations for the K th lamina of a stacking sequence comprising N lamina,

$$\begin{bmatrix} \sigma_x \\ \sigma_y \\ \sigma_{xy} \end{bmatrix}_k = \begin{bmatrix} \bar{Q}_{11} & \bar{Q}_{12} & \bar{Q}_{16} \\ \bar{Q}_{21} & \bar{Q}_{22} & \bar{Q}_{26} \\ \bar{Q}_{61} & \bar{Q}_{62} & \bar{Q}_{66} \end{bmatrix}_k \begin{bmatrix} \varepsilon_x - \alpha_x \Delta T - \beta_x \Delta m \\ \varepsilon_y - \alpha_y \Delta T - \beta_y \Delta m \\ 2(\varepsilon_{xy} - \alpha_{xy} \Delta T - \beta_{xy} \Delta m) \end{bmatrix}_k$$

The strains $\varepsilon_x^{(k)}$, $\varepsilon_y^{(k)}$ and $\varepsilon_{xy}^{(k)}$, can be rewritten in terms of the displacement components u , v and w resulting in the following equation,

$$\begin{bmatrix} \sigma_x \\ \sigma_y \\ \sigma_{xy} \end{bmatrix}_k = \begin{bmatrix} \bar{Q}_{ij} \end{bmatrix}_k \begin{bmatrix} \varepsilon_{x_0} + z\kappa_x - \alpha_x \Delta T - \beta_x \Delta m \\ \varepsilon_{y_0} + z\kappa_y - \alpha_y \Delta T - \beta_y \Delta m \\ 2(\varepsilon_{xy_0} + z\kappa_{xy} - \alpha_{xy} \Delta T - \beta_{xy} \Delta m) \end{bmatrix}_k$$

The stresses for the k th lamina can be redefined in terms of the membrane stress resultants N_x, N_y, N_{xy} and bending stress couples M_x, M_y, M_{xy} . Integrating over the thickness of the lamina as shown in Equation (2.47), we obtain Equation (2.49). In matrix notation this can be written as,

$$[N] = [A][\varepsilon_0] + [B][\kappa] - [N]^T - [N]^m$$

A similar set of equations can be found for the bending stress couples, that is,

$$[M] = [B][\varepsilon_0] + [D][\kappa] - [M]^T - [M]^m$$

transposing $[N]^T$, $[N]^m$, $[M]^T$ and $[M]^m$ from the right hand side to the left hand side of the stress resultant equations we can write:

$$[\bar{N}] = [N] + [N]^T + [N]^m = [A][\epsilon_0] + [B][\kappa]$$

$$[\bar{M}] = [M] + [M]^T + [M]^m = [B][\epsilon_0] + [D][\kappa]$$

The barred quantities are often referred to in the literature as the total force and moment resultants.

In some cases, it is advantageous to have the mid-plane strains and curvatures defined in terms of the stress resultants. Thus, inverting the above equations gives:

$$\begin{bmatrix} \epsilon_0 \\ \kappa \end{bmatrix} = \begin{bmatrix} a - b\alpha^{-1}b^T & b\alpha^{-1} \\ -d^{-1} & d^{-1} \end{bmatrix} \begin{bmatrix} \bar{N} \\ \bar{M} \end{bmatrix}$$

Thus for the case of plane stress anisotropic laminates, in the absence of transverse shear stress, the principal failure criteria can be interrogated as follows,

Maximum Stress Theory

- (1) Establish the stresses acting on the system
- (2) If the stresses do not coincide with the principal material direction they should be transformed according to the transformation law $[\sigma_L] = [T][\sigma_x]$
- (3) The stresses $[\sigma_L]$ should then be compared with the allowable stresses on a ply by ply basis to establish whether first ply failure has occurred.
- (4) The process of estimating whether laminate failure has occurred by introducing a selected post first ply failure criterion can then be evaluated.

Maximum Strain Theory

- (1) Establish the stresses acting on the system
- (2) Calculate the strains corresponding to the applied stresses
- (3) If the calculated strains do not coincide with the principal material directions they should be transformed according to the transformation law
- (4) The strains $[\epsilon_L]$ should then be compared with the allowable strains on a ply by ply basis in order to establish whether first ply failure has occurred.
- (5) The process of estimating whether laminate failure has occurred by introducing a selected post first ply failure criterion can then be evaluated.

Interactive Failure Criteria

- (1) Establish the stresses acting on the system
- (2) If the stresses do not coincide with the principal material directions they should be rotated using the transformation $[\epsilon_L] = [T][\epsilon_x]$

- (3) The stress $[\sigma_L]$ should then be inserted into the selected interactive failure criterion, that is, Tsai-Hill, Tsai-Wu, Hoffman and the criterion tested to ensure existence of a fail safe design on a ply by ply basis.
- (4) If a failed ply has been detected, an appropriate first ply failure assessment can be made and the composite system interrogated for laminate failure.

7.6 References

1. Rankine, W.J.M. (1858) *Applied Mechanics*, 1st edition, London.
2. Tresca, H. (1864) *Memoire su l'ecoulement des corps solides soumis a de fortes pressions*, Comptes Rendus, Paris, France, Vol. 59, 754.
3. Von Mises, R. (1913) *mechanik der festen Koerper im plastisch – deformablen zustand*, Goettinger Nachrichten, Mathematisch, Physikalische Klasse, Vol. 1913, 204-218.
4. Sandhu, R.S. (1972) *A Survey of Failure Theories of Isotropic and Anisotropic Materials*, AFFDL-TR-72-71, Wright-Patterson Air Force Base, Dayton, Ohio.
5. Stowell, E.Z. and Liu, T.S. (1961) *On the Mechanical Behavior of Fiber Reinforced Crystalline Solids*, Journal of the Mechanics and Physics of Solids. Vol. 9, 242-260.
6. Kelly, A. and Davies, G.J. (1965) *Metallurgical Reviews*, Vol. 10.
7. Waddoups, M.E. (1967) *Advanced Composite Material Mechanics for the Design and Stress Analyst*, General Dynamics, Ft. Worth, Texas, Report FZM-4763.
8. Hill, R. (1950) *The Mathematical Theory of Plasticity*, Oxford University Press.
9. Marin, J. (1957) *Theories of Strength for Combined Stresses and Non-Isotropic Materials*, J. of Aerospace Sciences, Vol. 24, 265-268.
10. Norris, C.B., *Strength of Orthotropic Materials Subjected to Combined Stress*, Forest Products Laboratory Report, 1816, 1950, 1962.
11. Azzi, V.D. and Tsai, S.W. (1965) *Anisotropic Strength of Components*, Experimental Mechanics, Vol. 5, 286-288.
12. Hoffman, O. (1967) *The Brittle Strength of Orthotropic Materials*, J. Composite Materials, Vol. 1, 200-206.
13. Tsai, S.W. and Wu, E.M. (1971) *A General Theory of Strength for Anisotropic Materials*, JI. Composite Materials, Vol. 5, 58-80.
14. Tsai, S.W. and Hahn, H.T. (1980) *Introduction to Composite Materials*, Technomic Publishing Company, Inc., Lancaster, Pa.
15. Burk, R.C. (1983) *Standard Failure Criteria Needed for Advanced Composites*, Astronautics and Aeronautics, Vol. 21, 58-62.

7.7 Problems

7.1. Consider the following laminate of equal ply thickness $0.0052''$

$$\begin{vmatrix} \theta = 30^\circ \\ \theta = 0^\circ \\ \theta = -30^\circ \end{vmatrix}$$

assume that the maximum strain theory governs failure, with the following inequalities given

$$|\epsilon_1| \leq 0.004$$

$$|\epsilon_2| \leq 0.003$$

$$|\gamma_{12}| \leq 0.010$$

Determine whether failure will occur at $z = 0$ for the following loadings.

$$N_x = 100 \text{ lb./in.} \quad M_x = 5 \text{ in.} \cdot \text{lb./in.}$$

The properties of an unidirectional layer are given by:

$$E_{11} = 29.2 \times 10^6 \text{ psi}$$

$$E_{22} = 2.4 \times 10^6 \text{ psi}$$

$$\nu_{12} = 0.223$$

$$\nu_{21} = 0.018$$

$$G_{12} = 0.83 \times 10^6 \text{ psi}$$

7.2. Consider the pure shear loading of a composite material at any angle θ with respect to the principal material directions. Use the Tsai-Hill criterion to find failure of the composite for this loading.

CHAPTER 8

JOINING OF COMPOSITE MATERIAL STRUCTURES

8.1 General Remarks

In the design of composite material structures, components must be joined in such a manner that the overall structure retains its structural integrity while performing its intended function, subjected to loads (static and dynamic) and environment (temperature, humidity).

The use of composite materials in complex structures rather than metals almost always significantly reduces the number of components, sometimes from hundreds to dozens, with the advantages of great savings in weight, cost, inspection, assembly, and increased reliability. Yet, joining is still required. Joining metallic structures is a well developed technology involving riveting, bolting, welding, gluing, brazing, soldering, and combinations thereof. However, for polymer matrix fiber reinforced composites only adhesive bonding and mechanical fasteners (bolts and rivets) are utilized. However, there has been some success in “welding” by melting and solidifying thermoplastic polymer matrix structural components at their interface.

Inherently, adhesive bonding is preferred because of the continuous connection, whereas in drilling the holes for bolts or rivets, fibers are cut, the joining is at discrete locations, and large stress concentrations occur around each hole drilled. However, in many structures, some structural components must be removed periodically for access to the interior (for example access to electronic components in an aircraft, etc.) so invariably some use of mechanical fasteners must be made. In this chapter both adhesive bonding and mechanical fastening are discussed and described in some detail.

8.2 Adhesive Bonding

8.2.1 INTRODUCTION

Adhesive bonding for joining materials began when the Egyptians used copper chloride poisoned casein adhesives in fabricating mummy cases. However, adhesive bonding for load bearing structures developed only several decades ago. One could say that the bonding of the plywood laminae of the British wooden Mosquito bomber of World War II might be the first aviation application. In the United States, Narmco developed the Metlbond adhesives in the early 1940's for the Consolidated Vultee B-36 bomber. Since that time the use of adhesive bonding has increased steadily.

The reasons why adhesive bonding in both metallic and composite material structures is so desirable compared to other joining methods are manifold according to Kuno [1]; they include:

1. Often, thinner gauge materials can be used with attendant weight savings and cost savings, for example, the case of adhesive bonding aluminum sheets of 0.508 mm (0.020") thickness, where 1.30 mm (0.051") thick sheets would be required for riveting.
2. Number of production parts can be reduced, and the design simplified.
3. Need for milling, machining and forming operation of details is reduced.
4. Large area bonds can be made with minimum work force without special skills.
5. Adhesive bonding provides a high strength to weight ratio with three times the shearing force of riveted or spot welded joints.
6. Aerodynamic smoothness and improved visual appearance.
7. Use as a seal, and/or corrosion preventer when joining incompatible adherends.
8. Excellent electrical and thermal insulation.
9. Superior fatigue resistance. Adhesive assemblies have shown fatigue life times twenty times better than riveted or spot welded structures of identical parts.
10. Damping characteristics and noise reduction are superior to riveted or spot welded assemblies.
11. Often, the adhesive is sufficiently flexible to allow for the variations in coefficients of thermal expansion when joining dissimilar materials.

Therefore, adhesive bonding is very desirable for use in composite material structures, and its use will be very beneficial from a weight, cost, reliability and flexibility of use. However, it is imperative that the ability to analyze, design and optimize these joints, of many configurations, subjected to generalized mechanical, thermal, and hygrothermal loads be fully developed.

8.2.2 SINGLE LAP JOINT

The single lap joint, shown in Figure 8.1, has been studied more extensively than any other configuration using many analytical, finite difference and finite element methods. Figure 8.1 shows a cross-section of two panels, referred to as adherends, joined together by adhesive.

Early methods of analysis for isotropic (metallic) adherends include those of Szepe [2], Volkersen [3], De Bruyne [4], Wang [5], and Goland and Reissner [6]. These are discussed in detail by Kutscha [7] and Kutscha and Hofer [8], who performed an excellent review to 1969. Kutscha and Hofer concluded that the present state of design in all bonded joints is simply that no rational procedure exists, and that such an approach must await further developments both in analytical methods and in materials characterization. Until that time design techniques will remain empirical and thus rely heavily on testing and experimental results.

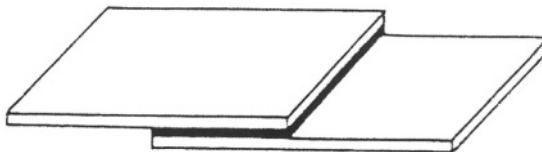


Figure 8.1. Single Lap Joint

Kutscha and Hofer [8] found that in a single lap joint with adherends of unequal thickness, the maximum shear stress will occur at “the point where the load enters the joint from the thinner adherend”. In a joint with equal thickness adherends the stress is the same at both ends of the overlap. Today the same conclusions are found, except that it is known that maximum shear stresses occur near to the end not at the end of the overlap, see Figure 8.3.

Kutscha and Hofer’s parametric studies show several important generalizations. Adhesive stresses decrease with increasing specimen width, up to about a four inch width, beyond which the stresses remain constant. Thus, wider joints designed on one inch wide data should be conservative because wider joints should be stronger than predicted. Also, the maximum stresses do not decrease significantly as the bonded area increases. As adhesive film thickness increases, more adhesive material is available to absorb differential straining and stresses decrease. As the shear modulus of the adhesive increases, the maximum stresses increase almost linearly with the shear modulus for values between 50,000 psi to 250,000 psi, the conventional range of values for structural adhesives. They also find that as the stiffness of the adherends increases, the resistance of the joint to bending increases, and therefore the maximum stresses decrease. Lastly, maximum stresses in the adhesive are relatively insensitive to the value of the Poisson’s ratio of the adherends. All of these early conclusions and generalizations hold today.

Kutscha and Hofer also define a “joint efficiency” that is very useful. It is defined for any bonded joint as the axial load divided by the nominal bonded area, divided by the strength of the weaker adherend without the joint. To not have the adhesive bond limit the load carrying capability of the structures joined, the joint efficiency must be 100% or greater.

It is interesting to note that fatigue tests conducted to 10^7 cycles were performed at 15 cycles per second, a frequency low enough to prevent significant heating in the viscoelastic adhesive.

In 1969, Lehman and Hawley [9] also analyzed and compared several methods of adhesive bonding including single lap, double lap, scarf and stepped lap adhesive joint configurations, shown in Figures 8.1 and 8.5 through 8.9. Their goal was to determine both static and fatigue strengths of these various configurations. Although transverse shear deformation, transverse normal strain, hygrothermal and viscoelastic effects were not considered, good agreement was found between analytical prediction and experimental results. However, their methods did include non-linear effects. Lehman and Hawley also found that the maximum joint strength occurs when the extensional stiffness of both adherends is the same. Also, they found that fatigue runout occurs when the maximum shear stress in the adhesive is below the shear stress proportional limit in the adhesive. Adhesive shear stresses above the proportional limit caused fatigue cracks in the adhesive that propagated through the joint causing failure. They also found that the residual strength of the fatigue specimens that survived runout usually exceeded static strength values. In 1972, Dickson, Hsu and McKinney [10] analyzed single lap joints, the double lap joint, and both the single doubler and double joints, including plasticity effects as well as transverse shear and transverse normal deformations. Also in 1972, Grimes and his colleagues [11] utilized a discrete element method and a continuum elasticity method to predict adherend stresses and joint strengths. Material non-linear

effects in adherends and adhesives were included in their study of single, double and step lap configurations. Experimental validation was also accomplished. In their analysis, the adhesive transverse normal and shear stresses obey a Ramberg-Osgood [12] approximation. Experimental verification of the two methods of analysis were made. Accurate predictions of adherend stresses and joint strength demonstrated for static loadings; however, Grimes notes that transverse shear stress, transverse normal strain, hygrothermal considerations and viscoelastic effects, although neglected, should be included. They also point out that small deflection theory is not valid for the continuum analysis due to the large deflections observed in joints under load. In predicting failure loads in the experimental program, Grimes used the maximum stress theory for the adhesive and for isotropic adherends; maximum strain theory was used for composite adherends, as discussed in Chapter 7, herein.

The work of Hart-Smith [13,14] on single lap joints in 1973 is also noted. The analysis involved a continuum model in which the adherends are elastic and the adhesive bond is elastic-plastic in shear while behaving elastically in transverse tension. Allowance was made for the peel (tensile) stresses at the ends of the adhesive, temperature differences between the adherends and differences in adherend stiffness. Transverse shear deformation, and transverse normal strain were not considered. Hart-Smith concludes that the influence of the adhesive on joint strength is determined by the shear strain energy to failure of the adhesive bond.

Hart-Smith [14] found that for composite adherends, fracture of 0° filaments close to the adhesives usually initiates an interlaminar shear failure within the laminates. He also found that for thicker adherends, the dominant failure modes are peel tensile stresses in the adhesive and the associated interlaminar tension stresses in the composite adherends.

He also pointed out that any adherend imbalance causes a significant strength reduction in a bonded joint, even compared to the strength of a balanced joint employing only the geometry of the weaker adherend of the unbalanced joint.

To characterize the stresses in the adhesive, Hart-Smith treated the transverse tension, σ_{adh} , as follows, looking at Figure 8.1

$$\sigma_{adh} = E_{adh} \frac{w_u - w_l}{\eta} \quad (8.1)$$

where E_{adh} is the adhesive tensile modulus, w_u and w_l are the lateral deformations of the adherends above and below the adhesive layer, and η is the adhesive thickness.

For the elastic shear behavior of the adhesive, τ_{adh} , the equation used is

$$\tau_{adh} = G_{adh} \frac{u_u - u_l}{\eta} \quad \text{for } \gamma \leq \gamma_e \quad (8.2)$$

where G_{adh} is the shear modulus of the adhesive, and u_u and u_l respectively are the in-plane displacements of the adherends above and below the adhesive layer, and γ is the

“engineering” shear strain. Hart-Smith then modeled the adhesive shear stress to be elastic-perfectly plastic, so that,

$$\tau_{adh} = \tau_p \text{ for } \gamma \geq \gamma_e \quad (8.3)$$

where τ_p is the adhesive shear failure stress, for shear strains beyond or greater than the elastic limit γ_e .

The rationale Hart-Smith uses for neglecting plasticity in tension in the adhesive is twofold. First, he asserts that for composite adherends, the adherend is much weaker in transverse tension than is the adhesive, hence it will fail before any plastic deformation of the adhesive will occur. Secondly, the adhesives, being long-chain polymers are essentially incompressible, and hence the adherend constraints on the adhesive suppress plastic deformation in tension or compression.

Hart-Smith also notes that when adherends have differing coefficients of thermal expansion, and when the joint operates at a temperature differing from the cure temperature, the joint load capacity usually is adversely affected.

Hart-Smith’s analysis establishes also that tough ductile adhesives produce much stronger joints than those which are stronger but more brittle.

Commencing 1973, publications by Renton and Vinson [15-22] and Renton, Vinson and Flaggs [23], dealt with analytical methods for analyzing stresses, strains and displacements in both the adhesive bond and adherends in single lap joints under in-plane static and dynamic loads. Transverse shear deformation, and transverse normal strain were included, as well as temperature effects in some of the publications referenced above. The methods of analysis were assumed to be linearly elastic only because it was generally agreed that for fatigue runout to occur, the maximum stresses in the adhesive must remain below the adhesive proportional limits in both tension and shear.

When the single lap joint of Figure 8.1 is subjected to an in-plane load it deforms as shown in Figure 8.2. Because of this response it is seen from a typical bonded joint shown in Figures 8.3 and 8.4 that shear stresses peak near to the ends of the adhesive bond, while transverse normal tensile stresses (peel stresses) peak at the ends of the bond length. In these figures the length of the adhesive bond is L .



Figure 8.2. Single Lap Joint in Tension

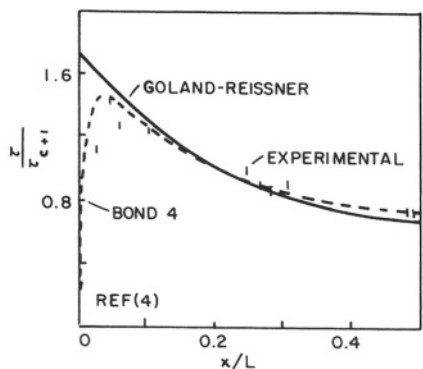


Figure 8.3. Comparison of Calculated Adhesive Shear Stresses With Experimental Data

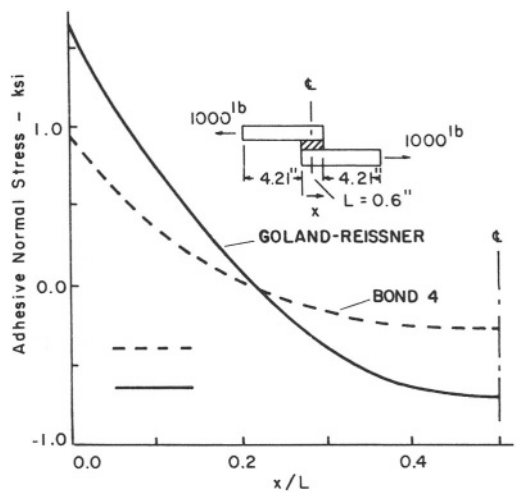


Figure 8.4. Comparison of Calculated Adhesive Normal Stresses

In 1974, Renton and Vinson reported on the results of a series of fatigue tests using a ductile adhesive, Hysol EA 951, and two different anisotropic adherend materials, subjected to constant amplitude and a two-block repeated load spectrum. The results showed that the proportional limit stress of the adhesive is a very important parameter. Fifty two unidirectional adherend specimens and fifty one angle ply fiberglass epoxy specimens were tested as well as nineteen Kevlar-49-epoxy specimens. It was found that the Kevlar-49 specimens were superior in performance. They also found that a 20-40% reduction in attainable loads associated with runout occurs when the angle ply construction is used compared with the unidirectional construction. Also in 4×10^6 cycles, a maximum design load corresponding to 26% of ultimate static load was attained for a lap length of 0.30 inches, and 20% for a lap length of 0.60 inches independent of ply orientation. No adhesive thickness effects on fatigue life were identified.

Early support for the Renton-Vinson methods of analysis, which were codified as BOND 3 and BOND 4 for single lap bonded joints, came from Sharpe and Muha [24]. They measured the shear strains in the adhesive layer of a single lap joint by monitoring the fringe pattern generated by a laser incident on imbedded single wires distributed along the adhesive layer. From this they calculated the shear stresses. They chose the single lap joint “because there are significant normal stresses present and it is presumed that the theory that can best predict the measurable shear stresses under these complicated conditions will be the best theory.” Comparing their experimental results with over twenty finite-element and closed form analytical solutions, they found the Renton-Vinson closed form solution of BOND 4 to agree the best with their experimental results. Figure 8.2 explicitly shows the comparisons made, while Figure 8.3 illustrates typical adhesive normal stresses. In each case corresponding results of the Goland-Reissner methods [6] are shown.

In 1975, Oplinger [25] published the results of his research. Oplinger’s classical paper went far to organize the plethora of publications that existed to that date. He compared and evaluated several analytic and finite element models of bonded joints, and concludes that transverse shear deformations, transverse normal strain, temperature effects, non-linear adherend and adhesive behavior, viscoelastic adhesive behavior and fracture mechanisms need to be included in modeling a bonded joint of any configuration.

Oplinger uses the concept of an ineffective length, defined as the lap length beyond which an increase in that dimension is ineffective in reducing peak adhesive shear and peel stresses. Equations for that length and those peak stresses will be given below.

In 1976, Wetherhold and Vinson [26,27] generalized the Renton-Vinson model to include hygrothermal effects in the adherend. Flaggs and Grossman [28] used a linear hereditary integral viscoelastic constitutive law for the analysis of composite adherend single lap joints under mechanical loading and/or transient hygrothermal exposure. The viscoelastic effects are significant. The Flaggs-Crossman approach allows the analysis of stresses in bonded joints over periods of years, utilizing creep relaxation data from experiments at various temperatures and moisture contents performed over periods of several minutes.

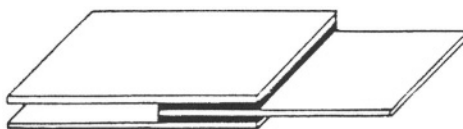


Figure 8.5. Double Lap Joint

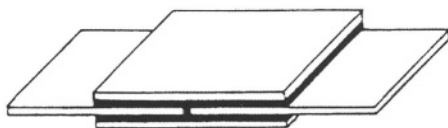


Figure 8.6. Double Doubler Joint

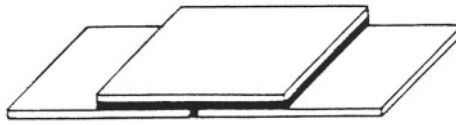


Figure 8.7. Single Doubler Joint

8.2.3 DOUBLE LAP JOINT AND DOUBLE DOUBLER JOINT

The double lap joint has also been studied by many researchers. There, however, is an ambiguity in the definition of the double lap joint of Figure 8.5, some calling Figure 8.6 a double lap joint.

Lehman and Hawley [9] were the first to show that double lap joints were more than twice as strong as single lap joints of the same lap length due to the symmetry of this configuration, which reduces bending in the adherends and transverse stresses across the adhesive. They also modified their linear analysis to account for plasticity in an approximate manner, which agreed well with experimental data.

8.2.4 SINGLE DOUBLER JOINT

Relatively little work has been performed on this configuration. This joint is shown in Figure 8.7. It is of importance in some repair procedures. Because of the asymmetry it results in high peel stresses, analogous to the single lap joint.

8.2.5 SCARF JOINTS

The scarf joint is depicted in Figure 8.8 below.

Its advantage is in aerodynamic smoothness, but the disadvantage is in the careful machining required to have a uniform bond line. Therefore, it is perhaps more useful for metallic adherends rather than those composed of composite materials. It has been found that for the best scarf joint the angle of the scarf is 7 to 9 degrees making for a long joint. Lehman and Hawley [9] found that the scarf joint and the stepped lap configurations have the capability of scale-up to transmit a load of any magnitude providing that the lap length is not restricted. They also found that in fatigue ($R = +0.05$, tension) scarf joints sustained stress levels 3.5 times greater than those of double lap joints. They found that the scarf joint approaches the ideals of strain compatibility in the adherends and uniform stress in the adhesive. One result of this is that adhesive ductility in scarf joints is less important than in other configurations.



Figure 8.8. Scarf Joint

Grimes [11] suggested in 1973 that a non-linear analysis for scarf joints is needed. Oplinger [25] states that both scarf and stepped lap joints provide efficient use of the full overlap length by allowing the peak adhesive stresses to be reduced as the overlap length increases, thus avoiding the “ineffective length” defined earlier.

8.2.6 STEPPED LAP JOINT

The stepped lap joint is shown in Figure 8.9. Lehman and Hawley [9] have found that stepped lap joints achieve higher average shear stresses than the scarf joint; also the strength of the stepped lap joint is not sensitive to the number of steps when the total lap length is held constant. In fact, they found that scarf and stepped lap joints are lighter in weight than other lap joints at all load levels. The stepped lap joint approximates the strain compatibility of the scarf joints. In Grimes' study [11] he assumes that no force is transmitted by the adhesive in the riser of the stepped-lap configuration.

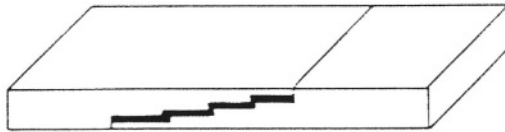


Figure 8.9. Stepped Lap Joint

8.2.7 ANALYSIS AND DESIGN OF SINGLE LAP AND DOUBLE LAP ADHESIVELY BONDED JOINTS

Oplinger [25] has provided a useful set of equations for the design and analysis of these joints. Assume that for in-plane loading, the axial strain, ϵ_x , is either constant across each adherend thickness shown in Figure 8.1

$$\epsilon_x = \frac{dU}{dx} = \frac{N_x}{A_{11}} \quad (8.4)$$

or is a linear function of the thickness coordinate z

$$\epsilon_x = \frac{N_x}{A_{11}} + \frac{M_x}{D_{11}} z \quad (8.5)$$

where all terms have been defined previously. The upper adherend shall have subscripts u ; the lower adherend will have subscripts l .

The equilibrium equations can be written as:

$$\frac{dN_u}{dx} + \tau_a = 0 \quad (8.6)$$

In the region of the bonded joint,

$$N_u + N_l = N_0 \quad (8.7)$$

where N_0 is the applied in-plane load per unit width to the structure.

$$\frac{dM_u}{dx} + Q_u - \frac{h_u \tau_a}{2} = 0 \quad (8.8)$$

$$\frac{dM_l}{dx} + Q_l - \frac{h_l \tau_a}{2} = 0 \quad (8.9)$$

$$\tau_a = \tau_u(x, -h_u/2) = \tau_l(x, +h_l/2) \quad (8.10)$$

Vertical equilibrium requires that,

$$\sigma_a = \frac{dQ_u}{dx} = -\frac{dQ_l}{dx} \quad (8.11)$$

The adhesive is modeled as a simple tension/compression spring and a shear spring, see Equations (8.1) and (8.2).

As a result of the above, two coupled ordinary differential equations in terms of the adhesive stresses can be obtained:

$$\frac{d^3 \tau_a}{dx^3} - \frac{\lambda^2}{h_u^2} \frac{d\tau_a}{dx} - \frac{\beta^2}{h_u^3} \sigma_a = 0 \quad (8.12)$$

$$\frac{d^4 \sigma_a}{dx^4} - 4 \frac{\Lambda^2}{h_u^4} \sigma_a - \frac{2C_v \beta^2}{h_u^3} \frac{d\tau_a}{dx} = 0 \quad (8.13)$$

If one defines $K_a = E_{adh} / \eta$ and $C_v = 1 + \nu_{adh}$ the parameters λ , Λ and β are given by:

Single Lap Joint:

$$\frac{\lambda^2}{h_u^2} = \frac{K_a}{2C_v} \left[\frac{1}{A_{11u}} + \frac{1}{A_{11l}} + \frac{h_u^2}{4D_{11u}} + \frac{h_l^2}{4D_{11l}} \right] \quad (8.14)$$

$$\frac{\Lambda^4}{h_u^4} = \frac{K_a}{4} \left[\frac{1}{D_{11_u}} + \frac{1}{D_{11_l}} \right] \quad (8.15)$$

$$\frac{\beta^2}{h_u^3} = \frac{K_a}{2C_v} \left[\frac{1}{2D_{11_u}} + \frac{1}{2D_{11_l}} \right] \quad (8.16)$$

Double Lap Joint:

$$\frac{\lambda^2}{h_u^2} = \frac{K_a}{2C_v} \left[\frac{1}{A_{11_u}} + \frac{2}{A_{11_l}} + \frac{h_u^2}{4D_{11_u}} \right] \quad (8.17)$$

$$\frac{\Lambda^4}{h_u^4} = \frac{K_a}{4D_{11_u}} \quad (8.18)$$

$$\frac{\beta^2}{h_u^3} = \frac{K_a}{4C_v} \frac{h_u}{D_{11_u}} \quad (8.19)$$

Using standard techniques, the solutions of Equations (8.12) and (8.13) are exponential functions of x and η is the root of a sixth degree polynomial obtained from (8.12) and (8.13). For a large class of bonded joints in which the adherend bending deformations are small compared to the axial stretching deformations, two roots are given approximately by $\pm \lambda$ and the remaining four roots are approximated by $\pm \Lambda(1 \pm i)$, where $i = (-1)^{1/2}$. For the cases of identical adherends (the best bonded joint) these roots are exact for the single lap joint case.

Oplinger also finds the maximum shear stresses and maximum peel stresses in the adhesive decrease with increased lap joint length, up to a length he defines as the “ineffective length”, l_{eff} , beyond which the peak stresses in the adhesive do not decrease. Therefore, l_{eff} , becomes a design goal in that at that length the peak stresses have their minimum value, but if the lap length is greater the peak adhesive stresses are not reduced, but the joint is heavier. So the ineffective length of the lap joint, l_{eff} , is given by

$$l_{\text{eff}} = \text{MAX}(3h_u / \lambda, 3h_u / \Lambda) \quad (8.20)$$

Defining the parameter ρ_u is given by,

$$\rho_u = \frac{E_{adh} h_u}{Q_{1l_u} \eta} \quad (8.21)$$

Then the parameters λ and Λ for the following cases are given by:

Single Lap, Identical Adherends

$$\lambda = 2(\rho_u / C_V)^{1/2}, \quad \Lambda = (6\rho_u)^{1/4} \quad (8.22)$$

Double Lap, $A_{1l_l} = 2A_{1l_u}$

$$\lambda = (\rho_u / 2C_V)^{1/2}, \quad \Lambda = (3\rho_u)^{1/4} \quad (8.23)$$

When the lap length is equal to or greater than the ineffective length, l_{eff} , then the peak stresses in the adhesive are:

Single Lap, Identical Adherends, l_{eff}

$$\frac{\sigma_{adh_{MAX}}}{\sigma_{u_0}} = \frac{k}{2} \Lambda^2 + 2k' \frac{h_u}{l} \Lambda \quad (8.24)$$

$$\frac{\tau_{adh_{MAX}}}{\sigma_{u_0}} = \left(\frac{1+3k}{8} \right) \lambda + 3(1-k) \quad (8.25)$$

where

$$\sigma_{u_0} = \frac{N_0}{h_u} \quad (8.26)$$

$$k = \frac{\cosh \mu}{\cosh \mu + 2\sqrt{2} \sinh \mu} \quad (8.27)$$

$$k' = \sqrt{2} k \mu \quad (8.28)$$

$$\mu = \frac{l}{2h_u} \left[\frac{3}{2} (1 - \nu_{12} \nu_{21}) \frac{N_0}{A_{1l_u}} \right]^{1/2} \quad (8.29)$$

Double Lap, $A_{1l_l} = 2A_{1l_u}$, $l \geq l_{\text{eff}}$

$$\frac{\tau_{\text{adh}_{\text{MAX}}}}{\sigma_{u_0}} = \frac{\lambda}{2}$$

$$\frac{\sigma_{\text{adh}_{\text{MAX}}}}{\sigma_{u_0}} = \left(-\frac{1}{2} + \frac{\Lambda}{\lambda} + \frac{\lambda^2}{2\Lambda^2} \right) \left(\frac{4\Lambda^4}{4\Lambda^4 + \lambda^4} \right) \frac{\lambda^2}{2} \quad (8.30)$$

The parameters k and k' in (8.26) and (8.27) reflect the bending of the single lap configurations due to load eccentricity.

Using (8.21) and (8.22), the above equations can be written in terms of ρ_u

Single Lap Joint:

$$\frac{\tau_{\text{adh}_{\text{MAX}}}}{\sigma_{u_0}} = \left(\frac{1+3k}{4} \right) \left(\frac{\rho_u}{C_v} \right)^{1/2} + 3(1-k) \quad (8.31)$$

$$\frac{\sigma_{\text{adh}_{\text{MAX}}}}{\sigma_{u_0}} = \frac{k}{2} (6\rho_u)^{1/2} + 2k' (6\rho_u)^{1/4} \quad (8.32)$$

Double Lap Joint:

$$\frac{\tau_{\text{adh}_{\text{MAX}}}}{\sigma_{u_0}} = \left(\frac{5}{8} \rho_u \right)^{1/2} \quad (8.33)$$

$$\frac{\sigma_{\text{adh}_{\text{MAX}}}}{\sigma_{u_0}} = \left[\frac{5}{2(3)^{1/2} C_v} \rho_u^{1/2} + \left(\frac{6}{5} C_v \right)^{1/2} \frac{1}{\rho_u^{1/4}} - \frac{1}{2} \right]$$

$$\times \frac{\frac{5}{4C_v} \rho_u}{\left[\frac{25}{12} \frac{\rho_u}{C_v^2} + 1 \right]} \quad (8.34)$$

In both joints the peak shear stress varies as $\rho_u^{1/2}$. The maximum peel stress in the single lap joint varies as $\rho_u^{1/4}$ for small ρ_u , and as $\rho_u^{1/2}$ for large ρ_u . For the double lap joint the peel stresses vary as $\rho_u^{1/4}$ for small ρ_u and as $\rho_u^{1/2}$ for large ρ_u . This suggests that in either joint ρ_u should be as small as possible.

Formulations including the effects of transverse shear deformation and transverse normal stresses have been given by Renton and Vinson [15-23].

Oplinger states that typical adhesive shear and peel strengths are on the order of 5-10 ksi, while composite adherend tensile strengths are typically on the order of 50-200 ksi. The ratio of peak adhesive shear stress to adherend tensile strength for a desirable joint design is thus

$$0.025 \leq \frac{\tau_{\text{adh_MAX}}}{\sigma_{u_0}} \leq 0.2 \quad (8.35)$$

However, this ratio cannot be reduced to less than about $\lambda/2$, or as shown above

$$\frac{\tau_{\text{adh_MAX}}}{\sigma_{u_0}} > \frac{1}{2} \left(\frac{5 \rho_u}{2 C_v} \right)^{1/2}$$

because of the “ineffective length” phenomenon, which prevents the interior region of the overlap from contributing much to the load transfer between adherends. See Figure 8.3.

The quantity

$$\left(\frac{\rho_u}{C_v} \right)^{1/2} = \left(\frac{G_{\text{adh}} h_u}{Q_{11_u} \eta} \right)^{1/2} \quad (8.36)$$

is on the order of unity or greater for typical joints so single lap and double lap joints cannot be designed to attain the ratios of (8.35).

Conversely, scarf and step lap joints provide for efficient use of the full overlap length of the joint by allowing peak adhesive stresses to be continually reduced as the overlap length increases, thus avoiding the “ineffective length” difficulty.

8.2.8 ANALYSIS OF A SCARF JOINT

For the scarf joint shown in Figure 8.8 where the thin adhesive bond line is cut at an angle α to the in-plane load direction, it is straightforward to show that

$$\frac{\tau_{\text{adh}}}{\sigma_0} = -\frac{\sin(2\alpha)}{2} \quad (8.37)$$

$$\frac{\sigma_{adh}}{\sigma_0} = \sin^2(2\alpha) \quad (8.38)$$

Since tangent $\alpha = \text{adherend thickness} / \text{lap length}$, then

$$\frac{\tau_{adh}}{\sigma_0} \cong -\frac{h}{l}; \quad \frac{\sigma_{adh}}{\sigma_0} \approx \left(\frac{h}{l}\right)^2 \quad (8.39)$$

Thus Oplinger finds that any shear stress concentration is relatively independent of the lap length, which means that the “ineffective length” handicap of single lap joints is surmounted if a scarf joint is used.

8.2.9 DESIGN CONSIDERATIONS

It is seen that the design and analysis of adhesively bonded joints is very complex. If an analytical approach is used it involves at least 26 equations and 26 unknowns, and after the roots of the equations are found, a computer program such as BOND 4 is needed to do design, analysis or optimization studies.

Many computer programs are available. Each has different assumptions, and concerns different configurations. One of the problems involved is the shape of the shear stress distribution, see Figure 8.3, which often requires double precision on the computer.

For very simplified preliminary design studies, the excellent paper by Oplinger [25] can often be used, as a starting reference.

Some general comments can be made regarding the design of bonded joints.

- Maximum shear stresses and normal stresses can be reduced by making the D_{11} and A_{11} of the adherends as large as possible.
- Regardless of the materials used, the values of D_{11} and A_{11} of the adherends on each side of the bond should be equal. Otherwise there will not be symmetry of either the adhesive shear and normal stress about the adhesive bond mid-length, with higher stress values resulting from the asymmetry.
- As Oplinger points out, there is a length of bond line beyond which no load capacity increase occurs, due to the nature of the shear stress distribution, Figure 8.3.
- If the bond line length is made larger and larger, then failure or yielding will occur in the adherends instead of in the adhesive bond.
- Hart-Smith [30] points out that if there is a debond of length L_1 at the end of a bond line of length L , then approximately one can simply analyze the same adhesive bond, but of length $L - L_1$. Additional practical design information is included.

Many other factors must be studied more in detail such as those addressed by Vinson [27] and the effects of viscoelasticity and plasticity in adhesively bonded

structures. As stated previously, Flaggs and Crossman [28] were the first to study the effects of viscoelasticity in adhesive bonded joints. Sen [29] studies followed.

8.3 Mechanical Fastening

8.3.1 INTRODUCTION

Almost all composite engineers philosophically agree that adhesive bonding is superior to mechanical fastening, primarily because of continuous joining, no fiber cutting, and no stress concentrations. Nevertheless, for structural components which must be removable or easily replaced, mechanical fastening has an important place.

8.3.2 REVIEW OF MECHANICAL FASTENING TECHNOLOGY

The early research on mechanical fasteners dealt with joining isotropic metallic or plastic structural components. In 1928, Bickley [31], in an excellent paper, studied the state of stress around a circular hole in an infinite elastic plate of uniform thickness subjected to prescribed in-plane tractions acting on the periphery of the hole.

Before 1969, the early studies treated only isotropic, thin classical flat structures under static loads. Neither dynamic nor thermal loads were considered, nor were nonlinear effects.

In 1969, Kutscha and Hofer [8], presented the first comprehensive treatment of mechanical fasteners in composite structures. Their analytical and experimental study included experimentally studying the load distribution and joint strength in fiberglass bolted joints and comparing them with analytical solutions. They also provide an inclusive literature survey for design procedures for joining with mechanical fasteners.

Kutscha and Hofer concluded that the most effective way to deal with bolted joints in isotropic materials is to employ semi-empirical methods for design. For composites the failure modes are so different (tensile, compressive, shear buckling or mixed modes) a complete stress analysis and failure envelope (in four dimensions) is required to even develop the semi-empirical procedures to design a given class of joints. They also list six recommendations for further research, which are inclusive.

A short time later Lehman and Hawley published an inclusive technical report [9], presenting the results of their studies on bonded and bolted joints in composite panels under static and dynamic loads. The bolted joint concepts they studied included laminates with plain holes and with reinforced holes using either a composite or a steel shim reinforcement, or steel bushings. They found the factors affecting bolted joint failures are laminate strength and stiffness, edge distance, fastener pitch, laminate thickness and fastener diameter. One interesting result from their study is that a combination bolted-bonded joint performed better than bolted joints or bonded joints alone, primarily because the combination causes a fundamental change in the failure mode. They found that bolted joints in composites are lighter than bolted joints in aluminum. However, bonded joints were found to be superior to bolted joints on a weight-efficiency basis.

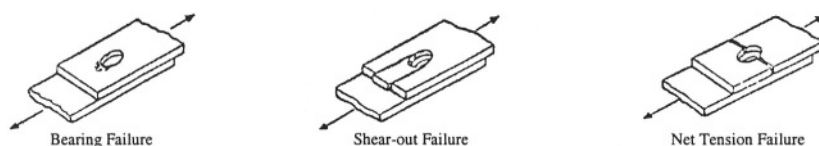


Figure 8.10. Potential Modes of Failure in Graphite/Epoxy Bolted Joint Specimen.

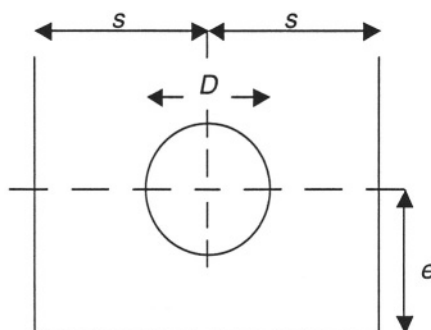


Figure 8.11. Dimensions of Mechanically Fastened Joint of Thickness, t .

They also concluded that their linear discrete element analysis did not adequately predict load-deformation characteristics of bolted joints. Agreement between test and linear theory for the basic fastener-sheet combination was poor. The discrepancy is probably due to nonlinear behavior associated with local filament buckling and matrix plasticity caused by high bearing stresses. They concluded that an extremely sophisticated nonlinear analysis is required to characterize the load-deformation behavior of bolted joints.

The three usual failure modes in mechanically fastened joints are net tension failure, shear out and bearing failure. These are shown for the single lap joint in Figure 8.10.

The bolted joints studied by Lehman and co-workers included both single and double lap configurations. The single lap joints were not penalized greatly strengthwise due to the asymmetry of the joint. In the double lap joint the use of bushings reduces the joint weight efficiency resulting in reduced effectiveness. Both the insertion of metal shims and thickened end designs resulted in weight effective joints. Although more difficult to fabricate, the shimmed joint produces a very compact, high strength joint. The thickened-end configuration, however, is a good general-purpose design. As stated above, the addition of adhesive bonding to a bolted joint gave strengths that were greater than similar joints using either bonding or bolting only. Specifically, bolted joints without bonding were less than 1/3 as strong in the fiberglass laminates and less than 1/5 as strong in the boron laminates. Shear-out failures were prevalent in all bolted joints except for the shim-reinforced and the combination bolted-bonded joints, even when the joint proportions were selected to produce bearing failures.

The shear stresses developed at failure decrease as edge distance, e , increases. Thus, increasing edge distance is an inefficient method of increasing joint strength.

However, for a given edge distance, joint strength increases approximately linearly with composite thickness until bolt bending effects reverse this trend.

Edge distances of 4.5 times the fastener diameter, d , were required to achieve a balance between shear-out and bearing strengths. Tensile failures through the fastener holes were precluded by a side distance, s , of twice the fastener diameter, d . A thickness-to-diameter ratio (t/d) of 0.8 results in maximum bearing strength. Maximum shear-out stresses were developed in a laminate containing 0° and $\pm 45^\circ$ layers in which $2/3$ of the laminae were $\pm 45^\circ$ to the load axis.

In their bolted joint tests, Lehman used bolts rather than pins so that the effects of bolt clamping friction were included. Consistent surface conditions and bolt torques were maintained to minimize scatter. Standard torques were used resulting in bolt stresses between 30 and 40 ksi. Standard specimen width was $1''$, while $3/16''$ and $1/4''$ bolts were used, hence s/D ratios were 2.63 and 2.00, respectively where s = distance from bolt center-line to the edge of the test piece. Lehman states that test results indicate that the full bearing stress will not be developed if D/t (where t is the laminate thickness) exceeds a value of two. Hence, a normal laminate thickness of 0.120 inches was selected. Lehman also stated that published test results show that the bearing stress increased with e/D ratio until a ratio 5 is reached, where e = edge distance. He chose $1/2''$, $3/4''$ and $1-1/4''$, such that the e/D ratio varied from 2.63 to 6.58. His tests show that the bolted joint strength increases linearly with e/D ratio up to a value of 4. Beyond that value, increasing the e/D ratio did not appreciably increase joint strength, regardless of t/D ratio.

Lehman concludes like Kutsche and Hofer that, semi-empirical methods are the most effective approach to rational joint design in composite materials.

Fatigue tests were conducted on both single and double lap bolted joints at a stress ratio of +0.05, wherein the maximum loads ranged from 60% to 80% of the static load capacities to reduce the possibility of runout. Boron reinforced specimens were cycled at 1800 cycles per minute and fiberglass-reinforced specimens were cycled at 900 rpm to minimize temperature effects. Even so the single lap joints suffered a 50°F temperature rise, and the double lap joints stabilized at 86°F Lehman found that the bolted double lap specimens produced the longest fatigue life (over the bolted single lap, single and double lap adhesive bonded, adhesive bonded scarf and adhesive bonded stepped lap joints) and in each case failure occurred in the aluminum alloy members through the bolt hole. The combination bolted and bonded joint of boron also performed well in fatigue.

In September 1974, Murphy and Lenoe [32] published an annotated bibliography on previous research on structural joints of all kinds, as well as interfaces. It was the first bibliography dealing with this subject.

In 1974 the Army Materials and Mechanics Research Center held a Symposium dealing primarily with the role of mechanics in the design of structural joints. At that meeting Van Siclen [33] presented design procedures for bolted joints in graphite epoxy laminates. His research had a dual purpose: one, to develop joint allowables and two, to evaluate the merits of alternative reinforcing concepts for improving joint strength. The approach Van Siclen used, similar to Lehman earlier, was to obtain and evaluate actual joint test data for Thornel 300/PR286, and from the data to establish semi-empirical procedures for predicting joint strength as a function of all pertinent variables. The

reinforcing concepts considered were metallic interleaves, externally bonded on metallic doublers, laminate cross-ply build ups and fiberglass “softening strips.”

Van Siclen states that “the main difficulty in designing mechanical joints in composite laminates is that the behavior of such joints in composites is not well understood. This is due in part, to the general complexities associated with composite materials and partly to the lack of understanding of mechanical joint behavior.”

Van Siclen also lists several references which are cogent to bolted joints, which are not discussed herein.

He discusses each of the geometric parameters which affect joint behavior which are edge distance (e), side distance (s), hole diameter (D) and laminate thickness (t), along with laminate properties which include fiber orientation, stacking sequence, and types of material systems.

He also points out that the type of fastener used has a great influence on joint strength. For example, when a countersunk fastener is used rather than a protruded head fastener, the bearing strength of the composite joint may be severely reduced.

Concerning net tension failure, the allowable stress for a laminate is significantly reduced as the s/D greater than 3 or 4 will not significantly increase the net tensile load a joint can carry.

Therefore the net tensile load a given joint can carry, P_{nt} , is given by

$$P_{nt} = F_{nt}(2s - D)t \quad (8.40)$$

where $2s$ is the specimen width, and F_{nt} is an empirical factor determined by experiments.

Van Siclen's equation for the shear-out strength, the maximum load P_{so} the joint can carry without shear-out failure is

$$P_{so} = F_{so}(2s - D)t \quad (8.41)$$

where F_{so} is an empirical factor determined by shear-out tests.

Van Siclen uses the obvious equation for the allowable bearing load on the joint P_{br} :

$$P_{br} = F_{bru} D t \quad (8.42)$$

where F_{bru} is the ultimate bearing strength for a given laminate determined from tests.

8.3.3 GENERAL DESIGN APPROACH

It is clear that the complexities associated with joints involving mechanical fasteners in composite material structures preclude a rational analytical solution at this time, and at any foreseeable time. To have an analytical solution would require a large finite element code which takes into account three dimensional effects, friction between bolt and the hole, hygrothermal effects, nonlinear laminate response, bolt bending, and

other factors. Even then practical considerations such as hole tolerances, and bolt torque actually applied would limit the usefulness of the results for design.

Therefore from a design standpoint it appears that the best approach to use is that of Van Siclen [33], wherein simple easy to use equations can be used, which necessitate that certain tests be performed.

For any given structural component, hopefully the material system, and the laminate orientation and number are decided on due to overall loading and environment for the component, rather than letting the joints control such decisions. Thus, material system, laminate orientation and thickness are predetermined before joint decisions are made or considered.

For that chosen laminate, tests described by Van Siclen should be performed to determine F_{nt} , the net tensile strength, F_{so} , the shear-out strength, and F_{br} the bearing strength for that particular laminate. In Van Siclen's [33] excellent paper, he presented the results of tests he performed on a $[0^\circ, \pm 45^\circ, 90^\circ]_S$ graphite epoxy laminate. The resulting curves are given in Figures 8.12, 8.13, and 8.14.

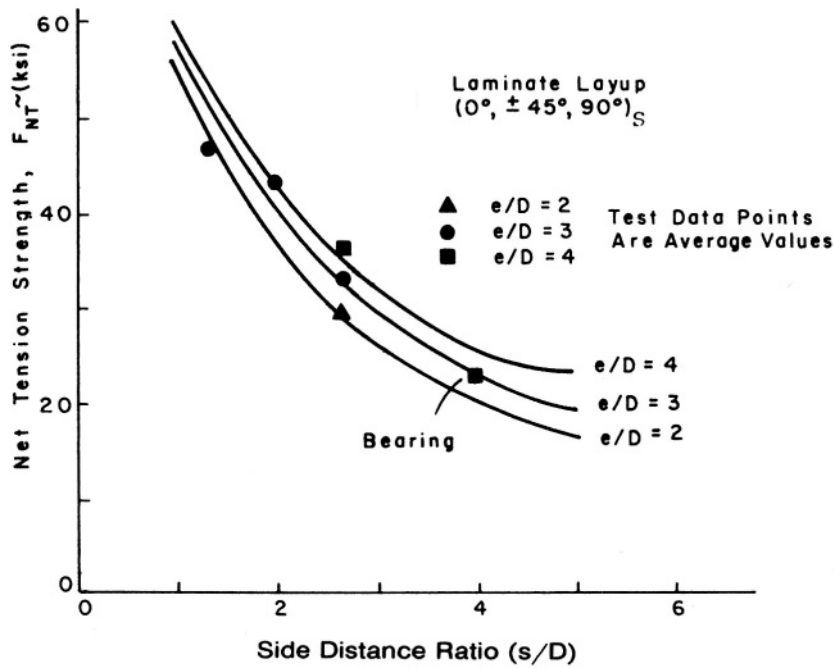


Figure 8.12. Net Tension Strength as a Function of (s / D) and (e / D)

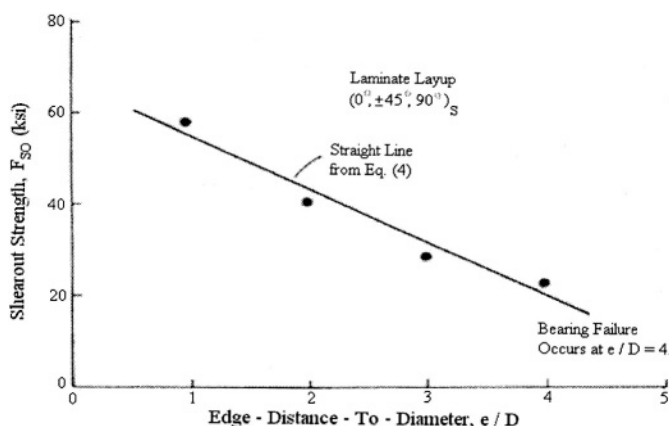


Figure 8.13. Shear-out Strength as a Function of Edge Distance

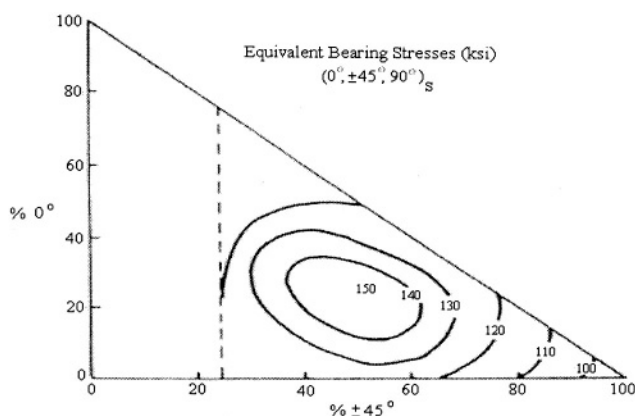


Figure 8.14. Bearing Strength in 10^3 psi as a Function of Laminate Properties

These results then are easily used with Equation (8.40) through (8.42) to design, analyze, and optimize any joint. If the structural component is to be subjected to hygrothermal loads, then these tests should be carried out under those conditions, because Kim and Whitney [34] have shown the deleterious effects of a hygrothermal environment. If there is a normal pressure due to bolt torquing then the tests should be performed with the intended torques applied because Stockdale and Matthews [35] have shown that such pressure can increase bearing strength by 40% to 100%. Also, the actual bolts considered should be used in these tests because Van Siclen [33] points out the differences in strength when countersunk fasteners or protruded head fasteners are used.

With those strengths available one can then select a fastener size to transmit the required load. It should be noted that it is generally agreed upon that $s/D = 1$ and $e/D = 2$ appear to be an optimum value in many cases. However, using the Van Siclen equations one can, to a certain extent, optimize the mechanically fastened joint.

If the laminate is too thin to transmit the required load then local stiffening is required. Alternative methods for stiffening have been discussed by Lehman and Hawley [9] and Oplinger and Gandhi [36] and additional testing could be required in the case of the stiffened configuration.

If the structure is subjected to fatigue loading it appears that a full cycle set of tests are required, although the preliminary design could be based upon a design for which there is no yielding in tension, shear-out, or bearing at the mean fatigue load.

As a data bank on the three strengths is built up for various material systems and ply orientations the amount of testing can be reduced.

Since stacking sequence does have a significant effect on joint strength, if the stacking sequence for a structural component could be modified then the optimum design may require a compromise between the stacking sequences best for the component primary purpose, and what is best for the joint strength.

Thus, the design of mechanically fastened joints is rather straightforward, and the optimization of joined structural components sufficiently complex that it is a challenge. In any case, simple analyses can be used, but some testing is required.

It should also be remembered that Lehman and Hawley [9] found the addition of adhesive bonding to a bolted joint gave strengths that are greater than similar joints using either bonding or bolting only. Hence, in a design this also can be investigated using the Van Siclen approach discussed above.

8.4 Recommended Reading

Other recommended reading for adhesive bonded joints includes that of Chamis and Murthy [37], Fujita et al [38], Tong [39], Running, Legon and Miskioglu [40], Mennetyen and Chamis [41], Liu, Raju and Yon [42], Lin and Jen [43], Pierron, Cerisier and Grediac [44], Turaga and Sun [45] and Zeng and Sun [46].

8.5 References

1. Kuno, James K. (1979) Structural Adhesives Continue to Gain Foothold in Aerospace and Industrial Use, Structural Adhesives and Bonding. *Proceedings of the Structural Adhesives Bonding Conference*, arranged by Technology Conferences Associates, El Segundo, California.
2. Szepe, F. (1966) Strength of Adhesive-Bonded Lap Joints with Respect to Temperature and Fatigue, *Experimental Mechanics*, Vol. 6, pp. 280-286.
3. Volkersen, O. (1944) Die Niet Kraft vertelung in Zug bean Spruchten Niet verb bind ungen mit Konstaanten Lasch enguerschnitten, *Luftfahrt forschungen*, Vol. 15, pp. 41-47.
4. De Bruyne, N.A. (1944) The Strength of Glued Joints, *Aircraft Engineering*, vol. 16, pp. 115-118.
5. Wang, D.Y. (1963) The Effect of Stress Distribution on the Fatigue Behavior of Adhesive Bonded Joints, *ASD-TDR-63-93*, AFML, July.

6. Goland, M. and Reissner, E. (1947) Stresses in Cemented Joints, *ASME Journal of Applied Mechanics*, Vol. 11, A-17-A-27.
7. Kutscha, D. (1964) Mechanics of Adhesive-Bonded Lap-Type Joints: Survey and Review, *AFML-TDR-64-298*, December.
8. Kutscha, D. and Hofer, K.E., Jr. (1969) Feasibility of Joining Advanced Composite Flight Vehicles, *AFML-TR-68-391*, January.
9. Lehman, G.M. and Hawley, A.V. (1969) Investigation of Joints in Advanced Fibrous Composites for Aircraft Structures, *AFFDL-TR-69-43*, Vol. 1, June.
10. Dickson, J.N., Hsu, T.M. and McKinney, J.M. (1972) Development of an Understanding of the Fatigue Phenomenon of Bonded and Bolted Joints in Advanced Filamentary composite Materials, Analysis Materials, *AFFDL-TR 72-64 (AD 750 132)*, Vol. 1, June.
11. Grimes, G.C., et al. (1972) The Development of Nonlinear Analysis Methods for Bonded Joints in Advanced Filamentary Composite Structures, *AFFDL-TR-72-97 (AD 905 201)*, September.
12. Ramberg, W. and Osgood, W.R. (1943) Description of Stress-Strain Curves by Three Parameters, *NACA TN 902*, July.
13. Hart-Smith, L.J. (1970) The Strength of Adhesive Bonded Single Lap Joints, *Douglas Aircraft Company IRAD Technical Report MDC-J0472*, April.
14. Hart-Smith, L.J. (1973) Adhesive-Bonded Single Lap Joints, *NASA-CR-112236*, January.
15. Renton, W.J. and Vinson, J.R. (1973) The Analysis and Design of Composite Material Bonded Joints Under Static and Fatigue Loadings, *AFOSR TR 73-1627*, August.
16. Renton, W.J. and Vinson, J.R. (1974) Fatigue Response of Anisotropic Adherend Bonded Joints, *AMMRC MA-74-8*, September.
17. Renton, W.J. and Vinson, J.R. (1974) The Analysis and Design of Anisotropic Bonded Joints, Report No. 2, *AFOSR TR-75-0125*, August.
18. Renton, W.J. and Vinson, J.R. (1975) On the Behavior of Bonded Joints in Composite Materials Structures, *Journal of Engineering Fracture Mechanics*, Vol. 7, pp. 41-60.
19. Renton, W.J. and Vinson, J.R. (1975) Fatigue Behavior of Bonded Joints in Composite Materials Structures, *AIAA Journal of Aircraft*, Vol. 12, No. 5, May, pp. 442-447.
20. Renton, W.J. and Vinson, J.R. (1975) The Efficient Design of Adhesive Bonded Joints, *Journal of Adhesion*, Vol. 7, pp. 175-193.
21. Renton, W.J., Pajerowski, J. and Vinson, J.R. (1975) On Improvement in Structural Efficiency of Single Lap Bonded Joints, *Proceedings of the Fourth Army Materials Technology Conference – Advances in Joining Technology*, September.
22. Renton, W.J. and Vinson, J.R. (1977) Analysis of Adhesively Bonded Joints Between Panels of Composite Materials, *Journal of Applied Mechanics*, April, pp. 101-106.
23. Renton, W.J., Flags, D.L. and Vinson, J.R. (1978) the Analysis and Design of Composite Materials Bonded Joints, Report No. III, *AFOSR –TR-78-1512*.
24. Sharpe, W.N., Jr. and Muha, T.J., Jr. (1978) Comparison of Theoretical Experimental Shear Stress in the Adhesive Layer of a Lap Joint Model, *AMMRC MS 74-8*.

25. Oplinger, D.W. (1975) Stress Analysis of Composite Joints, *Proceedings of the Fourth Army Materials Technology Conference – Advances in Joining Technology*, September .
26. Wetherhold , R.C. and Vinson, J.R. (1978) An Analytical Model for Bonded Joint Analysis in Composite Structures Including Hygrothermal Effects, *AFOSR TR 78-1337*.
27. Vinson, J.R. (1989) Adhesive Bonding of Polymer Composites, *Polymer Engineering and Science*, Mid-October, Vol. 29, No. 19, pp. 1325-1332.
28. Flaggs, D.L. and Crossman, F.W. (1979) Viscoelastic Response of a Bonded Joint Due to Hygrothermal Exposure, *Modern Developments in Composite Materials and Structures*, ASME.
29. Sen, J.K. (1977) Stress Analysis of Double Lap Joints Bonded with a Viscoelastic Adhesive, *Ph.D. Dissertation, Southern Methodist University*, May.
30. Hart-Smith, L.J. (1980) Further Development in the Design and Analysis of Adhesive Bonded Structural Joints, *Douglas Paper 6922 presented at the ASTM Symposium on Joining of Composite Materials*.
31. Bickley, W.G. (1928) The Distribution of Stress Round a Circular Hold in a Plate, *Royal society of London*, Vol. 227A, July 2, pp. 383-415.
32. Murphy, M.M. and Leno, E.M. (1974) Stress Analysis of Structural Joints and Interfaces, *A Selected Annotated Bibliography*, AMMRC MS 74-10.
33. Van Siclen, R.C. (1974) Evaluation of Bolted Joints in Graphite/Epoxy, *Proceedings of the Army Symposium on Solid Mechanics (AD 786543)*, September, pp. 120-138.
34. Kim, R.Y. and Whitney, J.M. (1976) Effect of Temperature and Moisture on Pin Bearing Strength of composite Laminates, *Journal of Composite Materials*, April, pp. 149-155.
35. Stockdale, J.H. and Matthews, F.L. (1976) The Effect of Clamping Pressure on Bolt Bearing Loads in Glass Fibre-Reinforced Plastics, *Composites*, January, pp. 34-38.
36. Oplinger, D.W. and Gandhi, K.R. (1974) Analysis Studies of Structural Performances in Mechanically Fastened Fiber-Reinforced Plates, *Proceedings of the Army Symposium on Solid Mechanics (AD 786-543)*, September.
37. Chamis, C.C. and Murthy, P.L. (1991) Simplified Procedures for Designing Adhesively Bonded Composite Joints, *Journal of Reinforced Plastics and Composites*, Vol. 10, January, pp. 29-41.
38. Fujita, A., Hamada, H., Maekowa, Z., Ohno, E., and Yokoyama, A. (1994) Mechanical Behavior and Fracture Mechanism in Flat Braided Composites, Part 3: Mechanically Fastened Joint in Flat Braided Bar, *Journal of Reinforced Plastics and Composites*, Vol. 13, August, pp. 740-755.
39. Tong, L. (1998) Failure of Adhesive-Bonded Composite Lap Joints With Embedded Cracks, *AIAA Journal*, Vol. 36, No. 3, March, pp. 448-456.
40. Running, D.M., Legon, J.B. and Miskioglu, I. (1999) Fastener Design for Transversely Loaded Composite Plates, *Journal of Composite Materials*, Vol. 33, No. 10, pp. 928-940.

41. Minnetyan, L. and Chamis, C.C. (1999) Progressive Fracture of Adhesively Bonded Composite Structures, *Theoretical and Applied Fracture Mechanics*, Vol. 31, pp. 75-84.
42. Liu, D., Raju, B.B. and Yon, J. (1999) Thickness Effects on Pinned Joints for Composites, *Journal of Composite Materials*, Vol. 33, No. 1, pp. 2-21.
43. Lin, W.H. and Jen, M.H. (1999) The Strength of Bolted and Bonded Single-Lapped Composite Joints in Tension, *Journal of Composite Materials*, Vol. 33, No. 7, pp. 640-666.
44. Pierron, F., Cerisier, F. and Grediac, M. (2000) A Numerical and Experimental Study of Woven Composite Pin-Joints, *Journal of Composite Materials*, Vol. 34, No. 12, pp. 1028-1054.
45. Turaga, U.V.R.S. and Sun, C.T. (2000) Failure Modes and Load Transfer in Sandwich T-Joints, *Journal of Sandwich Structures and Materials*, Vol. 2, July, pp. 1-21.
46. Zeng, Q.G. and Sun, C.T. (2001) Novel Design of a Bonded Lap Joint, *AIAA Journal*, Vol. 39, No. 10, October, pp. 1991.

8.6 Problems

- 8.1. a. For the laminate discussed by Van Siclen and the results presented in Figures 8.12, 8.13, and 8.14, if each ply is $0.0055''$ thick, using Figure 8.14 what total load (lbs) per bolt can be carried by a structure using $1/4''$ diameter bolt? (i.e. $P_{BR} = ?$)
 - b. Using Figure 8.13, if the construction has an edge distance, e , of $3/4''$, what side distance, s , is required to withstand the same load per bolt as in (a) above? (i.e. $P_{BR} = P_{SO}$, $s = ?$)
- 8.2. a. For the laminate discussed by Van Siclen in Figures 8.12 and 8.13, namely $[0^\circ, \pm 45^\circ, 90^\circ]_s$, if each lamina is $0.0055''$ thick, using Figure 8.14, what total load (lbs) per bolt can be carried by a structure using $5/8$ diameter bolts? (what is $P_{BR} = ?$)
 - b. Using Figure 8.13, if the construction has an edge distance, e , of $3/4''$, what side distance, s , is required to withstand the same load per bolt as in Problem 8.1 above? (that is $P_{BR} = P_{SO}$)
- 8.3. Consider a laminate composed of the composite of Figures 8.12, 8.13, and 8.14, $[0^\circ, \pm 45^\circ, 90^\circ]_s$, eight plies, hence $h = 0.044''$. If a $3/8''$ diameter bolt is used, with a side distance $s = 1''$, and $1''$ edge distance, e , in which mode of the three will the panel fail due to the bolt load; what is that failure value?
- 8.4. Why is adhesive bonding potentially better for joining composite material components together than using mechanical fasteners?
- 8.5. List six different types of adhesively bonded joints.
- 8.6. What are three types of failure in mechanically fastened joints?
- 8.7. What makes a combination of mechanically fastened and a bonded joint superior to either a mechanically bonded joint or an adhesively bonded joint separately?
- 8.8. What are five good design rules for designing a good bonded joint in composite

material structures?

- 8.9. What are five good rules to follow in designing good mechanically fastened joints in composite material structures?
- 8.10. Consider a laminate composed of a composite shown in Figures 8.12, 8.13 and 8.14, i.e., $[0^\circ, \pm 45^\circ, 90^\circ]_s$, eight plies, hence $h = 0.044''$. If a bolt of $1/4''$ diameter is used to fasten this laminate to another, where the side distance is $s = 3/4''$, and the edge distance is $e = 3/4''$, when an in-plane load P is applied, what is the maximum load P that the laminate can withstand, and in what mode will the laminate fail?
- 8.11. Consider a laminate composed of a composite shown in Figures 8.12, 8.13 and 8.14, i.e., $[0^\circ, \pm 45^\circ, 90^\circ]_s$, eight plies, hence $h = 0.044''$. If a bolt of $1/4''$ diameter is used to fasten this laminate to another, where the side distance is $s = 1''$, and the edge distance is $e = 1''$, when an in-plane load P is applied, what is the maximum load P that the laminate can withstand, and in what mode will the laminate fail?
- 8.12. For the laminate discussed by Van Siclen in Figures 8.12 and 8.13, namely $[0^\circ, \pm 45^\circ, 90^\circ]_s$, if each lamina is $0.0055''$ thick, using Figure 8.14 what total bearing load, P_{BR} , per bolt can be carried by this structure using $1/4''$ diameter bolts?
- 8.13. Using Figure 8.14, if the construction of Problem 8.12 has an edge distance, e , of $3/4''$, what side distance, s , is required to withstand the load per bolt found in Problem 8.12 above? (i.e., $P_{BR} = P_{SO}$)
- 8.14. Consider the laminate described by Figure 8.12, 8.13 and 8.14, composed of eight plies of ply thickness $h = 0.0055''$, hence laminated thickness totals $0.044''$. If a $3/8''$ diameter bolt is used, with a side distance of $s = 1''$, and an edge distance $e = 1''$, in which mode of the three will the panel fail due to the bolt load? What is that failure value?
- 8.15. Given a bolted joint between two graphite/epoxy panels of $[0^\circ, \pm 45^\circ, 90^\circ]_s$ construction as given in Figures in Chapter 8, if $D = 1/4''$, $e = 1/2''$, $s = 1/2''$, and $h = 0.0055''$, find the load carrying capacity in
- Net Tension
 - Shear-out
 - Bearing
- 8.16. Consider a single lap joint adhesively bonded in which the adherends are $0.1''$ thick, made of E-glass/epoxy whose properties are:

$$E_x = 8.8 \times 10^6$$

$$E_y = 3.6 \times 10^6$$

$$\nu_{xy} = 0.23$$

$$G_{xy} = 1.74 \times 10^6$$

$$\nu_{yx} = 0.094$$

What is the ineffective length defined by Oplinger if the adhesive is **0.005"** thick?

CHAPTER 9

INTRODUCTION TO COMPOSITE DESIGN

9.1 Introduction

Through the first eight chapters, the “trees” of composite structures has been treated, now to discuss the “forest”. Design is so multifaceted, all encompassing and so dependent upon the product, materials, manufacturing processes and the type of end use that it cannot be treated succinctly. However, it is hoped that the following will provide some insight.

➤ WHAT IS DESIGN? WHAT IS THE DESIGN PROCESS?

Design is an open ended, sequential iterative procedure with feedback from previous steps required to select the next step. The design process culminates with a set of working drawings, reports and calculations from which a component of a system, a system or a process can be fabricated/constructed.

➤ WHAT ARE SOME (EVALUATION OF DESIGN) DESIGN PROCESS MODELS?

Four differing models are shown below:

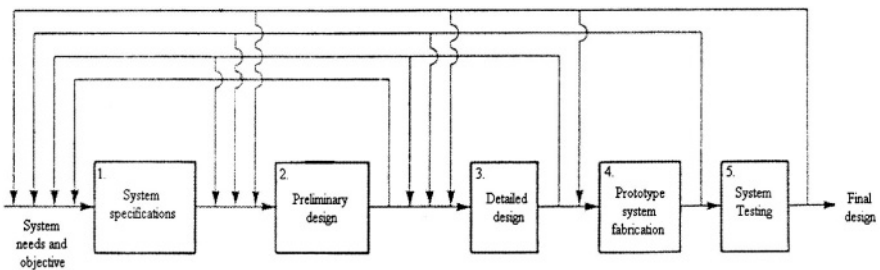


Figure 9.1. A System Evolution Model

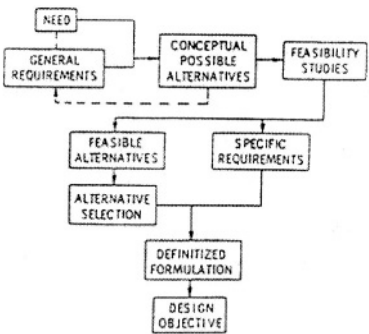


Figure 9.2. Schematic of the Evolution of the Design Objective

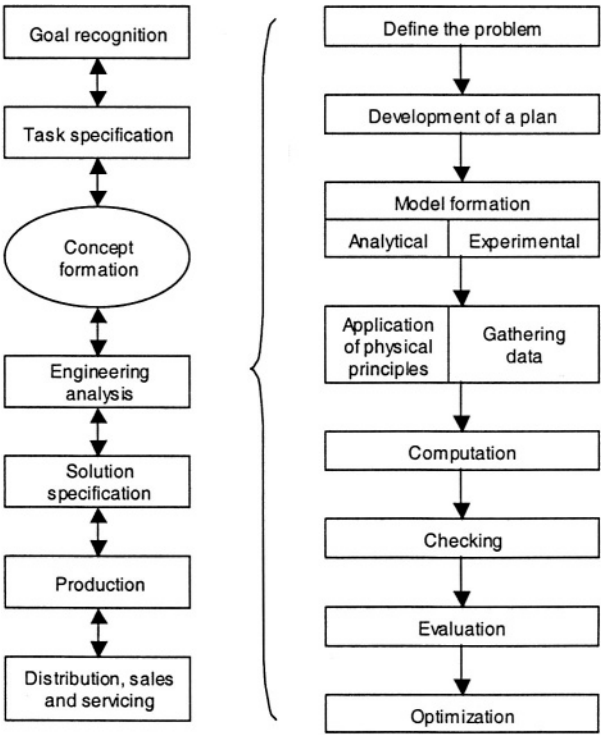


Figure 9.3. Block Diagram of the Design Process

➤ WHAT IS THE DIFFERENCE BETWEEN DESIGN AND ANALYSIS?

Analysis focuses on quantifying the performance/behavior of a component /system/process as related to a specific need/mission. The design problem is focused on calculating the size, shape and configuration of a component/system/process to meet

performance requirements for given specifications. Analysis capability must be available for the design process. If the trial design does not work, changes are made and a new design introduced until an acceptable design is developed meeting performance requirements of the given specifications. Optimization methods can play an important role in this process.

- WHAT IS THE DIFFERENCE BETWEEN CONVENTIONAL/TRADITIONAL DESIGN AND AN OPTIMUM DESIGN PROCESS?

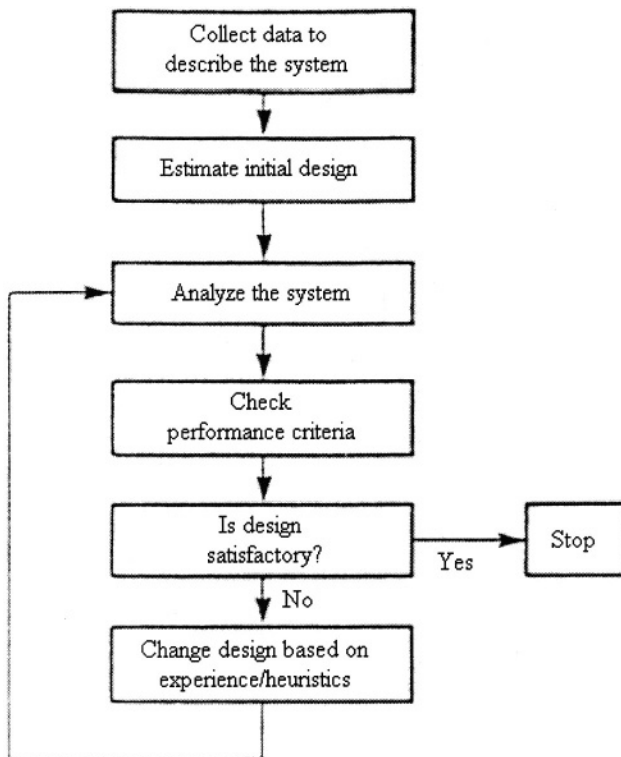


Figure 9.4. Conventional Design Process

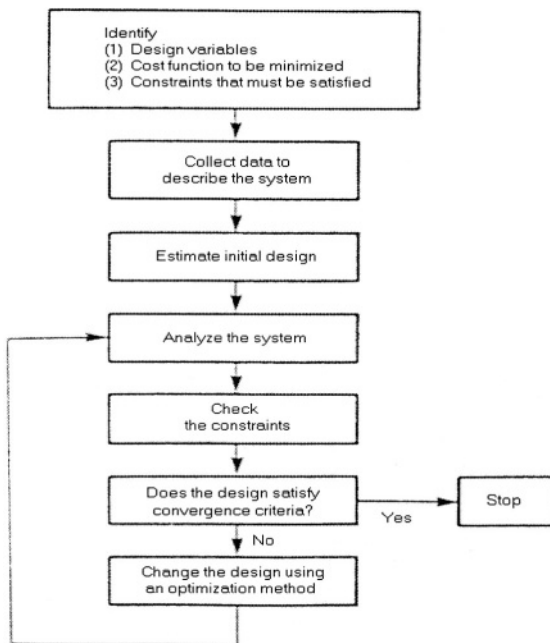


Figure 9.5. Optimum Design Process

The scarcity of resources and increased competitiveness nationally and internationally has focused increased attention on efficient, economical, safe and reliable designs. In addition, the advances in computer related technology such as computer-aided design, expert systems and artificial intelligence provide new opportunities in the design process. Thus, while the conventional design process can lead to uneconomical designs the optimum design process forces the designer to identify (recognize) a set of design variables, a cost function to be minimized and constraint functions.

Simplistically stated, the conventional design process is less formal while the optimization process is more organized using trend information to make decisions. The optimum design approach can be enhanced if designer experience (expert systems) and designer interaction (artificial intelligence) can be incorporated into the design process.

➤ WHAT ARE THE GOALS OF A DESIGNER INVOLVED WITH STRUCTURAL COMPOSITE MATERIAL DESIGN?

The goals of structural composite material design are the specifications of,

- The types of constituents and their quantities
- The ply sequences and orientation of fibers
- Selection of an appropriate component geometry
- Selection of a fabrication process

➤ WHAT DISCIPLINES MIGHT BE EMPLOYED IN THE DESIGN PROCESS?

Table 9.1. Summary of the Disciplines That Might Be Employed in the Design Process

I. Multilevel analysis for structural behavior	II. Structural analysis	III. Design
1. Micromechanics <ul style="list-style-type: none">a. ply thermoelastic propertiesb. ply uniaxial strengths	1. Classical methods	1. Conventional methods <ul style="list-style-type: none">a. handbook and design guidesb. trial and success
2. Ply combined-stress strength criterion	2. Matrix methods <ul style="list-style-type: none">a. forceb. displacement	2. Probabilistic methods
3. Laminate analysis <ul style="list-style-type: none">a. force balanceb. energyc. interply layer effectsd. transverse shear effectse. coupling responsesf. stress analysisg. edge effectsh. residual stresses	3. Finite-element methods	3. Optimization methods <ul style="list-style-type: none">a. parametric studiesb. structural synthesisc. simultaneous material and structural design
	4. Buckling	
	5. Vibrations	
	6. Impact	
	7. Statistical	

➤ WHAT IS A FRAMEWORK FOR DESIGNING STRUCTURAL COMPONENTS FROM FIBER COMPOSITES?

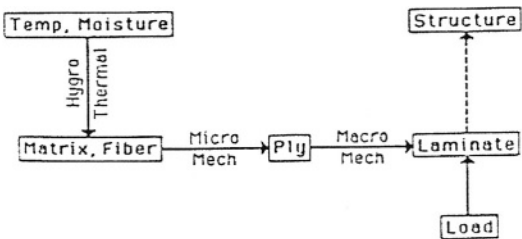


Figure 9.6. An Integrated Framework for Composites Design

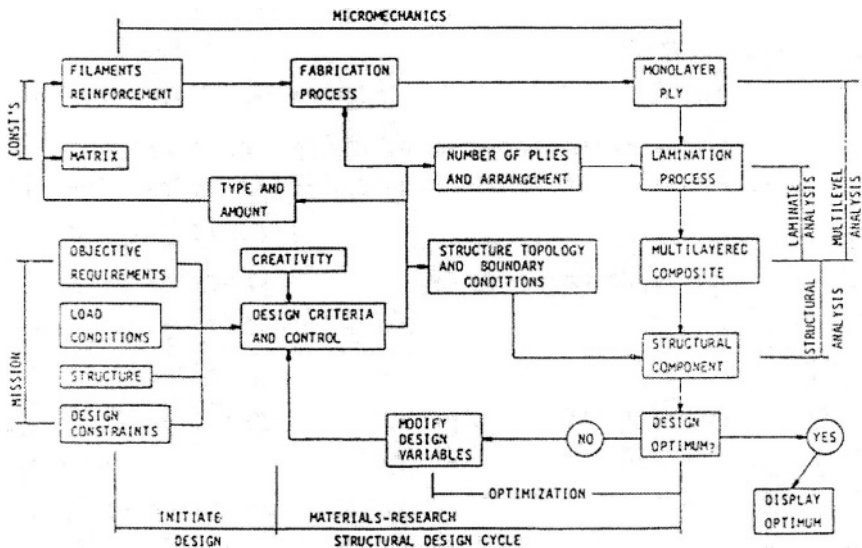


Figure 9.7. Schematic of Designing Structural Component From Fiber Composites

The above framework for designing structural components from fiber composites includes several additional elements, which are not included in the design process of conventional structural components. Three linkages are introduced for composites, these being hygrothermal analysis and data, micromechanics and macromechanics.

➤ WHAT ARE THE PRINCIPAL VARIABLE IN DESIGNING STRUCTURAL COMPONENTS FROM FIBER COMPOSITES?

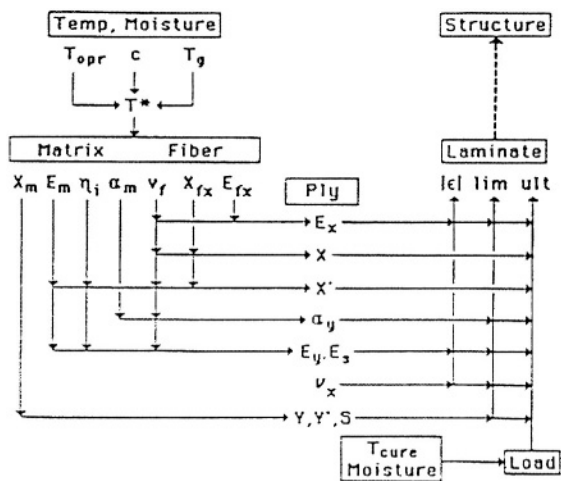


Figure 9.8. Principal Variables and Relations of Composites

The variables introduced can be defined.

➤ WHAT TYPES OF DATA ARE NEEDED IN A FIBER COMPOSITE DATA BANK?

Table 9.2. Composite Design Data Bank

1. Constituent properties	7. Creep
2. Unidirectional composite properties	8. Stress rupture
3. Environmental effects	9. Impact resistance
a. temperature	10. Viscoelastic behavior
b. moisture	11. Statistical data
c. vacuum	a. mean
4. Material nonlinearities	b. variance
5. Fatigue resistance	c. Weibull parameters
6. Notch sensitivity	

9.2 Structural Composite Design Procedures

➤ CONVENTIONAL/TRADITIONAL DESIGNS

- Trial and error process, requiring
 - Design Handbooks
 - Design Guides
 - Books, Technical Journals, Conference proceedings, professional society publications, government, industry, university reports
- Typical Data available
 - Elastic constants for unidirectional/angle ply composites
 - Ultimate/Limit stresses
 - Environmental properties, temperature, moisture, vacuum

➤ OPTIMAL DESIGN

- Parametric Studies, contour plots
- Index procedure, relate efficiency of structure to load conditions and pertinent design variables
- Structural synthesis, optimize some aspect of structure such as weight, cost, efficiency

➤ WHAT DOES A TYPICAL STRUCTURE CONSIST OF?

No matter how complex, any structure will consist of some assemblage of tension/compression members, torque tubes/rods, beams, frames, rings, membranes, plates, cylindrical and spherical shells, as shown below.

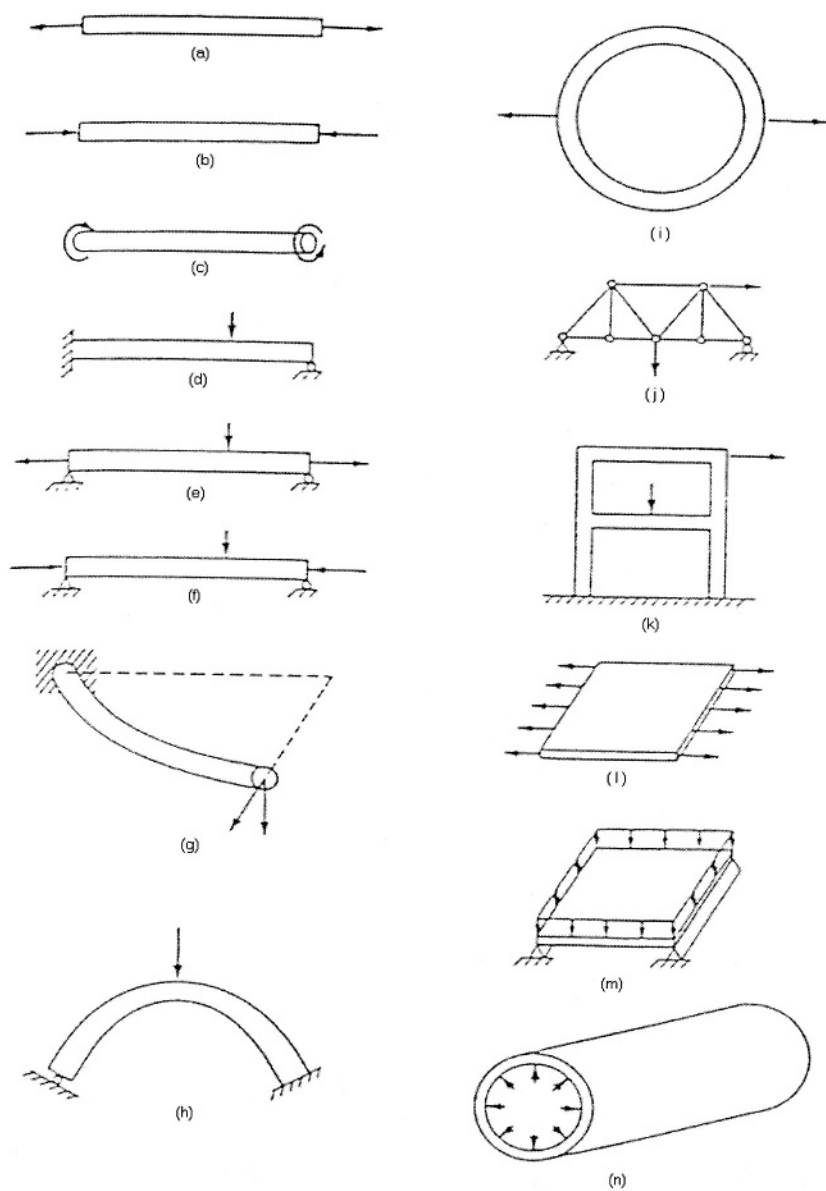


Figure 9.9.

➤ DESIGN OF A TRUSS/BAR MEMBER

As an example of the design process the following truss member is used. Returning to the block diagram of the design process.

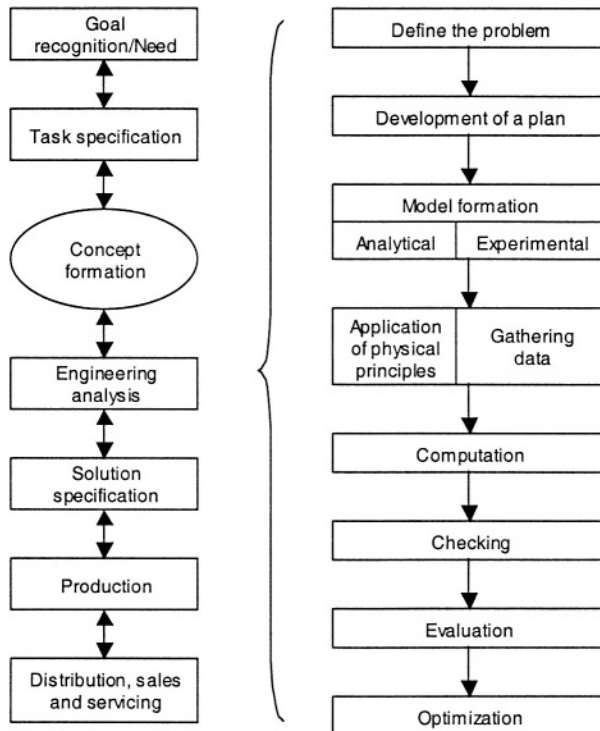


Figure 9.10. Block Diagram of the Design Process

Need: Design of a Truss/Bar member to carry tensile loads

Specifications: Tensile load requirement of 50 ksi Axial tension limited to 0.05 inches Bar geometry fixed at $1'' \times \frac{1}{2}'' \times 20''$

Concept Formation: The variables for design of the truss member are fiber type, fiber volume fraction and matrix material. Note that this flexibility would not occur using a monolithic material design.

9.3 Engineering Analysis

- Definition of problem: Design a bar $\left(1'' \times \frac{1}{2}'' \times 20''\right)$ to carry a load of 50 ksi while ensuring that the bar should not exceed 0.05 inches extension when subjected to load.
- Development of plan: Available for design of the composite (not possible for monolithic materials) is the selection of a matrix material, fiber type and fiber volume fraction.
- Model formation (Analytical/Experimental): In this example an analytical model will be used. Experiments can be introduced/used as proof tests of the selected design.
- Application of Physical Principles/Gathering Data: In this example the physical principles needed are the constitutive (stress-strain-deformation) relations for a structural component loaded uniaxially, that is, $\sigma_{iIT} = P/A$ and $\delta = \frac{PL}{AE}$ where the subscript i refers to the direction of loading/deformation that is, longitudinal, and the one direction and T refers to tension. The data needed here is information on the modulus of elasticity E_{iIT} and the ultimate strength σ of various composites. This can be obtained from the composite design data book.
- Computation: In this example the governing equations are,

$$\sigma_{iIT} = \frac{P}{A} = \frac{50,000 \text{ lbs}}{1/2 \text{ in}^2} = 10^5 \text{ psi} \quad (9.1)$$

and,

$$E_{iIT} = \frac{PL}{AE} = \frac{50,000 (20)}{1/2 (0.05)} = 40 \times 10^6 \text{ psi} \quad (9.2)$$

- Checking: In this simplistic example a checking of the computations is redundant however, the calculated σ_{iIT} and E_{iIT} could be reintroduced into the equations and a check made of for example, the load P in Equation (9.1) and similarly in Equation (9.2).
- Evaluation: Based upon the above calculations, since the modulus is high, referencing to the design data bank (see figure below) then a unidirectional boron-epoxy composite with a fiber volume ratio of 66% is selected

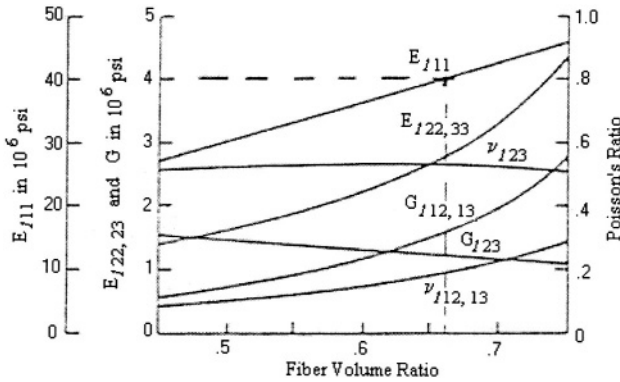


Figure 9.11. Theoretical Elastic Properties for Boron-Epoxy Unidirectional Composites. E = Young's Modulus, G = Shear Modulus, ν = Poisson's Ratio. Subscripts 1, 2, and 3 are along the fiber, transverse and through the thickness respectively (Chamis, 1968b).

From the figure blow, for a fiber volume fraction of 66%, the corresponding tensile strength in the uniaxial direction is given as, $\sigma_{11T} = 26$ ksi which is greater than the calculated value of 10 ksi. Thus the member is adequately designed.

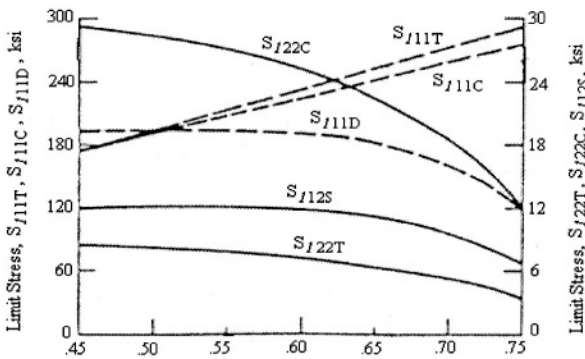


Figure 9.12. Theoretical Limit Stresses for Boron-Epoxy Unidirectional Composites. S_{11T} = Longitudinal Tensile, S_{11C} or S_{11D} = Longitudinal Compression, S_{12T} = Transverse Tension, S_{11C} = Transverse Compression, S_{12S} = Intralaminar Shear (Chamis, 1969c).

- **Optimization:** While the member has been adequately designed, the question of optimization for this example is not addressed. For example, a cost analysis of this composite system (which works) with that of another candidate system could be examined. Also, the current system while adequately designed from a modulus viewpoint is certainly oversized (factor of 2.6) from a strength point of view.

Thus there is much in the way of optimization that could be introduced in the example.

- Solution Specification: In this example, the proposed solution meets the required specifications. The solution could however be optimized.
- Production: In this example, a volume fraction of 66% represents a high degree of packing for the fibers. While in this example such a system could be fabricated, this issue can become an important consideration for other problems.
- Distribution, sales and servicing: In this example, a need has been identified thus distribution and sales are not considered. Service, i.e., reliability and safety of the component need to be addressed as the structural component is used in service over a period of time. In this case and as examples such non-destructive inspection tools as ultrasonics, X-ray radiography and thermography could be used.
- Summary: While the example cited is somewhat simplistic in its design concepts, each step of the design process has been addressed so that the student can relate to the thought process and to the sequence of events necessary to complete a successful design.

Appendix 1. Micromechanics

A. Elastic properties

For orthotropic materials in a plane state of stress, four technical engineering constants are generally needed as input into the constitutive equations in order to model the material behavior. In order to develop the analytical tools capable of modeling these material response parameters the subject of micromechanics is introduced. This topic is based principally upon the determination of overall material properties of lamina in terms of their respective constituent properties and volume fractions.

Assumptions

Fiber

- Homogeneous *
- Isotropic
- Linearly Elastic
- Regularly Spaced *
- Aligned

Matrix

- Homogeneous
- Isotropic
- Linearly Elastic *

Lamina

- Homogeneous
- Orthotropic
- Linearly Elastic *

A number of approaches are available for calculation purposes to establish the material properties of composites. Among these are,

Analytical approaches

Mechanics of Materials approach

Theory of Elasticity

- Self-Consistent Model

- Variational Principles

- Exact Solutions

Empirical Equations

Discussion of these different approaches can be found in a number of references as for example the following:

References

Mechanics of Materials Approach [1,2]

Theory of Elasticity

- Self-Consistent Model [3,4,5,6,7,8]

- Variational Methods [9,10,11,12]

- Exact Solutions [13,14,15,16,17,18,19]

Empirical Equations [20,21,22,23]

From the above approaches, two will be cited for further discussion as useful to students and design engineers.

Exact approach

The first approach employs so-called exact data. This may be properly labeled as a best method when compared with other available techniques. Inherent in this technique is the assumption that the fibers in the matrix are formally arranged in some fashion as for example the two patterns shown in Fig. 1.a,b. Other stacking/array sequences are also important and have been considered by investigators. An essential feature of this analytical methodology is the introduction of the so-called Representative Volume Element. The RVE represents the smallest reference control volume of material which contains a fiber (or fibers) surrounded by the matrix material. The RVE is considered to be both uniform and repetitive over the entire domain of the composite lamina with response characteristics representative of the composite. As indicated in the assumption for predicting the micromechanical behavior of composites, the effect of fiber arrangement/packing represents a fundamental building block in the modeling process. It appears that based upon investigation of this problem, that a hexagonal array model is

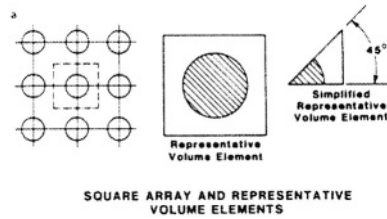


Figure 1. a. Square Array and Representative Volume Elements

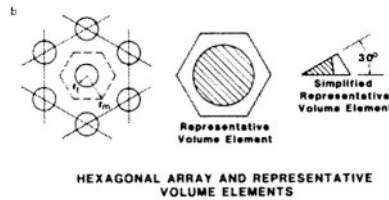


Figure 1. b. Hexagonal Array and Representative Volume Elements

more physically realistic than other geometrical arrayed models. The analytical process involved in thus determining the material properties follows the following process.

Exact analytical approach

Select an appropriate Fiber Array

Establish a representative RVE

Formulate an approximate Elastic Boundary Value Problem

Solve the formulated problem by means of

- Classical Stress Functions
- Series Solutions
- Numerical Methods (finite-differences)

Average the Elastic Fields to obtain the elastic constants

Results for calculating the four elastic constants using the “Exact” approach are noted below

$$E_L = E_f - (E_f - E_m)V_m$$

$$\begin{aligned}
E_T &= 2[(1-\nu_f + \nu_m)V_m] \\
&\times \left[(1-C) \frac{K_f(2K_m + G_m) - G_m(K_f - K_m)V_m}{(2K_m + G_m) + 2(K_f - K_m)V_m} \right. \\
&\quad \left. + C \frac{K_f(2K_m + G_f) - G_f - K_m)V_m}{(2K_m + G_f) - 2(K_m - K_f)V_m} \right] \\
\nu_{LT} &= (1-C) \frac{K_f \nu_f (2K_m + G_m)V_f + K_m \nu_m (2K_f + G_m)V_m}{K_f(2K_m + G_m) - G_m(K_f - K_m)V_m} \\
&\quad + C \frac{K_m \nu_m (2K_f + G_f)V_m + K_f \nu_f (2K_m + G_f)V_f}{K_f(2K_m + G_f) + G_f(K_m - K_f)V_m} \\
G_{LT} &= (1-C)G_m \frac{2G_f - (G_v - G_m)V_m}{2G_m + (G_f - G_m)V_m} \\
&\quad + CG_f \frac{(G_f + G_m) - (G_f - G_m)V_m}{(G_f + G_m) + (G_f - G_m)V_m}
\end{aligned}$$

Nomenclature

ν_f, ν_m = Poisson's ratio of fiber and matrix respectively
 K_f, K_m = Bulk Moduli for fiber and matrix respectively
 G_f, G_m = Shear Moduli for fiber and matrix respectively

$$K_f = \frac{E_f}{2(1-\nu_f)}, \quad K_m = \frac{E_m}{2(1-\nu_m)},$$

$$G_f = \frac{E_f}{2(1+\nu_f)}, \quad G_m = \frac{E_m}{2(1+\nu_m)}.$$

The quantity C relates to fiber spacing in the matrix with $C = 0$ representing a single isolated fiber while $C = 1$ corresponds to full contact by the fibers in the matrix. A summary of curves for different values of C and fiber/matrix types and fiber volume fractions have been plotted in Figures 2-20. These plots are displayed for the three

technical engineering constants which are functionally related to C , that is, E_T , G_{LT} and ν_{LT} . It should be noted that from practical considerations that C is generally small in magnitude.

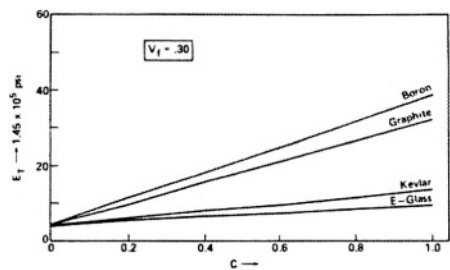


Figure 2.

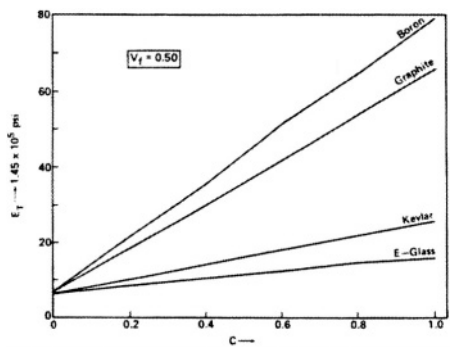


Figure 3.

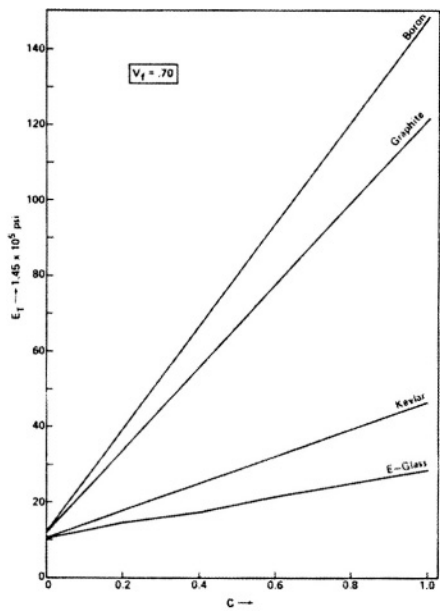


Figure 4.

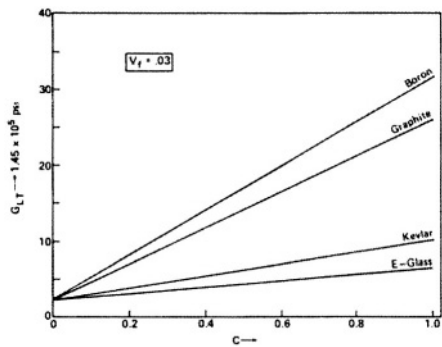


Figure 5.

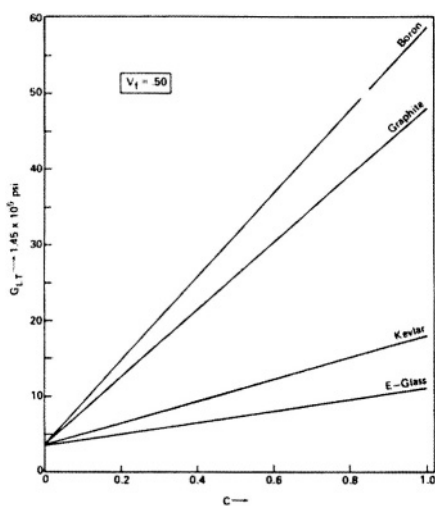


Figure 6.

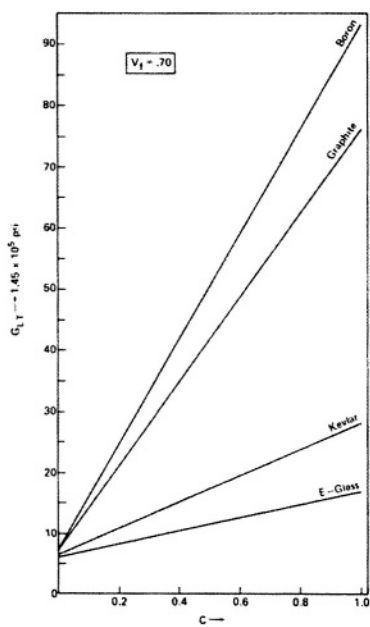


Figure 7.

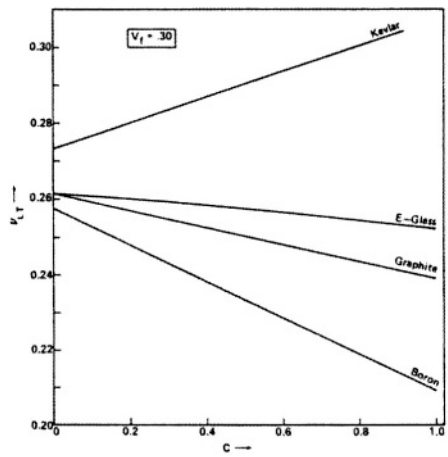


Figure 8.

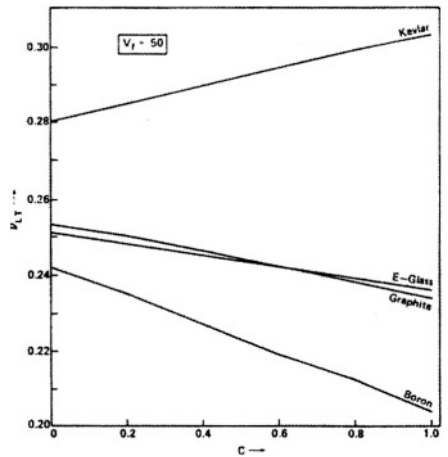


Figure 9.

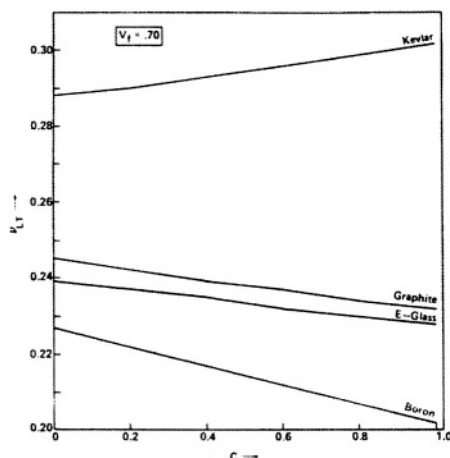


Figure 10.

Empirical equations

While the above equations represent useful formulae, they are not presented in a format which can be easily used by designers. For this reason, some compact and more rapid computational procedure is preferable. To this end the authors of Ref. [23] introduced simplifications in the formulae indicated above which take into account the,

- geometry of the fibers
- fiber packing geometry
- loading conditions

The validity of these simplifications can be measured by comparing the results of the restructured equations with those obtained using the more exact analytical procedures of micromechanics. Thus for predicting the four elastic constants for an orthotropic composite in a plan state of stress, the following equations can be used.

For the unidirectional modulus the rule of mixtures remains a satisfactory computational quantity. That is,

$$E_L = E_f V_f + E_m V_m$$

For the effective elastic moduli E_T or G_{LT} , the following formulae can be used

$$\frac{E_T}{E_m} = \frac{1 + \xi \eta V_f}{1 - \eta V_f}, \quad \frac{G_{LT}}{G_m} = \frac{1 + \xi \eta V_f}{1 - \eta V_f},$$

$$\eta = \frac{E_f / E_m - 1}{E_f / E_m + \xi}, \quad \eta = \frac{G_f / G_m - 1}{G_f / G_m + \xi}.$$

The factor ξ represents a measure of the constituent element packing geometry and loading conditions. For example, for the transverse modulus E_T , $\xi = 2$ is used while for calculation of the in-plane shear modulus G_{LT} a value of $\xi = 1$ is used. It should be noted that the values of ξ as given above provide reasonable predictions for the elastic constants up to certain volume fractions of fiber packing density and also for reasonable bounds on certain fiber geometries.

For predicting the fourth technical engineering constant, the major Poisson's ratio ν_{LT} , the rule of mixtures can again be used. Thus,

$$\nu_{LT} = \nu_f \nu_f + \nu_m \nu_m$$

When considering anisotropic and twisted fibers, such as yarns, a modification of the above formulae is necessary.

B. Physical properties

An important factor in determining the elastic properties of composites is knowledge concerning the proportion of constituent materials used in the respective lamina/laminates. These proportions can be given in terms of either weight fractions or volume fractions. From an experimental viewpoint, a measure of the weight fractions is easier to obtain than is the corresponding volume fractions of constituent elements. There is however, an analytical connection between these proportioning factors which allows conversion from weight to volume fraction and vice versa. Since volume fractions are key to elastic properties calculations, this connection remains important. The expressions necessary for this development follow.

Definitions

Volume Fractions	Weight Fraction
$V_f = \frac{v_f}{v_c}$	$W_f = \frac{w_f}{w_c}$
$V_m = \frac{v_m}{v_c}$	$W_m = \frac{w_m}{w_c}$

f, m, c refer to fiber, matrix, composite respectively

In order to interrelate the above quantities analytically, we make use of familiar density-volume relations. Thus,

$$\rho_c v_c = \rho_f v_f + \rho_m v_m \quad (1)$$

ρ refers to density

The above equation can be rewritten in terms of volume fractions by dividing thru by v_c . Thus,

$$\rho_c = \rho_f V_f + \rho_m V_m$$

Equation (1) can be couched alternately in terms of constituent weights so that,

$$\frac{w_c}{\rho_c} = \frac{w_f}{\rho_f} + \frac{w_m}{\rho_m}$$

Dividing the above equation by w_c we obtain

$$\rho_c = \frac{W_f}{\rho_f} + \frac{W_m}{\rho_m}$$

Introducing now the relationships between weight, volume and density, we have,

$$W_f = \frac{w_f}{w_c} = \frac{\rho_f v_f}{\rho_c v_c} = \frac{\rho_f}{\rho_c} V_f$$

$$W_m = \frac{w_m}{w_c} = \frac{\rho_m v_m}{\rho_c v_c} = \frac{\rho_m}{\rho_c} V_m$$

The relationship for V_f and V_m in terms of W_f and W_m can now be easily established by inverting the above relations. Further, while the current derivation has been limited by to two constituent elements, the extension to and the inclusion of multiple elements can be easily made.

A relation between weight and volume fractions of fiber or matrix can thus be analytically expressed in terms of the following equations

$$W_f = \frac{(\rho_f / \rho_m)}{(\rho_f / \rho_m)V_f + V_m} V_f \quad (2)$$

$$W_m = \frac{V_m}{\rho_f / \rho_m (1 - V_m) + V_m} \quad (3)$$

where,

W_f = Weight fraction of fibers

W_m = Weight fraction of matrix

V_f = Volume fraction of fibers

V_m = Volume fraction of matrix

ρ_f = Density of fiber

ρ_m = Density of matrix

ρ_c = Density of composite

Equations (2) has been plotted in Figure 11 for the following fiber types and corresponding fiber densities as shown in Table 1.

This figure is useful for converting between weight and volume fraction of fibers for respective materials. Other fiber types, with defined densities can be added to the plotted data as inferred by interpolation. It should be noted that for volume fractions of fiber greater than 75% care in the use of Figure 1 should be exercised. This is due to the fact that there are theoretical as well as practical limits which can be attached to the maximum allowable packing densities oriented with different fiber arrays. As specific examples for the most common arrays encountered the square and hexagonal, the maximum fiber volume fractions allowed would be 78% and 91% respectively. These results can be obtained from simple analysis which is included below for the two most common fiber packing geometries.

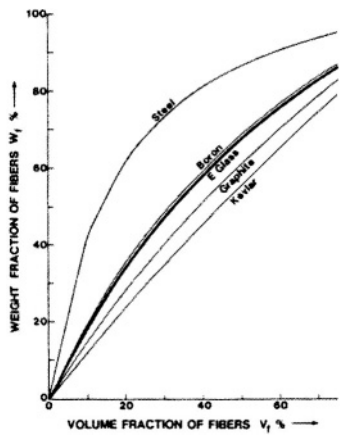


Figure 11.

Table I

Fiber Type	Density (gm/cm ³)
Kevlar 49	$\rho = 1.50$
Graphite	$\rho = 1.90$
E-glass	$\rho = 2.54$
Boron	$\rho = 2.63$
Steel	$\rho = 7.80$

Fiber Packing Geometry

1. Hexagonal Array:

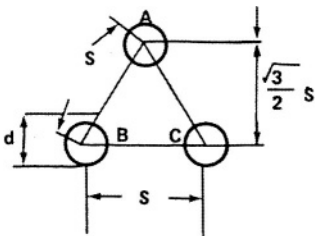


Figure 12.

Consider triangle ABC

$$A_{\text{total (area)}} = \frac{1}{2} s \left(\sqrt{\frac{3}{2}} s \right) = \sqrt{\frac{3}{4}} s^2$$

$$A_{\text{fiber (Area occupied by the fibers)}} = 3 \left(\frac{1}{6} \frac{\pi}{4} d^2 \right) = \frac{\pi}{8} d^2$$

Volume Fraction

$$V_f = \frac{A_{\text{fiber}}}{A_{\text{total}}} = \frac{\frac{\pi}{8} d^2}{\sqrt{\frac{3}{4}} s^2} = \frac{\pi}{2\sqrt{3}} = 0.907$$

2. Square Packing:

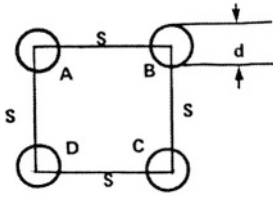


Figure 13.

Consider a square $ABCE$

$$A_{\text{total}} = S^2$$

$$A_{\text{fiber}} = 4 \times \left(\frac{\pi}{4} d^2 \times \frac{1}{4} \right) = \frac{\pi d^2}{4}$$

$$\therefore V_f = \frac{\pi}{4} = 0.785.$$

References

1. Ekvall, J.C. (1961) Elastic Properties of Orthotropic Monofilament Laminates, *ASME Aviation Conference*, Los Angeles, California, 61-AV-56.
2. Ekvall, J.C. (1966) Structural Behavior of Monofilament Composites, *AIAA/ASME 7th Structures, Structural Dynamics and Materials Conference*, Palm Springs, California, pp. 250.
3. Hill, R. (1965) Theory of Mechanical Properties of Fiber-Strengthened Materials – Self Consistent Model, *Journal of Mechanics and Physics of Solids*, Vol. 13, pp. 189.
4. Hill, R. (1965) A Self-Consistent Mechanics of Composite Materials, *Journal of Mechanics and Physics of Solids*, Vol. 13, pp. 213.
5. Whitney, J.M. (1966) Geometrical Effects of Filament Twist on the Modulus and Strength of Graphite Fiber-Reinforce Composite, *Textile Research Journal*, September, pp. 765.
6. Whitney, J.M. and Riley, M.B. (1966) Elastic Properties of Fiber Reinforced Composite Materials, *Journal of AIAA*, Vol. 4, pp. 1537.
7. Hashin, Z. (1968) Assessment of the Self-Consistent Scheme Approximation – Conductivity of Particulate Composites, *Journal of Composite Materials*, Vol. 2, pp. 284.
8. Hashin, Z. (1965) On Elastic Behavior of Fiber-Reinforced Materials of Arbitrary Transverse Phase Geometry, *Journal of Mechanism and Physics of Solids*, Vol. 13, pp. 119.

9. Paul, B. (1960) Prediction of Elastic Constants of Multiphase Materials, *Transactions of the Metallurgy Society of AIME*, Vol. 218, pp. 36.
10. Hashin, Z. and Rosen, W. (1964) The Elastic Moduli of Fiber-Reinforced Materials, *Journal of Applied Mechanism*, Vol. 31, June, pp. 223, Errate, Vol. 32, 1965, pp. 219.
11. Hashin, Z. and Shtrikman, S. (1963) A Variational Approach to the Theory of the Elastic Behavior of Multiphase Materials, *Journal Mechanics and Physics of Solids*, pp. 127.
12. Schapery, R.A. (1968) Thermal Expansion Coefficients of Composite Materials Based on Energy Principle, *Journal of Composite Materials*, Vol. 2, No. 3, pp. 380.
13. Adams, D.F. and Tsai, S.W. (1969) The Influence of Random Filament Packing on the Transverse Stiffness of Unidirectional Composites, *Journal of Composite Materials*, Vol. 3, pp. 368.
14. Adams, D.F. and Doner, D.R. (1967) Longitudinal Shear Loading of a Unidirectional Composite, *Journal of Composite Materials*, Vol. 1, pp. 4.
15. Adams, D.F. and Doner, D.R. (1967) Longitudinal Shear Loading of a Unidirectional Composite, *Journal of Composite Materials*, Vol. 1, pp. 152.
16. Chen, C.H. and Cheng, S. (1967) Mechanical Properties of Fiber-Reinforced Composites, *Journal of Composite Materials*, Vol. 1, pp. 30.
17. Behrens, E. (1968) Thermal Conductivity of Composite Materials, *Journal of Composite Materials*, Vol. 2, pp. 2.
18. Behrens, E. (1967) Elastic Constants of Filamentary Composite with Rectangular Symmetry, *Journal of Acoustical Society of America*, Vol. 47, pp. 367.
19. Foye, R.L. (1966) An Evaluation of Various Engineering Estimates of the Transverse Properties of Unidirectional Composites, *SAMPE*, Vol. 10, pp. 31.
20. Tsai, S.W. (1964) Structural Behavior of Composite Materials, *NASA CR-71*, July, National Aeronautical and Space Administration CR-71.
21. Halpin, J.C. and Tsai, S.W. (1967) Environmental Factors in Composite Materials Design, *AFML-TR-67-423 Air Force Materials Laboratory*, Wright-Patterson Air Force Base, Ohio.
22. Tsai, S.W., Adams, D.F. and Doner, D.R. (1966) Effect of Constituent Material Properties on the Strength of Fiber-Reinforced Composite Materials, *AFML-TR-66-190*, Air Force Materials Laboratory.
23. Ashton, J.E., Halpin, J.C. and Petit, P.H. (1969) *Primer on Composite Materials: Analysis*, Technomic Publishing Co., Inc., Stanford, Conn., pp. 113.

Appendix 2. Test Standards for Polymer Matrix Composites.

As can be discerned from the test material, the role of the engineer in controlling the design process using composite materials requires considerable expertise beyond traditional levels for establishing design criteria. A fundamental input into any design process is the requirement for obtaining the necessary materials properties data as well as establishing the overall material response in order to identify the types of failure events that can occur. Thus the data base for composites is an evolutionary process in which current accepted test standards are being reviewed and revisions adopted as well as composite modes of failure identified and tabulated.

As a ready means of access and awareness to the test procedures in current practice, test standards have been included. It should be mentioned that in general the engineer executes tests of the following type:

- A. *Interrogative*, that is, those examining some aspect, or is seeking fundamental information on certain properties, relations, or physical constants of materials, those using unique test apparatus.
- B. *Developmental*, that is, those tests required to obtain additional data to ensure meeting performance specifications on a selected material. In such cases both standard and modified standard test equipment may be used by the engineer.
- C. *Standardized*, that is, those tests which utilize controlled test procedures which have been adapted from sanctioned test committee and professional engineering society recommendations. Such tests are almost universally run using commercially available test equipment and with specific geometry specimens.

While all three of the aforementioned type of tests provide important data, it is the standardized test that we tend to rely upon when requiring data for materials. This is especially true since engineers in general wish to be able to duplicate specific tests using accessible equipment rather than designing totally unique test facilities. In view of these statements, the following standards given in Table 1 are provided which describe a number of common mechanical tests. Details concerning the test specimen geometry and procedures can be found in the appropriate standard.

Appreciation is expressed to Dr. Gregg Schoeppner, AFRL/MLBCM for his contribution to Appendix 2.

Mechanical/Physical Properties		Fibers	Yarns/Tows	Matrices	Continuous Composites	Discontinuous Composites
Tension	Modulus	D3379	D2256,D2343	D5934,D638	D3039,D5450,D5083,D3916	D3039,D638,D3916
Interlaminar	Strength	D3379	D2256,D2343	D638	D3039,D5450,D5083,D3916	D3039,D638,D3916
Compression	Strength			D695	D6415	
	Modulus			D695	D3410,D5449,D5467	D3410,D695
Shear	Modulus					
Interlaminar	Strength			D732	D3518,D5379,D5448	D3846,D4255,D5379
	Strength			D732	D2344	D3846,D4255,D5379
Poisson's Ratio (longitudinal)				D638	D3039,D5083	D3039,D5083
Damage Resist/Impact				D1822,D256	D6264	
CTE (long/transverse)				D696		
Moisture Diffusivity Coefficient						
Density				D792	D5229	D5229
Constituent	Voids				D792	D792
	Fibers				D2734	D2734
					D3171	D3171
Fatigue					D3479,D6115	D3479
Fracture Toughness Mode I						
Translaminar					D5528,D6115	
					E1922	
Dynamic & Loss Moduli & Creep				D4065		

Appendix 3. Properties of Various Polymer Composites.

Using such tests as described in the standards of Appendix 2, a listing of selected material properties for continuous filament unidirectional composites is included as Table A3-1 below.

The symbols used in Table A3-1 are:

- E_x Modulus of elasticity in the fiber direction
- E_y Modulus of elasticity perpendicular to the fiber direction
- ν_{xy} Major Poisson's ratio, i.e., $\nu_{xy} = (E_x / E_y) \nu_{yx}$
- G_{xy} In-plane shear stiffness
- \bar{X} Tensile strength in the fiber direction
- \bar{X}' Compressive strength in the fiber direction
- Y Tensile strength normal to the fiber direction
- Y' Compressive strength normal to the fiber direction
- S In-plane shear strength
- V_F Fiber volume fraction
- α_{11} Coefficient of thermal expansion in the fiber direction
- α_{22} Coefficient of thermal expansion perpendicular to the fiber direction
- β_{11} Coefficient of moisture expansion in the fiber direction
- β_{22} Coefficient of moisture expansion perpendicular to the fiber direction.

For conversion from the psi units used in Table A3-1 for stress and modulus of elasticity,

$$1 \text{ psi} = 6.89 \times 10^{-3} \text{ MPa (or MN/m}^2\text{)}$$

To determine the density of many of the composite materials given on the next page, use the Rule of Mixtures of Section 2.4 (pp. 51-52), along with the fiber densities given in Table 1 of Appendix 1 (pg. 387), and the polymer matrix densities given in Table 1.2 (pg. 8).

Properties of Various Polymer Composites

Composite Property	E-Glass/ Epoxy	S2- Glass/ Epoxy	Spectra/ 826 Epoxy	Kevlar 49/ Epoxy	Boron/ Epoxy	AS4/ 3501-6 Epoxy	T300/ 5208 Epoxy	IM6/ 3501-6 Epoxy	IM7/ 8551-7 Epoxy	GY70/ 930 Epoxy	AS4/ Peek (APC2)
E_x (10^6 psi)	5.6	7.5	4.5	11.0	30.0	20.0	20.0	25.0	24.0	47.1	19.4
E_y (10^6 psi)	1.4	1.7	0.5	0.8	2.7	1.3	1.5	1.6	1.2	0.9	1.3
G_{xy} (10^6 psi)	0.9	1.1	0.2	0.3	0.8	1.0	1.0	1.2	0.9	0.6	0.7
ν_{xy}	0.26	0.28	0.32	0.34	0.23	0.30	0.28	0.3	0.18	0.26	0.28
α_{11} (10^{-6} / °C)	4.0	4.0	-11.0	-4.0	4.5	-0.04	-0.04	-0.4	-0.4	-0.48	0.6
α_{22} (10^{-6} / °C)	16.0	16.0	120	57.0	20.0	18.0	18.0	18.0	18.0	18.0	29
β_{11} (10^{-4} / %M)	1.0	1.0	--	2.0	0.1	1.0	1.0	1.0	1.0	0.4	1.0
β_{22} (10^{-4} / %M)	3.0	3.0	--	3.5	3.0	3.5	3.5	3.5	3.5	3.4	2.0
\bar{X} σ_{1t} (10^3 psi)	155	230	160	200	230	310	225	400	370	110	310
Y σ_{2t} (10^3 psi)	4.5	8.8	1.2	4.3	8.8	7.5	5.8	8.1	7.4	3.8	11.6
S σ_{10t} (10^3 psi)	10.4	13.0	3.5	6.3	15.6	19.0	17.0	18.0	15.6	3.9	19.2
\bar{X}' σ_{1c} (10^3 psi)	88	125	12	40	425	210	230	223	275	102	160
Y' σ_{2c} (10^3 psi)	17	34	7	20	29	30	36	22	10	5	29

V_F nominally 60%

There is an increased use of various quasi-isotropic composite materials. Therefore the properties of a number of such materials are included as Table A3-2 below. These are taken from Pfund [1].

Table A3-2: Mechanical properties of various quasi-isotropic composite materials.

Material	Matrix	Fiber Weight Fraction	Laminate Specific Gravity	Tensile Strength lb/in ²	Tensile Modulus lb/in ² x 10 ⁶	Specific Tensile Strength	Specific Tensile Modulus	Compressive Strength lb/in ²	Compressive Modulus lb/in ² x 10 ⁶
1. E-glass mat	Polyester	0.29	1.42	12,050	0.87	8,486	0.61	16,675	0.81
2. E-glass mat	Polyester	0.33	1.44	13,630	1.08	9,465	0.75	17,690	1.04
3. E-glass W.R.	Polyester	0.50	1.63	27,550	1.99	16,902	1.22	21,750	2.03
4. S-glass W.R.	Polyester	0.50	1.64	63,800	2.90	38,902	1.77	30,450	-
5. Aramid K49, woven	Polyester	0.44	1.31	62,350	3.77	47,595	2.88	16,675	2.36
6. Carbon fiber, woven	Polyester	0.40	1.40	66,700	4.35	47,643	3.11	-	-
7. Aramid K49, woven	Epoxy	0.55	1.31	65,250	4.35	49,810	3.32	24,940	-
8. Carbon fiber, woven	Epoxy	0.59	1.47	79,750	7.98	54,250	5.43	52,200	-
9. K49/E-glass hybrid (C72/K200)	Polyester	0.40	1.46	34,800	1.81	23,835	1.24	24,650	2.14
10. K49/E-glass hybrid (C77/K200)	Polyester	0.45	1.49	36,400	2.05	24,430	1.38	22,185	2.29
11. Kevlar 49 (1350)	Polyester	0.42	1.293	53,850	2.80	-	-	16,675	2.60
12. Kevlar 49 (1350S, Twill weave)	Polyester	0.42	1.30	55,610	3.47	-	-	16,460	2.80
13. Aramid 900S (Twill weave)	Polyester	0.48	1.294	64,165	3.86	-	-	14,865	2.80
14. E-glass cloth, woven	Polyester	0.56	1.71	48,285	2.20	28,237	1.29	-	-
15. K49/E-glass hybrid (no mat)	Polyester	0.44	1.50	42,780	2.42	28,520	1.61	-	-

References

1. Pfund, B. (1999) *Designing and Building With Kevlar, Professional Boatbuilder*, January, p. 64.

Author Index

- Abrate, S. 14, 58, 78
Adams, D.F. 389
Arbocz, J. 235
Argyris, J. 54, 77
Ashton, J.E. 389
Azzi, V.D. 312, 321, 326, 331
- Baker, J.L. 253
Behrens, E. 389
Ben-Yosef, Y. 253, 254
Bert, C.W. 141, 142, 252-254
Bickley, W.G. 348
Birman, V. 253, 254
Bogdanovich, A.E. 36
Brull, M.A. 141, 243, 253
Burchill, P. 24, 36
Burk, R.C. 331
Burton, W.S. 54, 77
- Carlsson, L.A. 50, 77
Causbie, S.M. 285, 299
Challes, K. 36
Chamis, C.C. 354, 356, 357
Chao, W.C. 142
Chaturvedi, S.K. 78
Chen, C.H. 389
Cheng, S. 389
Chou, T.-W. 41, 52, 77, 78, 141
Christensen, R.M. 50, 57, 77, 78
Critchfield, M. 26, 36
Crossman, F.W. 141, 339, 348, 356
- Daniel, I.M. 57, 78
Daugherty, R.L. 173
Davies, G.J. 310, 331
DeBruyn, N.A. 334, 354
Dee, A.T. 200
Dickson, J.N. 335, 355
Dobyns, A.L. 116, 123, 124, 129, 142
Doner, D.R. 389
Dong, S.B. 252, 253
- Ekvall, J.C. 388
- Felgar, R., Jr. 132, 142, 183, 199, 200, 285, 299
Flaggs, D.L. 141, 337, 339, 343, 355, 356
Foye, R.L. 389
Fujita, A. 354, 356
- Gandhi, K.R. 354
Gellert, E. 24, 36
Gere, J. 164, 200
Ghosh, S.K. 135, 142
Goland, M. 334, 339, 355
Greenberg, J.B. 253, 254
Grimes, G.C. 335, 336, 341, 355
- Hahn, H.T. 50, 52, 77, 314, 331
Halpin, J.C. 50, 77, 389
Harris, C.E. 23, 36
Hart-Smith, L.J. 336, 337, 347, 355, 356
Hashin, Z. 50, 77, 388, 389
Hawley, A.V. 335, 341, 348, 350, 354, 355
Henderson, J. 129, 142
Hill, R. 311, 312, 326, 330, 331, 388
Hilton, H.H. 77, 79
Hofer, K.E. 334, 335, 348, 350, 355
Hoffman, O. 313, 314, 330, 331
Hsu, T.M. 335, 355
Hsu, Y.S. 253, 254
Huang, N.N. 54, 77
Hwu, C. 133, 142
- Inman, D.J. 129, 142
- Jen, M.M. 354, 357
Jones, D.L.C. 129, 140
Jones, R.M.
Jurf, R.A. 57, 78

- Kelly, A. 310, 331
 Kerr, A.D. 135, 142
 Kim, R.Y. 353, 356
 Koya, T. 260, 299
 Kuno, J.K. 333, 354
 Kutsche, D. 334, 335, 348, 350, 355

 LaBedz, R.H. 58, 78
 Lagace, P.A. 285, 299, 253, 354
 Larson, P.H. 76, 79
 Lee, C.K. 76, 79
 Legon, J.B. 354, 356
 Lehman, G.M. 335, 340, 341, 348, 349, 354, 355
 Leibowitz, M. 76-79
 Leissa, A.W. 121, 142
 Lenoe, E.M. 350, 356
 Levy, M. 102, 141
 Liber, T. 58, 78
 Lin, W.H. 354, 357
 Lindholm, V.S. 57, 77
 Liu, D. 354, 357
 Liu, T.S. 310, 331

 Marin, J. 311, 312, 331
 Marshall, I.H. 54, 77
 Matthews, F.L. 353, 356
 McKinney, J.M. 335, 355
 Mindlin, R.D. 75, 79
 Minnetyan, L. 354, 357
 Mirsky, I. 252, 253
 Miskioglu, I. 354, 356
 Moh, J.S. 133, 142
 Moon, F.C. 76, 79
 Morgan, S.L. 36
 Mouritz, A.P. 24, 27, 28, 36
 Mukhyapadyay, A.K. 138
 Muha, T.J. 339, 355
 Mura, T. 260, 299
 Murphy, M.M. 350, 356
 Murthy, P.L. 354, 356

 Nashif, A.D. 129, 142
 Nemeth, M.P. 253, 254
 Newill, J.F. 76, 79
 Nicholas, T. 58, 78

 Noor, A.K. 54, 76
 Norris, C.D. 312, 331
 Nosier, A. 253, 254

 Oplinger, D.W. 339, 341, 343, 346, 347, 354, 356
 Osgood, W.R. 336, 355

 Pagano, N.J. 66, 79
 Pajerowski, J. 355
 Paliwal, D.N. 135, 142
 Paul, B. 389
 Petit, P.H. 389
 Pipes, R.B. 50, 77, 78
 Potter, P.C. 36
 Preissner, E.C. 237, 253

 Rajapakse, Y.D.S. 58, 78
 Raju, B.B. 354, 357
 Ramberg, W. 336, 355
 Rankine, W.J.M. 306, 331
 Reddy, J.N. 141, 142, 253, 254
 Reddy, V.S. 142
 Reissner, E. 75, 76, 79, 286, 289, 293, 299, 334, 339, 355
 Renton, W.J. 334, 337, 338, 346
 Riley, M.B. 388
 Ross, C.A. 252, 254
 Roy, B.N. 252, 253
 Running, D.M. 354, 356

 Sandhu, R.S. 331
 Sankar, B.V. 253
 Schapery, R.A. 389
 Sen, J.K. 356
 Shames, I. 77
 Sharpe, W.N., Jr. 339, 355
 Shaw, D. 253, 254
 Sheinman, I. 253, 254
 Shen, C. 57
 Sherman, I. 253, 254
 Shuart, M.J. 23, 36
 Sierakowski, R.L. 36, 58, 78, 138, 252, 254
 Simites, G.J. 253, 254
 Sloan, J.G. 62, 68, 274, 299

- Smeltzer, S.S., III 253, 254
 Sokolnikoff, I.S. 36, 41, 77, 259, 299
 Sottos, N. 32
 Springer, G.S. 56, 78
 Starnes, J.H., Jr. 23, 36, 253, 254
 Stavsky, Y. 253, 254
 Stockdale, J.H. 353, 356
 Stowell, E.Z. 310, 331
 Sun, C.T. 252-254, 354, 357
 Szepe, F. 334, 354

 Taraga, U.Y.R.S. 354, 357
 Tasi, J. 252, 253
 Tauchert, T.R. 54, 77
 Tenek, L. 54, 77
 Timoshenko, S. 109, 141, 164, 200
 Tong, L. 354, 356
 Tresca, H. 331
 Tsai, S.W. 50, 66, 77, 78, 312, 313,
 321, 326, 330, 331, 389
 Tso, F.K.W. 252, 253
 Turvey, O.J. 54, 77

 Ulrich, D.R. 78

 Van Siclen, R.C. 350-354, 356
 Vinson, J.R. 41, 57, 58, 76-79, 106,
 109, 114, 138, 141, 142, 200, 230,
 243, 253, 254, 276, 285, 299, 337,
 338, 339, 346, 347, 356
 Vizzini, A.J. 253, 254
 Volkersen, O. 334, 354
 von Mises, R. 326, 331

 Waddoups, M.E. 331
 Walker, W.J. 78
 Waltz, T. 230, 253
 Wang, D.Y. 334, 354
 Warburton, G. 132, 142, 183, 200, 285,
 299
 Wetherhold, R.C. 339, 356
 White, J.C. 252, 253
 White, S. 32
 Whitney, J.M. 114, 141, 184, 200, 252-
 254, 353, 356
 Wilson, D.W. 58, 78, 141, 142

 Woinowski-Krieger, S. 109, 141
 Woldesenbet, E. 57, 78
 Wu, C.I. 299
 Wu, E.M. 314, 330, 331

 Yi, S. 77, 79
 Yon, J. 354, 357
 Young, D. 132, 142, 183, 199, 200,
 285, 299
 Yu, Y.Y. 76, 79

 Zeng, Q.G. 354, 357
 Zenkert, D. 138, 142
 Zukas, J.A. 58, 78

Subject Index

A380 super jumbo jet 23
acetals 7, 13
acoustic signature 27
acrylonitrile – butadiene styrene (ABS) 7, 13
adaptive structures
adhesive 281, 282, 333, 335-338, 340, 342, 343
 bonded joint 341, 347, 348
 ductility 340
 film thickness 335, 336
 peel strength 346
 shear stress 335-338, 347
 stresses 335, 342, 344
 tensile modulus 336
 thickness effects 338
 transverse normal stresses 336
adherends 334-337, 340, 347
advanced beam theory 184, 193
Advanced Enclosed Mast/Sensor (AEM/S)
aerodynamic smoothness 334, 340
aeroelastic tailoring 74
aerospace 19, 29
affine transformations 42
agriculture 32
AIAA 36
Airbus Industries 23
aircraft 19, 20, 22, 35, 89, 333
allowable
 bearing load 351
 loads 328
 strain 320, 321, 325, 330
 stress 34, 105, 111, 162, 184, 243, 247, 250, 306, 319, 322
Alta 25
aluminum 5, 23, 24, 27, 81, 350
 6061-T6 81
amplitude ratio 297
angle 11
 interlock composite 4
 ply laminate 34, 73, 338, 368
 of twist 137

- anisotropic 27, 34
 - compliance matrix 40, 41
 - elastic stiffness matrix 40, 41
 - elasticity 39
 - failure theory 309
 - fiber 52
 - laminate 330
 - materials 39, 40, 306, 309, 311
 - strength 309
 - tensor 40
- anisotropy 40, 259, 274, 311
- antenna 26, 27
- applied
 - lateral loads 135
 - load 243, 251
 - surface shear stresses 90, 91, 113
 - torque 243
- aramid fibers 7, 51, 141
- area moment of inertia 269
- Arleigh Burke destroyers (DDG 51) 27
- armored vehicle 32
- artificial intelligence 364
- A54
 - 3501-6 graphite/epoxy 394
 - Peek (APC42) 394
- aspect ratio 285
- ASTM
 - C393-62 293
 - D638 55
 - D3846 55
 - D5229-92 77
 - Test Standards 392
- asymmetric beam 183, 237
- asymmetry 184, 240, 340
- autoclave molding 12, 19
- automobile 24, 35
- Automotive Composite Alliance 24
- Avenger class MCMV 27
- axial
 - compression 244, 246, 251
 - displacements 178
 - equilibrium 178, 233
 - in-plane force 221
 - loads 184, 187, 243, 336
 - strain 341
 - stress resultant 178

- stretching deformations 343
- axially symmetric
 - cylindrical shell 240, 242, 243
 - in-plane loads 226
 - in-plane shear stresses 231
 - laminated shell 230
 - loads 222, 226, 228, 239-241
 - vibrations 252
- axle joint 304
- balanced joint 336
- ballistic protection 28
- balsa 28
- beam 59, 66, 67, 73, 76, 87, 108, 129, 155-160, 164-173, 179-183, 186, 190, 199, 215, 244, 259, 262, 266, 289, 292, 293, 303, 368, 369
 - assumptions 261, 264
 - behavior 183
 - bending 160, 261, 262, 264
 - bending moment 290
 - cross-section 292
 - equations 165, 199, 261
 - mode shapes 182
 - natural frequencies 183
 - on an elastic foundation 221
 - transverse shear resultant 290
 - vibrations 286, 293
- beam-column 156
- bending 106, 133, 138, 155, 244, 248, 251, 273, 290, 340, 345
 - boundary layer 227, 228, 230-234, 236, 237, 243
 - loads 135
 - moment 136, 161, 166, 170, 172, 243, 290
 - stiffness 293
 - stiffness matrix 246
 - strain energy 273
 - stresses 105, 117, 159, 266
- bending-shearing coupling 74
- bending-stretching coupling 73, 105, 113, 131, 138, 139, 180, 183, 185, 218, 276, 277
- bending-twisting coupling 73, 106, 139, 140, 276, 277
- biaxial
 - compressive load 133
 - stress state 236
- bicycles 31
- bi-harmonic operator 107
- bi-modular materials 141
- biodegradable composites 32
- biological tissue 141

- biomedical engineering 141
- bird strike 179
- blades 32
- blast 27, 28
- boat hulls 16, 28
- body forces 88, 89, 260, 287
- Boeing 23
- bolt 333, 351, 380
 - bending 350, 351
 - clamping friction 350
 - joint strength 350
 - torque 350, 351, 353
- bolted
 - double lap joint 350
 - joint 348-351
 - single lap joint 351, 353
- bolted-bonded joint 348-350
- boron
 - aluminum 151
 - epoxy 79-82, 394
 - epoxy unidirectional composite 372
 - fibers 8, 387
 - laminates 349, 350
- boundary condition 94, 95, 103, 105, 107, 108, 113, 114, 120, 121, 131, 132, 159, 160, 163, 165, 167-169, 172, 173, 179, 182, 190, 191, 196, 199, 222, 233, 235, 265, 266-268, 278, 283, 285, 286, 293, 296
- box beam 135, 136
- braided
 - composite 4, 34
 - preforms 12
- brazing 333
- breakage 305
- bridge deck 28-30
- brittle materials 309, 313
- buckled plate 132
- buckling 35, 57, 130-132, 135, 138, 140, 155, 158, 179, 197-199, 243, 244, 246, 248, 250-252, 259, 260, 274, 282, 365
 - analysis 244
 - loads 35, 39, 53, 88, 92, 131, 132, 134, 135, 156, 198, 199, 244, 246, 247, 274, 282, 284
 - modes 131, 132, 138, 198, 199
 - pressure 249
 - resistance 141
 - stress 243
- buildings 28

- bulk
 - matrix 305
 - modulus 39, 50, 378
- bulkheads 28
- buses 24
- bushings 348, 349

- cable stayed bridge 30, 31
- canards 32
- cantilevered beam 162, 163, 172, 184, 267, 268, 283
- carbon
 - fibers 25, 27-29
 - fiber polymeric laminate 23
 - nanotubes 32
 - steel 5
- carbon-carbon composites 6
- cargo door assembly 24
- carrier film sheets 21
- Cartesian coordinate system 42, 43, 66, 217, 206, 293
- catalyst 16
- centrifugal forces 88
- ceramic 76
 - matrix 7
 - composite 6
- characteristic beam functions 285
- chasses 35
- chemical storage tanks 19
- chopped
 - fiber composite 3, 23
 - fiber reinforcements 5, 17
 - rovings 21
- chopper/spray gun 17
- circular
 - cylindrical shell 215-217, 222-224, 226, 228, 232, 240, 241, 243, 276
 - hole 348
- circumferential
 - coordinates 215
 - loads 231
 - stiffness 231
- clamped edge 94, 105, 109, 110, 114, 160, 168-170, 222, 232, 233, 235-239, 264, 282, 285, 286
- clamped-clamped beam 173, 184, 184, 267
- clamped-free beam 170, 183, 184, 283
- clamped-simply supported beam 172, 183, 267
- Class A finish 16

classical

- beam 160, 182, 197, 294
- beam theory 70, 94, 155, 156, 182, 290, 292, 295, 298
- plate theory 70, 91, 93, 94, 96, 111-113, 115, 124, 139, 215, 272
- shell theory 70, 215
- theory 68, 69, 91, 92, 96, 106, 111, 112, 120, 130, 135, 138, 182, 183, 252, 282, 290

cloth 20

clutch disks 24

cockpit cover 28

cold working 39

coefficient of

- hygrothermal expansion 55, 59, 64, 276, 337, 393
- moisture expansion 393
- thermal expansion 1, 8, 53, 55, 59, 64, 192, 276, 334, 393

cold press molding 15, 16

collapse 35, 243

column 58, 87, 155, 160, 198, 199

combine 32

combined axial compression and

- bending 250
- external pressure 251
- hydrostatic pressure 251
- torsion 252

combined loading 250, 316

- failure theories 306
- strength theories 306

commercial aircraft 22

compatibility equations 33, 34, 40, 66, 112

complete orthogonal set of functions 95

compliance matrix 46, 50, 316

Composite Worldwide Inc. 28

compressive

- failure mode 348
- failure strength 313
- loads 131, 132, 135, 155, 158, 188, 199, 243, 244, 315
- mechanical properties 140
- modulus of elasticity 8, 184
- stiffness 141
- strength 305, 312, 315, 393
- stresses 324
- transverse loads 315
- yield strength 306, 312, 314, 316

compression 320, 323, 325, 337

- members 368, 369
- molding 12-15

- concentrated load 155, 168, 170, 171, 266, 267, 278
 - boundary conditions 259
- conical shell 215
- conservative system 119, 294
- Consolidated Vultee B-36 Bomber 333
- constant amplitude load 338
- constituent properties 367
- constitutive equations 33, 34, 40, 42, 63, 66, 67, 76, 87, 92, 112, 132, 138, 155, 156, 178, 183, 185, 194, 195, 218, 239, 246, 274, 275, 371, 375
- contact molding 17
- continuous
 - fibers 5, 6, 11
 - laminating process 21
 - load 167, 227
- contour plots 368
- contraction 55
- control
 - element 40, 41, 88
 - volume 41
- convolution integral 124-126
- coordinate stretching 106
- copper 1, 5
 - chloride 333
- core 276, 281, 282
 - depth 281
 - material 281, 282
 - shear instability 138
- Correspondence Principle 58
- corrosion 24, 32, 35
 - prevention 334
 - resistance 27-29, 31
- corrugations 21
- countersunk fasteners 351, 353
- coupled differential equations 183, 185
- cosine load 118
- costs 12, 15, 17, 25, 27, 333, 334
- crack propagation 305
- cracks 58
- crash loads 119
- creep 56, 141, 367
 - relaxation 339
- critical
 - buckling load 245, 248, 282, 284, 285
 - load 131, 246
 - pressure 248, 249

- torque 250
- cross-link 7, 15
- cross-ply laminates 34, 74, 75, 98, 99, 101, 133, 138
- cure temperature 337
- curvature 69, 73, 74, 87, 97, 105, 125, 140, 155, 156, 166, 215, 273, 280, 285, 330
- curvilinear coordinate system 43, 217
- cut-off saw 21
- cyclic loading 35, 119, 179
- cylindrical
 - shell 215, 228, 233, 244, 246, 248, 252, 368, 369
 - woven composite 4
- d'Alembert's Principle 120, 180, 184
- damage 35, 304
- damping 27, 75, 119, 129, 334
- debond 347
- decks 28
- defects 305
- deflection functions 273
- deformation (displacement) 39, 66, 68, 75, 112, 133, 141, 158, 185, 189, 190, 192, 196, 215, 218, 232, 259-261, 270, 274, 276, 278, 279, 286, 288-292, 294, 296, 329, 337
- degradation 304
- density 52, 387
- design 33, 34, 58, 63, 65, 92, 94, 104, 105, 111, 129, 131, 132, 156, 173, 180, 182, 199, 216, 228, 233, 236, 249, 250, 259, 268, 270, 271, 303-305, 309, 316, 318, 323, 328, 333, 334, 338, 341, 346-353, 361-373, 391
- design driver 303, 304
- destroyer 27
- differential
 - equation 242
 - operator 173
- dilatational 65
 - energy 309
 - strain 41, 64
- direction cosine 43
- discontinuity 168
- discontinuous
 - boundary conditions 259
 - fiber reinforced composite 5
 - flexural stiffness 167
 - load 165
 - thickness 267
- displacement tensor 48
- distortion energy criterion 308, 309, 326
- double

- doubler joint 335, 339, 340
- lap joint 335, 336, 339-341, 344-346, 349, 350
- sine series 132
- drive shaft 24
- ductile
 - adhesives 338
 - materials 309
 - matrices 309
 - metals 311
- Duhamel integral 124
- dynamic
 - deformations 289
 - effects 119, 180, 286
 - loads 35, 57, 119, 120, 124, 125, 129, 132, 179, 180, 184, 193, 199, 333, 348
 - magnification load factor 129
- edge
 - delamination 305
 - displacement 230
 - distance 348-351, 353
 - effects 365
 - load solutions 222, 225, 243
 - moment 223-225
 - shear load 224
 - shear resultant 224
- effective shear resultant 95
- E-glass epoxy 98, 99, 191, 209, 212, 230, 358, 394
 - cross-ply composite 99, 100
 - laminate 101
- E-glass fibers 6, 28, 387
- E-glass/mat polyester 395
 - W.R. polyester 395
- eigenfunctions 132, 199
- eigenvalue problem 119, 120, 124, 132, 199, 259, 284
- Einsteinian notation 89
- elastic
 - body 260
 - constants 52
 - energy 308
 - foundation 115, 135, 221
 - foundation modulus 221
 - instability 35, 155, 179, 244
 - limit 337
 - perfectly plastic characterization 336
 - stiffness matrix 45
 - strain energy density function 57

elasticity

- equations 65, 217, 289
- matrix 44
- tensor 42, 43

electrical

- field intensity vector 75
- insulation 334
- potential 76
- signature 27
- transmission tower 268, 271

electromagnetic shielding 25

electro-rheological fluids 75

elliptical coordinate system 43

empirical factor 244, 247, 248, 351

energy

- methods 87, 259
- principles 261
- theorems 260
- solutions 266

engineering

- analysis 371
- plastics 5
- shear strain 43

environmental effects 35, 310, 329, 367, 368

epoxy 7, 8, 13, 19, 24, 28, 29, 32, 52, 57, 58, 82, 309

equations of motion 293, 294

equilibrium equations 33, 34, 40, 66, 76, 87-91, 112, 132, 133, 138, 156, 157, 183, 184, 193, 217, 239, 240, 259, 260, 286, 289, 290, 292, 323, 341

equivalent lateral pressure 221

esthetic considerations 239

Euler coefficient 117

Euler-Lagrange equations 264, 286

exact solution 95

excessive wear 304

expert systems 364

experimental considerations 252

explosion 57

exponential

- data 247
- decay 223-227, 234
- function 343
- pulse loading 127, 129

extensional stiffness 136, 293, 335

- behavior 183
- matrix 73, 135, 246
- strain 41

- external pressure 243, 248, 249, 251
- extrusion 11
- fabric 21
 - reinforced composite 5
- fabrication 39, 305, 364, 366
- face 276, 281, 282
 - dimpling 138
 - material 281, 282
 - thickness 281
 - wrinkling instability 138
- failsafe 323, 328, 330
 - design 325
- failure 198, 199, 243, 303-307, 309-314, 322, 326, 347
 - analysis 305, 316, 328
 - characterization 304
 - criterion 303, 306, 312, 314, 315, 318, 321, 326-328, 330
 - envelope 306, 328, 329, 348
 - initiation 304, 305
 - loads 336
 - mechanisms 305
 - modes 131, 198, 305, 336, 348, 349
 - strength 309, 310
 - stress 162, 247, 250
- fasteners 348-351
- fatigue 26, 27, 35, 350
 - cracks 335
 - damage 180
 - failure 119
 - life 334-350
 - resistance 334, 367
 - run-out 335, 337, 338, 350
 - specimens 335
 - strength 335
 - stress 27
 - tests 335, 338, 350
- fiber 4, 21, 25, 27, 29, 304, 365, 367, 375
 - buckling 140
 - cutting 348
 - dominated failure 305
 - failure 328
 - materials 140
 - optics 5
 - orientation 246, 305, 351
 - packing geometry 378, 389
 - placement 19

- properties 51
- reinforced composite 3, 5, 13, 14, 16, 39, 62, 309, 312
- volume fraction 98, 372, 393
- fiberglass 11, 26, 29
 - boats 28
 - bolted joints 348
 - laminates 349
 - mat 32
- filament winding 11-13, 19, 20
- fins 32
- fire 27, 28
- finite difference methods 334
- finite element methods 334, 339, 351, 365, 377
- first ply failure 328, 330
- fishing rods 10, 31
- flammability 28
- flange plate 282
- flaw 304, 305
 - dominated failure 305
- flexural
 - natural frequencies 295
 - stiffness 97, 107, 110, 132, 165, 218, 228, 240, 262, 273, 293
 - stiffness matrix 73, 135, 246, 278
 - vibrations 293
- FM 73M adhesive 56
- FM 300 adhesive 56
- foam core 25, 28, 276
- forced vibration 119, 124
- forcing function 120, 173, 181, 243
- Ford Excursion SUV 24
- forensic analysis 182
- forging 39
- forming 334
- forming block 20, 21
- forward swept wings 23
- foundation modulus 115
- fracture 306
 - criteria 236
 - stress 250
- frames 368, 369
- free
 - body diagram 108
 - edge 94, 105, 115, 160, 168, 169, 222, 264, 282, 285, 286
 - vibration 121, 252, 293, 295
- free-free beam 183
- Freedonia Group, Inc. 21

- French Navy 26
- frequency
 - equations 297, 298
 - tunable hybrid composite material 26
- friction 351
- frigate 26, 27
- fuel
 - consumption 24
 - storage tank 24
- functionally graded materials 32
- fundamental frequency 121, 182
- funnel 27

- Galerkin's method 173, 175
- Gaussian curvature 273
- gel coat 14-17
- general anisotropy 47
- generalized Navier approach 96
- geometric perturbation 108
- glass 11, 16
 - polyester composite 55, 56
 - transition temperature 9, 55
- glazing panels 21
- golf clubs 10, 31
- governing differential equations 106, 107, 138-140, 159, 172, 178, 180, 189, 194, 197, 215-217, 219, 226, 239-241, 259, 264, 286, 291, 294
- graphite-epoxy 30, 80, 209, 210, 352
 - cross-ply laminate 101
 - laminate 100, 101
- graphite fibers 4, 51, 80, 82, 387
- gravitational forces 88
- Green-Gauss Divergence Theorem 288
- Green's Functions 171, 172
- guitars 32
- GY 70/339 graphite epoxy 80, 83, 84
- GY 70/930 graphite epoxy 394
- gyroscopes 35

- half range sine series 96
- halogenated polyester 7
- Hamilton's Principle 286, 293
- hand lay-up 12, 13, 16-18, 28, 32
- harmonic oscillations 179, 180, 296
- hatches 28
- heated steel die 20, 21
- helicopters 20, 26

- hereditary integral 339
- hexagonal array 377, 387
- high
 - explosive blast load 129
 - modulus graphite/epoxy 81
 - strain rate effects 35, 37
 - strength graphite/epoxy 81
- highway system 28, 297
- Hill's criterion 311
- Hinnoy 25
- HM-S graphite 82
- Hoffman failure criterion 315, 330
- homogeneous
 - algebraic equations 176
 - anisotropic material 306
 - boundary conditions 173, 259
 - equations 120, 131, 181, 198
 - lamina 304
 - laminated 304
 - orthotropic material 306
 - shell equations 226
 - solution 227
- honeycomb core 28
- Hooke's Law 62, 307, 320, 325
- hull structure 25
- human bone 39
- humidity 239, 310, 329, 333
- hybrid composite 3, 6, 25, 26, 40, 52
- hydraulic
 - head 109
 - pressure 110
- hydrogen storage cylinders 24
- hydrostatic pressure 248, 249, 251, 309
- hygrothermal 54, 191, 365
 - analysis 366
 - effects 53, 55-57, 60, 62, 68, 76, 91-93, 156, 157, 162, 178, 259, 274, 335, 336, 339, 351
 - environment 55, 353
 - load 186, 193, 274, 334, 353
 - solutions 55, 77, 93
 - strain 75, 275
- Hysol EA951 adhesive 338
- I-beam 20
- IM6/3501-6 graphite epoxy 394
- IM7/8551-7 graphite/epoxy 56, 394

- impact 32, 40, 58, 179, 180, 365
 - loading 27, 119, 179
 - resistance 16, 367
- in-plane shear
 - stiffness 393
 - strength 393
- indicial equation 103
- ineffective length 341, 343, 344, 346, 347
- infrastructure 28, 29
- initial
 - displacement 294
 - imperfection 244
 - stresses 310
 - velocity 294
- injection
 - molding 12, 13, 15, 16
 - screw 15
- integration by parts 291
- in-plane
 - boundary conditions 115
 - buckling load 283, 285
 - compressive load 156
 - displacement 113, 130, 139, 158, 177, 183, 221, 222, 278, 336
 - dynamic load 337
 - forces 72
 - loads 113, 130-132, 157, 159, 197, 198, 274, 283, 337, 341, 342
 - shear load 132
 - shear modulus 280, 282
 - shear strength 276, 277, 280, 282
 - shear stresses 99, 280
 - shear test 276
 - stiffness 218, 278
 - strain 130
 - strain energy 273
 - stress 98
 - stress resultant 72, 74
 - tensile load 152
 - tractions 348
- integral equations 172
- intelligent material 76
- interactive
 - equations 250-252
 - failure criterion 310, 311, 315, 316, 326, 327, 330
 - failure envelope 329
 - failure modes 315
 - yield criterion 311

- infrared signature 27
- interface 350
 - dominated failure 305
- interior environment 239
- interlaminar
 - shear failure 336
 - shear stress 90, 91, 230
 - tensile stresses 336
- internal pressure 232, 233
- interply layer effects 365
- isopolyester 28
- isothermal strain 60, 76, 275
- isotropic 34, 51, 74, 97, 348, 375
 - adherends 336
 - beam 162, 164, 261
 - material 39, 40, 159, 160, 162, 215, 276, 280, 287, 293, 305, 306, 348
 - plate 96, 102, 103, 106, 107, 109, 120, 121, 124
 - yield criterion 311
- isotropy 47
- iteration 270
- jacket wrap system 28
- John Deere 32
- joint 352
 - efficiency 335, 343, 346, 351
 - load capacity 337
- kayak paddles 31
- Kevlar 4, 25
 - fibers 7, 28, 141, 387
- Kevlar 49/epoxy composite 81, 144, 148, 206, 394
 - specimen 338
- Kevlar 49/E-glass hybrid polyester composite 395
- Kevlar 49 woven
 - epoxy composite 395
 - polyester composite 395
- kinematic
 - motion 304
 - relations 67
- kinetic energy 119, 293, 294
- Kirchoff edge condition 94, 95, 115
- ladder side rail 20, 282
- Lagrangian 293
- lamina 3, 57, 58, 63, 66, 67, 69, 70, 74, 75, 87, 90, 97, 98, 105, 117, 125, 159, 218, 231, 246, 274, 280, 304, 305, 311, 316, 318, 322-324, 328, 329, 375, 384
 - failure 304, 305, 316

- strength 315, 316, 324
- laminate 58, 66, 69, 70, 75, 87, 97, 231, 274, 276, 278, 280, 305, 311, 328, 336, 350, 351, 365, 367, 384
 - analysis 65, 365
 - failure 304, 305, 330, 331
 - equations 329, 353
 - strength 328, 348
 - stiffness 348
 - thickness 348, 351
- laminated
 - material 164, 215, 259, 276
 - plate 67, 70, 71, 91, 96, 97, 105, 111-114, 117, 124, 131, 138, 276, 280
 - shell 228, 230, 252
 - structures 69, 73, 74, 226, 246
- landing craft 24
- Landsort 25
- lap
 - joints 341
 - length 338, 340, 341, 343, 344, 347
- Laplace transformation 37
- large strains 311
- large amplitude
 - deflection 336
 - vibration 120
- lateral
 - displacement 68, 109, 112-115, 130, 131, 139, 183, 197, 221, 241, 267, 278, 283, 285, 297, 336
 - distributed load 93, 97, 102, 104, 113, 116, 117, 122, 125, 131, 155-157, 159, 165, 168, 171, 172, 184, 186, 198, 217, 261, 267, 274, 289, 292, 293
 - load coefficient 116
- layered orthotropic shell 75
- Levy
 - approach 140
 - solution 94, 102, 103, 105, 106
- limit stress 368
- lineal element 67, 68, 122
- linear
 - elasticity theory 130, 191, 197
 - vibrations 25
- liquid injection molding 59
- load 365
 - analysis 303
 - deformation behavior 349
 - discontinuity 165, 167
- local
 - failure modes 305

- fiber instability 315, 349
- Lockheed Martin 23
- long chain polymer 337
- longitudinal
 - axis 243
 - inertia 185
 - stress 306
- Los Angeles County Metropolis Transportation Authority 24
- Love's First Approximation 216
- macromechanics 365, 366
- macroscopic 1, 87
 - yield criterion 309
- magnetic
 - forces 88
 - signature 25, 27
- manufacturing processes 11, 12, 16, 17, 19, 244, 361
- margin of safety 34
- marine fenders 3
- mass 180
 - density 123, 124, 180, 185, 294
- mast 26, 27, 31
- master creep curve 56
- mat 28
- mat reinforcement 16, 20, 21
- material
 - coordinate system 64
 - invariants 66
 - nonlinearities 367
 - point 40, 87, 88
 - property perturbation 108
- matrix 5, 6, 50, 365, 367, 378
 - dominated failure modes 305, 315, 316
 - dominated properties 57
 - materials 140, 333
 - methods 365
 - properties 51
 - swelling 54
- maximum
 - axial stress
 - bearing strength 350
 - bending stress 110
 - circumferential stress 236
 - curvature 162
 - deflections 35, 92, 97, 108-111, 122, 130, 132, 161, 164, 166, 172, 173, 179, 184, 197, 199, 265, 268, 351

- distortion energy 236
- joint strength 335
- loads 350
- normal stresses 347
- peel stresses 343, 346
- principal stresses 236
- principal stress failure theory 233, 306, 308, 310, 315, 316, 318, 321, 322, 325-327, 330, 336
- shear stress 308, 335, 343, 347
- shear stress theory 236, 308, 309
- shear-out stresses 350
- strain 308
- strain theory 307, 308, 310, 315, 316, 320-322, 325-327, 330, 336
- stress 34, 97, 108-111, 117, 130, 132, 161, 162, 164, 166, 167, 173, 179, 197, 199, 234, 266, 268, 270, 325, 337
- stress couple 109, 111, 164
- stress resultants 329
- stress state 237
- McLauren series 130
- mechanical
 - fastened joint 349, 353
 - fastener 333, 348, 351
 - fastener load 189, 193
 - joint behavior 351
 - loads 334, 339
 - properties 55, 191
- membrane 108, 368, 369
 - displacements 228, 237
 - failure criterion 306
 - loads 329
 - shell theory 233, 236
 - solution 236
 - stress 228, 236, 237
- metal 39, 306, 309, 333
 - matrix composites 5, 6, 7, 309
- metallic
 - adherends 340
 - components 348
 - doublers 351
 - interleaves 351
- Metlbond adhesive 331
- Metton 203
- micro
 - buckling 305
 - mechanical failure 304
 - mechanical strength theory 305

- mechanics 304, 316, 365, 366, 375
- microscopic shear failure modes 315, 316
- middle surface 292
 - displacement 68, 72, 114, 158
 - strain 69, 73, 87
- mid-plane
 - asymmetric 114, 183, 226, 239, 241
 - asymmetric beam 186, 189
 - asymmetric cylindrical shell 239, 242, 243
 - asymmetric structure 184
 - asymmetry 138, 183, 184, 239, 277
 - asymmetry parameter 184
 - strain 73, 178, 330
 - symmetric beam 184
 - symmetric cylindrical shell 243
 - symmetric laminate
 - symmetric plate
 - symmetry 91, 92, 99, 105, 106, 112, 113, 121, 122, 124, 130, 131, 139, 156, 157, 159, 162, 164, 178, 180, 186, 197, 198, 218, 245, 247, 276, 280
- mid span deflection 293
- military aircraft 22, 23
- milling 334
- mine countermeasure vessel (MCMV) 25, 27
- mineral fibers 9
- minimum weight 250, 251
- mixed mode failure 348
- mode shapes 122, 182
- moderately thick beams 286, 289, 293
- modes of failure 311
- modulus of elasticity 39, 47, 53, 54, 58, 216, 261, 268, 393
- Mohr's circle 59
- moisture 35, 55, 57, 365, 367, 368
 - absorption 55
 - effects 55, 156, 191, 259, 339
 - equilibrium (saturation) 55
 - shift factor 57, 58
 - strain 76
 - stress couples 76
 - stress resultant 76
- moment
 - curvature relations 140
 - equations 184
 - equilibrium 90, 91, 295
- monococque
 - beams 261
 - construction 280

- plate 109, 111, 276
- monolithic materials 306, 309
- Mosquito bomber 333
- multifunctional materials 32
- mummy cases 333
- musical instruments 32
- N dimensional failure envelope 306
- nanotubes 32
- NARMCO 2387 epoxy 8
- National Aviation and Space Agency (NASA) 244, 253
- natural
 - boundary conditions 222, 264, 292, 294
 - circular frequency 121, 122, 181, 182, 298
 - flexural vibrations 120, 122
 - frequencies 35, 39, 53, 92, 119-124, 130-132, 141, 156, 180-183, 197-199, 296-298
 - vibrations 119-122, 132, 199, 252
- naval ships 24, 26, 27
- Navier
 - approach 105, 106, 116, 123, 140
 - problem 96
 - series solutions 94, 95, 98, 131
- negative shear fiber orientation 324
- net
 - tensile load 351
 - tensile strength 352
 - tension failure 349, 351
- Newton's Laws of Motion 293
- nickel aluminum bronze alloy 27
- normal pressure 353
- noise reduction and suppression 25, 27, 334
- nonhomogeneity 108
- nonlinear
 - analysis 197, 341
 - behavior 111, 349
 - effects 119, 122, 130, 180, 335
 - response 351
 - vibrations 120
- non-nuclear blast loading 129
- normal
 - modes of vibration 120, 196
 - stress 292, 339
- notch sensitivity 367
- nuclear blast load 127
- nylon 7, 8, 18

nylon 6 13
 nylon 6/6 13

off axis

 composite strength 322
 specimen 324

one time dynamic load 119

open mold 17, 28

Opsay 25

optimization 370, 372

 design process 364
 methods 363, 365

orthogonal

 anisotropy 44
 interlock 4
 set of functions 173
 woven composite 4

orthotropic

 cylindrical shell 252
 elasticity tensor 46
 lamina 320
 laminate 103
 material 45, 53, 228, 276, 310, 320, 375
 plate 96, 102, 103, 112, 114
 relationship 218
 sandwich 103

outfall structures 31

overall

 buckling 138
 buckling strength 27
 loading 352

overlap length 341, 346

overpressure 127

overstressing 131, 180, 198, 246, 248-252

PAN based carbon fibers 10

panel 66, 87, 111, 112, 119, 274, 276, 277, 334

parametric studies 365, 368

partial differentiation 260

particular solution 104, 105, 120, 172, 222, 226, 227

particulate composite 2

patrol boats 24, 25

peak stresses 343

peel stresses 336, 337, 343, 344, 346

permanent deformation 199

personnel boats 24

- perturbation 106, 108
 - parameters 108
 - solutions 94, 105, 106, 241, 243
 - techniques 108, 242, 243
- piezoelectric
 - effects 76
 - face layers 76
 - laminate 76
 - material 32, 76, 77
 - PVDF layer 76
 - stress couple 76
 - stress resultant 76
 - tensor 76
- pilings
- pins 350
- pipes 11, 19, 20
- plain holes 348
- plane strain bulk modulus 51
- plane stress 307, 308, 311-313, 316, 321, 328-330, 375
- plastic
 - deformation 119, 337
 - structural components 348
- plasticity 337, 347
 - effects 335
- plate 59, 66, 67, 70, 71, 73, 76, 81, 87, 96, 102, 105, 106, 108, 112, 114, 116, 122, 124, 132, 138, 139, 172, 243, 244, 259, 273-275, 293, 303, 309, 348, 368, 369
 - on an elastic foundation 115
 - thickness 111
- ply 69, 89, 91, 98, 246-250, 305, 328, 330, 365, 367
 - distribution 328
 - failure 329
 - orientation 246, 338
 - sequence 364
 - strength 365
 - thermoelastic properties 365
- plywood 333
- point failure envelope 306
- Poisson's ratio 8, 39, 47, 52, 81, 110, 156, 159, 164, 178, 292, 335, 378, 393
- polybutadiene 7
- polycarbonate 7, 13
- polycrystalline materials 39
- polyester 7, 8, 13, 28, 74
 - BMC 13
 - SMC 13
- polyethylene 7, 8
- polyimide 80-82

- polymer 7, 55, 58, 76
 - matrix composite 5, 6, 54, 56-58, 391
- polymeric matrix 52, 53
- polynomial 279, 343
- polyphenylene
 - oxide 13
 - sulphide (PPS) 7, 13
- polypropylene 7, 13
- polystyrene 7, 13
- polysulphone 7
- polyurethane 7, 13
- polyvinyl
 - alcohol 18
 - chloride (PVC) 7, 8, 25
- portable bridge 29, 30
- positive
 - shear fiber orientation 324
 - shear stresses 324
- post first ply failure criterion 330
- potential energy 119, 260, 268, 269, 274, 276, 277, 282, 284
- power boats 28
- preform 13, 16, 58
 - molding 13
- prepreg 58, 59
- pressure
 - bag molding 18, 19
 - bottle 11
 - hulls 27
 - vessel 19
- prestressed reinforcement 29
- principal
 - directions 318-320, 323, 329, 330
 - material axes 58, 61, 62, 310, 322, 324
 - strain 307, 311
 - stresses 306-309, 311
- prismatic bar 33
- probabilistic methods 365
- projectiles 32
- proof test 371
- propeller 27
- proportional limit 335, 338
- protruded head fasteners 351, 353
- pure shear stress test 310
- pull rolls 21
- pultrusion 11-13, 20, 29

- quasi-isotropic 109, 191, 233
 - laminate 232, 234
 - panel 109, 111
- racing boats 28
- radar 28
 - cross-section 26, 27
- Ramberg-Osgood law 336
- random
 - fiber preform 12
 - mat composite 55-57
- reaction injection molding 12
- rebar 29
- rectangular cross-section 135, 262, 289, 293
- rectangular plate 58, 68, 87, 95, 110, 120, 121, 130, 138, 139, 272, 276, 277, 285
 - test specimen 276
- recurring dynamic load 119
- recycle 31
- reduced bending stiffness 184, 186, 200, 240
- reinforced
 - concrete structures 28
 - holes 348
 - reaction transfer molding 13
 - thermoplastic composite 24
 - thermoset molding composite 15
- reinforcing mat 16, 21
- Reissner functional 291, 293
- Reissner's Variational Theorem 259, 286, 289, 293, 295
- relative humidity 55
- reliability 333, 334
- repeated roots 103
- representative volume element (RVE) 376, 377
- residual
 - strength 335
 - stresses 304, 310, 365, 369
- resin injection molding 29
- resin transfer molding 12-15, 28, 232
- resonances 35, 180
- rings 368, 369
- rivets 333, 334
- rocket cases 11, 19
- rods 11, 20, 87, 155, 158, 160, 177, 179
- room temperature cure 15, 17
- rotation 67, 68, 72, 112-115, 133, 183, 195, 218, 244, 290, 296
- rotatory inertia 124, 125, 182, 185, 252, 286, 293, 295, 298
- roving 11, 19-21, 28

RTM composite 23, 232, 234

Royal

Norwegian Navy 25

Swedish Navy 25, 26

rubber matrix 141

rudders 27

rule of mixtures 51, 383

S2 glass/epoxy 394

safety factor 27

sandwich

construction 25, 32, 278, 281

panel 26, 27, 75, 90, 112, 138, 276, 280-282

structures 65, 68

scarf joint 335, 340, 341, 346, 347, 350

SCRIMP 28

seams 244

self consistent model 376

semi

empirical methods 348, 350

infinite shell 222-224

series solution 377

service life 27

S-glass

epoxy 80, 317-319

fibers 6, 28

W.R. polyester 395

S-2 glass fibers 6, 23

shape memory alloys 76

shear 337

behavior 336

buckling 348

deformation theory 69

factor 75

loads 199

modulus 39, 49, 51, 58, 280, 293, 335, 336, 378

proportional limit 335

resultant 87, 170, 237

strain 41, 49, 56, 337, 339

strain energy to failure 336

spring 342

strength 55, 56, 280, 281, 312, 324

stress 49, 55, 277, 292, 305, 324, 337, 339, 341

stress concentration 335

test 46, 48, 55, 314, 316

- shear out
 - failure 349, 351
 - strength 350-353
 - tests 351
- sheet molding compounds (SMC) 13, 24
- shell 57, 66-68, 72, 87, 129, 172, 215, 217, 219, 233-235, 239, 243, 245, 251, 259, 293, 303, 309
 - failure 243
 - stresses 247
 - structures 69, 244, 252
 - theory 75, 89, 215, 253, 286
 - vibrations 252
- shim 348, 349
 - reinforced joint 349
- ship 28
 - funnels 27
 - shock 27
 - loading 179
- short
 - fiber composite 40, 52
 - time creep properties 58
 - time properties 57, 58
- side distance 350, 351
- simple
 - clamped beam 183
 - simple beam 183, 184, 187, 190, 195, 196
 - simple column 198
 - support 124, 160, 168
- simply supported
 - beam 167, 182, 295, 296, 298
 - edge 94, 95, 102, 105, 106, 108, 109, 110, 114, 116, 121, 122, 124, 131-133, 169-171, 181, 222, 232, 233, 236-238, 264, 266, 282, 283, 285, 286
 - plate 94, 98, 123
- simultaneous linear equations 134
- sine pulse load 125, 126
- single
 - doubler joint 340
 - ply lamina 306
 - ply strength 315
 - lap joint 334
- single ply
 - lamina 306
 - strength 315
- single layer plate 96
- skeletal matrix 2
- Skjold surface effect ship 25

- small deflection theory 336
- smart materials 75
- smoke 28
- soak time 55, 56
- softening strip 351
- soldering 333
- solid mechanics
- sonar 28
- Sonic Cruiser 23
- special orthotropy 121, 122, 124, 226, 228, 239, 244, 277, 280, 316
- specially orthotropic plates 130, 282
- Spectra 826/epoxy 394
- Spectra 900 fiber 203
- spherical
 - coordinate system 93, 293
 - shells 368, 369
- spinning 39
- spindles 20
- sports 31
- spot welded joint 334
- spray lay-up 12, 13, 17, 28
- spring 231
 - constant 115
- square array 377
- stability 244
- stacking sequence 70, 73, 92, 218, 231, 329
- stainless steel 5
- standard torques 350
- static
 - loads 129, 178, 180, 194, 195, 333, 336, 348, 352
 - material properties 54
 - strength 335
- statistical
 - analysis 365
 - data 367
- stealth 25, 239
- steel 24, 26, 27, 73, 80, 387
 - shaft 27
- stepped
 - lap joint 335, 336, 340, 341, 346, 350
 - pulse load 126, 127
 - triangular pulse loading 127
- stiffness 55, 57, 316, 335
 - critical structure 129, 161, 179
 - matrix 46, 61, 276
 - to density ratio 39

stitched

glass fiber fabric 24

preform 12

strain 39, 41, 44, 60, 65, 66, 68, 75, 141, 261, 272, 275, 287, 294, 320, 329, 330, 335, 337

curvature matrix 68

displacement relations 33, 34, 40, 65, 66, 75, 87, 112, 138, 185, 193, 197, 262, 264, 274, 275, 286, 290

dominated failure theory 310, 326

energy 260, 262, 273, 275, 276, 285

energy density function 43, 260, 262, 272, 274, 287

energy density to failure 57

space 306, 326, 327

tensor 41-43, 47, 48, 75

to failure 57

strength 55, 56, 58, 117, 243, 270, 305, 309, 316, 335

analysis 305

critical structure 129, 161, 179

degradation 316

of materials 324

reduction 336

theory 303

to density ratio 39

to weight ratio 11, 334

stress 39, 44, 65, 69, 88, 98, 117, 125, 158, 167, 232, 249, 250, 259, 261, 272, 287, 288, 291, 294, 306, 323, 325, 328-330, 335-337

analysis 32, 53, 303, 348, 365

boundary conditions 290

component 246, 290, 313

concentration 315, 333

couple 69, 70, 73, 87, 89, 97, 109, 117, 156, 215, 221, 222, 237, 238, 290, 292

displacement relations 286

dominated failure theory 310, 326

free temperature 53

redistribution 305

resultant 69, 70, 87, 89, 215, 219, 221, 243, 292, 329

rupture 317

space 306, 326, 327

strain curve 317

strain relations 33, 34, 40, 41, 65, 75, 112, 194, 218, 261, 264, 274, 286, 288, 329

tensor 41-43, 47, 48

stretching 273, 290

shearing coupling 73, 276, 277

structural

- ceramics 5
- components 316, 366, 367
- configuration 303
- coordinate system 64
- discontinuity 167
- element 306, 307, 309, 316, 328
- failure 181
- integrity 28, 105, 180, 333
- mechanics 75, 259
- reaction injection molding (SRIM) 16
- systems 309
- vibrations 129

submarines 27

substructural failure 304

superalloys 5

superposition 191

integral 124

superstructure 26

surface

- imperfection 304
- loading 273, 276
- shear stresses 91, 157, 217, 219
- stresses 88
- traction 41, 260, 262, 287

surfacing veil 20, 21

symmetric

- beam 162, 183
- laminate 74

T300

/934 graphite epoxy 149

/5208 graphite epoxy 100, 200, 204, 206, 230, 254, 394

tailgate 24

tape 57, 269

lay-up 12

tapered

- beam 268
- tower 271
- wall thickness 271

temperature 54-56, 239, 310, 329, 333, 365, 367, 368

control 20

shift factor 56, 57

tennis racket 10, 31

- tensile
 - failure 313, 348, 350
 - load 135, 158, 177, 312, 313, 315, 370
 - mechanical properties 140
 - modulus of elasticity 8, 9, 184
 - stiffness 141
 - strength 9, 55, 56, 305, 372, 393
 - test 33, 47, 48, 55
 - yield strength 306, 312, 314, 326
- tension 320, 323, 325, 337
 - compression spring 342
 - members 368, 369
- tensor 41
 - strain 61
- textile composite 52
- theorem of minimum
 - complementary energy 259
 - potential energy 140, 259-261, 264-268, 272, 274, 276, 277, 282, 283, 286, 293
- theory of elasticity 33, 376
- thermal
 - considerations 53
 - effects 55, 56, 59, 61, 75, 156, 191, 259, 274
 - gradient 58
 - insulation 29, 334
 - load 191, 334, 338
 - signature 25
 - strain 53, 75, 275
 - stress 53
 - stress couple 75
 - stress resultant 75
- thermoelastic
 - problem 55
 - solutions 76
- thermoform preform 12
- thermoplastic
 - polymer matrix 333
 - resins 7, 11, 13, 15, 21, 31
- thermoset FRP 15, 24, 31
- thermosetting resins 7, 11, 13, 31, 309
- thickened end joints 349
- thickness
 - shear mode 297
 - to diameter ratio 350
- thin walled structures 57, 68, 87, 286
- third order tensor 75
- Thornel 300/PR286 graphite/epoxy

three

dimensional effects 351

point bend test 293

time dependent loads 179, 180

time-temperature-moisture effects 56, 57

tires 141

titanium 1

Toho rayon 10

topology 215

torque tubes/rods 368, 369

torsion

buckling 250

loads 135, 137, 243, 250

torsional stiffness 137

matrix 135

total

ply discount 328

strain 75, 275

work term 273

toxicity 28

tough ductile adhesive 337

tracing constants 295

transformation

equations 319, 323

law 330

matrix 323

of variables 259

translation 66, 183, 290

transverse

force equilibrium 295

inertia 295

isotropy 47

modulus 51

normal deformation 335

normal strain 252, 272, 335-337

normal stress 62, 252, 286, 289, 290, 292, 293, 295, 337, 340, 346

properties 328

shear coefficient 112, 123

shear correction factor 194

shear deformation 59, 62, 67, 74, 75, 92-94, 106, 111, 113, 114, 116, 120-122,

124, 127, 132, 135, 138-140, 156, 157, 160, 180, 182, 183, 193,

196, 197, 199, 216, 218, 252, 259, 272, 274, 278, 286, 289, 290,

292, 293, 295, 298, 335-337, 346, 365

shear deformation shape factor 113, 116

shear force 223-225

shear modulus 50, 216

- shear resultant 69, 74, 237-239, 290
 - shear stresses 74, 98, 330
 - tension 315, 336, 337
- transversely isotropic 50, 62, 312, 316
- triangular pulse loading 126, 127
- trial function 268, 285
- trigonometric terms 227
- trimming 16
- trucks 24
- truss/bar member 370
- Tsai-Hill failure criterion 315, 330
- Tsai-Wu fracture criterion 315, 330
- tub/shower unit 17
- tube 11
- turbine blade 20
- twisted fibers 384
- twisting 139
 - deformations 72
 - stretching coupling 73, 276
- twists 72
- two dimensional fracture analysis 306
- ultimate
 - bearing strength 351
 - compressive stress 303, 306
 - shear strength 55, 56
 - shear stress 303, 306
 - static load 338
 - strength 8, 53, 56, 111, 119, 309, 322, 368
 - tensile stress 303, 306
- ultra high modulus graphite epoxy 80
- underwater shock
 - damage 28
 - explosion 57
 - loading (UNDLX) 25
 - resistance 25
- uniaxial
 - compression test 307, 310, 316
 - lamina 315
 - laminate 317
 - stress state 308
 - tensile test 307, 310, 316
 - yield strain 307
- unidirectional 34, 98, 247
 - adherend specimen 338
 - composite properties 367

- construction 338, 368
 - lamina 65
 - laminate 73, 99
- uniform
 - compressive in-plane load 282
 - convergence 96
 - flexural stiffness 170
 - lateral load 98, 109, 110, 118, 160, 184, 264, 266, 283
 - load 167, 172, 195
 - taper 268
- U.S.
 - Department of Energy 24
 - Navy 26, 27
- USS Radford 26
- United Kingdom 27, 32
- unsaturated polyester 7
- vacuum 367, 368
 - assisted resin transfer molding (VARTM) 14, 24
 - bag
 - molding 12, 18, 19, 32
- variable
 - cross-section 173
 - thickness 267
 - wall thickness 268
- variation 260, 262, 264, 269, 279, 287, 291
- variational
 - methods 260
 - operations 260, 278
 - principles 293, 376
 - problems 286
 - theorem 289
- vectorial distance 69
- vehicular loads 119
- veil 20
- vent hood 17
- vertical stabilizer 23
- very flexible composites 52
- vibration 75, 129, 179, 198, 252, 259, 286, 294, 365
 - control 129
 - damping 129
 - measurement 129
 - modes 132, 181, 199
 - stability 129
- vinylester 7, 24, 25, 28
- Visby 25-27

- viscoelastic
 - adhesive 335
 - analysis 57
 - behavior 367
 - constitutive law 339
 - effects 56, 335, 336, 339
- viscoelasticity 56, 57, 141, 347, 348
- voids 304, 305
- volume 260
 - fraction 51, 52, 384-387
- von Mises criterion 308

- wall thickness 243, 244, 269
- wave number 297
- wavelength 121
- Weibull parameters 367
- weight 339
 - efficiency 348
 - fraction 52, 384-387
 - savings 334
- weighting
 - factor 75
 - functions 74
- welding 333
- whiskers 2, 5, 9
- wind energy 32
- winding machines 20
- wings 135
- wood 39
- woven
 - fabrics 28
 - fiber composites 3, 4, 34
 - preform 12
 - roving 16, 17

- X-29 aircraft 23
- X-36 advanced research vehicle 23

- yarns 389
- yield 309, 312
 - criterion 236, 308, 326
 - point 307
 - strain 57
 - strength 119, 306, 309, 322
 - stress 27, 53, 57, 111

Mechanics

SOLID MECHANICS AND ITS APPLICATIONS

Series Editor: G.M.L. Gladwell

Aims and Scope of the Series

The fundamental questions arising in mechanics are: *Why?*, *How?*, and *How much?* The aim of this series is to provide lucid accounts written by authoritative researchers giving vision and insight in answering these questions on the subject of mechanics as it relates to solids. The scope of the series covers the entire spectrum of solid mechanics. Thus it includes the foundation of mechanics; variational formulations; computational mechanics; statics, kinematics and dynamics of rigid and elastic bodies; vibrations of solids and structures; dynamical systems and chaos; the theories of elasticity, plasticity and viscoelasticity; composite materials; rods, beams, shells and membranes; structural control and stability; soils, rocks and geomechanics; fracture; tribology; experimental mechanics; biomechanics and machine design.

1. R.T. Haftka, Z. Gürdal and M.P. Kamat: *Elements of Structural Optimization*. 2nd rev.ed., 1990
ISBN 0-7923-0608-2
2. J.J. Kalker: *Three-Dimensional Elastic Bodies in Rolling Contact*. 1990 ISBN 0-7923-0712-7
3. P. Karasudhi: *Foundations of Solid Mechanics*. 1991 ISBN 0-7923-0772-0
4. *Not published*
5. *Not published.*
6. J.F. Doyle: *Static and Dynamic Analysis of Structures*. With an Emphasis on Mechanics and Computer Matrix Methods. 1991 ISBN 0-7923-1124-8; Pb 0-7923-1208-2
7. O.O. Ochoa and J.N. Reddy: *Finite Element Analysis of Composite Laminates*.
ISBN 0-7923-1125-6
8. M.H. Aliabadi and D.P. Rooke: *Numerical Fracture Mechanics*. ISBN 0-7923-1175-2
9. J. Angeles and C.S. López-Cajún: *Optimization of Cam Mechanisms*. 1991
ISBN 0-7923-1355-0
10. D.E. Grierson, A. Franchi and P. Riva (eds.): *Progress in Structural Engineering*. 1991
ISBN 0-7923-1396-8
11. R.T. Haftka and Z. Gürdal: *Elements of Structural Optimization*. 3rd rev. and exp. ed. 1992
ISBN 0-7923-1504-9; Pb 0-7923-1505-7
12. J.R. Barber: *Elasticity*. 1992 ISBN 0-7923-1609-6; Pb 0-7923-1610-X
13. H.S. Tzou and G.L. Anderson (eds.): *Intelligent Structural Systems*. 1992
ISBN 0-7923-1920-6
14. E.E. Gdoutos: *Fracture Mechanics*. An Introduction. 1993 ISBN 0-7923-1932-X
15. J.P. Ward: *Solid Mechanics*. An Introduction. 1992 ISBN 0-7923-1949-4
16. M. Farshad: *Design and Analysis of Shell Structures*. 1992 ISBN 0-7923-1950-8
17. H.S. Tzou and T. Fukuda (eds.): *Precision Sensors, Actuators and Systems*. 1992
ISBN 0-7923-2015-8
18. J.R. Vinson: *The Behavior of Shells Composed of Isotropic and Composite Materials*. 1993
ISBN 0-7923-2113-8
19. H.S. Tzou: *Piezoelectric Shells*. Distributed Sensing and Control of Continua. 1993
ISBN 0-7923-2186-3
20. W. Schiehlen (ed.): *Advanced Multibody System Dynamics*. Simulation and Software Tools. 1993
ISBN 0-7923-2192-8
21. C.-W. Lee: *Vibration Analysis of Rotors*. 1993 ISBN 0-7923-2300-9
22. D.R. Smith: *An Introduction to Continuum Mechanics*. 1993 ISBN 0-7923-2454-4
23. G.M.L. Gladwell: *Inverse Problems in Scattering*. An Introduction. 1993 ISBN 0-7923-2478-1

Mechanics

SOLID MECHANICS AND ITS APPLICATIONS

Series Editor: G.M.L. Gladwell

24. G. Prathap: *The Finite Element Method in Structural Mechanics*. 1993 ISBN 0-7923-2492-7
25. J. Herskovits (ed.): *Advances in Structural Optimization*. 1995 ISBN 0-7923-2510-9
26. M.A. González-Palacios and J. Angeles: *Cam Synthesis*. 1993 ISBN 0-7923-2536-2
27. W.S. Hall: *The Boundary Element Method*. 1993 ISBN 0-7923-2580-X
28. J. Angeles, G. Hommel and P. Kovács (eds.): *Computational Kinematics*. 1993 ISBN 0-7923-2585-0
29. A. Curnier: *Computational Methods in Solid Mechanics*. 1994 ISBN 0-7923-2761-6
30. D.A. Hills and D. Nowell: *Mechanics of Fretting Fatigue*. 1994 ISBN 0-7923-2866-3
31. B. Tabarrok and F.P.J. Rimrott: *Variational Methods and Complementary Formulations in Dynamics*. 1994 ISBN 0-7923-2923-6
32. E.H. Dowell (ed.), E.F. Crawley, H.C. Curtiss Jr., D.A. Peters, R. H. Scanlan and F. Sisto: *A Modern Course in Aeroelasticity*. Third Revised and Enlarged Edition. 1995 ISBN 0-7923-2788-8; Pb: 0-7923-2789-6
33. A. Preumont: *Random Vibration and Spectral Analysis*. 1994 ISBN 0-7923-3036-6
34. J.N. Reddy (ed.): *Mechanics of Composite Materials*. Selected works of Nicholas J. Pagano. 1994 ISBN 0-7923-3041-2
35. A.P.S. Selvadurai (ed.): *Mechanics of Poroelastic Media*. 1996 ISBN 0-7923-3329-2
36. Z. Mróz, D. Weichert, S. Dorosz (eds.): *Inelastic Behaviour of Structures under Variable Loads*. 1995 ISBN 0-7923-3397-7
37. R. Pyrz (ed.): *IUTAM Symposium on Microstructure-Property Interactions in Composite Materials*. Proceedings of the IUTAM Symposium held in Aalborg, Denmark. 1995 ISBN 0-7923-3427-2
38. M.I. Friswell and J.E. Mottershead: *Finite Element Model Updating in Structural Dynamics*. 1995 ISBN 0-7923-3431-0
39. D.F. Parker and A.H. England (eds.): *IUTAM Symposium on Anisotropy, Inhomogeneity and Nonlinearity in Solid Mechanics*. Proceedings of the IUTAM Symposium held in Nottingham, U.K. 1995 ISBN 0-7923-3594-5
40. J.-P. Merlet and B. Ravani (eds.): *Computational Kinematics '95*. 1995 ISBN 0-7923-3673-9
41. L.P. Lebedev, I.I. Vorovich and G.M.L. Gladwell: *Functional Analysis*. Applications in Mechanics and Inverse Problems. 1996 ISBN 0-7923-3849-9
42. **J. Menčík**: *Mechanics of Components with Treated or Coated Surfaces*. 1996 ISBN 0-7923-3700-X
43. D. Bestle and W. Schiehlen (eds.): *IUTAM Symposium on Optimization of Mechanical Systems*. Proceedings of the IUTAM Symposium held in Stuttgart, Germany. 1996 ISBN 0-7923-3830-8
44. D.A. Hills, P.A. Kelly, D.N. Dai and A.M. Korsunsky: *Solution of Crack Problems*. The Distributed Dislocation Technique. 1996 ISBN 0-7923-3848-0
45. V.A. Squire, R.J. Hosking, A.D. Kerr and P.J. Langhorne: *Moving Loads on Ice Plates*. 1996 ISBN 0-7923-3953-3
46. A. Pineau and A. Zaoui (eds.): *IUTAM Symposium on Micromechanics of Plasticity and Damage of Multiphase Materials*. Proceedings of the IUTAM Symposium held in Sèvres, Paris, France. 1996 ISBN 0-7923-4188-0
47. A. Naess and S. Krenk (eds.): *IUTAM Symposium on Advances in Nonlinear Stochastic Mechanics*. Proceedings of the IUTAM Symposium held in Trondheim, Norway. 1996 ISBN 0-7923-4193-7
48. **D. Ieşan** and A. Scalia: *Thermoelastic Deformations*. 1996 ISBN 0-7923-4230-5

Mechanics

SOLID MECHANICS AND ITS APPLICATIONS

Series Editor: G.M.L. Gladwell

49. J.R. Willis (ed.): *IUTAM Symposium on Nonlinear Analysis of Fracture*. Proceedings of the IUTAM Symposium held in Cambridge, U.K. 1997 ISBN 0-7923-4378-6
50. A. Preumont: *Vibration Control of Active Structures*. An Introduction. 1997 ISBN 0-7923-4392-1
51. G.P. Cherepanov: *Methods of Fracture Mechanics: Solid Matter Physics*. 1997 ISBN 0-7923-4408-1
52. D.H. van Campen (ed.): *IUTAM Symposium on Interaction between Dynamics and Control in Advanced Mechanical Systems*. Proceedings of the IUTAM Symposium held in Eindhoven, The Netherlands. 1997 ISBN 0-7923-4429-4
53. N.A. Fleck and A.C.F. Cocks (eds.): *IUTAM Symposium on Mechanics of Granular and Porous Materials*. Proceedings of the IUTAM Symposium held in Cambridge, U.K. 1997 ISBN 0-7923-4553-3
54. J. Roorda and N.K. Srivastava (eds.): *Trends in Structural Mechanics*. Theory, Practice, Education. 1997 ISBN 0-7923-4603-3
55. Yu.A. Mitropolskii and N. Van Dao: *Applied Asymptotic Methods in Nonlinear Oscillations*. 1997 ISBN 0-7923-4605-X
56. C. Guedes Soares (ed.): *Probabilistic Methods for Structural Design*. 1997 ISBN 0-7923-4670-X
57. D. François, A. Pineau and A. Zaoui: *Mechanical Behaviour of Materials*. Volume I: Elasticity and Plasticity. 1998 ISBN 0-7923-4894-X
58. D. François, A. Pineau and A. Zaoui: *Mechanical Behaviour of Materials*. Volume II: Viscoplasticity, Damage, Fracture and Contact Mechanics. 1998 ISBN 0-7923-4895-8
59. L.T. Tenek and J. Argyris: *Finite Element Analysis for Composite Structures*. 1998 ISBN 0-7923-4899-0
60. Y.A. Bahei-El-Din and G.J. Dvorak (eds.): *IUTAM Symposium on Transformation Problems in Composite and Active Materials*. Proceedings of the IUTAM Symposium held in Cairo, Egypt. 1998 ISBN 0-7923-5122-3
61. I.G. Goryacheva: *Contact Mechanics in Tribology*. 1998 ISBN 0-7923-5257-2
62. O.T. Bruhns and E. Stein (eds.): *IUTAM Symposium on Micro- and Macrostructural Aspects of Thermoplasticity*. Proceedings of the IUTAM Symposium held in Bochum, Germany. 1999 ISBN 0-7923-5265-3
63. F.C. Moon: *IUTAM Symposium on New Applications of Nonlinear and Chaotic Dynamics in Mechanics*. Proceedings of the IUTAM Symposium held in Ithaca, NY, USA. 1998 ISBN 0-7923-5276-9
64. R. Wang: *IUTAM Symposium on Rheology of Bodies with Defects*. Proceedings of the IUTAM Symposium held in Beijing, China. 1999 ISBN 0-7923-5297-1
65. Yu.I. Dimitrienko: *Thermomechanics of Composites under High Temperatures*. 1999 ISBN 0-7923-4899-0
66. P. Argoul, M. Frémond and Q.S. Nguyen (eds.): *IUTAM Symposium on Variations of Domains and Free-Boundary Problems in Solid Mechanics*. Proceedings of the IUTAM Symposium held in Paris, France. 1999 ISBN 0-7923-5450-8
67. F.J. Fahy and W.G. Price (eds.): *IUTAM Symposium on Statistical Energy Analysis*. Proceedings of the IUTAM Symposium held in Southampton, U.K. 1999 ISBN 0-7923-5457-5
68. H.A. Mang and F.G. Rammerstorfer (eds.): *IUTAM Symposium on Discretization Methods in Structural Mechanics*. Proceedings of the IUTAM Symposium held in Vienna, Austria. 1999 ISBN 0-7923-5591-1

Mechanics

SOLID MECHANICS AND ITS APPLICATIONS

Series Editor: G.M.L. Gladwell

69. P. Pedersen and M.P. Bendsøe (eds.): *IUTAM Symposium on Synthesis in Bio Solid Mechanics*. Proceedings of the IUTAM Symposium held in Copenhagen, Denmark. 1999
ISBN 0-7923-5615-2
70. S.K. Agrawal and B.C. Fabien: *Optimization of Dynamic Systems*. 1999
ISBN 0-7923-5681-0
71. A. Carpinteri: *Nonlinear Crack Models for Nonmetallic Materials*. 1999
ISBN 0-7923-5750-7
72. F. Pfeifer (ed.): *IUTAM Symposium on Unilateral Multibody Contacts*. Proceedings of the IUTAM Symposium held in Munich, Germany. 1999
ISBN 0-7923-6030-3
73. E. Lavendelis and M. Zakrzhevsky (eds.): *IUTAM/IFTToMM Symposium on Synthesis of Non-linear Dynamical Systems*. Proceedings of the IUTAM/IFTToMM Symposium held in Riga, Latvia. 2000
ISBN 0-7923-6106-7
74. J.-P. Merlet: *Parallel Robots*. 2000
ISBN 0-7923-6308-6
75. J.T. Pindera: *Techniques of Tomographic Isodyne Stress Analysis*. 2000
ISBN 0-7923-6388-4
76. G.A. Maugin, R. Drouot and F. Sidoroff (eds.): *Continuum Thermomechanics*. The Art and Science of Modelling Material Behaviour. 2000
ISBN 0-7923-6407-4
77. N. Van Dao and E.J. Kreuzer (eds.): *IUTAM Symposium on Recent Developments in Non-linear Oscillations of Mechanical Systems*. 2000
ISBN 0-7923-6470-8
78. S.D. Akbarov and A.N. Guz: *Mechanics of Curved Composites*. 2000
ISBN 0-7923-6477-5
79. M.B. Rubin: *Cosserat Theories: Shells, Rods and Points*. 2000
ISBN 0-7923-6489-9
80. S. Pellegrino and S.D. Guest (eds.): *IUTAM-IASS Symposium on Deployable Structures: Theory and Applications*. Proceedings of the IUTAM-IASS Symposium held in Cambridge, U.K., 6–9 September 1998. 2000
ISBN 0-7923-6516-X
81. A.D. Rosato and D.L. Blackmore (eds.): *IUTAM Symposium on Segregation in Granular Flows*. Proceedings of the IUTAM Symposium held in Cape May, NJ, U.S.A., June 5–10, 1999. 2000
ISBN 0-7923-6547-X
82. A. Lagarde (ed.): *IUTAM Symposium on Advanced Optical Methods and Applications in Solid Mechanics*. Proceedings of the IUTAM Symposium held in Futuroscope, Poitiers, France, August 31–September 4, 1998. 2000
ISBN 0-7923-6604-2
83. D. Weichert and G. Maier (eds.): *Inelastic Analysis of Structures under Variable Loads*. Theory and Engineering Applications. 2000
ISBN 0-7923-6645-X
84. T.-J. Chuang and J.W. Rudnicki (eds.): *Multiscale Deformation and Fracture in Materials and Structures*. The James R. Rice 60th Anniversary Volume. 2001
ISBN 0-7923-6718-9
85. S. Narayanan and R.N. Iyengar (eds.): *IUTAM Symposium on Nonlinearity and Stochastic Structural Dynamics*. Proceedings of the IUTAM Symposium held in Madras, Chennai, India, 4–8 January 1999
ISBN 0-7923-6733-2
86. S. Murakami and N. Ohno (eds.): *IUTAM Symposium on Creep in Structures*. Proceedings of the IUTAM Symposium held in Nagoya, Japan, 3–7 April 2000. 2001
ISBN 0-7923-6737-5
87. W. Ehlers (ed.): *IUTAM Symposium on Theoretical and Numerical Methods in Continuum Mechanics of Porous Materials*. Proceedings of the IUTAM Symposium held at the University of Stuttgart, Germany, September 5–10, 1999. 2001
ISBN 0-7923-6766-9
88. D. Durban, D. Givoli and J.G. Simmonds (eds.): *Advances in the Mechanis of Plates and Shells The Avinoam Libai Anniversary Volume*. 2001
ISBN 0-7923-6785-5
89. U. Gabbert and H.-S. Tzou (eds.): *IUTAM Symposium on Smart Structures and Structonic Systems*. Proceedings of the IUTAM Symposium held in Magdeburg, Germany, 26–29 September 2000. 2001
ISBN 0-7923-6968-8

Mechanics

SOLID MECHANICS AND ITS APPLICATIONS

Series Editor: G.M.L. Gladwell

90. Y. Ivanov, V. Cheshkov and M. Natova: *Polymer Composite Materials – Interface Phenomena & Processes*. 2001 ISBN 0-7923-7008-2
91. R.C. McPhedran, L.C. Botten and N.A. Nicorovici (eds.): *IUTAM Symposium on Mechanical and Electromagnetic Waves in Structured Media*. Proceedings of the IUTAM Symposium held in Sydney, NSW, Australia, 18-22 Januari 1999. 2001 ISBN 0-7923-7038-4
92. D.A. Sotiropoulos (ed.): *IUTAM Symposium on Mechanical Waves for Composite Structures Characterization*. Proceedings of the IUTAM Symposium held in Chania, Crete, Greece, June 14-17, 2000. 2001 ISBN 0-7923-7164-X
93. V.M. Alexandrov and D.A. Pozharskii: *Three-Dimensional Contact Problems*. 2001 ISBN 0-7923-7165-8
94. J.P. Dempsey and H.H. Shen (eds.): *IUTAM Symposium on Scaling Laws in Ice Mechanics and Ice Dynamics*. Proceedings of the IUTAM Symposium held in Fairbanks, Alaska, U.S.A., 13-16 June 2000. 2001 ISBN 1-4020-0171-1
95. U. Kirsch: *Design-Oriented Analysis of Structures. A Unified Approach*. 2002 ISBN 1-4020-0443-5
96. A. Preumont: *Vibration Control of Active Structures. An Introduction (2nd Edition)*. 2002 ISBN 1-4020-0496-6
97. B.L. Karihaloo (ed.): *IUTAM Symposium on Analytical and Computational Fracture Mechanics of Non-Homogeneous Materials*. Proceedings of the IUTAM Symposium held in Cardiff, U.K., 18-22 June 2001. 2002 ISBN 1-4020-0510-5
98. S.M. Han and H. Benaroya: *Nonlinear and Stochastic Dynamics of Compliant Offshore Structures*. 2002 ISBN 1-4020-0573-3
99. A.M. Linkov: *Boundary Integral Equations in Elasticity Theory*. 2002 ISBN 1-4020-0574-1
100. L.P. Lebedev, I.I. Vorovich and G.M.L. Gladwell: *Functional Analysis. Applications in Mechanics and Inverse Problems (2nd Edition)*. 2002 ISBN 1-4020-0667-5; Pb: 1-4020-0756-6
101. Q.P. Sun (ed.): *IUTAM Symposium on Mechanics of Martensitic Phase Transformation in Solids*. Proceedings of the IUTAM Symposium held in Hong Kong, China, 11-15 June 2001. 2002 ISBN 1-4020-0741-8
102. M.L. Munjal (ed.): *IUTAM Symposium on Designing for Quietness*. Proceedings of the IUTAM Symposium held in Bangkok, India, 12-14 December 2000. 2002 ISBN 1-4020-0765-5
103. J.A.C. Martins and M.D.P. Monteiro Marques (eds.): *Contact Mechanics*. Proceedings of the 3rd Contact Mechanics International Symposium, Praia da Consolação, Peniche, Portugal, 17-21 June 2001. 2002 ISBN 1-4020-0811-2
104. H.R. Drew and S. Pellegrino (eds.): *New Approaches to Structural Mechanics, Shells and Biological Structures*. 2002 ISBN 1-4020-0862-7
105. J.R. Vinson and R.L. Sierakowski: *The Behavior of Structures Composed of Composite Materials*. Second Edition. 2002 ISBN 1-4020-0904-6

1. J. Buckmaster, T.L. Jackson and A. Kumar (eds.): *Combustion in High-Speed Flows*. 1994 ISBN 0-7923-2086-X
2. M.Y. Hussaini, T.B. Gatski and T.L. Jackson (eds.): *Transition, Turbulence and Combustion*. Volume I: Transition. 1994 ISBN 0-7923-3084-6; set 0-7923-3086-2
3. M.Y. Hussaini, T.B. Gatski and T.L. Jackson (eds.): *Transition, Turbulence and Combustion*. Volume II: Turbulence and Combustion. 1994 ISBN 0-7923-3085-4; set 0-7923-3086-2
4. D.E. Keyes, A. Sameh and V. Venkatakrishnan (eds.): *Parallel Numerical Algorithms*. 1997 ISBN 0-7923-4282-8
5. T.G. Campbell, R.A. Nicolaides and M.D. Salas (eds.): *Computational Electromagnetics and Its Applications*. 1997 ISBN 0-7923-4733-1
6. V. Venkatakrishnan, M.D. Salas and S.R. Chakravarthy (eds.): *Barriers and Challenges in Computational Fluid Dynamics*. 1998 ISBN 0-7923-4855-9
7. M.D. Salas, J.N. Hefner and L. Sakell (eds.): *Modeling Complex Turbulent Flows*. 1999 ISBN 0-7923-5590-3